SYNTHESIS AND CHARACTERIZATION OF NEW PALLADIUM-BIS(OXAZOLINE) COMPLEXES. CATALYTIC ACTIVITIES IN COUPLING AND CARBONYLATION REACTIONS

BY

MANSUR BALA IBRAHIM

A Dissertation Presented to the

DEANSHIP OF GRADUATE STUDIES

KING FAHD UNIVERSITY OF PETROLEUM & MINERALS

DHAHRAN, SAUDI ARABIA

In Partial Fulfillment of the
Requirements for the Degree of

DOCTOR OF PHILOSOPHY

In

CHEMISTRY

DECEMBER, 2015

KING FAHD UNIVERSITY OF PETROLEUM & MINERALS

DHAHRAN- 31261, SAUDI ARABIA

DEANSHIP OF GRADUATE STUDIES

This thesis, written by MANSUR BALA IBRAHIM under the direction his thesis advisor and approved by his thesis committee, has been presented and accepted by the Dean of Graduate Studies, in partial fulfillment of the requirements for the degree of **DOCTOR OF PHILOSOPHY IN CHEMISTRY.**

Dr. Bassam El Ali
(Advisor)

10/12/2015

Dr Al-Saadi Abdulaziz
Department Chairman

Dr. Mohammed Fettouhi
(Co-Advisor)

Dr. Salam A. Zummo
Dean of Graduate Studies

Sk. Asraf Ali

Dr. Shaikh A. Ali
(Member)

20/12/15

Date

Dr. Mohammed Wazeer
(Member)

Dr. Abdul Rahman Al-Arfaj
(Member)

Dedicated to my Family

ACKNOWLEDGMENTS

Alhamdulillah. Peace and blessings to our beloved prophet Muhammad sallallahu alaihi wasallam, his companions, members of his house hold and all those who followed their path in righteousness.

It is a great pleasure to express sincere appreciation to my advisor, Prof. Bassam El Ali. His passion and keenness to support his students had been solely the main reason behind the successful and timely completion of this work. His deep knowledge of the subject matter, scientific approach, careful scrutiny, constructive criticism and scholarly advice were particularly helpful in accomplishing this great task.

My deep appreciation to the committee members; Dr Mohammed B. Fettouhi (Co-Advisor), Prof. Shaikh A. Ali, Prof. Mohammed Wazeer and Prof. Abdul Rahman Al-Arfaj for their guidance and constructive advice towards the successful completion of this project.

I would also like to thank Dr Mohammed B. Fettouhi for conducting the X-ray crystallographic analysis presented in this thesis.

I am obliged to express my gratitude to Dr. S.M. Shakil Hussain (Center for Petroleum and Minerals) and Dr. Rami Suleiman (Center of Research Excellence in Corrosion) for their contributions at various stages of my research. Their inspirations, timely suggestions and enthusiasm have been greatly acknowledged.

To my parents: No words can convey, no act of appreciation can express, no gift can represent what your care and support have been to me. Please accept this piece as an

expression of my heartfelt appreciation for everything you've done for me from my childhood through the present time. May Allah continue to bless you with good health, long life and happiness than your heart can embrace.

To my loving wife, you have always been my strength. Thank you for being such a caring and understanding wife. I just hope I can keep you happy forever. May Allah bless our little princess, Aisha.

I would also like to acknowledge with deep appreciation the invaluable assistance I received from all the faculty and staff members of Chemistry department, my lab colleagues Ibrahim and Dr. Imran and all members of catalysis research group.

To my In-laws, sister, brothers and friends, thank you for your prayers and well wishes.

My gratitude goes to the King Fahd University of Petroleum and Minerals and the Kingdom of Saudi Arabia for given me the chance to study and for funding this research.

Finally, appreciations to my employer, Bayero University Kano, Nigeria, for the study fellowship to accomplish this program.

TABLE OF CONTENTS

ACKNOWLEDGMENTS..... VI

TABLE OF CONTENTS VIII

LIST OF TABLES.....XIII

LIST OF FIGURES..... XV

LIST OF ABBREVIATIONS XVIII

ABSTRACT XX

ملخص الرسالة..... XX

CHAPTER 1 INTRODUCTION AND LITERATURE REVIEW 1

1.1 General Introduction..... 1

1.2 Literature background..... 3

1.2.1 Bis(oxazoline) (BOX) ligands 3

1.2.2 Metal-bis(oxazoline) complexes 6

1.2.3 Mixed ligand metal-bis(oxazoline) complexes 7

1.2.4 Water soluble metal complexes 7

1.2.5 Supported palladium-bis(oxazoline) catalysts 8

1.3 Coupling reactions 9

1.3.1 Suzuki-Miyaura cross coupling reactions 10

1.3.2 Mizoroki-Heck coupling reaction 16

1.3.3 Sonogashira coupling reaction..... 21

1.4 Carbonylation reactions..... 26

1.4.1Alkoxycarbonylation of alkynes..... 27

1.4.2 Aminocarbonylation of alkynes 29

1.5 Problem identification 30

1.6 Objectives of the present work 31

CHAPTER 2 BIS(OXAZOLINE) LIGANDS AND PALLADIUM-BIS(OXAZOLINE) COMPLEXES: SYNTHESIS AND CHARACTERIZATIONS.....33

2.1 Introduction 33

2.2 Experimental 33

2.2.1 Materials and instruments 33

2.2.2 General procedure for the synthesis of bis(oxazoline) 34

2.2.3 General procedure for the synthesis of palladium-bis(oxazoline) (Pd-BOX) complexes 40

2.2.4 X-ray structure analysis 46

2.3 Results and discussions 56

2.3.1 Synthesis of BOX ligands 56

2.3.2 Synthesis of palladium-BOX complexes 57

CHAPTER 3 WATER SOLUBLE AND MIXED LIGAND PALLADIUM-BIS(OXAZOLINE) COMPLEXES: SYNTHESIS AND CHARACTERIZATION 72

3.1 Introduction 72

3.2 Experimental 73

3.2.1 Materials and Instrumentation 73

3.2.2 General procedure for the synthesis of hydroxyl and carboxylate functionalized BOX- ligands 74

3.2.3. General procedure for the synthesis of hydroxyl and carboxylate functionalized palladium- bis(oxazoline) complexes 76

3.2.4 General procedure for the synthesis of palladium-bis(oxazoline)-phosphine mixed ligand complexes 78

3.3 Results and discussions 81

3.3.1 The synthesis of water soluble bis(oxazoline) ligands 81

3.3.2 The synthesis of water soluble palladium-bis(oxazoline) complexes 82

3.3.3 The synthesis of palladium-bis(oxazoline)-phosphine mixed ligand complexes 83

CHAPTER 4 SUPPORTED BOX LIGANDS AND SUPPORTED PALLADIUM-BOX CATALYSTS: SYNTHESIS AND CHARACTERIZATION 87

4.1 Introduction 87

4.2 Experimental 89

4.2.1 Materials and Instrumentation 89

4.2.2 Synthesis of supported bis(oxazoline) ligand 89

4.2.3 General procedure for the synthesis of supported palladium-BOX catalysts 91

4.3 Results and discussions 92

4.3.1 Merifield's resin supported Pd-BOX catalyst 94

4.3.2 Silica supported Pd-BOX catalyst 99

CHAPTER 5 APPLICATIONS OF PALLADIUM-BIS(OXAZOLINE) COMPLEXES AS CATALYSTS IN COUPLING REACTIONS 105

5.1 Introduction 105

5.2 Experimental 106

5.2.1 General procedure for homogeneous palladium bis(oxazoline) catalyzed Suzuki-Miyaura coupling reaction 107

5.2.2 General procedure for homogeneous palladium-bis(oxazoline) catalyzed Mizoroki-Heck coupling reaction 111

5.2.3 General procedure for homogeneous palladium-bis(oxazoline) catalyzed Sonogashira coupling reaction 115

5.2.4 General procedure for supported palladium-bis(oxazoline) catalyzed Suzuki-Miyaura coupling reaction 122

5.2.5 General procedure for supported Pd-BOX catalyzed Mizoroki-Heck coupling reaction 123

5.2.6 General procedure for supported Pd-BOX catalyzed Sonogashira coupling reaction 124

5.2.7 General procedure for catalyst recycling using dialysis bag 124

5.3 Results and Discussions 125

5.3.1 Palladium-bis(oxazoline) catalyzed Suzuki-Miyaura coupling reaction 125

5.3.2 Pd-BOX catalyzed Mizoroki-Heck coupling reactions of Alkenes with aryl iodides 138

5.3.3 Palladium-bis(oxazoline) catalyzed Sonogashira coupling reaction of iodobenzene with alkynes 146

5.3.4 Supported palladium-bis(oxazoline) as catalyst for Suzuki-Miyaura coupling reaction 160

5.3.5 Catalytic activities of supported palladium-bis(oxazoline) in Mizoroki-Heck coupling reaction 167

5.3.6 Catalytic activities of supported palladium-bis(oxazoline) in Sonogashira coupling reaction 176

5.4 Characterization of the used supported palladium-bis(oxazoline) catalysts 182

5.4.1 Characterization of the used supported palladium-bis(oxazoline) catalysts using FT-IR 182

5.4.2 Analysis of the used supported palladium-bis(oxazoline) catalysts using ICP-MS 184

5.4.3 Analysis of the used supported palladium-bis(oxazoline) catalysts using XPS 184

5.5 Palladium leaching test 186

CHAPTER 6 CATALYTIC CARBONYLATION REACTIONS 187

6.1 Introduction 187

6.2 Experimental 188

6.2.1 Materials and Instrumentation 188

6.2.2 General procedure for alkoxycarbonylation and aminocarbonylation of alkynes 189

6.2.3 General procedure for alkoxycarbonylation of aryl halide 190

6.2.4 General procedure for amino carbonylation of aryl halide 190

6.3 Results and discussions 191

6.3.1 Evaluation of the catalytic activity of the new Pd-BOX-PR_3 complexes in the alkoxycarbonylation of alkynes 191

6.3.2 Evaluation of the catalytic activity of the new Pd-BOX-PR_3 complexes in the aminocarbonylation of alkynes 208

6.3.3 Evaluation of the catalytic activity of the newly prepared supported palladium-BOX catalysts in the alkoxycarbonylation of aryl iodides 212

6.3.4Supported palladium-BOX catalyst for aminocarbonylation of aryl iodides: Recycling ability of the catalyst 221

6.4 Characterization of the used supported palladium-bis(oxazoline) catalysts 227

6.4.1 Characterization of the used supported palladium-bis(oxazoline) catalysts using FT-IR 227

6.4.2 Analysis of the used supported palladium-bis(oxazoline) catalysts using ICP-MS 229

6.4.3 Analysis of the used supported palladium-bis(oxazoline) catalysts using XPS 230

6.5 Palladium leaching test 232

CHAPTER 7 CONCLUSIONS 234

REFERENCES 237

APPENDICES 254

VITAE 316

LIST OF TABLES

TABLE 1. Crystallographic Data for Pd-BOX-1 and Pd-BOX-2.....48
TABLE. 2. Crystallographic Data for Pd-BOX-3 and Pd-BOX-4.....49
TABLE 3. Crystallographic Data for Pd-BOX-5 and Pd-BOX-6.....50
TABLE 4. Crystallographic Data for Pd-BOX-7.....51
TABLE 5. Selected bond lengths (Å) and bond angles (°) for Pd-BOX-1 and Pd-BOX-2.....52
TABLE 6. Selected bond lengths (Å) and bond angles (°) for Pd-BOX-3 and Pd-BOX-4.....53
TABLE 7. Selected bond lengths (Å) and bond angles (°) for Pd-BOX-5 and Pd-BOX-6.....54
TABLE 8. Selected bond lengths (Å) and bond angles (°) for Pd-BOX-7.....55
TABLE 9. Suzuki-Miyaura Coupling Reaction of 4-Iodoacetophenone with Phenylboronic Acid. Optimization of Reaction Conditions. 128
TABLE 10. Suzuki-Miyaura Coupling Reaction of Various Aryl Halides with Different Arylboronic Acids Using Pd-BOX-1 as a Catalyst.....132
TABLE 11. Mizoroki-Heck Coupling Reactions of Iodobenzene with Styrene. 139
TABLE 12. Mizoroki-Heck Coupling Reactions of Styrene Derivatives with Aryl Iodides Using Pd-BOX-6 as Catalyst.....143
TABLE 13. Palladium-Catalyzed Sonogashira Coupling Reaction of Iodobenzene with Phenylacetylene. Optimization of the Reaction Conditions. 148
TABLE 14. Sonogashira Coupling Reactions of Aryl Iodides with Aryl Alkynes Catalyzed by Pd-BOX-1.....151
TABLE 15. Sonogashira Coupling Reaction of Aryl Iodides with Dialkynes. Synthesis of Bis(Phenyl Ethynyl)-Benzene Derivatives (BPEB'S).....154
TABLE 16. Sonogashira Coupling Reactions of Aryl Iodide with Alkyl Alkyne.....156
TABLE 17. Sonogashira Coupling Reaction of Aryl Iodide and Diiodobenzene with Alkynes 159
TABLE 18. Suzuki-Miyaura Coupling Reaction of Various Aryl Halides with Different Arylboronic Acids Using Pd-BOX-12 (Recycled Catalyst).....165

TABLE 19. Mizoroki-Heck Coupling Reactions of Aryl Iodides with Alkynes Using Supported Palladium Bis(Oxazoline) as Catalyst. 173
TABLE 20. Sonogashira Coupling Reaction of Various Aryl Iodides with Different Alkynes Using Merifield's Resin Supported Palladium-Bis(Oxazoline) Catalyst. 180
TABLE 21. Palladium-Catalyzed Methoxycarbonylation of Phenylacetylene. Effect of Solvent. 193
TABLE 22. Palladium-Catalyzed Methoxycarbonylation of Phenylacetylene. Effect of Temperature. 195
TABLE 23. Palladium-Catalyzed Alkoxycarbonylation of Phenylacetylene. Effect of the Type of Pd-Catalyst. 197
TABLE 24. Palladium Catalyzed Alkoxycarbonylation of Phenylacetylene with Various Alcohols. 199
TABLE 25. Palladium Catalyzed Methoxycarbonylation of Alkyne. Effect of Various Alkynes. 201
TABLE 26. Palladium Catalyzed Aminocarbonylation of Phenylacetylene. Effect of Type of Pd-Catalyst. 209
TABLE 27. Palladium-Bis(Oxazoline) Catalyzed Aminocarbonylation Reaction of Phenylacetylene. Effect of Various Amines. 211
TABLE 28. Palladium-Bis(Oxazoline) Catalyzed Methoxycarbonylation of Iodobenzene. Optimization of Reaction Conditions using Supported Catalysts 214
TABLE 29. Alkoxycarbonylation Reaction of Iodobenzene Using Pd-BOX-12 As Catalyst. Effect of Different Substrates 219
TABLE 30. Aminocarbonylation of Iodobenzene. Recycling Ability Of Merifield's Resin Supported Palladium-Bis(Oxazoline) (Pd-BOX-12) Catalyst 222
TABLE 31. Aminocarbonylation of Iodobenzene. Recycling Ability of Silica Supported Palladium-Bis(Oxazoline) (Pd-BOX-13) Catalyst. 223
TABLE 32. Aminocarbonylation of Iodobenzene Using Pd-BOX-12 as Catalyst. Effect of Different Substrates. 225
TABLE 33. Comparison of Percentage of Palladium in the Fresh and the Used

Supported Catalysts.....230

LIST OF FIGURES

Figure 1: Some Examples of Bis(Oxazoline) Ligands 5
Figure 2. Catalytic Cycle for Palladium Catalyzed Suzuki-Miyaura Cross Coupling Reaction.....11
Figure 3. Catalytic Cycle for Palladium Catalyzed Mizoroki-Heck Cross Coupling Reaction.....17
Figure 4. Catalytic Cycle for Palladium Catalyzed Sonogashira Cross Coupling reaction.....23
Figure 5. ORTEP Diagram of Pd-BOX-1 Showing the Atomic Labeling Scheme. Displacement Ellipsoids are Drawn at the 30 % Probability Level. 59
Figure 6. ORTEP Diagram of Pd-BOX-2 Showing the Atomic Labeling Scheme. Thermal ellipsoids are drawn at the 30% probability level. 61
Figure 7: ORTEP Diagram of Pd-BOX-3 Showing the Atomic Labeling Scheme. Dichloromethane Molecule has been Omitted for Clarity. Thermal ellipsoids are drawn at the 30% probability level. 63
Figure 8: ORTEP Diagram of Pd-BOX-4 Showing the Atomic Labeling Scheme. Thermal ellipsoids are drawn at the 30% probability level 66
Figure 9: Inherent Chirality in Palladium-Bis(Oxazoline) Complexes 66
Figure 10: ORTEP Diagram of Pd-BOX-5 Showing the Atomic Labeling Scheme. Thermal ellipsoids are drawn at the 30% probability level 68
Figure 11: ORTEP Diagram of Pd-BOX-6 Showing the Atomic Labeling Scheme. Thermal ellipsoids are drawn at the 30% probability level 70
Figure 12: ORTEP Diagram of Pd-BOX-7 Showing the Atomic Labeling Scheme. Thermal ellipsoids are drawn at the 30% probability level. 71
Figure 13: ^{1}H NMR Spectra in CD_2Cl_2 of (a) BOX ligand (b) Pd-BOX-1 (c) Pd-BOX-10……...……85
Figure 14. FT-IR Spectrum of Unmodified Merifield's Resin 95
Figure 15. FT-IR Spectrum of Merifield's Resin Supported BOX Ligand 96

Figure 16. FT-IR Spectra of Merifield's Resin Supported Pd-BOX Complex (Pd-BOX-12). 96
Figure 17: Scanning Electron Micrograph of (a) Merifield's Resin (b) Merifield's Resin Supported BOX Ligand (c) Merifield's Resin Supported Pd-BOX Complex 98
Figure 18: XPS Spectrum of Pd-BOX-12 (Pd3d) 99
Figure 19. FT-IR Spectra of Unmodified Benzyl Silica Support....100
Figure 20. FT-IR Spectra of Silica Supported BOX Ligand. 101
Figure 21. FT-IR Spectra of Silica Supported Pd-BOX Complex. 101
Figure 22: Scanning Electron Micrograph of (a) Benzyl Chloride Silica (b) Benzyl Silica Supported Bis(Oxazoline) Ligand (BOX-10) (c) Benzyl Silica Supported Palladium(II) Bis(Oxazoline) Complex (Pd-BOX-11).....103
Figure 23: XPS Spectrum of Pd-BOX-13 (Pd3d) 104
Figure 24: Pd-BOX-1 Catalyzed Suzuki-Miyaura Coupling Reaction of Iodobenzene with *p*-Tolyl boronic Acid. Recycling Ability of the Catalyst System 137
Figure 25: Merifield's Resin Supported Palladium-Bis(Oxazoline) Complex Catalyzed Suzuki-Miyaura Coupling Reaction of Iodobenzene with *p*-Tolylboronic Acid. Recycling Ability of The Catalyst. 162
Figure 26: Silica Supported Palladium-Bis(Oxazoline) Complex Catalyzed Suzuki-Miyaura Coupling Reaction of Iodobenzene with *p*-Tolylboronic Acid. Recycling Ability of the Catalyst. 162
Figure 27: Merifield's Resin Supported Palladium-Bis(Oxazoline) Complex Catalyzed Mizoroki-Heck Coupling Reaction of Iodobenzene with Methylacrylate. Recycling Ability of the Catalyst System. 168
Figure 28: Silica Supported Palladium-Bis(Oxazoline) Complex Catalyzed Mizoroki-Heck Coupling Reaction of Iodobenzene with Styrene. Recycling Ability of the Catalyst System. 170
Figure 29: Merifield's Resin Supported Palladium-Bis(Oxazoline) Complex Catalyzed Sonogashira Coupling Reaction of Iodobenzene with Phenylacetylene. Recycling Ability of the Catalyst System. 177
Figure 30: Silica Supported Palladium-Bis(Oxazoline) Complex Catalyzed

Sonogashira Coupling Reaction of Iodobenzene with Phenylacetylene. Recycling Ability of the Catalyst System. 178
Figure 31. FT-IR Spectrum of Used Pd-BOX-12 recovered from Suzuki-Miyaura Coupling Reaction.....183
Figure 32. FT-IR Spectrum of Used Pd-BOX-13 Recovered from Suzuki-Miyaura Coupling Reaction.....183
Figure 33: XPS Spectra of used Pd-BOX-12 showing Pd 3d. Spectrum of fresh catalyst is displayed on the left 185
Figure 34: XPS Spectra of used Pd-BOX-13 showing Pd 3d. Spectrum of fresh catalyst is displayed on the left 185
Figure 35: DFT/B3LYP-D3/Def2-TZVP Computed Total Electronic Energies (Etot, au), Zero-Point Energies (ZPE, kcal/mol) and Optimized Structures in Acetonitrile for the Intermediates 3Hgem, 3Htrans, 5Agem and 5Atrans. 205
Figure 36: Optimized structures and computed total electronic energies (Etot, au) for transition states TS2H/3Hgem and TS2H/3Htrans. 207
Figure 37: Methoxycarbonylation Reaction of Iodobenzene. Recycling Ability of Merifield's Resin Supported Palladium-Bis(Oxazoline) (Pd-BOX-12) Catalyst. 216
Figure 38: Methoxycarbonylation Reaction of Iodobenzene. Recycling Ability of Silica Supported Palladium-Bis(Oxazoline) (Pd-BOX-12) catalyst. 216
Figure 39. FT-IR Spectrum of Pd-BOX-12 catalysts Recovered from Alkoxycarbonylation Reaction 228
Figure 40: FT-IR Spectrum of Pd-BOX-13 catalysts Recovered from Alkoxycarbonylation Reaction 228
Figure 41: XPS Spectrum of Pd-BOX-12 Recovered from Alkoxycarbonylation reaction Showing the Pd 3d, (right specturum) Spectrum of fresh catalyst is displayed on the left.....231
Figure 42: XPS Spectrum of Pd-BOX-13 Recovered from Alkoxycarbonylation reaction showing the Pd 3d (right specturum). Spectrum of fresh catalyst is displayed on the left.....231

LIST OF ABBREVIATIONS

BOX	:	Bis(oxazoline)
d	:	doublet
dba	:	dibenzylidene acetone
dppb	:	1,4-bis(diphenylphosphinobutane)
dppp	:	1,4-bis(diphenylphosphinopropane)
DMF	:	dimethyl formamide
DMSO	:	dimethyl sulfoxide
EtOAc	:	ethyl acetate
FT	:	Fourier transform
GC	:	Gas chromatography
GC-MS	:	Gas chromatography-mass spectroscopy
h	:	hour
ICP	:	Inductively coupled plasma
IR	:	Infra red
J	:	coupling constant
Me	:	Methyl

NMR	:	Nuclear magnetic resonance
OAc	:	acetate ion
Pd-BOX	:	Palladim-bis(oxazoline)
Ph	:	phenyl
OPh	:	phenoxy
Phos	:	phosphine
ppb	:	part per billion
ppm	:	part per million
psi	:	per square inch
r.t.	:	room temperature
SEM	:	Scanning electron microscopy
TGA	:	Thermo gravimetric analysis
XPS	:	X-ray photoelectron spectroscopy

ABSTRACT

Full Name : [Mansur Bala Ibrahim]

Thesis Title : [Synthesis and Characterization of New Palladium – Bis(Oxazoline) Complexes. Catalytic Activities in Coupling and Carbonylation Reactions]

Major Field : [Chemistry]

Date of Degree : [December, 2015]

In the present study, the synthesis of new bis(oxazoline) ligands (**BOX-1** to **BOX-7**) including water soluble (**BOX-8** and **BOX-9**) and supported ligands (**BOX-10** and **BOX-11**) were carried out. The synthesis of palladium bis(oxazoline) complexes (**Pd-BOX-1** to **Pd-BOX-7**), water soluble palladium-bis(oxazoline) complexes (**Pd-BOX-8** and **Pd-BOX-9**), palladium-bis(oxazoline)-phosphine mixed ligand complexes (**Pd-BOX-10** and **Pd-BOX-11**) and supported palladium-bis(oxazoline) catalysts (**Pd-BOX-12** and **Pd-BOX-13**) were also carried out. The new BOX ligands and Pd-BOX catalysts were characterized with various spectroscopic and analytical techniques. The X-ray crystal structures of the complexes (**Pd-BOX-1** to **Pd-BOX-7**) showed that the palladium ion is bound to the nitrogen atoms of the two heterocycles of the bidentate ligand and two halide or acetate ions are in a distorted square planar geometry. The coordination to the palladium ion allowed the non C_2-symmetric bis(oxazoline) ligand-based complexes (**Pd-BOX-2** to **Pd-BOX-6**) to acquire a rigid backbone curvature and an inherent chirality. The **Pd-BOX** catalysts were effective in the Suzuki-Miyaura coupling reactions of arylboronic acids with aryl iodides, aryl bromides and aryl chlorides, Mizoroki-Heck coupling reactions of aryl halides with terminal alkenes, and copper free Sonogashira coupling reaction of aryl halides with terminal alkynes. A wide range of functional groups as substituents on the arylboronic acids, aryl halides, alkenes and alkynes were considered. The palladium bis(oxazoline) complexes were also active in the alkoxycarbonylation and aminocarbonylation reactions of aryl iodides. The **Pd-BOX** catalysts demonstrated exceptional air and moisture stability. The mixed ligand complexes (**Pd-BOX10** and **Pd-BOX-11**) were applied as catalysts in the alkoxycarbonylation and aminocarbonylation reactions of alkynes. The process of carbonylation has produced the *gem*-α,β-unsaturated ester/amide isomer in high regioselectivity and excellent yields. The supported palladium-bis(oxazoline) catalysts showed excellent recycling ability in most cross coupling and carbonylation reactions.

ملخص الرسالة

الإسم الكامل : منصور بالا إبراهيم

عنوان الرسالة : توليف وتوصيف معقدات بلاديوم-بس أوكسازولين جديدة وتطبيقاتها كحفازات في تفاعلات الإقتران والكربنلة

التخصص الرئيس : الكيمياء

تاريخ الدرجة : ديسمبر, ٢٠١٥

تم - في هذه الدراسة – إجراء توليف متصلات بس أوكسازولين جديدة (بوكس1 إلى بوكس 7) منها الذائب في الماء (بوكس 8 وبوكس9) والمتصلات المدعمة (بوكس10 وبوكس11). كما تم أيضا توليف معقدات بلاديوم- بس أوكسازولين (بلاديوم بوكس1 إلى بلاديوم بوكس 7) ومعقدات البلاديوم- بس أوكسازولين القابلة للذوبان في الماء (بلاديوم بوكس8 وبلاديوم بوكس 9) ومعقدات البلاديوم- بس أوكسازولين ذات المتصلات المختلطة (بلاديوم بوكس10 وبلاديوم بوكس 11) و حفازات معقدات البلاديوم- بس أوكسازولين المدعمة (بلاديوم بوكس12 وبلاديوم بوكس 13). تم تمييز متصلات البوكس ومعقدات البلاديوم- بوكس الجديدة باستخدام التقنيات التحليلية والطيفية المختلفة. أظهرت هياكل بلورات الأشعة السينية للمعقدات (بلاديوم بوكس1 إلى بلاديوم بوكس 7) أن أيون البلاديوم منضم إلى ذرات النيتروجين من الحلقتين غير المتجانستين للمتصلات ثنائية الربط واثنين من أيونات الهاليد أو الخلات وفي هندسة مستوية مربعة مشوهة. سمح تناسق أيون البلاديوم للمعقدات المستندة إلى متصلة البس أوكسازولين غير المتناظرة في الحصول على انحناء جامد في العمود الفقري واللاتناظرية الأصيلة. كانت حفازات معقدات البلاديوم- بس أوكسازولين فعالة في تفاعلات اقتران سوزوكي - ميروا لأحماض أريل البورون مع يود الأريل، بروميد الأريل وكلوريدات الأريل، وتفاعلات اقتران هيك - ميزوروكي لهاليدات الأريل مع الألكاينات الطرفية، وتفاعل اقتران سوناجوشوري الخالي من النحاس لهاليدات الأريل مع الألكاينات الطرفية. اعتبرت مجموعة واسعة من المجموعات الوظيفية كمجموعات فرعية على أحماض أريل البورون، هاليدات الأريل والألكينات والألكاينات. وقد كانت معقدات البلاديوم- بس أوكسازولين نشطة أيضا في تفاعلات كربنلة الألكوكسي وكربنلة الأمين ليود الأريل. أظهرت حفازات بلاديوم- بس أوكسازولين استقرارا إستثنائيا في الهواء والرطوبة. تم تطبيق المعقدات ذات المتصلات المختلطة (بلاديوم بوكس 10 و بلاديوم بوكس 11) كحفازات في تفاعلات كربنلة الألكوكسي وكربنلة الأمين للألكاينات. وقد أنتجت عملية الكربنلة أيزومر جيم ألفا، بيتا استر / أميد غير المشبعة في إنتقائية عالية وعوائد ممتازة. أظهرت حفازات البلاديوم- بس أوكسازولين المدعمة قدرة إعادة تدوير ممتازة في معظم تفاعلات الاقتران المتقاطع والكربنلة

CHAPTER 1

INTRODUCTION AND LITERATURE REVIEW

1.1 General Introduction

Despite the important advancements in transition metal catalyzed coupling and carbonylation reactions, still most organic synthesis as well as industrial processes involving the use of coupling and carbonylation reactions can be improved. Presently, the majority of industries, including fine chemicals, pharmaceuticals and related industries employ cross coupling reaction at one or more stages of production. In this regard, the development of more efficient, economically viable and environmentally benign catalysts constitutes a vital issue for attaining a sustainable industrial processes today and in the future.

In most catalytic coupling reactions, transition-metal complexes derived from phosphine ligands play a dominating role. Though, several reports have described the successful use of phosphine with palladium complexes in catalyzing Suzuki-Miyaura, Mizoroki-Heck, Sonogashira as well as carbonylative coupling reactions, these ligands have numerous limitations due to the difficulty in their synthesis, high cost, toxicity, and low air and moisture stability [1-3]. In certain catalytic reactions, phosphine ligands can be replaced by nitrogen ligands. Contrary to phosphine ligands, the nitrogen-based ligands are significantly inexpensive. Most of them are derived from primary amines. The vast number

of primary amines available can be used for their production. Moreover, the nitrogen based ligands are easy to synthesize, non-toxic and stable to air and moisture [4].

Taking into consideration these substantial advantages, the interest towards the use of nitrogen donor ligands with palladium to catalyze the cross coupling and carbonylation reactions has been increasing rapidly. The bis(oxazoline) (BOX) were selected as the ligands of choice in this work.

In general, most palladium catalyzed coupling reacions are considered to follow a similar mechanism and careful selection of ligand can facilitate the important steps of the catalytic cycle. For instance; strong donating ligands increases the electron density around the metal centre, thereby accelerating the oxidative addition of the catalyst to the substrate. The oxidative addition step is generally believed to be the rate determining step. The elimination step can be accelerated by the use of bulky ligands. This will lead to the overall increase in the rate of the coupling reaction.

The bis(oxazoline) ligands are considered suitable ligands for the coupling reactions because of the presence of two nitrogen binding sites which originates from two oxazoline rings joined through an aromatic ring. These makes the BOX ligand highly electron rich and a strong σ-donor. Consequently, the electron density around the metal center will be greatly increased and as a result, the oxidative addition step of the catalytiv cycle will be accelerated. Moreover, the bulkiness of the BOX ligand will aid the elimination step.

1.2 Literature background

1.2.1 Bis(oxazoline) (BOX) ligands

Since early nineties, Bis(oxazolines) (BOX) ligands have attracted considerable attention in coordination chemistry and catalysis [5]. They are structurally related to the C_2 symmetric semicorrins [6]. BOX ligands are described as either C_2 symmetric or non C_2 symmetric and are based on two oxazoline rings joined together by a spacer, which is an aromatic or aliphatic moiety. Because of their importance and wider applications, easy and flexible synthesis, excellent selectivity [7] and ability to coordinate with a large number of metals [8], several BOX ligands have been synthesized and investigated.

The use of oxazoline as a ligand for transition metal catalyzed reactions started after the successful hydrosilylation of prochiral ketones with diphenylsilane using thiazolidines as co-catalysts [8]. The thiazolidine group was replaced with an oxazoline group in the enantioselective monophenylation of meso diol with $Ph_3Bi(OAc)_2$ [9].

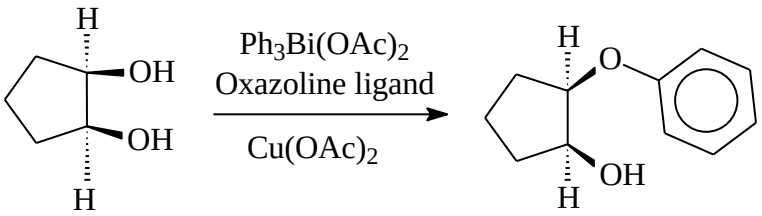

50 % ee
56 % yield

Nishiyama successfully produced a rhodium complex of a pyridine bis(oxazoline) ligand. Having three nitrogen binding sites, the pyridine-BOX forms a tricoordinated complex

with bite angle 158.7^{o} with rhodium (III) chloride. This complex was found to be efficient catalyst for asymmetric hydrosilylation of ketones [10].

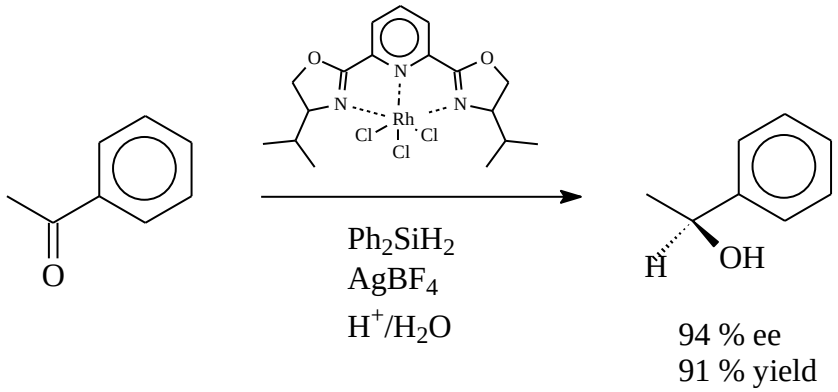

A general method for the synthesis of BOX complexes was later reported [11], and in 1991, two communications were published in the journal of American chemical society on asymmetric cyclopropanation of alkenes using chiral Cu(I)-BOX [12] and on enantioselective Diels-Alder reaction using chiral Fe(III)-BOX [13] complexes as catalysts.

Since then, a considerable number of BOX ligands and their metal complexes have been synthesized and investigated. In order to provide an insight into the structural diversity of BOX ligands, a few examples are presented in Figure 1. More detailed examples can be found in related reviews [8, 14]

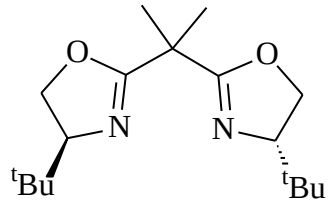

1

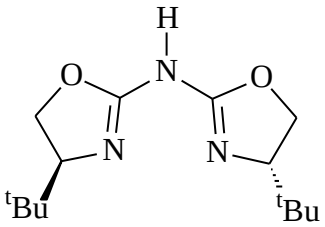

2

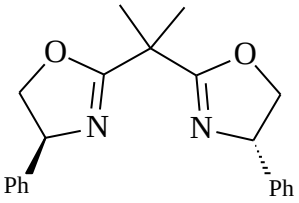

3

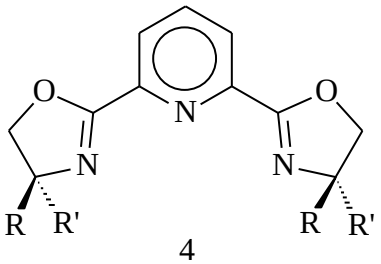

4

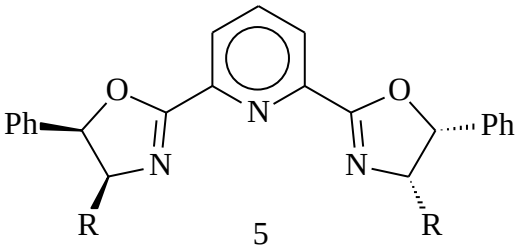

5

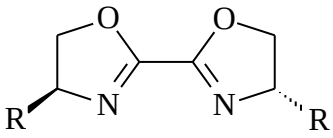

6

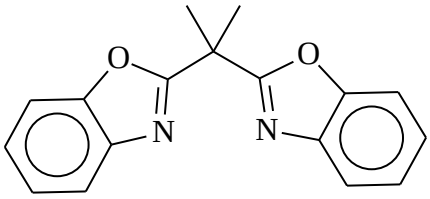

7

Figure 1: Some Examples of Bis(Oxazoline) Ligands: 1 [13]; 2 [15]; 3 [16]; 4 [17]; 5 [18]; 6 [19]; 7 [20, 21].

1.2.2 Metal-bis(oxazoline) complexes

Like most transition metal complexes, a metal-BOX complex is obtained when a solution of BOX ligand reacts with a solution of transition metal salt. BOX ligands are predominantly bidentate, except in few cases where they act as monodentate ligands.

Metal-BOX complexes usually form a conformationally constrained chelate in which the substituents on oxazoline rings are in close proximity to the donor nitrogen. This provides a strong directing effect on the catalytic site and high selectivity in the catalyzed reaction [22]. Moreover, in the case of C_2-symmetric ligands, the axial C_2-symmetry minimizes the number of possible transition states for a particular reaction. This enhances the rate of the reaction being catalyzed.

BOX ligands can form tetracoordinated complexes with distorted square planar or tetrahedral geometry [23].

Monodentate BOX Complexes

There are few literature reports on metal complexes in which a BOX ligand serves as monodentate. An example is the Cu-BOX complex in which the ligand occupy a bridging position between two linearly coordinated Cu (I) ions [24]. Another example of a monodentate BOX ligand is a singly stranded linearly coordinated optically active polymer of BOX with silver trifluoromethane sulfonate. The crystal structure of this coordination polymer reveals the silver ion as coordinated to two nitrogen atoms from two different BOX ligands [25].

Bidentate BOX Complexes

In general, BOX ligands with one or more carbon atom(s) as a spacer between two oxazoline moieties act as bidentate ligands. They coordinate with the metal ion through their two nitrogen atoms. This type of metal-BOX complexes are by far the most popular in catalysis, and Cu(II) is the leading cation involved in their formation [24].

1.2.3 Mixed ligand metal-bis(oxazoline) complexes

Our literature survey does not reveal any complex of palladium or any other metal with bisoxazoline and phosphine as mixed ligands. However, the ligands are commonly used separately in the transition metal catalyzed coupling and carbonylative coupling reactions. The "soft" P-ligand exhibits to some extent π-acceptor properties, while the "hard" N-ligand is dominantly acting as σ-donor [26]. This different feature associated with each ligand is expected to provide a unique reactivity to the metal complexes.

1.2.4 Water soluble metal complexes

The increasing concern about safety and environmental protection lead to increasing interest in developing greener chemistry. The main objective is to design safer chemistry and chemical processes and to limit waste and toxicity. The studies in this area have led to the development of cleaner and relatively benign chemical processes. The major interest has been in the development of methods that avoid or minimize the use of traditional organic solvents for chemical synthesis. The methods developed include solventless processes [27], reactions in supercritical carbon dioxide [28], reactions in ionic liquids and perfluorinated solvents [29] and reactions in aqueous media [30].

Organic synthesis in water is rapidly gaining importance because it is considered as environmental benign process due to the non-toxic nature of aqueous media. Water is traditionally avoided in organometallic catalyzed reactions due to the reactivity of many metal-carbon bonds in water. However, several processes involving aqueous phase catalysis were recently developed. Among the early examples of such processes include catalytic hydrogenation, hydroformylation and water tolerant acid –base catalysis [31, 32]

The Suzuki-Miyaura coupling reaction is one of the most versatile methods of carbon-carbon bond formation. Due to the high water solubility of arylboronic acids and low toxicity of reagents and by-products compared to other coupling methods, Suzuki coupling is an ideal reaction to be performed in aqueous system. Over the last few years, there has been a considerable attention for this reaction in aqueous medium and various water soluble catalysts have been developed [33-36].

1.2.5 Supported palladium-bis(oxazoline) catalysts

Homogeneous catalysts are widely accepted for their high selectivity, activity and low catalysts loading. However, homogeneous catalysts are accompanied with certain disadvantages. These include, among others, difficulty in separation and reuse. Thus, it adds cost to the production cycle [37]. Moreover, most transition metal catalysts are toxic, hence an efficient separation procedure is particularly desirable for applications in pharmaceutical and related industries. The best approach towards solving the separation problem is the immobilization of the catalyst on solid support. This method has received enormous attention over the past few decades [38]. There are many approaches to

immobilization, however, grafting metal complex on solid support via covalent bond is the preferred method [39, 40].

The first method reported for the immobilization of bis(oxazoline) complex was non covalent attachment through ionic exchange between a cationic metal complex and anionic support [41, 42]. The support used in this context was a nafion-silica nanocomposite [43]. The main disadvantage of this heterogenization technique is the leaching of the ligand.

The covalent attachment involves a chemical modification of the ligand and Burguette [44, 45] reported an immobilization of BOX complex through homo and copolymerization.

Silica immobilized BOX ligands were also reported using partially pre-capped silica material. The product is then post capped after attaching the ligand to the silica support [46].

1.3 Coupling reactions

Catalytic coupling of organic compounds by various transition metals represents an important method of carbon – carbon bond generation. It has been particularly useful in the synthesis of various compounds including natural products, pharmaceutical products, and industrial raw materials. Different nucleophiles having various metals, such as magnesium, lithium, boron and zinc bonded to carbon can be coupled with different electrophilic substrates.

Originally, carbon-carbon bond forming reactions require harsh conditions and have low functional group tolerance. The development of transition metal-catalysis lead to more selective mild conditions for the construction of carbon-carbon bonds.

1.3.1 Suzuki-Miyaura cross coupling reactions

The Suzuki-Miyaura cross coupling reaction involves the coupling of vinyl, aryl halides or triflates with organoboron reagents. The organoboron reagent is typically in the form of a boronic acid or ester, and requires activation by a base to enable its transmetallation. Since the invention by Suzuki and Miyaura in 1981, Suzuki –Miyaura coupling reaction has gained enormous attention and wide application in chemical, pharmaceutical and related industries. This has been attributed to the exceptionally high yield of products, high functional group tolerance and easy separation of non-toxic boronic acid side product especially with the use of palladium catalysts. In view of the importance of their invention, Akira Suzuki and other workers in the field of coupling reactions were in 2010 awarded a nobel prize in chemistry.

Suzuki-Miyaura coupling reaction is usually a three step reaction. The first step is the ***oxidative addition***, which involves the addition of the halide to the palladium to form an organo-palladium specie. The second step is the ***transmetallation,*** which involves rapid isomerization of the cis-organo palladium specie to the trans isomer. The addition of the aryl boronate forming a biaryl palladium complex also takes place at this step. The final step is the ***reductive elimination***, which involves release of the final biaryl product and regeneration of the palladium catalyst [47, 48].

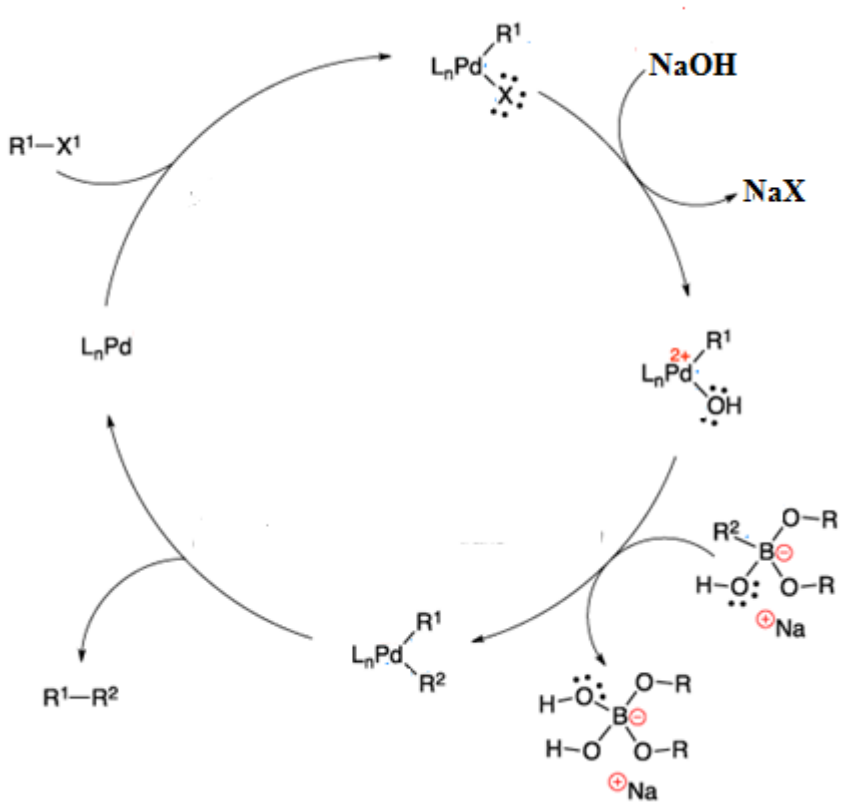

Figure 2. Catalytic Cycle for Palladium Catalyzed Suzuki-Miyaura Cross Coupling Reaction [48b]

Since the initial discovery of Suzuki Miyaura coupling reaction, a plethora of papers have been published on the development and application of various homogenous and heterogenous palladium complexes for the coupling reactions of diversely functionalized substrates. Among the recent and interesting developments were the study on the palladium-catalyzed cross-coupling reaction of 1,1-diboryl-1-alkenes with electrophiles by Shimizu and coworkers, 2005. The coupling reaction afforded the corresponding (*E*)-alkenyl boronates as single diastereomer. The method was efficient and completely stereocontrolled for the production of triarylalkenes and the whole transformation was

carried out sequentially in one pot. The method was also applied in the stereoselective preparation of polysubstituted 1, 3-dienes [49].

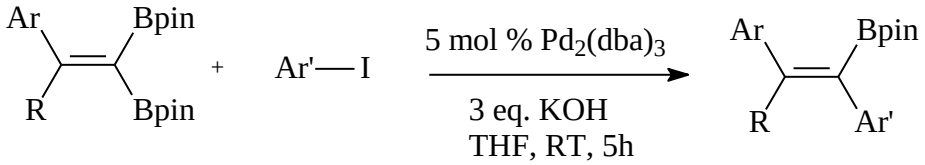

The use of bulky bis-phenanthrylN-heterocyclic carbene (NHC) based palladium acetate complex in the coupling of various aryl and vinyl chlorides with organoboron compounds was reported. The NHC based palladium-complex efficiently catalyze Suzuki–Miyaura coupling reaction of electron rich substrates such as aryl and vinyl chorides including unactivated and di-ortho substituted aryl chlorides. Using THF as a solvent and at room temperature, excellent yields of the cross coupling products were obtained. Tri and tetra-ortho substituted products were also efficiently produced under mild reaction conditions [50].

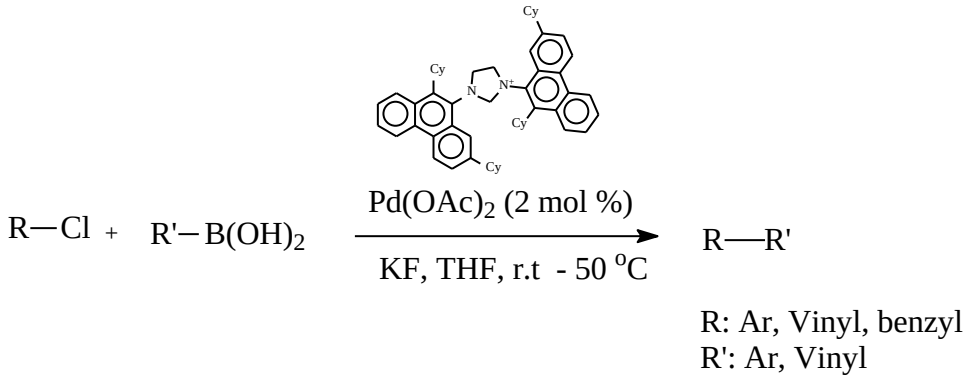

A new catalytic system based on $Pd(OAc)_2$/guanidine was studied in the room temperature Suzuki coupling of aryl boronic acids with a wide range of aryl halides and activated aryl chlorides. The catalytic system was found to have a great tolerance to a wide range of

sensitive functional groups, such as CHO, NO_2, OMe, CF_3, and COOMe on both substrates [51].

New air-stable chlorido phosphino palladium complexes were studied for Suzuki-Miyaura coupling reactions of a variety of heteroatom substituted heteroaryl chlorides with a diverse range of aryl/heteroaryl boronic acids. The reactions were found to be influenced by the nature of the base and the solvent employed. The catalytic activity of the complex was also found to increase with the increase in basicity of the phosphine ligand. The catalysts display exceptional performance for the cross-coupling reaction and this is attributed to their unique combination of electronic and steric properties [52].

Another interesting report is the Suzuki-Miyaura coupling of aryl tosylates catalyzed by an array of indolyl phosphine-palladium catalysts. A catalyst loading of 0.2 mol % was found to be sufficient for coupling of nonactivated aryl tosylate. Using this protocol, room temperature coupling was also possible. The catalytic system was extended to other boron nucleophiles, including trifluoroborate salts and boronate esters [53].

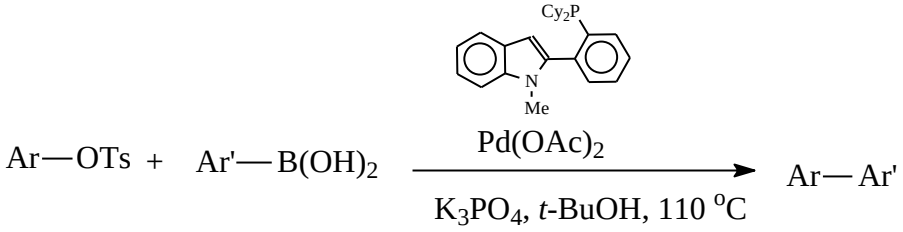

The coupling of aryl halides with various potassium trifluoroboratohomoenolates was reported. The enolate esters were synthesized from the conjugate addition of bis(pinacolato)diboron to unsaturated carbonyl compounds. The methods developed allow the cross-coupling of ketone and amide homoenolates with various aryl halides [54].

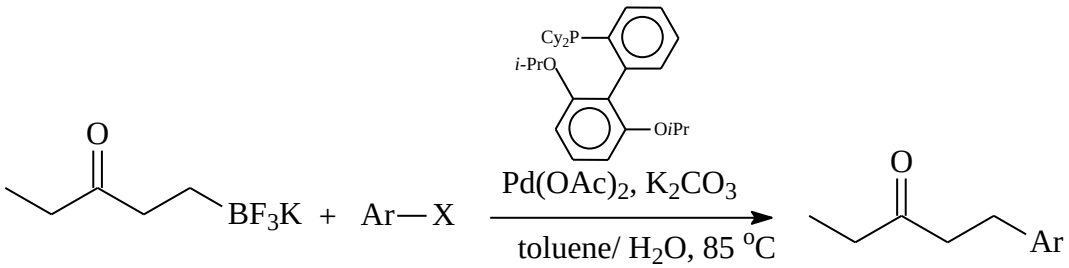

A new class of glyoxal bis-hydrazones derived from C_2-symmetric hydrazines was reported as efficient ligands for the asymmetric Suzuki-Miyaura cross-coupling to biaryls. The catalysts provide an unprecedented combination of activity and stereochemical control. The reactions yielded products in near quantitative yields with short reaction times and high enantioselectivity. Furthermore, the high activity of the catalysts enabled the reactions to be performed at temperature as low as 20 °C. The high enantioselections were due to restricted Pd-C(aryl) bond rotations in the oxidative addition and transmetalation intermediates [55].

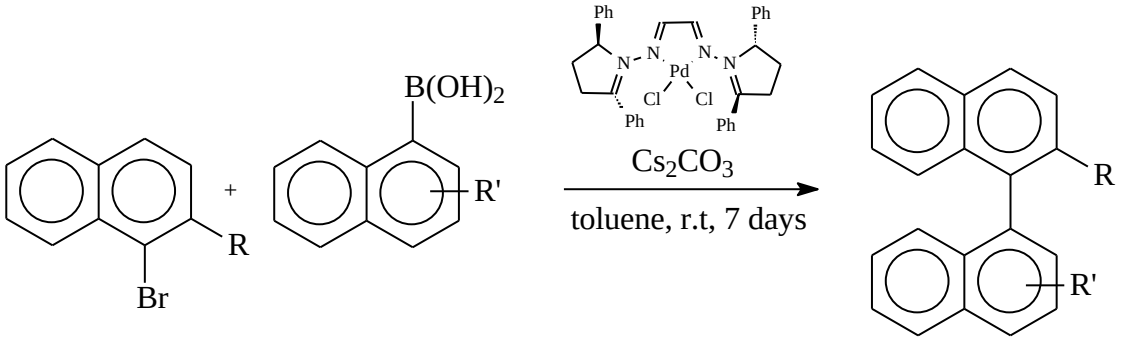

Palladium-catalyzed cross-coupling reaction of potassium alkenyltrifluoroborates with organic halides in aqueous solvent was also reported. The reaction conditions were found to be appropriate for the synthesis of styrene unsymmetrical stilbenes, and

alkenylbenzenes. Ligand free $Pd(OAc)_2$ or the 4-hydroxyacetophenone oxime derived palladacycle, which are efficient sources of Pd nanoparticles, acted as precatalyst using 1mol % Pd loading. The coupling with alkenyltrifluoroborates took place in a stereoselective manner without isomerization of the C-C double bond. The mild reaction conditions allow the separation and recycling of the Pd catalyst [56].

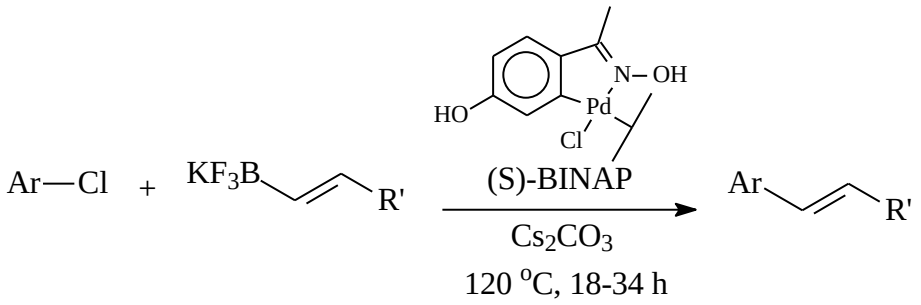

Palladium-catalyzed Suzuki-type cross-coupling of aryl and heteroaryl mesylates with potassium aryl and heteroaryltrifluoroborates was also studied. The catalytic system was found to be effective for the coupling of a range of mesylate substrates containing various common functional groups. The system was also feasible in using heteroaryl mesylates and trifluoroborate salts as electrophiles and nucleophiles, respectively. Vinyl and alkyltrifluoroborates were also coupled successfully [57].

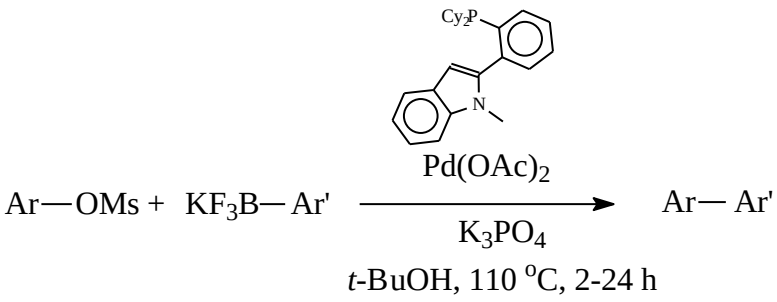

More literature on various catalytic systems for Suzuki-Miyaura coupling reaction can be found in the following references [58 - 64].

1.3.2 Mizoroki-Heck coupling reaction

Mizoroki-Heck reaction is the C-C coupling between aryl/ vinyl halides or triflates with terminal alkenes using palladium-catalyst and in the presence of a base. This reaction is of great importance as it allows the substitution reaction on planar carbon centers and it is the most efficient route toward the synthesis of internal alkenes from terminal alkenes [65, 66].

Heck reaction emerges from the pioneering work by Fujiwara (1967), Heck (1969) and Mizoroki (1971). Fujiwara studied the palladium catalyzed coupling reaction of arenes with alkenes. Heck studied the palladium catalyzed coupling of arylmercuric halides with alkenes. Then Mizoroki reported the palladium catalyzed coupling reaction of aryl halide with styrene [67, 68, 69]. Since the initial discovery of Mizoroki-Heck coupling reaction, it has received enormous attention and has been developed from both synthetic and mechanistic point of view as summarized in the relevant reviews [65, 66, 70, 71].

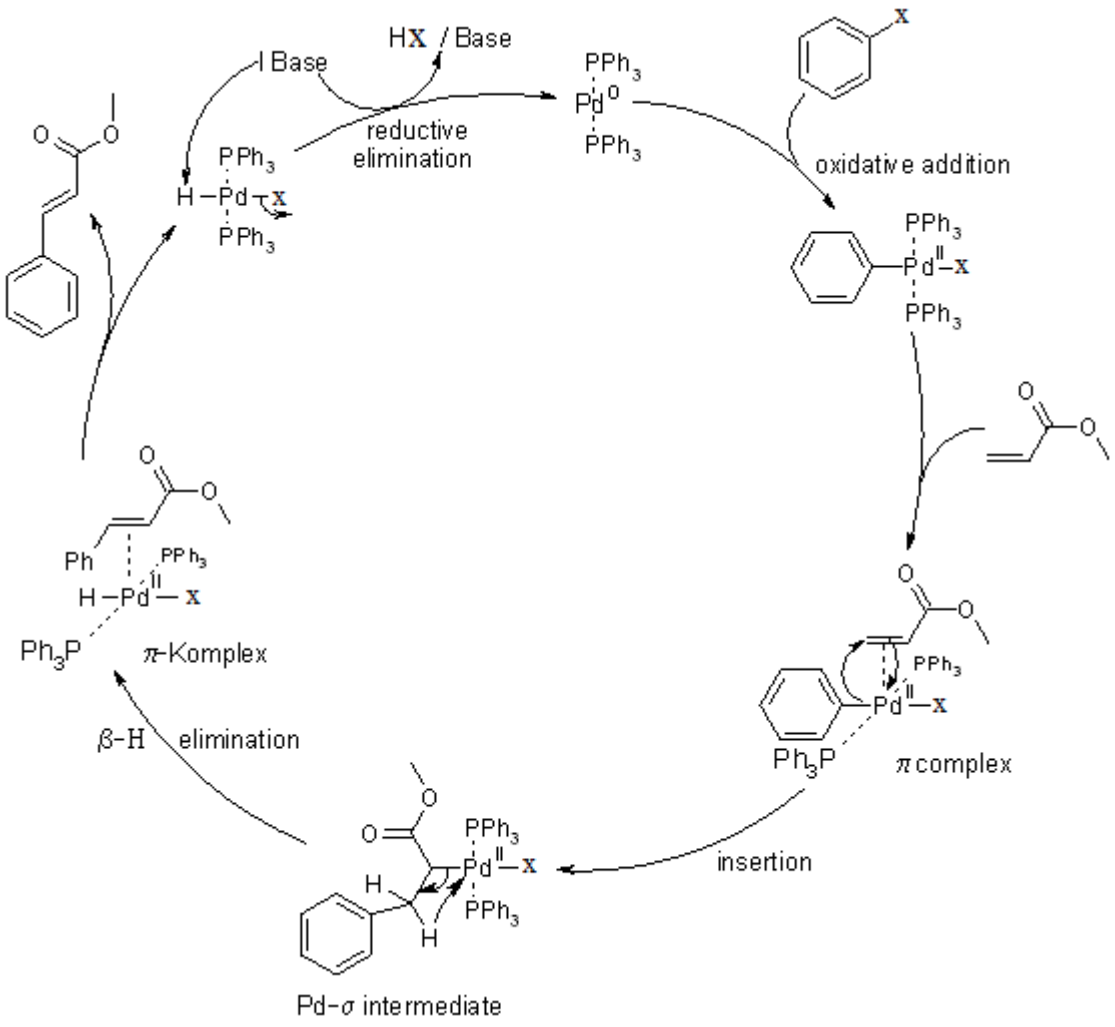

Figure 3. Catalytic Cycle for Palladium Catalyzed Mizoroki-Heck Cross Coupling Reaction [71b].

Among the recent developments was the use of a new type of triaryl phosphine-functionalized imidazolium salt and its palladium complex generated in-situ in the Heck reaction. The catalyst has proven to be highly efficient for the coupling of a wide array of aryl bromides and iodides with acrylates. The catalytic system was also efficient in the coupling of 4-bromotoluene with various styrene derivatives. The reason for high activity was related to the bulky substituents on the N-phenyl ring of the phoshphine-functionalized NHC ligands [72].

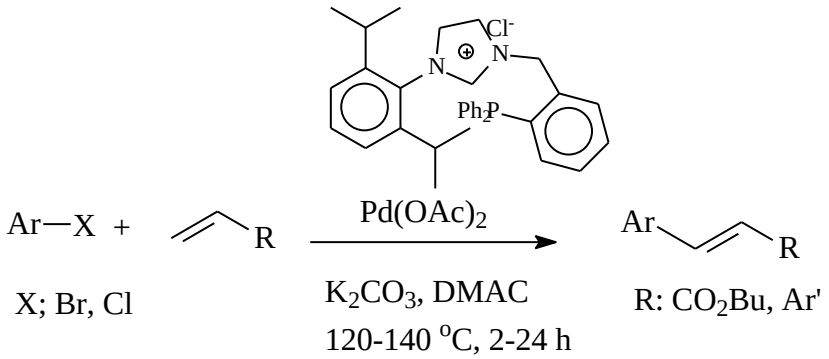

Heck reactions can also take place simultaneously with other organic transformations. For example, the one-step synthesis of 2-vinylic indoles and their tricycle derivatives takes place via an efficient Pd-catalyzed tandem Buchwald-Hartwig/Heck reaction. A gem dibromovinyl aniline unit was used as a readily available starting material. A rapid access to a wide range of substituted 2-vinylic indoles was realized. Intramolecular version of this reaction was also applied in the construction of interesting cyclic compounds including pyrido and azepino indole derivatives [73].

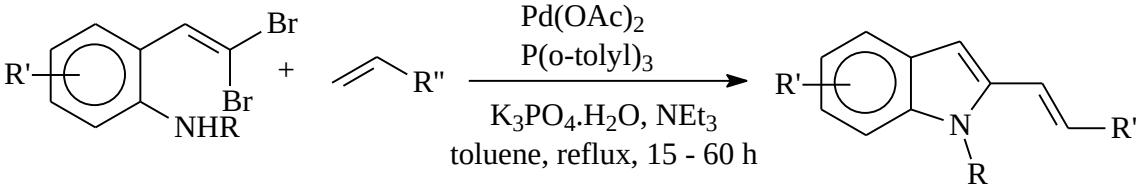

A catalytic system based on *meso*-2,4-bis(diphenylphosphino)pentane (*m*BDPP) with palladium was studied in the regioselective internal arylation of electron-rich olefins with aryl bromides. The effect of the ligand *m*BDPP was found to be of steric origin, and the enhanced R-regioselectivity observed was due to the palladium as an electron-deficient entity exchanging from Pd-DPPP to Pd-*m*BDPP. This interchange of ligand with steric and

electronic properties and their effects on olefin coordination and aryl insertion in Heck reaction effected the regio-control which has been tackled using triflates, halide scavengers, or ionic liquids [74].

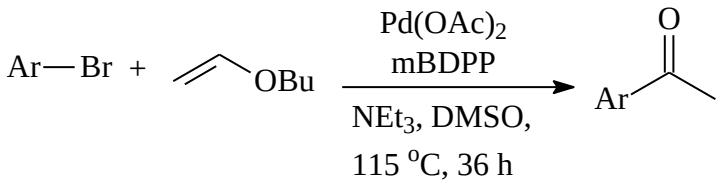

Brønsted acid-base ionic liquid (GILs) based on guanidine and acetic acid as a ligand, was used for palladium-catalyzed Heck reactions. The catalyst was tested on several representative aryl halides with electron-withdrawing or electron donating substituents. The result shows satisfactory regioselectivities and yields. The catalyst was recyclable and was re-used up to five times without bearing any loss in catalytic activity [75].

A nonionic amphiphile such as Triton X-100 or the vitamin E based PTS, both of which form nano micelles in water were found to promote Heck cross coupling of non-water-soluble partners at ambient temperatures. This finding reveals that Heck coupling can be effected without the use of co-solvents, ionic liquids, sonication, electrochemisty, or water-soluble phosphines [76].

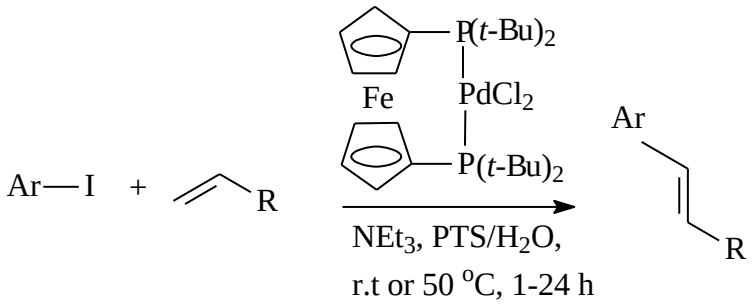

A hemilabile 1,3-bis(diphenylphosphino) propane monoxide (dpppO) ligand was reported as a highly regioselective ligand for the palladium catalyzed vinylation of electron-rich olefins with bromo- and chlorostyrenes. The method enables reaction of more challenging olefins within short reaction times and lower palladium loadings. The reaction was feasible in common solvents with no halide scavengers, ionic liquids or ionic additives. In contrast to the related arylation reactions, the vinylation was proposed to proceed via the neutral Heck mechanism [77].

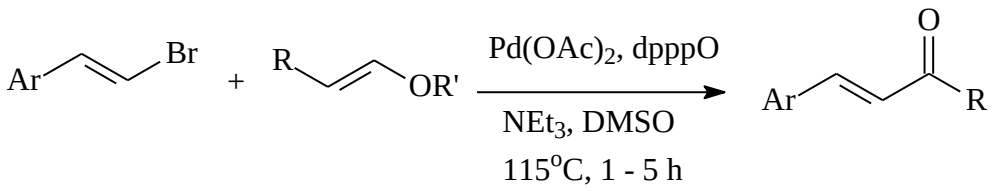

Trifunctional *N,N,O*-tridentate amido/pyridyl carboxylate ligated Pd(II) complexes were found to be excellent catalyst for Heck reaction at room-temperature. The amidate donor-functional group was found to be a good supporting functionality, enhancing the thermal stability and at the same time enhances the activity of the palladium catalysts in C-C cross-coupling reactions**.** These catalysts, compared to many of the previous phosphine-free

catalysts, are air- and heat-stable, have long lifetimes and do not require cocatalysts to achieve high catalytic activity [78].

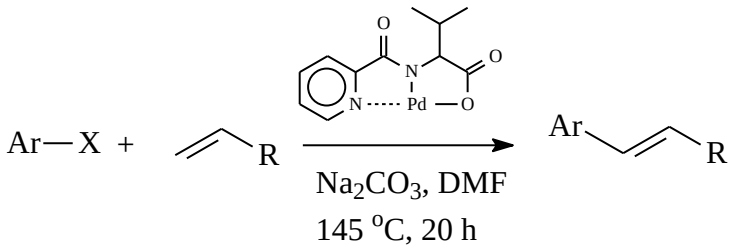

More literature on various catalytic systems for Mizoroki-Heck coupling reaction can be found in the following references [79 - 85]

1.3.3 Sonogashira coupling reaction

The Sonogashira coupling reaction is the reaction of organic halides (aryl or vinyl halides) with terminal alkynes. It provides a powerful tool for the construction of carbon-carbon bond in molecules with triple bond [86 – 91]. The importance of the alkynes is directly associated with their reoccurrence in a wide range of natural products and other biologically active substances [92], their versatility as intermediates for the production of materials for advanced engineering applications such as conducting polymers and non-linear optical devices and liquid crystals [93-95]. Owing to their importance, the development of methods for incorporating triple bonds to molecules remains an important objective [96].

Sonogashira coupling reaction follows the general mechanism: oxidative addition of the organohalide to the Pd(0) or Pd(II) to form a Pd(II) or Pd(IV) complex, respectively. This is then followed by the transmetalation with the organocopper reagent, formed from the terminal alkyne and the copper catalyst. The halide on the palladium complex is then replaced by the alkynyl anion and the copper halide catalyst is regenerated. The final step is the reductive elimination. This involves the release of the final coupled product and subsequent regeneration of the palladium catalyst [97].

In general, the Sonogashira cross coupling reaction, which represents the leading method for the production of internal alkynes, is catalyzed by palladium complexes with the combination of copper salts and a large excess of amine as a base [98]. However, the presence of copper(I) co-catalysts could result in the formation of some copper(I) acetylides in situ that leads to the oxidative homo-coupling of alkynes [98-100]. To avoid the homocoupling reactions, serious efforts were made, including the employment of new active palladium complexes as catalysts in the Sonogashira cross coupling reaction. Problems associated with the copper free systems include the frequent requirement for high palladium catalysts loading, excess of base and rigorously dried organic solvent [101, 102].

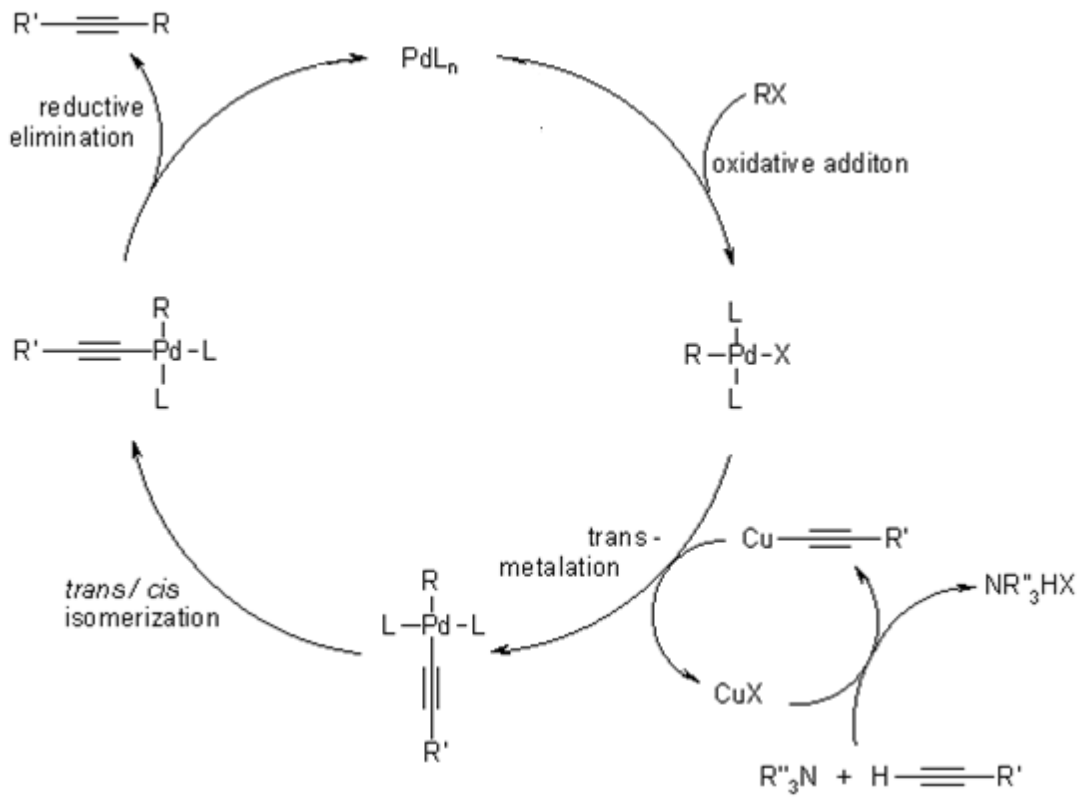

Figure 4. Catalytic Cycle for Palladium Catalyzed Sonogashira Cross Coupling reaction [102b]

In the past few decades, various researchers focused on the development of new catalytic systems and modification of the original Sonogashira procedure to allow for more selectivity, high functional groups tolerance and ability to couple unreactive substrates. Among the recent developments, includes a copper free system for the Sonogashira coupling of aryl iodide with acetylenes in aqueous solvent and under aerobic condition. The use of 1 mol% palladium chloride in the presence of pyrrolidine allows the coupling reaction of an array of aryl iodides with diversely functionalized alkyl and aryl alkynes [103].

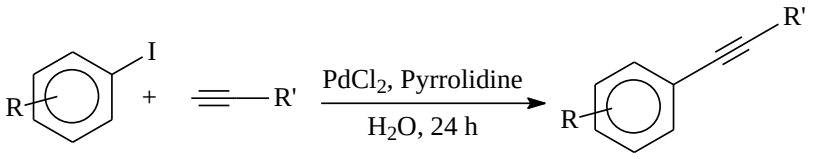

Another interesting example is the solvent, copper and ligand free system for the Sonogashira coupling using ball milling. The catalyst employed was either $Pd(OAc)_2$ or $Pd(PPh_3)_4$ and a sterically hindered base (1,4-diazabicyclo[2,2,2]octane, DABCO). It was found that the use of $Pd(OAc)_2$ as catalyst and SiO_2 as a grinding auxiliary, efficiently catalyzed the coupling of aryl iodide with various acetylenes. However, the coupling of aryl bromides with aryl acetylenes was effected using Al_2O_3 as auxiliary and $Pd(PPh_3)_4$ as catalyst [104].

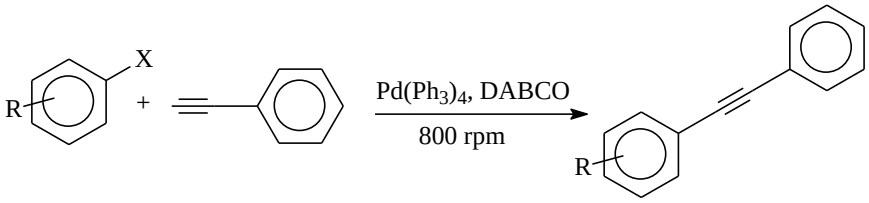

A tandem Sonogashira coupling of aryl iodides with alkynols was used to produce hydroxyl functionalized internal alkynes. This protected alkyne was further reacted with another mole of aryl iodide to produce diarylalkyne. Such tandem reactions are applicable in the synthesis of polymers and oligomers [105].

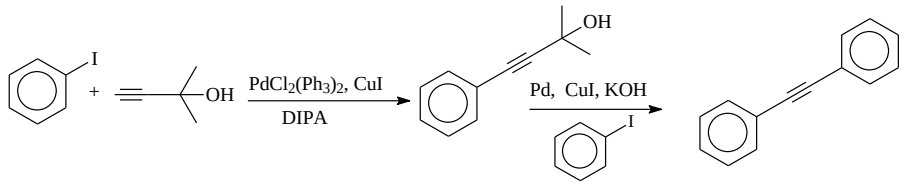

Sonogashira coupling reaction was reported as a step in the total synthesis of many drugs and biologically active compounds. For instance, in the synthesis of altenicline, a drug used in the treatment of Parkinson's disease. The drug was synthesized from nicotine. A Sonogashira coupling of dihalonicotine with triisopropyl silyl acetylene yields an important pre-cursor for the synthesis of Altinicline [106].

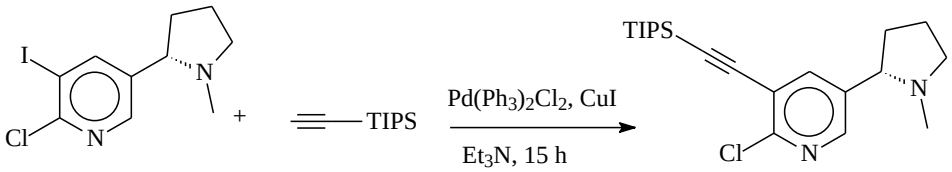

Aerobic oxidative coupling of terminal alkynes with alkyl zinc in the presence of palladium catalyst have successfully been developed [107, 108].

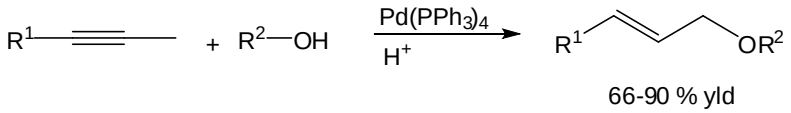

An environmentally benign palladium catalysed phosphine and copper free Sonogoshira reaction in aqueous medium was reported by Liu in 2011. The reaction worked well in water with ethanol as co-solvent. $K_3PO_4 \cdot 7H_2O$ and NaOH, as bases, provided better

conversions than carbonates and amines. The process shows good to excellent conversions for a range of substrates with different substitution pattern and different electronic properties [86].

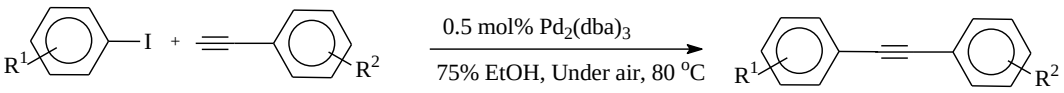

1.4 Carbonylation reactions

The carbonylation of alkynes in the presence of protic nucleophile was first discovered in the 1930's [109, 110]. It is considered a powerful synthetic method for the industrial production of value added bulk and fine chemicals. Depending on the type of nucleophile involved, a range of products can be synthesized. These include various linear, branched and cyclic α, β-unsaturated carboxylic acids, esters and amides [111, 112]. The products of carbonylation reaction are widely applied as starting raw materials for the production of monomers for polymers, liquid crystals, light sensitive and electrically conductive materials, flavors, fragrances and pharmaceuticals [111-116].

Although many transition metal complexes are active catalyst for carbonylation reactions, palladium complexes are the most widely used. The use of Pd-complexes as catalyst for carbonylation reactions are covered in the relevant reviews [117-119].

1.4.1 Alkoxycarbonylation of alkynes

The alkoxycarbonylation of terminal alkynes is a one step process for the synthesis of α, β-unsaturated carboxylic acids and their derivatives [120]. Unless a highly regioselective catalyst is employed, the process gives a mixture of *gem* and *trans* products [120, 121].

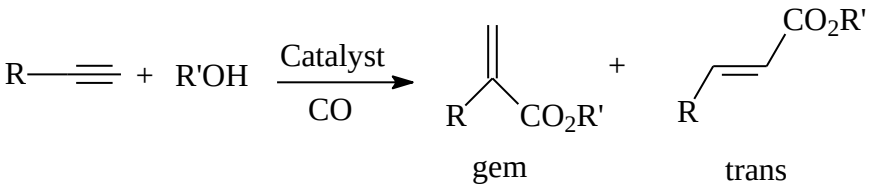

The regioselecivity of alkoxycarbonylation reaction is usually controlled by the catalytic system and other reaction parameters. For instance, the use of $Pd(dba)_2$ /*p*-TSOH in the presence of PPh_3 favors the formation of the *gem* ester [122]. Similarly, the hydroesterification of alkynes and alkynols with formate ester using $Pd(OAc)_2$/dppb/PPh_3/*p*-TSOH, as catalyst, selectively yielded the branched ester in excellent yield [123].

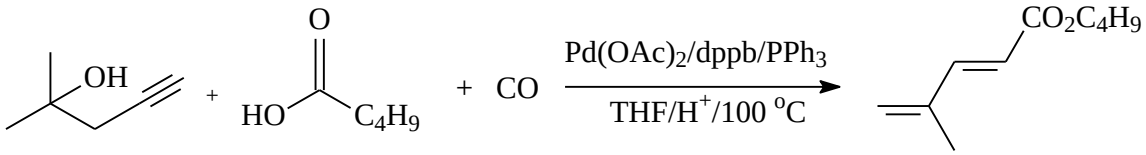

On the other hand, various catalytic systems have been developed that worked selectively towards the linear α, β-unsaturated ester. For instance, the regioselective carbonylation of terminal alkynes to the corresponding linear α, β-unsaturated ester was achieved using $Pd(dba)_2$ /dppb as catalyst [124].

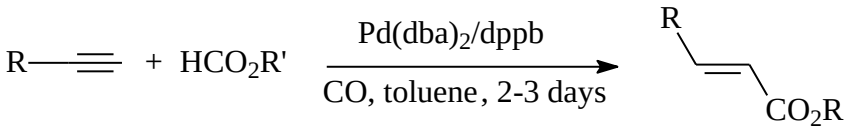

Similarly, the trans α, β-unsaturated ester was found to be the predominant product in the methoxycarbonylation of terminal alkynes using $Pd(OAC)_2$/dppb/*p*-TSOH as catalytic system [125].

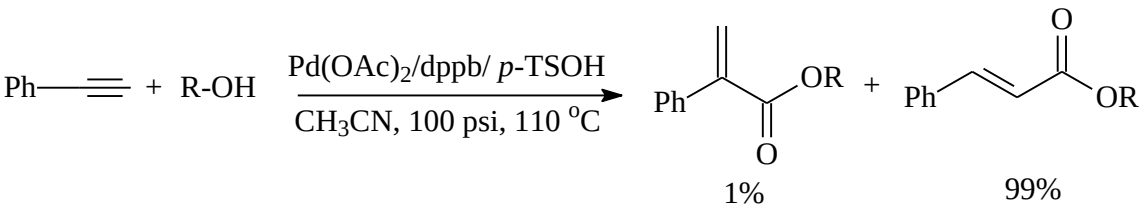

The intermolecular methoxycarbonylation is a valuable method for the direct transformation of terminal alkynes into β-methoxy acrylates. This is a common structure found in many antibiotics, dihydrokawain and tetronic acids [126]. A catalytic system based on $Pd(TFA)_2$ with BOX ligand has been found to effectively catalyze the

intermolecular methoxycarbonylation of terminal alkynes. The system was reported to be tolerant to wide range of functionalities including ketal and acetal protecting groups, free hydroxyl groups and glycosidic bonds [126].

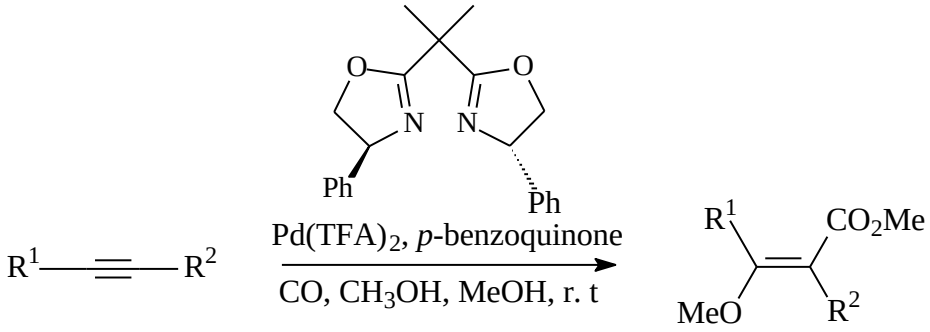

1.4.2 Aminocarbonylation of alkynes

Aminocarbonylation is considered the most efficient, atom economical and cleaner synthetic method for the production of acrylamides from carbonylative coupling of alkynes with amines. It is considered more efficient than most of the conventional methods for the synthesis of amides. Similar to the alkoxycarbonylation, aminocarbonylation of alkynes can result in either *gem* or *trans*-α, β-unsaturated amides. However, the selectivity can be tuned to the desired isomer by using the appropriate catalytic system. In this regard, the regioselective aminocarbonylation of propargylamine was achieved using Pd(0) as catalyst, to yield the corresponding *trans*-α, β-unsaturated amide [127].

On the other hand, the use of $Pd(OAc)_2$/2-$PyPPh_2$/ CH_3SO_3H as catalyst system for the aminocarbonylation of phenylacetylene with n-butylamine afforded the corresponding *gem*-acrylamide as the predominant product [128].

Another system that favours *gem* selectivity is the use of $Pd(OAc)_2$/dppp in ionic liquid (IL) for the aminocarbonylation of terminal alkynes [129].

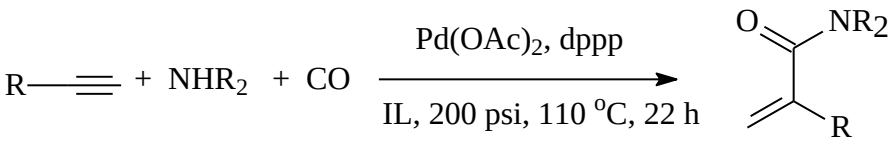

The *gem* product was also realized as the predominant product from the carbonylation of phenylacetylene with various amines using $Pd(OAc)_2$/dppb/*p*-TSOH/CH_3CN as catalyst system [125].

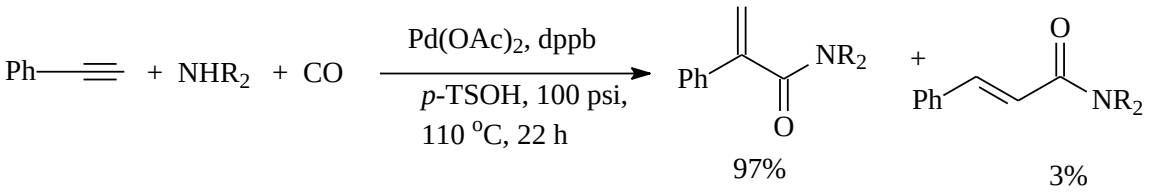

1.5 Problem identification

A plethora of research papers and patents have been published on cross coupling and carbonylation reactions catalyzed by homogenous metal-phosphine complexes [130]. On the contrary, the use of nitrogen donor ligands in palladium catalyzed cross coupling and carbonylative coupling reactions is limited [4, 131]. The following are some of the problems associated with homogeneous phosphine complexes.

- They are generally toxic, air and moisture sensitive.
- Their applications in catalytic coupling and carbonylation reactions require the use of rigorously dried organic solvents.
- Phosphine ligands are generally expensive and very difficult to synthesize

Contrary to phosphine ligands and their complexes, their nitrogen based counterparts are:

- Generally non-toxic, air and moisture stable
- Can be used as catalyst in aqueous solvents and neat water as reaction medium
- Flexible, easy to synthesize and less expensive [4].

The current research is focused on the development of nitrogen donor ligands, in this context, dinitrogenated bis(oxazoline) ligands [12, 13, 127-132]. The C_2-symmetric chiral bis(oxazoline) ligands have been extensively studied with different metal ions in asymmetric catalysis [133]. Nevertheless, there is limited number of reports describing the synthesis of non C_2 and achiral bis(oxazoline) ligands, their palladium complexes and applications in cross coupling and carbonylative coupling reactions [134].

1.6 Objectives of the present work

The investigation in this research includes:

1. Synthesis and characterization of new bis(oxazoline) ligands and their palladium(II) complexes
2. Synthesis and characterization of palladium-bis(oxazoline)-phosphine mixed ligands complexes
3. Synthesis and characterization of water soluble palladium-bis(oxazoline) complexes
4. Synthesis and characterization of supported palladium-bis(oxazoline) complexes
5. Evaluation of the synthesized new complexes in fundamental organic cross coupling reactions such as Suzuki-Miyaura, Heck-Mizoroki and Sonogashira coupling reactions.

6. Evaluation of the synthesized new complexes in the carbonylation reactions such as alkoxycarbonylation and aminocarbonylation of alkynes and aryl halides.

CHAPTER 2

Bis(oxazoline) ligands and palladium bis(oxazoline) complexes: Synthesis and characterizations

2.1 Introduction

Bis(oxazolines) (BOX) are nitrogen-based ligands which are generally non-toxic, stable to air/moisture, modular, and less expensive than phosphine ligands [4]. They are well known bidentate ligands where the binding sites are normally the two nitrogen centers. A good number of C_2-symmetric chiral bis(oxazoline) ligands and their complexes with different metal ions have been extensively studied [133]. However, only few examples that describe the synthesis of non-chiral bis(oxazoline) ligands and their palladium complexes have been reported [134]. In this chapter, we present the synthesis and characterization of seven new bis(oxazoline) (BOX) ligands and their corresponding palladium(II) (Pd-BOX) complexes. The X-ray crystal structure of these new complexes is also presented.

2.2 Experimental

2.2.1 Materials and instruments

Materials for the synthesis of ligands and palladium complexes were purchased from Sigma Aldrich and were used as received. All solvents used in the synthesis were distilled

before their use. The products were purified using flash column chromatography packed with 60 F Silica gel from Fluka Chemie AG (Buchs, Switzerland).

^{1}H and ^{13}C NMR spectral data were obtained using 500 MHz NMR machine (Joel 1500 model). Chemical shifts were recorded in ppm using tetramethyl silane (TMS) as reference and $CDCl_3$ as solvent. IR spectra were recorded in wave numbers (cm^{-1}) using FT-IR spectrometer (Perkin-Elmer 16F model). Elemental analyses were performed on Perkin Elmer Series 11 (CHNS/O) Analyzer 2400. Merck 60 F_{254} silica gel plates (250 µm layer thickness) were used for thin-layer chromatography (TLC) analyses. A Varian Saturn 2000 GC-MS machine was used to analyze the products.

2.2.2 General procedure for the synthesis of bis(oxazoline)

The following general procedure was followed for the synthesis of ligands (**BOX-1 to BOX-7**):

A solution of phthalonitrile (or its derivative) (4.0 mmol) and zinc triflate (5.0 mol%, 0.2 mmol) in dried chlorobenzene (30 mL) was stirred at room temperature for 15 minutes. A solution of the appropriate amino alcohol (8.0 mmol) in dry chlorobenzene (5 mL) was slowly added. The temperature was raised to 135 ^{o}C and the reaction mixture was refluxed for 24 hours. The product of the reaction was dissolved in 30 mL of dichloromethane and extracted twice with distilled water (2 x 20.0 mL). The aqueous layer was then separated and the combined organic layers were dried with anhydrous sodium sulfate. The dichloromethane was removed using a rotary evaporator to obtain the impure product, which was then purified using silica gel column chromatography with dichloromethane/ether as eluent

2,2'-(1,2-phenylene)bis(4,4-dimethyl-4,5-dihydrooxazole) (BOX-1)

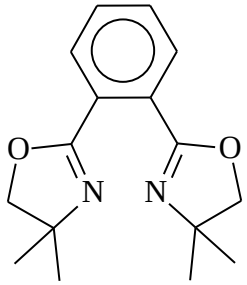

BOX-1

Colorless oil; isolated yield (82 %); ^{1}H NMR (500 MHz, $CDCl_3$) δ (ppm): 7.26 - 7.24 (m, 2H, C*H*-4,5 arom), 6.96 - 6.94 (m, 2H, C*H*-3,6 arom), 3.55 (s, 4H, OCH_2 x 2), 0.88 (s, 12H, CH_3x4), ^{13}C NMR (125 MHz, $CDCl_3$) δ (ppm): 27.03 (*C*H_3 x 4), 66.81 (*C* x 2), 72.80 (O*C*H_2 x2), 127.64 (*C*-1,2 arom), 128.56 (*C*-3,6 arom), 129.11 (*C*-4,5 arom), 161.12 (O*C*=N); IR (*v cm^{-1})* 2965, 1662, 1266, 1190; GC-MS m/z 273 (M^{+1}) Anal. Calc. for $C_{16}H_{20}N_2O_2$, (272.35) (%): C, 70.56; H, 7.40; N, 10.29. Found: C, 70.51; H, 7.43; N, 10.23.

2,2'-(4-methylbenzene-1,2-diyl)bis(4,4-dimethyl-4,5-dihydro-1,3-oxazole) (BOX-2)

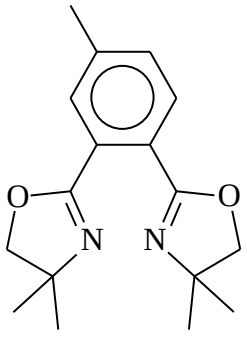

BOX-2

Yellow oil, isolated yield (87 %); ^{1}H NMR (500 MHz, $CDCl_3$) δ (ppm): 7.50 (d, *J* = 7.93 Hz, 1H, C-5 arom), 7.41 (s, 1H, C-3 arom), 7.12 (d, *J* = 7.93 Hz, 1H, C-6 arom), 3.92 (s,

4H, OC*H*$_2$ x 2), 2.24 (s, 3H, C*H*$_3$ on arom), 1.25 (s, 12H, NC(C*H*$_3$)$_2$ x 2); ^{13}C NMR (125 MHz, $CDCl_3$) δ (ppm); 20.8 (CH_3 on arom), 27.8 (NC(*C*H$_3$)$_2$ x 2), 67.5 (N*C*(CH$_3$)$_2$ x 2), 79.1 (O*C*H$_2$), 79.2 (O*C*H$_2$), 125.4, (C-2 arom), 128.2 (C-1 arom), 129.4 (C-3 arom), 130.0 (C-5 arom), 130.5 (C-6 arom), 140.3 (C-4 arom), 162.1 (C-4'), 162.4 (C-1'); IR (CH_2Cl_2) υ (cm^{-1}) 2930, 1655, 1460, 1354, 1266, 1085, 969, 830, 735; GC-MS m/z 287 (M^{+1}). Anal. Calcd. for $C_{17}H_{22}N_2O_2$ (%): C, 71.3; H, 7.7; N, 9.8. Found: C, 71.0; H, 7.7; N, 9.9.

2,2'-(4-nitro-1,2-phenylene)bis(4,4-dimethyl-4,5-dihydrooxazole) (BOX-3)

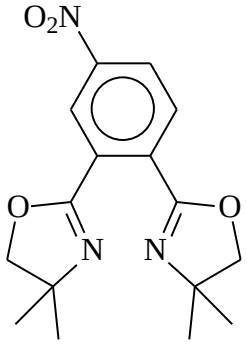

BOX-3

Green solid, isolated yield (88 %); ^{1}H NMR (500 MHz, $CDCl_3$) δ (ppm): 8.56 (s, 1H, C-3 arom), 8.28 (d, *J* = 6.1 Hz, 1H, C-5 arom), 7.89 (d, *J* = 8.5 Hz, 1H, C-6 arom), 4.09 (s, 4H, OC*H*$_2$ x 2), 1.38 (s, 12H, NC(C*H*$_3$)$_2$ x 2); ^{13}C NMR (125 MHz, $CDCl_3$) δ (ppm); 28.0 (NC(*C*H$_3$)$_2$ x 2), 68.5 (N*C*(CH$_3$)$_2$ x 2), 80.0 (O*C*H$_2$ x 2), 124.7 (C-3 arom), 124.9 (C-5 arom), 130.4 (C-2 arom), 131.1 (C-6 arom), 134.5 (C-1 arom), 148.5 (C-4 arom), 160.1 (C-4'), 160.5 (C-1'); IR (CH_2Cl_2) υ (cm^{-1}) 2932, 1659, 1530, 1352, 1266, 1185, 1043, 968, 736; GC-MS m/z 318 (M^{+1}). Anal. Calcd. for $C_{16}H_{19}N_3O_4$, (%): C, 60.5; H, 6.0; N, 13.2. Found: C, 60.6; H, 6.0; N, 13.3.

2,2'-(4-Phenoxy-1,2-phenylene)bis(4,4-dimethyl-4,5- dihydrooxazole) (BOX-4)

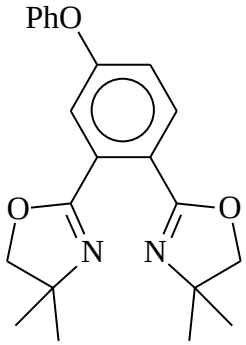

BOX-4

Greenish oil; isolated yield (94 %); ^{1}H NMR (500 MHz, $CDCl_3$) d (ppm): 7.64 (d, J = 8.5 Hz, 1H), 7.28–7.24 (m, 3H), 7.06 (t, J = 7.9 Hz, 1H), 6.98–6.92 (m, 3H), 3.97 (s, 4H, OCH_2 x 2), 1.29 (s, 12H, NC(CH_3)$_2$ x 2); ^{13}C NMR (125 MHz, $CDCl_3$) d (ppm); 28.0 (NC(CH_3)$_2$ x 2), 67.7 (NC(CH_3)$_2$), 67.9 (NC(CH_3)$_2$), 79.3 (OCH$_2$), 79.4 (OCH$_2$), 119.4, 119.6, 123.0, 124.0, 129.8, 130.6, 131.5, 156.0, 158.8, 161.6, 161.7; IR ν (cm^{-1}) 2969, 1656, 1488, 1354, 1233,1078, 974, 737; GC–MS m/z 365 (M^{+1}); Anal. Calc. for $C_{22}H_{24}N_2O_3$ (364.44): C, 72.51; H, 6.64; N, 7.69. Found: C, 72.44; H, 6.52; N, 7.87.

2,2'-(4-Phenoxy-1,2-phenylene)bis(4-isopropyl-4,5- dihydrooxazole) (BOX-5)

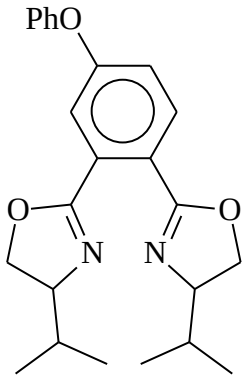

BOX-5

Colorless oil; isolated yield (86 %); ^{1}H NMR (500 MHz, $CDCl_3$) d (ppm): 7.71 (d, J = 8.9 Hz, 1H), 7.30–7.34 (m, 3H), 7.13 (t, J = 7.3 Hz, 1H), 6.08–7.04 (m, 3H), 4.35 (t, J = 17.3 Hz, 2H, NC*H* x 2), 4.00–4.08 (m, 4H, OCH_2 x 2), 1.84 (m, 2H, isopropyl C*H* x 2), 1.01 (d, J = 6.1 Hz, 6H, isopropyl CH_3 x 2), 0.92 (d, J = 6.7 Hz, 6H, isopropyl CH_3 x 2); ^{13}C NMR (125 MHz, $CDCl_3$) d (ppm): 18.1 (isopropyl *C*H_3 x 2), 19.0 (isopropyl *C*H_3 x 2), 32.5 (isopropyl *C*H), 32.6 (isopropyl *C*H), 70.4 (O*C*H_2), 70.6 (O*C*H_2), 72.9 (N*C*H), 73.0 (N*C*H), 119.4, 119.5, 119.6, 122.9, 124.0, 129.9, 130.5, 130.6, 131.6, 131.7, 156.0, 158.9, 163.0, 163.1; IR *v* (cm^{-1}) 2959, 2926,1653, 1589, 1489, 1355, 1224, 1090, 736; GC–MS m/z 393 (M^{+1}); Anal. Calc. for $C_{24}H_{28}N_2O_3$ (392.50): C, 73.44; H, 7.19; N, 7.14.Found: C, 73.54; H, 7.04; N, 7.37.

***R,R-2,2'-benzene-1,2-diylbis(4-ethyl-4,5-dihydro-1,3-oxazole) (*BOX-6)**

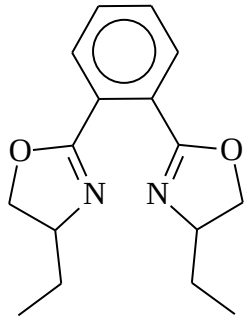

BOX-6

Yellow oil; isolated yield (87 %); ^{1}H NMR (500 MHz, $CDCl_3$) δ (ppm): 7.72 - 7.69 (m, 2H, C*H*-4,5 arom), 7.45 - 7.43 (m, 2H, C*H*-3,6 arom), 4.43-4.39 (m, 2H), 4.21-4.18 (m, 2H), 4.00-3.96 (m, 2H), 1.77 - 1.71 (m, 2H) , 1.63 - 1.57 (m, 1H), 0.99 (t, *J* = 7.35, 6H, (NCHCH_2CH_3 x2),); ^{13}C NMR (125 MHz, $CDCl_3$) δ (ppm); 10.08 (NCHCH_2*C*H_3 x2), 28.37 (NCH*C*H_2CH_3 x2), 68.30 (N*C*(CH_2CH_3)$_2$ x 2), 72.56 (O*C*H_2 x2), 128.45 (*C*-1,2 arom), 129.72 (*C*-3,6 arom), 130.27 (C-4,5 arom), 163.75 (O*C*=N) IR (*v* cm^{-1}) 2967, 1661,

1256, 1192; GC-MS m/z 273 (M^{+1}) Anal. Calc. for $C_{16}H_{20}N_2O_2$, (272.15): C, 70.56; H, 7.40; N, 10.29. Found: C, 70.54; H, 7.33; N, 10.31.

2,2'-(4-iodobenzene-1,2-diyl)bis(4,4-dimethyl-4,5-dihydro-1,3-oxazole) (BOX-7)

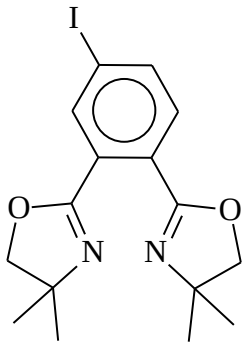

BOX-7

Waxy solid, isolated yield (94 %); ^{1}H NMR (500 MHz, $CDCl_3$) δ (ppm): 8.01 (s, 1H, C-3 arom), 7.73 (d, *J* =10 Hz, 1H, C-5 arom), 7.38 (d, *J* = 10 Hz, 1H, C-6 arom), 3.99 (s, 2H,OCH_2), 3.98 (s, 2H,OCH_2),1.30 (s, 6H, C*H*$_3$ x 2); 1.29 (s, 6H, C*H*$_3$ x 2); ^{13}C NMR (125 MHz, $CDCl_3$) δ (ppm); 27.95 (*C*H_3 x 4), 67.92 (N*C*H x 2), 79.40 (O*C*H_2 x 2), 96.12 (C-4 arom), 127.89 (C-1 arom), 130.11 (C-2 arom), 130.97(C-6 arom), 138.26 (C-5 arom), 139.07 (C-3 arom), 160.82 (C-4'), 161.47 (C-1'); IR (KBr) υ (cm^{-1}) 2963, 2884, 1642, 1458, 1398, 1352, 1303, 1194, 1089, 1039, 964, 824, 723; GC-MS m/z 398 (M^+); Anal. Calc. for $C_{16}H_{19}IN_2O_2$ (398.24): C, 48.26; H, 4.81; N, 7.03. Found: C, 48.44; H, 4.88; N, 7.22.

2.2.3 General procedure for the synthesis of palladium-bis(oxazoline) (Pd-BOX) complexes

The following general procedure was followed for the synthesis of palladium-bis(oxazoline) complexes (**Pd-BOX-1 to Pd-BOX-7**).

In a 25-mL round bottom flask flushed with nitrogen was charged 0.5 mmol of the appropriate palladium(II) salt (in 8 mL DMF) and 0.5 mmol of BOX ligand. The reaction mixture was stirred at room temperature for 6 h. The progress of the reaction was monitored by TLC until no free BOX was observed. The solvent was separated using rotary evaporator. The impure product was dissolved in CH_2Cl_2 and layered with hexane to obtain pure crystals. The crystals were separated and washed with ether and characterized with different spectroscopic techniques including ^{1}H and ^{13}C NMR, elemental analysis, IR spectroscopy and single crystal X-ray crystallography [135-137].

Dichlorido(2,2'-(1,2-phenylene)bis(4,4-di-methyl-4,5-dihydrooxazole)-N,N')palladium (II) (Pd-BOX-1)

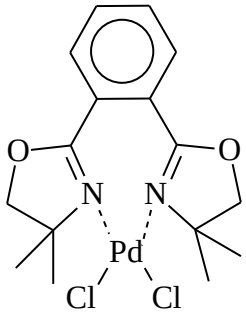

Pd-BOX-1

Pale yellow needle shape crystals; yield (81 %); m.p. (252 ^{o}C), ^{1}H NMR (500 MHz, DMSO) δ (ppm): 7.95 (s, 4H, C*H*-3,4,5,6 arom), 4.39 (s, 4H, OCH_2 x 2), 1.52 (s, 6H, NC(CH_3)$_2$), 1.57 (s, 6H, NC(CH_3)$_2$, ^{13}C NMR (125 MHz, $CDCl_3$) δ (ppm); 27.8 (NC(*C*H_3) x 4), 70.8 (N*C*), 80.5 (O*C*H_2), 125.5 (C-1,2 arom), 129.5 (C-3,4 arom), 132.9 (C-5,6 arom), 163.9.(OCN); IR (KBr) (*ν cm^{-1}*): 2968, 1632, 1260, 1193.; Anal. Calc. for $C_{16}H_{20}Cl_2N_2O_2Pd$, (449.67) (%): C, 42.74; H, 4.48; N, 6.23, Found: C, 42.71; H, 4.46; N, 6.29.

Dichlorido(2, 2'-(4-methyl-1,2-phenylene)bis(4,4-dimethyl-4,5-dihydrooxazole) -N,N')-palladium(II) (Pd-BOX-2)

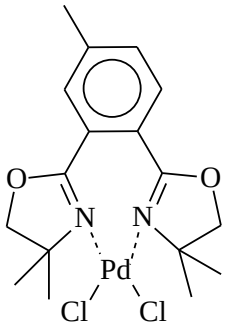

Pd-BOX-2

Pale yellow solid; yield (85 %); m.p. (230-232 ^{o}C), ^{1}H NMR (500 MHz, $CDCl_3$) δ (ppm): 7.70 (d, *J* = 7.9 Hz, 1H, C-5 arom), 7.61 (s, 1H, C-3 arom), 7.54 (d, *J* = 7.9 Hz, 1H, C-6 arom), 4.32-4.23 (m, 4H, OCH_2 x 2), 2.51 (s, 3H, CH_3 on arom), 1.75 (s, 6H, NC(CH_3)$_2$), 1.62 (s, 3H, NC(C*H*$_3$), 1.59 (s, 3H, NC(C*H*$_3$); ^{13}C NMR (125 MHz, $CDCl_3$) δ (ppm); 21.5 (CH_3 on arom), 28.2 (NC(*C*H_3), 28.3 (NC(*C*H_3), 28.8 (NC(*C*H_3), 28.9 (NC(*C*H_3), 71.1 (N*C*(CH_3)$_2$), 71.2 (N*C*(CH_3)$_2$), 80.8 (O*C*H_2), 80.9 (O*C*H_2), 123.1 (C-2 arom), 125.9 (C-1 arom), 129.0 (C-3 arom), 130.8 (C-5 arom), 132.0 (C-6 arom), 143.7 (C-4 arom), 164.2

(C-4'), 164.3 (C-1'); IR (CH_2Cl_2) υ (cm^{-1}): 2973, 1637, 1457, 1374, 1122, 1068, 958, 829, 730; Anal. Calc. for $C_{18}H_{25}Cl_2N_2O_2Pd$, (478.73): C, 45.16; H, 5.26; Cl, 14.81; N, 5.85; Found: C, 45.51; H, 5.21; N, 5.89.

Diacetato(2,2'-(4-nitro-1,2-phenylene)bis(4,4-dimethyl-4,5-dihydrooxazole)-N,N')-palladium(II) (Pd-BOX-3)

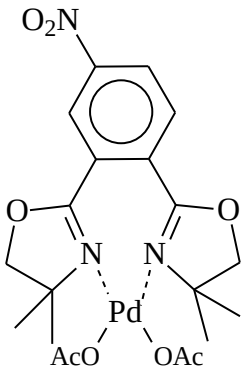

Pd-BOX-3

Green solid; yield (92 %), m.p. 149 °C; ^{1}H NMR (500 MHz, $CDCl_3$) δ (ppm): 8.72 (s, 1H, C-3 arom), 8.52 (d, *J* = 8.8 Hz, 1H, C-5 arom), 8.10 (d, *J* = 8.5 Hz, 1H, C-6 arom), 4.38-4.27 (m, 4H, OCH_2 x 2), 1.74 (s, 3H, NC(C*H*$_3$), 1.73 (s, 3H, NC(C*H*$_3$), 1.63 (s, 3H, NC(C*H*$_3$), 1.61 (s, 3H, NC(C*H*$_3$), 1.42 (s, 3H, OCOC*H*$_3$), 1.41 (s, 3H, OCOC*H*$_3$); ^{13}C NMR (125 MHz, $CDCl_3$) δ (ppm); 22.8 (OCO*C*H_3 x 2), 26.2 (NC(*C*H_3), 26.3 (NC(*C*H_3), 29.2 (NC(*C*H_3 x 2), 70.3 (N*C*$(CH_3)_2$ x 2), 80.9 (O*C*H_2 x 2), 125.5 (C-3 arom), 126.0 (C-5 arom), 127.8 (C-2 arom), 131.5 (C-1 arom), 132.1 (C-6 arom), 149.5 (C-4 arom), 162.8 (C-4'), 163.1 (C-1'), 177.9 (O*C*OCH$_3$), 178.0 (O*C*OCH$_3$). IR (KBr) υ (cm^{-1}): 2980, 1651, 1605, 1533, 1500, 1376, 1329, 1222, 1172, 1129, 1063, 951, 713. Anal. Calc. for $C_{20}H_{25}N_3O_8Pd$ (%): C, 44.3; H, 4.6; N, 7.8; Found: C, 44.3; H, 4.7; N, 7.7. UV-Vis: $\lambda_{max}(CH_2Cl_2)$/nm: 360; $\varepsilon_{A,}$ 5926 $L.mol^{-1}cm^{-1}$.

Dichlorido(2,2'-(4-phenoxy-1,2-phenylene)bis(4,4-dimethyl-4,5-dihydrooxazole)-N,N') palladium(II) (Pd-BOX-4)

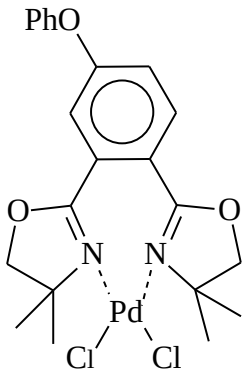

Pd-BOX-4

Yellow solid; yield (89 %); mp (242-243 ^{o}C); ^{1}H NMR (500 MHz, $CDCl_3$) δ (ppm): 7.74 (d, *J* = 8.8 Hz, 1H), 7.46 (t, *J* = 8.2 Hz, 2H), 7.30 (d, *J* = 2.4 Hz, 1H), 7.27 (t, *J* = 7.6 Hz, 1H), 7.22 (d, *J* = 2.4 Hz, 1H), 7.15 (d, *J* = 7.6 Hz, 2H), 4.30–4.19 (m, 4H, OCH_2 x 2), 1.75 (s, 3H, NC(CH_3), 1.73 (s, 3H, NC(CH_3), 1.61 (s, 3H, NC(CH_3), 1.58 (s, 3H, NC(CH_3); ^{13}C NMR (125 MHz, CDCl3) δ (ppm); 28.2 (NC(*C*H_3), 28.3 (NC(*C*H_3), 29.0 (NC(*C*H_3), 29.1 (NC(*C*H_3), 71.2 (N*C*$(CH_3)_2$), 71.5 (N*C*$(CH_3)_2$), 80.8 (O*C*H_2), 80.9 (O*C*H_2), 118.7, 119.2, 120.7, 125.7, 127.8, 130.5, 132.6, 154.3, 161.5, 163.7, 164.0; IR *ν* (cm^{-1}) 2972, 1637, 1582, 1486, 1372, 1236, 1063, 961, 729; Anal. Calc. for $C_{22}H_{24}Cl_2N_2O_3Pd$ (541.77): C, 48.77; H, 4.47; N, 5.17. Found: C, 48.83; H, 4.66; N, 5.29 %. UV-Vis: $\lambda_{max}(CH_2Cl_2)$/nm: 301; $\varepsilon_{A,}$ 1003 L.mol^{-1}cm^{-1}.

Dichlorido(2,2'-(4-phenoxy-1,2-phenylene)bis(4-isopropyl-4,5-dihydrooxazole)-N,N0)palladium(II) (Pd-BOX-5)

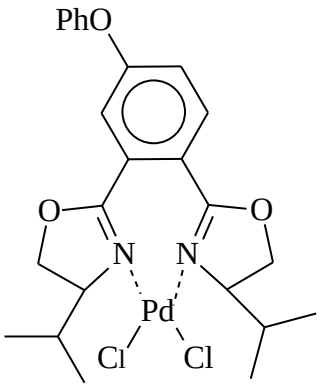

Pd-BOX-5

Orange solid; yield (90 %) mp (235-236 ^{o}C); ^{1}H NMR (500 MHz, $CDCl_3$) δ (ppm): 7.90 (d, *J* = 8.6 Hz, 1H), 7.50-7.45 (m, 3H), 7.31-7.27 (m, 2H), 7.18-7.14 (m, 2H), 4.96-4.92 (m, 2H, NC*H* x 2), 4.62-4.54 (m, 2H, OCH_2 x 2), 4.42-4.35 (m, 2H, OCH_2 x 2), 2.69 (m, 2H, isopropyl C*H* x 2), 1.31 (d, *J* = 7.0 Hz, 6H, isopropyl CH_3 x 2), 0.91 (d, *J* = 6.7 Hz, 6H, isopropyl CH_3 x 2); ^{13}C NMR (125 MHz, CDCl3) δ (ppm): 16.1 (isopropyl *C*H_3 x 2), 20.3 (isopropyl *C*H_3 x 2), 30.7 (isopropyl *C*H x 2), 69.4 (O*C*H_2 x 2), 71.0 (N*C*H), 71.3 (N*C*H), 117.7, 120.4, 120.5, 120.7, 121.0, 125.6, 126.4, 130.5, 133.1, 134.6, 154.2, 161.7, 164.5, 164.8; IR *v* (cm^{-1}): 3063, 2963, 1640, 1585, 1484, 1380, 1228, 1064, 692; Anal. Calc. for $C_{24}H_{28}Cl_2N_2O_3Pd$ (569.82): C, 50.59; H, 4.95; N, 4.92. Found: C, 50.28; H, 4.88; N, 5.11 %. UV-Vis: $\lambda_{max}(CH_2Cl_2)$/nm: 299; $\varepsilon_{A,}$ 2157 $L.mol^{-1}cm^{-1}$.

Dibromido(2,2'-(4-methyl-1,2-phenylene)bis(4,4-dimethyl-4,5-dihydrooxazole)-N, N')palladium(II) (Pd-BOX-6)

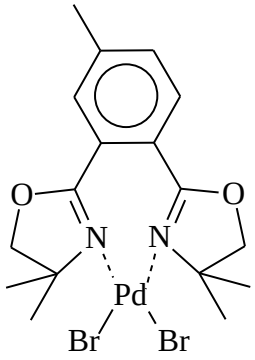

Pd-BOX-6

Brown solid; yield (89 %), m.p (232-234 ^{o}C); ^{1}H NMR (500 MHz, $CDCl_3$) δ (ppm): 7.69 (d, *J* = 7.9 Hz, 1H, C-5 arom), 7.59 (s, 1H, C-3 arom), 7.52 (d, *J* = 7.9 Hz, 1H, C-6 arom), 4.31-4.23 (m, 4H, OC*H*$_2$ x 2), 2.49 (s, 3H, C*H*$_3$ on arom), 1.77 (s, 6H, NC(C*H*$_3$)$_2$), 1.58 (s, 3H, NC(C*H*$_3$), 1.55 (s, 3H, NC(C*H*$_3$); ^{13}C NMR (125 MHz, $CDCl_3$) δ (ppm); 21.5 (CH_3 on arom), 28.9 (NC(*C*H$_3$), 29.0 (NC(*C*H$_3$ x 2), 29.1 (NC(*C*H$_3$), 71.1 (N*C*(CH$_3$)$_2$), 71.2 (N*C*(CH$_3$)$_2$), 80.9 (O*C*H$_2$), 81.0 (O*C*H$_2$), 123.1, (C-2 arom), 125.9 (C-1 arom), 130.1 (C-3 arom), 130.6 (C-5 arom), 133.3 (C-6 arom), 143.7 (C-4 arom), 164.0 (C-4'), 164.1 (C-1').; IR (KBr) υ (cm^{-1}): 2969, 2920, 1630, 1457, 1374, 1327, 1207, 1122, 1067, 961, 830, 722; Anal. Calc. for $C_{17}H_{22}Br_2N_2O_2Pd$ (%): C, 36.9; H, 4.0; N, 5.1. Found: C, 37.0; H, 4.0; N, 5.0; UV-Vis: $\lambda_{max}(CH_2Cl_2)$/nm: 383; $\varepsilon_{A,}$ 12650 $L.mol^{-1}cm^{-1}$.

Dichlorido(2,2'-(1,2-phenylene)bis(4-ethyl-4,5-dihydrooxazole)-N,N')-palladium(II) (Pd-BOX-7)

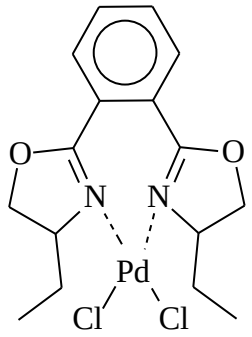

Pd-BOX-7

Yellow solid; isolated yield (90 %); ^{1}H NMR (500 MHz, $CDCl_3$) δ (ppm): 7.87 - 7.85 (m, 2H, C*H* arom), 7.76 - 7.74 (m, 3H, C*H* arom), 4.80 - 4.66 (m, 2H), 4.34 - 4.28 (m, 2H), 4.17-4.14 (m, 1H), 2.75 - 2.70 (m, 1H), 2.65 - 2.60 (m, 1H), 2.25 - 2.19 (m, 1H), 2.02 - 1.96 (m, 1H), 1.87- 1.81 (m, 1H) , 1.10 – 1.02 (m, 6H, ($NCHCH_2CH_3$ x2),); ^{13}C NMR (125 MHz, $CDCl_3$) δ (ppm); 8.97 ($NCHCH_2CH_3$), 10.10 ($NCHCH_2CH_3$), 26.70 ($NCHCH_2CH_3$) 27.56 ($NCHCH_2CH_3$), 66.32 ($NC(CH_2CH_3)$, 70.30 ($NC(CH_2CH_3)$, 73.07 (OCH_2), 74.50 (OCH_2), 124.42 (*C*- arom), 124.96 (*C*- arom), 125.64 (*C*- arom), 130.57 (*C*- arom), 131.55 (*C*- arom), 132.94 (*C*- arom), 164.36 (O*C*=N), 165.90 (O*C*=N); IR (*ν cm^{-1}*): 2960, 2873, 1645, 1589, 1458, 1385, 1340, 1301, 1246, 1133, 944, 781; Anal. Calc. for $C_{16}H_{20}Cl_2N_2O_2Pd$, (447.99): C, 42.74; H, 4.48; N, 6.23. Found: C, 42.63; H, 4.69; N, 6.61.

2.2.4 X-ray structure analysis

A Single crystal of Pd-BOX-**1** was mounted on a APEXII Bruker-AXS diffractometer for data collection (MoK_α radiation source, λ = 0.71073 Å), at the Centre de Diffractométrie

(CDIFX), Université de Rennes 1, France. The data were collected at 150 K, using SMART and the integration was performed using SAINT [138]. X-ray intensity data for Pd-BOX-2 to Pd-BOX-7 were collected on a Bruker-AXS Smart Apex system equipped with a graphite monochromatized MoK_α radiation ($\lambda = 0.71073$Å). The data were collected using SMART and the integration was performed using SAINT [138]. An empirical absorption correction was carried out using SADABS [139]. The structures were solved by direct methods with SHELXS-97 and refined by full-matrix least squares procedures on F^2 using the program SHELXL-97 [140]. All non-hydrogen atoms were refined anisotropically. Hydrogen atoms were placed at calculated positions using a riding model. Molecular graphic was generated using ORTEP-3 [141]. Crystal data and details of the data collection are summarized in tables.

TABLE 1. Crystallographic Data for Pd-BOX-1 and Pd-BOX-2

Compound	**Pd-BOX-1**	**Pd-BOX-2**
Chemical formula	$C_{16}H_{20}Cl_2N_2O_2Pd$	$C_{17}H_{22}Cl_2N_2O_2Pd$
Formula weight	449.64	463.67
Crystal system	monoclinic	Monoclinic
Space group	P $2_1/c$	$P2_1/n$
Temperature (K)	150	296
Radiation	MoKα (λ = 0.71073 Å)	
ρ_{calc} (g.cm^{-3})	1.685	1.582
a (Å)	13.9850(6)	8.0861(4)
b (Å)	7.8175(4)	23.7532(13)
c (Å)	16.4400(7)	10.4338(6)
β (°)	99.486(2)	103.6820(10)
V (Å^3)	1772.8(1)	1947.16(18)
Z	4	4
Refl. collect. / Uniq.	14898 / 4040	26395 / 4845
Refl. obser. [$I > 2\sigma(I)$]	3819	4140
R (int)	0.0315	0.0272
Data / restr/ parameter.	4040 / 0 / 212	4845 / 0 / 222
Goodness-of-fit on F^2	1.037	1.027
R indices [$I > 2\sigma(I)$]	$R_1 = 0.0241$; $wR_2 = 0.0486$	$R_1 = 0.0259$; $wR_2 = 0.0594$
R indices (all data)	$R_1 = 0.0265$; $wR_2 = 0.0494$	$R_1 = 0.0336$; $wR_2 = 0.0630$
Largest diff. peak hole (e Å^{-3})	0.433, -0.482	0.430, -0.257

TABLE. 2. Crystallographic Data for Pd-BOX-3 and Pd-BOX-4

Compound	**Pd-BOX-3**	**Pd-BOX-4**
Chemical formula	C_{21} H_{27} Cl_2 N_3 O_8 Pd	$C_{22}H_{24}Cl_2N_2O_3Pd.$ $0.25H_2O$
Formula weight	626.76	546.24
Crystal system	monoclinic	Triclinic
Space group	P $2_1/c$	P-1
Temperature (K)	296	120
Radiation	MoKα (λ = 0.71073 Å)	
ρ_{calc} (g.cm^{-3})	1.551	1.619
a (Å)	11.0974(7)	9.639(1)
b (Å)	18.991(1)	13.045(2)
c (Å)	12.7396(8)	18.610(3)
β (°)	91.926(1)	85.894(2)
V (Å^3)	2683.3(3)	2240.9(5)
Z	4	4
Refl. collect. / Uniq.	36216 / 6665	30241 / 11093
Refl. obser. [$I > 2\sigma(I)$]	4502	8638
R(int)	0.0750	0.0453
Data / restr./ parameter.	6665 / 0 / 322	11093 / 4 / 650
Goodness-of-fit on F^2	1.111	1.094
R indices [$I > 2\sigma(I)$]	R_1 = 0.0536; wR_2 = 0.1109	R_1=0.0712; wR_2= 0.1869
R indices (all data)	R_1 = 0.0799; wR_2 = 0.1270	R_1 = 0.0906; wR_2 = 0.1980
Largest diff. peak hole (e Å^{-3})	0.894, -0.802	3.978, -2.539

TABLE 3. Crystallographic Data for Pd-BOX-5 and Pd-BOX-6

Compound	**Pd-BOX-5**	**Pd-BOX-6**
Chemical formula	$C_{24}H_{28}Cl_2N_2O_3Pd$	$C_{17}H_{22}Br_2N_2O_2Pd$
Formula weight	569.78	552.59
Crystal system	Triclinic	monoclinic
Space group	P-1	P $2_1/n$
Temperature (K)	296	120
Radiation	MoKα (λ = 0.71073 Å)	
ρ_{calc} (g.cm^{-3})	1.521	1.872
a (Å)	9.9207(6)	9.881(2)
b (Å)	12.2824(7)	17.233(3)
c (Å)	12.3884(7)	11.612(2)
α (°)	108.988(1)	
β (°)	110.775(1)	97.273(3)
γ (°)	101.803(1)	
V (Å^3)	1244.1(1)	1961.2(6)
Z	2	4
Refl. collect. / Uniq.	17140 / 6173	25922 / 4904
Refl. obser. [$I > 2\sigma(I)$]	4690	4004
R(int)	0.0201	0.0449
Data / restr./ parameter.	6173 / 0 / 330	4904 / 0 / 222
Goodness-of-fit on F^2	1.034	1.123
R indices [$I > 2\sigma(I)$]	$R_1 = 0.0561$; $wR_2 = 0.1630$	$R_1 = 0.0371$; $wR_2 = 0.0776$
R indices (all data)	$R_1 = 0.0711$; $wR_2 = 0.1756$	$R_1 = 0.0518$; $wR_2 = 0.0820$
Largest diff. peak hole (e Å^{-3})	1.746, -0.392	0.894, -0.802

TABLE 4. Crystallographic Data for Pd-BOX-7

Compound	**Pd-BOX-7**
Chemical formula	$C_{16}\ H_{20}\ Cl_2\ N_2\ O_2\ Pd$
CCDC #	1040966
Formula weight	449.64
Crystal system	Orthorhombic
Space group	$P\ 2_1\ 2_1\ 2_1$
Temperature (K)	296
Radiation	MoKα (λ = 0.71073 Å)
ρ_{calc} (g.cm^{-3})	1.683
a (Å)	7.3897(18)
b (Å)	10.408(3)
c (Å)	23.068(6)
V (Å^3)	1774.3(7)
Z	4
Refl. collect. / Uniq.	20361 / 4419
Refl. obser. [$I > 2\sigma(I)$]	3272
R(int)	0.0845
Data / restr./ parameter.	4419 / 0 /210
Goodness-of-fit on F^2	0.984
R indices [$I > 2\sigma(I)$]	$R_1 = 0.0533$; $wR_2 = 0.0700$
R indices (all data)	$R_1 = 0.0837$; $wR_2 = 0.0733$
Largest diff. peak hole (e Å^{-3})	0.703, -0.362

TABLE 5. Selected bond lengths (Å) and bond angles (°) for Pd-BOX-1 and Pd-BOX-2

Pd-BOX-1		Pd-BOX-2	
Bond lengths	**Bond angles**	**Bond lengths**	**Bond angles**
Pd1-N12.0290(17)	N1-Pd1-N2 87.51(7)	Pd1-N1 2.0315(17)	N1-Pd1-N2 87.35(7)
Pd1-N2 2.0353(18)	N1-Pd1-Cl1 91.06(5)	Pd1-N2 2.0477(18)	N1-Pd1-Cl1 91.84(5)
Pd1-Cl1 2.2851(5)	N2-Pd1-Cl1 175.77(5)	Pd1-Cl1 2.2751(6)	N2-Pd1-Cl1178.56(6)
Pd1-Cl2 2.2893(5)	N1-Pd1-Cl2 179.23(5)	Pd1-Cl2 2.2924(6)	N1-Pd1-Cl2177.04(5)
N1 C1 1.282(3)	N2-Pd1-Cl2 93.24(5)	N1-C1 1.277(3)	N2-Pd1-Cl2 92.37(5)
N2 C12 1.282(3)	Cl1-Pd1-Cl2 88.20(2)	N1-C2 1.508(3)	Cl1-Pd1-Cl2 88.38(2)
N2 C14 1.511(3)	C3 N1 Pd1 128.07(13)	N2-C13 1.278(3)	C1-N1-C2 107.34(18)
O2 C12 1.350(3)	C12 N2 C14 107.37(18)	N2-C15 1.511(3)	C1-N1-Pd122.01(14)
O2 C13 1.468(3)	C12 N2 Pd1 123.18(15)	O1-C1 1.339(3)	C2-N1-Pd1 130.65(14)
	C14 N2 Pd1 129.45(14)	O1-C5 1.465(3)	C13-N2 C15108.42(19)
	C12 O2 C13 104.40(17)	O2-C13 1.349(3)	C13-N2-Pd1123.72(16)
		O2-C14 1.447(4)	C15-N2-Pd1127.81(16)
			C1-O1-C5 104.05(18)
			C13-O2-C14 105.9(2)

TABLE 6. Selected bond lengths (Å) and bond angles (°) for Pd-BOX-3 and Pd-BOX-4

Pd-BOX-3		Pd-BOX-4	
Bond lengths	**Bond angles**	**Bond lengths**	**Bond angles**
Pd1-N1 2.020(3)	N1-Pd1-N2 88.01(11)	Pd1-N1 2.031(5)	N1-Pd1-N2 87.6(2)
Pd1-N2 2.022(3)	O1-Pd1-N1 92.94(11)	Pd1-N2 2.056(5)	N1-Pd1-Cl 176.3(2)
Pd1-O1 2.001(2)	O1-Pd1-N2 177.56(10)	Pd1-Cl12.295(2)	N2-Pd1-Cl2 91.7(2)
Pd1-O4 1.996(2)	O4-Pd1-O1 87.22(10)	Pd1-Cl22.280(2)	N1-Pd1-Cl1 91.5(1)
N1 C9 1.272(4)	O4-Pd1-N1 172.94(10)	N1-C5 1.273(7)	N2-Pd1-Cl1174.0(1)
N1 C7 1.511(4)	O4-Pd1-N2 91.56(11)	N2-C12 1.264(7)	Cl2-Pd1-Cl1 88.8(7)
N2 C16 1.286(4)	C9 N1 C7 107.7(3)	N2 C14 1.510(8)	C12 N2 Pd1 119.3(4)
N2 C18 1.500(4)	C9 N1 Pd1 121.9(2)		C14 N2 Pd1 132.0(4)
C7 C8 1.534(5)	C7 N1 Pd1 130.2(2)		C5 O1 C4 105.5(5)
C17 C18 1.539(5)	C16 N2 C18 108.9(3)		C12O2 C13 105.4(5)
	C16 N2 Pd1 122.7(2)		
	C18 N2 Pd1 128.4(2)		

TABLE 7. Selected bond lengths (Å) and bond angles (º) for Pd-BOX-5 and Pd-BOX-6

Pd-BOX-5		**Pd-BOX-6**	
Bond lengths	**Bond angles**	**Bond lengths**	**Bond angles**
Pd1-N1 2.018(4)	N1-Pd1-N2 88.5(2)	Pd1-N1 2.063(3)	N2-Pd1-N1 86.94(12)
Pd1-N2 2.041(4)	N1-Pd1-Cl1 88.3(1)	Pd1-N2 2.045(3)	N2-Pd1-Br1 175.70(9)
Pd1-Cl1 2.285(2)	N2-Pd1-Cl1 176.7(1)	Pd1-Br1 2.416(7)	N1-Pd1-Br1 91.69(9)
Pd1-Cl2 2.286(2)	N1-Pd1-Cl2 178.3(1)	Pd1Br2 2.416(7)	N2-Pd1-Br2 92.02(9)
N1-C1 1.274(6)	N2-Pd1-Cl2 91.3(1)	N1 C5 1.284(5)	N1-Pd1Br2173.10(10)
N2-C7 1.273(6)	Cl1-Pd1-Cl2 91.9(8)	N1 C1 1.507(5)	Br1-Pd1-Br2 88.845(19)
N2 C9 1.497(8)	C1 N1 C3 108.3(4)	N2 C13 1.282(5)	C5 N1 C1 107.5(3)
O1 C1 1.342(6)	C1 N1 Pd1 125.8(3)	N2 C15 1.495(5)	C5 N1 Pd1 118.5(3)
O1 C2 1.447(7)	C3 N1 Pd1 125.8(3)	O1 C5 1.351(5)	C1 N1 Pd1 133.6(3)
O2 C7 1.333(7)	C7 N2 C9 108.7(5)	O1 C4 1.458(5)	C13 N2 C15 108.6(3)
O2 C8 1.473(8)	C7 N2 Pd1 124.4(3)	O2 C13 1.345(4)	C13 N2 Pd1 119.5(3)
		O2 C14 1.466(5)	C15 N2 Pd1 131.7(2)
			C5 O1 C4 105.1(3)
			C13 O2 C14 105.7(3)

TABLE 8. Selected bond lengths (Å) and bond angles (º) for Pd-BOX-7

Bond distances (Å)		**Bond angles (°)**	
Pd1-N1	2.014(3)	N1-Pd1-N2	86.71(13)
Pd1-N2	2.015(3)	N1-Pd1-Cl2	177.01(10)
Pd1-Cl2	2.2742(13)	N2-Pd1-Cl2	90.40(10)
Pd1-Cl1	2.2886(12)	N1-Pd1-Cl1	92.42(10)
N1-C5	1.276(5)	N2-Pd1-Cl1	176.34(10)
N1-C3	1.487(6)	Cl2-Pd1-Cl1	90.51(6)
N2-C12	1.262(5)	C5-N1-C3	107.4(4)
N2-C14	1.475(5)	C5-N1-Pd1	123.8(3)
O1-C5	1.353(5)	C3-N1-Pd1	128.7(3)
O1-C4	1.465(5)	C12-N2-C14	109.3(3)
O2-C12	1.345(5)	C12-N2-Pd1	125.8(3)
O2-C13	1.450(6)	C14-N2-Pd1	124.9(2)
		C5-O1-C4	106.4(3)
		C12-O2-C13	105.9(3)

2.3 Results and discussions

2.3.1 Synthesis of BOX ligands

The Bis(oxazoline) ligands (**BOX-1 to BOX-7**) were prepared as shown in Scheme 1. The treatment of amino alcohol with 0.5 mmol equivalent of phthalonitrile or its derivative in the presence of zinc triflate afforded the corresponding BOX ligand in excellent isolated yield. ^{1}H and ^{13}C NMR chemical shifts for BOX ligands **(BOX-1 to BOX-7)** were consistent with the formerly proposed structures.

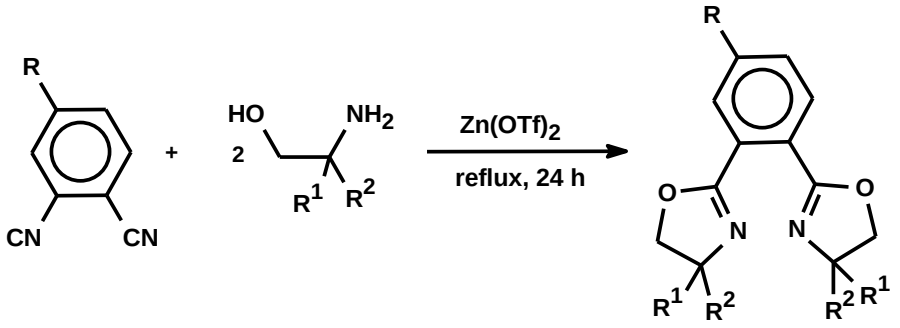

BOX	R	R^1, R^2
BOX-1	H	CH_3, CH_3
BOX-2	CH_3	CH_3, CH_3
BOX-3	NO_2	CH_3, CH_3
BOX-4	OPh	CH_3, CH_3
BOX-5	OPh	H, $CH(CH_3)_2$
BOX-6	H	H, CH_2CH_3
BOX-7	I	CH_3, CH_3

Scheme 1. Synthesis of bis(oxazoline) ligands (**BOX-1 to BOX-7**)

2.3.2 Synthesis of palladium-BOX complexes

The palladium-bis(oxazoline) complexes (**Pd-BOX-1 to Pd-BOX-7)** were prepared from the reaction of BOX ligand (**BOX-1 to BOX-7**) with the appropriate palladium(II) salt (Scheme 2).

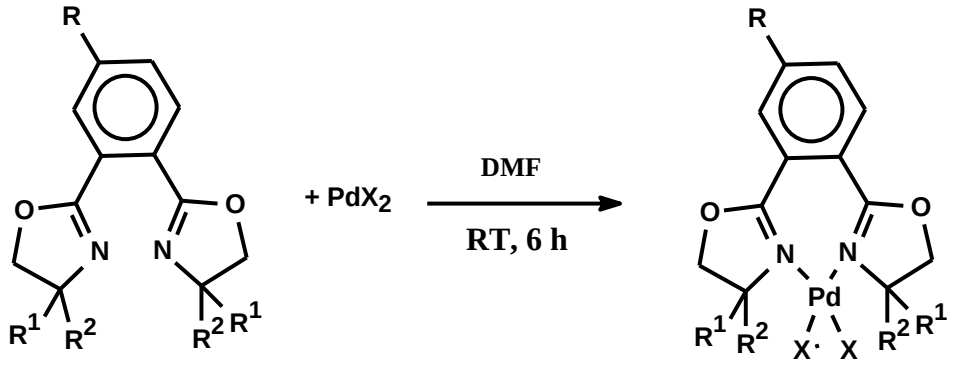

Pd-BOX	Δν (cm^{-1})*	R	R^1, R^2	X
Pd-BOX-1	30	H	CH_3, CH_3	Cl
Pd-BOX-2	18	CH_3	CH_3, CH_3	Cl
Pd-BOX-3	54	NO_2	CH_3, CH_3	OAC
Pd-BOX-4	19	OPh	CH_3, CH_3	Cl
Pd-BOX-5	13	OPh	H, $CH(CH_3)_2$	Cl
Pd-BOX-6	25	CH_3	CH_3,CH_3	Br
Pd-BOX-7	16	H	H, CH_2CH_3	Cl

Scheme 2. Synthesis of palladium-bis(oxazoline) complexes **(Pd-BOX-1 to Pd-BOX-7)**

*Coordination shift: $\nu_{C=N}^{free\ ligand}$ - $\nu_{C=N}^{complex}$

2.3.2.1 Dichlorido(2,2'-(1,2-phenylene)bis(4,4-di-methyl-4,5-dihydrooxazole)-N,N')palladium(II) (Pd-BOX-1)

The palladium complex **Pd-BOX-1** was prepared from the reaction of **BOX-1** with bis(benzonitrile) palladium(II) chloride. The complex was purified by recrystallization from dichloromethane by adding hexane. A single crystal suitable for X-ray was grown from DMF solution. The complex was obtained in form of needle shape air stable crystals. In order to confirm the coordination of $PdCl_2$ to the BOX-1 ligand, ^{1}H and ^{13}C NMR were first adopted. Indeed, all the proton and carbon resonances have shifted in a certain scale compared to their position in the free ligand. For example, in the spectrum of the free ligand, the methyl groups attached to the oxazoline rings were observed as a single peak with chemical shift of 0.88 ppm. In the spectrum of the complex, the single peak resolved into two peaks with each individual peak integrating for six protons. The signal shifted down field from 0.88 ppm to 1.52 ppm and 1.57 ppm. Similar trends were observed in the ^{13}C spectrum. The formation of Pd-BOX-1 from BOX-1 was further confirmed from the respective FT-IR data. The shift in the positon of -*C*=*N*- band from 1662 cm^{-1} in the spectrum of BOX-1 ligand to 1632 cm^{-1} in the spectrum of Pd-BOX-1 complex is an indication that the ligand is coordinated to the palladium.

X-ray crystal structure of Pd-BOX-1

The **Pd-BOX-1** complex crystallizes in the $P2_1/c$ space group and the palladium ion is bonded to the nitrogen atoms of the two oxazoline heterocycles in addition to two chloride ions. The geometry is distorted square planar and the corresponding cis-angles are in range of 87.51(7) - 93.24(5)° (figure 2). The Pd-N and Pd-Cl bond distances (table 5) are similar to those reported for other chloridobis(oxazoline)palladium complexes [137, 142-144]. The two oxazoline heterocycles are tilted from the benzene ring spacer plane due to coordination to the palladium ion. The dihedral angles, between the NCO moiety planes of each of the two oxazoline heterocycles and the benzene ring spacer mean plane are 48.57(9)° and 51.46(8)° respectively. The legless chair-type structure of the complex is characterized by a dihedral angle of 78.60(7)° between the chair seat [PdN_2Cl_2] moiety and the chair back benzene ring spacer.

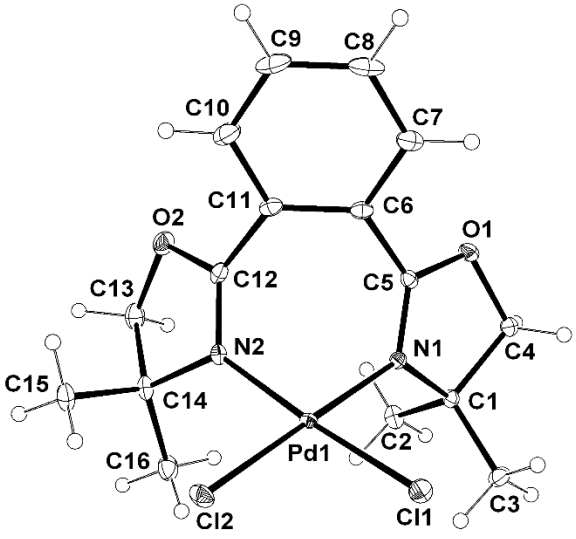

Figure 5. ORTEP Diagram of Pd-BOX-1 Showing the Atomic Labeling Scheme. Displacement Ellipsoids are Drawn at the 30 % Probability Level.

2.3.2.2 Dichlorido(2, 2'-(4-methyl-1,2-phenylene)bis(4,4-dimethyl-4,5-dihydrooxazole) -N,N')-palladium(II) (Pd-BOX-2)

The palladium complex **Pd-BOX-2** was prepared using the general procedure described in section 2.2.3 on page 38. It was recrystallized from dichloromethane by adding hexane. A single crystal suitable for X-Ray crystallography was grown from DMF solution. The complex was obtained as needle shape crystals. In order to confirm the coordination of $PdCl_2$ to BOX-2 ligand, ^{1}H and ^{13}C NMR were used. It was observed from both the proton and carbon spectra that all the proton and carbon resonances have shifted in a certain scale compared to their position in the free ligand. For example, in the spectrum of BOX-2, the methyl groups attached to the oxazoline rings were observed as a single resonance with chemical shift of 1.25 ppm. In the spectrum of Pd-BOX-2 complex, the single peak resolved into three distinctive singlets at 1.75 ppm, 1.62 ppm and 1.59 ppm integrating for six, three and three protons respectively. Similar trends were observed in the ^{13}C spectrum. The splitting of a single peak in to three peaks, together with change in chemical shift, confirms the formation of Pd-BOX-2 from BOX-2. Furthermore, from the FT-IR data, the -*C=N*- band shifted from 1655 cm^{-1} to 1637 cm^{-1} due to complexation.

X-ray crystal structure of Pd-BOX-2

The molecular structure of Pd-BOX-2 is given in Figure 6. The complex crystallizes in the P-1 space group with two molecules in the asymmetric unit. The palladium ion is bound to the nitrogen atoms of the two oxazoline heterocycles of the bidentate ligand and two chloride ions in a distorted square planar geometry. The cis-bond angles are in the range: 87.35(7) - 91.84(5) ° (table 5) and the Pd-N and Pd-Cl bond distances are similar to those found in other bis(oxazoline) palladium complexes [142, 143, 146].

Interestingly and despite the fact that the ligand is achiral, the coordination to the palladium ion allows this non C_2-symmteric bis(oxazoline) ligand-based complex to acquire a rigid backbone curvature and the molecule resembles a chair with the [PdN_2Cl_2] moiety being the seat and the benzene ring spacer being the back of the chair (Figure 6). This rigid curvature generates an inherent chirality in the complex and the two mirror images are not superimposable. The complex crystallizes as a pseudoracemate and the packing disorder of the two enantiomers in the structure was modeled using a two-site occupancy for the methyl group substituent.

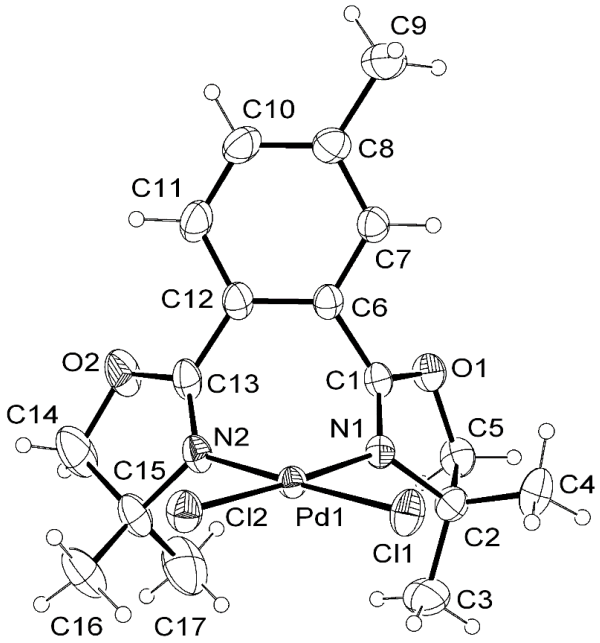

Figure 6. ORTEP Diagram of Pd-BOX-2 Showing the Atomic Labeling Scheme. Thermal ellipsoids are drawn at the 30% probability level.

2.3.2.3 Diacetato (2,2'-(4-nitro-1,2-phenylene)bis(4,4-dimethyl-4,5-dihydrooxazole)-N,N')-palladium(II) (Pd-BOX-3)

The palladium complex **Pd-BOX-3** was prepared from the reaction of BOX-3 with palladium(II) acetate using the general procedure described in section 2.2.3 on page 38. The complex was recrystallized from dichloromethane by adding hexane. A single crystal suitable for X-ray crystallography was grown from dichloromethane solution. In order to confirm the coordination of $Pd(OAc)_2$ to BOX-3 ligand, ^{1}H and ^{13}C NMR were used. It was observed from both the proton and carbon spectra that all the proton and carbon resonances have shifted in a certain scale compared to the spectrum of the free ligand. For example, in the spectrum of BOX-3 ligand, the methyl groups attached to the oxazoline rings were observed as a single resonance with chemical shift of 1.38 ppm. In the spectrum of Pd-BOX-3 complex, the single peak resolved into four distinctive singlets with the chemical shifts of 1.74 ppm, 1.73 ppm, 1.63 and 1.61 ppm with each singlet integrating for three protons. Additional peaks were observed at 1.42 ppm and 1.41 ppm which are due to the CH_3 of the acetate ion. Similar changes were observed in the ^{13}C spectrum of the complex when compared with the free ligand. The splitting of a single peak in to four together with the change in chemical shift value and the appearance of the acetate peaks confirms the formation of Pd-BOX-3 from BOX-3. Furthermore, from the FT-IR data, the -*C=N*- band which appears at 1659 cm^{-1} in the spectrum of the free ligand shifted to 1605 cm^{-1} and there is presence of additional bands at 1533 cm^{-1} and 1500 cm^{-1} assignable to -*C=O*- stretching.of the acetate ligands.

X-ray crystal structure of Pd-BOX-3

The **Pd-BOX-3** complex crystallizes in the $P2_1/c$ space group. Similarly to Pd-BOX-1, the geometry around the palladium ion is distorted square planar with cis-angles in the range 87.22(10)° - 92.94(11)° (Figure 7). The Pd-N and Pd-O bond lengths are similar to those reported for bis(oxazoline) bis(trifluoroacetato)palladium complexes [145] and the Pd-N bond lengths are significantly shorter than those of Pd-BOX-1 (Table 6) likely due to the difference in σ and π donor effects of the acetate and chloride ligands. As expected by steric effect the two acetato acyl groups lie on opposite sides of the $[PdN_2O_2]$ plane. The complex adopts a chair structure with a rigid curvature inducing inherent chirality and the compound crystallizes as a racemic dichloromethane solvate.

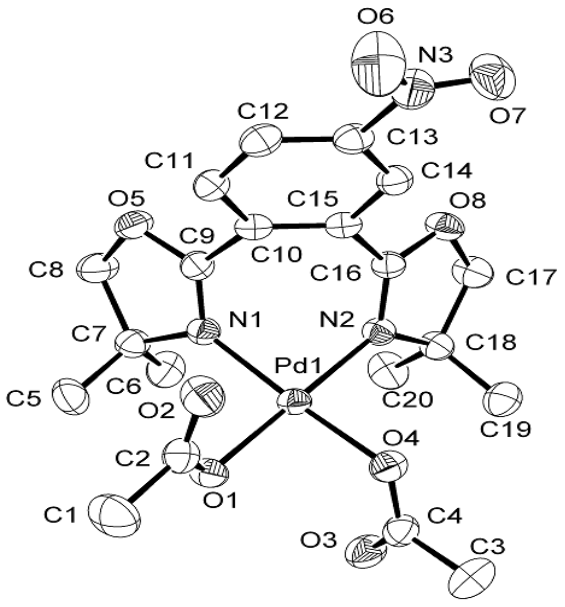

Figure 7: ORTEP Diagram of Pd-BOX-3 Showing the Atomic Labeling Scheme. Dichloromethane Molecule has been Omitted for Clarity. Thermal ellipsoids are drawn at the 30% probability level.

2.3.2.4 Dichlorido(2,2'-(4-phenoxy-1,2-phenylene)bis(4,4-dimethyl-4,5-dihydrooxazole)-N,N') palladium(II) (Pd-BOX-4)

The palladium complex **Pd-BOX-4** was prepared from the reaction of **BOX-4** with bis(benzonitrile) palladium(II) chloride using the general procedure described in section 2.2.3 on page 38. The complex was recrystallized from dichloromethane by adding hexane. A single crystal suitable for X-Ray crystallography was grown from CH_2Cl_2 solution. In order to confirm the complex formation, ^{1}H and ^{13}C NMR were used. It was observed from both the proton and carbon spectra that all the proton and carbon resonances have shifted in a certain scale compared to the spectrum of the free ligand. For instance, in the spectrum of BOX-4 ligand, the methyl groups attached to the oxazoline rings were observed as a single resonance with chemical shift of 1.29 ppm. In the spectrum of Pd-BOX-4 complex, the single peak resolved into four distinctive singlets with the chemical shifts of 1.75 ppm, 1.73 ppm, 1.61 and 1.58 ppm with each singlet integrating for three protons. Similar changes were observed in the ^{13}C spectrum of the complex when compared with the free ligand. The splitting of a single peak in to four, and the change in the value of chemical shift confirms the formation of Pd-BOX-4 from BOX-4. Furthermore, from the FT-IR data, the -*C=N*- band which appears at 1656 cm^{-1} in the spectrum of the free ligand shifted to 1637 cm^{-1} after complexation.

X-ray crystal structure of Pd-BOX-4

The Pd-BOX-4 complex crystallizes in the P-1 space group with two molecules in the asymmetric unit. The palladium ion is bound to the nitrogen atoms of the two oxazoline heterocycles of the bidentate ligand and two chloride ions in a distorted square planar geometry. The cis-bond angles are in the range: 87.6(2) - 91.7(2) ° (table 6) and the Pd-N and Pd-Cl bond distances are similar to those found in other bis(oxazoline) palladium complexes [142, 143, 146]. The dihedral angles, between each of two oxazoline heterocycles and the benzene ring spacer mean planes are (41.5(2) °, 42.7(3) °) and (44.9(3) °, 47.5(2) °) for the two molecules respectively.

Interestingly and despite the fact that the ligand is achiral, the coordination to the palladium ion allows this non C_2-symmteric bis(oxazoline) ligand-based complex to acquire a rigid backbone curvature and the molecule resembles a chair with the [PdN_2Cl_2] moiety being the seat and the benzene ring spacer being the back of the chair. The dihedral angle between the mean planes of the two moieties is 87.4(2) ° and 85.7(2) ° for the two molecules respectively (Figure 8). This rigid curvature generates an inherent chirality in the complex and the two mirror images are not superimposable (Fgure 9). The complex crystallizes as a pseudoracemate and the packing disorder of the two enantiomers in the structure was modeled using a two-site occupancy for the phenoxy group substituent. The phenyl ring of the phenoxy group is twisted from coplanarity with the benzene ring spacer with a torsion angle of 83(1) ° and 85(1) ° for the two molecules respectively (Figure 9).

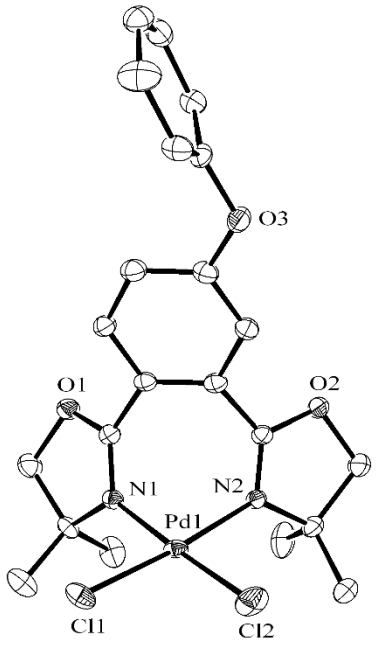

Figure 8: ORTEP Diagram of Pd-BOX-4 Showing the Atomic Labeling Scheme. Thermal ellipsoids are drawn at the 30% probability level

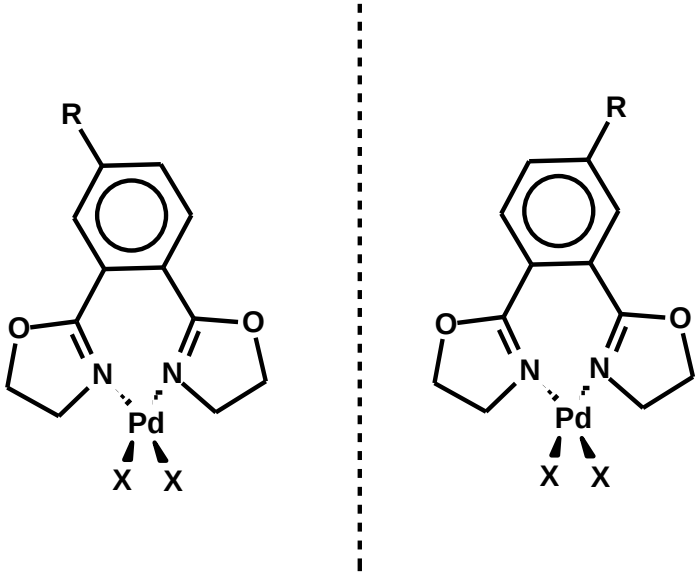

Figure 9: Inherent Chirality in Palladium-Bis(Oxazoline) Complexes

2.3.2.5 Dichlorido(2,2'-(4-phenoxy-1,2-phenylene)bis(4-isopropyl-4,5-dihydrooxazole)-N,N') palladium(II) (Pd-BOX-5)

The palladium complex **Pd-BOX-5** was prepared from the reaction of **BOX-5** with bis(benzonitrile) palladium(II) chloride using the general procedure described in section 2.2.3 on page 38. The complex was recrystallized from dichloromethane by adding hexane. A single crystal suitable for X-ray crystallography was grown from CH_2Cl_2 solution. In order to confirm the complex formation, ^{1}H and ^{13}C NMR were used. It was observed from both the proton and carbon spectra that all the proton and carbon resonances have shifted in a certain scale compared to the spectrum of the free ligand. Furthermore, from the FT-IR data, the -*C=N*- band which appears at 1653 cm^{-1} in the spectrum of the free ligand shifted to 1640 cm^{-1} due to complexation.

X-ray crystal structure of Pd-BOX-5

Pd-BOX-5 crystallizes also in the P-1 space group and the asymmetric unit contains a single molecule with a distorted square planar geometry (Figure 10). The cis-bond angles around the palladium ion are in the range 88.3(1) - 91.97(8)° (table 7) and the Pd-N and Pd-Cl bonds lengths are in normal ranges. The dihedral angles, between each of the two oxazoline heterocycles and the benzene ring spacer mean plane are 40.0(3)° and 42.2(3)° respectively (Table 7). The complex presents a rigid curvature in a chair-like mode. The dihedral angle between the mean planes of $[PdN_2Cl_2]$ moiety and the benzene ring spacer is 78.4(1)°. The complex crystallizes as a pseudoracemate. The packing disorder of the two enantiomers (R, S) and (S, R) in the crystal structure was modeled using a two-site occupancy for the phenoxy group substituent lowering the symmetry of the ligand. The

phenyl ring of the phenoxy pendant arm is not coplanar with the benzene ring spacer showing a torsion angle of 83(1)° (Figure 10).

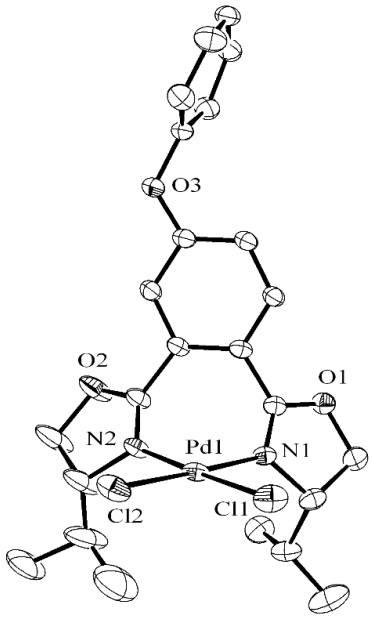

Figure 10: ORTEP Diagram of Pd-BOX-5 Showing the Atomic Labeling Scheme. Thermal ellipsoids are drawn at the 30% probability level

2.3.2.6 Dibromido(2,2′-(4-methyl-1,2-phenylene)bis(4,4-dimethyl-4,5-dihydrooxazole)-N,N′)palladium(II) (Pd-BOX-6)

The palladium complex **Pd-BOX-6** was prepared from the reaction of **BOX-2** with palladium(II) bromide using the general procedure described in section 2.2.3 on page 38. The complex was recrystallized from dichloromethane by adding hexane. A single crystal of Pd-BOX-4 suitable for X-ray crystallography was grown from DMF solution. In order to confirm the complex formation, ^{1}H and ^{13}C NMR were used. It was observed from both the proton and carbon spectra that all the proton and carbon resonances have shifted in a

certain scale compared to the spectrum of the free ligand. For example, in the spectrum of BOX-2, the methyl groups attached to the oxazoline rings were observed as a single resonance with chemical shift of 1.25 ppm. In the spectrum of Pd-BOX-6 complex, the single peak resolved into three distinctive singlets at 1.77 ppm, 1.58 ppm and 1.55 ppm integrating for six, three and three protons respectively. Similar trends were observed in the ^{13}C spectrum. The splitting of a single peak in to three peaks, together with change in chemical shift, confirms the formation of Pd-BOX-6 from BOX-2. Furthermore, from the FT-IR data, the -*C=N*- band which appears at 1655 cm^{-1} in the spectrum of the free ligand shifted to 1630 cm^{-1} after complexation.

X-ray structure of Pd-BOX-6

The **Pd-BOX-6** complex crystallizes in the $P2_1/n$ space group. The palladium ion is bonded to the nitrogen atoms of the two oxazoline heterocycles in addition to two bromide ions with a distorted square planar geometry (Figure 11). The corresponding cis-angles are in range of 86.94(12) - 92.02(9)°. The Pd-N and Pd-Br bond distances (Table 7) are similar to those reported for other bis(oxazoline)palladium complexes [137, 146] and bromido(diimine)palladium complexes [147, 148] respectively. Bonding to the metal ion results in a tilting of the two oxazoline heterocycle planes from the benzene ring spacer. The dihedral angles, between the mean planes of each of the two oxazoline heterocycles and the benzene ring spacer mean plane are 38.0(3)° and 48.1(2)°. The metal complex structure is reminiscent of a chair with the $[PdN_2Br_2]$ moiety being the seat and the benzene ring spacer being the back of the chair (Figure 11). The dihedral angle between the two moieties is 88.1(1)°. Despite the achirality of the ligand, this rigid chair curvature, together

with the unsymmetrical substitution of the benzene spacer, generates an inherent chirality in the molecule and the complex crystallizes as a racemic [137].

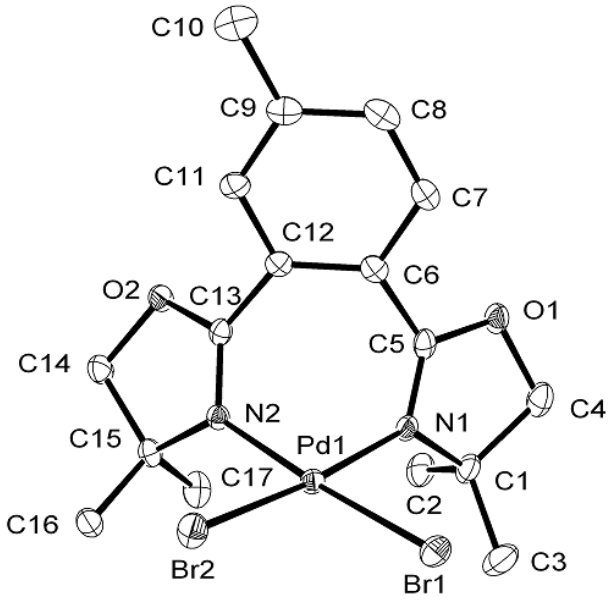

Figure 11: ORTEP Diagram of Pd-BOX-6 Showing the Atomic Labeling Scheme. Thermal ellipsoids are drawn at the 30% probability level

2.3.2.7 Dichlorido(2,2'-(1,2-phenylene)bis(4-ethyl-4,5-dihydrooxazole)-N,N')-palladium(II) (Pd-BOX-7)

The palladium complex **Pd-BOX-7** was prepared from the reaction of **BOX-6** with bis(benzonitrile) palladium(II) chloride using the general procedure described in section 2.2.3 on page 38. The complex was purified by recrystallization from dichloromethane by adding hexane. A single crystal suitable for X-ray was grown from DMF solution. The complex was obtained in form of yellow, needle shape air stable crystals. In order to confirm the coordination of $PdCl_2$ to the BOX-6 ligand, ^{1}H and ^{13}C NMR spectroscopy

were used. All the proton and carbon resonances have shifted in a certain scale compared to their position in the free ligand. For example, in the ^{1}H NMR spectrum of BOX-6, the CH_3 group were observed as a triplet with chemical shift of 0.99 ppm. In the ^{1}H NMR spectrum of the Pd-BOX-7 complex, the triplet resolved into a multiplet peak with a chemical shift range of 1.10 -1.02 ppm. Similar trends were observed in the ^{13}C spectrum. The formation of Pd-BOX-7 from BOX-6 was further confirmed from the respective FT-IR data. The shift in the positon of -*C=N*- band from 1661 cm^{-1} in the spectrum of BOX-6 ligand to 1645 cm^{-1} in the spectrum of Pd-BOX-7 complex is an indication that the ligand is coordinated to the palladium.

X-ray structure of Pd-BOX-7

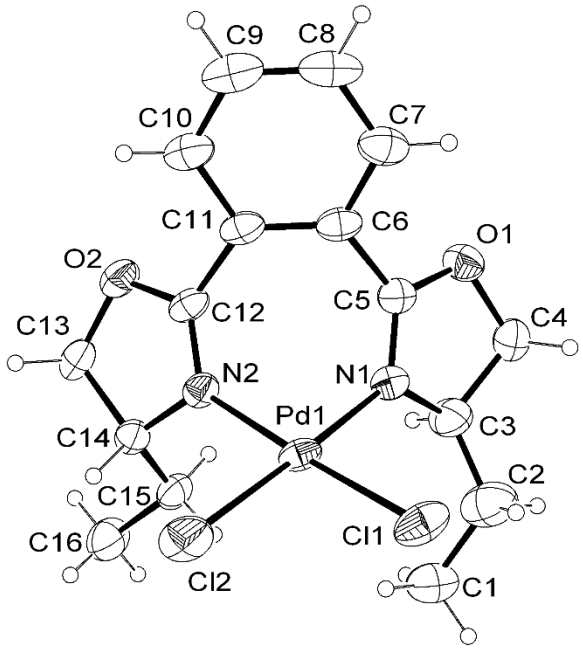

Figure 12: ORTEP Diagram of Pd-BOX-7 Showing the Atomic Labeling Scheme. Thermal ellipsoids are drawn at the 30% probability level.

CHAPTER 3

Water soluble and mixed ligand palladium-bis(oxazoline) complexes: synthesis and characterization

3.1 Introduction

In this chapter, the synthesis and characterization of two new water soluble bis(oxazoline) ligands, which have hydroxyl and carboxylate functionalities, and their dichloridopalladium(II) complexes are described. The synthesis and characterization of two new palladium-bis(oxazoline)-phosphine (Pd-BOX-PR_3) mixed ligand complexes are also described. Although, a number of mixed ligand complexes of nitrogen and phosphine donors have been reported [149 - 152], the complexes described in this chapter are, to the best of our knowledge, the first examples of cationic mixed ligand palladium complexes of bis(oxazoline) and phosphine.

3.2 Experimental

3.2.1 Materials and Instrumentation

Materials for the synthesis of ligands and complexes were purchased from Sigma Aldrich company, US and were used as received. All solvents (reagent grade) used in the synthesis were distilled before use. The products were purified using flash column chromatography packed with Silica gel 170-400 Mesh, Fisher chemical (Fisher scientific, US). ^{1}H, ^{13}C NMR and ^{31}P spectral data were obtained using 500 MHz NMR machine (Joel 1500 model). Chemical shifts were recorded in ppm using tetramethyl silane (TMS) as reference for ^{1}H and ^{13}C spectra and phosphoric acid as reference for ^{31}P spectrum. CD_2Cl_2 and DMSO were used as NMR solvent. IR spectra were recorded in wave numbers (cm^{-1}) using FT-IR spectrometer (Perkin-Elmer 16F model). Merck 60 F_{254} silica gel plates (250 µm layer thickness) were used for thin-layer chromatography (TLC) analyses. A Varian Saturn 2000 GC-MS machine equipped with 30 m capillary column was used to analyze the products. Molecular weight of the complexes were established using electrospray ionization mass spectrometer (ESI-MS). The analyses were performed on an LTQ-Orbitrap mass spectrometer (Thermo Scientific, San Jose, CA, USA) equipped with a HESI-II electrospray source (ESI-MS) using a metal spray needle.

3.2.2 General procedure for the synthesis of hydroxyl and carboxylate functionalized BOX-ligands

2,2'-(4-iodobenzene-1,2-diyl)bis(4,4-dimethyl-4,5-dihydro-1,3-oxazole **(BOX-7)** (0.50 mmol), $PdCl_2$ (0.025 mmol, 5.0 mol%), K_2CO_3 (1.0 mmol, 2.0 mol equivalent), DMF (2 mL), distilled water (2 mL) and the appropriate phenylboronic acid (0.60 mmol), were added in a 10.0 mL round bottom flask. The mixture was stirred at 70 ^oC for 6 h. After completion of the reaction, the mixture was cooled down and acidified with 1 M HCl. The acidified solution was extracted 3 times with EtOAc and the combined EtOAc extract was dried using anhydrous $MgSO_4$. The solvent was removed under reduced pressure and the product was purified by silica gel column chromatography using hexane-EtOAc (1:9) as eluent.

3,4'-bis(4,4-dimethyl-4,5-dihydro-1,3-oxazol-2-yl)biphenyl-4-ol (BOX-8)

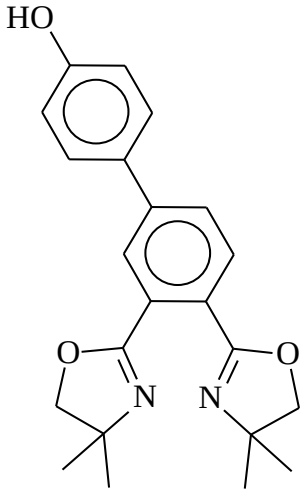

BOX-8

Light brown oil, yield (90 %); ^1H NMR (500 MHz, $CDCl_3$) δ (ppm): 7.81 (s, 1H), 7.79 (d, *J* = 10 Hz, 1H), 7.57 (d, *J* = 10 Hz, 1H), 7.25 (s, 2H), 6.82 (d, *J* = 10 Hz, 2H), 4.18 (s, 2H,

OCH_2), 4.14 (s, 2H, OCH_2),1.51 (s, 6H, $NC(CH_3)_2$), 1.44 (s, 6H, $NC(CH_3)_2$); ^{13}C NMR (125 MHz, $CDCl_3$) δ (ppm); 28.0 ($NC(CH_3)_2$), 28.1 ($NC(CH_3)_2$), 67.7 ($NC(CH_3)_2$), 67.9 ($NC(CH_3)_2$), 79.6 (OCH_2), 79.9 (OCH_2), 116.1, 116.2, 125.7, 127.9, 128.2, 130.3, 130.4, 143.4, 157.3, 162.5, 164.1; IR (KBr) υ (cm^{-1}) 3189, 2968, 2929, 2893, 1650, 1605, 1522, 1460, 1358, 1276, 1177, 1098, 964, 829. GC-MS m/z 364 (M^+); Anal. Calc. for $C_{22}H_{24}N_2O_3$ (364.44): C, 72.51; H, 6.64; N, 7.69. Found: C, 72.25; H, 6.38; I; N, 7.52.

3,4'-bis(4,4-dimethyl-4,5-dihydro-1,3-oxazol-2-yl)biphenyl-4-carboxylic acid (BOX-9)

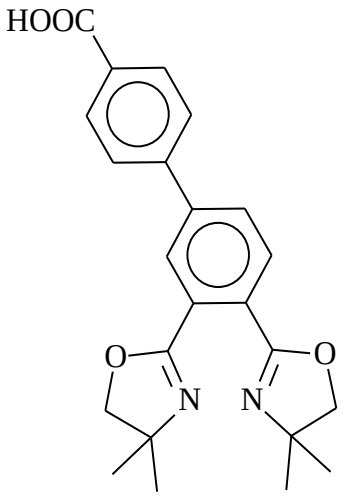

BOX-9

Yellow solid, yield (89 %); ^1H NMR (500 MHz, DMSO) δ (ppm): 8.03-7.77 (m, 7H), 4.05 (s, 4H, OCH_2 x2), 1.28 (s, 6H, $NC(CH_3)_2$), 1.27 (s, 6H, $NC(CH_3)_2$); ^{13}C NMR (125 MHz, DMSO) δ (ppm); 27.9 ($NC(CH_3)_2$), 28.0 ($NC(CH_3)_2$), 68.0 ($NC(CH_3)_2$ x 2), 78.8 (OCH_2), 79.0 (OCH_2), 127.2, 127.7, 128.9, 129.4, 130.2, 130.4, 130.6, 140.1, 142.4, 160.7, 161.1, 167.2; IR (KBr) υ (cm^{-1}) 3389, 2966, 2925, 1700, 1651, 1602, 1463, 1361, 1315, 1045, 951, 843, 757, 728. GC-MS m/z 392 (M^+); Anal. Calc. for $C_{23}H_{24}N_2O_4$ (%): C, 70.39; H, 6.16; N, 7.14; Found: C, 70.11; H, 6.51; N, 7.39.

3.2.3. General procedure for the synthesis of hydroxyl and carboxylate functionalized palladium-bis(oxazoline) complexes

The hydroxyl and carboxylate functionalized **Pd-BOX** complexes were synthesized using the general procedure described in section 2.2.3

Dichlorido(3,4-bis(4,4-dimethyl-4,5-dihydro-1,3-oxazol-2-yl)biphenyl-4-ol-N,N') palladium(II) (Pd-BOX-8)

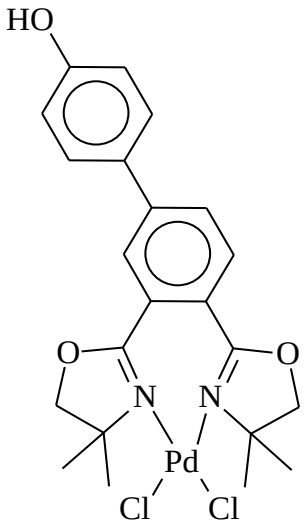

Pd-BOX-8

Yellow solid, yield (92 %); ^{1}H NMR (500 MHz, DMSO) δ (ppm): 9.98 (s, 1H), 8.15 (s, 1H), 7.95 (s, 1H), 7.72 (s, 2H,) 6.91 (s, 2H), 4.39 (s, 4H, OC*H*$_2$ x2), 1.59 (s, 6H, NC(CH$_3$)$_2$), 1.56 (s, 6H, NC(CH$_3$)$_2$); ^{13}C NMR (125 MHz, DMSO) δ (ppm); 27.8 (NC(*C*H$_3$)$_2$), 28.0 (NC(*C*H$_3$)$_2$), 70.7 (N*C*(CH$_3$)$_2$), 70.8 (N*C*(CH$_3$)$_2$), 80.7 (O*C*H$_2$), 80.9 (O*C*H$_2$), 116.2, 123.3, 126.5, 126.8, 127.8, 128.6, 129.5, 130.5, 144.2, 158.7, 163.4, 164.1; IR (KBr) υ (cm^{-1}) 3308, 2972, 2926, 1635, 1601, 1522, 1498, 1458, 1373, 1330, 1265, 1217, 1177, 1125,

1072, 952, 827, 716. Anal. Calc. for $C_{22}H_{24}Cl_2N_2O_3Pd$ (%): C, 48.77; H, 4.47; N, 5.17; Found: C, 48.62; H, 4.71; N, 5.24.

Dichlorido(3,4'-bis(4,4-dimethyl-4,5-dihydro-1,3-oxazol-2-yl)biphenyl-4-carboxylic acid-N,N') palladium(II) (Pd-BOX-9)

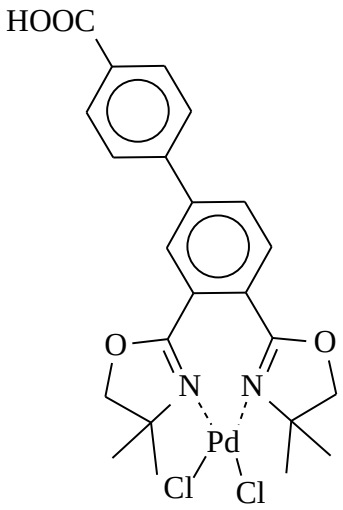

Pd-BOX-9

Yellow solid, yield (90 %); ^{1}H NMR (500 MHz, DMSO) δ (ppm): 8.29 (s, 2H), 8.07-7.98 (m, 5H), 4.40 (s, 4H, OC*H*$_2$ x2), 1.58 (s, 6H, NC(C*H*$_3$)$_2$), 1.54 (s, 6H, NC(C*H*$_3$)$_2$); ^{13}C NMR (125 MHz, DMSO) δ (ppm); 28.0 (NC(*C*H$_3$)$_2$), 28.5 (NC(*C*H$_3$)$_2$), 71.2 (N*C*(CH$_3$)$_2$ x 2), 81.2 (O*C*H$_2$ x 2), 127.2, 127.9, 128.2, 130.6, 130.9, 131.4, 141.6, 143.4, 164.1, 167.4; IR (KBr) ν (cm^{-1}) 3471, 2972, 2318, 1710, 1636, 1460, 1373, 1328, 1259, 1220, 1170, 1124, 1071, 952, 843, 776. Anal. Calc. for $C_{23}H_{24}Cl_2N_2O_4Pd$ (%): C, 48.48; H, 4.25; N, 4.92; Found: C, 44.31; H, 4.27; N, 4.79.

3.2.4 General procedure for the synthesis of palladium-bis(oxazoline)-phosphine mixed ligand complexes

To a stirred solution of *Dichlorido(2,2'-(1,2-phenylene)bis(4,4-di-methyl-4,5-dihydrooxazole)-N,N')palladium (II)* (**Pd-BOX-1**) (prepared in section 2.2.3) (0.25 mmol) in 10 ml dichloromethane, a stoichiometric amount of the proper phosphine (0.25 mmol) (dissolved in 2 ml dichloromethane) was added. The resulting mixture was stirred for 30 minutes at room temperature. Subsequently, the solvent was removed using rotavary evaporator at reduced pressure. The resulting solid product was dissolved in dimethylformamide (5 ml). A stoichiometric amount (0.25 mmol) of silver perchlorate ($AgClO_4$) was added and the mixture was stirred in the dark for 30 minutes. After complete reaction, the mixture was filtered to remove the AgCl precipitate. The solvent was removed under reduced pressure to give the appropriate mixed ligand complex. The product was dissolved in dichloromethane and layered with *n*-hexane in order to obtain pure microcrystals [153]. The products were characterized using various spectroscopic and analytical techniques and the molecular weights were established on the basis of ESI-MS analyses.

Chlorido(2,2'-(1,2-phenylene)bis(4,4'-dimethyl-4,5-dihydrooxazole)-N,N') triphenylphosphino palladium(II) perchlorate (Pd-BOX-10)

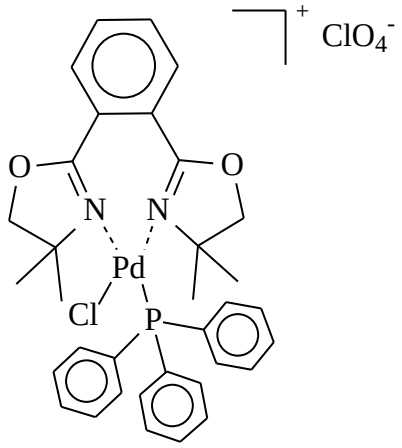

Pd-BOX-10

Yellow solid; yield (72 %); m.p. 230 ºC; ^{1}H NMR (500 MHz, CD_2Cl_2) δ (ppm) 8.11 (d, *J* = 7.6 Hz, 1H, C*H* arom), 8.00 (m, *J* = 5.2 Hz, 1H, C*H* arom), 7.81 (d, *J* = 3.05Hz, 2H, C*H* arom), 7.56 (m, , 3H, C*H* arom), 7.46 (m, 12H, C*H* arom), 4.51 (d, *J* = 8.85 1H, OC*H*),), 4.40 (d, *J* = 8.85 1H, OC*H*),), 4.33 (d, *J* = 8.85 1H, OC*H*),), 3.49 (d, *J* = 8.85 1H, OC*H*), 1.73 (s, 3H, NC(CH_3)), 1.66 (s, 3H, NC(CH_3), 1.49 (s, 3H, NC(CH_3), 0.73 (s, 3H, NC(CH_3), ^{13}C NMR (125 MHz, CD_2Cl_2) δ (ppm); 24.35 (NC(*C*H_3)), 27.81 (NC(*C*H_3)), 29.46 (NC(*C*H_3)), 31.20 (NC(*C*H_3)), 71.47 (N*C*), 72.66 (N*C*), 81.25 (O*C*H_2), 82.44 (O*C*H_2), 125.37, 127.53, 128.54, 129.16, 130.08, 131.11, 132.46, 132.48, 133.47, 134.28, 134.70, 165.98, 166. ^{31}P NMR (500 MHz, CD_2Cl_2) δ (ppm); 21.34 (*P*Ph_3) IR (KBr) (*ν cm*$^{-1}$) 3043, 2974, 2914, 2356, 1626, 1442,1373, 1324, 1093, 949, 750, 701, 622, 527, ESI-MS, 676.5, Anal. Calc. for $C_{34}H_{35}Cl_2N_2O_6PPd$ (775.95) (%): C, 52.63; H, 4.55; N, 3.61, Found: C, 52.41; H, 4.49; N, 3.60.

Chlorido(2,2'-(1,2-phenylene)bis(4,4'-dimethyl-4,5-dihydrooxazole)-N,N') tris(p-methoxy phenylphosphino) palladium(II) perchlorate (Pd-BOX-11)

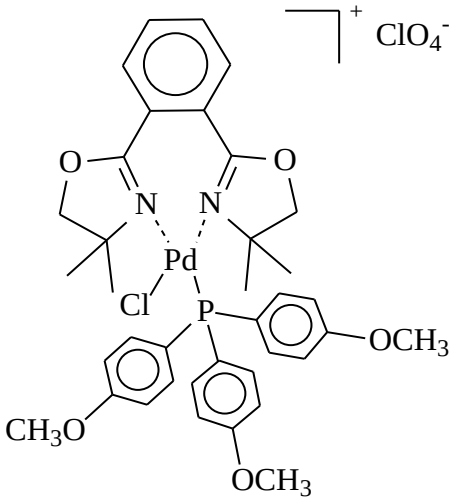

Pd-BOX-11

Yellow solid, yield (69 %); m.p. 215 ^{o}C; ^{1}H NMR (500 MHz, CD_2Cl_2) δ (ppm) 8.08 (d, *J* = 7.9 Hz, 1H, C*H* arom), 7.97 (m, 1H, C*H* arom), 7.82 (d, *J* = 3.7Hz, 2H, C*H* arom), 7.35(m, , 6H, C*H* arom), 6.91 (m, 6H, C*H* arom), 4.48 (d, *J* = 8.6 1H, OC*H*), 4.39 (d, *J* = 8.8 1H, OC*H*),), 4.30 (d, *J* = 8.6 1H, OC*H*), 3.84 (s, 9H, (OCH_3)) 3.56 (d, *J* = 9.2 1H, OC*H*), 1.73 (s, 3H, NC(CH_3)), 1.65 (s, 3H, NC(CH_3), 1.48 (s, 3H, NC(CH_3), 0.81 (s, 3H, NC(CH_3), ^{13}C NMR (125 MHz, CD_2Cl_2) δ (ppm); 24.37 (NC(*C*H_3)), 27.74 (NC(*C*H_3)), 29.40 (NC(*C*H_3)), 30.98 (NC(*C*H_3)), 55.98 (O*C*H_3), 71.42 (N*C*), 80.90 (O*C*H_2), 82.29 (O*C*H_2), 114.61, 114.71, 114.84, 120.23, 130.13, 131.05, 133.41, 134.16, 136.20, 136.30, 136.42, 162.76, 162.96; ^{31}P NMR (500 MHz, CD_2Cl_2) δ (ppm); 18.87 ((*p*-MeO-C_6H_4)$_3$P); IR (KBr) (*v* cm^{-1}) 3062, 2973, 2840, 1897, 1634, 1592, 1567, 1500, 1458, 1407, 1373, 1292, 1260, 1180, 1096, 1020, 942, 828, 800, 717, 623, 541; ESI-MS, 765, Anal. Calc. for $C_{37}H_{42}Cl_2N_2O_9PPd$ (867.03) (%): C, 51.25; H, 4.88; N, 3.23, Found: C, 51.42; H, 4.76; N, 3.40.

3.3 Results and discussions

3.3.1 The synthesis of water soluble bis(oxazoline) ligands

The hydroxyl and carboxylate functionalized bis(oxazoline) ligands (**BOX-8** and **BOX-9**) were prepared as shown in scheme 3. The palladium catalyzed Suzuki-Miyaura coupling reaction of *2,2'-(4-iodobenzene-1,2-diyl)bis(4,4-dimethyl-4,5-dihydro-1,3-oxazole)* **(BOX-7)** with 1.0 mol equivalent of 4-hydroxy phenylboronic acid and with 4-carboxy phenyl boronic acid lead to the hydroxyl (**BOX-8**) and carboxylate (**BOX-9**) functionalized bis(oxazoline) ligands respectively. ^{1}H and ^{13}C NMR chemical shifts together with the FT-IR spectral data were found to be consistent with the proposed structures.

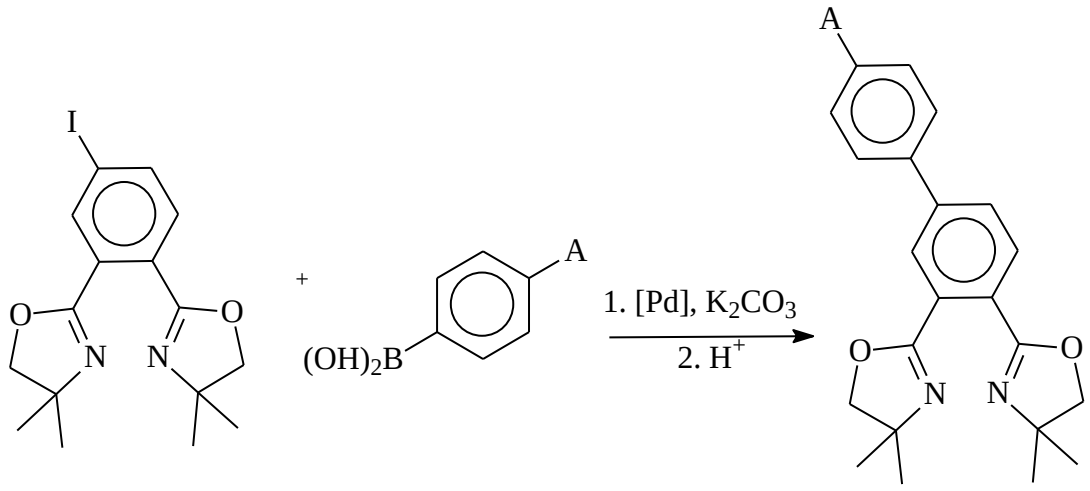

A: OH : **BOX-8**
A: COOH: **BOX-9**

Scheme 3. Synthesis of hydroxyl and carboxylate functionalized bis(oxazoline) ligands (**BOX-8** and **BOX-9**)

3.3.2 The synthesis of water soluble palladium-bis(oxazoline) complexes

The palladium complexes **Pd-BOX-8** and **Pd-BOX-9** were prepared from the reaction of **BOX-8 and BOX-9** respectively with bis(benzonitrile) palladium(II) chloride. The complexes were purified by recrystallization. They were obtained in form of yellow powders that are stable to air and moisture. The coordination of $PdCl_2$ to the BOX ligands was confirmed using ^{1}H and ^{13}C NMR spectroscopy. The protons and carbon resonances of both complexes were shifted in a certain scale when compared with the spectra of the free ligands. The FT-IR data show a shift in the position of -*C=N*- band in both complexes due to complexation.

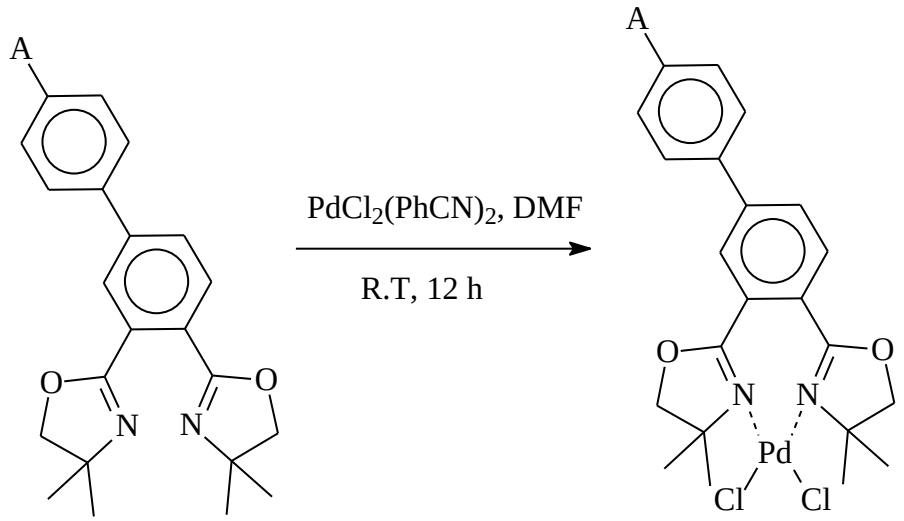

Scheme 4. Synthesis of hydroxyl and carboxylate functionalized palladium-bis(oxazoline) complexes (**Pd-BOX-8** and **Pd-BOX-9**)

3.3.3 The synthesis of palladium-bis(oxazoline)-phosphine mixed ligand complexes

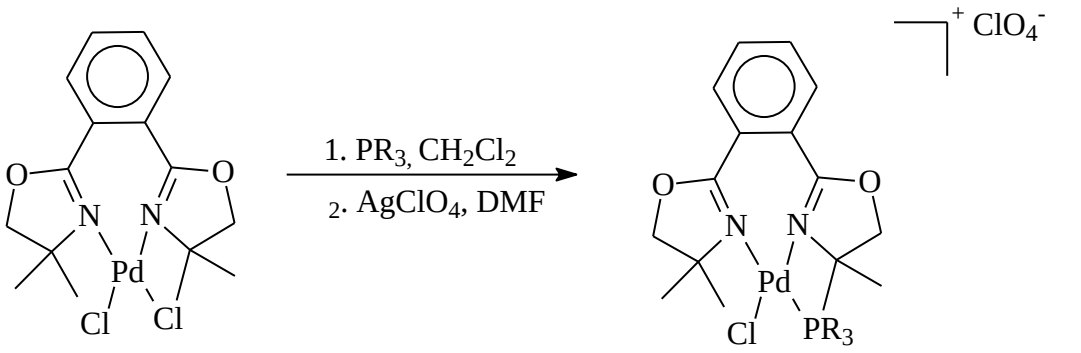

Pd-BOX-1

Pd-BOX-10: R=PPh_3

Pd-BOX-11: R=P(*p-OMe*-Ph)$_3$

Scheme 5. Synthesis of palladium bis(oxazoline) phosphine mixed ligand complexes

Pd-BOX-1 complex was prepared as shown in scheme 2 (section 2.3.2). **Pd-BOX-10** and **Pd-BOX-11** were obtained by introducing the appropriate phosphine to **Pd-BOX-1 (**Scheme 5**)**. ^{1}H and ^{13}C NMR chemical shifts for both the BOX-1 ligand and Pd-BOX-1 were consistent with the formerly reported structures. The BOX ligand is a symmetrical molecule, hence the two oxazoline moieties behave in a similar manner: A single peak was observed for the methyl protons with a chemical shift of 0.88 ppm, integrating for 12 protons. Also, the six methylenic protons appeared as a singlet with chemical shift of 3.55 ppm (Fig. 13a). In the spectrum of palladium BOX complex (Pd-BOX-1), both the methyl and methylene protons were deshielded and were observed in the downfield region due to complexation. Unlike in the spectrum of the free ligand, here, the two oxazoline moieties behave differently. Two singlets were observed in the methyl region each integrating for six protons. The methylenic protons appear as two separate AB spin systems, with each

doublet integrating for two protons (Fig. 13b). In the spectra of Pd-BOX-phosphine mixed ligand complexes (Pd-BOX-10 and Pd-BOX-11), there is further splitting of both the methyl and methylenic protons due to complete loss of symmetry in the molecules (Scheme 5). In the spectrum of Pd-BOX-10 complex, four singlets were observed in the methyl region (Fig. 13c) with each singlet integrating for three protons. One of the four singlets appear further upfield as opposed to the three remaining singlets which resonate in nearly the same chemical shift as in Pd-BOX-1. The methylenic protons appear as four different doublets integrating for one proton each (Fig. 13c). Similar to the methyl protons, one out of the four doublets appear further upfield likely because of magnetic anisotropy effects: one methyl and one hydrogen are in the shielding region of a phenyl group of the phosphine. The protons due to the aromatic spacer of the BOX and the aromatic phosphines appeared in the aromatic region and were slightly downfield compared to their positions in the free state. The proton NMR spectrum of Pd-BOX-11 shows a similar pattern to the spectrum of Pd-BOX-10 with additional singlet peak at 3.84 ppm which was assigned to the *p*-methoxy substituent.

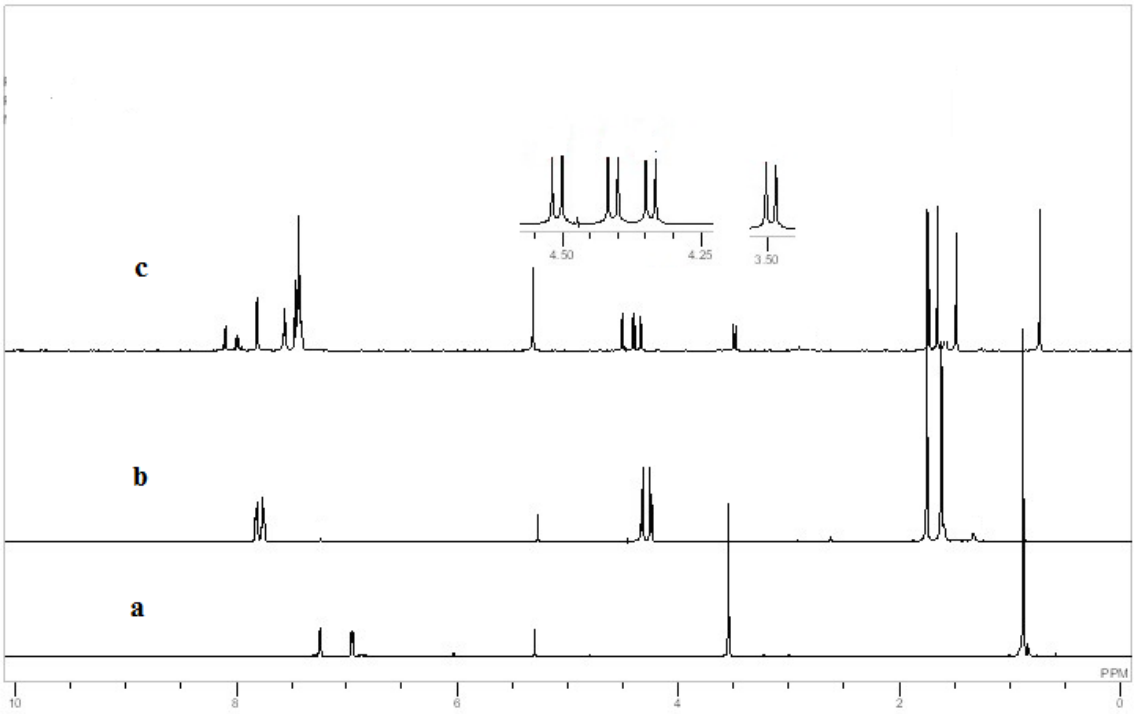

Figure 13: ^{1}H NMR Spectra in CD_2Cl_2 of (a) BOX ligand (b) Pd-BOX-1 (c) Pd-BOX-10.

The carbon-13 NMR spectra for the BOX ligand, Pd-BOX complex and the mixed ligand Pd-BOX-phosphine complexes were consistent with the proposed structures and were in entire agreement with the spectra of other known BOX ligands and Pd-BOX complexes [135-137]. For instance, in the spectra of Pd-BOX-10 and Pd-BOX-11, two sets of carbon signals were detected in the aromatic region. The weak signals represent the benzene spacer of the BOX ligand and the intense signals represent the triphenyl phosphine and *o*-methoxy triphenylphosphine ligands for Pd-BOX-10 and Pd-BOX-11 respectively. A downfield shift was observed in the resonance of the imino carbon (-*C*=*N*-) in the spectrum of Pd-BOX-1, Pd-BOX-10 and Pd-BOX-11.

Similarly, in the ^{31}P NMR spectra, the phosphorous resonances were observed at 21.3 ppm and 18.9 ppm for Pd-BOX-10 and Pd-BOX-11 respectively. This is a further confirmation that the phosphine ligands are coordinated to form the mixed ligand complexes.

Analysis of Pd-BOX-10 and Pd-BOX-11 using ESI-MS

We described in section 2.3.2.1 the crystal structure of Pd-BOX-1 [135]. The attempts to grow the crystals of Pd-BOX-10 and Pd-BOX-11 complexes were unsuccessful. We considered ESI-MS as a suitable technique to establish the molecular weight of our new mixed ligand complexes. ESI-MS is a mass spectroscopic technique that is generally considered suitable for organometallic compounds and transition metal complexes. This is due to the ability of electrospray ionization to generate gas phase ions that are similar in structure to the ions in solution [154]. It is a soft ionization technique in which a very little residual energy is retained by the analyte and hence, the chemical specie remains intact after ionization [154, 155]. The molecular weights obtained were in entire agreement with the calculated molecular weight. This results together with the information acquired from other spectroscopic techniques are consistent with the proposed molecular structure of the new complexes (Scheme 5).

CHAPTER 4

Supported BOX ligands and supported palladium-BOX catalysts: Synthesis and characterization

4.1 Introduction

As clearly stated in the preceding chapters of this thesis, the synthesized complexes are intended to be used as catalysts for the coupling and carbonylative coupling reactions. We have described in detail (chapter two and chapter three) the synthesis and characterization of palladium(II) bis(oxazoline) complexes. Since the complete removal and recycling of homogeneous catalysts represents complex and costly processes, the use of immobilized catalysts will be the good option for industries that have concerns over metal contamination [156]. In addition to the easy removal from the reaction products, the immobilized catalyst offers the potential to be recycled and reused in a continuous flow reactor [157]. The ability to separate and reuse the supported catalyst makes it more viable alternative especially from economical point of view. Taking into consideration these substantial advantages, the interest towards the use of immobilized complexes has been increasing rapidly. In this chapter, we described the synthesis and characterization of supported palladium(II) bis(oxazoline) complexes.

The selection of the support for the immobilization of BOX complexes was guided by the following criteria:

- ✓ The support should be inexpensive and readily available.
- ✓ The type of chemical bond linking the support with the Pd-BOX complex should be stable under the conditions that will be encountered during the catalytic applications.
- ✓ The support should be tolerant to the standard conditions of the coupling and carbonylation reactions (temperature, base, solvents).

Merifield's resin and 4-chlorobenzyl functionalized silica gel were considered as suitable supports for the following reasons:

Polystyrene based supports are inexpensive, readily available, mechanically robust and chemically inert. Polystyrene immobilized catalysts have been reported to possess high recycling ability and inertness to most of the standard conditions encountered during coupling reactions [3, 100, 158].

Similarly, silica supports are characterized with easy accessibility, high porosity and excellent stability. Many silica supported transition metal complexes have been reported to show excellent properties in catalysis of organic reactions and transformations [156, 159].

4.2 Experimental

4.2.1 Materials and Instrumentation

Materials for the synthesis of ligands and palladium complexes were purchased from Sigma Aldrich and were used as received. All solvents used in the synthesis were distilled before their use. Merifield's peptide resin (50 – 100 mesh, extent of labelling: 2.5-4.0 mmol/g Cl^- loading, 1% crosslinked with divinylbenzene) and 4-benzyl chloride functionalized silica gel (200-400 mesh, extent of labelling: 1.2 mmol/g loading) were purchased from Sigma - Aldrich.

Solid state NMR spectral data was recorded using CP-MAS on a Bruker Avans 400 MHz machine. IR spectra were recorded in wave numbers (cm^{-1}) using FT-IR spectrometer (Perkin-Elmer 16F model). Elemental analyses were performed on Perkin Elmer Series 11 (CHNS/O) Analyzer 2400. Palladium loading was estimated using inductively coupled plasma- mass spectrometer, X-series 2 ICP-MS, thermos scientifc. Thermal stability of the supported ligands and complexes were established using thermogravimetry (TG) (Perkin-Elmer TGA 7, US) analysis at a heating rate of 10 $^oC\ min^{-1}$ through to 700 ^oC under nitrogen atmosphere. The morphology of the supports, supported ligands and supported complexes were studied using scanning electron microscope, JEOL JSM6610LV SEM.

4.2.2 Synthesis of supported bis(oxazoline) ligand

The following procedure was adopted for the synthesis of merifield's resin and benzyl silica supported bis(oxazoline) ligands.

NaH (0.50 mmol) was added in one portion to a stirred solution of *3,4-bis(4,4-dimethyl-4,5-dihydro-1,3-oxazol-2-yl)biphenyl-4-ol* ***(BOX-8)*** (prepared in section 3.2.2) (0.31 mmol) in dry DMF in a dry flask. The mixture was stirred for 2 h at room temperature and under argon atmosphere. The appropriate support (0.30 mmol) was added and the mixture was stirred at 90 ºC for 12 h. The solid product was filtered and washed successively with methanol, water, acetone and dichloromethane. The product was dried at room temperature under vacuum [157].

Merifield's resin supported BOX ligand (BOX-10)

Yellow solid; yield (91 %); ^{13}C NMR: δ 28.2, 41.7, 67.9, 80.3, 91.4, 120-140 (several signals), 168.8; IR: ν_{max} (cm^{-1}) 3081, 3024, 2965, 2923, 1652, 1604, 1517, 1491, 1452, 1351, 1311, 1244, 1086, 1036, 825, 759, 699, Anal. C, 80.68; H, 6.36; N, 3.80

Benzyl silica supported BOX ligand (BOX-11)

Yellow solid, yield (93 %); ^{13}C NMR: δ 28.6, 67.5, 80.3, 120-140 (several signals), 190.7, 195.4; IR: ν_{max} (cm^{-1}), 2971, 2933, 2387, 1661, 1606, 1522, 1498, 1460, 1361, 1323, 917, 799, 697; Anal. C, 15.85; H, 1.68; N, 1.40.

4.2.3 General procedure for the synthesis of supported palladium-BOX catalysts

4.2.3.1 Procedure for the synthesis of merifield's resin supported palladium(II) bis(oxazoline) catalyst (Pd-BOX-12)

The Merrifield resin supported bis(oxazoline) ligand (***BOX-10***) (0.30 mmol, 0.12 g) was stirred in ethanol for 30 min. An ethanolic solution of bis(benzonitrile) palladium(II) chloride (0.3 mmol, 0.11 g) was added and the resulting mixture was stirred at 50 ^{o}C for 12 h. The solid product was filtered, washed thoroughly with ethanol and dried in a vacuum [160].

Merifield's resin supported palladium(II) bis(oxazoline) catalyst (Pd-BOX-12)

Dark brown solid, yield (95 %); ^{13}C NMR: δ 27.5, 41.4, 70.5, 81.7, 96.1, 120-140 (several signals), 182.3; IR: ν_{max} (cm^{-1}) 3056, 3021, 2919, 2844, 1634, 1599, 1494, 1452, 1371, 1327, 1221, 1178, 1068, 1011, 950, 824, 757, 699; Anal. C, 62.84; H, 4.83; N, 2.99. Metal loading from ICP-MS: 6.7 % corresponding to 0.6 mmol/g.

4.2.3.2 Procedure for the synthesis of benzyl silica supported palladium(II) bis(oxazoline) catalyst (Pd-BOX-13)

The silica supported bis(oxazoline) ligand (***BOX-11***) (0.30 mmol, 0.25 g) was stirred in anhydrous toluene for 30 min. A solution of bis(benzonitrile) palladium(II) chloride (0.30 mmol, 0.12 g) in toluene was added and the resulting mixture was stirred at 90 ^{o}C for 12 h. The solid product was filtered, washed thoroughly with ethanol and dried in a vacuum.

Benzyl silica supported palladium(II) bis(oxazoline) catalyst (Pd-BOX-13)

Brown solid, 90 % yield; ^{13}C NMR: δ 28.6, 67.6, 80.5, 120-140 (several signals), 189.9, 195.9 IR: ν_{max} (cm^{-1}) 2971, 2361, 1643, 1086, 943, 795, Anal. C, 12.78; H, 1.58; N, 1.29. The metal loading of the polymer supported palladium catalyst which was determined using ICP-MS, was found to be 2.8 % corresponding to 0.30 mmol/g.

4.3 Results and discussions

The iodofunctionalized BOX ligand (**BOX-7**) was considered as suitable candidate for immobilization. This is attributed to the simplicity with which various functionalities could be introduced, for instance, through coupling reaction. **BOX-7** was successfully coupled with 4-hydroxyphenylboronic acid to obtain the hydroxyl functionalized BOX ligand (**BOX-8**). The hydroxyl functionalized BOX ligand has then reacted with the appropriate support to obtain the immobilized BOX ligand. The immobilized BOX ligands were further reacted with bis(benzonitrile) palladium(II) chloride to result in the supported palladium(II)-BOX catalysts.

It is worth mentioning that the ether bond was considered suitable for linking the BOX ligand to the support. Whereas most functional groups such as esters and amides can easily be hydrolyzed under the standard conditions of coupling reaction (which involves the use of bases such as KOH and K_2CO_3), the ether link is particularly stable to the reaction conditions and thus, expected to prevent leaching of the ligand during the catalytic application.

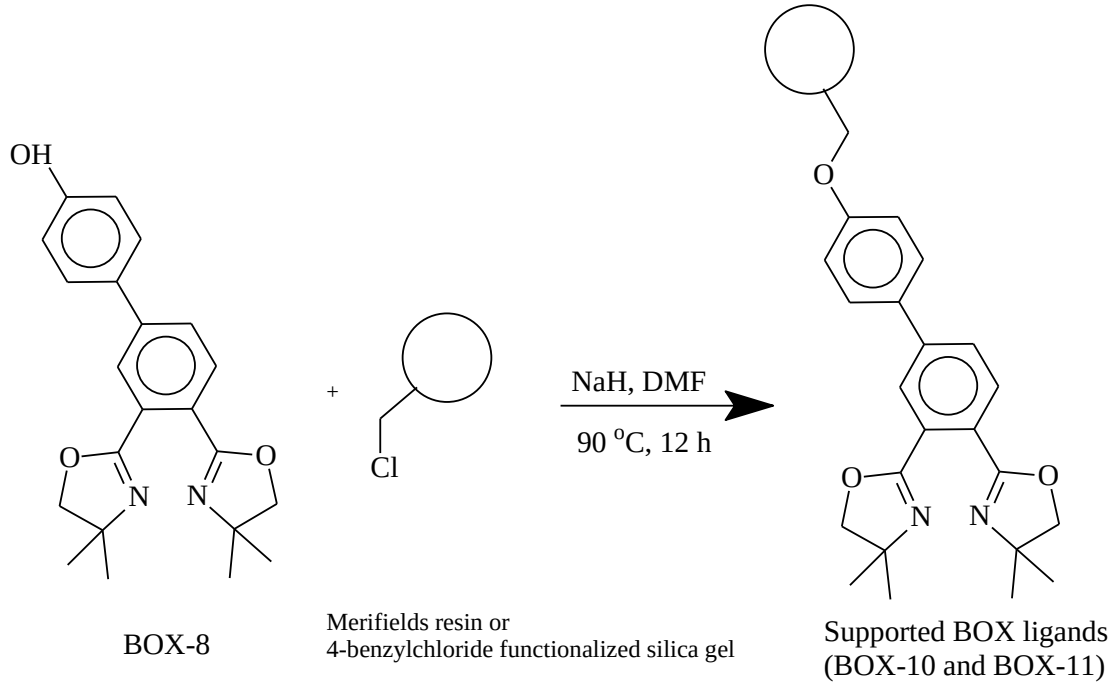

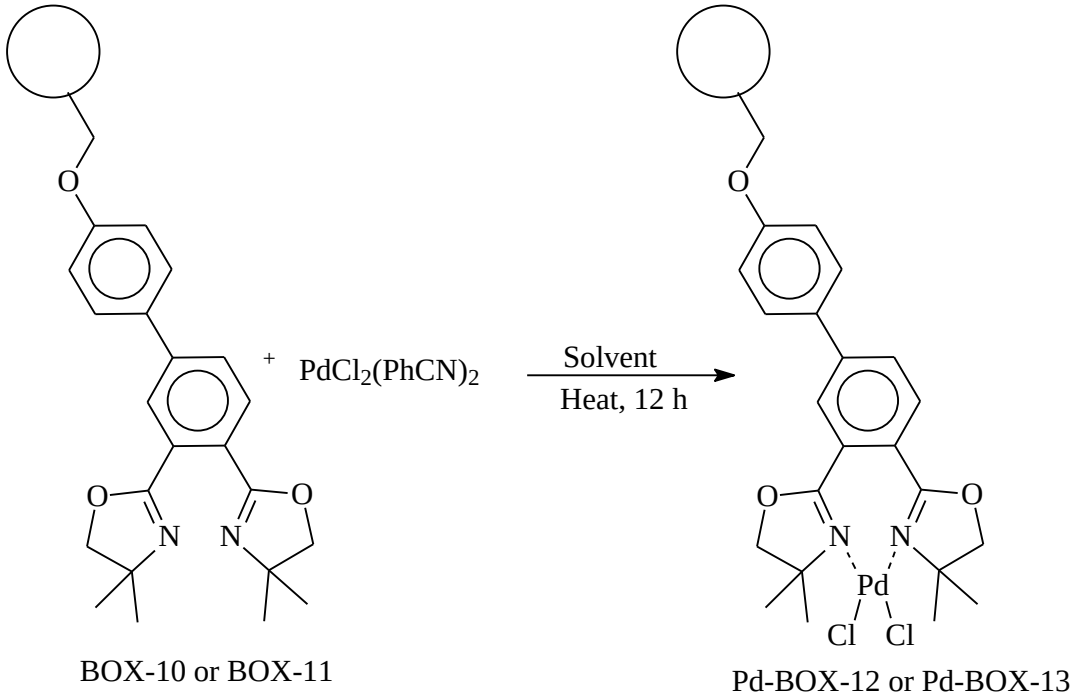

Scheme 6: Synthesis of supported bis(oxazoline) ligands and their dichloridopalladium(II) catalysts

4.3.1 Merifield's resin supported Pd-BOX catalyst

The functionalization of merifield's resin with the bis(oxazoline) ligand (**BOX-8**) to form merifield's resin supported BOX ligand **(BOX-10)** followed by subsequent complexation with palladium chloride to form the merifield's resin supported dichloridopalladium(II) bis(oxazoline) catalyst (**Pd-BOX-12**) was shown in scheme 6. The formation of the supported catalyst was confirmed by FT-IR, CP-MAS ^{13}C NMR, elemental analysis and ICP-MS. The catalyst was further characterized with scanning electron microscopy (SEM) and thermogravimetric analysis (TGA).

4.3.1.1 Characterization of the merifield's resin supported BOX ligand and its dicholoridopalladium(II) complex using FT-IR

The sharp C-Cl peak at 1264 cm^{-1} [160] which was observed in the FT-IR spectrum of the unmodified merifield resin (Figure 14) is no longer present after the introduction of the bis(oxazoline) ligand (Figure 15). This is consistent wth the fact that all the chloro groups attached to the resin were successfully replaced with the BOX ligand. The formation of resin supported bis(oxazoline) ligand was further confirmed by the appearance of a strong band at 1652 cm^{-1} in the spectrum of the resin bound BOX ligand (Figure 15). This peak was initially absent in the spectrum of the unmodified merifield's resin (Figure 14). This band is due to the stretching of imino *(-C=N-)* bond of the oxazoline ring. The *-C=N-* stretching band shifted to 1634 cm^{-1} on complexation with palladium (Figure 16). The shift in the position of the *-C=N-* band ($\Delta\nu = 18cm^{-1}$) confirms the coordination of palladium with the supported ligand. The position of the *-C=N-* band in the supported ligand and the

observed shift after coordination entirely agress with the previously reported data [135-137].

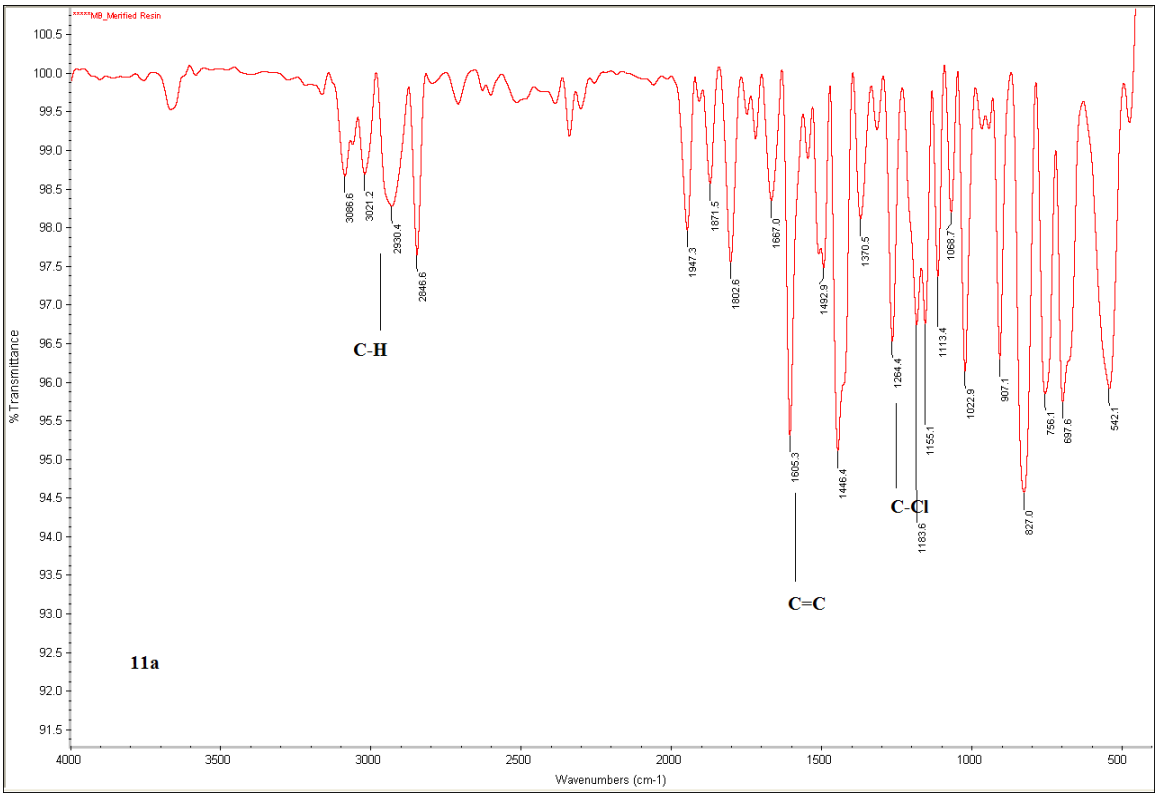

Figure 14. FT-IR Spectrum of Unmodified Merifield's Resin

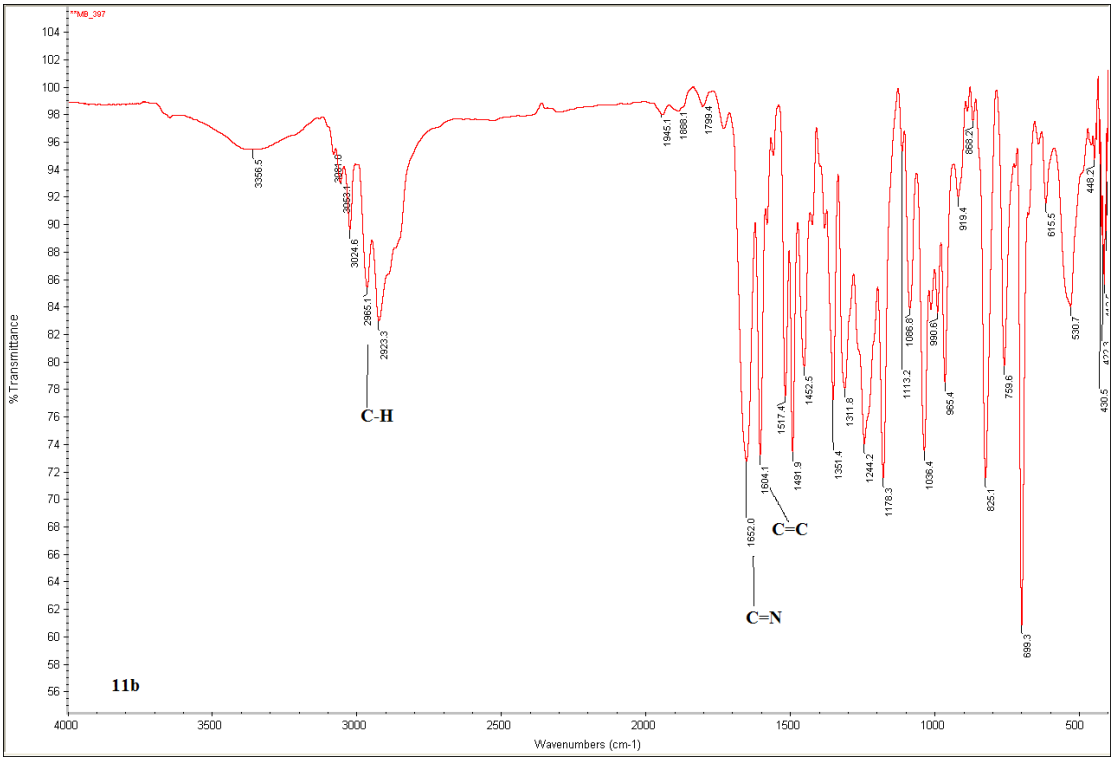

Figure 15. FT-IR Spectrum of Merifield's Resin Supported BOX Ligand

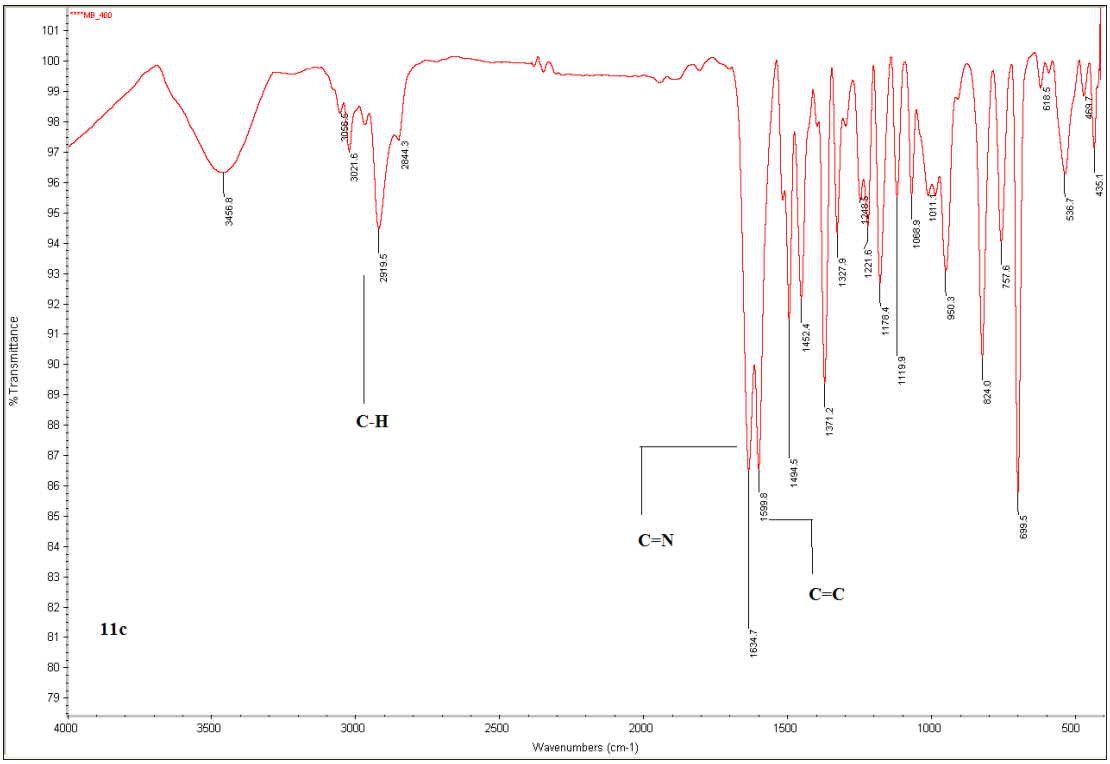

Figure 16. FT-IR Spectra of Merifield's Resin Supported Pd-BOX Catalyst (Pd-BOX-12).

4.3.1.2 Characterization of the merifield's resin supported BOX ligand and its dichloridopalladium(II) catalyst using CP-MAS ^{13}C NMR

The merifield resin supported BOX ligand and its palladium catalyst were further analyzed using solid state ^{13}C NMR. The spectra of the polymer bound ligand and its palladium catalyst were in entire agreement with those reported for other homogenous and supported bis(oxazoline) ligands and complexes. For instance, the resonance due to imino carbon (-*C*=N) was observed at 168.8 in the spectrum of the supported ligand. This band shifted to 182.3 after complexation [160, 135-137].

4.3.1.3 Analysis of the merifield's resin supported dichloridopalladium(II)-bis(oxazoline) catalyst using ICP-MS

The palladium loading on the merifield resin supported dichloridopalladium(II)-BOX catalyst was estimated using ICP-MS and was found to be 6.7 %. This corresponds to 0.6 mmol of palladium(II) per gram of the supported catalyst.

4.3.1.4 Analysis of the merifield's resin supported BOX ligand and its dichoridopalladium(II) catalyst using TGA

The thermal stability of both the merifield's resin supported ligand and its palladium catalyst was established from thermogravimetric analysis (figure A-III-1, A-III-3 and A-III-5). The merifield's resin supported BOX ligand and its dichloridopalladium(II) complex were found to possess high thermal stability with decomposition temperature of 370 ^{o}C.

4.3.1.5 Analysis of the merifield's resin supported BOX ligand and its dichloridopalladium(II) catalyst using scanning electron microscopy (SEM)

In order to assess the morphology of the merifield's resin, merifield's resin supported BOX ligand and the merifield's resin supported with dichloridopalladium(II)-BOX complex, SEM micrographs were recorded for a single bead of pure merifield's resin (Figure 17a), the supported BOX ligand (Figure 17b) and the supported dichloridopalladium(II) complex (Figure 17c). As expected, the smooth and flat microsphere surfaces of the merifiled's resin have been broken to a rough and irregular surface after incorporation of the BOX ligand and then the Pd-BOX complex. The morphological changes observed were similar to what was reported for other polystyrene supported ligand and their palladium complexes [100, 160].

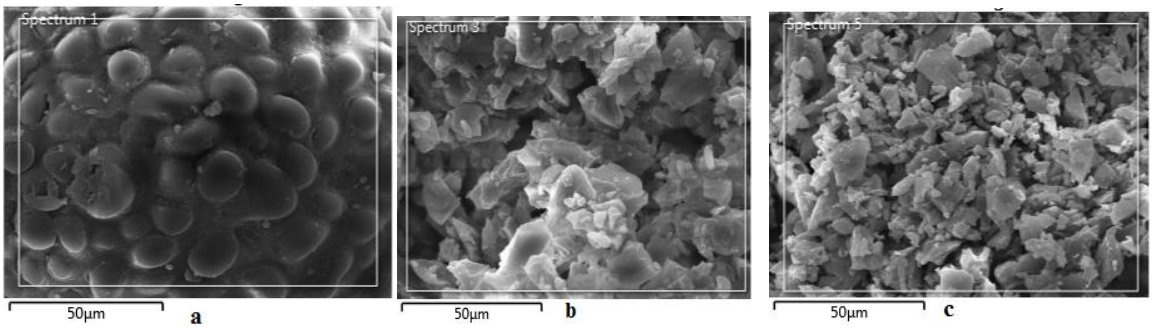

Figure 17: Scanning Electron Micrograph of (a) Merifield's Resin (b) Merifield's Resin Supported BOX Ligand (c) Merifield's Resin Supported Pd-BOX Catalyst

4.3.1.6 Characterization of the merifield's resin supported palladium-bis(oxazoline) (Pd-BOX-12) catalyst using X-ray photoelectron spectroscopy (XPS)

In the XPS spectrum of Pd-BOX-12 catalyst (Figure 18.), palladium peaks were observed in the range of 335 to 341 eV. Two distinctive 3d peaks were identified. The first peak with binding energy of 334.98 eV ($Pd3d_{5/2}$) and the second peak with binding energy of 340.28 ($Pd3d_{3/2}$). These peaks correspond to palladium(II) forms, and this confirms that palladium(II) is the main form of palladium in the supported catalyst [161, 162].

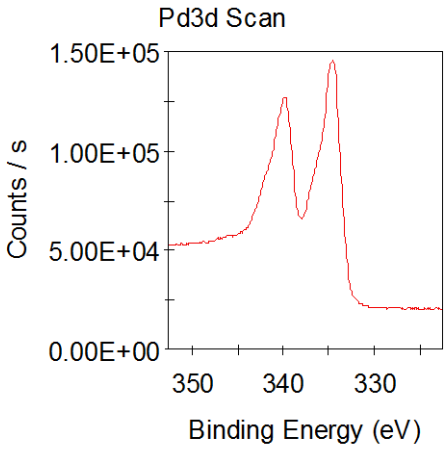

Figure 18: XPS Spectrum of Pd-BOX-12 (Pd3d)

4.3.2 Silica supported Pd-BOX catalyst

The functionalization of benzyl silica support with the bis(oxazoline) ligand (***BOX-8***) to form the silica supported bis(oxazoline) ligand (***BOX-11***) followed by complexation with palladium chloride to form the silica supported dichloridopalladium(II) bis(oxazoline) catalyst (***Pd-BOX-13***) was shown in scheme 6 . The formation of the required products

was confirmed by FT-IR, CP-MAS NMR, elemental analysis and inductively coupled plasma-mass spectrometry (ICP-MS). The product was further characterized with scanning electron microscopy (SEM) and thermogravimetric analysis (TGA).

4.3.2.1 Characterization of silica supported bis(oxazoline) ligand and its palladium(II) catalyst using FT-IR

FT-IR analysis of the silica supported bis(oxazoline) ligand reveals a strong band at 1661 cm^{-1} (Figure 20). This band was initially absent in the unmodified benzyl silica support (Figure 19). This band reflects *–C=N-* stretching in the oxazoline ring. The appearance of this additional band is an indication that the BOX ligand has been incorporated into the silica support matrix. The *–C=N-* stretching band shifted to 1643 cm^{-1} on complexation with palladium [Figure 21]. [135-137].

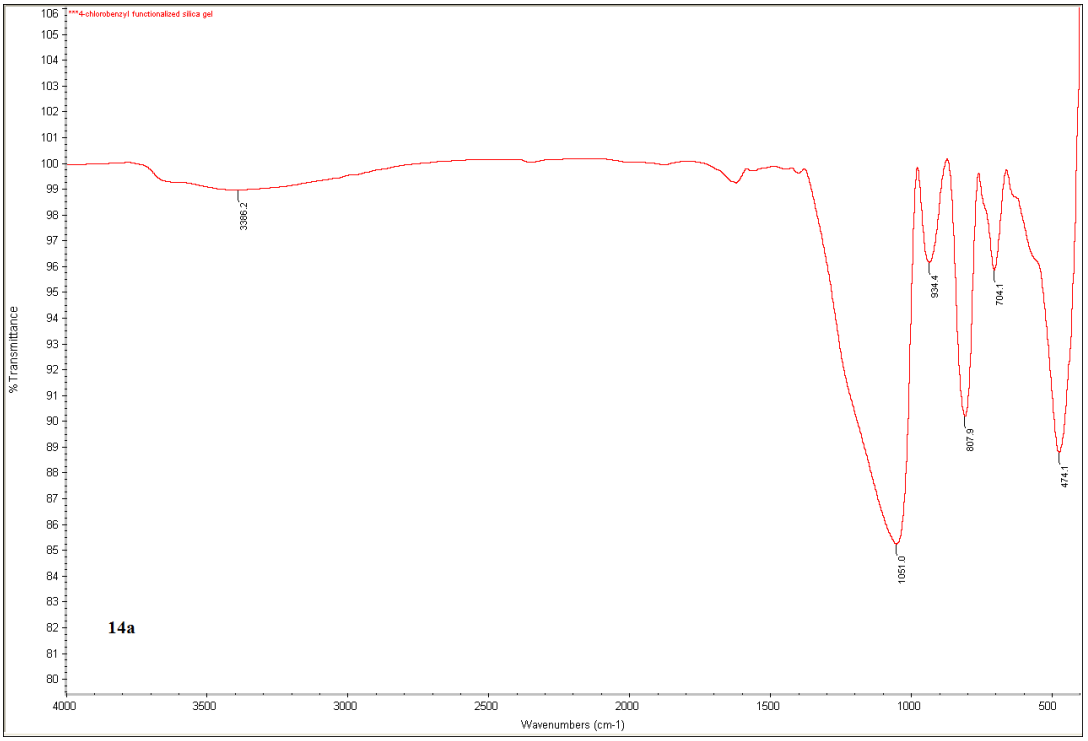

Figure 19. FT-IR Spectra of Unmodified Benzyl Silica Support

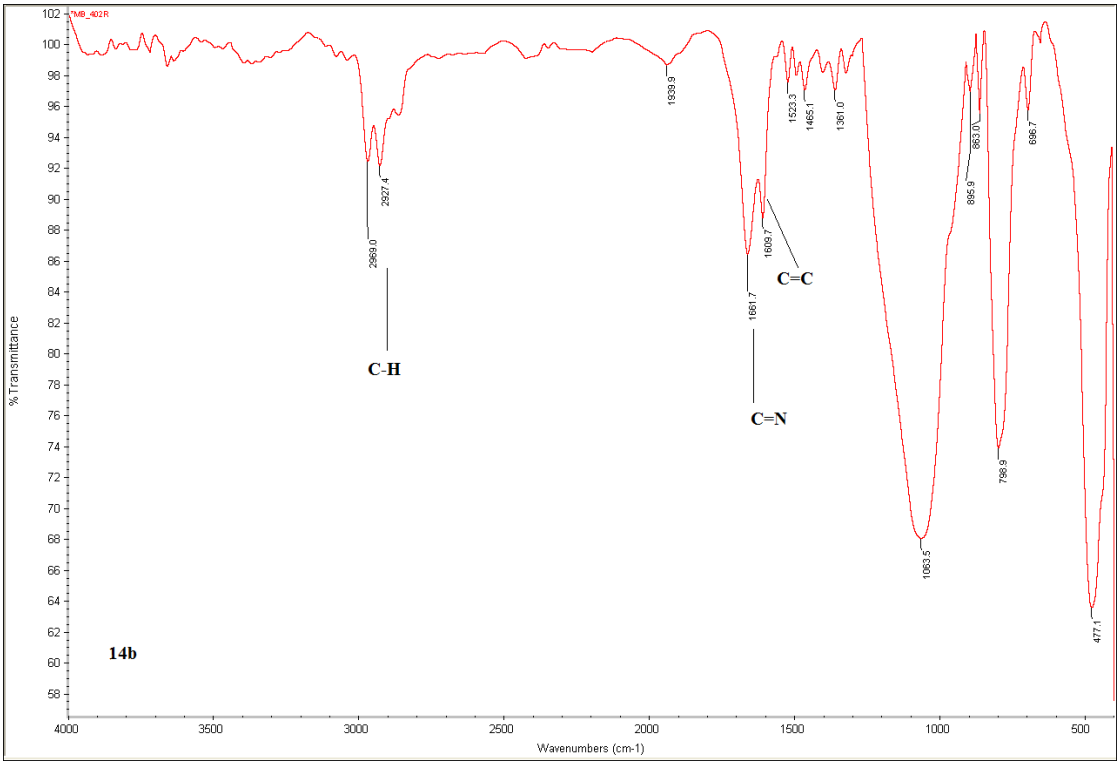

Figure 20. FT-IR Spectra of Silica Supported BOX Ligand.

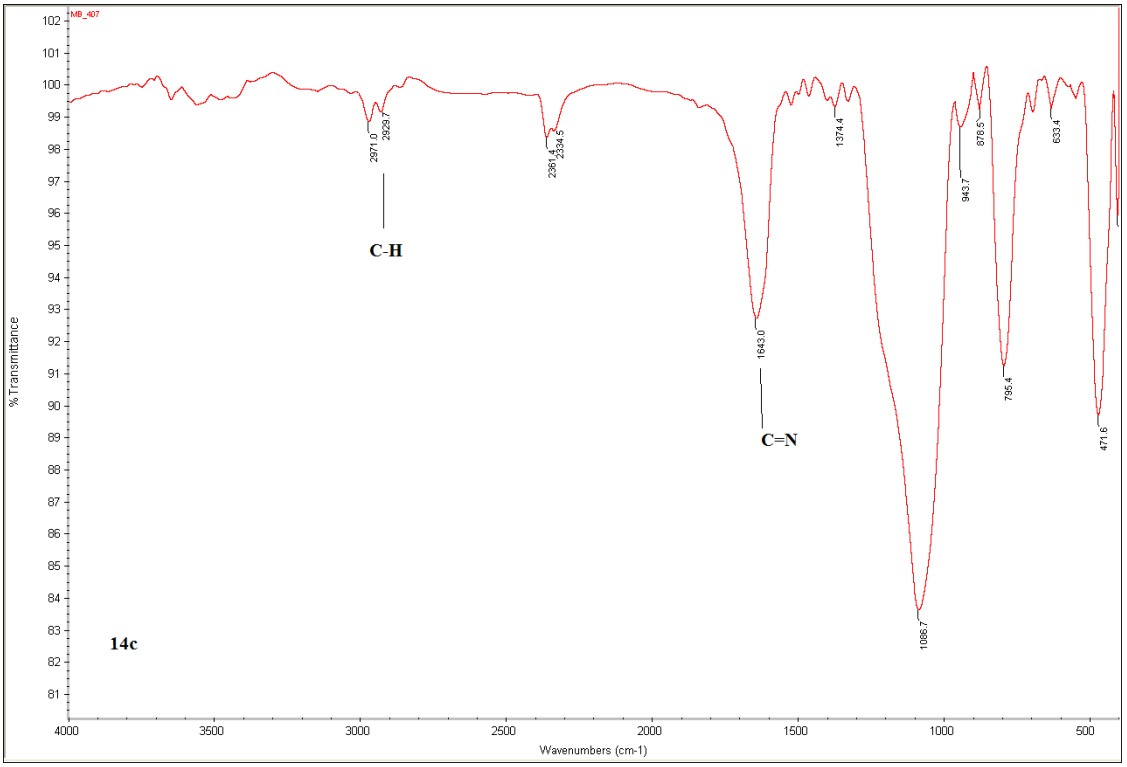

Figure 21. FT-IR Spectra of Silica Supported Pd-BOX Catalyst.

4.3.2.2 Characterization of silica supported BOX ligand and its dichloridopalladium(II) catalyst using CP-MAS ^{13}C NMR

The silica supported ligand and its palladium(II) complex were further characterized using solid state ^{13}C NMR. The spectra of the silica bound ligand and its palladium(II) complex were in entire agreement with those reported for other known bis(oxazoline) and supported bis(oxazoline) ligands and their complexes. For instance, the resonance due to imino carbon (-*C*=N) was observed at 195 ppm in the spectrum of the silica supported ligand. This band slightly shifted to 196 ppm after complexation [160, 135-137].

4.3.2.3 Analyis of silica supported dichloridopalladium(II) catalyst using ICP-MS

The palladium loading of the silica supported dichloridopalladium(II) bis(oxazoline) catalyst was determined using ICP-MS and was found to be 2.8 %. This corresponds to 0.3 mmol palladium per gram of the supported catalyst.

4.3.2.4 Analyis of silica supported BOX ligand and its palladium(II) catalyst using TGA

The thermal stability for the silica supported BOX ligand and its palladium(II) catalyst was determined using TGA (figure A-III-2, A-III-4 and A-III-6). Both the supported ligand and its palladium complex showed a decomposition temperature of ~150 ^{o}C indicating a good thermal stability. However, silica supported palladium-bis(oxazoline) catalyst is less stable as compared to the merifield resin supported palladium-bis(oxazoline) catalyst (decomposition temperature, 370 ^{o}C).

4.3.2.5 Analyis of silica supported BOX ligand and its dichloridopalladium(II) catalyst using SEM

In order to assess the morphology of the benzyl silica support, the silica supported BOX ligand and its palladium(II) catalyst, SEM micrographs were recorded for a pure benzyl chloride silica support, silica supported bis(oxazoline) ligand (***BOX-10***) and silica supported palladium(II)-bis(oxazoline) catalyst (***Pd-BOX-11***). As expected, the smooth and flat surfaces of the benzyl silica supports (Figure 22a), have been broken to a rough and irregular surface after incorporation of the metal complex (Figure 22c) [163 -166].

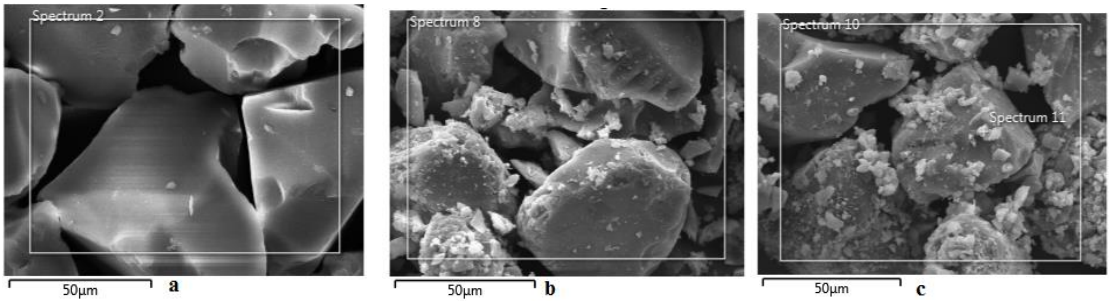

Figure 22: Scanning Electron Micrograph of (a) Benzyl Chloride Silica (b) Benzyl Silica Supported Bis(Oxazoline) Ligand (BOX-10) (c) Benzyl Silica Supported Palladium(II) Bis(Oxazoline) Catalyst (Pd-BOX-11)

4.3.2.6 Characterization of silica supported palladium-bis(oxazoline) (Pd-BOX-13) catalyst using X-ray photoelectron spectroscopy (XPS)

In the XPS spectrum of Pd-BOX-13 catalyst (Figure 23), palladium peaks were observed in the range of 335 to 342 eV. Two distinctive 3d peaks were identified. The first peak with binding energy of 336.08 eV ($Pd3d_{5/2}$) and the second peak with binding energy 341.38 ($Pd3d_{3/2}$). These data are consistent with palladium(II) forms, and this confirms that palladium (II) is the main form of palladium in the supported catalyst [161, 162].

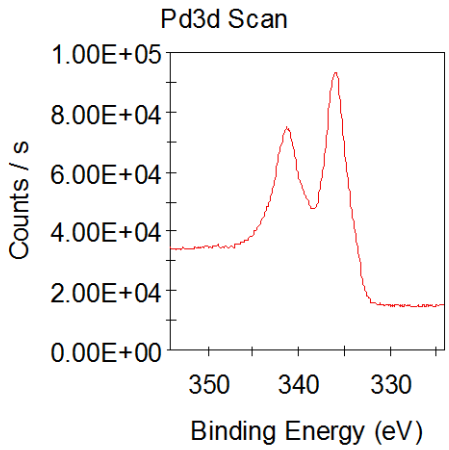

Figure 23: XPS Spectrum of Pd-BOX-13 (Pd3d)

CHAPTER 5

Applications of palladium-bis(oxazoline) complexes as catalysts in coupling reactions

5.1 Introduction

Cross coupling reactions have been considered among the best direct route for the synthesis of biaryls [167], internal alkenes and alkynes. Palladium complexes have been the most effective and versatile catalysts for Suzuki-Miyaura, Mizoroki-Heck and Sonogashira coupling reactions [168]. This effectiveness has been attributed to the feasible and facile interchange between Pd(II) and Pd(IV) or Pd(0) and Pd(II) species. Furthermore, although palladium complexes can tolerate a broad range of functional groups [168, 169], they are more effective catalysts in the presence of suitable ligands [170]. Though several reports have described the successful use of phosphine ligands with palladium complexes in catalyzing Suzuki-Miyaura, Mizoroki-Heck and Sonogashira coupling reactions, these ligands have numerous limitations due to the difficulty in synthesis, high cost, toxicity, and low air and moisture stability [1-3]. On the contrary, the nitrogen-based ligands are significantly inexpensive, easy to synthesize, non-toxic and stable to air and moisture [4]. Taking into consideration these substantial advantages, the interest towards the use of nitrogen donor ligands with palladium to catalyze cross coupling reactions has been increasing rapidly. Though ligands such as N-heterocyclic carbenes, oximes and

bis(amides) have been recognized to be efficient [170], the application of bis(oxazolines) as ligands in coupling reactions has not yet been widely explored.

In this chapter, detailed application of the newly synthesized palladium-bis(oxazoline) complexes (Pd-BOX-1 to Pd-BOX-7) and the supported palladium-bis(oxazoline) complexes (Pd-BOX-12 and Pd-BOX-13) in the Suzuki-Miyaura coupling reactions of arylboronic acids with aryl iodides, aryl bromides and aryl chlorides, Mizoroki-Heck coupling reactions of aryl iodides with alkenes and Sonogashira coupling reaction of aryl iodides with alkynes is described.

5.2 Experimental

Materials and Instrumentation

Aryl halides, arylboronic acids, alkenes and alkynes were purchased from Sigma Aldrich, US and were used as received. All solvents (reagent grade) used in the synthesis were distilled before use. The products were purified using flash column chromatography packed with Silica gel 170-400 Mesh, Fisher chemical (Fisher scientific, US). Merck 60 F_{254} silica gel plates (250 µm layer thickness) were used for thin-layer chromatography (TLC) analyses.

^{1}H and ^{13}C NMR spectral data were obtained using 500 MHz NMR machine (Joel 1500 model). Chemical shifts were recorded in ppm using tetramethyl silane (TMS) as reference. $CDCl_3$ and DMSO-d_6 were used as NMR solvents. IR spectra were recorded in wave numbers (cm^{-1}) using FT-IR spectrometer (Perkin-Elmer 16F model). A Varian Saturn 2000 GC-MS machine equipped with 30 m capillary column was used to analyze the

products. Agilent 6890 Gas chromatography (GC) was used to monitor the reactions and analyze the products.

5.2.1 General procedure for homogeneous palladium bis(oxazoline) catalyzed Suzuki-Miyaura coupling reaction

Palladium complex (0.20 mol %, 0.0020 mmol), aryl halide (1.0 mmol), aryl boronic acid (1.5 mmol), potassium carbonate (2.0 mmol), dimethylformamide (4.0 mL) and distilled water (4.0 mL) were added in a 15 mL round bottom flask. The mixture was stirred at room temperature under air. The progress of the reaction was monitored by the gas chromatography. After the completion of the reaction, the product was extracted 3 times with 5 mL of ethyl acetate. The combined organic extract was dried using anhydrous $MgSO_4$. The solvent was then removed under reduced pressure using a rotary evaporator. The product was further purified by column chromatography using hexane-EtOAc (8:2).

The characterization data of the compounds were in entire agreement with those reported in literature [137, 171 -175].

4-Acetylbiphenyl (3a):

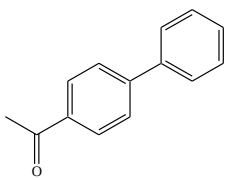

Yield 98 %; ^{1}H NMR (500 MHz, $CDCl_3$) δ (ppm): 8.01 (d, *J* = 8.2 Hz, 2H, CH), 7.67 (d, *J* = 8.2 Hz, 2H, CH), 7.61 (d, *J* = 7.3 Hz, 2H, CH), 7.46 (t, *J* = 7.3 Hz, 2H, CH), 7.39 (t, *J* = 7.0 Hz, 1H, CH), 2.62 (s, 3H, CH_3); ^{13}C NMR (125 MHz, $CDCl_3$) δ (ppm): 197.8, 145.6, 139.8, 135.8, 128.9, 128.8, 128.2, 127.2, 127.1, 26.6; GC-MS m/z 196 (M^+).

1-(4'-Methylbiphenyl-4-yl)ethanone (3b):

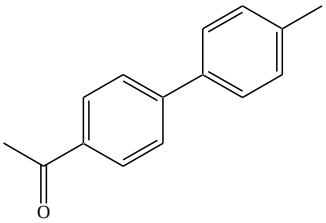

Yield 99 %; ^{1}H NMR (500 MHz, $CDCl_3$) δ (ppm): 8.01 (d, *J* = 8.5 Hz, 2H, CH), 7.67 (d, *J* = 8.5 Hz, 2H, CH), 7.53 (d, *J* = 8.3 Hz, 2H, CH), 7.28 (d, *J* = 8.3 Hz, 2H, CH), 2.63 (s, 3H, CH_3), 2.40 (s, 3H, CH_3); ^{13}C NMR (125 MHz, $CDCl_3$) δ (ppm): 197.8, 145.7, 138.2, 136.9, 135.7, 135.5, 129.7, 128.9, 128.7, 127.1, 126.9, 26.6, 21.2; GC-MS m/z 210 (M^+).

1-(4'-Hydroxybiphenyl-4-yl)ethanone (3c):

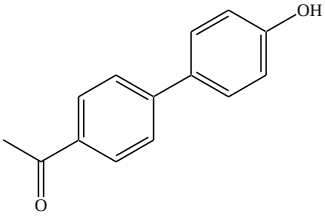

Yield 97 %; ^{1}H NMR (500 MHz, DMSO) δ (ppm): 9.8 (s, 1H, OH) 7.95 (s, 2H, CH), 7.72 (s, 2H, CH), 7.58 (s, 2H, CH), 6.85 (s, 2H, CH), 2.56 (s, 3H, CH_3); ^{13}C NMR (125 MHz, DMSO) δ (ppm): 197.7, 144.7, 136.0, 134.7, 129.6, 129.0, 128.3, 126.0, 116.0, 26.8; GC-MS m/z 212 (M^+).

1-[4-(1,3-Benzodioxol-5-yl)phenyl]ethanone (3d):

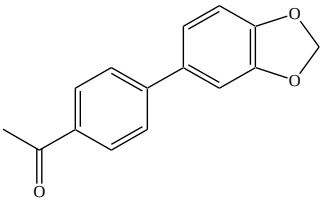

Yield 97 %; ^{1}H NMR (500 MHz, $CDCl_3$) δ (ppm): 7.98 (d, *J* = 8.6 Hz, 2H, CH), 7.58 (d, *J* = 8.6 Hz, 2H, CH), 7.08 (d, *J* = 7.9 Hz, 2H, CH), 6.88 (d, *J* = 7.9 Hz, 1H, CH), 5.99 (s, 2H, CH_2), 2.60 (s, 3H, CH_3); ^{13}C NMR (125 MHz, $CDCl_3$) δ (ppm): 197.7, 148.3, 147.8, 145.4, 135.5, 134.0, 128.9, 126.7, 121.0, 108.7, 107.6, 101.3, 26.6; GC-MS m/z 240 (M^+).

4-Nitrobiphenyl (3e):

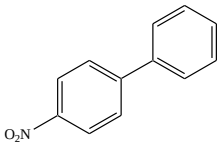

Yield 96 %; ^{1}H NMR (500 MHz, $CDCl_3$) δ (ppm): 8.26 (d, *J* = 7.0 Hz, 2H, CH), 7.71 (d, *J* = 7.0 Hz, 2H, CH), 7.61 (d, *J* = 7.6 Hz, 2H, CH),

7.49 (t, *J* = 7.6 Hz, 2H, CH), 7.44 (s, 1H); ^{13}C NMR (125 MHz, $CDCl_3$) δ (ppm): 147.5, 146.9, 138.6, 129.0, 128.8, 127.6, 127.2, 124.0; GC-MS m/z 199 (M^+).

Biphenyl-4-ol (3f):

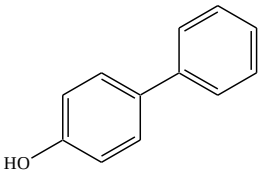

Yield 96 %; ^{1}H NMR (500 MHz, DMSO-d_6) δ (ppm): 7.53 (s, 2H, CH), 7.45 (s, 2H, CH), 7.38 (s, 2H, CH), 7.25 (s, 1H, CH), 6.83 (s, 2H, CH); ^{13}C NMR (125 MHz, DMSO-d_6) δ (ppm): 129.0, 127.9, 126.6, 126.1, 115.9; GC-MS m/z 170 (M^+).

4-Methylbiphenyl (3g):

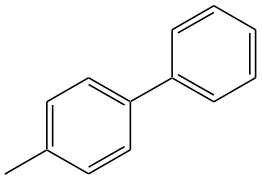

Yield 95 %; ^{1}H NMR (500 MHz, $CDCl_3$) δ (ppm): 7.57 (d, *J* = 7.6 Hz, 2H, CH), 7.49 (d, *J* = 8.2 Hz, 2H, CH), 7.42 (t, *J* = 7.3 Hz, 2H, CH), 7.31 (t, *J* = 7.6 Hz, 1H, CH), 7.24 (d, *J* = 8.5 Hz, 2H, CH), 2.39 (s, 3H, CH_3); ^{13}C NMR (125 MHz, $CDCl_3$) δ (ppm): 141.1, 138.3, 137.0, 129.5, 128.7, 127.0, 21.1; GC-MS m/z 168 (M^+).

4-Methoxybiphenyl (3h):

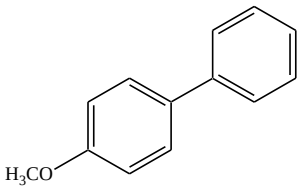

Yield 93 %; ^{1}H NMR (500 MHz, $CDCl_3$) δ (ppm): 7.52-7.60 (m, 4H, C-H), 7.43(t, *J* = 7.8 Hz, 2H, C-H), 7.29 (t, *J* = 7.0 Hz, 1H, CH), 6.98 (d, *J* = 9.5Hz, 2H, CH), 3.87 (s, 3H, CH_3), , ^{13}C NMR (125 MHz, $CDCl_3$) δ (ppm): 159.1, 138.3, 133.7, 132.6, 128.7, 128.1,126.7, 126.6, 114.1, 55.3; GC-MS m/z 184 (M^+).

4-Aminobiphenyl (3i):

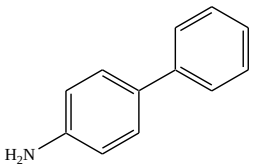

Yield 94 %; ^{1}H NMR (500 MHz, $CDCl_3$) δ (ppm): 7.51 (d, *J* = 8.5 Hz, 2H, CH), 7.39 – 7.35 (m, 4H, CH), 7.24 (t, *J* = 7.3 Hz, 1H, CH),

6.72 (d, *J* = 7.9 Hz, 2H, CH), 3.68 (s, 2H); ^{13}C NMR (125 MHz, $CDCl_3$) δ (ppm): 145.8, 141.1, 131.5, 128.6, 127.9, 126.3, 126.2, 115.3; GC-MS m/z 169 (M^+).

Biphenyl-4-carbaldehyde (3k):

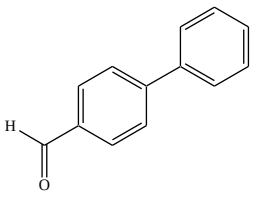

Yield 99 %; ^{1}H NMR (500 MHz, $CDCl_3$) δ (ppm): 10.04 (s, 1H, CHO), 7.94 (d, *J* = 8.6 Hz, 2H, CH), 7.74 (d, *J* = 8.2 Hz, 2H, CH), 7.62 (d, *J* = 8.2 Hz, 2H, CH), 7.46 (t, *J* = 7.1 Hz, 2H, CH), 7.40 (t, *J* = 7.3 Hz, 1H, CH); ^{13}C NMR (125 MHz, $CDCl_3$) δ (ppm): 191.9, 147.2, 139.7, 135.1, 130.2, 128.9, 128.6, 128.4, 127.6, 127.3, 127.1; GC-MS m/z 182 (M^+).

Biphenyl-4-carbonitrile (3l):

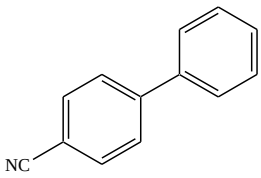

Yield 98 %; ^{1}H NMR (500 MHz, $CDCl_3$) δ (ppm): 7.70 (d, *J* = 8.3 Hz, 2H, CH), 7.66 (d, *J* = 8.3 Hz, 2H, CH), 7.57 (d, *J* = 8.2 Hz, 2H, CH), 7.47 (t, *J* = 7.6 Hz, 2H, CH), 7.42 (d, *J* = 7.3 Hz, 1H, CH); ^{13}C NMR (125 MHz, $CDCl_3$) δ (ppm): 145.6, 139.1, 135.6, 132.5, 129.0, 128.6, 127.7, 127.2, 118.9; 110.8 GC-MS m/z 179 (M^+).

4-Ethoxybiphenyl (3m):

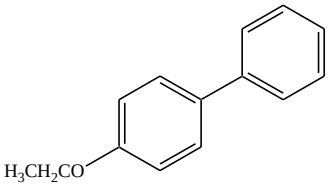

Yield 87; ^{1}H NMR (500 MHz, $CDCl_3$) δ (ppm): 7.50 - 7.55 (m, 4H, C-H), 7.50 (t, *J* = 8.8 Hz, 2H, C-H), 7.39 (t, *J* = 9.1 Hz, 1H, CH), 7.0 (d, *J* = 11 Hz, 2H, CH), 4.13 (q, *J* = 8.8 Hz 2H, CH_2), 1.52 (t, *J* = 8.8 Hz 3H, CH_3) , ^{13}C NMR (125 MHz, $CDCl_3$) δ (ppm): 140.9, 133.7, 128.8, 128.2, 126.8, 126.7, 114.8, 63.6, 14.9; GC-MS m/z 198 (M^+).

Biphenyl (3n):

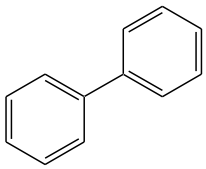

Yield 72 %; ^{1}H NMR (500 MHz, $CDCl_3$) δ (ppm): 7.59-7.57 (m, 4H, CH), 7.43-7.40 (m, 4H, CH), 7.34-7.32 (m, 2H, CH); ^{13}C NMR (125 MHz, $CDCl_3$) δ (ppm): 141.2, 128.7, 127.2, 127.1; GC-MS m/z 154 (M^+).

4'-Methylbiphenyl-4-carbaldehyde (3o):

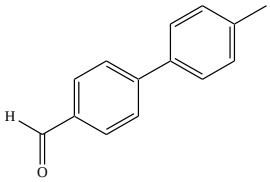

Yield 96 %; ^{1}H NMR (500 MHz, $CDCl_3$) δ (ppm): 9.9 (s, 1H, CHO), 7.9 (d, *J* = 8.3 Hz, 2H, CH), 7.68 (d, *J* = 8.3 Hz, 2H, CH), 7.48 (d, *J* = 7.9 Hz, 2H, CH), 7.22 (d, *J* = 7.9 Hz, 2H, CH), 2.36 (s, 3H, CH_3); ^{13}C NMR (125 MHz, $CDCl_3$) δ (ppm): 191.9, 147.2, 138.5, 136.8, 134.9, 130.3, 130.2, 129.7, 129.4, 127.4, 127.2, 126.8, 21.2; GC-MS m/z 196 (M^+).

5.2.2 General procedure for homogeneous palladium-bis(oxazoline) catalyzed Mizoroki-Heck coupling reaction

Palladium complex (0.010 mmol), aryl halide (1.0 mmol), styrene (1.5 mmol), KOH (2.0 mmol), DMF (3.0 mL) and distilled water (1.0 mL) were added in a 15 mL round bottom flask. A condenser was attached and the mixture was stirred at 90 ºC. The progress of the reaction was monitored by the gas chromatography. After the completion of the reaction, the product was extracted 3 times with 5 mL of ethyl acetate. The combined organic extract was dried using anhydrous $MgSO_4$. The solvent was then removed under reduced pressure using a rotary evaporator. The product was further purified by column chromatography using hexane-EtOAc (7:3) as eluent.

The characterization data of the compounds were in entire agreement with those reported in literature [137, 175].

***(E)*-Stilbene (5a)**:

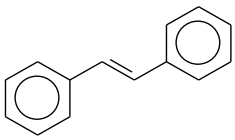

Yield 96 %; ^{1}H NMR (500 MHz, $CDCl_3$) δ (ppm): 7.64 (d, *J* = 7.3 Hz, 4H), 7.48 (t, *J* = 7.3 Hz, 4H), 7.39 (t, *J* = 7.3 Hz, 2H), 7.24 (s, 2H); ^{13}C NMR (125 MHz, $CDCl_3$) δ (ppm): 137.2, 128.6, 127.5, 126.5; GC-MS m/z 180 (M^+).

4-Methoxy-trans-stilbene (5b):

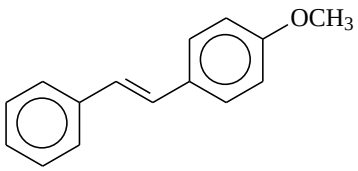

Yield 95 %; ^{1}H NMR (500 MHz, $CDCl_3$) δ (ppm): 7.48-7.46 (m, *J* = 7.3 Hz, 4H), 7.32 (t, *J* = 7.3 Hz, 2H), 7.22 (t, *J* = 7.3 Hz, 1H), 7.05 (d, *J* = 16 Hz, 1H), 6.95 (d, *J* = 16 Hz, 1H), 6.88 (d, *J* = 8.6 Hz, 2H), 3.80 (s, 3H); ^{13}C NMR (125 MHz, $CDCl_3$) δ (ppm): 137.6, 130.1, 128.6, 128.2, 127.7, 127.2, 126.6, 126.2, 114.1, 55.3; GC- MS m/z 210 (M^+).

1-[4-(2-Phenylethenyl)phenyl]ethanone (5c):

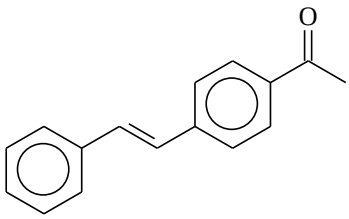

Yield 96 %; ^{1}H NMR (500 MHz, $CDCl_3$) δ (ppm): 7.93 (d, *J* = 8.3 Hz, 2H), 7.57 (d, *J* = 8.3 Hz, 2H), 7.52 (d, *J* = 7.3 Hz, 2H), 7.37 (t, *J* = 7.3 Hz, 2H), 7.28 (t, *J* = 7.3 Hz, 1H), 7.20 (d, *J* = 16.5 Hz, 1H), 7.12 (d, *J* = 16.5 Hz, 1H); 2.59 (s, 3H) ^{13}C NMR (125 MHz, $CDCl_3$) δ (ppm): 197.5, 141.2, 136.7, 135.9, 131.4, 128.9, 128.8, 128.3, 127.4, 126.8, 126.4, 26.6; GC- MS m/z 222 (M^+).

1-Chloro-4-[(1E)-2-phenylethenyl (5d):

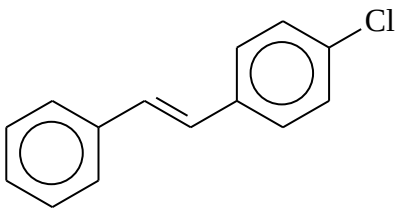

Yield 94 %; ^{1}H NMR (500 MHz, $CDCl_3$) δ (ppm): 7.49 (d, *J* = 7.3 Hz, 2H), 7.42 (d, *J* = 8.6 Hz, 2H), 7.35 (t, *J* = 7.6 Hz, 2H), 7.30 (d, *J* = 8.3 Hz, 2H), 7.26 (t, *J* = 8.3 Hz, 1H), 7.0 (d, *J* = 4.3 Hz, 2H); ^{13}C NMR (125 MHz, $CDCl_3$) δ (ppm): 136.9, 135.8, 133.2, 129.3, 128.9, 128.8, 128.7, 128.6, 127.9, 127.7, 127.6, 127.5, 127.4, 126.6, 126.5, 126.4; GC- MS m/z 214 (M^+).

1-[4-[2-(4-Methylphenyl)ethenyl]phenyl]ethanone (5e):

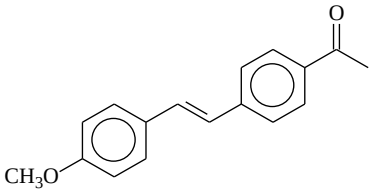

Yield 97 %; ^{1}H NMR (500 MHz, $CDCl_3$) δ (ppm): 7.97 (d, *J* = 8.3 Hz, 2H), 7.59 (d, *J* = 8.3 Hz, 2H), 7.52 (d, *J* = 8.8 Hz, 2H), 7.22 (d, *J* = 16.2 Hz, 2H), 7.03 (d, *J* = 16.5 Hz, 1H), 6.95 (d, *J* = 8.8 Hz, 1H), 3.88 (s, 3H), 2.64 (s, 3H); ^{13}C NMR (125 MHz, $CDCl_3$) δ (ppm): 197.5, 159.8, 142.4, 136.1, 135.5, 131.0, 129.4, 128.8, 128.1, 126.1, 125.3, 114.2, 55.3, 26.6; GC- MS m/z 252 (M^+).

(*E*)-Methyl cinnamate (5g):

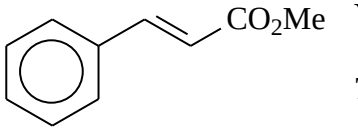

Yield 96 %; white solid; ^{1}H NMR (500 MHz, $CDCl_3$) δ (ppm): 7.68 (d, *J* = 15.9 Hz, 1H, CH), 7.51 – 7.49 (m, 2H, CH arom.), 7.38 – 7.35 (m, 3H, CH arom), 6.43 (d, *J* = 16.2 Hz, 1H, CH), 3.79 (s, 3H, CH_3). ^{13}C NMR (125 MHz, $CDCl_3$) δ (ppm): 167.4 , 144.8, 134.4, 130.3, 129.5, 129.1, 128.9, 117.8, 51.7; GC-MS m/z 162 (M^+).

(*E*)-Methyl 3-(4-nitrophenyl)acrylate (5h):

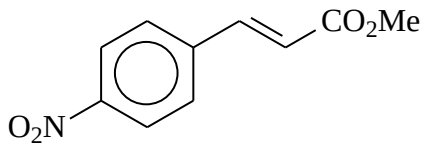

Yield 97 %; yellow solid; ^{1}H NMR (500 MHz, $CDCl_3$) δ (ppm): 8.22 (d, *J* = 8.9 Hz, 2H, CH arom), 7.70-7.63

(m, 3H), 6.53 (d, *J* = 16.2 Hz, 1H, CH), 3.81 (s, 3H, CH_3); ^{13}C NMR (125 MHz, $CDCl_3$) δ (ppm): 166.4 (C), 148.5, 141.8, 140.4, 128.6, 124.1, 124.0, 122.0, 52.0 (CH_3); GC-MS m/z 207 (M^+).

(*E*)-Methyl 3-(4-acetylphenyl)acrylate (5i):

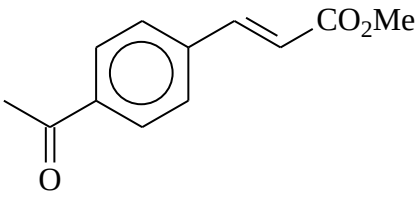

Yield 96 %; white solid; ^1H NMR (500 MHz, $CDCl_3$) δ (ppm): 7.92 (d, *J* = 6.4 Hz, 2H, CH arom), 7.66 (d, *J* = 16.2 Hz, 1H, CH), 7.56 (d, *J* = 6.7 Hz, 2H, CH arom), 6.48 (d, *J* = 15.9 Hz, 1H, CH), 3.78 (s, 3H, CH_3), 2.57 (s, 3H, CH_3); ^{13}C NMR (125 MHz, $CDCl_3$) δ (ppm): 197.2 (C), 166.8 (C), 143.2 (CH), 138.6 (C), 137.9 (C), 128.8 (CH), 128.1 (CH), 120.2 (CH), 51.8(CH_3), 26.6 (CH_3); GC-MS m/z 205 (M^{+1}).

(*E*)-Methyl 3-(4-aminophenyl)acrylate (5j):

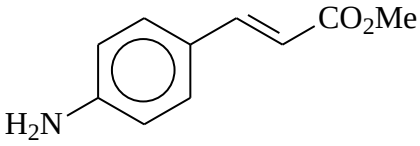

Yield 94 %; yellow solid; ^1H NMR (500 MHz, $CDCl_3$) δ (ppm): 7.58 (d, *J* = 15.9 Hz, 1H, CH), 7.31 (d, *J* = 5.8 Hz, 2H, CH arom), 6.61 (d, *J* = 8.5 Hz, 2H, CH arom), 6.21 (d, *J* = 15.9 Hz, 1H, CH), 3.97 (s, 2H, NH_2), 3.75 (s, 3H, CH_3); ^{13}C NMR (125 MHz, $CDCl_3$) δ (ppm): 168.1 (C), 148.8, 145.1, 129.8, 124.4, 114.7 (CH), 113.0 (CH), 51.4 (CH_3); GC-MS m/z 197 (M^+).

(*E*)-Methyl 3-(4-methoxyphenyl)acrylate (5k):

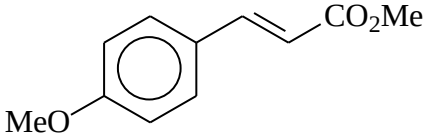

Yield 94 %; white solid; ^1H NMR (500 MHz, $CDCl_3$) δ (ppm): 7.63 (d, *J* = 15.9 Hz, 1H, CH), 7.44 (d, *J* = 5.8 Hz, 2H, CH arom), 6.87 (d, *J* = 5.8 Hz, 2H, CH arom), 6.29 (d, *J* = 15.9 Hz, 1H, CH), 3.79 (s, 3H, CH_3), 3.77 (s, 3H, CH_3). ^{13}C NMR (125 MHz,

$CDCl_3$) δ (ppm): 167.6 (C), 161.2 (C), 144.3 (CH), 129.6 (CH), 126.9 (C), 115.1 (CH), 114.1 (CH), 55.1 (CH_3), 51.4 (CH_3); GC-MS m/z 192 (M^+).

5.2.3 General procedure for homogeneous palladium-bis(oxazoline) catalyzed Sonogashira coupling reaction

In a 10 mL round bottom flask, palladium complex (0.010 mmol) was dissolved in acetonitrile (2 mL). Aryl halide (1.0 mmol), alkyne (1.2 mmol), KOH (2.00 mmol) and distilled water (2 mL) were added. The mixture was stirred at room temperature (or 60 ^oC) for the required time. After completion of the reaction, the product was extracted three times with ethyl acetate (5 mL). The combined organic layer was dried with anhydrous sodium sulfate. The product was analyzed with GC and GC-MS. The product was further purified using column chromatography with hexane-ethyl acetate as eluent. The characterization data were in entire agreement with the previously reported literature [135, 136, 104, 176-180].

Diphenylacetylene (7a):

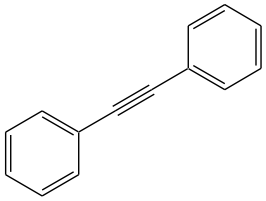

Yield 97 %; ^1H NMR (500 MHz, $CDCl_3$) δ (ppm): 7.60-7.56 (m, 5H), 7.45-7.33 (m, 5H); ^{13}C NMR (125 MHz, $CDCl_3$) δ (ppm): 131.6, 128.3, 128.2, 123.2, 89.3; GC-MS m/z 178 (M^+).

1-nitro-4-(phenylethynyl)benzene (7b):

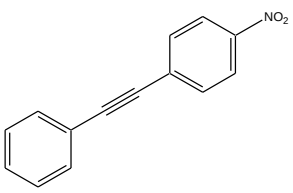

Yield 95 %; ^1H NMR (500 MHz, $CDCl_3$) δ (ppm): 8.20 (d, *J* = 8.8 Hz, 2H), 7.64 (d, *J* = 9.2 Hz, 2H), 7.54 (d, *J* = 7.6 Hz, 2H), 7.37 (s, 3H); ^{13}C NMR (125 MHz, $CDCl_3$) δ (ppm):132.3, 132.2,

131.9, 131.8, 131.7, 130.3, 129.3, 129.2, 128.6, 128.5,128.4, 123.7, 123.6, 123.5, 122.0, 94.7, 87.5.

1-[4-(Phenylethynyl)phenyl]ethanone (7c):

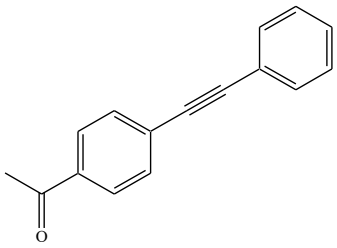

Yield 97 %; ^{1}H NMR (500 MHz, $CDCl_3$) δ (ppm): 7.92 (d, *J* = 8.6 Hz, 2H), 7.59 (d, *J* = 8.6 Hz, 2H), 7.54 - 7.52 (m, 2H), 7.35 - 7.34 (m, 3H), 2.60 (s, 3H) ; ^{13}C NMR (125 MHz, $CDCl_3$) δ (ppm):197.3, 136.1, 131.7, 131.6, 128.8, 128.4, 128.3, 128.2, 128.1, 122.6, 92.7, 88.6, 26.6; GC-MS m/z 220 (M^+).

4-(phenylethynyl)benzonitrile (7d):

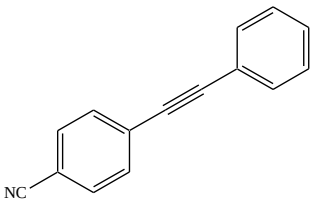

Yield 98 %; ^{1}H NMR (500 MHz, $CDCl_3$) δ (ppm): 7.62 - 7.57 (m, 4H), 7.53 - 7.51 (m, 2H), 7.37 – 7.35 (m, 3H); ^{13}C NMR (125 MHz, $CDCl_3$) δ (ppm): 132.0, 131.7, 129.1, 128.5, 128.2, 122.2, 118.5, 111.4, 93.7, 87.7; GC-MS m/z 203 (M^+).

4-(phenylethynyl)benzaldehyde (7e):

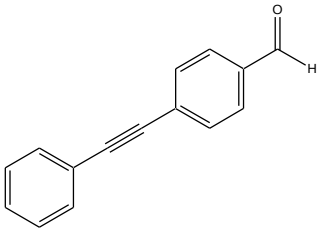

Yield 97 %; ^{1}H NMR (500 MHz, $CDCl_3$) δ (ppm): 10.00 (s, 1H), 7.85 (d, *J* = 8.5 Hz, 2H), 7.66 (d, *J* = 8.5 Hz, 2H), 7.57 – 7.52 (m, 2H), 7.36 – 7.34 (m, 3H), ^{13}C NMR (125 MHz, $CDCl_3$) δ (ppm):191.4, 135.4, 132.1, 132.0, 131.8, 131.7, 129.6, 129.5, 128.9, 128.5, 128.4, 122.5, 93.4, 88.4.

4-[(4-formylphenyl)ethynyl]benzonitrile (7f):

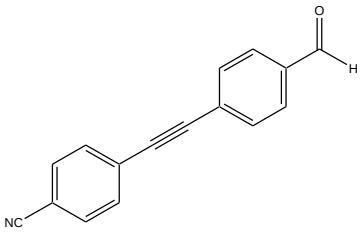

Yield 97 %; ^{1}H NMR (500 MHz, $CDCl_3$) δ (ppm): 10.00 (s, 1H), 7.88 (d, *J* = 8.5 Hz, 2H), 7.68 – 7.62 (m, 6H), ^{13}C NMR (125 MHz, $CDCl_3$) δ (ppm):191.3, 135.9, 132.3, 132.2, 132.1, 129.7, 129.6, 128.3, 127.4, 118.3, 112.2, 92.4, 91.2.

1-Methoxy-4-(phenylethynyl)benzene (7h):

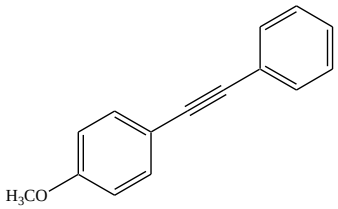

Yield 93 %; ^{1}H NMR (500 MHz, $CDCl_3$) δ (ppm): 7.49 (d, *J* = 5.8 Hz, 2H), 7.45 (d, *J* = 8.9 Hz, 2H), 7.30 (d, *J* = 7.3 Hz, 3H), 6.86 (d, *J* = 8.9 Hz, 2H), 3.81 (s, 3H); ^{13}C NMR (125 MHz, $CDCl_3$) δ (ppm):138.2, 133.0, 131.4, 128.4, 127.9, 123.6, 113.9, 55.3; GC-MS m/z 208 (M^+).

1-{4-[(4-methylphenyl)ethynyl]phenyl}ethanone:

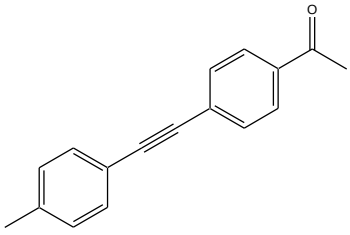

Yield 97 %; ^{1}H NMR (500 MHz, $CDCl_3$) δ (ppm): 7.99 (d, *J* = 8.5 Hz, 2H), 7.65 (d, *J* = 8.9 Hz, 2H), 7.50 (d, *J* = 8.2 Hz, 2H), 7.23 (d, *J* = 7.7 Hz, 2H), 2.66 (s, 3H), 2.44 (s, 3H) ; ^{13}C NMR (125 MHz, $CDCl_3$) δ (ppm):197.4, 139.1, 135.9, 131.6, 131.5, 129.2, 128.4, 128.3, 128.2, 93.0, 880, 26.6, 21.6.

4-(phenylethynyl)aniline (7i):

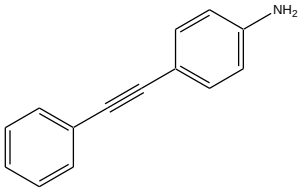

Yield 95 %; ^{1}H NMR (500 MHz, DMSO-d_6) δ (ppm): 7.42 (d, *J* = 7.1 Hz, 2H), 7.37-7.31 (m, 3H), 7.17 (d, *J* = 7.9 Hz, 2H), 6.54 (d, *J* = 8.3 Hz, 2H); 5.54 (s, 2H); ^{13}C NMR (125 MHz, $CDCl_3$) δ (ppm): 149.6, 132.7, 130.9, 128.8, 127.9, 123.5, 113.9, 108.2, 91.4.

1-Methyl-4-(phenylethynyl)benzene (7j):

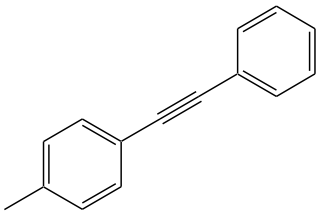

Yield 95 %; ^{1}H NMR (500 MHz, $CDCl_3$) δ (ppm): 7.52 (d, *J* = 9.5 Hz, 2H), 7.41 (d, *J* = 8.3 Hz, 2H), 7.33 - 7.30 (m, 3H), 7.14 (d, *J* = 8.6 Hz, 2H), 2.36 (s, 3H); ^{13}C NMR (125 MHz, $CDCl_3$) δ (ppm):138.4, 131.7, 131.6, 131.5, 131.4, 131.3, 129.0, 128.9, 128.3,128.1, 127.9, 123.4, 120.1, 89.5, 88.7, 21.5; GC-MS m/z 192 (M^{+}).

1-(phenylethynyl)-4-(trifluoromethyl)benzene (7k):

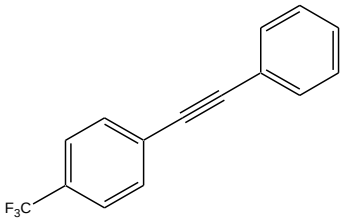

Yield 97 %; ^{1}H NMR (500 MHz, $CDCl_3$) δ (ppm): 7.60 (d, *J* = 5.8 Hz, 4H), 7.54 - 7.52 (m, 2H), 7.36 - 7.34 (m, 3H); ^{13}C NMR (125 MHz, $CDCl_3$) δ (ppm):131.8, 131.7, 131.6, 128.8, 128.5, 128.4, 127.0, 125.3, 125.2, 122.5, 91.7, 87.9.

4,4'-ethyne-1,2-diyldianiline (7l):

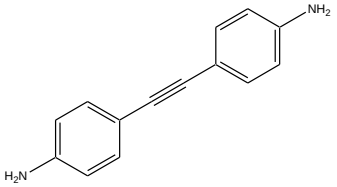

Yield 95 %; ^{1}H NMR (500 MHz, DMSO) δ (ppm): 7.08 (d, *J* = 8.3 Hz, 4H), 6.50 (d, *J* = 8.2 Hz, 4H), 5.40 (s, 4H); ^{13}C NMR (125 MHz, $CDCl_3$) δ (ppm): 148.7, 132.0, 113.7, 113.6, 109.5.

4,4'-benzene-1,4-diylbisbut-3-yn-1-ol:

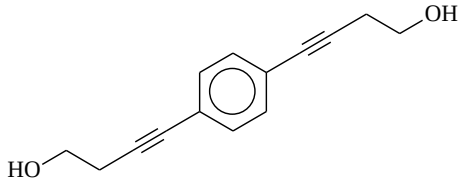

White solid, Yield 96 %; ^{1}H NMR (500 MHz, $CDCl_3$) δ (ppm): 7.32 (s, 4H), 4.91 (s, 2H), 3.54-3.57 (m, 4H), 2.54 (t, J = 6.8Hz, 4H); ^{13}C NMR (125 MHz, $CDCl_3$) δ (ppm):131.4, 122.7, 90.4, 80.7, 59.7, 23.3; GC-MS m/z 214 (M^{+1})

1-[4-(4-phenylbut-1-yn-1-yl)phenyl]ethanone (7q):

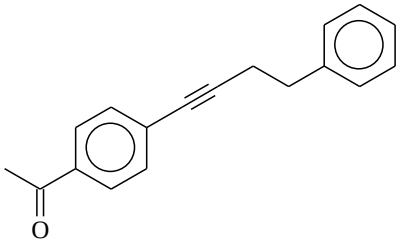

Yield 97 %; ^{1}H NMR (500 MHz, $CDCl_3$) δ (ppm): 7.82 (d, *J* = 8.6 Hz, 2H), 7.39 (d, *J* = 8.6 Hz, 2H), 7.28 - 7.19 (m, 5H), 2.89 (t, J = 7.4 Hz, 2H), 2.68 (t, 7.6 Hz, 2H), 2.53 (s, 3H); ^{13}C NMR (125 MHz, $CDCl_3$) δ (ppm):197.3, 140.4, 135.7, 131.6, 128.8, 128.5, 128.4, 128.1, 126.4, 93.3, 80.8, 34.8, 26.5, 21.7; GC-MS m/z 248 (M^{+}).

1-[4-(5-phenylpent-1-yn-1-yl)phenyl]ethanone (7r):

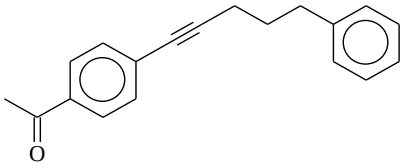

Yield 97 %; ^{1}H NMR (500 MHz, $CDCl_3$) δ (ppm): 7.90 (d, *J* = 8.6 Hz, 2H), 7.48 (d, *J* = 8.2 Hz, 2H), 7.31 - 7.29 (m, 2H), 7.26 - 7.22 (m, 3H), 2.81 (t, J = 7.35 Hz, 2H), 2.59 (s, 3H), 2.46 (t, J = 7.1 Hz, 2H), 1.95 (m, J = 7.3 Hz, 2H); ^{13}C NMR (125 MHz, $CDCl_3$) δ (ppm):197.3, 141.4, 135.7, 131.6, 128.9, 128.5, 128.4, 128.2, 125.9, 93.7, 80.6, 34.8, 30.0, 26.5, 18.9; GC-MS m/z 262 (M^{+}).

4-(hex-1-yn-1-yl)benzonitrile (7w):

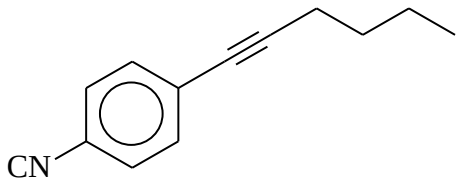

Yield 96 %; ^{1}H NMR (500 MHz, $CDCl_3$) δ (ppm): 7.54 (d, J = 8.6 Hz, 2H), 7.43 (d, J = 8.3 Hz, 2H), 2.41 (t, J = 7.0 Hz, 2H), 1.58 (m, 2H); 1.46 (m, 2H), 0.93 (t, J = 7.3 Hz, 3H); ^{13}C NMR (125 MHz, $CDCl_3$) δ (ppm):132.0, 129.2, 118.7, 110.7, 95.7, 79.4, 30.5, 22.0, 19.2, 13.6, GC-MS m/z 146 (M^{+1}).

(5-chloropent-1-yn-1-yl)benzene (7x):

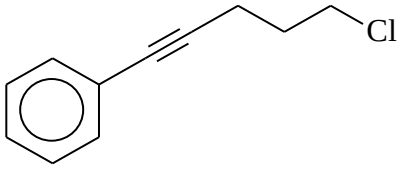

Yield 96 %; ^{1}H NMR (500 MHz, $CDCl_3$) δ (ppm): 7.36-7.34 (m, 2H), 7.25 – 7.21 (m, 3H), 3.67 (t, J = 6.4 Hz, 2H), 2.56 (t, J = 6.7 Hz, 2H), 2.02 (m, 2H); ^{13}C NMR (125 MHz, $CDCl_3$) δ (ppm):131.6, 128.3, 128.2, 127.8, 127.6, 123.5, 88.04, 81.5, 43.7, 31.4, 16.8, GC-MS m/z 178 (M^{+1}).

6-phenylhex-5-ynenitrile (7y):

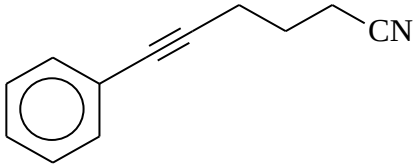

Yield 96 %; ^{1}H NMR (500 MHz, $CDCl_3$) δ (ppm): 7.34-7.32 (m, 2H), 7.24 – 7.22 (m, 3H), 2.53 (t, J = 6.7 Hz, 2H), 2.49 (t, J = 7.3 Hz, 2H), 1.89 (m, 2H); ^{13}C NMR (125 MHz, $CDCl_3$) δ (ppm):131.5, 128.2, 127.9, 123.1, 119.1, 86.8, 82.3, 24.6, 18.5, 16.1, GC-MS m/z 169 (M^{+1}).

4-phenylbut-3-yn-1-ol (7ac):

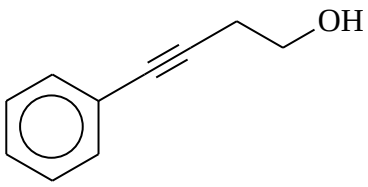

Yield 96 %; ^{1}H NMR (500 MHz, $CDCl_3$) δ (ppm): 7.39-7.37 (m, 2H), 7.27 – 7.25 (m, 2H), 3.77 (t, J = 6.1Hz, 2H), 2.65 (t, J = 6.1Hz, 2H); ^{13}C NMR (125 MHz, $CDCl_3$) δ (ppm):131.6, 128.2, 127.8, 123.3, 86.4, 82.3, 61.0, 23.7, GC-MS m/z 146 (M^{+1}).

1,4-di(hex-1-yn-1-yl)benzene:

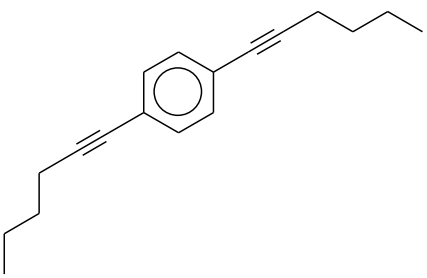

Yellow oil, Yield 96 %; ^{1}H NMR (500 MHz, $CDCl_3$) δ (ppm): 7.24 (s, 4H), 2.36 (t, *J* = 7.0 Hz, 4H), 1.53 (m, 4H), 1.42 (m, 4H), 0.89 (t, *J* = 7.3 Hz, 6H); ^{13}C NMR (125 MHz, $CDCl_3$) δ (ppm):131.3, 123.2, 91.8, 80.3,

30.8, 22.0, 19.2, 13.6; IR (CH_2Cl_2, *v* cm^{-1}*);*3055, 2935, 2394, 2301, 1712, 1657, 1405, 1265, 1064, 740; GC-MS m/z 238 (M^{+1}).

6, 6'-benzene-1,4-diylbishex-5-ynenitrile :

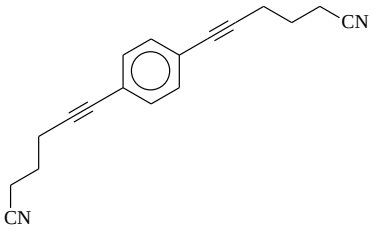

Yellow oil, Yield 95 %; ^{1}H NMR (500 MHz, $CDCl_3$) δ (ppm): 7.29 (s, 4H), 2.59 (t, *J* = 6.7 Hz, 4H), 2.53 (t, *J* = 7.3 Hz, 4H), 1.94 (m, 4H); ^{13}C NMR (125 MHz, $CDCl_3$) δ (ppm):132.2, 123.5, 119.8, 89.4, 82.8, 25.2, 19.3, 16.9; IR (CH_2Cl_2, *v* cm^{-1}*);* GC-MS m/z 260 (M^{+1}).

1,4-bis(5-chloropent-1-yn-1-yl)benzene :

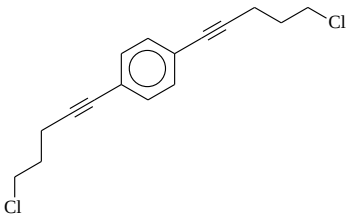

Yellow oil, Yield 96 %; ^{1}H NMR (500 MHz, $CDCl_3$) δ (ppm): 7.24 (s, 4H), 4.0 (t, *J* = 6.4 Hz, 4H), 2.54 (t, *J* = 6.7 Hz, 4H), 1.98 (m, 4H); ^{13}C NMR (125 MHz, $CDCl_3$) δ (ppm):131.3, 122.9, 89.7, 81.2, 43.7, 31.3, 16.9; IR (*v* cm^{-1}) 2947, 2230, 1915, 1706, 1501, 1437, 1283, 1064; GC-MS m/z 279 (M^{+1}).

1,4-bis(3,5-dimethyl-1-hex-1-yn-3-ol)benzene :

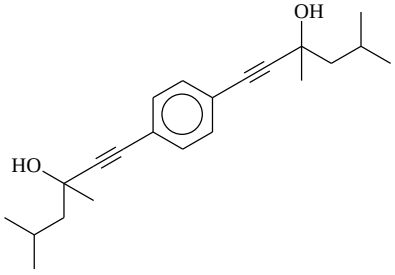

Yellow viscous oil, Yield 93 %; ^{1}H NMR (500 MHz, $CDCl_3$) δ (ppm): 7.31 (s, 4H), 1.98 (m, 2H), 1.67 (d, *J* = 6.2 Hz, 4H), 1.55 (s, 6H); 1.03 (d, *J* = 4.6 Hz, 12H), ^{13}C NMR (125 MHz, $CDCl_3$) δ (ppm):131.4, 122.6, 95.0, 83.1, 68.5, 51.9, 30.9, 25.2, 24.2; IR (*v* cm^{-1}) 3373, 2953, 2225, 1910, 1658, 1457, 1367, 1153, 926, 834; GC-MS m/z 326 (M^{+1}).

1,1'-(octa-1,7-diyne-1,8-diyldibenzene-4,1-diyl)diethanone :

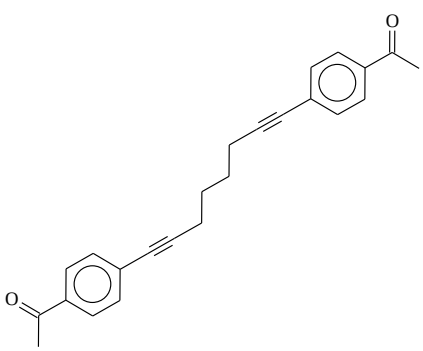

White solid, Yield 92 %; ^{1}H NMR (500 MHz, $CDCl_3$) δ (ppm): 7.85 (d, *J* = 8.6 Hz, 4H), 7.44 (d, *J* = 8.3 Hz, 4H), 2.56 (s, 6H), 2.49 (t, *J* = 6.4 Hz, 4H), 1.79 (m,4H), ^{13}C NMR (125 MHz, $CDCl_3$) δ (ppm):197.4, 135.7, 131.7, 128.9, 128.1, 93.6, 80.5, 27.7, 26.6, 19.1; GC-MS m/z 342 (M^+).

1,4-di(hex-1-yn-1-yl)benzene :

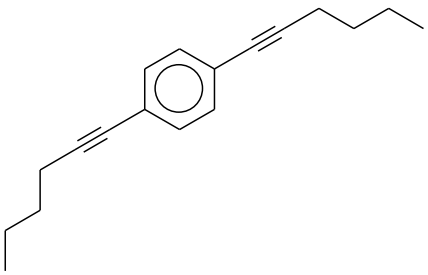

Yellow oil, Yield 96 %; ^{1}H NMR (500 MHz, $CDCl_3$) δ (ppm): 7.24 (s, 4H), 2.36 (t, *J* = 7.0 Hz, 4H), 1.53 (m, 4H), 1.42 (m, 4H), 0.89 (t, *J* = 7.3 Hz, 6H); ^{13}C NMR (125 MHz, $CDCl_3$) δ (ppm):131.3, 123.2, 91.8, 80.3, 30.8, 22.0, 19.2, 13.6; IR (CH_2Cl_2, *v* cm^{-1}*);*3055, 2935, 2394, 2301, 1712, 1657, 1405, 1265, 1064, 740; GC-MS m/z 238 (M^{+1}).

5.2.4 General procedure for supported palladium-bis(oxazoline) catalyzed Suzuki-Miyaura coupling reaction

Aryl halide (1.0 mmol), aryl boronic acid (1.2 mmol), potassium carbonate (2.0 mmol), DMF (2.0 mL) and distilled water (2.0 mL) were added in a 10 mL round bottom flask. Immobilized palladium bis(oxazoline) catalyst contained in a dialysis bag (0.0050 mmol) was introduced. The mixture was stirred at 80 ^{o}C. The progress of the reaction was monitored by the gas chromatography. After completion of the reaction, the catalyst bag

was removed and dialyzed in DMF to extract all the products. The combined solutions was extracted with ethyl acetate. The combined ethyl acetate extract was dried over anhydrous magnesium sulfate. The solvent was removed under reduced pressure using a rotary evaporator. The crude product was purified by silica gel column chromatography using hexane-EtOAc as eluent.

5.2.5 General procedure for supported Pd-BOX catalyzed Mizoroki-Heck coupling reaction

A mixture of aryl halide (1.0 mmol), alkene (1.5 mmol), KOH (2.0 mmol), DMF (2.0 mL) and distilled water (2.0 mL) was added in a 10 mL round bottom flask. Immobilized palladium bis(oxazoline) catalyst contained in a dialysis bag (0.0050 mmol) was introduced. The mixture was stirred at 80 ^{o}C. The progress of the reaction was monitored by the gas chromatography. After the completion of the reaction, the catalyst bag was removed and dialyzed in DMF to extract all the products. The combined solutions was extracted with ethyl acetate. The combined ethyl acetate extract was dried over anhydrous magnesium sulfate. The solvent was removed under reduced pressure using a rotary evaporator. The crude product was purified by silica gel column chromatography using hexane-EtOAc as eluent.

5.2.6 General procedure for supported Pd-BOX catalyzed Sonogashira coupling reaction

A mixture of aryl halide (1.0 mmol), alkyne (1.5 mmol), KOH (2.00 mmol) acetonitrile (2 mL) and distilled water (2 mL) were added to a flask. Immobilized palladium bis(oxazoline) catalyst contained in a dialysis bag (0.0050 mmol) was introduced. The mixture was stirred at 60 ^{o}C for the required time. After completion of the reaction, the catalyst bag was removed and dialyzed in acetonitrile to extract all the products. The combined solutions was extracted with ethyl acetate. The combined ethyl acetate extract was dried over anhydrous magnesium sulfate. The solvent was removed under reduced pressure in a rotary evaporator. The residue was purified using column chromatography with hexane-EtOAc as eluent to afford the cross coupling product in excellent yield.

5.2.7 General procedure for catalyst recycling using dialysis bag

The reusability of the supported palladium bis(oxazoline) catalyst was studied for Suzuki-Miyaura, Mizoroki-Heck and Sonogashira cross coupling reactions. Membrane piece was soaked in distilled water for five minutes and squeezed open. The bag was tied from the bottom. The required quantity of the catalyst and a magnetic stir bar were placed. The bag was then tied from the top. The catalyst bag was placed in a flask containing the appropriate reactants. The flask was mounted on a hot plate equipped with magnetic stirring. At the end of each circle, the catalyst bag was removed from the reaction flask and dialysed in a fresh solvent to remove all traces of reactants and product. The catalyst bag was then placed in another flask containing fresh substrates for the subsequent run. The same cleaning

procedure was repeated after each cycle. After the sixth cycle, the catalyst was removed from the dialysis bag, washed successively with water, acetone and methanol. The catalyst was dried in an oven at 100 ^{o}C and then placed in a new dialysis bag for subsequent cycles.

5.3 Results and Discussions

5.3.1 Palladium-bis(oxazoline) catalyzed Suzuki-Miyaura coupling reaction

The catalytic activities of the new palladium-bis(oxazoline) catalyst in Suzuki-Miyaura coupling reactions of arylboronic acids and aryl halides were carefully studied. Different arylboronic acids and aryl iodides, aryl bromides and aryl chlorides were considered in this reaction.

In order to optimize the experimental conditions, different experiments were performed at room temperature and under aerobic condition using 4-iodoacetophenone and phenylboronic acid as model substrates, and various palladium catalysts including Pd-BOX catalysts. The effect of varying the solvents was primarily investigated by using Pd-BOX-1 as a catalyst and the results are summarized in table 9. Low conversion (25 %) was observed when neat DMF was used as a solvent (Table 9, entry 1). However, the addition of water drastically increased the yield of the product. A full conversion was obtained at the equal ratio of DMF: H_2O (1:1) (Table 9, entry 2). The yield decreased severely to 18 % in neat water (Table 9, entry 3). Other solvent systems such as dioxane-water and acetonitrile-water gave low yields (38 % and 28 %, respectively) (Table 9, entries 4 and 5).

The presence of a base is essential for the palladium-catalyzed cross coupling reactions because it promotes the transmetallation in the catalytic cycle [167]. A control experiment in the absence of any base has only yielded traces of product (Table 9, entry 6). Various common bases such as K_2CO_3, Et_3N, KOH, KH_2PO_4 and K_3PO_4 (Table 9, entries 2, 7-10) were considered. Excellent yields were obtained with K_2CO_3 and K_3PO_4 (Table 9, entries 2 and 10). On the other hand, the activity of the catalyst system showed a weaker performance when Et_3N (20%), KOH (50%) or KH_2PO_4 (6%) was used as a base (Table 9, entries 7-9).

In addition, we have compared the catalytic activities of various palladium complexes under the same coupling reactions. As expected, only traces of product were observed when the reaction was performed in the absence of a palladium catalyst (Table 9, entry 11). We have examined the Suzuki-Miyaura coupling reaction by considering all the newly synthesized Pd-BOX complexes (Pd-BOX-1 to Pd-BOX-7) and some commercially available palladium(II) complexes having bidentate nitrogen donor ligands such as (2, 2'-bipyridine) dichloridopalladium(II) ($PdCl_2$-Bipy) and (1,10-phenanthroline) dichoridopalladium(II) ($PdCl_2$-Phen), and also bis(triphenylphosphino) dichloridopalladium(II), $Pd(PPh_3)_2Cl_2$, and bis(benzonitrile) dichloridopalladium(II), $Pd(PhCN)_2Cl_2$, under the optimized experimental conditions. The results showed that all Pd-BOX complexes gave excellent yields of products [Pd-BOX-2 (97%), Pd-BOX-3 (96%) Pd-BOX-4 (97%), Pd-BOX-5 (98%), Pd-Box-6 (97%) and Pd-BOX-7 (97%)] (Table 9, entries 12 - 17). On the other hand, a lower yield was obtained with $PdCl_2$-Phen (40%), $Pd(PPh_3)_2Cl_2$ (47%), $Pd(PhCN)_2Cl_2$ (68%) and only traces of product were detected with $PdCl_2$-Bpy (Table 9, entries 18, 19, 20 and 21). The results illustrate that the

type and the structure of the dinitrogenated ligands play a key role in the catalyst activity towards Suzuki-Miyaura cross coupling reactions. The bisoxazolines (BOX) ligands demonstrated prominently higher performance over many well-known dinitrogenated ligands, specifically 2,2'-bipyridine, 1,10-phenanthroline and pyridine triazole [137]. Moreover, the air and moisture stable Pd-BOX catalysts showed advantages in terms of the catalytic activity, the diversity of substrates, the reaction temperature, and the reaction time as compared to catalyst system based on palladium-phosphine complexes [181-183]. The high performance of this new system was then further compared to a recent study [184], where an active ligand-free system for the Suzuki-Miyaura coupling reaction in aqueous DMF was reported. Nonetheless, a higher catalyst loading (1.0 mol%) and a longer reaction time are required for bromo substrates.

TABLE 9. Suzuki-Miyaura Coupling Reaction of 4-Iodoacetophenone with Phenylboronic Acid. Optimization of Reaction Conditions.

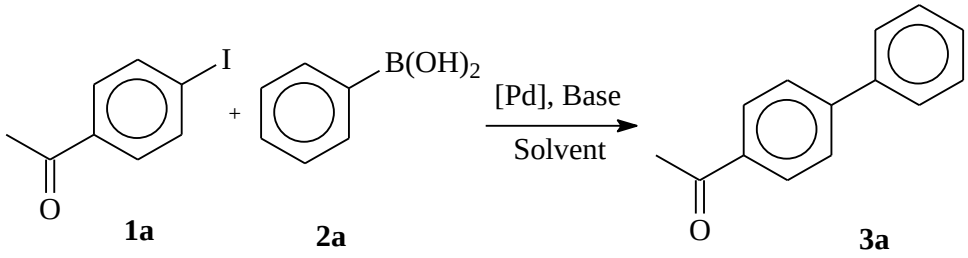

1a **2a** **3a**

Entry	Pd-Complex	Solvent-(mL)	Base	Yield (%)[b]
1	Pd-BOX-1	Neat DMF	K_2CO_3	25
2	Pd-BOX-1	DMF-H_2O (1:1)	K_2CO_3	98
3	Pd-BOX-1	Neat H_2O	K_2CO_3	18
4	Pd-BOX-1	Dioxane-H_2O (1:1)	K_2CO_3	38
5	Pd-BOX-1	CH_3CN-H_2O (1:1)	K_2CO_3	28
6	Pd-BOX-1	DMF-H_2O (1:1)	-	Traces
7	Pd-BOX-1	DMF-H_2O (1:1)	Et_3N	20
8	Pd-BOX-1	DMF-H_2O (1:1)	KOH	50
9	Pd-BOX-1	DMF-H_2O (1:1)	KH_2PO_4	6
10	Pd-BOX-1	DMF-H_2O (1:1)	K_3PO_4	95
11	-	DMF-H_2O (1:1)	K_2CO_3	Traces
12	Pd-BOX-2	DMF-H_2O (1:1)	K_2CO_3	97
13	Pd-BOX-3	DMF-H_2O (1:1)	K_2CO_3	96
14	Pd-BOX-4	DMF-H_2O (1:1)	K_2CO_3	96
15	Pd-BOX-5	DMF-H_2O (1:1)	K_2CO_3	98
16	Pd-BOX-6	DMF-H_2O (1:1)	K_2CO_3	97
17	Pd-BOX-7	DMF-H_2O (1:1)	K_2CO_3	97
18	$PdCl_2$-Bpy	DMF-H_2O (1:1)	K_2CO_3	Traces
19	$Pd(PPh_3)_2Cl_2$	DMF-H_2O (1:1)	K_2CO_3	47

20	$Pd(PhCN)_2Cl_2$	DMF-H_2O (1:1)	K_2CO_3	68
21	$PdCl_2$-Phen	DMF-H_2O (1:1)	K_2CO_3	40

a. Reaction conditions: [Pd] (0.0020 mmol), phenylboronic acid (1.50 mmol), 4-iodoacetophenone (1.0 mmol), base (2.0 mmol), solvent (8.0 mL), 20 minutes, R. T.

b. Isolated yield.

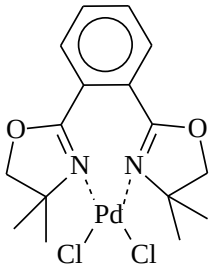

Pd-BOX-1

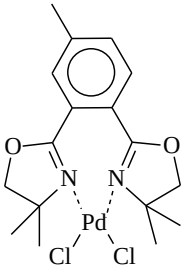

Pd-BOX-2

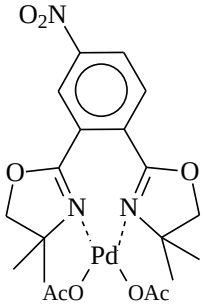

Pd-BOX-3

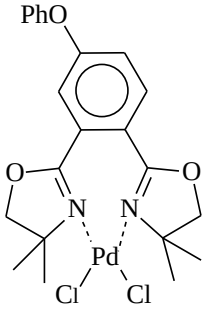

Pd-BOX-4

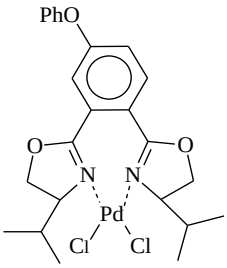

Pd-BOX-5

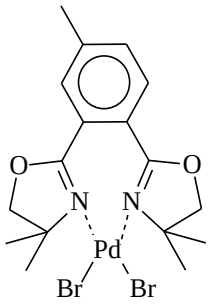

Pd-BOX-6

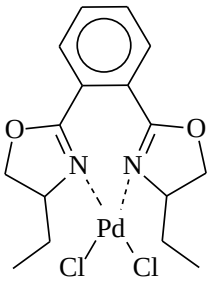

Pd-BOX-7

The exceptional catalytic activity observed with Pd-BOX complexes could be attributed to both electronic and steric effects. Electronic effects are induced by the aromatic spacer and the oxazoline rings, which enrich the palladium center [185]. While the steric effects originate from the substituents on the oxazoline rings, they provide kinetic stability to the intermediate complex, which supports an effective reductive elimination [170]. Another factor that might play an important role is the solubility of Pd-BOX complexes in the solvent. Whereas many palladium complexes with dinitrogenated ligands are less soluble in DMF-H_2O, the presence of the polar oxazoline rings in BOX enhances the solubility of Pd-BOX complexes. This advantage may result in increasing the rate of the oxidative addition and the reductive elimination steps.

The above-mentioned results encouraged us to examine the Suzuki-Miyaura coupling reactions of a broad range of substrates to determine the specificity and scope of substrates in the presence of Pd-BOX as a catalyst and DMF-H_2O (1:1) as a solvent system at room temperature. Thus, various arylboronic acids were reacted with a diverse array of arylhalides including aryl iodides, aryl bromides and aryl chlorides, and the results are summarized in table 10. Aryl iodides having either activating or deactivating groups reacted smoothly affording the cross coupling products in excellent isolated yields (93-99%) (Table 10, entries 1-9). Various functional groups were tolerated with the new catalytic system. Interestingly, the catalytic system worked effectively in the coupling of hydroxyl phenylboronic acid with aryl iodide affording the corresponding product in almost quantitative yield (Table 10, entries 3 and 6). The coupling reactions were also successful at room temperature with aryl bromides having activating and deactivating groups (CHO, COR, CN CH_3, OCH_3) leading to the corresponding biphenyl products in

high isolated yields (Table 10, entries 11-14). However, lower reactivity was observed with the aryl chlorides. Thus, a higher temperature (110 ^{o}C) and longer reaction time were required to obtain excellent yields (Table 10, entries 15-19).

The effect of varying the substituents on the arylboronic acids was also investigated. In contrast to aryl halides, arylboronic acids containing electron donating substituents react slightly faster than those with electron withdrawing substituents. However, the overall electronic effect of the arylboronic acids with the Pd-BOX-catalyzed Suzuki-Miyaura reaction was rather not very significant.

TABLE 10. Suzuki-Miyaura Coupling Reaction of Various Aryl Halides with Different Arylboronic Acids Using Pd-BOX-1 as a Catalyst.

Entry	Aryl halide 1a-l	Arylboronic acid 2a-e	Coupling Product 3a-o	Time (min)	Yield (%)[b]
1	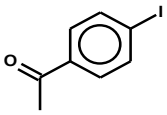 **1a**	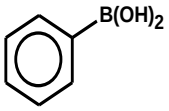 **2a**	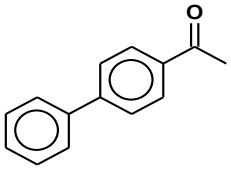 **3a**	20	98
2	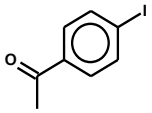 **1a**	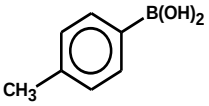 **2b**	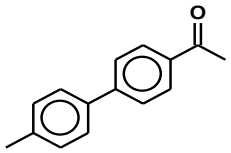 **3b**	20	99
3	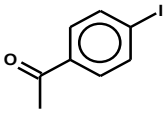 **1a**	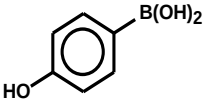 **2c**	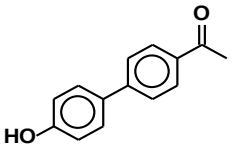 **3c**	20	97
4	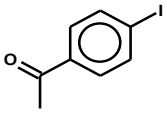 **1a**	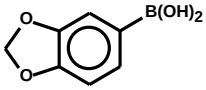 **2d**	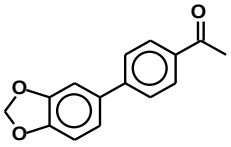 **3d**	20	97
5	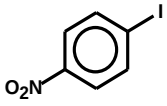 **1b**	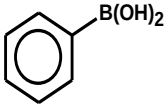 **2a**	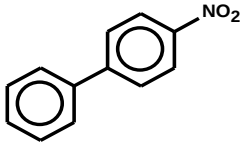 **3e**	20	96
6	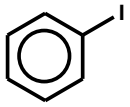 **1c**	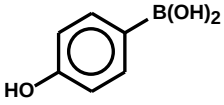 **2c**	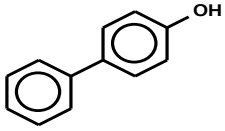 **3f**	20	96

a. Reaction Conditions: Pd-BOX-1 (0.0020 mmol), arylboronic acid (1.5 mmol), aryl halide (1.0 mmol), K_2CO_3 (2.0 mmol), DMF (4.0 mL), H_2O (4.0 mL), R.T.

7	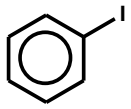 **1c**	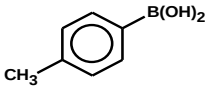 **2b**	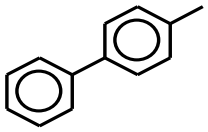 **3g**	90	95
8	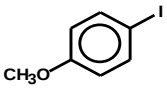 **1d**	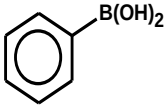 **2a**	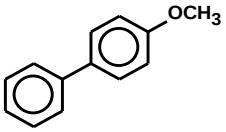 **3h**	90	93
9	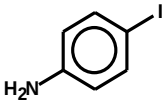 **1e**	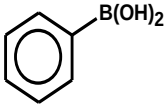 **2a**	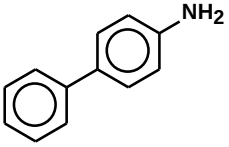 **3i**	90	94
10	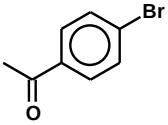 **1f**	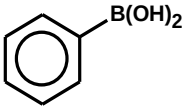 **2a**	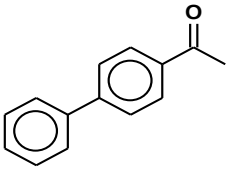 **3a**	60	99
11	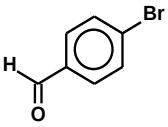 **1g**	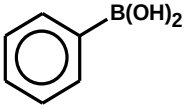 **2a**	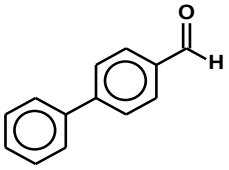 **3k**	60	99
12	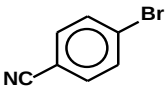 **1h**	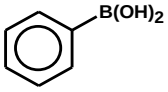 **2a**	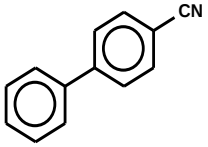 **3l**	60	98
13	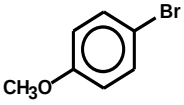 **1i**	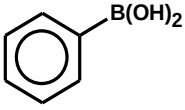 **2a**	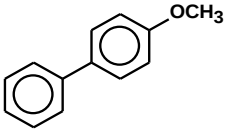 **3h**	120	95
14	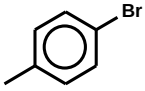 **1j**	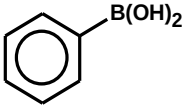 **2a**	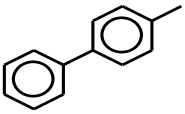 **3g**	120	98

b.Isolated Yield.
c. 110 ^{o}C.

15[c]	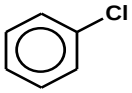 **1k**	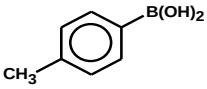 **2b**	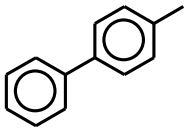 **3g**	12 h	89
16[c]	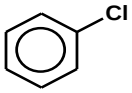 **1k**	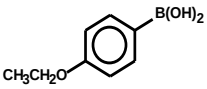 **2e**	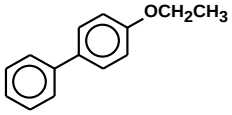 **3m**	12 h	87
17[c]	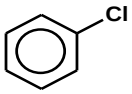 **1k**	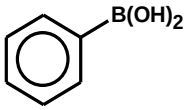 **2a**	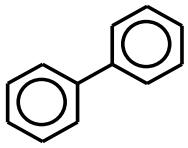 **3n**	12 h	72
18[c]	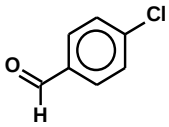 **1l**	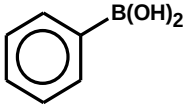 **2a**	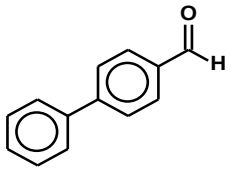 **3k**	12 h	95
19[c]	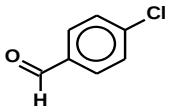 **1l**	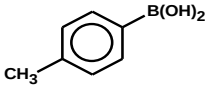 **2b**	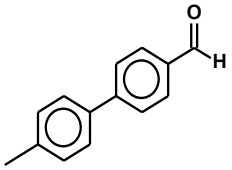 **3o**	12 h	96

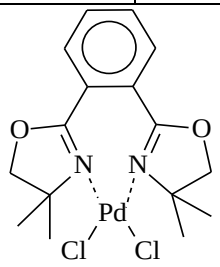

Pd-BOX-1

Suzuki-Miyaura coupling reaction of p-tolylboronic acid with iodobenzene. Recycling ability of the catalyst system

Homogeneous catalysis is widely accepted for the high selectivity, activity and low catalyst loading. However, homogeneous catalysts are associated with the difficulty in separating

and reuse of the transition metal catalyst, which leads to the increase of the cost of production [37].

Nowadays, most chemical industries are turning towards systems that can be easily recycled. The recycling ability of the homogeneous catalytic system comprising Pd-BOX in DMF-H_2O was investigated in the Suzuki-Miyaura coupling reaction of iodobenzene with p-tolylboronic acid at 70 ^oC for 1 h. The results of the recycling experiments are presented on the Figure 24.

After the first cycle of the coupling reaction, the product was extracted three times (3 x 5 ml) with n-hexane. The DMF-aqueous phase was charged with a fresh substrate and a base and the coupling reaction was carried out again under the same experimental conditions. Remarkably, the catalytic system could be recycled for at least twelve times without bearing any loss in the catalytic activity. We have not been able yet to identify the stable and active palladium intermediate species in the catalytic cycle, which was responsible for the high recycling ability of the catalyst system. More studies are required in order to identify such palladium active species. However, it is important to mention that the high recycling ability of the catalytic system is so far limited to non-polar substrates, since the products can be easily separated by extraction without any loss of the Pd-BOX catalyst from the DMF-H_2O phase. The turnover frequency of the Pd-BOX-1 is estimated for the 12 cycles as 3000/h. In order to confirm the efficiency of the Pd-BOX-1 catalyst, we have conducted an experiment with a ratio of iodobenzene (4.0 mmol) to Pd-BOX-1 catalyst (0.002 mmol) equal to 2000 for 40 minutes. A complete conversion of iodobenzene and excellent isolated yield of product (98%) were observed. Again, the turnover frequency of the Pd-BOX-1 catalyst in the later experiment is estimated as 3000/h.

These interesting preliminary results urged us to undertake a further research study that led to the development of a supported catalyst system which is a more general recycling system and was applied on a wide range of substrates. The application of the supported palladium-bis(oxazoline) system will be described in the later part of this chapter.

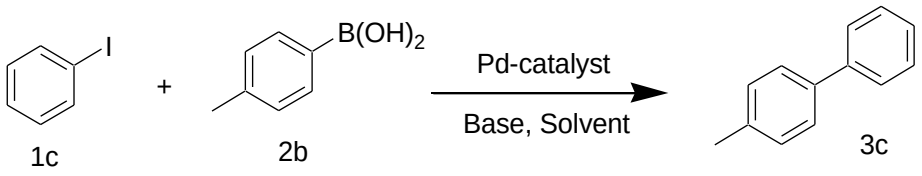

1c + 2b → 3c

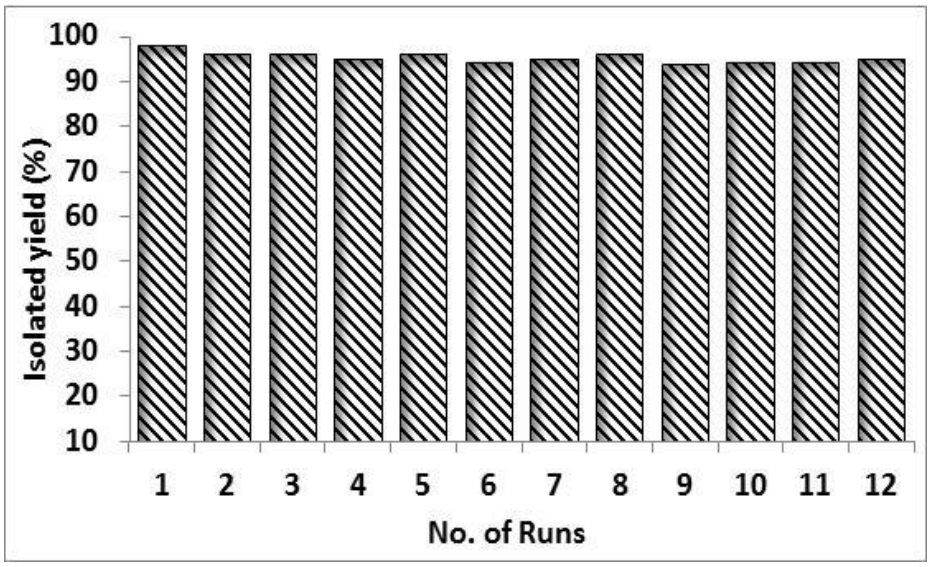

Figure 24: Pd-BOX-1 Catalyzed Suzuki-Miyaura Coupling Reaction of Iodobenzene with *p*-Tolyl boronic Acid. Recycling Ability of the Catalyst System

Reaction conditions: Pd-BOX-1 (0.0040 mmol), p-tolylboronic acid (1.5 mmol), iodobenzene (1.0 mmol), K_2CO_3 (2.0 mmol), DMF (4.0 mL), H_2O (4.0 mL), 70 ^oC, 1 h.

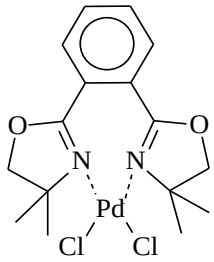

Pd-BOX-1

5.3.2 Pd-BOX catalyzed Mizoroki-Heck coupling reactions of Alkenes with aryl iodides

The cross coupling reactions of aryl halides with olefins catalyzed by palladium complexes, known as Mizoroki-Heck reaction, is a well-known and widely used methodology for the regioselective synthesis of unsaturated compounds under mild conditions [186, 187].

The catalytic activities of the new palladium-bis(oxazoline) complexes in Mizoroki-Heck coupling reactions of alkenes and aryl halides were carefully studied. Several aryl halides styrenes and acrylates were also considered in this reaction.

In order to determine the most suitable experimental conditions, iodobenzene and styrene were considered as model substrates (Table 11). Different palladium catalysts including Pd-BOX complexes were used. The effect of varying the solvents was investigated by using Pd-BOX-6 as a catalyst. In the absence of water (neat DMF, Table 11, entry 1), only 50% isolated yield was achieved. However, in DMF-H_2O (3:1 mL) (Table 11, entry 2), the coupling product was obtained in quantitative yield. Only traces of product were detected in neat water (Table 11, entry 3).

TABLE 11. Mizoroki-Heck Coupling Reactions of Iodobenzene with Styrene.

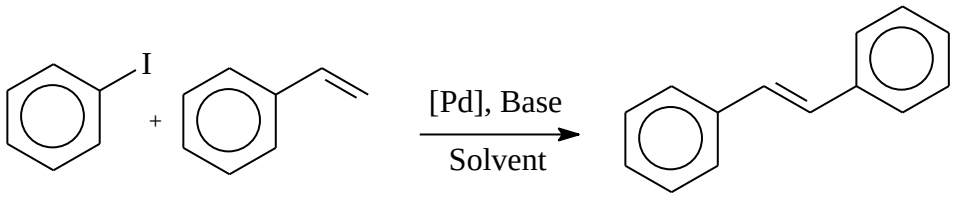

1c **4a** **5a**

Entry	Pd-Complex	Solvent	Base	Yield (%)[b]
1	Pd-BOX-6	Neat DMF (4 mL)	KOH	50
2	Pd-BOX-6	DMF-H_2O (3-1 mL)	KOH	99
3	Pd-BOX-6	Neat water	KOH	9
4	Pd-BOX-6	Dioxane-H_2O (3-1 mL)	KOH	20
5	Pd-BOX-6	DMF-H_2O (3-1 mL)	K_2CO_3	84
6	Pd-BOX-6	DMF-H_2O (3-1 mL)	Et_3N	64
7	-	DMF-H_2O (3-1 mL)	KOH	Traces
8	Pd-BOX-1	DMF-H_2O (3-1 mL)	KOH	95
9	Pd-BOX-2	DMF-H_2O (3-1 mL)	KOH	97
10	Pd-BOX-3	DMF-H_2O (3-1 mL)	KOH	98
11	Pd-BOX-4	DMF-H_2O	KOH	98

		(3-1 mL)		
12	Pd-BOX-5	DMF-H_2O (3-1 mL)	KOH	96
13	Pd-BOX-7	DMF-H_2O (3-1 mL)	KOH	96
14	$PdCl_2$- Bpy	DMF-H_2O (3-1 mL)	KOH	70
15	$PdCl_2$- Phen	DMF-H_2O (3-1 mL)	KOH	56
16	$Pd(PPh_3)_2Cl_2$	DMF-H_2O (3-1 mL)	KOH	80
17	$Pd(PhCN)_2Cl_2$	DMF-H_2O (3-1 mL)	KOH	62

a.Reaction conditions: [Pd] (0.010 mmol), iodobenzene (1.00 mmol), styrene (1.50 mmol), KOH (2.00 mmol), solvent (4 mL), 90 ^oC, 2 h.

b.Isolated yield.

In addition, we have compared the catalytic activity of various palladium complexes in the Mizoroki-Heck coupling reaction. As expected, no product was formed when the reaction was performed in the absence of palladium catalyst (Table 11, entry 7). We have examined Mizoroki-Heck coupling reaction by considering Pd-BOX complexes (Pd-BOX-1 to Pd-BOX-7) [188], and some commercially available palladium complexes having bidentate nitrogen donor ligands such as $PdCl_2$-Bipy and $PdCl_2$-Phen, and also $Pd(PPh_3)_2Cl_2$ and $Pd(PhCN)_2Cl_2$ under the optimized experimental conditions [189]. All Pd-BOX complexes gave again excellent isolated yields (96-98%) of product (Table 11, entries 8 to 13). However, lower isolated yields were obtained with $PdCl_2$-Bpy (70%) and $PdCl_2$-Phen (56%), $Pd(PPh_3)_2Cl_2$ (80%) and $Pd(PhCN)_2Cl_2$ (62%) (Table 11, entries 14-17).

Amino oxazolines were previously used as potential ligands for Mizoroki-Heck coupling reaction [189, 190]. However, higher temperature (140 ^oC) and longer reaction time (40 h) were required to reach high conversions. We can conclude that the new Pd-BOX catalysts showed to certain extent higher catalytic activity in the Mizoroki-Heck coupling reaction at relatively milder reaction conditions of temperature and reaction time as compared to palladium nitrogen or palladium phosphine [72, 191] catalysts, where longer reaction time (6-40 h) and higher temperature (120-140 ^oC) are sometimes applied to obtain high yield.

The coupling reaction was then extended to a broad range of substrates to determine the scope of the newly developed catalytic system. Thus, various aryl halides were reacted with different styrene derivatives and with methyl acrylate. The results are summarized in table 12. As expected, the time required to complete the reaction depends on the substituent attached to either the aryl iodide and/or the alkene. Aryl iodides having either activating or deactivating groups as substituent reacted smoothly affording the cross coupling product

in excellent isolated yield. The reaction of iodobenzene with methyl acrylate (Table 12, entry 7) under the optimized reaction condition led to the hydrolysis of the ester and the corresponding carboxylic acid was obtained. The hydrolysis of the ester was avoided when the reaction was conducted in neat DMF. Though, longer reaction time (12 h) was required. Various aryl esters were obtained in excellent isolated yield (Table 12, entries 8-12).

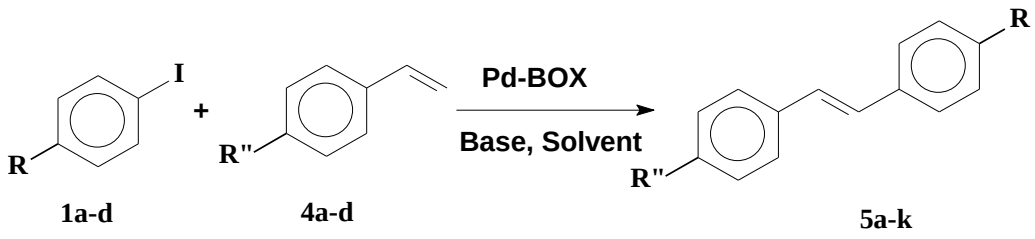

1a-d **4a-d** **5a-k**

Eq. 4

TABLE 12. Mizoroki-Heck Coupling Reactions of Styrene Derivatives with Aryl Iodides Using Pd-BOX-6 as Catalyst.

Entry	Aryl Iodide 1a-d	Olefin 4a-d	Coupling Product 5a-k	Time (h)	Yield (%)[b]
1	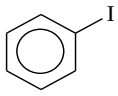 **1c**	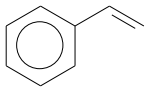 **4a**	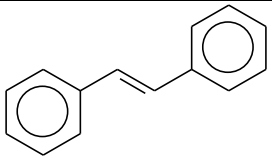 **1a**	2	99
2	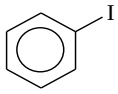 **1c**	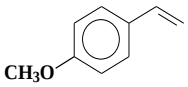 **4b**	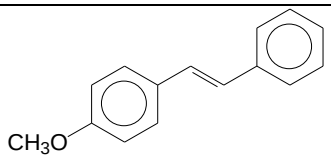 **5b**	1.5	96
3	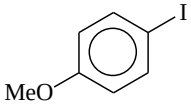 **1d**	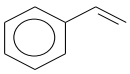 **4a**	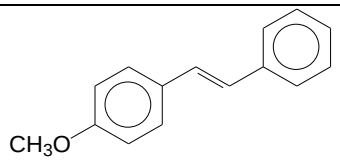 **5b**	2.5	96
4	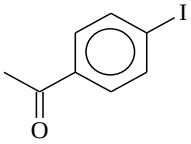 **1a**	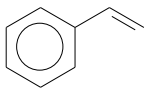 **4a**	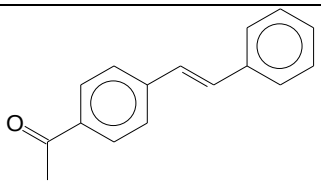 **5c**	2	96

a. Reaction Conditions: **Pd-BOX-6** (0.0100 mmol), Aryl iodide (1.00 mmol), styrene derivative (1.50 mmol), KOH (2.00 mmol), DMF-H_2O (3-1 mL), 90 ^oC.

5	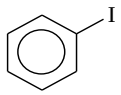 **1c**	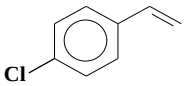 **4c**	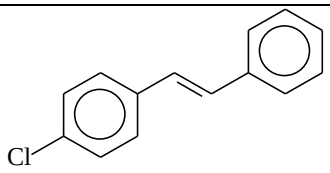 **5d**	2	96
6	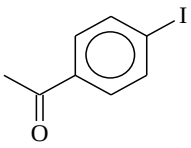 **1a**	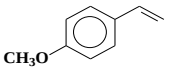 **4a**	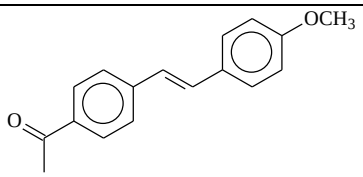 **5e**	1	98
7	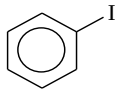 **1c**	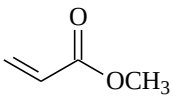 **4d**	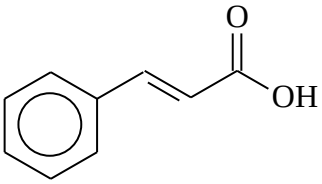 **5f**	2	95
8[c]	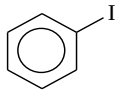 **1c**	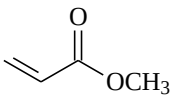 **4d**	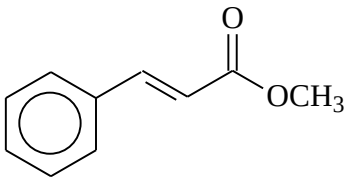 **5g**	12	96
9[c]	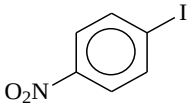 **1b**	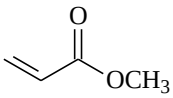 **4d**	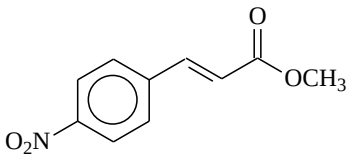 **5h**	12	97
10[c]	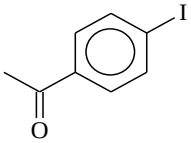 **1a**	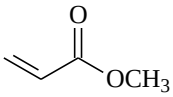 **4d**	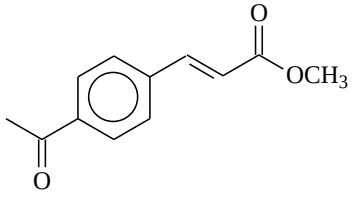 **5i**	12	96

b. Isolated yield.

c. Reaction Conditions: **Pd-BOX-4** (0.0100 mmol), aryl halide (0.500 mmol), olefin (0.750 mmol), K_2CO_3 (2.00 mmol), DMF (5.0 mL), 70 ^oC, 12 h.

11[c]	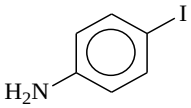 **1e**	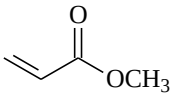 **4d**	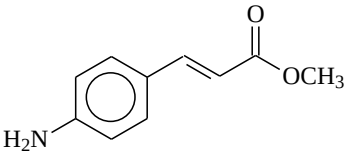 **5j**	12	94
12[c]	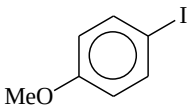 **1d**	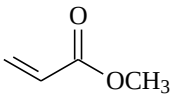 **4d**	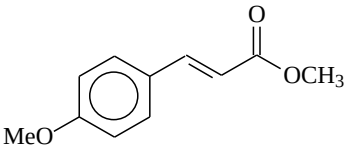 **5k**	12	94

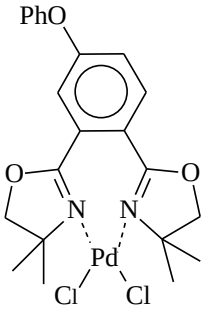

Pd-BOX-4

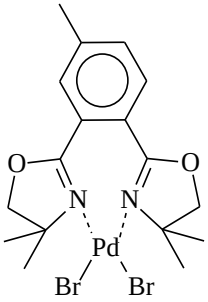

Pd-BOX-6

5.3.3 Palladium-bis(oxazoline) catalyzed Sonogashira coupling reaction of iodobenzene with alkynes

The catalytic activity of the new Pd-BOX complexes in Sonogashira coupling reactions of alkynes and aryl halides was carefully studied. The coupling reaction of several aryl iodides with various aryl alkynes, alkyl alkynes and dialkynes were evaluated.

In order to determine the best experimental conditions, different experiments were performed at room temperature and under aerobic conditions using iodobenzene and phenylacetylene as model substrates, and various palladium catalysts including Pd-BOX complexes. The results are summarized in table 13. The effect of varying the solvents was also investigated by using Pd-BOX-1 as catalyst. Similar to the Suzuki-Miyaura coupling reaction only trace of products was observed with neat water as solvent (Table 13, entry 1). It was observed that there is a gradual increase in the yields of the product when DMF was used with water as solvent (Table 13, entries 2 and 3). Remarkably, the change of the solvent to CH_3CN-H_2O led to excellent isolated yields (Table 13, entries 4 and 5). The yields decreased severely to traces in neat acetonitrile (Table 13, entry 6). Other solvent systems such as CH_3OH-H_2O gave lower yields (Table 13, entry 7).

The presence of a base is essential for palladium catalyzed Sonogashira cross coupling reaction [167]. A control experiment in the absence of any base has only yielded to traces of product (Table 13, entry 8). Bases such as KOH, NaOH, K_2CO_3, Et_3N (Table 13, entries 5, 9-11) were tested. Excellent isolated yields were (94% and 90%) obtained with KOH and NaOH, respectively (Table 13, entries 5 and 9). However, much lower yields (60%

and 47%) in product were observed with K_2CO_3 and Et_3N, respectively (Table 13, entries 10 and 11).

Having the optimized experimental reaction conditions, we have examined the Sonogashira cross coupling reaction by considering other palladium- bis(oxazoline) complexes (Pd-BOX-2 to Pd-BOX-7) (Table 13, entries 12 and 13) [135, 136] and also commercially available palladium(II) complexes and palladium(II) salts such as (2, 2'-bipyridine) dichloridopalladium(II) ($PdCl_2$-Bipy) and (1,10-phenanthroline) dichoridopalladium(II) ($PdCl_2$-Phen) (Table 13, entries 19-23). As illustrated in Table 13 (entry 18), we have observed no coupling product in the absence of palladium catalyst, indicating that palladium is necessary for the cross coupling reaction. It was found that the nature of the palladium complex had a pronounced impact on the catalyzed reaction. $Pd(OAc)_2$ (75%) (Table 13, entry 20) turned out to be slightly higher in activity than $PdCl_2$ (69%) (Table 13, entry 19), $PdCl_2$-Bipy (40%) (Table 13, entry 21) and $PdCl_2$-Phen (20%) (Table 13, entry 22). Remarkably, the yields in cross coupling products were excellent with Pd-BOX complexes as catalysts (Table 13, entries 5, 12 to 17).

TABLE 13. Palladium-Catalyzed Sonogashira Coupling Reaction of Iodobenzene with Phenylacetylene. Optimization of the Reaction Conditions.

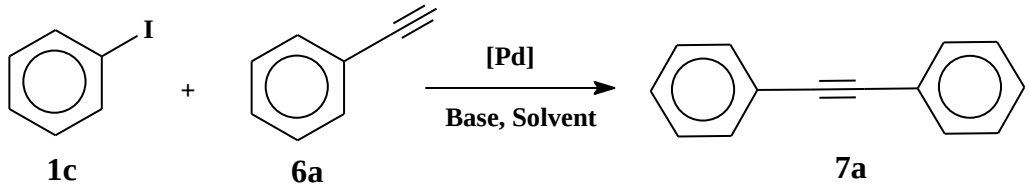

1c **6a** **7a**

Entry	Pd Complex	Solvent	Base	Yield (%)[b]
1	Pd-BOX-1	Neat H_2O (4 mL)	KOH	Traces
2	Pd-BOX-1	DMF-H_2O (3-1 mL)	KOH	27
3	Pd-BOX-1	DMF-H_2O (2-2 mL)	KOH	35
4	Pd-BOX-1	CH_3CN-H_2O (3-1 mL)	KOH	80
5	Pd-BOX-1	CH_3CN-H_2O (2-2 mL)	KOH	94
6	Pd-BOX-1	Neat CH_3CN (4 mL)	KOH	Traces
7	Pd-BOX-1	CH_3OH-H_2O (2-2 mL)	KOH	15
8	Pd-BOX-1	CH_3CN-H_2O (2-2 mL)	-	Traces
9	Pd-BOX-1	CH_3CN-H_2O (2-2 mL)	NaOH	90
10	Pd-BOX-1	CH_3CN-H_2O (2-2 mL)	K_2CO_3	60
11	Pd-BOX-1	CH_3CN-H_2O (2-2 mL)	Et_3N	47
12	Pd-BOX-2	CH_3CN-H_2O (2-2 mL)	KOH	90
13	Pd-BOX-3	CH_3CN-H_2O (2-2 mL)	KOH	93
14	Pd-BOX-4	CH_3CN-H_2O (2-2 mL)	KOH	93
15	Pd-BOX-5	CH_3CN-H_2O (2-2 mL)	KOH	94
16	Pd-BOX-6	CH_3CN-H_2O (2-2 mL)	KOH	94
17	Pd-BOX-7	CH_3CN-H_2O (2-2 mL)	KOH	93
18	-	CH_3CN-H_2O (2-2 mL)	KOH	Traces

19	$PdCl_2$	CH_3CN-H_2O (2-2 mL)	KOH	69
20	$Pd(OAc)_2$	CH_3CN-H_2O (2-2 mL)	KOH	75
21[c]	Pd-Bipy	CH_3CN-H_2O (2-2 mL)	KOH	40
22[d]	Pd-Phen	CH_3CN-H_2O (2-2 mL)	KOH	20
23	$PdCl_2(PPh_3)_2$	CH_3CN-H_2O (2-2 mL)	KOH	43

a. Reaction Conditions: Pd-catalyst (0.01 mmol), iodobenzene (1.00 mmol), phenylacetylene (1.50 mmol), Base (2.00 mmol), Solvent (4mL), RT, 2 h.

b. Isolated yield**.**

c. $PdCl_2$-Bipy = (2, 2'-bipyridine)dichloridopalladium(II).

d. $PdCl_2$-Phen = (1, 10-phenanthroline)dichoridopalladium(II).

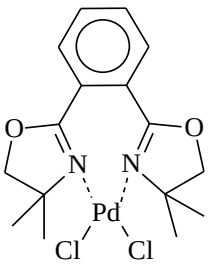

Pd-BOX-1

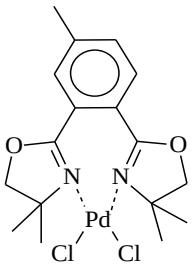

Pd-BOX-2

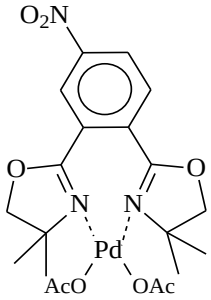

Pd-BOX-3

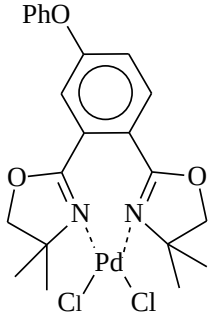

Pd-BOX-4

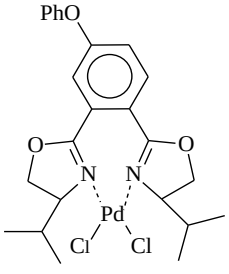

Pd-BOX-5

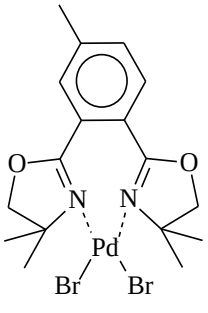

Pd-BOX-6

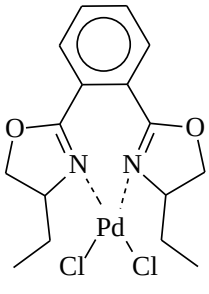

Pd-BOX-7

Pd-BOX catalyzed Sonogashira cross coupling reactions of aryl iodide with aryl alkynes

Under the optimized experimental conditions (1 mol% Pd-BOX-1, 2 equiv. KOH, 1:1 CH_3CN-H_2O, R.T), we have screened a wide range of aryl iodides with a wide array of structurally and electronically different aryl alkynes (Table 14). With respect to the aryl iodides, both activated and deactivated aryl iodides reacted smoothly with alkynes bearing electron withdrawing and electron donating substituents. The cross coupling products were obtained in excellent yields. The coupling of phenylacetylene with deactivated aryl iodides (Table 14, entries 2-5) afforded high yields of internal acetylenes after 1 h. Similarly, the coupling of 4-iodobenzonitrile with 4-ethynyl benzaldehyde (Table 14, entry 6) afforded the corresponding internal alkyne in 1 h. The coupling reactions of activated aryl iodides such as 4-iodoanisole (Table 14, entry 8) and 4-iodoaniline (Table 14, entry 9) were completed within 3 h. The synthesis of 4,4'-diaminodiphenylacetylene was achieved quantitatively from the reaction of 4-iodoaniline with 4-ethynylaniline (Table 14, entry 13).

TABLE 14. Sonogashira Coupling Reactions of Aryl Iodides with Aryl Alkynes Catalyzed by Pd-BOX-1.

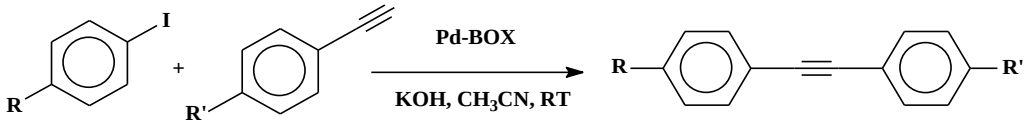

1a - 1m **6a - 6e** **7a - 7l**

Entry	Aryl Iodide 1a – 1m	Aryl Alkyne 6a – 6e	Product 7a – 7l	Time (h)	Yield (%)[b]
1	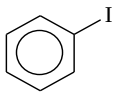 **1c**	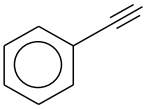 **6a**	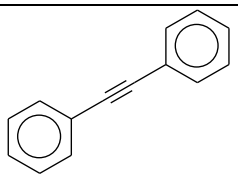 **7a**	2	94
2	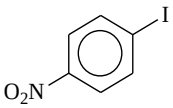 **1b**	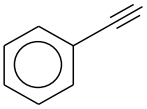 **6a**	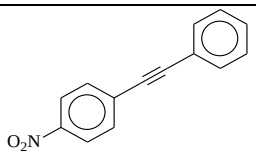 **7b**	1	98
3	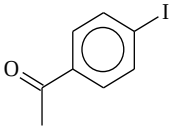 **1a**	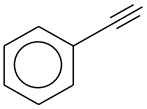 **6a**	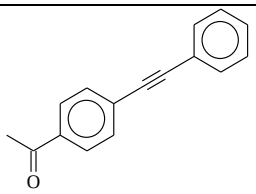 **7c**	1	96
4	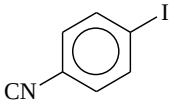 **1h**	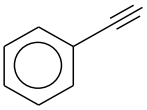 **6a**	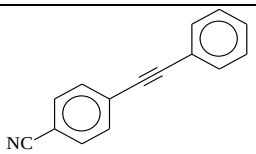 **7d**	1	97
5	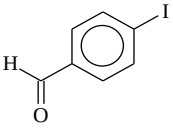 **1m**	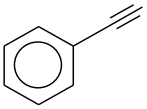 **6a**	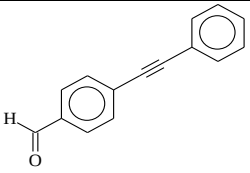 **7e**	1	95
6	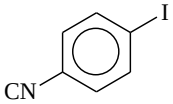 **1h**	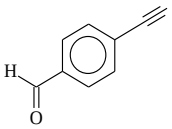 **6b**	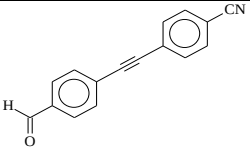 **7f**	1	98

7	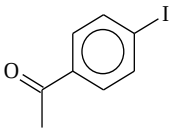 **1a**	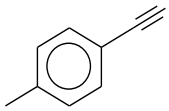 **6c**	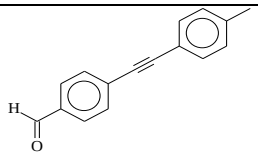 **7g**	1	98
8	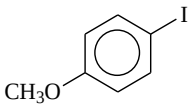 **1d**	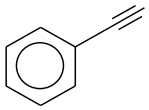 **6a**	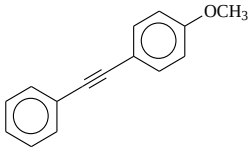 **7h**	3	91
9	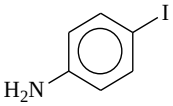 **1e**	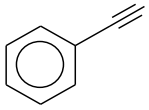 **6a**	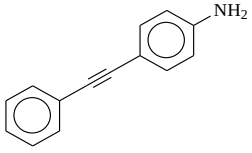 **7i**	4	90
10	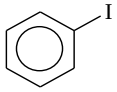 **1c**	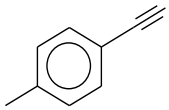 **6c**	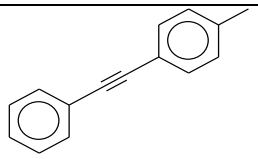 **7j**	2	93
11	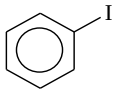 **1c**	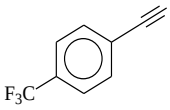 **6d**	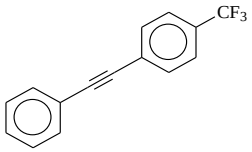 **7k**	3	88
12	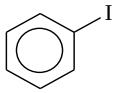 **1c**	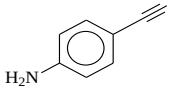 **6e**	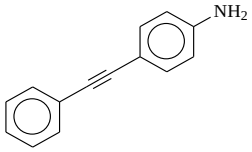 **7i**	3	96
13	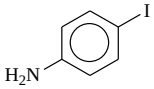 **1e**	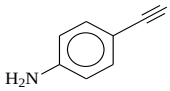 **6e**	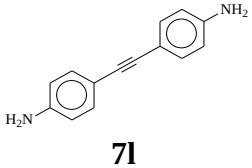 **7l**	4	88

a. Reaction Conditions: Pd-BOX-1 (0.01 mmol), aryl iodide (1.00 mmol), alkyne (1.50 mmol), KOH (2.00 mmol), CH_3CN-H_2O (2-2 mL), RT.

b. Isolated yield.

Pd-BOX catalyzed Sonogashira coupling reactions of aryl iodides with Aryl dialkynes. Synthesis of Bis(phenyl ethynyl)-benzene derivatives (BPEBs)

Bis(phenyl ethynyl)-benzene derivatives have been widely recognized as important component of liquid crystals for electronic displays [192-194]. They found wide applications in the production of note book computer screens, mobile phones, flat screen monitors and LCD televisions. BPEBs are characterized with high clearing point, high melting point and large values of optical anisotropy [195-197]. Our new catalyst system based on Pd-BOX-1 was successfully applied in the synthesis of this important class of compounds (Table 15). 1,3 and 1,4-Bis(phenylethynyl)-benzenes were obtained from the reactions of aryl iodides with 1,3- and 1,4-diethynyl benzenes (Table 15). The complete conversions were observed after 1-3 h of reactions (Table 15, entries 1, 2, 4), depending on the nature of substituents. The desired cross coupling products were isolated in excellent yields. It is worth mentioning at this point that the reactions were carried out at room temperature and the palladium catalysts showed particular air and moisture stability. This free phosphine catalytic system represents a significant advantage where the reactions are carried out in air. Moreover, the reactions were carried out in the absence of copper, therefore, no homo-coupling products of the alkynes were detected. Hence, the cross coupling products were obtained in excellent yields.

TABLE 15. Sonogashira Coupling Reaction of Aryl Iodides with Dialkynes. Synthesis of Bis(Phenyl Ethynyl)-Benzene Derivatives (BPEB'S).

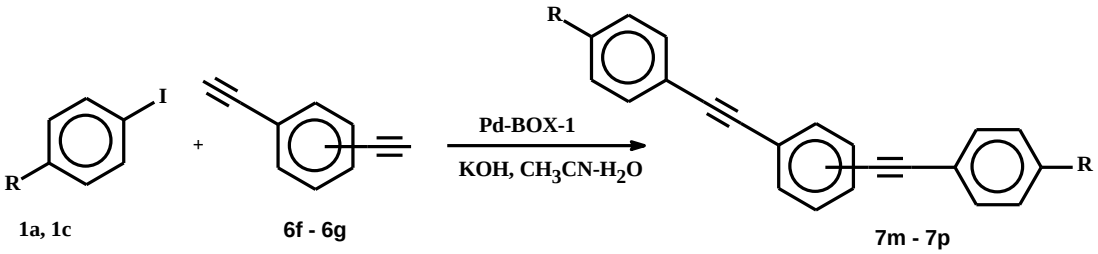

Entry	Aryl Iodide 1a, 1c	Aryl Dialkyne 6f – 6g	Time (h)	Yield (%)[b]
1	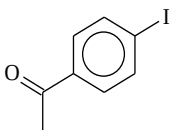 **1a**	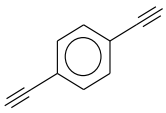 **6f**	1	97
2	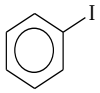 **1c**	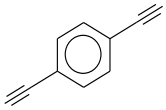 **6f**	3	90
3	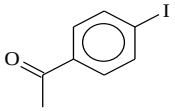 **1a**	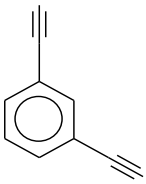 **6g**	2	97
4	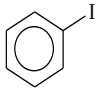 **1c**	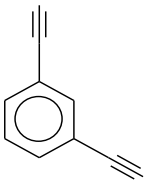 **6g**	3	89

a. Reaction Conditions: Pd-BOX-1 (0.01 mmol), aryl iodide (1.00 mmol), alkyne (0.50 mmol), KOH (2.00 mmol), CH_3CN-H_2O (2-2mL), r.t.

b. Isolated yield**.**

Sonogashira coupling reaction of aryl iodide with alkyl alkynes: Effect of various substituents

The Sonogashira cross coupling of aryl iodides with alkyl alkynes using palladium phosphine catalysts has been widely studied [87, 90, 198]. On the other hand, there are only few reports on copper and phosphine free Sonogashira cross coupling of aryl iodides with alkyl alkynes [100, 177, 199], and in few cases, high temperature was used and low yields of products were observed [87]. Interestingly, the Pd-BOX complexes were highly active in the cross coupling reactions of aryl iodides with alkyl alkynes at 60 ^{o}C. For instance, the coupling reactions of 4-iodoacetophenone with various alkyl alkynes were achieved to give the expected internal acetylenes in excellent isolated yield (Table 16, entries 1-5). The reactions rates were found to be unaffected by the length of the alkyl chain, however, phenyl substituted alkyl alkynes were more reactive (Table 16, entries 1-2). In fact, 4-iodobenzonitrile reacted with 1-hexyne in a similar manner (Table 16, entry 6). Other interesting examples are the cross coupling reaction of trimethylsilyl acetylene (Table 16, entry 11) and triphenyl silyl acetylene (Table 16, entry 12) under the same reaction conditions. The reactions have led predominantly to the corresponding aryl silyl acetylenes. These results indicated that the new catalytic system having Pd-BOX is highly effective in the coupling reactions of aryl iodides with terminal acetylenes through activation of the C-Si bond [89, 200]. Simlarly, silyloxy acetylene reacted in a comparable manner. However, the silyloxy group was hydrolyzed under the reaction conditions to give the corresponding alkynol (Table 16, entry 13). The cross coupling reaction of iodobenzene with terminal alkynol was also successful and produced the desired product in 87% isolated yield (Table 16, entry 14).

TABLE 16. Sonogashira Coupling Reactions of Aryl Iodide with Alkyl Alk

yne Catalyzed by Pd-BOX-1.

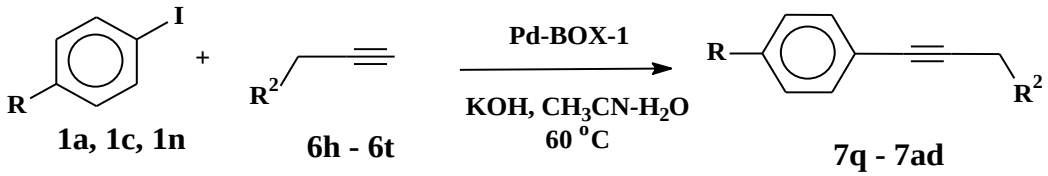

1a, 1c, 1n **6h - 6t** **7q - 7ad**

Entry	Aryl Iodide 1a, 1c, 1n	Alkyl Alkyne 6h – 6t	Product 7q – 7ad	Time (h)	Yield (%)[b]
1	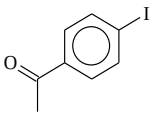 **1a**	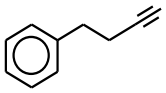 **6h**	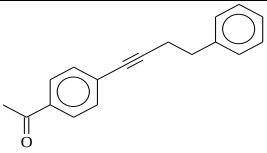 **7q**	2	98
2	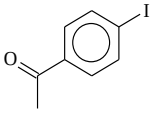 **1a**	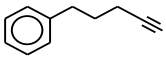 **6i**	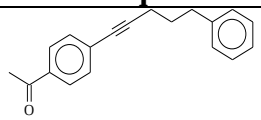 **7r**	2	96
3	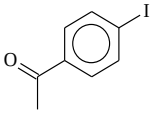 **1a**	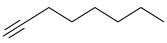 **6j**	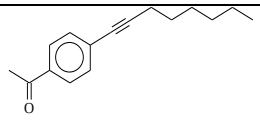 **7s**	3	95
4	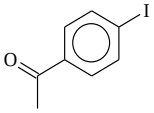 **1a**	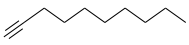 **6k**	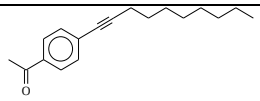 **7t**	3	96
5	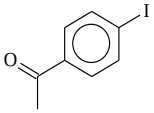 **1a**	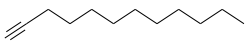 **6l**	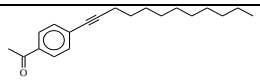 **7u**	3	90
6	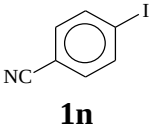 **1n**	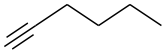 **6m**	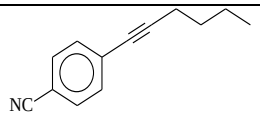 **7v**	3	93
7	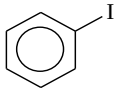 **1c**	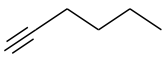 **6m**	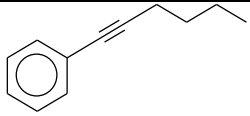 **7w**	4	80

8	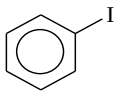 **1c**	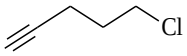 **6n**	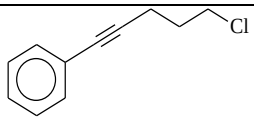 **7x**	4	95
9	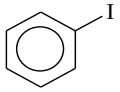 **1c**	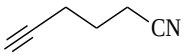 **6o**	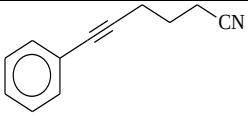 **7y**	4	90
10	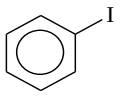 **1c**	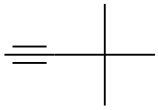 **6p**	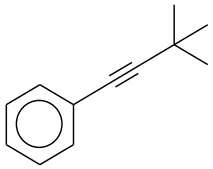 **7z**	4	92
11	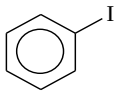 **1c**	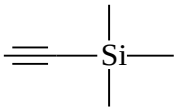 **6q**	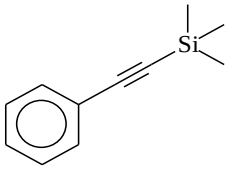 **7aa**	4	93
12	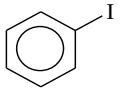 **1c**	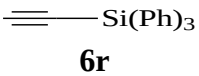 **6r**	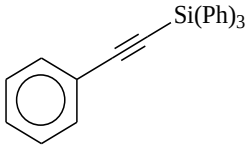 **7ab**	4	95
13	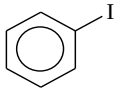 **1c**	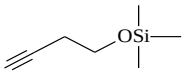 **6s**	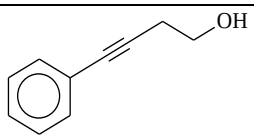 **7ac**	4	90
14	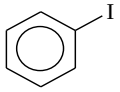 **1c**	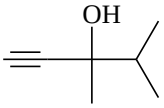 **6t**	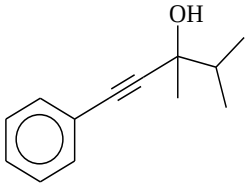 **7ad**	4	87

a. Reaction Conditions: Pd-BOX-1 (0.01 mmol), aryl iodide (1.00 mmol), alkyl alkyne (1.50 mmol), KOH (2.00 mmol), CH_3CN-H_2O (2-2 mL), 60 ^oC.

b. Isolated yield

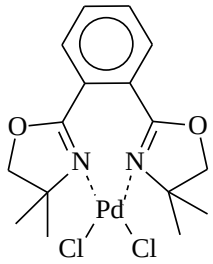

Pd-BOX-1

Pd-BOX catalyzed Sonogashira coupling reaction of aryl diiodide with different alkyl and aryl alkynes

We have further evaluated the Sonogashira coupling reaction of diiodobenzene with aryl and alkyl alkynes. Amazingly, the reaction worked to give new internal alkynes in excellent isolated yields (Table 17). The reactions of 1,4-diiodobenzene with phenylacetylene or 4-ethynyl aniline (Table 17, entries 1 and 2) yielded successfully the corresponding bis(phenylethynyl)-benzene derivatives. Similarly, the reaction of 1,4-diiodobenzne with various alkyl alkynes gave excellent yields of the corresponding symmetrically disubstituted alkynyl benzenes (Table 17, entries 3-7). Alkynols and alkyndiols represent excellent building blocks for the synthesis of wide variety of industrially and pharmaceutically important heterocycles [201]. The representative dialkyndiols, 4,4'-benzene-1,4-diylbisbut-3-yn-1-ol (table 17, entry 6) and 1,1'-benzene-1,4-diylbis-(3,4-dimethylpent-1-yn-3-ol) (Table 17, entry 7), were successfully synthesized from the coupling of 1,4-diiodobenzene with 1-trimethylsiloxy-3-butyne and 3,5-dimethylhex-1-yn-3-ol, respectively. Likewise, under the same conditions, the terminal dialkyl alkyne, octa-1,7-diyne, coupled smoothly with 2 equivalent of 4-iodoacetophenone to afford the corresponding internal dialkynyl ketone in excellent yield (Table 17, entry 8).

TABLE 17. Sonogashira Coupling Reaction of Aryl Iodide and Diiodobenzene with Alkynes

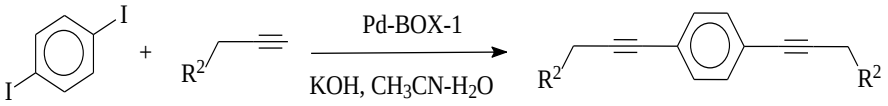

Entry	Ar-I	Alkyne	Yield (%)[b]
1	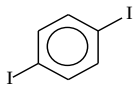 **1o**	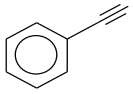 **6a**	95[c]
2	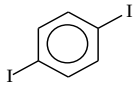 **1o**	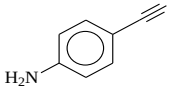 **6e**	96[c]
3	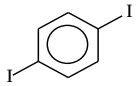 **1o**	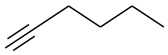 **6m**	96
4	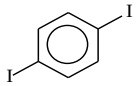 **1o**	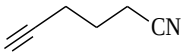 **6o**	95
5	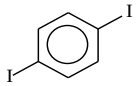 **1o**	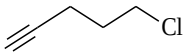 **6n**	96
6	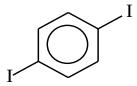 **1o**	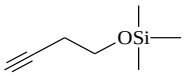 **6s**	90
7	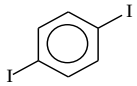 **1o**	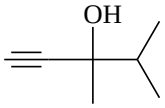 **6t**	93
8	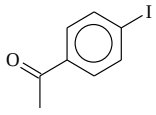 **1o**	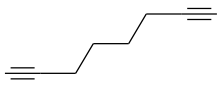 **6u**	95[c]

a. Reaction Conditions: Pd-BOX-1 (0.01 mmol), p-diiodobenzene (0.50 mmol), alkyne (1.5 mmol), KOH (2.00 mmol), CH_3CN-H_2O (2-2mL), 60 °C, 12 h.

b. Isolated yield

c. 5 h

5.3.4 Supported palladium-bis(oxazoline) as catalysts in Suzuki-Miyaura coupling reaction

The catalytic activities of the new supported palladium-bis(oxazoline) catalysts (Pd-BOX-12 and Pd-BOX-13) in Suzuki-Miyaura coupling reaction of arylboronic acids and aryl halides was carefully studied. In general, Suzuki-Miyaura coupling reaction catalyzed by supported palladium catalysts follow similar mechanism with the homogeneous catalyst [202]. For this reason, we adopted a previously optimized reaction condition based on homogeneous Pd-BOX complexes ([Pd]/K_2CO_3/DMF-H_2O) (section 5.3.1) [203]. Several arylboronic acids with aryl iodides, aryl bromides and aryl chlorides were considered in this reaction.

Suzuki-Miyaura coupling reaction of p-tolylboronic acid with iodobenzene. Recycling ability of the supported catalysts

The recycling ability of the new supported palladium-bis(oxazoline) catalysts in DMF-H_2O was investigated in the Suzuki-Miyaura coupling reaction of iodobenzene with p-tolylboronic acid at 80 ^oC for 2 h. As previously explained, the supported catalyst was packaged in a membrane tube fabricated from a commercially available dialysis bag. The membrane allows the migration of molecules with low molecular weight. This means only the reactants and products can smoothly pass through the membrane. The transport of both reactants and products in and out of the membrane is driven by concentration gradient and temperature of the reaction (80 ^oC), these resulted in relatively slower reaction rate [204, 205]. The results of the recycling experiments are presented on Figures 25 and 26 for Pd-BOX-12 and Pd-BOX-13, respectively. Remarkably, the two supported catalysts could be

recycled up to twelve times without bearing any loss in their catalytic activities. The turnover numbers were estimated for the 12 cycles as 2242 and 2278, while the turnover frequencies were estimated as 1121/h and 1139 for merifield's resin supported palladium-bis(oxazoline) catalyst (Pd-BOX-12) and silica supported palladium-bis(oxazoline) catalyst (Pd-BOX-13) respectively. In order to confirm the efficiency of the supported catalysts, we have conducted an experiment with a ratio of iodobenzene (12.0 mmol) to supported palladium-bis(oxazoline) catalyst (0.005 mmol) equal to 2400 for 2 hours. A complete conversion of iodobenzene and excellent and isolated yield 98% and 96% were obtained for the Pd-BOX-12 and Pd-BOX-13 catalysts respectively. Again, the turnover number of the supported palladium-bis(oxazoline) catalysts in the later experiments are estimated as 2352 and 2304, while the turnover frequencies are estimated as 1176/h and 1152/h for the Pd-BOX-12 and the Pd-BOX-13 catalysts respectively.

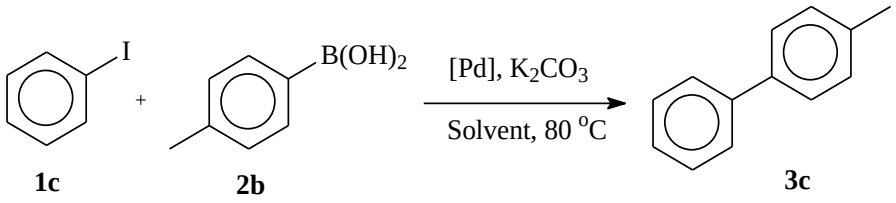

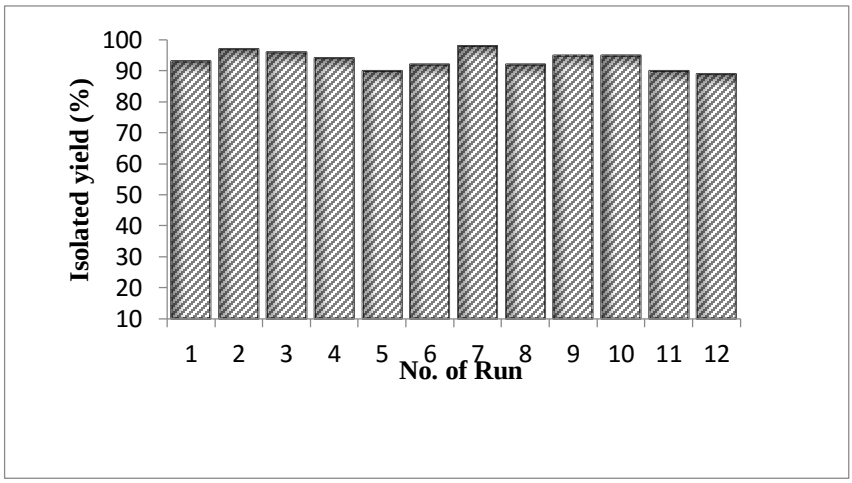

Figure 25: Merifield's Resin Supported Palladium-Bis(Oxazoline) as Catalyst Suzuki-Miyaura Coupling Reaction of Iodobenzene with *p*-Tolylboronic Acid. Recycling Ability of The Catalyst.

Reaction conditions: [Pd] (0.0050 mmol), p-tolylboronic acid (1.5 mmol), iodobenzene (1.0 mmol), K_2CO_3 (2.0 mmol), DMF (3.0 mL), H_2O (3.0 mL), 80 °C, 2 h.

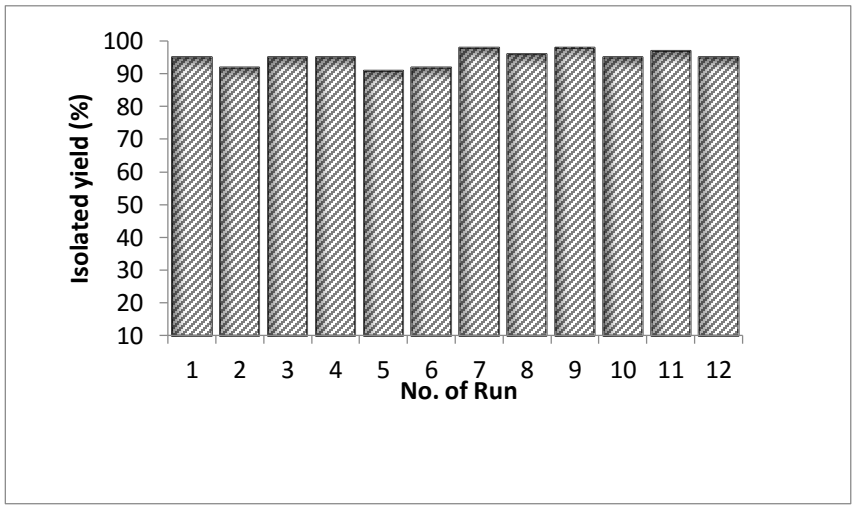

Figure 26: Silica Supported Palladium-Bis(Oxazoline) as Catalyst Suzuki-Miyaura Coupling Reaction of Iodobenzene with *p*-Tolylboronic Acid. Recycling Ability of the Catalyst.

Reaction conditions: [Pd] (0.0050 mmol), p-tolylboronic acid (1.5 mmol), iodobenzene (1.0 mmol), K_2CO_3 (2.0 mmol), DMF (3.0 mL), H_2O (3.0mL), 80 °C, 2 h

Suzuki-Miyaura coupling reactions of various phenylboronic acids and arylhalides using supported palladium-bis(oxazoline) catalysts

We have mentioned in a previous section (section 5.3.1) that the homogeneous Pd-BOX complexes exhibit high activities for the Suzuki-Miyaura coupling of diversely functionalized aryl halides including aryl iodides, aryl bromides and aryl chrorides with a wide array of arylboronic acids. Our homogeneous catalytic system was found to be tolerant to a variety of functional groups on both the aryl halides and the arylboronic acids. The literature studies reveal that the majority of investigations on the recycling ability of supported catalysts are restricted to the reaction of the same substrates throughout the catalytic cycles. We have envisaged that, the use of the recycled catalyst for reactions of different substrates in each cycle is worth investigating. The high recycling ability realized with the new supported catalysts in the Suzuki-Miyaura coupling reaction of iodobenzene with p-tolylboronic acid encouraged us to examine the recycling ability of this new system in the Suzuki-Miyaura coupling of broad range of substrates using DMF-H_2O (1:1) as a solvent system and K_2CO_3 as a base. Thus, various aryl halides including aryl iodides, aryl bromides and aryl chlorides were coupled successfully with various arylboronic acids. At the end of each reaction, the catalyst bag was removed from the reaction mixture and dialyzed in DMF to remove all traces of reactants and products before taking it to the next catalytic run with new substrates.

Aryl iodides having either activating or deactivating groups reacted smoothly, affording the cross coupling products in excellent isolated yields (92-98%) (Table 18, entries 1-7). Various functional groups were tolerated with the new supported catalytic system. The coupling reactions were also successful with both activated and deactivated aryl bromides

(CHO, CH_3) leading to the corresponding biphenyl products in high isolated yields (Table 18, entries 8 and 9). It is worth mentioning that all the reactions of arylboronic acids with aryl iodides and aryl bromides were conducted with the same recycled catalyst. Aryl chlorides however, were observed to possess lower reactivity. They required relatively higher temperature (110 ^oC) which was unsuitable for the dialysis bag. Thus the coupling reaction of aryl chlorides were conducted using a fresh catalyst and without dialysis bag. A longer reaction time (12 h) was necessary to obtain high yields (Table 18, entries 10 and 11).

The effect of varying the substituents on the arylboronic acids was also investigated. In contrast to aryl halides, the overall electronic effect of the arylboronic acids with the supported palladium-bis(oxazoline) catalyzed Suzuki-Miyaura reaction was rather insignificant.

TABLE 18. Suzuki-Miyaura Coupling Reaction of Various Aryl Halides with Different Arylboronic Acids Using Pd-BOX-12 (Recycled Catalyst).

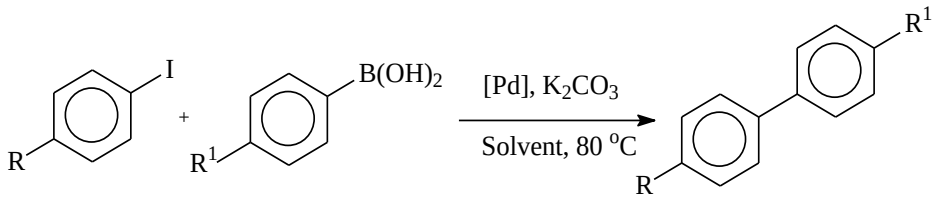

Entry	Arylhalide 1a – 1l	Phenylboronic acid 2a – 2f	Time (h)	Yield (%)[b]
1	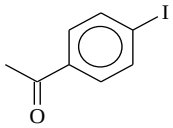 **1a**	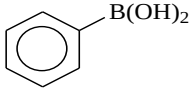 **2a**	2	96
2	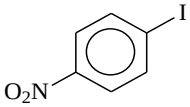 **1b**	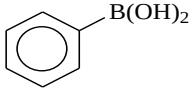 **2a**	2	94
3	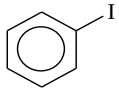 **1c**	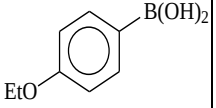 **2e**	2	95
4	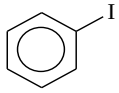 **1c**	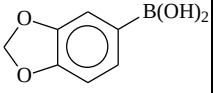 **2d**	2	95
5	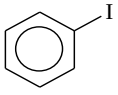 **1c**	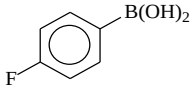 **2f**	2	93
6	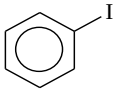 **2b**	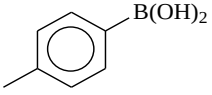	2	95

	1c			
7	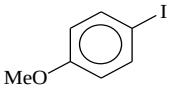 **1d**	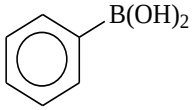 **2a**	4	92
8	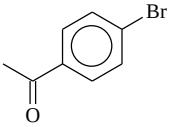 **1f**	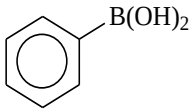 **2a**	3	94
9	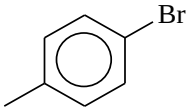 **1j**	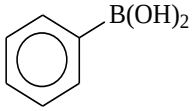 **2a**	5	90
10[c]	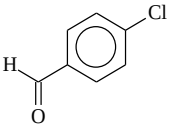 **1l**	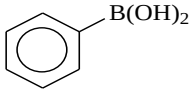 **2a**	12	95
11[c]	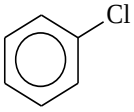 **1k**	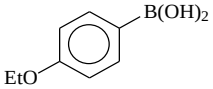 **2e**	12	92

a. Reaction Conditions: [Pd] (0.005 mmol), arylboronic acid (1.2 mmol), aryl halide (1.0 mmol), K_2CO_3 (2.0 mmol), DMF (3.0 mL), H_2O (3.0 mL), 80 ^oC.

b. Isolated Yield

c. 110^oC, using a fresh catalyst

5.3.5 Catalytic activities of supported palladium-bis(oxazoline) in Mizoroki-Heck coupling reaction

The catalytic activities of the new supported palladium-bis(oxazoline) catalysts in Mizoroki-Heck coupling reaction of various olefins and aryl halides was carefully studied. Based on our previous investigation using homogeneous palladium bis(oxazoline) catalyst (section 5.3.2), we adopted an optimized reaction condition ([Pd]/KOH/DMF-H_2O). The cross coupling reactions of various aryl iodides with styrene, acrylic acid, acrylate and acrylamide were considered.

Mizoroki-Heck coupling reaction of methylacrylate with iodobenzene. Recycling ability of Merifield's resin supported palladium-bis(oxazoline) catalyst

The recycling ability of the new Merifield's resin supported palladium-bis(oxazoline) catalysts in Mizoroki-Heck coupling reaction of iodobenzene with methylacrylate was investigated. Interestingly, the supported catalyst could be recycled up to ten times without significant loss in catalytic activity. The turnover number of the merifield's resin supported palladium-bis(oxazoline) catalyst was estimated for the 10 cycles as 1800, while the turnover frequency was found to be 300/h. In order to confirm the efficiency of the merifield's resin supported palladium-bis(oxazoline) catalyst, we have conducted an experiment with a ratio of iodobenzene (10.0 mmol) to supported palladium-bis(oxazoline) catalyst (0.005 mmol) equal to 2000 for 6 hours. A complete conversion of iodobenzene and excellent isolated yield of product (93 %) was observed. The turnover number of the Merifield's resin supported palladium-bis(oxazoline) catalysts in the later experiment was estimated as 1860, while the turnover frequency was found as 310/h.

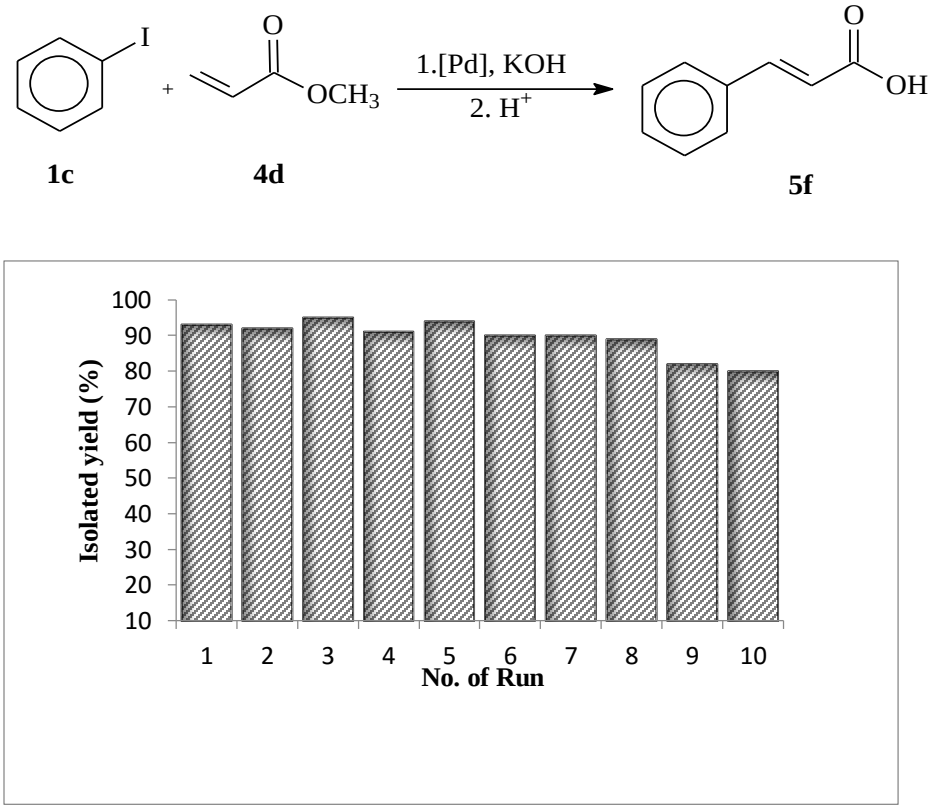

Figure 27: Merifield's Resin Supported Palladium-Bis(Oxazoline) as Catalyst for Mizoroki-Heck Coupling Reaction of Iodobenzene with Methylacrylate. Recycling Ability of the Catalyst System.

Reaction conditions: [Pd] (0.0050 mmol), methylacrylate (1.5 mmol), iodobenzene (1.0 mmol), KOH (2.0 mmol), DMF (3.0 mL), H_2O (3.0 mL), 80 ^oC, 6 h.

Mizoroki-Heck coupling reaction of styrene with iodobenzene. Recycling ability of silica supported palladium-bis(oxazoline) catalyst

The recycling ability of the new silica supported palladium-bis(oxazoline) catalyst in Mizoroki-Heck coupling reaction of iodobenzene with styrene was investigated. The supported catalyst could be recycled up to ten times without significant loss in catalytic activity. The turnover number of the silica supported palladium-bis(oxazoline) catalyst was estimated for the 10 cycles as 1804, while the turnover frequency was found to be 301/h. In order to confirm the efficiency of the silica supported palladium-bis(oxazoline) catalyst, we have conducted an experiment with a ratio of iodobenzene (10.0 mmol) to silica supported palladium-bis(oxazoline) catalyst (0.005 mmol) equal to 2000 for 6 hours. A complete conversion of iodobenzene and excellent isolated yield of product (93 %) was observed. Again, the turnover number of the silica supported palladium-bis(oxazoline) catalysts in the later experiment was estimated as 1860, while the turnover frequency was found as 310/h.

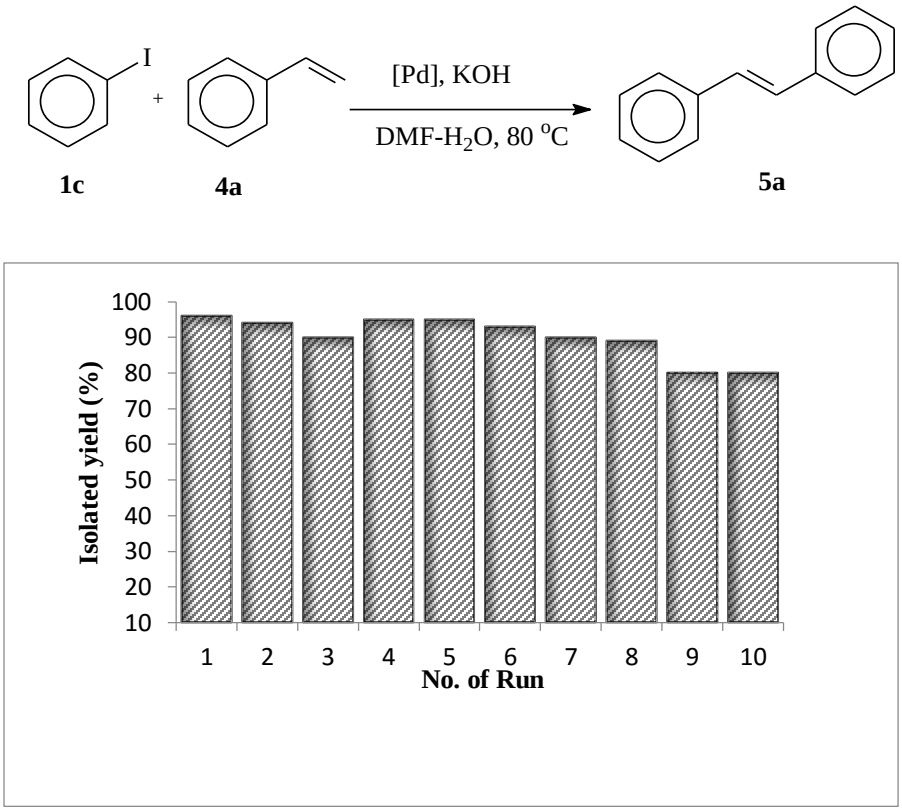

Figure 28: Silica Supported Palladium-Bis(Oxazoline) as Catalyst Mizoroki-Heck Coupling Reaction of Iodobenzene with Styrene. Recycling Ability of the Catalyst System.

Reaction conditions: [Pd] (0.0050 mmol), styrene (1.5 mmol), iodobenzene (1.0 mmol), KOH (2.0 mmol), DMF (3.0 mL), H_2O (3.0 mL), 80 ^oC, 6 h.

Mizoroki-Heck coupling reaction of various alkenes with iodobenzene catalyzed by supported palladium-bis(oxazoline) catalysts . Recycling ability for different substrates.

As we mentioned previously (section 5.3.2), homogeneous palladium-bis(oxazoline) catalysts exhibit high catalytic activity for the Mizoroki-Heck coupling reaction of diversely functionalized aryl iodides with a wide array of terminal alkenes. Our homogeneous catalyst system can tolerate a variety of functional groups on both the aryl iodides and the alkenes. The high recycling ability realized with the new supported catalyst

in the Mizoroki Heck coupling of iodobenzene with styrene and with methylacrylate encouraged us to examine the recycling ability of the supported catalysts in the Mizoroki-Heck coupling of a broad range of substrates using DMF-H_2O (1:1) as a solvent system and KOH as a base. Thus, various aryl halides including aryl iodides and aryl bromides were coupled successfully with various styrene derivatives and with acrylates. The silica supported catalyst was employed in the coupling of aryl halides with styrene derivatives, while the merifield's resin supported catalyst was used in the coupling of aryl halides with acrylate, acrylic acid and acrylamide (the two supported catalyst show similar activity and recycling ability). At the end of each reaction, the catalyst was removed from the reaction mixture and dialysed in DMF to remove all traces of reactants and products before taking it to the next catalytic run.

Aryl iodides having either activating or deactivating groups reacted smoothly with styrene, affording the cross coupling products in excellent isolated yields (90-98%) (Table 19, entries 1-5). Aryl bromides also reacted smoothly at relatively higher temperature (100 ^oC) to give the corresponding coupling product in good yields (Table 19, entries 6 and 7). Various functional groups were tolerated with the new supported catalyst system. It is worth mentioning that the aryl iodides were coupled to styrene (Table 19, entries 1 - 5) using the same recycled catalyst. Aryl bromides however, were observed to possess lower reactivity. They required relatively higher temperature (100 ^oC) which was unsuitable for the dialysis bag. Thus the coupling reaction of aryl bromides were conducted using a fresh catalyst and excluding the dialysis bag.

Similarly, the coupling reactions of aryl halides with methyl acrylate, acrylic acid and acrylamide was investigated (Table 19, entries 8 - 16) using the merifield's resin supported

catalyst. Under the optimized reaction conditions, the acrylates and acrylamides were hydrolyzed to the corresponding salts of the carboxylic acids. The aryl propenoic acids were obtained after acidic work up. Aryl iodides having either activating or deactivating groups reacted smoothly with acrylates, to give the cross coupling products in excellent isolated yields (90 – 96 %) (Table 19, entries 8 - 14). The coupling reactions of aryl bromides were conducted at 100 ^{o}C, using a fresh catalyst and without dialysis bag. Also, good isolated yields of the coupling products were obtained.

The effect of varying the substituents on the olefins was also investigated. In contrast to aryl halides, the overall electronic effect of the alkenes with the supported palladium-bis(oxazoline) catalyzed Mizoroki - Heck coupling reaction was rather insignificant.

TABLE 19. Mizoroki-Heck Coupling Reactions of Aryl Iodides with Alkynes Using Supported Palladium Bis(Oxazoline) as Catalyst.

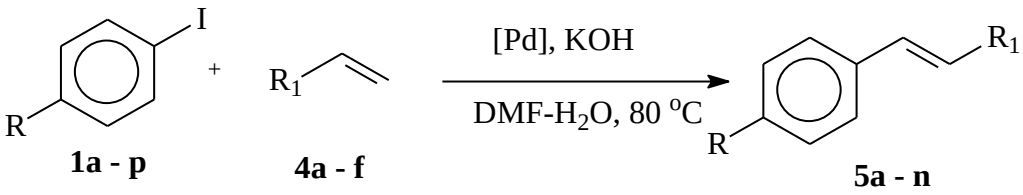

1a - p **4a - f** **5a - n**

Entry	Aryl halide 1a-p	Alkyne 4a-f	Coupling Product 5a-n	Yield (%)[b]
1	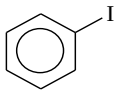 **1c**	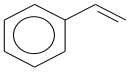 **4a**	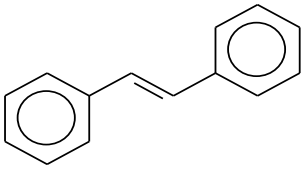 **5a**	96
2	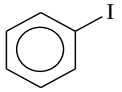 **1c**	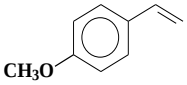 **4b**	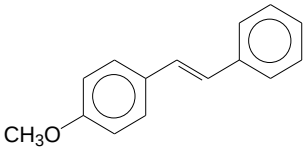 **5b**	96
3	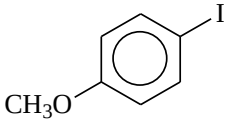 **1d**	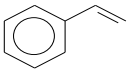 **4a**	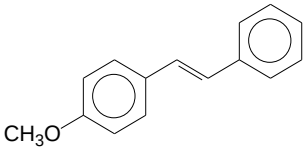 **5b**	90
4	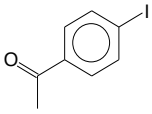 **1a**	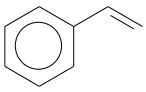 **4a**	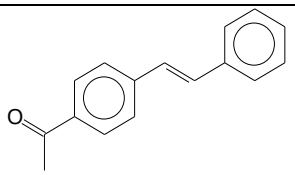 **5c**	97

a. Reaction conditions: [Pd] (0.0050 mmol), alkyne (1.5 mmol), iodobenzene (1.0 mmol), KOH (2.0 mmol), DMF (3.0 mL), H_2O (3.0 mL), 80 °C, 6 h.
b. Entries 8 – 16 were obtained after acid workup.
c. Entries 6, 7, 15 and 16 were reacted at 100 °C

5	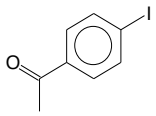 **1a**	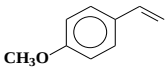 **4b**	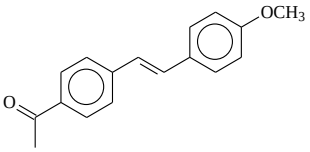 **5e**	98
6	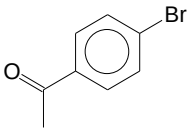 **1f**	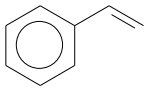 **4a**	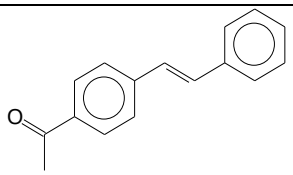 **5c**	92
7	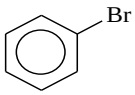 **1p**	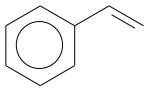 **4a**	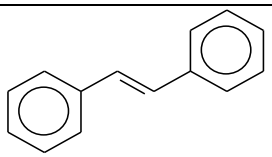 **5a**	82
8	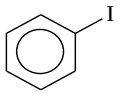 **1c**	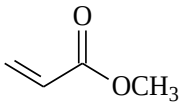 **4d**	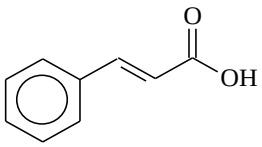 **5f**	91
9	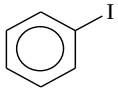 **1c**	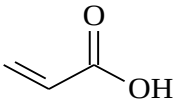 **4e**	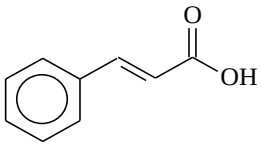 **5f**	96
10	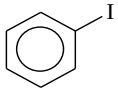 **1c**	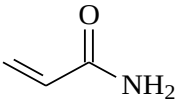 **4f**	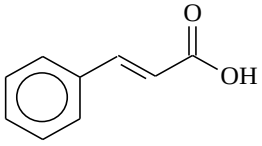 **5f**	90
11	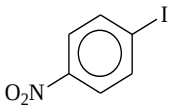 **1b**	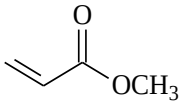 **4d**	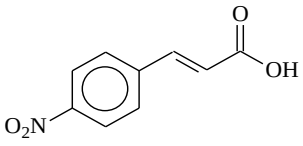 **5l**	91

12	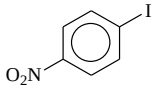 **1b**	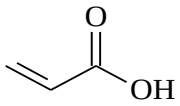 **4e**	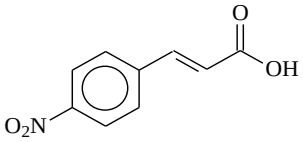 **5l**	94
13	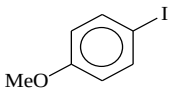 **1d**	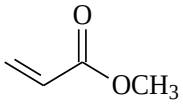 **4d**	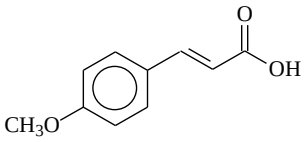 **5m**	90
14	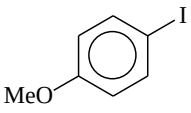 **1d**	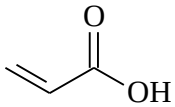 **4e**	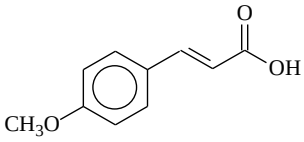 **5m**	93
15	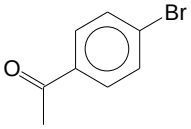 **1f**	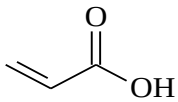 **4e**	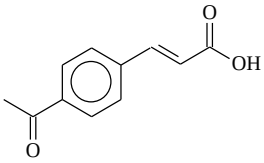 **5n**	88
16	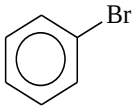 **1p**	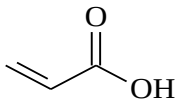 **4e**	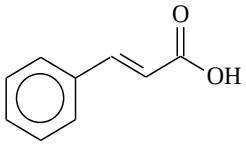 **5f**	80

5.3.6 Catalytic activities of supported palladium-bis(oxazoline) in Sonogashira coupling reaction

The catalytic activities of the new supported palladium-bis(oxazoline) catalyst in Sonogashira coupling reactions of alkynes and aryl halides was carefully investigated. Based on our previous findings using homogeneous palladium bis(oxazoline) catalysts (section 5.3.3), we have adopted the optimized catalytic system [Pd]/KOH/CH_3CN-H_2O. The coupling reactions of various aryl iodides with aryl and alkyl alkynes were considered in this reaction.

Sonogashira coupling reaction of phenylacetylene with iodobenzene. Recycling ability of the supported catalyst system

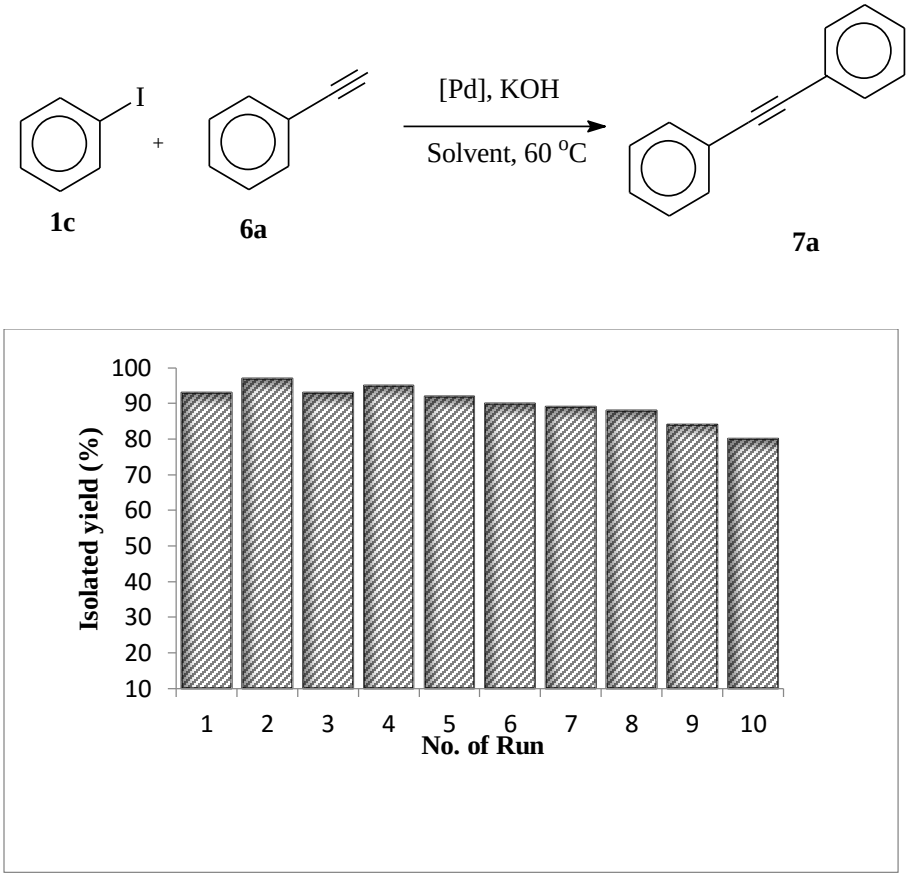

Figure 29: Merifield's Resin Supported Palladium-Bis(Oxazoline) as Catalyst for Sonogashira Coupling Reaction of Iodobenzene with Phenylacetylene. Recycling Ability of the Catalyst System.

Reaction conditions: [Pd] (0.0050 mmol), phenylacetylene (1.5 mmol), iodobenzene (1.0 mmol), KOH (2.0 mmol), acetonitrile (2.0 mL), H_2O (2.0 mL), 60 °C, 6 h

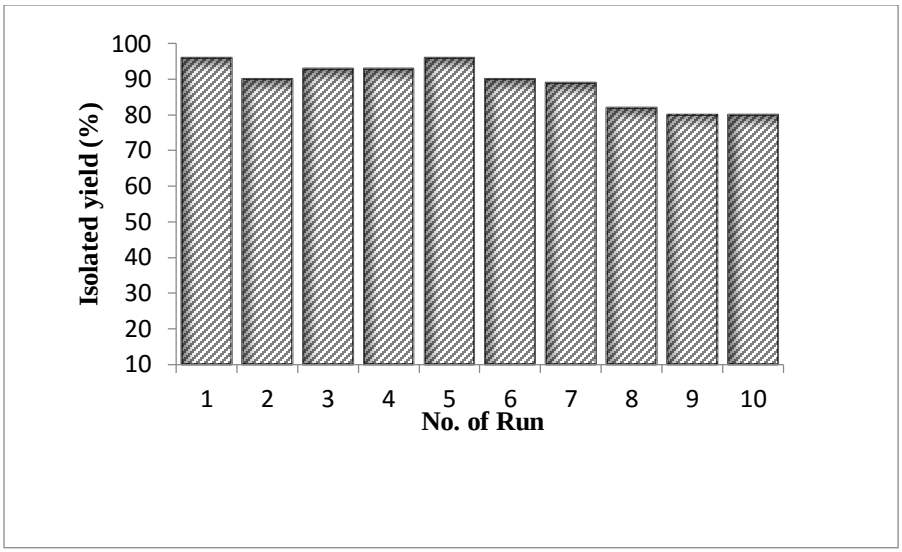

Figure 30: Silica Supported Palladium-Bis(Oxazoline) as Catalyst for Sonogashira Coupling Reaction of Iodobenzene with Phenylacetylene. Recycling Ability of the Catalyst System.

Reaction conditions: [Pd] (0.0050 mmol), phenylacetylene (1.5 mmol), iodobenzene (1.0 mmol), KOH (2.0 mmol), acetonitrile (2.0 mL), H_2O (2.0 mL), 60 ^oC, 6 h.

The recycling ability of the new supported palladium-bis(oxazoline) catalysts in Sonogashira coupling reaction of iodobenzene with phenylacetylene was investigated. Interestingly, both the merifield's resin (Figure 29) and the silica supported palladium-bis(oxazoline) (Figure 30) catalysts could be recycled up to ten times without significant loss in their catalytic activities. The turnover numbers of the supported palladium-bis(oxazoline) catalysts were estimated for the 10 cycles as 1802 and 1780, while the turnover frequencies were found to be 300/h and 297/h for the merifield's resin and silica supported palladium-bis(oxazoline) catalysts, respectively. In order to confirm the efficiency of the supported palladium-bis(oxazoline) catalysts, we have conducted an experiment with a ratio of iodobenzene (10.0 mmol) to supported palladium-bis(oxazoline) catalyst (0.005 mmol) equal to 2000 for 6 hours. A complete conversion of iodobenzene and excellent isolated yield of product (96% using merifield's resin supported catalyst and

95% using silica supported catalyst) were observed in each case. The turnover numbers of the merifield's resin and the silica supported palladium-bis(oxazoline) catalysts in the later experiment is estimated as 1920 and 1900, while the turnover frequencies were found to be 320 and 317/h respectively.

Sonogashira coupling reactions of various arylhalides and alkynes using the supported palladium-bis(oxazoline) catalysts. Recycling ability for different substrates.

The high recycling ability of the supported palladium-bis(oxazoline) catalysts in the Sonogashira coupling reaction of iodobenzene with phenylacetylene urged us to extend the scope of the coupling reaction to various electronically different aryl halides and alkynes.

We studied the Sonogashira coupling reaction of 4-iodoacetophenone with phenylacetylene using the merifield's resin supported palladium-bis(oxazoline) catalyst. The corresponding internal acetylene was obtained in almost quantitative yield (95%) (Table 20, entry 1). The catalyst was dialysed in acetonitrile and the purified catalyst was used again for the coupling of iodobenzene with p-tolylacetylene. Interestingly, the reaction worked to give excellent yield (90%) of the expected product (Table 20, entry 2). The same procedure was repeated for the supported catalyst. The same catalyst was then used in the coupling of phenylacetylene with 4-iodoanisole and with 4-iodoaniline (Table 20, entries 4 and 5). The corresponding internal acetylenes were also isolated in excellent yields (89% and 90%).

We have also tested the recycled catalyst in the Sonogashira coupling reaction of iodobenzene with alkyl alkynes. For instance, the coupling reaction of iodobenzene with 5-chloro-1-pentyne led to excellent yield (91%) of the coupling product (Table 20, entry

6). Similarly, 5-cyano-1-pentyne was successfully coupled with iodobenzene (93%) (Table 20, entry 7).

TABLE 20. Sonogashira Coupling Reaction of Various Aryl Iodides with Different Alkynes Using Merifield's Resin Supported Palladium-Bis(Oxazoline) Catalyst.

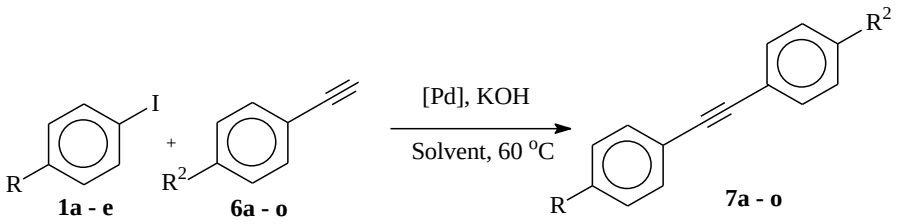

Entry	Arylhalide 1a – e	Alkyne 6a - o	Time (h)	Yield (%)[b]
1	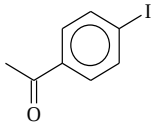 **1a**	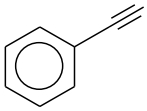 **6a**	2	95
2	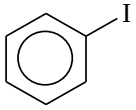 **1c**	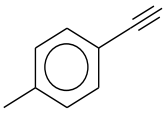 **6c**	4	90
3	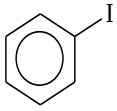 **1c**	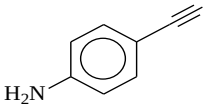 **6e**	4	94
4	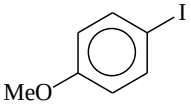 **1d**	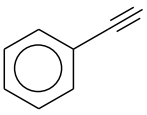 **6a**	5	89
5	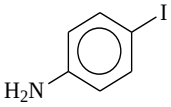	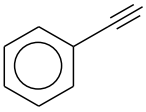	5	90

	1e	6a		
6	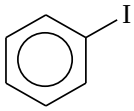 **1c**	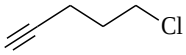 **6n**	12	91
7	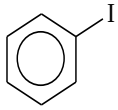 **1c**	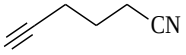 **6o**	12	93

a. Reaction

Conditions: [Pd] (0.005 mmol), alkyne (1.5 mmol), aryl halide (1.0 mmol), KOH (2.0 mmol), CH3CN (2.0 mL), H2O (2.0 mL), 60 oC.

b. Isolated Yield.

5.4 Characterization of the used supported palladium-bis(oxazoline) catalysts

The ability to reuse the supported palladium-bis(oxazoline) catalysts several times and in various reactions without significant loss in their catalytic activities demonstrates their high stabilities. The interesting results realized with the supported catalysts urged us to carry out further investigations to asses any change in the structure of the used catalysts in comparison with the unused catalysts. The catalysts recovered after the 12^{th} cycle of the Suzuki coupling reaction and the 10^{th} cycle of both the Heck and the Sonogashira coupling reactions were washed successively with distilled water, acetone and methanol. The catalysts were then dried in an oven at 100 ^{o}C prior to analysis. The purified catalysts were analyzed with FT-IR, XPS and the amount of palladium was established using ICP-MS.

5.4.1 Characterization of the used supported palladium-bis(oxazoline) catalysts using FT-IR

The catalysts were pressed in to pellets with KBr and analysed using FT-IR. The FT-IR spectra for the recovered merifield's resin and the silica supported palladium-bis(oxazoline) (Pd-BOX-12 and Pd-BOX-13) (Figure 31 and Figure 32 respectively) catalysts were found to be similar with the spectra of the unused catalysts.

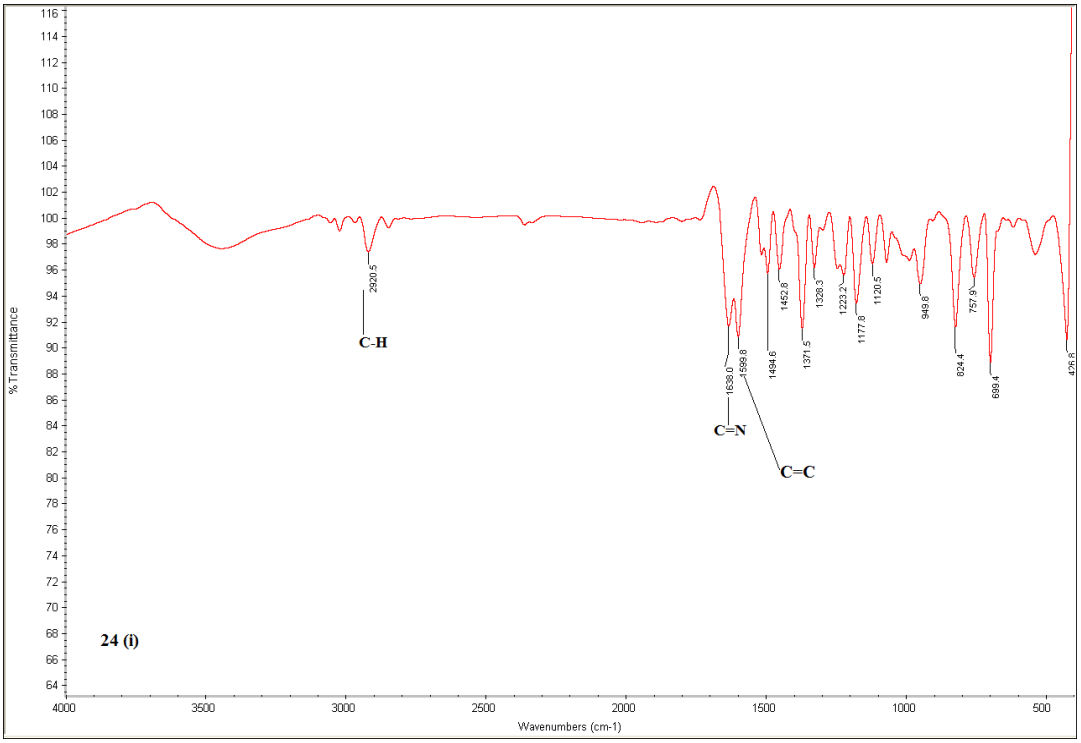

Figure 31. FT-IR Spectrum of Used Pd-BOX-12 recovered from Suzuki-Miyaura Coupling Reaction

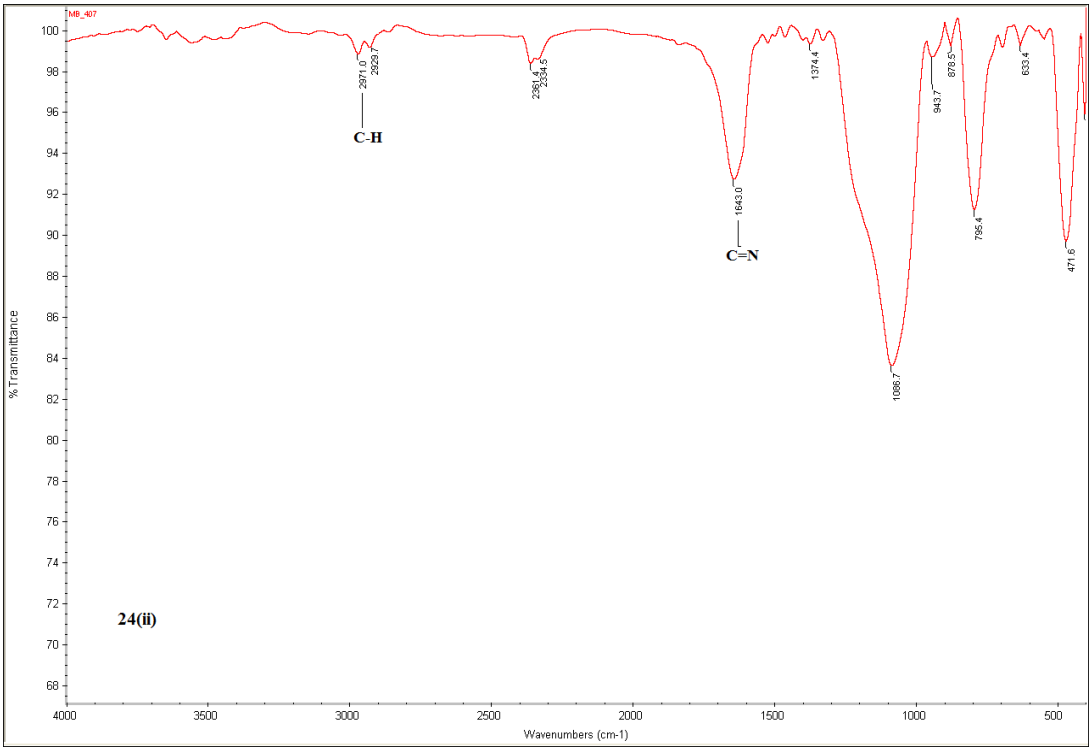

Figure 32. FT-IR Spectrum of Used Pd-BOX-13 Recovered from Suzuki-Miyaura Coupling Reaction

5.4.2 Analysis of the used supported palladium-bis(oxazoline) catalysts using ICP-MS

The percentages of palladium on **Pd-BOX-12** and **Pd-BOX-13** recovered from the Suzuki-Miyaura and the Mizoroki-Heck coupling reactions were found to be similar to the amount of palladium on the fresh catalysts (Table 20b). This results further justifies the high recycling ability observed with the new supported catalysts.

TABLE 20b: Comparison of the Percentage of Palladium in the Fresh and the Used Supported Palladium-Bis(Oxazoline) Catalysts.

	Fresh catalyst (%)	Recovered catalyst	
		Suzuki- Miyaura coupling reaction (%)	Mizoroki-Heck coupling reaction (%)
Pd-BOX-12	6.7	6.2	6.2
Pd-BOX-13	2.8	2.3	2.4

5.4.3 Analysis of the used supported palladium-bis(oxazoline) catalysts using XPS

The XPS studies of the supported palladium-bis(oxazoline) catalysts, Pd-BOX-12 (Figure 33) and Pd-BOX-13 (Figure 34) recovered after the tenth cycle of the Sonogashira coupling reaction shows that the oxidation state of palladium remains unchanged after the catalytic

applications. Similar to the unused supported catalysts, the 3d spectrum resolved in to $3d_{5/2}$ and $3d_{3/2}$ spin orbit pairs with binding energies 334.58 eV and 339.78eV (Pd-BOX-12) and 336.18 and 341.68 (Pd-BOX-13) respectively [161, 162].

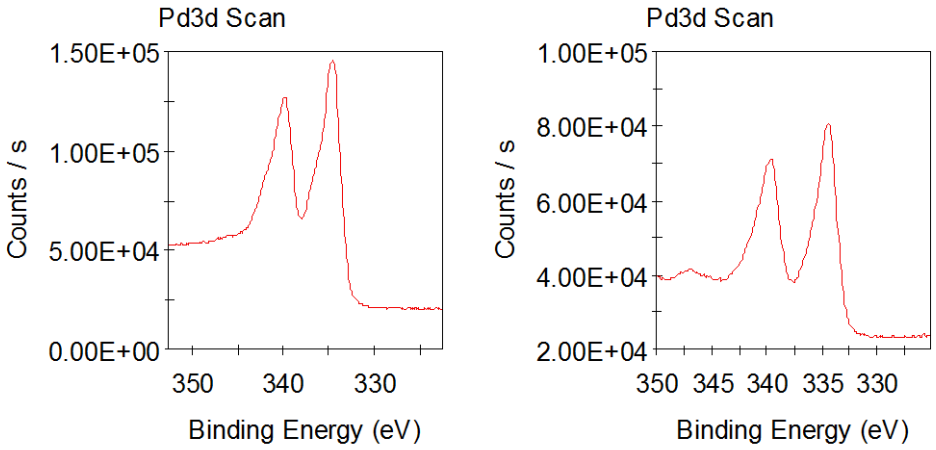

Figure 33: XPS Spectra of used Pd-BOX-12 showing Pd 3d. Spectrum of fresh catalyst is displayed on the left

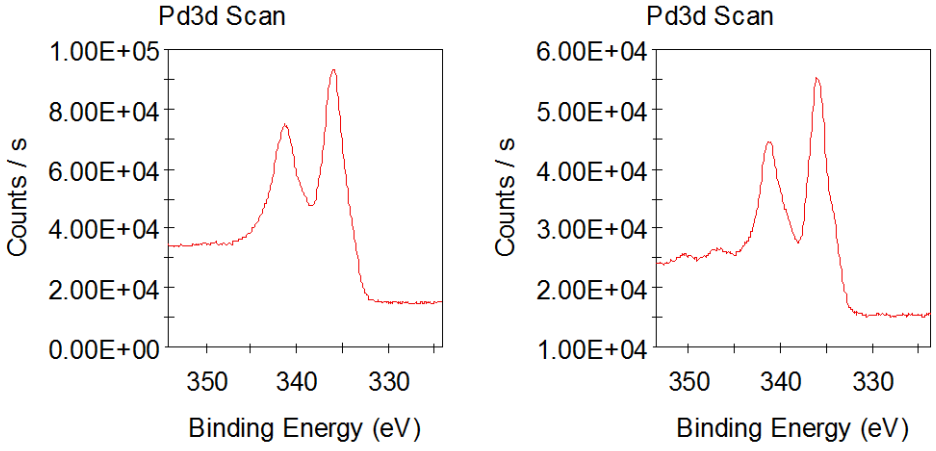

Figure 34: XPS Spectra of used Pd-BOX-13 showing Pd 3d. Spectrum of fresh catalyst is displayed on the left

5.5 Palladium leaching test

The main objective of supporting a homogeneous catalyst is to enable its easy separation from the product and to minimize the level of contamination caused by the toxic metal. The possible palladium leaching into the products was analyzed using ICP-MS. After the twelfth cycle of the Suzuki-Miyaura coupling reaction and the tenth cycle of the Mizoroki-Heck and the Sonogashira coupling reactions, the products of each reaction were combined in separate containers. Samples from each coupling product were taken for the analysis. The samples were digested using concentrated nitric acid. The solutions were then analyzed using ICP-MS.

The results of the ICP-MS analysis indicates that the concentration of palladium in the products were below 10 ppb for all the samples analyzed. These results indicate that less than 0.5 % of the total palladium on the supported catalysts was leached into the products. These results clearly indicate the high stability of the supported catalysts towards the cross coupling reactions under the prescribed reaction conditions.

CHAPTER 6

CATALYTIC CARBONYLATION REACTIONS

6.1 Introduction

Palladium catalyzed carbonylation reactions of alkynes (reductive carbonylation) and aryl halides (carbonylative coupling) in the presence of an alcohol or an amine as nucleophile represent major industrial processes for the production of value-added bulk and fine chemicals. It is a versatile synthetic pathway which allows to obtain a wide range of linear, branched and cyclic carboxylic acids and their derivatives in one step and from easily accessible starting materials [111-114]. The products of alkoxycarbonylation and aminocarbonylation reactions are extensively used as building blocks for various materials ranging from polymers [115], light sensitive and electrically conductive materials, detergents, flavours, fragrances and various pharmaceuticals [116].

Highly active and selective catalysts are necessary for the successful carbonylation reactions. Palladium complexes are considered the most efficient catalysts for carbonylation reactions. This is attributed to their high activity under mild reaction conditions. Most of the catalytic systems used in carbonylation reactions are generated in-situ from a palladium salt, a phosphine ligand and a weakly coordinating acid [113, 125, 206]. Various catalytic systems [207, 208, 122] have been used in the carbonylation reactions at low CO pressure. However, many systems are associated with relatively low activity and often give a mixture of products.

In this chapter, the catalytic activities of new palladium-bis(oxazoline)-phosphine mixed ligand complexes (Pd-BOX-10 and Pd-BOX-11) in alkoxycarbonylation and amino carbonylation reactions of alkynes are presented. Similarly, the catalytic activities of supported palladium-bis(oxazoline) complexes (Pd-BOX-12 and Pd-BOX-13) in the alkoxycarbonylation and aminocarbonylation reactions of aryl halides were also investigated.

6.2 Experimental

6.2.1 Materials and Instrumentation

Aryl halides, alkynes, amines and alcohols were purchased from Sigma Aldrich company and Farchan laboratories (Florida, USA) and were used as received. All solvents (reagent grade) used in the synthesis were distilled before use. The products were purified using flash column chromatography packed with Silica gel 170-400 Mesh (Fisher scientific, US). Merck 60 F_{254} silica gel plates (250 µm layer thickness) were used for thin-layer chromatography (TLC) analyses.

^{1}H and ^{13}C NMR spectral data were obtained using 500 MHz NMR machine (Joel 1500 model). Chemical shifts were recorded in ppm using tetramethyl silane (TMS) as a reference. $CDCl_3$ and DMSO-d_6 were used as NMR solvents. IR spectra were recorded in wave numbers (cm^{-1}) using FT-IR spectrometer (Perkin-Elmer 16F model). A Varian Saturn 2000 GC-MS machine equipped with 30 m capillary column was used to analyze the products. Agilent 6890 Gas chromatography (GC) was used to monitor the reactions and analyze the products.

6.2.2 General procedure for alkoxycarbonylation and aminocarbonylation of alkynes

A basic stainless steel autoclave equipped with a glass liner, gas inlet valve and pressure gauge was used for the carbonylation reactions. Pd-complex (0.0200 mmol) dissolved in 2 ml of acetonitrile, *p*-TsOH (0.300 mmol), alkyne (2.00 mmol) and alcohol (8.00 mmol) or amine (2.00 mmol) were added to the glass liner followed by the addition of 8 ml of acetonitrile. The glass liner was then placed in 45 ml autoclave. The autoclave was vented three times with CO and then pressurized to 100 psi CO. The mixture was heated to the required temperature (110^{o}C for alkoxycarbonylation and 120^{o}C for aminocarbonylation) and maintained at this temperature under stirring for the required time. After the reaction is complete, the mixture was cooled down to room temperature and the excess of CO was released under fume hood. The mixture was filtered and the filtrate was immediately analyzed with GC and GC-MS [125].

6.2.2.1 Computational Details of the alkoxycarbonylation of alkynes

Theoretical calculations employed Gaussian 09, Revision D.01, package [209], and used the B3LYP functional application [210]. Geometries of reactants, transition states and products were fully optimized considering solvent corrections using def2-SVP basis set [211] for all atoms, and characterized with frequency calculations (no and a single imaginary frequency for minima and transition states, respectively). The solvation effect was included in the optimization process using the polarizable continuum model (PCM) [212] method with the united atom for Universal Force Field (UFF) radii and the parameters for acetonitrile. The dispersion effect was also included in the geometry

optimization step by using the D3 atom by atoms correction of Grimme [213]. The final energies reported in this article were obtained from single-point calculations by using a larger basis set (def2-TZVP) for all atoms (Effective core potential was added to the Pd atom). Zero-point energy corrections (ZPE), derived from the frequency calculations, were added to the total energies of all proposed species in the mechanistic study.

6.2.3 General procedure for alkoxycarbonylation of aryl halide

A basic stainless steel autoclave equipped with a glass liner, gas inlet valve and pressure gauge was used for the reaction. Immobilized palladium catalyst (0.005 mmol based on palladium), iodobenzene (1.0 mmol), KOH (2.0 mmol) and alcohol (5.0 ml) were added in the glass liner which was then placed in 45 mL autoclave. The autoclave was vented three times with CO and then pressurized to 100 psi CO. The mixture was heated to 100 ^{o}C and maintained at this temperature under stirring for the required time. After the reaction is complete, the mixture was cooled down to room temperature and the excess of CO was released under fume hood. The catalyst was carefully separated from the product. The product mixture was immediately analyzed with GC and GC-MS. The recovered catalyst was carefully washed and dried under vacuum in a desiccator before next use.

6.2.4 General procedure for amino carbonylation of aryl halide

A basic stainless steel autoclave equipped with a glass liner, gas inlet valve and pressure gauge was used for the reaction. Immobilized palladium catalyst (0.005 mmol based on palladium), iodobenzene (1.0 mmol), amine (2.0 mmol), triethylamine (3.0 mmol), and acetonitrile (5.0 ml) were added to the glass liner. The glass liner was then placed in 45

mL autoclave. The autoclave was vented three times with CO and then pressurized to 100 psi CO. The mixture was heated to 120 ^{o}C and maintained at this temperature under stirring for the required time. After the reaction is complete, the mixture was cooled down to room temperature and the excess of CO was released under fume hood. The catalyst was carefully separated from the product. The product mixture was immediately analyzed with GC and GC-MS. The recovered catalyst was carefully washed and dried under vacuum in a desiccator before next use.

6.3 Results and discussions

6.3.1 Evaluation of the catalytic activity of the new Pd-BOX-PR_3 complexes in the alkoxycarbonylation of alkynes

The reaction of terminal alkynes with alcohol in the presence of carbon monoxide as carbonyl source (alkoxycarbonylation) is a well-known methodology for the synthesis of α,β-unsaturated esters. In our investigation, we have chosen the methoxycarbonylation of phenylacetylene (**6a**) using Pd-BOX as a catalyst as a model reaction. Two α,β-unsaturated ester isomers, *gem* (**9a**) and *trans* (**10a**), are expected as products from this reaction. We have studied the influence of various reaction parameters including solvent, temperature and type of palladium catalyst.

A preliminary alkoxycarbonylation reaction of phenylacetylene with methanol (**8a**) using the catalyst system (Pd-BOX-1/*p*-TsOH) yielded only trace amounts of products. The in-situ introduction of triphenylphosphine as a co-ligand resulted in a higher catalytic activity

and improved the conversion of phenylacetylene. This shows that the presence of a coordinated phosphine ligand is necessary for the progress of the alkoxycarbonylation reaction.

6.3.1.1 Effect of solvent

We have investigated the effect of various solvents on the catalytic activity and selectivity of the model reaction using the catalyst system Pd-BOX-10/*p*-TsOH. A complete conversion and an excellent selectivity towards the formation of the *gem* isomer **9a** were achieved with acetonitrile as a solvent (Table 21, entry 1). The conversion of the alkyne and the selectivity in *gem* isomer have decreased severely to 43% and 75%, respectively, when DMF was used as a solvent (Table 21, entry 2). A further decrease in the conversion of phenylacetylene to 28% was observed with *n*-hexane as a solvent, with a selectivity of 90% in favor of **9a** isomer (Table 21, entry 3). Poor conversion and poor selectivity were obtained when the reaction was performed in neat methanol (Table 21, entry 5). The coordination of anions to the cationic palladium center is reported to be very weak in non-polar solvents [214]. The reason for the higher activity of the alkoxycarbonylation reaction in acetonitrile is not yet quite understood but it is possible that this solvent plays the role of both the solvent and the co-ligand in the catalytic cycle [116, 125].

TABLE 21. Palladium-Catalyzed Methoxycarbonylation of Phenylacetylene. Effect of Solvent.

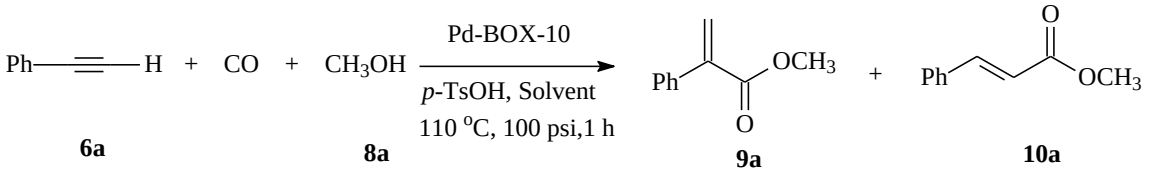

6a **8a** **9a** **10a**

Entry	Solvent	Conversion[b] %	Product Distribution[b] %	
			9a	**10a**
1	Acetonitrile	99	97	3
2	DMF	43	75	25
3	*n*-hexane	28	90	10
4	Toluene	65	92	8
5	Methanol	10	65	35

a Reaction conditions: Pd-BOX-10 (0.02 mmol), *p*-TsOH (0.30 mmol), solvent (10 ml), phenylacetylene (2.0 mmol), methanol (8.0 mmol), CO (100 psi),110 °C, 1 h.
b Determined by GC based on phenylacetylene.

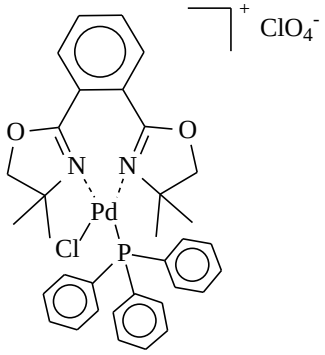

Pd-BOX-10

6.3.1.2 Effect of Temperature

After determining the best solvent for the reaction, we have studied the effect of varying the temperature on the conversion and the selectivity of the methoxycarbonylation reaction

of phenylacetylene using the catalytic system (Pd-BOX-10/*p*-TsOH/CH_3CN). The catalytic activity was found to be highly temperature dependent. The conversion has dropped significantly from 99% to 40% when the temperature was lowered from 110 ^oC (Table 22, entry 5) to 60 ^oC (Table 22, entry 1) and decreased to 70 % at 90 ^oC (Table 22, entry 3). The selectivity was not significantly affected by changing the reaction temperature.

TABLE 22. Palladium-Catalyzed Methoxycarbonylation of Phenylacetylene. Effect of Temperature.

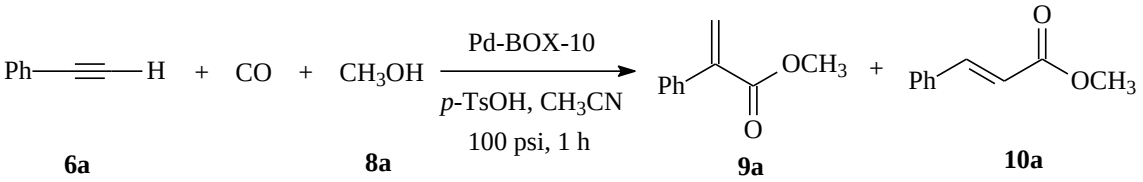

6a **8a** **9a** **10a**

Entry	Temperature (°C)	Conversion[b] %	Product Distribution[b] %	
			9a	**10a**
1	60	40	95	5
2	70	58	94	6
3	90	70	98	2
4	100	90	98	2
5	110	99	97	3

a. Reaction conditions: Pd-BOX-10 (0.02 mmol), *p*-TsOH (0.30 mmol), acetonitrile (10 ml), phenylacetylene (2.0 mmol), methanol (8.0 mmol), CO (100 psi), 1 h.
b. Determined by GC based on phenylacetylene.

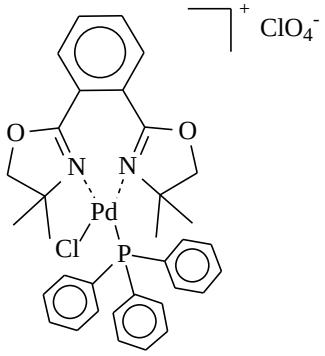

Pd-BOX-10

6.3.1.3 Effect of the type of palladium complex

The presence of a catalyst is essential for the progress of carbonylation reactions. Palladium complexes are known to catalyze the carbonylation reactions, however, the efficiency and selectivity in such reactions depend strongly on the type of palladium precursor, the attached ligand and other reaction parameters.

The effect of the type of palladium complex and the ligand on the methoxycarbonylation of phenylacetylene was investigated. The results are summarized in Table 23. Only traces of products were observed with Pd-BOX-1 as a catalyst. There was a remarkable increase in the product yield (from traces to 75 %) when triphenylphosphine was used as a co-ligand (Table 23, entries 2 and 3). The mixed ligand palladium complexes (Pd-BOX-10 and Pd-BOX-11) (Table 23, entries 4 and 5) gave full conversion with 97% and 98% selectivity, respectively, towards the **9a**. To highlight more the excellent activity of our newly prepared mixed ligand complexes, we have compared them with some commercially available palladium complexes and salts such as $Pd(PPh_3)_2Cl_2$ (Table 23, entry 6) (54%), $Pd(PhCN)_2Cl_2$ (Table 23, entry 7) (traces), $Pd(OAc)_2$ (Table 23, entry 8) (traces) and $Pd(OAc)_2/PPh_3$ (Table 23, entry 9) (74%). The low catalytic activity or the inactivity observed with most commercial palladium complexes and salts is an indication of the significance of the new mixed ligand complexes on the alkoxycarbonylation reaction. The high catalytic activity achieved with the new mixed ligand complexes is higher than the activity of the individual complexes combined (Pd-BOX-1 and $Pd(Ph_3)_2Cl_2$) and is a clear indication of a synergistic relationship between the donor nitrogen and phosphorous ligand.

TABLE 23. Palladium-Catalyzed Alkoxycarbonylation of Phenylacetylene. Effect of the Type of Pd-Catalyst.

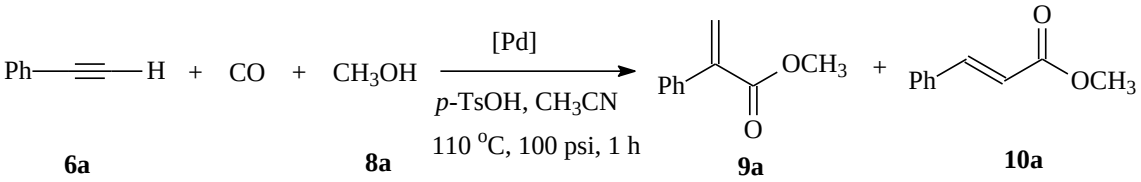

6a **8a** **9a** **10a**

Entry	Catalyst	Conversion[b] %	Product distribution[b] (%)	
			9a	**10a**
1	Pd-BOX-1	Traces	-	-
2[c]	Pd-BOX-1/PPh_3	75	90	10
3[d]	Pd-BOX-1/PPh_3	90	90	10
4	Pd-BOX-10	99	97	3
5	Pd-BOX-11	99	98	2
6	$Pd(PPh_3)_2Cl_2$	54	92	8
7	$Pd(PhCN)_2Cl_2$	Traces	-	-
8	$Pd(OAc)_2$	Traces	-	-
9	$Pd(OAc)_2/PPh_3$	74	95	5

[a] Reaction conditions: [Pd] (0.02 mmol), *p*-TsOH (0.3 mmol), acetonitrile (10 ml), phenylacetylene (2.0 mmol), methanol (8.0 mmol), CO (100 psi),110 ◦C, 1 h
[b] Determined by GC based on phenylacetylene.
[c] 0.02 mmol PPh_3 was added
[d] 0.04 mmol PPh_3 was added

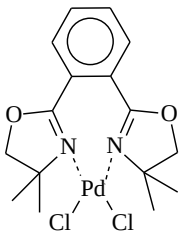

Pd-BOX-1

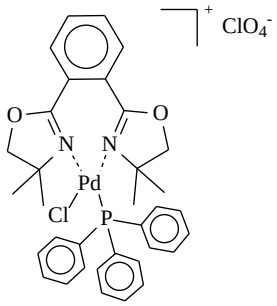

Pd-BOX-10

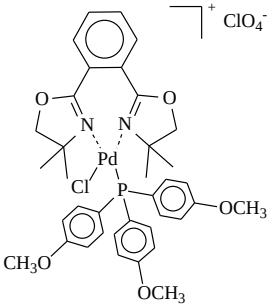

Pd-BOX-11

6.3.1.4 Effect of the type of alcohol

We have extended the scope of our study by considering various linear and branched alcohols as nucleophiles in the alkoxycarbonylation of phenylacetylene (Table 24, entries 1-7). Interestingly, the activity and selectivity were not affected by the length of the carbon chain or the presence of branching in the alcohol nucleophile. All the reactions worked with high selectivity towards the formation of the *gem*-α,β-unsaturated ester (**9**).

TABLE 24. Palladium Catalyzed Alkoxycarbonylation of Phenylacetylene with Various Alcohols.

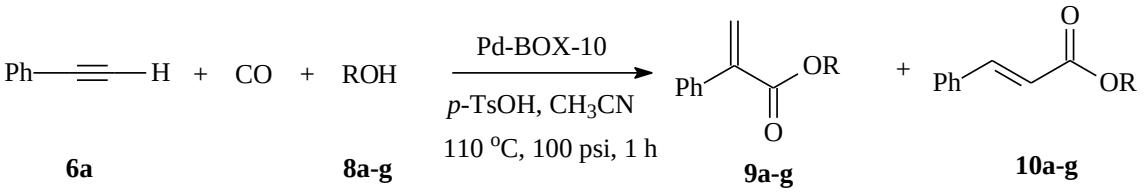

6a **8a-g** **9a-g** **10a-g**

Entry	**Alcohol**	Conversion[b] %	Product Distribution[b] (%)	
			9	10
1	Methanol **8a**	99	97	3
2	Ethanol **8b**	99	98	2
3	Propanol **8c**	99	97	3
4	Butanol **8d**	99	96	4
5	Isopropanol **8e**	99	96	4
6	Isobutanol **8f**	99	97	3
7	Isopentanol **8g**	99	97	3

a .Reaction conditions: Pd-BOX-10 (0.02 mmol), *p*-TsOH (0.30 mmol), acetonitrile (10 ml), phenylacetylene (2.0 mmol), alcohol (8.0 mmol), CO (100 psi),110 ◦C, 1 h

b. Determined by GC based on phenylacetylene.

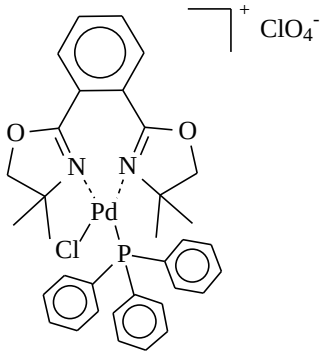

Pd-BOX-10

6.3.1.5 Effect of the type of alkyne

We have further evaluated the new catalytic system in the alkoxycarbonylation of electronically different alkynes. Interestingly, the palladium-bis(oxazoline)-phosphine mixed ligand complexes were highly active in the alkoxycarbonylation reactions of various alkynes. For instance, the methoxycarbonylation of 4-ethynylanisole (**6v**) and 4-ethynyltoluene (**6c**) were achieved to give excellent conversions and very high selectivity in the expected *gem* α,β-unsaturated esters **9** (table 25, entries 2 and 3). Similarly, the methoxycarbonylation of the deactivated aryl alkyne (4-ethynylbenzaldehyde) (**6b**) and of the alkyl alkyne (1-decyne) (**6l**) were also achieved with high conversions and selectivities (table 25, entries 4 and 5). Owing to the lower reactivity of these unactivated alkynes, a longer reaction time was required to achieve high conversions.

Table 25. Palladium Catalyzed Methoxycarbonylation of Alkyne. Effect of Various Alkynes.

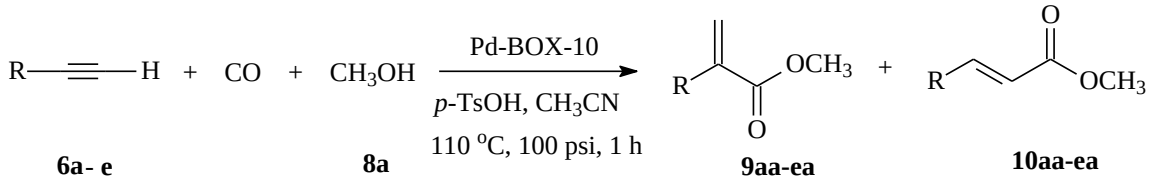

6a- e **8a** **9aa-ea** **10aa-ea**

Entry	Alkyne	Conversion[b] %	Product distribution[b] %	
			9	**10**
1	Phenylacetylene **6a**	99	97 **9aa**	3 **10aa**
2	4-Ethynyltoluene **6c**	98	98 **9ba**	2 **10ba**
3	4-Ethynylanisole **6v**	99	94 **9ca**	6 **10ca**
4[c]	4-Ethynylbenzaldehyde **6b**	79	95 **9da**	5 **10da**
5[c]	1-Decyne **6l**	76	98 **9ea**	2 **10ea**

a. Reaction conditions: Pd-BOX-10 (0.02 mmol), *p*-TsOH (0.3 mmol), acetonitrile (10 ml), alkyne (2.0 mmol), methanol (8.0 mmol), CO (100 psi), 110 °C, 1 h

b. Determined by GC based on alkyne

c. 6 h

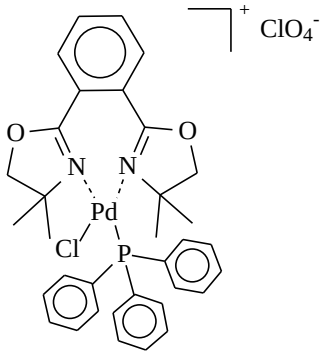

Pd-BOX-10

6.3.1.6 Proposed mechanism of the catalytic cycle

Two reaction pathways can be proposed for our palladium-catalyzed alkoxycarbonylation reaction of phenylacetylene: one is based on a palladium-hydride active species (hydride cycle) [125, 214] and the other one is initiated by a palladium-alkoxy active species (alkoxy cycle) [215]. The above two mechanisms were reported to be the plausible mechanisms for a variety of alkoxycarbonylation reactions of different unsaturated substrates [216-218]. Based on the results of the screening of the different reaction parameters reported above, we can propose a hydride mechanism (Scheme 7) for our catalyst systems, where the active start-up intermediate proposed for this cycle is the Pd(II)-hydridochlorido bis(oxazoline) complex (**1H**). This intermediate is produced via reaction of Pd-BOX-10/11 complex with *p*-TsOH. The experimental results shown in Table 23 proved the requirement of the presence of both phosphine and chloro ligands to initiate the catalytic activity of palladium precursors in the alkoxycarbonylation of phenyleacetylene. The hydride catalytic cycle involves the following steps: i) alkyne coordination and insertion ii) CO addition and insertion and iii) methanolysis of the Pd-acyl species. The catalytic activity has been found to be independent of the type of alcohol employed as reaction nucleophile (Table 24). This evidence rules out a methanolysis reaction path as termination reaction [215].

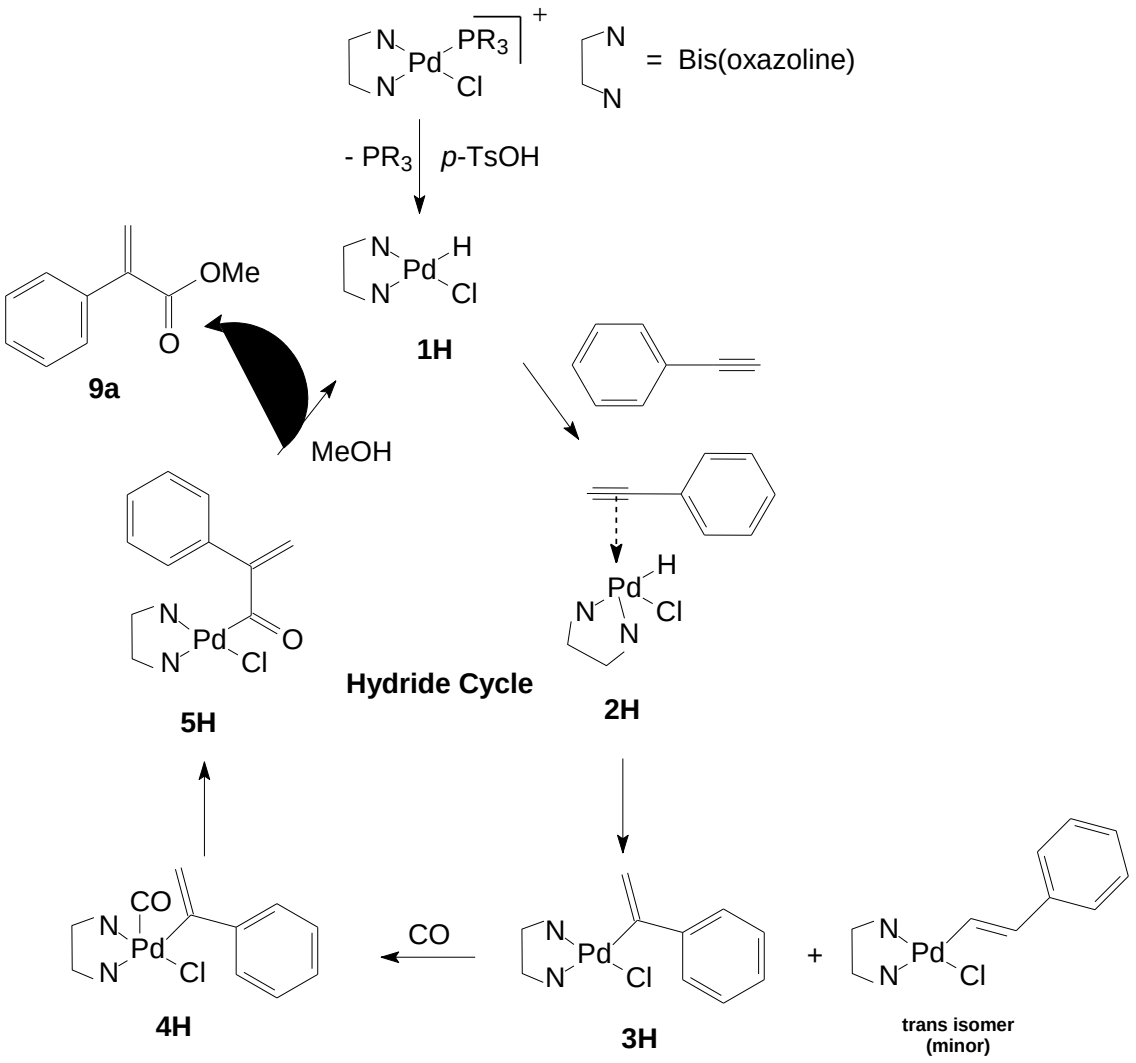

Scheme 7. Alkoxycarbonylation of phenylacetylene by a bis(oxazoline) chloridohydrido Pd(II) complex.

In order to get insight on the hydride mechanism we proposed above and to address the origin of the interesting regioselectivity of our catalyst system, we decided to carry out a computational investigation on the energy of key regioselective intermediates that might exist in both the hydride (**3H**$_{gem}$ and **3H**$_{trans}$) and alkoxy cycles (**5A**$_{gem}$ and **5A**$_{trans}$). Key regioselective intermediates for the alkoxy cycle are only shown for simplicity and the full cycle is reported elsewhere in literature [215, 217]. Recent progress in computational

chemistry has shown that many important chemical and physical properties of the species involved in catalytic reactions can be predicted by this technique [219]. This ability is especially important with respect to homogenously catalyzed reactions, where the isolation of key intermediates is usually difficult to achieve. The optimized geometries for the intermediates $\mathbf{3H_{gem}}$ and $\mathbf{3H_{trans}}$ shown in Figure 27 are distorted square planers (N-Cl-C-N dihedral angles are 0.2° and 1.8°, respectively) , and the phenyl ring of the vinyl moiety is in an opposite direction to the phenyl ring of the bis(oxazoline) moiety in the two intermediates. The Pd-N1/N2 distances in $\mathbf{3H_{gem}}$ and $\mathbf{3H_{trans}}$ are (2.042/2.146 Å) and (2.048/2.149 Å), respectively which are in perfect agreement with crystallographic data of Pd-BOX-1 complex reported earlier [135]. Results in Figure 27 indicated also clearly that the regioselectively of the reaction can be addressed successfully based only on hydride intermediates where the $\mathbf{3H_{gem}}$ isomer was thermodynamically more stable than $\mathbf{3H_{trans}}$ by 1.84 kcal/mol. For the alkoxy key regioselective intermediates, the *trans* isomer $\mathbf{5A_{trans}}$ was more stable than the *gem* intermediate $\mathbf{5A_{gem}}$ by a 11.27 kcal/mol which is against our experimental findings.

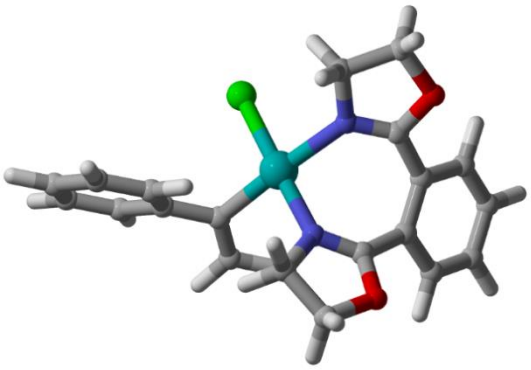 **3H*gem***	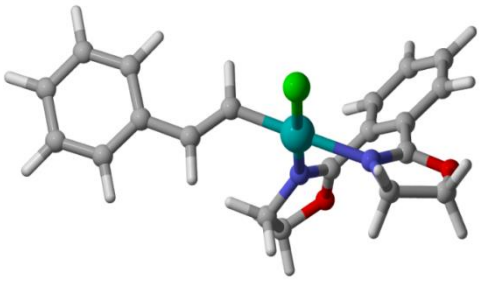 **3H*trans***
E_{tot}(au) = -1622.2676054, ZPE = 220.95128	E_{tot}(au) = -1622.2646303, ZPE = 220.92755
*Energy difference (kcal/mol) = **-2.69**	
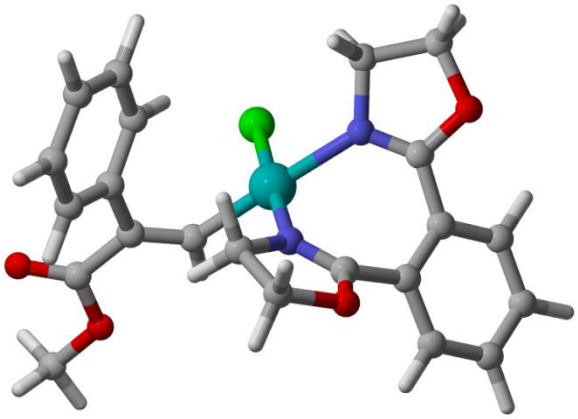 **5A$_{gem}$**	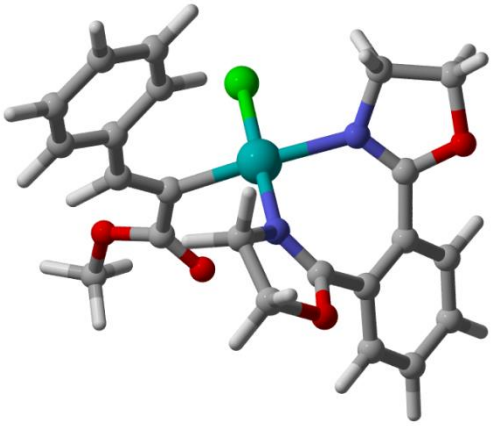 **5A$_{trans}$**
E_{tot}(au) = -1850.2579174, ZPE = 247.97046	E_{tot}(au) = -1850.2623196, ZPE = 248.03890
Energy difference (kcal/mol) = **2.69**	

* Energy difference = [E_{tot}(***gem***)-E_{tot}(***trans***)] x 627.51

Figure 35: DFT/B3LYP-D3/Def2-TZVP Computed Total Electronic Energies (Etot, au), Zero-Point Energies (ZPE, kcal/mol) and Optimized Structures in Acetonitrile for the Intermediates 3Hgem, 3Htrans, 5Agem and 5Atrans.

The transition states for the formation of the intermediates **3H$_{gem}$** and **3H$_{trans}$** were also located (**TS2H/3H$_{gem}$** and **TS2H/3H$_{trans}$**) and the results shown in Figure 35 revealed a small energy difference between the above two transition states (0.89 kcal/mol) and hence no kinetic control over the regioselectivity of our catalytic system. This result is in agreement with our previous computational findings on the olefin insertion process in the alkoxycarbonylation of propyne using palladium bisphosphines complex [220]. It is also worth mentioning here that energy difference of about 1 kcal/mol is in the range of the known accuracy limitations of the computational method used in this study.

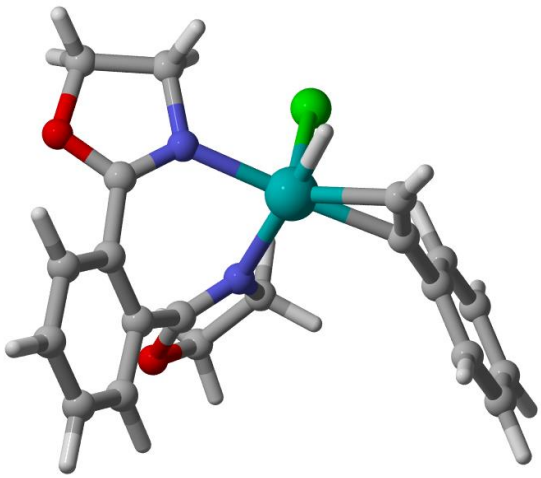 **TS2H/3H$_{gem}$**	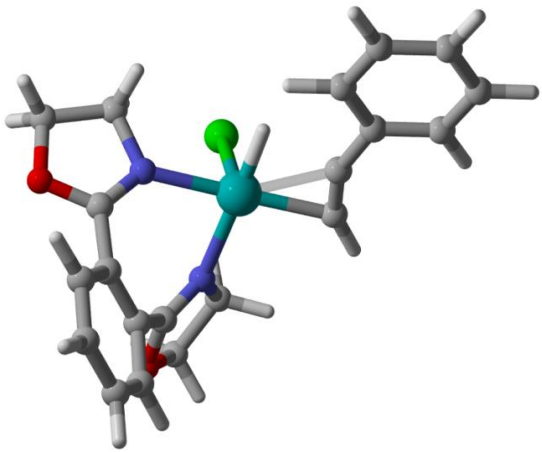 **TS2H/3H$_{trans}$**
E_{tot}(au) = -1622.1942759, ZPE = 216.29705	E_{tot}(au) = -1622.1954388, ZPE = 216.12919
Energy difference (Kcal/mol) = **0.89**	

Figure 36: Optimized structures and computed total electronic energies (Etot, au) for transition states TS2H/3Hgem and TS2H/3Htrans.

6.3.2 Evaluation of the catalytic activity of the new Pd-BOX-PR_3 complexes in the aminocarbonylation of alkynes

The reaction of terminal alkynes with amines in the presence of carbon monoxide as carbonyl source (aminocarbonylation) is an important industrial method for the synthesis of α,β-unsaturated amides. In our investigation, we have chosen the aminocarbonylation of phenylacetylene (**6a**) with diisobutylamine (**11a**) as a model reaction. We have adopted a catalytic system based on $pTsO_3H$-CO-CH_3CN [217] and we have studied the influence of various palladium catalysts (Table 26).

The effect of the type of palladium complex and the ligand on the aminocarbonylation of phenylacetylene was investigated. The results are summarized in Table 26. Only traces of products were observed with Pd-BOX-1 as a catalyst. The mixed ligand palladium complexes (Pd-BOX-10 and Pd-BOX-11) (Table 26, entries 2 and 3) yields also traces of product. There was a remarkable increase in the conversion of phenylacetylene (from traces to 67 %) when dppb was used as a co-ligand (Table 26, entry 4). We have further evaluated some commercially available palladium complexes and salts (Table 26, entries 5-8). Results obtained shows that all the palladium complexes worked only in the presence of diphosphine as co ligand. We have then studied Pd-BOX-3/dppb as catalyst for the aminocarbonylation of phenylacetylene. High conversion of iodobenzene and excellent regioselectivity towards the formation of *gem* α,β-unsaturated amide was achieved (Table 26, entry 10). Based on the latter result, we have adopted (Pd-BOX-3)-dppb-$pTsO_3H$-CO-CH_3CN as the optimum catalytic system for the aminocarbonylation reaction.

TABLE 26. Palladium Catalyzed Aminocarbonylation of Phenylacetylene. Effect of Type of Pd-Catalyst.

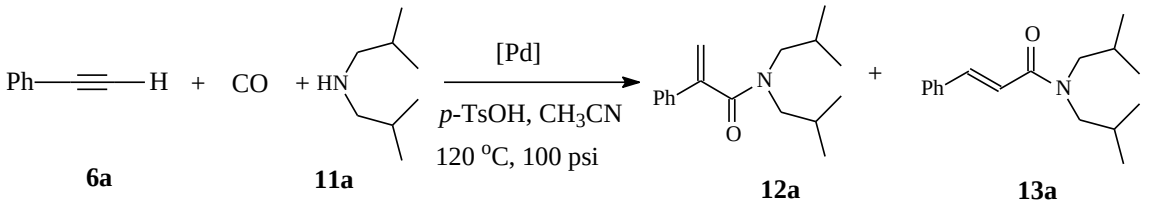

6a **11a** **12a** **13a**

Entry	Catalyst	% Conversion[b]	Product distribution (%)[b]	
			12a	**13a**
1	Pd-Box-**1**	Traces		
2	Pd-Box-**10**	Traces	-	-
3	Pd-Box-**11**	Traces		
4	Pd-Box-**10**/dppb	67	97	3
5	$Pd(PPh_3)_2Cl_2$	Traces	-	-
6	$Pd(PhCN)_2Cl_2$	Traces	-	-
7	$Pd(OAc)_2$	Traces	-	-
8	$Pd(OAc)_2$/dppb	65	97	3
9	Pd-BOX-**1**/dppb	25	90	10
10	Pd-BOX-**3**/dppb	90	98	2

a Reaction conditions: [Pd] (0.02 mmol), *p*-TsOH (0.3 mmol), acetonitrile (10 ml), phenylacetylene (2.0 mmol), DIBA (2.2 mmol), CO (100 psi), 120 ◦C, 6 h

b Determined by GC base on phenylacetylene.

c Amount of dppb added: 0.08 mmol

6.3.2.1 Evaluation of the catalytic activity of the newly prepared Pd-BOX complexes in the aminocarbonylation of alkynes. Effect of various amines

We have studied the effect of various primary and secondary amines as nucleophiles in the aminocarbonylation of phenylacetylene with the catalytic system (Pd-BOX-3)-dppb-$pTsO_3H$-CO-CH_3CN (Table 27, entries 1-4). The reactivity was found to depend on the type of the amine employed. Diisobutylamine (Table 27, entry 1) (99) was found to be the most reactive. The conversion of phenylacetylene was found to decrease when isobutylamine was employed as a nucleophile (Table 27, entry 2) (48%). This could be due to the less nucleophilicity of primary amine when compared with the secondary amine. The use of benzylamine as a nucleophile was also successful and yielded selectively, the *gem* amide (Table 27, entry 3). Diethylamine was also less reactive than isobutylamine (50%) (Table 27, entry 4). All the reactions worked with high selectivity towards the *gem*-α,β-unsaturated amides (**12**).

Table 27. Palladium-Bis(Oxazoline) Catalyzed Aminocarbonylation Reaction of Phenylacetylene. Effect of Various Amines.

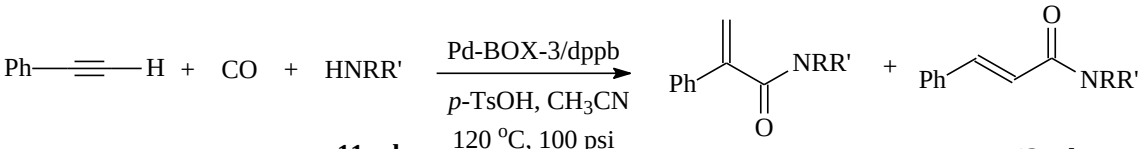

6a **11a-d** **12a-d** **13a-d**

Entry	Amine	% Conversion[b]	Product distribution[b]	
			12a-d	**13a-d**
1	Diisobutylamine **11a**	99	97	3
2	Isobutylamine **11b**	48	98	2
3	Benzylamine **11c**	80	99	1
4	Diethylamine **11d**	50	97	3

a Reaction conditions: Pd-BOX-3 (0.02 mmol), dppb (0.08mmol) *p*-TsOH (0.3 mmol), acetonitrile (10 ml), phenylacetylene (2.0 mmol), amine (2.2 mmol), CO (100 psi), 120°C, 20h

b Determined by GC based on phenylacetylene.

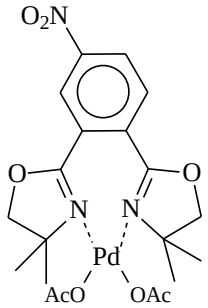

Pd-BOX-3

6.3.3 Evaluation of the catalytic activity of the newly prepared supported palladium-BOX catalysts in the alkoxycarbonylation of aryl iodides

Palladium-catalyzed alkoxycarbonylation reaction of aryl halides is a versatile reaction for the synthesis of various aromatic carboxylic acids and their derivatives. The reaction is of synthetic value due to the exceptionally low cost of carbon monoxide and from the diversity of aromatic esters that can be achieved by selecting the proper alcohol. In our investigation, we have chosen the methoxycarbonylation of iodobenzene (**1c**) using Pd-BOX-12 as a catalyst. We have studied the influence of various reaction parameters including temperature, base, solvent, and type of palladium catalyst.

A preliminary alkoxycarbonylation reaction of iodobenzene with methanol (**8a**) using the catalytic system (Pd-BOX-12)/KOH/CH_3OH/70 ^oC (Table 28, entry 1) yielded 50% of methyl benzoate after 3 h reaction. The catalytic activity was found to be highly temperature dependent. The yield of methylbenzoate increased significantly from 50 % to 85 % when the temperature was raised from 70 ^oC (Table 28, entry 1) to 100^oC (Table 28, entry 2) and to 90 % yield at 110 ^oC (Table 28, entry 3). Full conversion of iodobenzene and almost quantitative yield of the ester was obtained on raising the temperature to 120^oC (Table 28, entry 4). The selectivity was not affected by changing the reaction temperature.

We further screened various bases using the optimized temperature. Potassium hydroxide gave excellent yield (99%) of the product (Table 28, entry 4). Similarly, full conversion and almost quantitative yield was obtained with NaOH (Table 28, entry 5). Potassium carbonate gave 96% of the methyl benzoate (Table 28, entry 6). The use of an organic base such as triethylamine resulted in excellent yield of the required ester (93%) (Table 28, entry

7). We have then studied the optimized reaction using acetonitrile as a solvent and methanol as a nucleophile (Table 28, entry 8). Comparable excellent yield of the ester was achieved.

The effect of the type of palladium catalyst on the methoxycarbonylation of iodobenzene was investigated. No product was obtained in the absence of palladium catalyst (Table 28, entry 9). The supported palladium-bis(oxazoline) complexes (Pd-BOX-12 and Pd-BOX-13) (Table 28, entries 4 and 10) yielded full conversion and 100% selectivity in favor of the methyl benzoate. Similar high conversions and excellent selectivities were achieved with the homogeneous palladium-bis(oxazoline) complexes (Pd-BOX-1, Pd-BOX-3 and Pd-BOX-6) (Table 28, entries 11-13). We have further compared the catalytic activities of our newly prepared palladium-bis(oxazoline) complexes with some commercially available palladium complexes and salts such as $Pd(PPh_3)_2Cl_2$ (table 28, entry 14) (96%), $Pd(PhCN)_2Cl_2$ (table 28, entry 15) (99%) and $Pd(OAc)_2$ (table 28, entry 16) (95%). Interestingly, the palladium salts and complexes were similar in activity to our newly prepared palladium-bis(oxazoline) complexes. However, the newly prepared supported palladium-bis(oxazoline) complexes possess the potential of being recycled and reused several times for the same or similar reaction. Consequently, the supported palladium-bis(oxazoline) complexes possess higher TON and TOF than most commercially available palladium complexes and salts.

TABLE 28. Palladium-Bis(Oxazoline) Catalyzed Methoxycarbonylation of Iodobenzene. Optimization of Reaction Conditions using Supported Catalysts

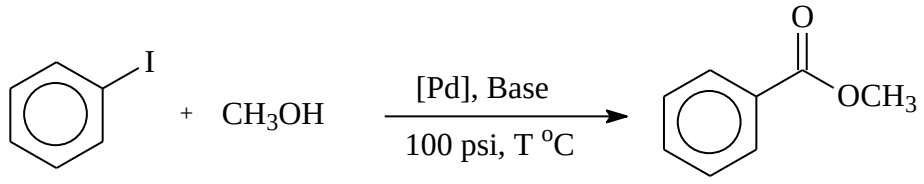

1c **8a** **14a**

Entry	Pd-Complex	Solvent (5 mL)	Base	Temperature (°C)	Yield (%)[b]
1	Pd-BOX-12	Neat CH_3OH	KOH	70	50
2	Pd-BOX-12	Neat CH_3OH	KOH	100	85
3	Pd-BOX-12	Neat CH_3OH	KOH	110	90
4	Pd-BOX-12	Neat CH_3OH	KOH	120	99
5	Pd-BOX-12	Neat CH_3OH	NaOH	120	99
6	Pd-BOX-12	Neat CH_3OH	K_2CO_3	120	96
7	Pd-BOX-12	Neat CH_3OH	Et_3N	120	93
8	Pd-BOX-12	CH_3CN/CH_3OH	KOH	120	99
9	-	Neat CH_3OH	KOH	120	Trace
10	Pd-BOX-13	Neat CH_3OH	KOH	120	96
11	Pd-BOX-1	Neat CH_3OH	KOH	120	99
12	Pd-BOX-3	Neat CH_3OH	KOH	120	99
13	Pd-BOX-6	Neat CH_3OH	KOH	120	99
14	$Pd(PPh_3)_2Cl_2$	Neat CH_3OH	KOH	120	96
15	$Pd(PhCN)_2Cl_2$	Neat CH_3OH	KOH	120	99
16	$Pd(OAc)_2$	Neat CH_3OH	KOH	120	95

a. Reaction conditions: [Pd] (0.0050 mmol), iodobenzene (1.0 mmol), Solvent (5.0 mL), Base (2.0 mmol), CO (100 psi), 3 h
b. GC Yield.

6.3.3.1 Supported palladium-BOX catalysts catalyzed methoxycarbonylation of iodobenzene: Recycling ability of the supported catalysts

The recycling ability of the new supported palladium-bis(oxazoline) catalysts (**Pd-BOX-12** and **Pd-BOX-13**) was investigated in the methoxycarbonylation reaction of iodobenzene at 100 psi CO pressure and a temperature of 100 ^{o}C for 6 h. The results of the recycling experiments are presented on Figures 37 and 38 for the supported complexes **Pd-BOX-12** and **Pd-BOX-13,** respectively. Remarkably, the two supported catalysts could be recycled up to ten times devoid of substantial loss in their catalytic activities. The turnover number of the supported complexes **Pd-BOX-12** and **Pd-BOX-13** were estimated for the 10 cycles as 1884 and 1880, respectively, while the turnover frequency for the supported complexes were estimated as 314/h and 313/h for the supported catalysts **Pd-BOX-12** and **Pd-BOX-13,** respectively. In order to confirm the effectiveness and the high activities realized with the supported catalysts, we have conducted experiments with the amount of iodobenzene equal to the total amount used in all the ten cycles (10.0 mmol) using the same quantity of supported palladium-bis(oxazoline) catalyst (0.005 mmol) (substrate to catalyst ratio equals to 2000). Excellent yield of methyl benzoate were recorded for **Pd-BOX-12** (95%) and **Pd-BOX-13** (91%) catalysts. Similarly, the turnover number of the supported palladium-bis(oxazoline) catalysts in the later experiments were estimated as 1860 and 1820, while the turnover frequencies were estimated as 310/h and 303/h for the supported palladium-bis(oxazoline) catalysts **Pd-BOX-12** and **Pd-BOX-13** catalysts, respectively.

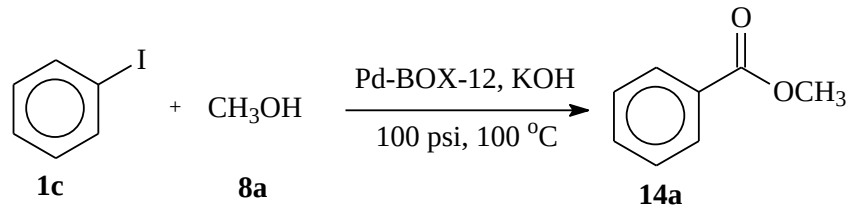

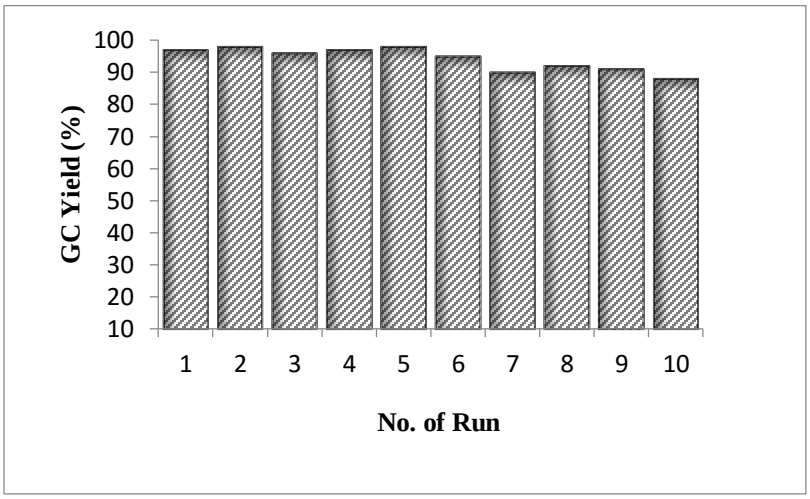

Figure 37: Methoxycarbonylation Reaction of Iodobenzene. Recycling Ability of Merifield's Resin Supported Palladium-Bis(Oxazoline) (Pd-BOX-12) Catalyst.

Reaction conditions: [Pd] (0.0050 mmol), iodobenzene (1.0 mmol), methanol (5.0 mL), KOH (2.0 mmol), CO (100 psi), 100 °C, 6 h

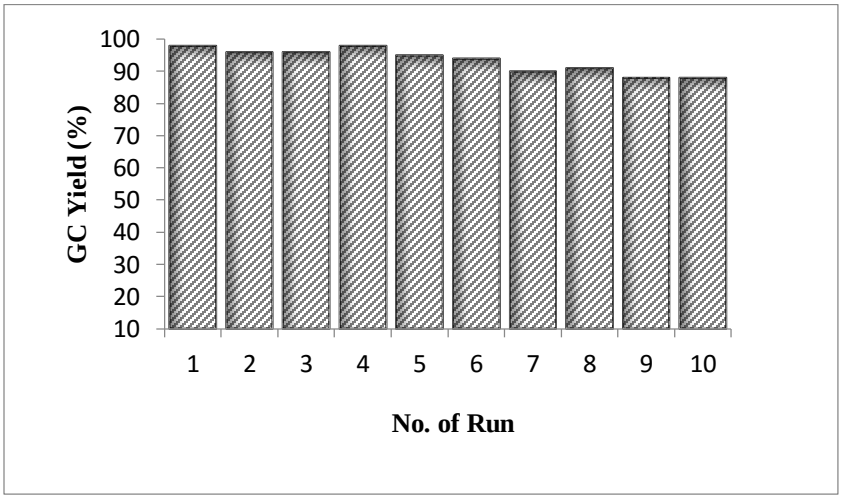

Figure 38: Methoxycarbonylation Reaction of Iodobenzene. Recycling Ability of Silica Supported Palladium-Bis(Oxazoline) (Pd-BOX-12) catalyst.

Reaction conditions: [Pd] (0.0050 mmol), iodobenzene (1.0 mmol), methanol (5.0 mL), KOH (2.0 mmol), CO (100 psi), 100 °C, 6 h

6.3.3.2 Supported palladium-BOX complex catalysed alkoxycarbonylation of aryl iodides: Effect of various substrates

The excellent recycling ability realized with the new supported palladium-bis(oxazoline) complexes in the methoxycarbonylation of iodobenzene encouraged us to study the scope of the new catalytic system and to examine its recycling ability in the alkoxycarbonylation reaction of a broad range of substrates using a CO pressure of 100 psi and KOH as a base. Thus, the alkoxycarbonylation of iodobenzene with various alcohols including aliphatic (primary, secondary and tertiary aliphatic alcohols) as well as aromatic alcohols were studied (Table 29). The catalyst used in the first example (Table 29, entry 1) was carefully separated, washed with methanol and dried in an oven at 100 ^{o}C. The recovered catalyst could be again used in the alkoxycarbonylation of aryl iodide if the same cleaning and drying procedure after each reaction are applied. However, a fresh catalyst was used for the study with various substrates. All the alcohols studied gave excellent conversion, and in some cases the corresponding esters were isolated in excellent yields. Primary aliphatic alcohols (Table 29, entries 1-3) reacted smoothly to yield the corresponding aromatic ester. The reactivity of primary alcohols was not affected by the length of the carbon chain. Secondary and tertiary aliphatic alcohols (Table 29, entries 4 and 5), however, were relatively less reactive compared to the primary alcohols and therefore longer reaction time was necessary to achieve their full conversions. In the alkoxycarbonylation reactions, the alcohol served as a nucleophile and also as a solvents for the reaction. The alkoxycarbonylation reaction of iodobenzene with phenol was carried-out using acetonitrile as solvent (Table 29, entry 7)

The electronic effect of aryl iodides were also studied in the same carbonylation reaction. Both activated and deactivated aryl iodides worked effectively to lead to the corresponding

aromatic ester. The presence of a deactivating group on the aryl iodide enhanced its reactivity and the corresponding ester was isolated in excellent yield (Table 29, entry 9). Similarly, 4-iodoanisole reacted smoothly to yield methyl 4-methoxybenzoate (Table 29, entry 10). The methoxycarbonylation of 1,4-diiodobenzene was also successful and yields dimethylbenzene-1,4-dicarboxylate (Table 29, entry 11)

TABLE 29. Alkoxycarbonylation Reaction of Iodobenzene Using Pd-BOX-12 As Catalyst. Effect of Different Substrates.

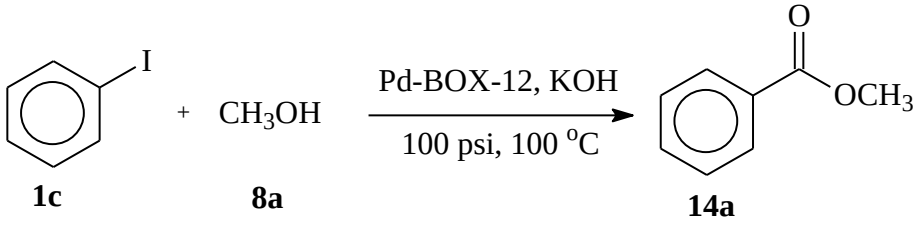

1c **8a** **14a**

Entry	Arylhalide 1c, d, p	Alcohol 8a – k	Product (ester) 14a – k	Time (h)	Conversion (%)[c]
1	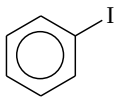 **1c**	CH_3OH **8a**	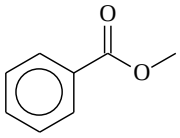 **14a**	6	99
2	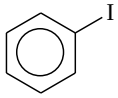 **1c**	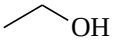 **8b**	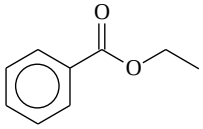 **14b**	6	99
3	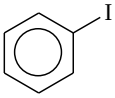 **1c**	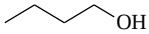 **8d**	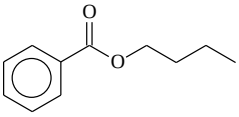 **14c**	6	96
4	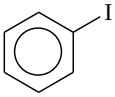 **1c**	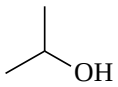 **8e**	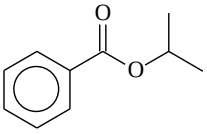 **14d**	12	95
5	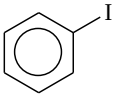 **1c**	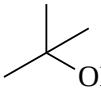 **8h**	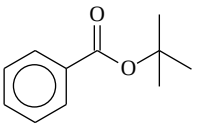	12	99 (92)

			14e		
6	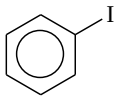 **1c**	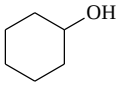 **8i**	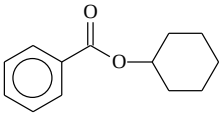 **14f**	12	99
7[b]	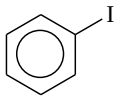 **1c**	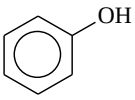 **8j**	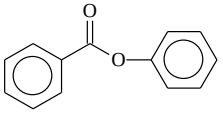 **14g**	6	99 (95)
8	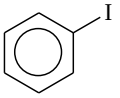 **1c**	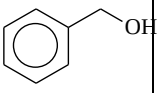 **8k**	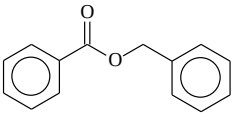 **14h**	6	99 (92)
9	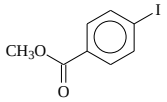 **1p**	CH_3OH **8a**	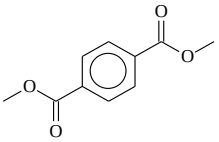 **14i**	6	99 (94)
10	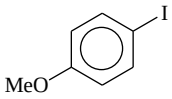 **1d**	CH_3OH **8a**	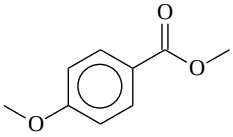 **14j**	6	96 (90)
11	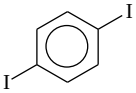 **1o**	CH_3OH **8a**	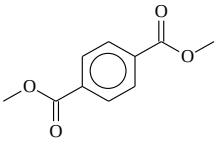 **14i**	12	99 (92)

a. Reaction conditions: Pd-BOX-12 (0.005 mmol), aryl iodide (1.0mmol), alcohol (5 ml), KOH (2.00 mmol), CO (100 psi), 100 °C
b. Phenol (2.0 mmol), CH_3CN (5.0 mL), 120 °C
c. Percent conversion based aryl iodide
d. Isolated yield is given in bracket

6.3.4 Supported palladium-BOX catalysts for aminocarbonylation of aryl iodides: Recycling ability of the catalyst

Palladium-catalyzed aminocarbonylation of aryl halides is a widely used methodology in the synthesis of carboxamides from easily accessible starting materials. Various amides including those with bulky N-substitutions can easily be accessed by selecting the proper aryl iodide and amine [220]. We have tested the catalytic activities of the new supported palladium-bis(oxazoline) complexes in the aminocarbonylation of aryl iodides. Various amines were considered in this reaction.

The recycling ability of the new supported palladium-bis(oxazoline) complexes (**Pd-BOX-12** and **Pd-BOX-13**) was also investigated in the aminocarbonylation reaction of iodobenzene with diisobutylamine (DIBA) in the presence of trimethylamine as a base at 100 psi CO pressure and a temperature of 120 ^{o}C for 6 h. The results of the recycling experiments are presented on tables 30 and 31 for the supported complexes **Pd-BOX-12** and **Pd-BOX-13,** respectively. The two supported complexes were recycled up to six times without showing significant loss in their catalytic activities. However, a drop in activity to 61 % and 56 % conversions of iodobenzene were observed with supported complexes **Pd-BOX-12** and **Pd-BOX-13** respectively, during the seventh cycle.

TABLE 30. Aminocarbonylation of Iodobenzene. Recycling Ability Of Merifield's Resin Supported Palladium-Bis(Oxazoline) (Pd-BOX-12) Catalyst

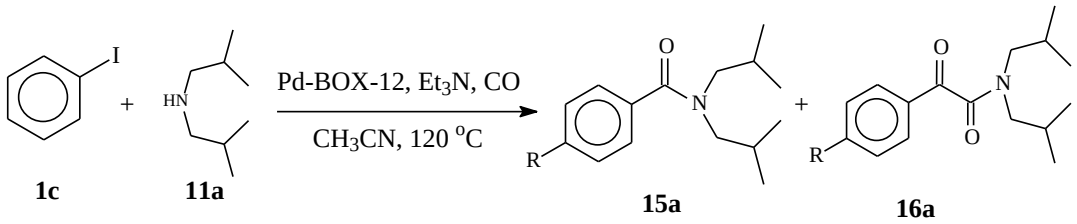

1c **11a** **15a** **16a**

Run	% Conversion[b]	Product distribution[b]	
		15a	**15b**
1	99	96	4
2	99	95	5
3	99	96	4
4	92	96	4
5	88	96	4
6	85	96	4
7	61	95	5

[a] Reaction conditions: Pd-BOX-12 (0.005 mmol), iodobenzene (1.0 mmol), DIBA (2.0 mmol), Et_3N (3.0 mmol), acetonitrile (5.0 ml), CO (200 psi), 120 °C, 6 h.

[b] Determined by GC based on iodobenzene.

TABLE 31. Aminocarbonylation of Iodobenzene. Recycling Ability of Silica Supported Palladium-Bis(Oxazoline) (Pd-BOX-13) Catalyst.

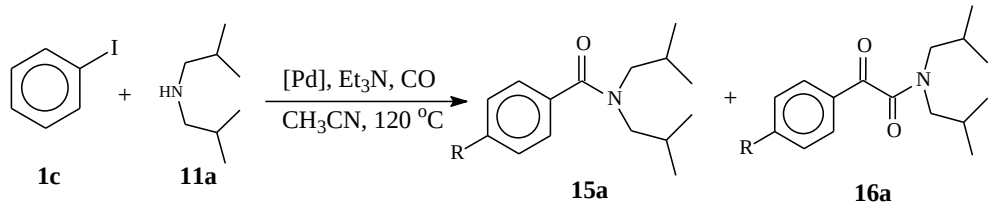

1c **11a** **15a** **16a**

Run	% Conversion[b]	Product distribution[b]	
		15a	**15b**
1	99	96	4
2	98	96	4
3	99	95	5
4	95	96	4
5	90	96	4
6	85	95	5
7	56	96	4

a.Reaction conditions: Pd-BOX-12 (0.005 mmol), iodobenzene (1.0 mmol), DIBA (2.0 mmol), Et_3N (3.0 mmol), acetonitrile (5.0 ml), CO (200 psi), 120 °C, 6 h.
b.Determined by GC based on iodobenzene.

6.3.4.1 Supported palladium-BOX complexes catalysed aminocarbonylation of aryl iodides: Effect of various substrates

We have extended the scope of the aminocarbonylation reaction by considering various amines including primary and secondary amines as nucleophiles and various aryl iodides (Table 32, entries 1-7). The rate of the aminocarbonylation reaction was found to depend on the type of the amine employed. For instance, secondary amines such as diisobutylamine and dicyclohexylamine reacted smoothly with iodobenzene (Table 32, entries 1 and 2). The reaction of iodobenzene with diisobutylamine yielded the corresponding carboxamide (96%) and a ketocarboxamide (4%). However, the reaction of iodobenzene with dicyclohexylamine yielded the carboxamide as the only product. The aminocarbonylation of iodobenzene with aniline as nucleophile was also successful and yielded selectively *N*-phenylbenzamide as sole product (Table 32, entry 3). The catalyst system also give excellent conversions in the aminocarbonylation of iodobenzene with primary amines as nucleophiles (Table 32, entries 4 and 5). However, in contrast to secondary amines, primary amines show relatively poor selectivity and a mixture of carbonylation and double carbonylation products were obtained.

The effect of substituent on the aryl iodide was also investigated in the aminocarbonylation reaction. Interestingly, the supported palladium-bis(oxazoline) complexes were highly active in the aminocarbonylation reactions of both activated and unactivated aryl iodides. For instance, the aminocarbonylation of 4-iodoanisole (**1d**) and methyl 4-iodobenzoate (**1p**) with diisobutylamine were achieved to give excellent conversions and very high selectivities in the expected carboxamides (Table 32, entries 6 and 7).

TABLE 32. Aminocarbonylation of Iodobenzene Using Pd-BOX-12 as Catalyst. Effect of Different Substrates.

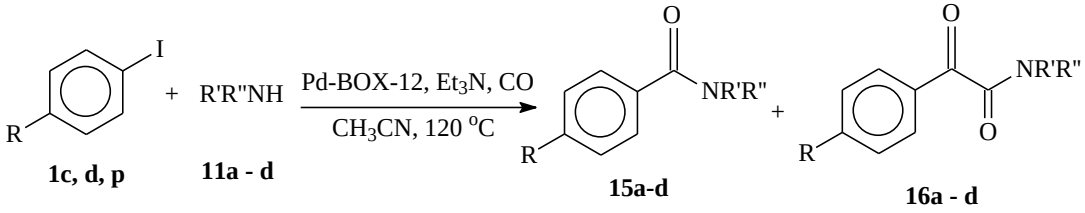

1c, d, p **11a - d** **15a-d** **16a - d**

Entry	Aryl halide 1 c, d, p	Amine 11a – 11f	Conversion[b] %	Product Distribution[b] %	
				15a-d	16a-d
1	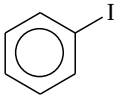 **1c**	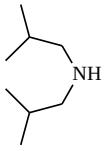 **11a**	99	96	4
2	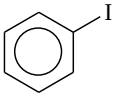 **1c**	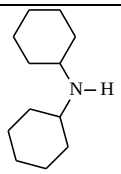 **11b**	99	100	0
3	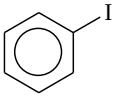 **1c**	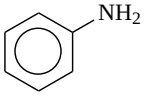 **11e**	99	100	0
4	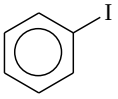 **1c**	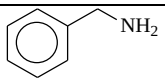 **11c**	99	40	35
5	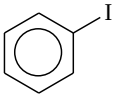 **1c**	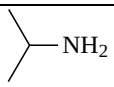 **11f**	99	38	30
6	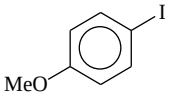 **1d**	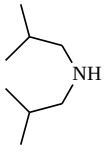 **11a**	99	96	4
7	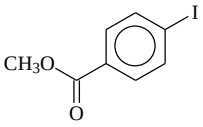 **1p**	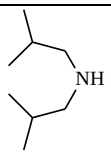 **11a**	99	93	7

8	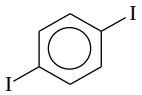 **1o**	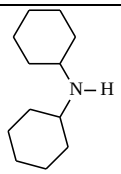 11b	99	100	0

a. Reaction conditions: Pd-BOX-12 (0.005 mmol), Aryliodide (1.0 mmol), amine (2.0 mmol), Et_3N (3.00 mmol), CO (100 psi), 120 °C, 6 h.
b. Percent conversion determined by GC based on aryl iodide

6.4 Characterization of the used supported palladium-bis(oxazoline) catalysts

The ability to reuse the supported palladium-bis(oxazoline) complexes several times and in various reactions without significant loss in their catalytic activities demonstrates their high stabilities. The interesting results realized with the supported catalysts urged us to carry out further investigations to asses any change in the physical and chemical structures of the used catalysts in comparison with the unused complexes. The recovered catalysts from all the two applications were analyzed with FT-IR, XPS and the amount of palladium was established using ICP-MS.

6.4.1 Characterization of the used supported palladium-bis(oxazoline) catalysts using FT-IR

The recovered palladium-bis(oxazoline) catalysts were washed successively with distilled water, acetone and methanol. The catalysts were then dried in an oven at 100 ^{o}C prior to analysis. The dried catalysts were pressed in to disc with KBr and analysed using FT-IR. The FT-IR spectra for the recovered merifield's resin and the silica supported palladium-bis(oxazoline) catalysts were found to be similar with the spectra of the unused catalysts (Figure 39 and Figure 40).

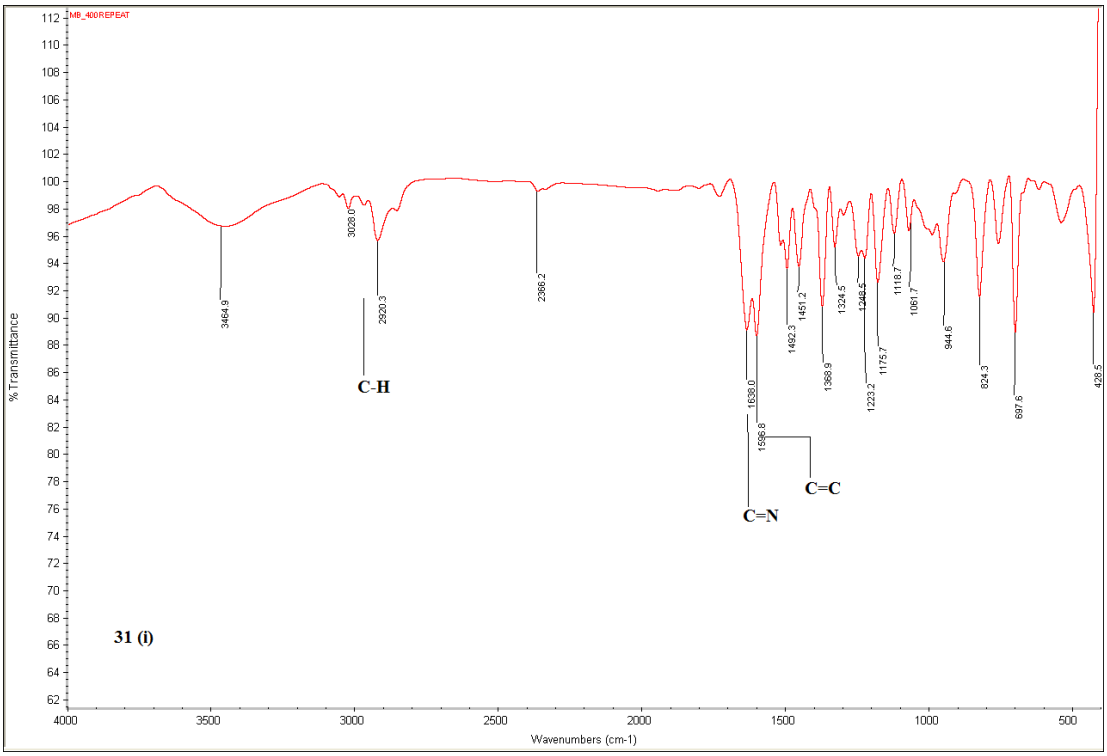

Figure 39. FT-IR Spectrum of Pd-BOX-12 catalysts Recovered from Alkoxycarbonylation Reaction

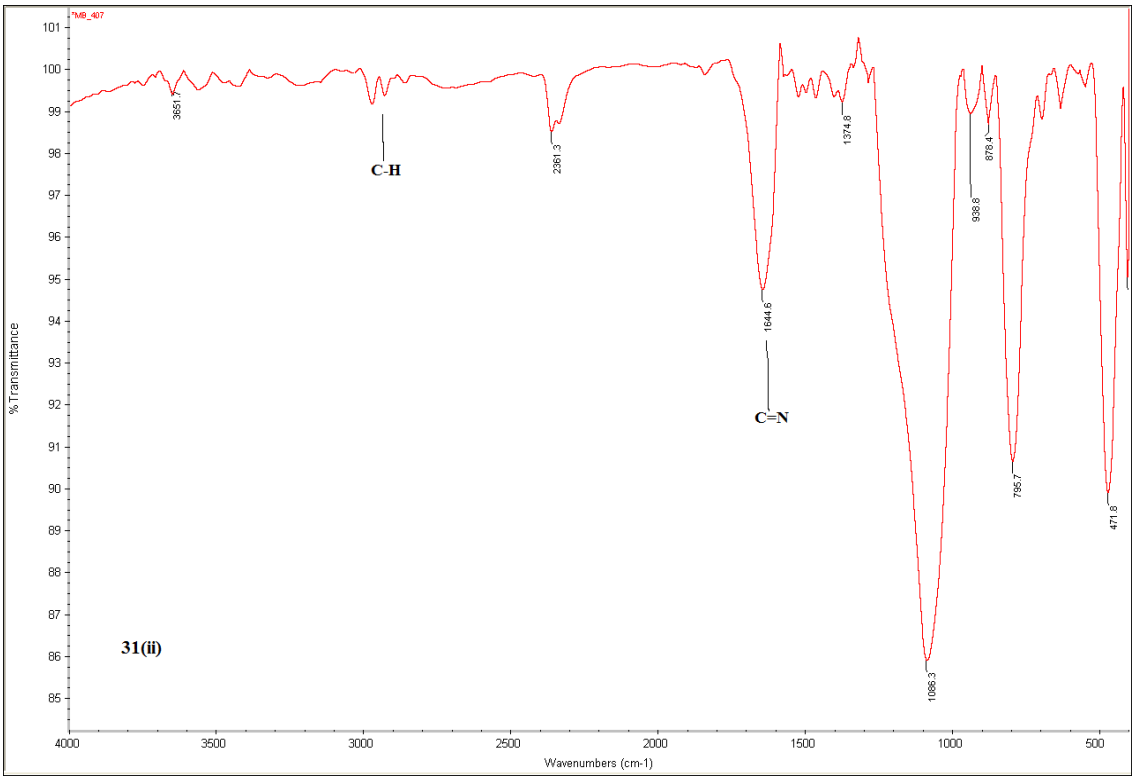

Figure 40: FT-IR Spectrum of Pd-BOX-13 catalysts Recovered from Alkoxycarbonylation Reaction

6.4.2 Analysis of the used supported palladium-bis(oxazoline) catalysts using ICP-MS

The percentages of palladium on **Pd-BOX-12** and **Pd-BOX-13** recovered after the tenth cycle of the alkoxycarbonylation reaction were determined using ICP-MS and were found to be 6.0% and 2.2%, respectively. Whereas, the amount of palladium on **Pd-BOX-12** and **Pd-BOX-13** recovered after the seventh cycle of the aminocarbonylation reaction were estimated as 5.1% and 1.9%, respectively.

These results indicate that the amount of palladium on the supported catalysts recovered from alkoxycarbonylation reactions are similar to the amount of palladium in the unused catalyst and could be the reason for the high recycling ability observed in the alkoxycarbonylation reaction.

On the other hand, the amount of palladium on the supported catalysts recovered from aminocarbonylation reaction were much less than the amount of palladium on the unused supported complexes (there is 24 % and 32 % losses of palladium from **Pd-BOX-12** and **Pd-BOX-13** respectively). This could be the reasons for the decreased in catalytic activities observed in the later cycles of the aminocarbonylation.

TABLE 33. Comparison of Percentage of Palladium in the Fresh and the Used Supported Catalysts

	Fresh catalyst (%)	**Catalyst recovered from alkoxycarbonylation (%) (after 10 cycles)**	**Catalyst recovered from aminocarbonylation (%) (after 7 cycles)**
Pd-BOX-12	6.7	6.0	5.1
Pd-BOX-13	2.8	2.2	1.9

6.4.3 Analysis of the used supported palladium-bis(oxazoline) catalysts using XPS

The XPS studies of the supported palladium-bis(oxazoline) catalysts Pd-BOX-12 (Figure 41) and Pd-BOX-13 (Figure 42), recovered after the tenth cycle of the alkoxycarbonylation reaction shows that the oxidation state of palladium remains unchanged after the catalytic application. Similar to the unused supported catalysts, the 3d spectrum resolved in to $3d_{5/2}$ and $3d_{3/2}$ spin orbit pairs with binding energies 334.88 eV and 339.98 eV (Pd-BOX-12) and 336.28 eV and 341.58 eV (Pd-BOX-13) respectively [161, 162].

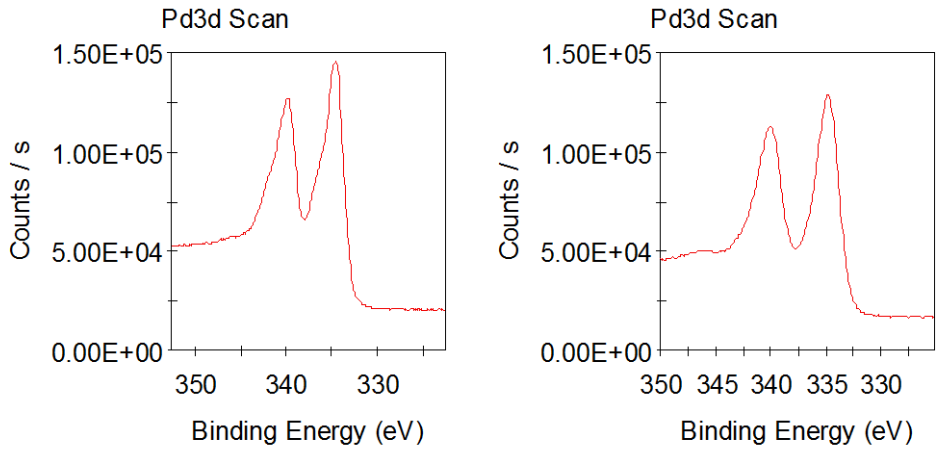

Figure 41: XPS Spectrum of Pd-BOX-12 Recovered from Alkoxycarbonylation reaction Showing the Pd 3d, (right specturum) Spectrum of fresh catalyst is displayed on the left

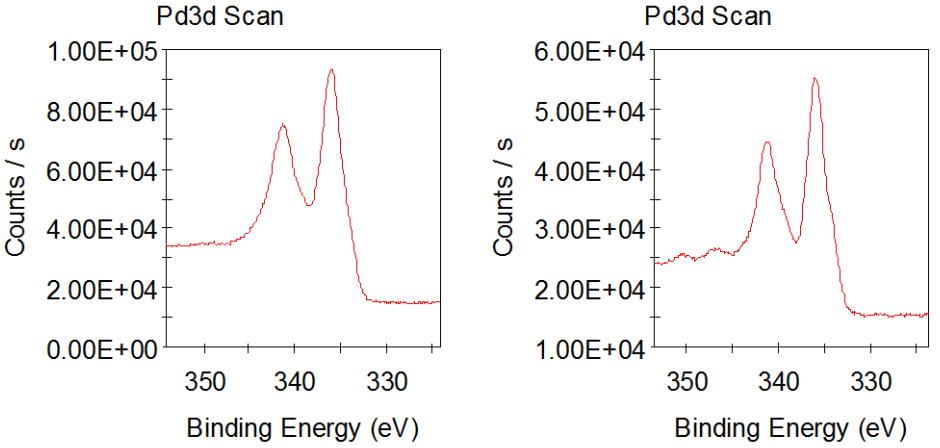

Figure 42: XPS Spectrum of Pd-BOX-13 Recovered from Alkoxycarbonylation reaction showing the Pd 3d (right specturum). Spectrum of fresh catalyst is displayed on the left

6.5 Palladium leaching test

The main objective of supporting a homogeneous catalyst is to enable its easy separation from the product and to minimize the level of contamination caused by the toxic metal. The possible palladium leaching into the product was analyzed using ICP-MS. After the tenth cycle of the alkoxycarbonylation and the seventh cycle of the aminocarbonylation, the products of each reaction were combined in separate containers. Samples were taken from each reaction for the analysis. The samples were digested using concentrated nitric acid. The solutions were then analyzed with inductively coupled plasma mass spectrometry (ICP-MS).

The results of the ICP-MS analysis show that the concentration of palladium in the products are 2.0 ppb and 2.3 ppb for Pd-BOX-12 and Pd-BOX-13 catalyzed alkoxycarbonylation, respectively. This means less than 0.1 % of the total palladium on the supported complexes was leached into the solution. On the other hand, the amount of palladium that leached into the solution during the aminocarbonylation reactions were 195.0 ppb and 166.0 ppb for Pd-BOX-12 and Pd-BOX-13, respectively. These amounts were estimated as 3.4 % and 1.2 % of the total palladium on the supported catalysts, respectively. These results clearly show that the palladium leaching during aminocarbonylation reaction was significantly higher than the alkoxycarbonylation, which explains the reason for the relatively lower recycling ability encountered during the aminocarbonylation reaction as compared to the alkoxycarbonylation reaction. The higher leaching of palladium observed with the aminocarbonylation reaction could be the result of palladium coordination to the amine

(either trimethylamine used as base or the amine nucleophile). This results in the formation of homogeneous complexes that are highly soluble in the liquid phase [221].

CHAPTER 7

CONCLUSIONS

1. The synthesis and characterization of five new non C_2-symmetric and two new C_2-symmetric bis(oxazoline) ligands (**BOX-1** to **BOX-7**) were accomplished. We have also synthesized five new dichlorido palladium-bis(oxazoline) complexes (**Pd-BOX-1, Pd-BOX-2, Pd-BOX-4, Pd-BOX-5 and Pd-BOX-7**), one new diacetato palladium-bis(oxazoline) (**Pd-BOX-3**) complex and one new dibromido palladium-bis(oxazoline) complex (**Pd-BOX-6**). The X-ray crystal structures of the seven new complexes (**Pd-BOX-1** to **Pd-BOX-7**) were determined. The coordination to the palladium ion allows the non C_2-symmetric bis(oxazoline) ligand-based complexes (**Pd-BOX-2** to **Pd-BOX-6**) to acquire a rigid backbone curvature and an inherent chirality.
2. The synthesis and characterization of two new water soluble bis(oxazoline) ligands (**BOX-8** and **BOX-9**) and their diclorido palladium complexes (**Pd-BOX-8** and **Pd-BOX-9**) were achieved.
3. The synthesis and characterization of two new cationic palladium-bis(oxazoline) phosphine mixed ligand complexes (**Pd-BOX-10** and **Pd-BOX-11**) were also accomplished.
4. The synthesis and characterization of two new supported bis(oxazoline) ligands (**BOX-10 and BOX-11**) and their diclorido palladium(II) complexes (**Pd-BOX-12 and Pd-BOX-13**) were achieved.

5. Palladium-bis(oxazoline) complexes (**Pd-BOX-1** to **Pd-BOX-7)** showed outstanding catalytic activities in various important cross coupling reactions including Suzuki-Miyaura, Mizaroki-Heck and Sonogashira cross coupling reactions. Various biaryl, internal alkenes and internal alkynes compounds have been synthesized in excellent isolated yields. The catalytic system can tolerate a wide range of substituents on the arylhalides, arylboronic acids, styrene derivatives and alkynes. Moreover, the new palladium-bis(oxazoline) complexes were highly efficient in the synthesis of various internal alkynes from the Sonogashira cross coupling reactions of aryl halides with a wide range of aryl and alkyl alkynes in the absence of copper.
6. The alkoxycarbonylation and aminocarbonylation of terminal alkynes proceeded smoothly with the newly synthesized palladium-bis(oxazoline) phosphine mixed ligand complexes (**Pd-BOX-10** and **Pd-BOX-11**). The new catalytic system showed high catalytic activity and excellent selectivity (>97%) towards the *gem*-α,β-unsaturated esters and *gem*-α,β-unsaturated amides under mild reaction conditions and low CO pressure. DFT calaculations on possible intermediates revealed that the regioselectivity of our palladium-catalyzed alkoxycarbonylation reaction is mainly determined by the stability of the complex [Pd(II)(N_2)(C_2H_3Ph)]. The kinetic data for the formation of the two key complexes show no difference between the *gem* and *trans* isomers which predict the regioselectivity to be a thermodynamically controlled process.
7. The supported palladium-bis(oxazoline) complexes (**Pd-BOX-12** and **Pd-BOX-13**) showed excellent catalytic activities in various important cross coupling

reactions including Suzuki-Miyaura, Mizoroki-Heck and Sonogashira cross coupling reactions. The supported palladium-bis(oxazoline) complexes showed excellent recycling ability in most of the cross coupling reactions.

8. The alkoxycarbonylation and aminocarbonylation reactions of aryl iodides proceeded smoothly with the newly synthesized supported palladium-bis(oxazoline) complexes (**Pd-BOX-12** and **Pd-BOX-13**). The supported palladium-bis(oxazoline) complexes showed excellent recycling ability in alkoxycarbonylation reaction of aryl iodides and moderate recycling ability in aminocarbonylation reaction of aryl iodides.

References

[1] Marziale, A. N.; Faul, S. H. ; Reiner, T. ; Schneider, S. ; Eppinger, J. *Green Chem*. **2010**, 12, 35.

[2] Connelly-Espinosa, P.; Morales-Morales, D. *Inorg. Chim. Acta* **2010,** 363, 1311.

[3] Islam, S. M.; Mondal, P.A.; Roy, S.; Mondal, S.; Hossain, D. *Tetrahedron Lett*. **2010**, 51, 2067.

[4] Banik, B.; Tairai, A.; Shahnaz, N. ; Das, P. *Tetrahedron Lett*. **2012**, 53, 5627.

[5] Gómez, M.; Muller, G.; Rocamora, M. *Coord. Chem. Rev.* **1999**, 769, 193

[6] Paltz, A.; *Acc. Chem. Res* **1993**, 26, 339.

[7] Desimoni, G.; Faita G.; Quadrelli, P. *Chem. Rev.* ***2003****,103*, 3119.

[8] Rasappan, R.; Laventine, D.; Reiser, O. *Co.ord Chem. Rev*. **2008**, 252, 702.

[9] Brunner, H.; Obermann, U.; Wimmer, P. *Organometallics*, **1989**, 8:3, 821.

[10] Nishiyama, H.; Sakaguchi, H.; Nakamura, T.; Horihata, M.; Kondo, M.; Itoh, K.; *Organometallics*, **1989**, 8:3, 846.

[11] Lowenthal, R. E.; Abiko, A.; Masamune, S. *Tetrahedron Lett.* **1990**, *31*:42, 6005.

[12] Corey, E. J.; Imai, N.; Zhang, H.Y. *J. Am. Chem. Soc*. **1991**, *113*, 728.

[13] Evans, D. A.; Woerpel, K. A.; Hinman, M. M.; Faul, M. M.; *J. Am. Chem. Soc*. **1991**, *113*:2, 726.

[14] Desimoni, G.; Faita, G.; Jorgensen, K.K. *Chem. Rev*. **2006**, 106, 3561.

[15] Glos, M.; Reiser, O. *Org. Lett*. **2000**, 2, 2045.

[16] Matsumura, Y.; Maki, T.; Murakami, S.; Onomura, O. *J. Am. Chem. Soc*. **2003**, 125, 2052

[17] Nishiyama, H. ; Kondo, M. ; Nakamura, T. ; Itoh, K. ; *Organometallics*, **1991**, 10, 500.

[18] Davies, I. W. ; Gerena, L. ; Lu, N. ; Lassen, R. D. ; Reider P.J. *J. Org. Chem*. **1996**, 61, 9629.

[19] Helmchen, G. ; Krotz, A. ; Ganz, K. T. ; Hansen, D. *Syn. Lett.* **1991** 257.

[20] Sibi, M. P. ; Ji, J. *J. Org. Chem*. **1997**, 62, 3800.

[21] Park, J. K.; Kim, S. W.; Hyeon, T.; Kim, B. M. *Tetrahedron: Asymmetry*. **2001**, 12, 2931.

[22] Whitesell, J. K. *Chem. Rev*.**1989**, 89, 1581.

[23] Thorhauge, J.; Roberson, M.; Hazell, R. G.; Jørgensen, K. A. *Chem. Eur. J*. **2002**, 8, 1888.

[24] Brunner, H. *Angew. Chem. Int. Ed*. **1983**, 22, 897

[25] Evans, D. A.; Woerpel, K. A.; Scott, M. J. *Angew. Chem., Int. Ed.* **1992**, *31*, 430.

[26] Espinet, P.; Soulantica, K. *Coord. Chem. Rev*. **1999**, 499, 193.

[27] Tanaka, K. *Angew. Chem. Int. Ed*. **2003**, 42, 4851.

[28] Jessop, P. G.; Leitner, W. Chemical synthesis using supercritical fluids, **2007**, 1-36; Wiley-VCH.

[29] Gladysz, J. A.; Curran, D. P. *Tetrahedron*, **2002**, 3823.

[30] Li, C. *Chem. Rev*. **2005**, 105, 3095.

[31] Shimizu, S.; Shirakawa, S.; Sasaki, Y.; Hirai, C. *Angew. Chem. Int. Ed*. **2000**, 39, 1256.

[32] Varma, R. S. Org. Chem. Highlights, **2007** http://www.organic-chemistry.org/ Highlights/2007/01February.shtm.

[33] Churruca, F.; SanMartin, R.; In´es, B.; Tellitu, I.; Dom´ınguez, E. *Adv. Synth. Catal*. **2006**, 348, 1836.

[34] Hall, D. G. 2005, Wiley-VCH.

[35] Anderson, K. W.; Buchwald, S. L.; *Angew. Chem., Int. Ed*. **2005,** 44, 6173.

[36] Jin-Heng L.; Xi-Chao H.; Yun L.; Ye-Xiang X. *Tetrahedron*, **2006**, 62, 31.

[37] Afsharpour, M.; Mahjoub, A. R.; Amini, M. M. *Applied Catalysis A: General*, **2007,** 327, 205

[38] Valodkar, V. B.; Gopal, L.; Ravindranathan, M.; Ram, R.N.; Rama, H.S. *J. Mol. Catal. A: Chemical*, **2003**, 202, 47

[39] Song, E. ; Le, S. G. *Chem. Rev*. **2002,** 102, 3495

[40] Jia, M. A.; Berger, S. M.; Giegengack, H.; Schulze, S.; Thiel, W. R. *Chem. Mater*. **2004**, 16, 877.

[41] Maurya, M. R.; Kumar, A.; Manikandan, P.; Chand, S. *Applied Catalysis A: General*, **2004**, 277, 45.

[42] Fraile, J. M.; García, J. I.; Mayoral, J.; Tarnai, T. *Tetrahedron Asymmetry*. **1997,** 8, 2089.

[43] Fraile, J. M; García, J. I.; Harmer, M. A.; Herrerías, C. I.; Mayoral, J.; Reiser, O.; Werner, H.; *J. Mater. Chem*. **2002**, 12, 3290.

[44] Burguete, M. I.; Fraile, J. M.; Garcia, J. I.; Garcia-Verdugo, E.; Luis, S. V.; Mayoral, J. A. *Org. Lett*. **2000,** 2, 3905.

[45] Burguete, M. I.; Fraile, J. M.; Garcia, J. I.; Garcia-Verdugo, E.; Herrerias, C. I.; Luis, S. V.; Mayoral, J. A. *J. Org. Chem.* **2006,** 66, 8893

[46] Lee, S. S.; Hadinoto, S.; Ying, J. Y. *Adv. Synth. and Catal*. **2006**, 348, 1248.

[47] J. G. de Vries, A. H. M. de Vries, The Power of High-Throughput Experimentation in Homogeneous Catalysis Research for Fine Chemicals, Eur. J. Org. Chem. 2003, 799-811

[48] Ridgway, B. H.; Woerpel, K. A. *J. Org. Chem*. **1998**, 63, 458. (b) Miyaura, N.; Yamada, K.; Suzuki, A. *Tetrahedron Letters* **1979**, *20*, 3437

[49] Shimizu, M.; Nakamaki, C.; Shimono, K.; Schelper, M.; Kurahashi, T.; and Hiyama T. *J. Am. Chem. Soc*. **2005**, 127, 12506

[50] Song, C.; Ma, Y.; Chai, Q.; Ma, C.; Jiang, W and Andrus, M. B. *Tetrahedron*, **2005**, 61, 7438

[51] Li, S.; Lin, Y.; Cao, J. and Zhang S. *J. Org. Chem*. **2007**, 72, 4067

[52] Liron, F.; Fosse, C.; Pernoler, A and Roulland, E.; *J. Org. Chem.* **2007**, 72, 2220

[53] So, C.M.; Lau, C.P.; Chan, A. S and Kwong, F. Y.; *J. Org. Chem*. **2008**, 73, 7731

[54] Molander, G. A. and Petrillo, D. E.; *Org. Lett.* **2008**, 10, 9

[55] Bermejo A.; Ros, A.; Fernadez, R. and Lassaletta, J. M. *J. Am. Chem. Soc*. **2008**, 130:47, 15799

[56] Alacid, E.; Najer, C. *J .Org. Chem*. **2009**, 74, 2321

[57] Chow, W. K.; So, C. M.; Lau, C. P.; Kwong, F. Y., *J. Org. Chem.* **2010**, 75, 5109

[58] Liu, L.; Zhang, Y.; and Wang, Y. *J. Org. Chem*. **2005**, 70, 6122

[59] Marion, N.; Navarro, O.; Mei, J.; Stevens, E. D.; Scott, N.M.; and Nolan, S.P. *J. Am. Chem. Soc*. **2006**, 128, 4101

[60] Guram, A. S.; Wang, X.; Bunel, E. E, Faul, M.M.; Larsen, R. D and Martinelli, M. J.; *J. Org. Chem*. **2007**, 72, 5104

[61] Lipshutz, B. H.; Petersen, T. B.; Abela, A. R. *Org. Lett*. **2008**, 10, 1333

[62] Fujihara, T.; Yoshida, S.; Terao, J.; Tsuji, Y. *Org. Lett*. **2009,** 11, 10

[63] Han, J.; Liu, Y.; Guo, R. *J. Am. Chem. Soc.* **2009**, 1316.

[64] Bakherad, M.; Keivanloo, A.; Bahramin, B.; Jajarmi, S.; *J. Organomet. Chem*., **2013**, 74, 206

[65] Shibasaki, M. and Vogl, E.M. *J. Organomet. Chem.* **1999**, 576, 1.

[66] Loiseleur, O., Hayashi, M., Keenan, M. *et al. J. Organomet. Chem.* **1999**, 576, 16.

[67] Moritani, I.; Fujiwara, Y. *Tetrahedron Letters*, **1967**, 8:12, 1119.

[68] Fujiwara, Y.; Noritani, I.; Danno, S.; Asano, R.; Teranishi, S. *J. Am. Chem. Soc*. **1969**, 91:25, 7166

[69] Heck, R. F. *J. Am. Chem. Soc*. **1969**, 91:24, 6707.

[70] Link, J.T. *Org. React.* **2002**, 60, 157

[71] Oestreich, M. *Eur. J. Org. Chem*. **2005**, 783. (b) Heck reaction, retrieved from http://www.organic-chemistry.org/namedreactions/heck-reaction.shtm

[72] Wang, A.E.; Xie, J.; Wang, L.; Zhou Q. *Tetrahedron,* **2005,** 61, 259.

[73] Fayol A.; Fang Y.; Lautens, M.; *Organic Letters*, **2006**, 8:19, 4203.

[74] Liu S.; Berry, N.; Thomson, N.; Pettman, A.; Hyder Z.; Mo, J.; Xio J. *J. Org Chem*. **2006**, 71, 7467

[75] Li, S.; Lin, Y.; Xie, H.; Zhang S, and Xu, J.; *Org let*. **2006,** 8, 3

[76] Lipshutz, B. H.; Taft, B. R. *Org. Lett.* **2008**, *10*, 1329

[77] McConville M.; Saidi O.; Blacker J.; Xiao J.; *J. Org. Chem*. **2009,** 74:7, 2693

[78] Kantam M.L.; Srinivas, P.; Yadav, J.; Likhar P. R and Bhargava, S. *J. Org. Chem.* **2009,** 74, 13

[79] Lie, H. J.; Wang, L.; *Eur. J Org. Chem*. **2006**, 5099

[80] Karimi, B.; Enders D. *Org. Lett.* **2006**, 8, 6

[81] Ranu B. C.; Chattopadhyay, K.; *Org. Lett*. **2007**, 9, 12

[82] Cui, X.; Li, J.; Zhang, Z, Fu, Y.; Liu l.; Guo, Q. *J. Org. Chem*, **2007**, 72, 24

[83] Ruan, J.; Saidi, O.; Iggo, J. A.; Xiao J. *J. Am. Chem Soc*. **2008**, 130, 10510

[84] Kantchev, E.B.; Peh, G.; Zhang, C.; Ying, J. Y. *Org. Lett,* **2008,** 10, 18

[85] Weiss, M. E.; Kreis L. M.; Lamber, A.; Carreira E. M. *Angrew Chem. Int. Ed*. **2011**, 50, 11125

[86] Lui, C.; Bao, F.; Ni, Q. *Arkivoc xi*, **2011**, 60.

[87] Guan, J. T.; Weng, T. Q.; Yu, G.; Liu, S. H. *Tetrahedron Lett*. **2007**, *48*, 7129.

[88] Komaromi, A.; Novak, Z. *Chem. Comm*. **2008**, 4968.

[89] Huang, H.; Liu, H.; Jiang, H.; Chen , K. *J. Org. Chem*. **2008**, *73*, 6037.

[90] Gu, Z. ; Li, Z. ; Liu, Z. ; Wang, Y.; Liu, C. ; Xiang, J. *Catal. Comm*, **2008**, *9*, 2154.

[91] Casado, M. A.; Fazal, A.; Oro, L. A. *Arab. J. Sc. Eng.*, **2013**, *38*, 1631.

[92] Leadbeater, N. E.; Tominack, B. J. *Tetrahedron*, **2003**, *44*, 8653.

[93] Hamajima, A.; Isobe, M.; *Org. Lett*. **2006**, *8*, 1205.

[94] Mujahidin, D.; Doye, S. *Eur. J. Org. Chem*. **2005**, 2689.

[95] Hajipour, A. R.; Zade, Z. S.; Azizi, G. *Appl.Organometal.Chem*. **2014**, *28*, 696.

[96] Mathias, E.; Gregory, C. F. *J. Am. Chem. Soc*. **2003**, *125*, 13642.

[97] Sonogashira, K.; Toda, Y.; Haghira, N. *Tetrahedron letters*, **1975**, 16, 4467

[98] Chinchilla, R.; Najera, C. *Chem. Rev*. **2007**, *107*, 874.

[99] Siemsen, P.; Livingstone, R.C.; Diederich, F. *Angew. Chem. Int. Ed*. **2000**, *39*, 2633.

[100] Bakherad, M.; Keivanloo, A.; Bahramian, B.; Jajarmi, S. *Appl. Catal. A: General* **2010**, *390*, 135.

[101] Hundertmark, T.; Littke, A. F.; Buchwald, S.L.; Fu, G. C. *Org. Lett*. **2000**, *2*, 1729.

[102] Eckhardt, M.; Fu, G. C. *J.Am.Chem.Soc*. **2000**, *39*, 2632 (b) Sonogashira coupling, retrived from http://www.organic-chemistry.org/namedreactions/sonogashira-coupling.shtm

[103] B. Liang, M. Dai, J. Chen, Z. Yang, *J. Org. Chem*. **2005**, 70, 391

[104] Thorwirth, R.; Stolle, A.; Ondruschka, B. *Green Chem.*, **2010**, 12, 985

[105] Novák, Z.; Nemes, P.; Kotschy, A. *Org. Lett.* **2004**, 6, 4917

[106] Wagner, F.; Comins, D. *J. Org. Chem*. **2006**, 71, 8673.

[107] Chen, M.; Zhen, X.; Li, W.; He, J.; Lei, A. *J. Am. Chem. Soc*. **2010**, *132*, 4101.

[108] Chen, M.; Zhen, X.; Li, W.; He, J.; Lei, A. *J. Am. Chem. Soc*. **2010**, *132*, 4101.

[109] Reppe, W; Ann, **1948**, 560, 1

[110] Roelen, O.; Angew. Chem. A. 60, 1948, 3, 213

[111] Jayasree, S.; Seayad, A.; Gupte, S. P.; Chaudhari, R. V. *Catalysis Letters*, **1999**, 5, 8213

[112] El Ali, B. and Alper, H. *Transition metals for organic synthesis: Building blocks and fine chemicals* (eds. M. Beller and C. Bolm); Wiley-VCH verlage GMBH, **2004** weinheim, Germany

[113] Scrivanti, A.; Matteoli, U.; Beghetto, V.; Antonaroli, S.; Scarpelli, R.; Crociani, B. *J. Mol. Catal. A: Chem.* **2001,** 170, 51

[114] El Ali, B.; Alper, H.; in: M. Beller, C. Bolm (Eds.), *Transition Metals for Organic Synthesis*, Vol. 1, VCH, Weinheim, **1998**, 57.

[115] Claufield, M. J.; Qiao, G. G.; Solomon, D. H. *Chem. Rev*. **2002**, 102, 3067

[116] Bianchini, C.; Mantovani, G.; Meli, A.; Oberhauser, W.; Bruggeller, P. and Stampfi, T. *J. Chem. Soc., Dalton Trans.,* **2001**, 690

[117] Zeni, G. and Larock, R.C. *Chem. Rev*. **2006,** 106, 4644.

[118] Zeni, G. and Larock, R.C. *Chem. Rev*. **2004**, 104, 2285.

[119] Nakamura, I. and Yamamoto, Y. *Chem. Rev*, **2004,** 104, 2127.

[120] Tsuji, J. *Palladium Reagents and Catalysts*; Wiley: New York, **1996**, 471.

[121] Bird, C. W. *Chem. Rev.* **1962**, *62*, 283.

[122] Kushino Y.; Itoh, K.; Miura, M.; Nomura, M. *J. Mol. Cat*. **1994**, 89, 151

[123] El Ali, B.; Alper, H. *J. Mol. Cat*. **1995**, 96, 197

[124] Alper, H.; Maldonado, M. S.; Lin, I. J. B. *J. Mol. Cat*. **1988**, 49, L27

[125] Suleiman, R.; Tijjani, J., El Ali, B. *Appl. Organometal. Chem*. **2010**, *24*, 38

[126] Kato, K.; Motodate,S.; Mochida, T.; Kobayashi, T.; Akita, H.; *Angew. Chem. Int. Ed.* **2009**, 48, 3326

[127] Imada, Y.; Vasopolo, G.; Alper, H. *J. Org. Chem*. **1996**, 61, 7982

[128] Matteoli, U., Scrivanti, A. and Beghetto, V. *J. Mol. Cat A: Chemical*, **2004**, 213, 183.

[129] Li, Y.; Alper, H.; Yu, Z. *Org. Lett.* **2006**, 8, 5199

[130] Garcia-Melchor, M. ; Ujaque, G. ; Maseras, F. ; Lledos, A. *Catal. Met. Comp*. **2011**, 37, 57.

[131] Shahnaz, N.; Banik, B.; Das, P. *Tet. Lett.* **2013,** 54, 2886.

[132] Desimoni, G. ; Faita, G. ; Jorgensen, K. A. *Chem. Rev.* **2011,** 111, 284.

[133] Ghosh, A. K. Mathivanan, P.; Cappiello, J. *Tetrahedron: Asymmetry*. **1998,** 9, 1.

[134] Takemoto, T.; Iwasa, S.; Hamada, H.; Shibatomi, K.; Kameyama, M.; Motoyama, Y.; Nishiyama, H. *Tetrahedron Lett*. **2007**, 48, 3397.

[135] Ibrahim, M. B.; El Ali, B.; Fettouhi, M.; Ouahab, L. *Appl. Organometal. Chem***, 2015,** 29, 400.

[136] Ibrahim, M. B.; Shakil Hussain, S. M.; Fazal, A.; Fettouhi, M.; El Ali, B. *J. Coord. Chem.* **2015**, 68:3, 432.

[137] Shakil-Hussein, S. M.; Ibrahim, M. B.; Fazal, A.; Suleiman, R.; Fettouhi, M.; El Ali B. *Polyhedron***, 2014,** 70, 39.

[138] Bruker, SMART and SAINT, Bruker Axs Inc. Madison. Wisconsin, USA, **2006**.

[139] Sheldrick, G. M. SADABS, Bruker AXS Inc., Madison, Wisconsin, USA, **2002**.

[140] Sheldrick, G. M. *Acta Cryst*. **2008,** A64, 112.

[141] Farrugia, L. *J. Appl. Crystallogr*. **1997**,30, 565.

[142] El Hatimi, A.; Gomez, M.; Jansat, S.; Muller, G.; Font-Bardia, M.; Solans, X. *J. Chem. Soc., Dalton Trans*. **1998**, 4229.

[143] Gottumukkala, A. L. ; Matcha, K. ; Lutz, M. ; de Vries, J. G. ; Minnaard, A. J. *Chem. Eur. J.* **2012**, 18, 6907.

[144] Foltz, C. ; Enders, M. ; Bellemin-Laponnaz, S. ; Wadepohl, H. ; Gade. L. H. *Chem. Eur. J.* **2007**, 13, 5994.

[145] Kato, K.; Matsuba, C.; Kusakabe, T.; Takayama, H.; Yamamura, S.; Mochida, T.; Akita, H. ; Peganova, T.A.; Vologdin, N.V.; Gusev. O.V. *Tetrahedron*, **2006,** 62, 9988.

[146] Abu-Surrah, A. S. ; Kettunen, M. ; Lappalainen, K. ; Piironen, U. ; Klinga, M. ; Leskela, M. *Polyhedron*, **2002**, 21, 27.

[147] Ruiyun G.; Portscheller, J. L.; Day, V. W.; Malinakova, H. C.; *Organometallics*, **2007**, 26, 3874.

[148] Hage, R.; deGraaff, R. A. G.; Haasnoot, J.G.; Kieler, K.; Reedijk, J. *Acta Crystallogr.; Sect.C: Cryst. Struct. Commun.* **1990**, 46, 2349.

[149] Romm, I.P.; Kravtzova, S.V.; Perepelokova, T.I.; Kalinovskiy, I.O.; Buslaeva, T.M.; Petrov, E.S. *Russ. J. Coord. Chem*. **1995**, 21, 708.

[150] Belykh, L.B.; Goremyka, T.V.; Zinchenko, S.V.; Rokhin, A.V.; Ratovshii, G.V. Schmidt, F.K. *Russ. J. Coord. Chem.*, **2002**, 28, 664.

[151] Montoya, V.; Pons, J.; Solans, X.; Font-bardia M.; Ros, J.; *Inorg. Chim. Acta*, **2005**, 358, 2312.

[152] Asma, M.; Badshah, A.; Ali, S.; Sohail, M. *Transition Met. Chem*. **2006**, 31, 556.

[153] Bortoluzzi, M.; Paolucci, G.; Pitteri, B.; Vavasori, A.; and Bertolasi, V. *Organometallics* **2009**, 28, 3247

[154] Gianelli, L.; Amendola, V.; Fabbrizzi, L.; Pallavicini, P.; Mellerio, G. G. *Rapid Commun. Mass Spectrom.* **2001**, 15, 2347.

[155] Yunker, L.P.E.; Stoddard, R. L.; McIndoe, J. S. *J. Mass Spectrom*. **2014**, 49, 1.

[156] Polshettiwar, V.; Len, C.; Fihri, A. *Coord. Chem. Rev*. ***2009***, 253, 2599

[157] Hallamn, K.; Moberg, C. *Tetrahedron: Asymmetry*, **2001**, 12, 1475

[158] He, Y.; Cai, C. *J. Organomet. Chem*. **2011**, 696, 2689

[159] Shimizu, K. I.; Koizumi, S.; Hatamachi, T.; Yoshida, H.; Komai, S.; Kodama, T.; Kitayama, Y. *J. Catal*. **2004**, 228, 141

[160] Bakherad, M.; Bahramian, B.; Nasr-Isfahani, H.; Kievanloo, A.; Sang, G. *Chin. J. Chem.* **2009**, 27, 353

[161] Yeap, H. N; Mian, W.; Hong, H.; Christina, L. L. C. *Chem. Commun*., **2009**, 5530

[162] Hajipour, A. R.; Shirdashtzade, Z.; Azizi, G. *J. Chem. Sci*. **2014**, 126, 1, 85

[163] Trilla, M.; Pleixats, R.; Wong Chi Man, M.; Bied, C.; Moreau, J.J.E. *Tetrahedron Lett*. **2006**, 47, 2399

[164] Trilla, M.; Pleixats, R.; Wong Chi Man, M.; Bield, C.; Moreau, J.J.E. *Adv. Synth. Catal*. **2008**, 350, 577

[165] Gruber-Woelfler, H.; Radaschitz, P.F.; Feenstra, P.W.; Haas, W.; Khinas, J. G. *J. Catal*. **2012**, 286, 30

[166] Antony, R.; Tembe, G. L.; Ravindranathan, M.; Ram, R.N. *J. Appl. Polym. Sci.*, **2003**, 90, 370

[167] Zhang, G.; Luan, Y.; Han, X.; Wang, Y.; Wen, X.; Ding, C. *Appl. Organomet. Chem*. **2014**, 28, 332.

[168] Lyons, T. W.; Sanford, M. S. *Chem. Rev*. **2010**, 110, 1147

[169] Rao, G. K.; Kumar, A.; Kumar, S.; Dupare, U. B.; Singh, A. K. *Organometallics*, **2013**, 32, 2452

[170] Szilvasi, T. ; Veszpremi, T. ; *ACS Catal*. **2013**, 3, 1984.

[171] Wolfe, J. P.; Singer, R. A.; Yang, B. H.; Buchwald, S. L. *J. Am. Chem. Soc.* **1999**, 121, 9550.

[172] Marziale, A. N.; Jantke, D.; Faul, S.H.; Reiner, T.; Herdweck, E.; Eppinger, J. *Green Chem.*, **2011**, 13, 169.

[173] Kylmala, T. ; Kuuloja, N. ; Xu, Y. ; Rissanen, K. ; Franzen, R. *Eur. J. Org. Chem*. **2008**. 4019.

[174] Fan, L.; Yi, R.; Yu, L.; Wu, Y.; Chen, T.; Guo, R. *Catal Sci. Technol*. **2012**, 2, 1136.

[175] Srinivas, K.; Srinivas, P.; Prathima, P.S.; Balaswamy, K.; Srihadar, B.; Rao, M.M. *Catal. Sci. Technol*. **2012,** 2, 1180.

[176] Chih-chung, T.; Mungyuen, L.; Bingli,M.; Sarah, W.; Alan, S. C.; *Chem. Lett.* **2011**, 40:9 955.

[177] Bakherad, M.; Keivanloo, A.; Samangooei, S.; Omidian, M. *J. Organometal. Chem*. **2013**, *740*, 78.

[178] Feng, Z.; Yu, S.; Shang, Y. *Appl. Organometal. Chem*. **2008**, *22*, 577.

[179] Shingo, A.; Motohiro, S.; Yuki, S.; Hirojiki, S.; Takuya, Y.; Aiky, O. *Chem. Lett*. **2011**, *40*:9, 925.

[180] Korzec, M.; Bartczak, P.; Niemczyk, A.; Szade, J.; Kapkowski, M.; Zenderowska, P.; Balin, K.; Lelarko, J.; Polariski, J. *J. Catalysis*, **2014**, *313*, 1.

[181] Jindabot, S.; Teerachanan, K.; Thongkam, P.; Kiatisevi, S.; Khamnaen, T.; Phiriyawirut, P.; Charoenchaidet, S.; Sooksimuang, T.; Kongsaeree, P.; Sangtrirutnugal, P. *J. Organomet. Chem.*, **2014**, 750, 35.

[182] Dai, Q.; Gao, W.; Liu, D.; Kapes, L. M.; Zhang, X. *J. Org. Chem.* **2006**, 71, 3928;

[183] Sabounchei, S. J.; Ahmadi, M.; Nasri, Z. *J. Coord. Chem.*, **2013**, 66, 411;

[184] Wang, Q. F.; Zhou, R.; Zheng, X.; Fu, H.; Chen, H.; Li, R. *Appl. Organometal. Chem.*, **2013,** 27, 232.

[185] Ke, H.; Chen, X.; Zou, G. *Appl. Organomet. Chem*. **2014**, 28, 54.

[186] Diao, Y.; HAO, R.; Kou, J.; Teng,M.; Huang, G.; Chen, Y. *Appl. Organomet. Chem.*, **2013** 9, 546.

[187] Vladimir, V. G.; Howard, A. *Organometallics*, **1993**, 12, 1890.

[188] Lin, B. ; Huang, S. ; Wu, W. ; Mou, C. ; Tsai, F. *Molecules*, **2010,** 15, 1957

[189] Saiyed, A. S.; Joshi, R. S.; Bedekar**,** A. V. *Journal of chemical research*, **2011,** 35, 408

[190] Saiyed, A. S.; Bedekar, A. V. *Tetrahedron Letters*, **2010**, 51, 6227

[191] Jung, E.; Park, K.; Kim, J.; Jung, H.T.; Oh, I.K.; Lee, S. *Inorg. Chem. Commun*., **2010**, 13, 1329

[192] Levitus M.; Schmieder K.; Ricks H.; Shimizu K. D.; Bunz U. H. F.; Garcia-Garibay M.A.; *J. Am. Chem. Soc.* **2001**, *123*, 4259.

[193] Beeby, A.; Findlay, K.; Low P.J.; Marder T. B. A. *J. Am. Chem. Soc*. **2002**, *124*, 8280.

[194] Schwab P. F. H.; Smith, J. R.; Michl, J. *Chem. Rev*. **2005**, *105*, 1197.

[195] Tanaka T.; Sekine, C.; Ashida, T.; Ishitobi, M.; Konya, N.; Minai, M.; Fujisawa, K. *Liq. Cryst.* **2000**, *346*, 209.

[196] Liao, Y. M. ; Chen, H. L. ; Hsu, C. S.; Gauza, S.; Wu, S. T. *Liq. Cryst*. **2007**, *34*, 507.

[197] Li, N.; Li, Z.; Zhang, X.; Hua, R. *Int. J. Mol. Sci*. **2013**, *14:12*, 23257.

[198] Feuerstein, M.; Doucet, H.; Santelli, M. *Tetrahedron Lett*. **2004**, *45*, 8443.

[199] Bakherad, M.; Keivanloo, A.; Samangooei, S. O. *Tetrahedron Lett*. **2012**, *53*, 5773

[200] Yi, C.Y.; Hua, R. M.; *J. Org. Chem*. **2006**, *71*, 2535.

[201] Alcaide, B.; Almendros, P.; Alonso, J. M. *Org. Biomol. Chem.*, **2011**, *9*, 4405.

[202] Sarkar M. S, Rahman M. L, Yusoff, M. M. *RSC Adv*. **2015**, 5, 1295

[203] Karmee, S. K.; Roosen, C.; Kohlmann, C.; Lutz, S.; Greiner L.; Leitner, W. *Green Chem.* **2009**, 11, 1052

[204] Gaab, M.; Bellemin-Laponnaz, S.; Gade, L. H. *Chem. Eur. J*. **2009**, 15, 5450

[205] Willemsen, J. S, van Hest, J. C. M.; Rutjes, F. P. J. T. *Beilstein J. Org. Chem*. **2013**, 9, 960

[206] Drent, E.; Arnoldy, P.; Budzelaar, P.H.M. *J. Organomet. Chem*. **1993**, 455, 247.

[207] Itoh, K.; Miura, M. and Nomira M. *Tetrahedron Lett*. **1992**,33, Page 5369

[208] Zargarain, D. and Alper, H., *Organometallics* **1993,** 12, Page 712

[209] Frisch, M. J.; Trucks, G. W.; Schlegel, H. B.; Scuseria, G. E.; Robb, M. A.; Cheeseman, J. R. Scalmani, G.; Barone, V.; Mennucci, B.; Petersson, G. A.; Nakatsuji, H.; Caricato, M.; Li, X.; Hratchian, H. P.; Izmaylov, A. F.; Bloino, J. ; Zheng, G.; Sonnenberg, J. L.; Hada, M.; Ehara, M.; Toyota, K.; Fukuda, R.; Hasegawa, J.; Ishida, M.; Nakajima, T.; Honda, Y.; Kitao, O.; Nakai, H.; Vreven, T.; Montgomery, J. A. Jr., Peralta, J. E.; Ogliaro, F.; Bearpark, M.; Heyd, J. J.; Brothers, E.; Kudin, K. N.; Staroverov, V. N.; Kobayashi, R.; Normand, J.; Raghavachari, K.; Rendell, A.; Burant, J. C. ; Iyengar, S. S.; Tomasi, J.; Cossi, M.; Rega, N.; Millam, J. M.; Klene, M.; Knox, J. E..; Cross, J. B.; Bakken, V.; Adamo, C.; Jaramillo, J.; Gomperts, R.; Stratmann, R. E.; Yazyev, O.; Austin, A. J.; Cammi, R.; Pomelli, C.; Ochterski, J. W.; Martin, R.L.; Morokuma, K.; Zakrzewski, V. G.; Voth, G. A.; Salvador, P.; Dannenberg, J. J.; Dapprich, S.; Daniels, A. D.; Farkas, Ö. ; Foresman, J. B.; Ortiz, J. V. ; Cioslowski, J.; Fox, D. J. **2013**, Gaussian, Inc., Wallingford CT.

[210] a) Lee, C.; Yang, W.; Parr, R. G. *Phys. Rev. B.* **1998**, 37, 785. b) Becke, A.D. *J. Chem. Phys.*, **1993**, 98, 1372. c) Becke, A.D. *J. Chem. Phys*., **1993**, 98, 5648.

[211] Weigend, F.; Ahlrichs, R. *Phys. Chem. Chem. Phys*. **2005**, 7, 3297.

[212] a) Barone, V.; Cossi, M. *J. Phys. Chem. A* **1998**, 102, 1995 b) Cossi, M.; Rega, N.; Scalmani, G.; Barone, V. *J. Comput. Chem*. **2003,** 24, 669.

[213] Grimme, S.; Antony, J.; Ehrlich, S.; Krieg, H. *J. Chem. Phys*. **2010**, 132, 154104.

[214] Tijani, J. ; Suleiman, R. ; El Ali, B. *Appl.Organomet. Chem*. **2008**, 22, 553.

[215] Bettucci, L.; Bianchini, C.; Oberhauser, W.; Vogt, M.; Grützmacher, H. *Dalton Trans*. **2010**, 36, 6509.

[216] El Ali, B.; Alper, H. *J. Mol. Cat*. **1991**, 67, 29.

[217] Suleiman, R.; Ibdah, A.; El Ali, B. *J. Organometal. Chem.*, **2011**, 696, 2355.

[218] Klaus, S.; Neumann, H.; Jiao, H.; Wangelin, J. A.; Gördes, D.; Strübing, D.; Hübner, S.; Hateley, M.; Weckbecker, C.; Huthmacher, K.; Riermeier, T.; Beller, M. *J. Organometal. Chem.,* **2004**, 689, 3685.

[219] Niu, S.; Hall, M. B. *Chem. Rev*. **2005**, 100, 353.

[220] Takacs, A.; Abreu, A. R.; Peixoto, A. F.; Pereira, M.; Kollar, L. *Synth. Commun.* **2009**, 39, 1534.

[221] Ji, Y.; Jain, S.; Davis, R. J. *J. Phys. Chem. B*, **2005**, 109, 17232

Appendices

A. I: NMR of ligands, complexes and some coupling reaction products

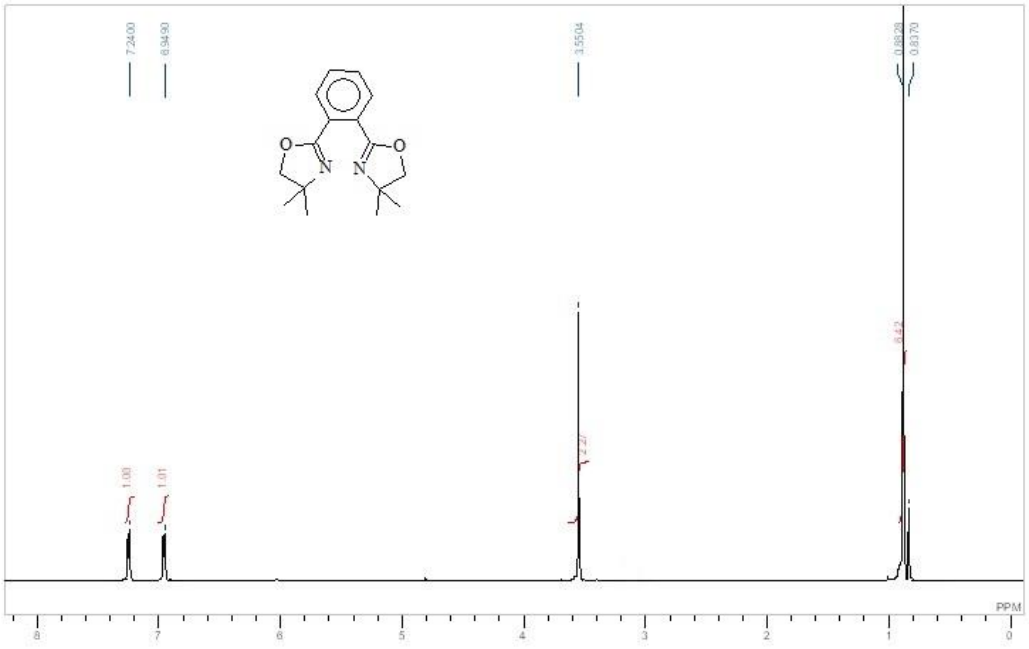

Figure AI-1: ^{1}H NMR Spectrum of BOX-1

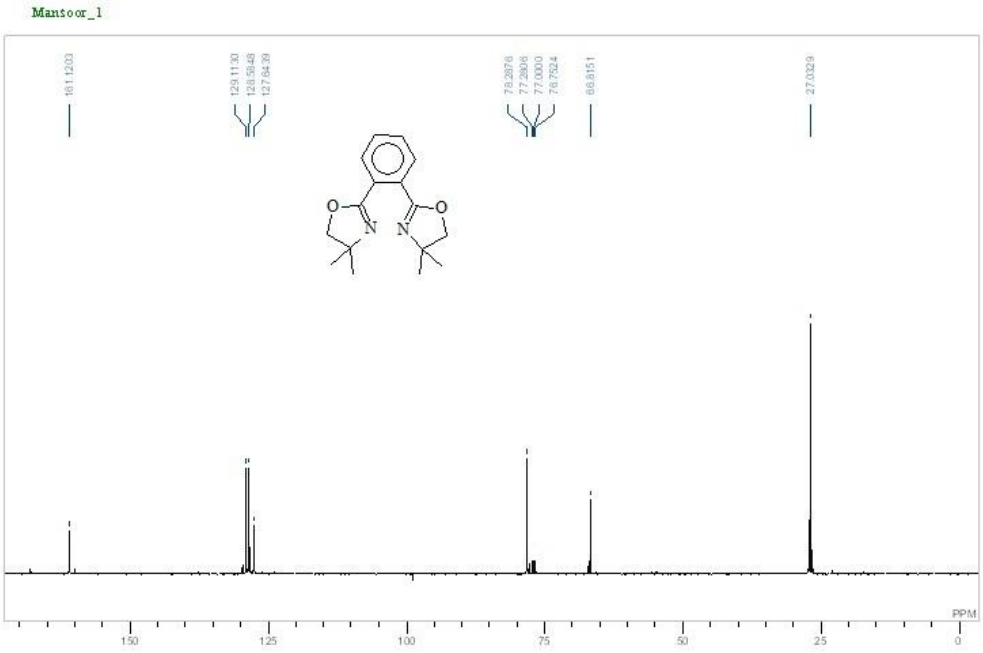

Figure A-I-2: ^{1}3C NMR Spectrum of BOX-1

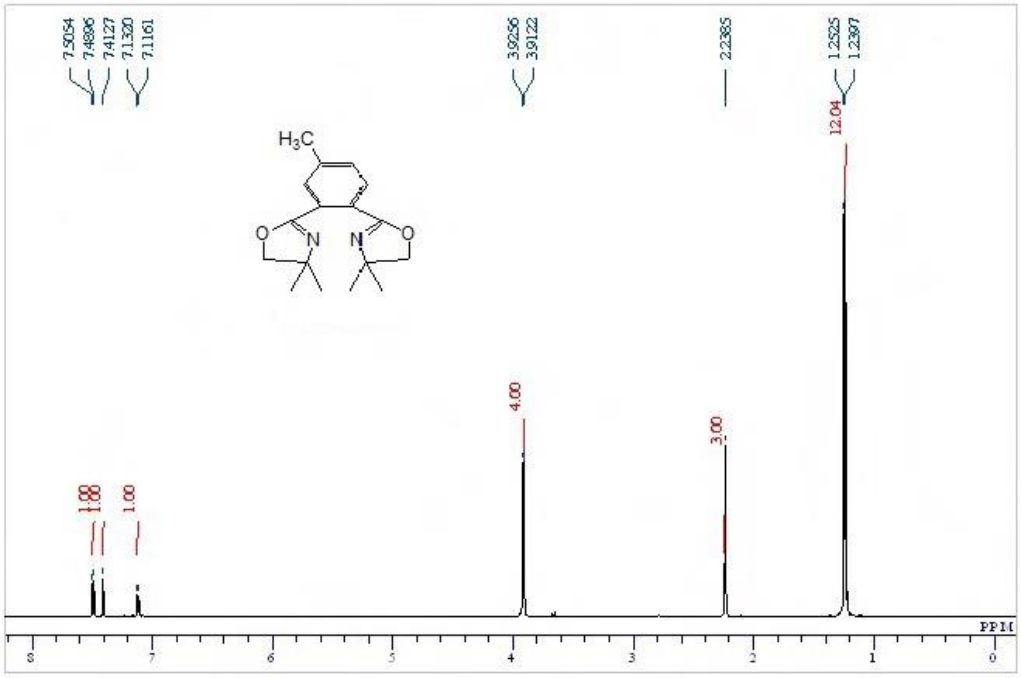

Figure A-I-3: [1]H NMR Spectrum of BOX-2

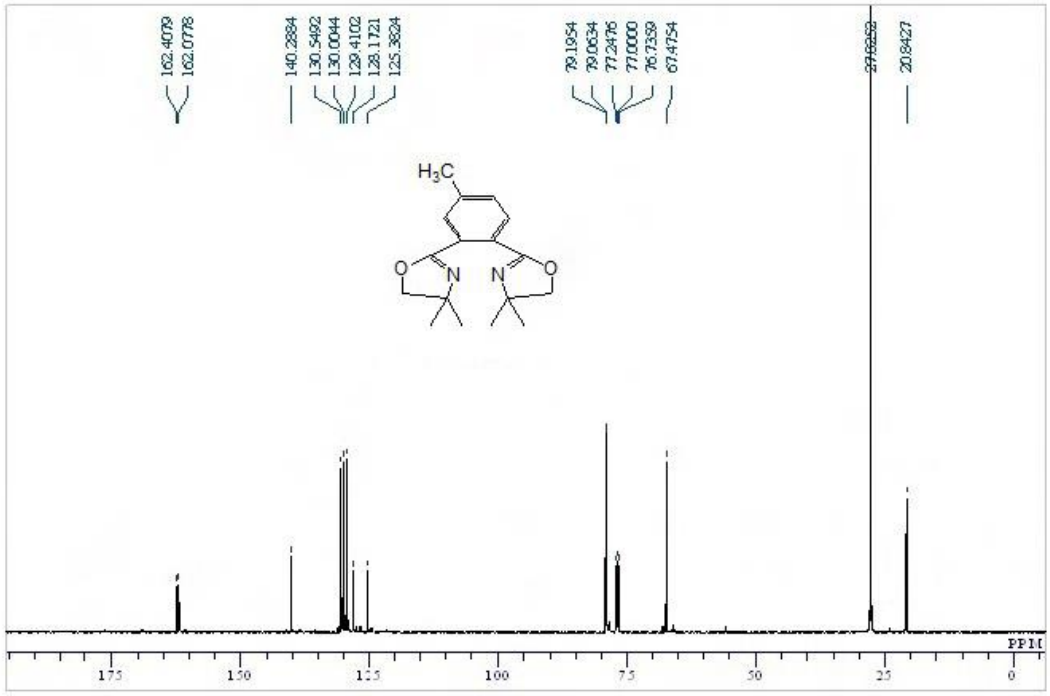

Figure A-I-4:[1]3C NMR Spectrum of BOX-2

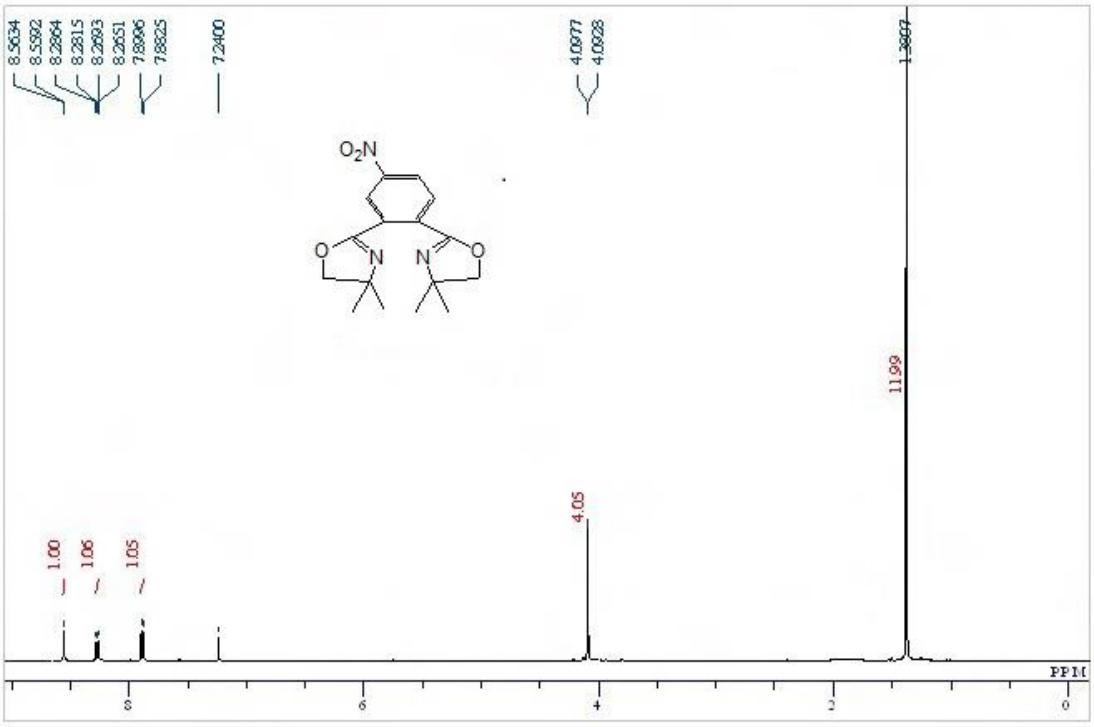

Figure A-I-5: ^{1}H NMR Spectrum of BOX-3

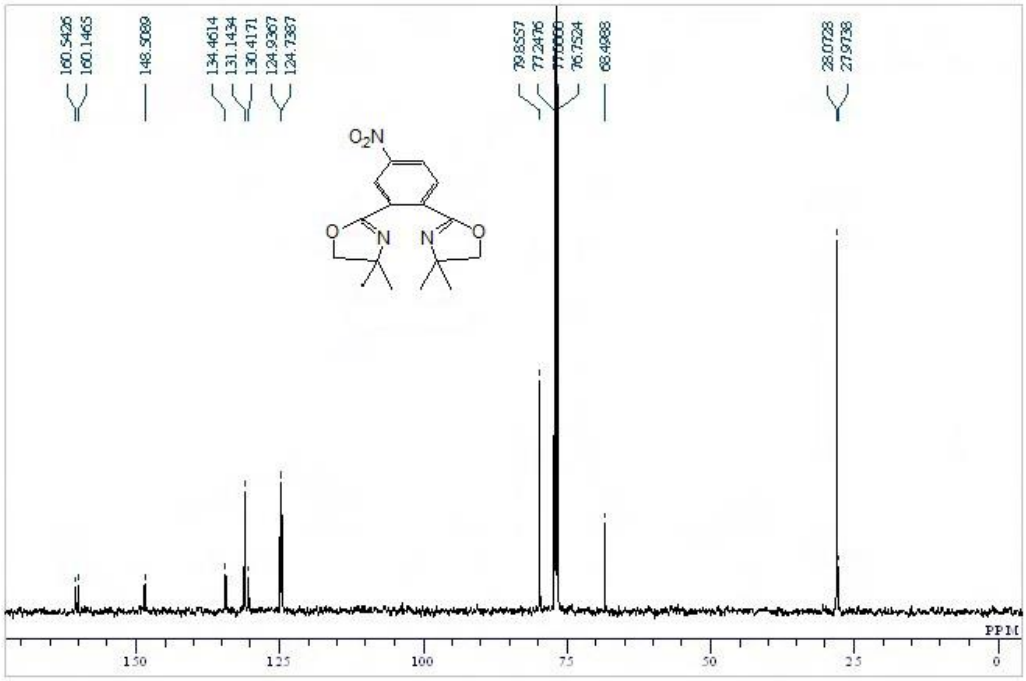

Figure A-I-6: ^{1}3C NMR Spectrum of BOX-3

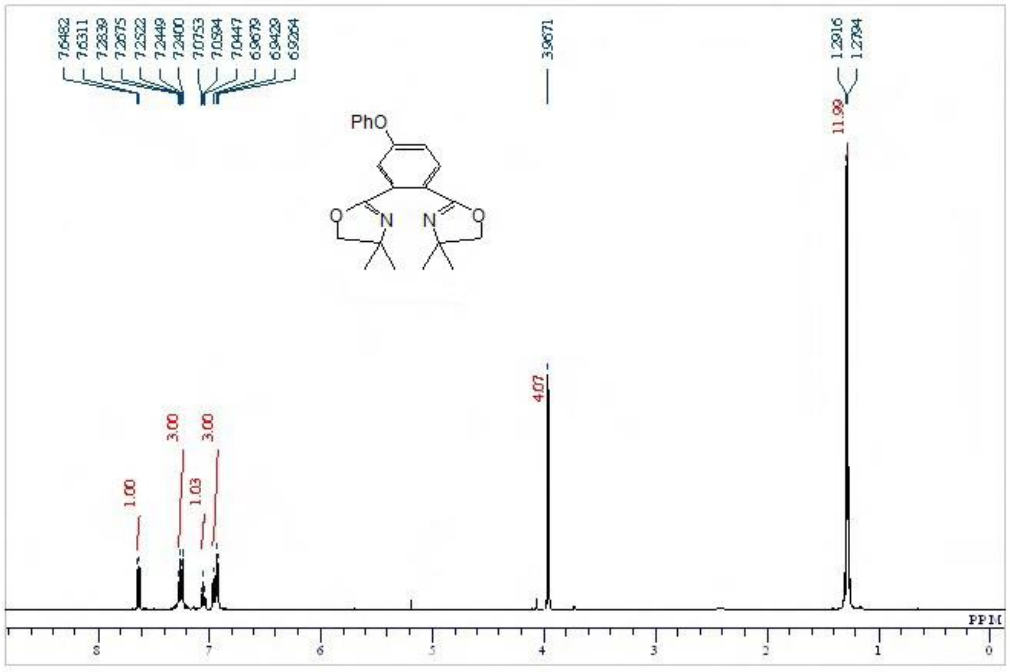

Figure A-I-7:[1]H NMR Spectrum of BOX-4

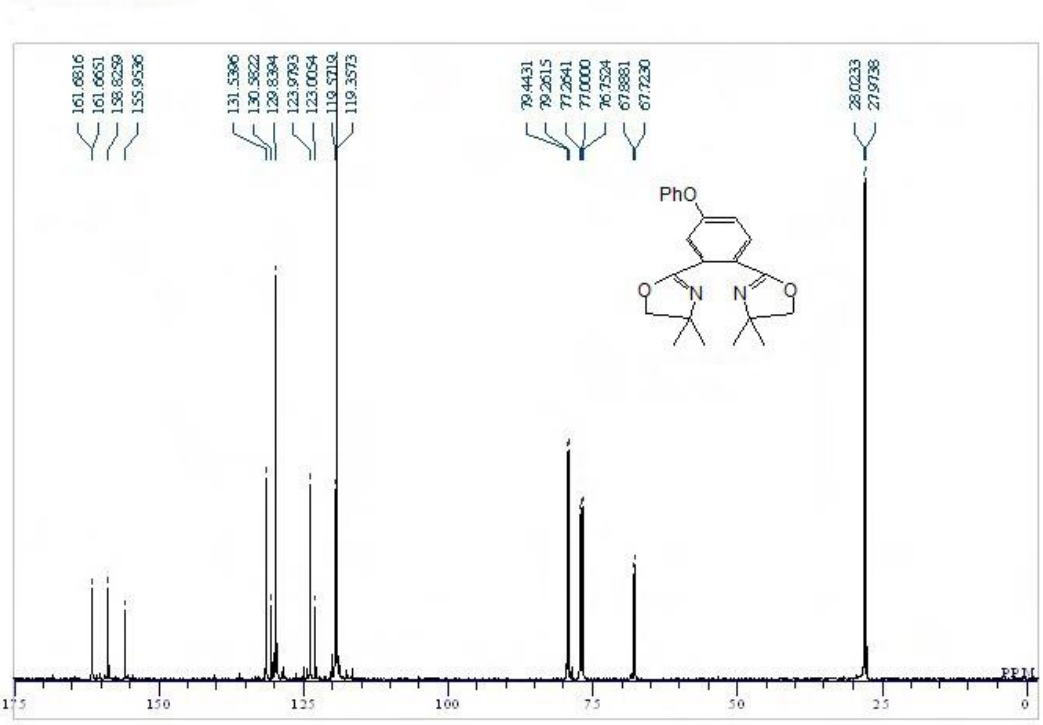

Figure A-I-8:[13]C NMR Spectrum of BOX-4

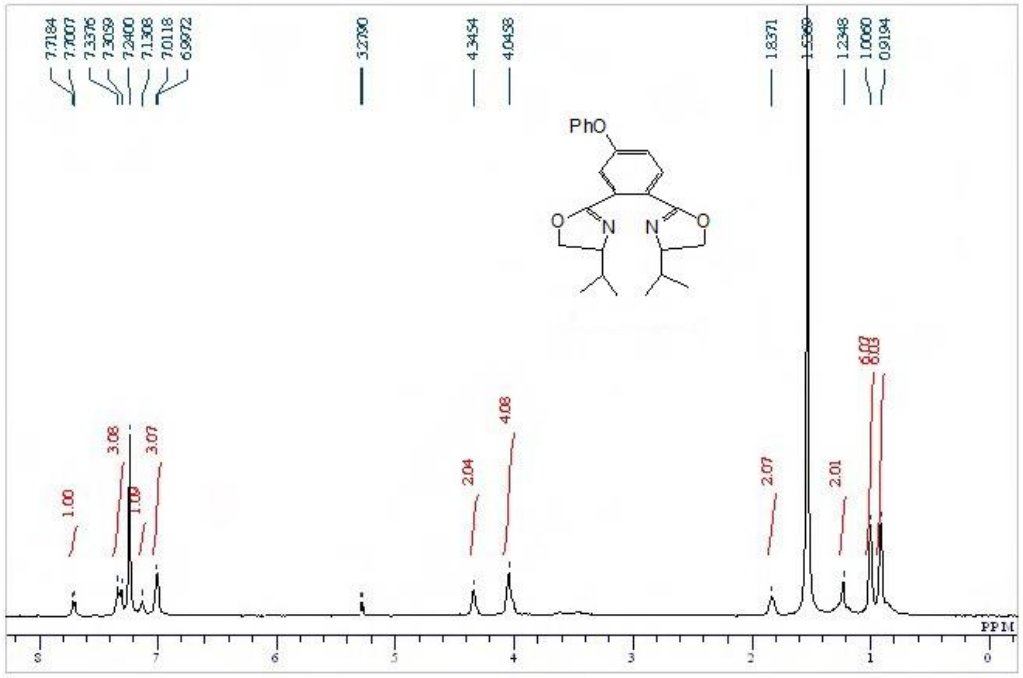

Figure A-I-9:[1]H NMR Spectrum of BOX-5

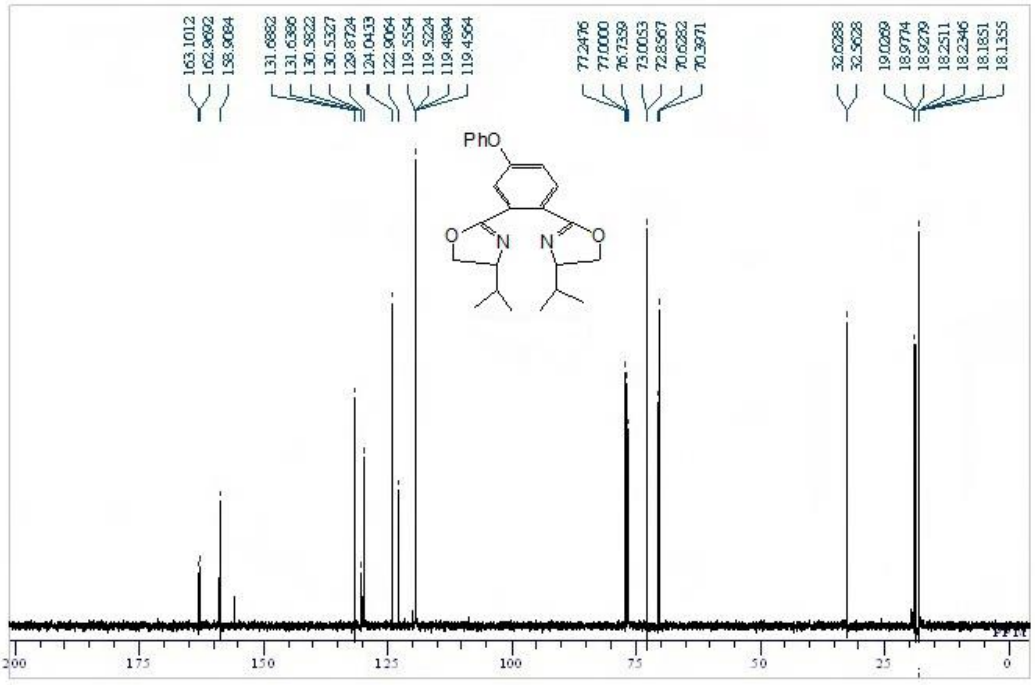

Figure A-I-10:[1]H NMR Spectrum of BOX-5

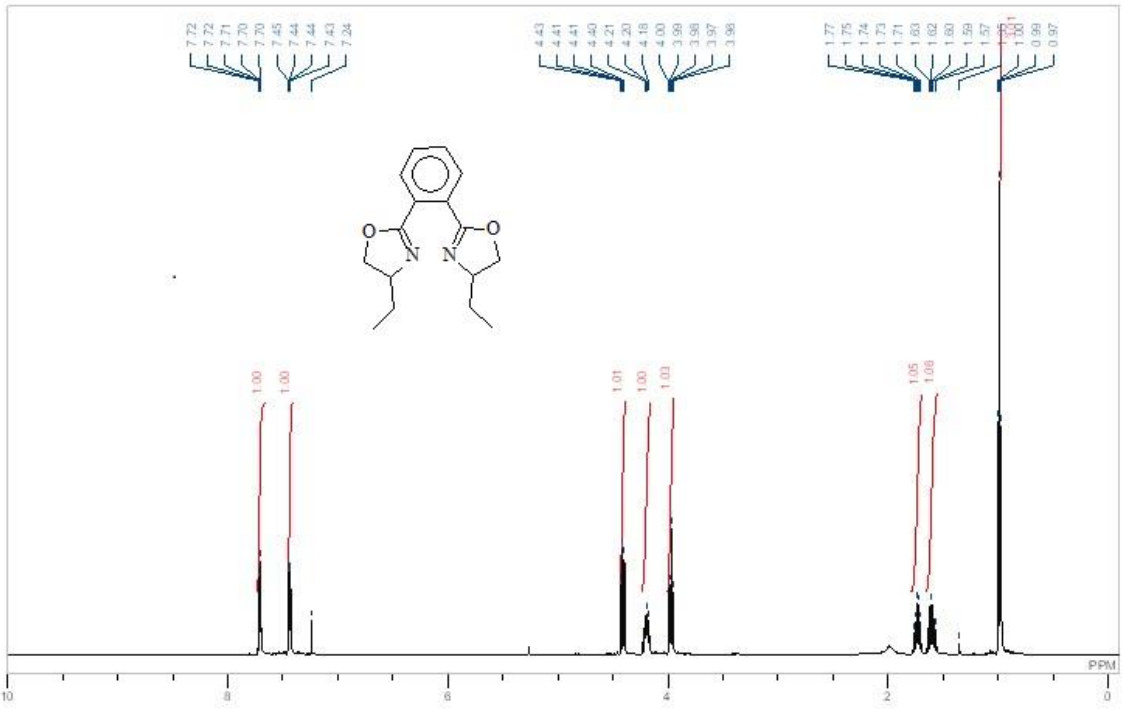

Figure A-I-11: ^{1}H NMR Spectrum of BOX-6

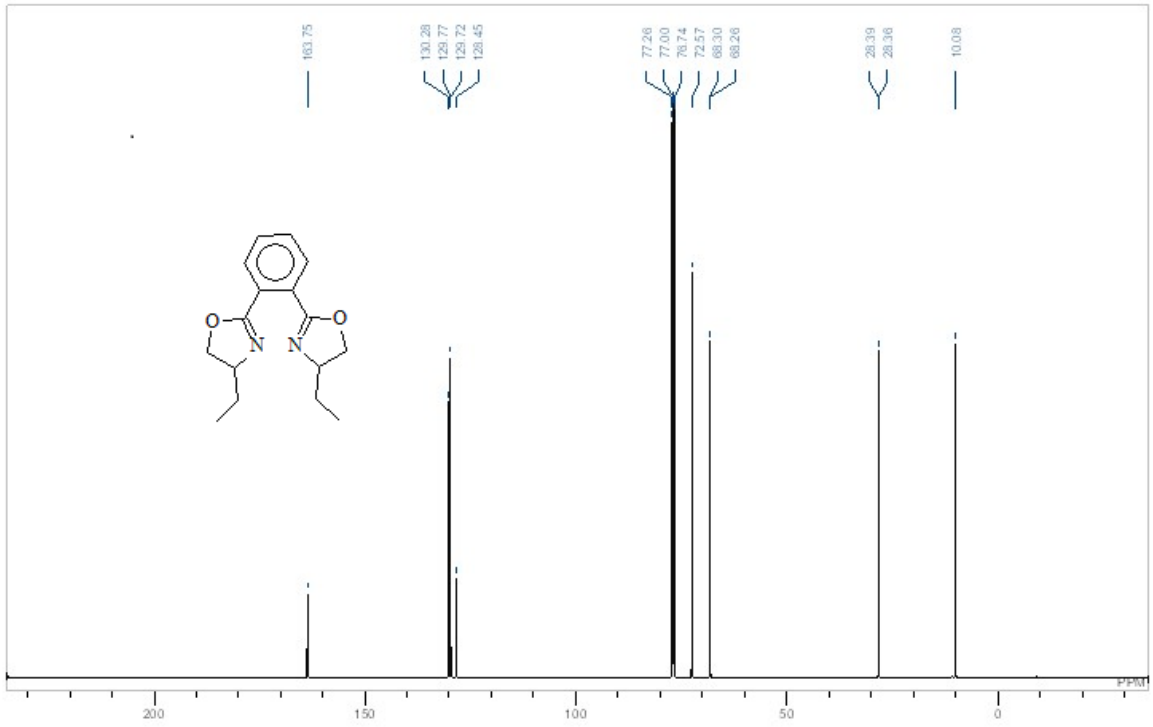

Figure A-I-12: ^{1}H NMR Spectrum of BOX-6

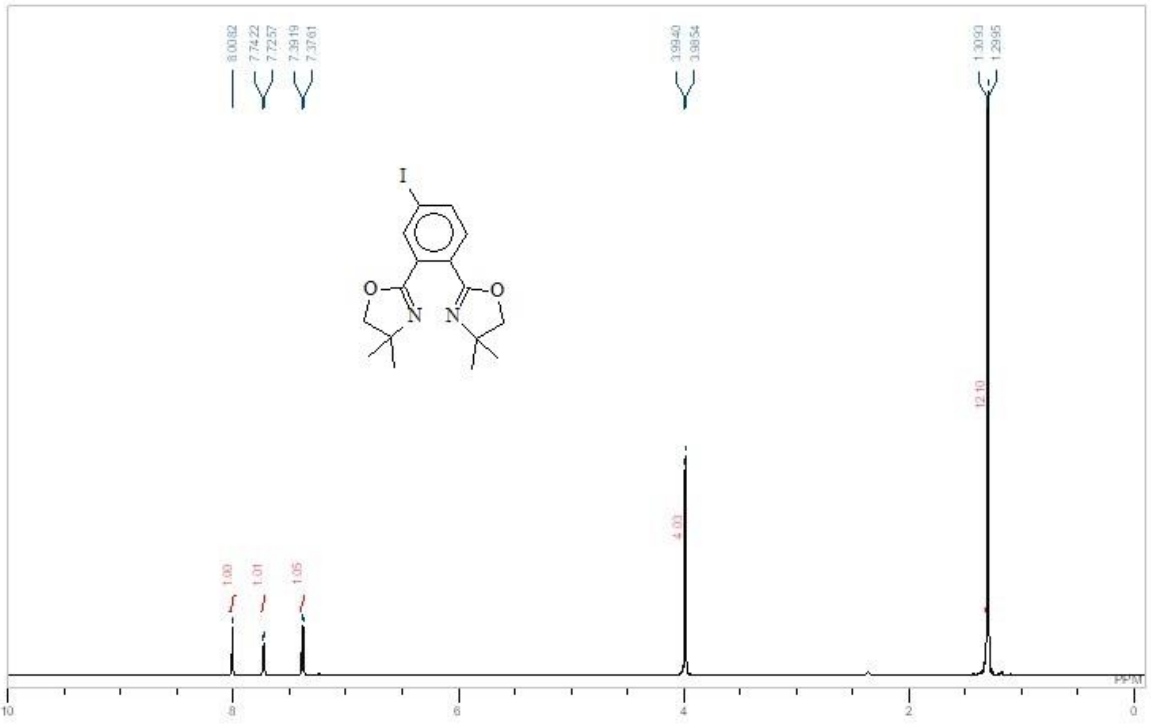

Figure A-I-13:[1]H NMR Spectrum of BOX-7

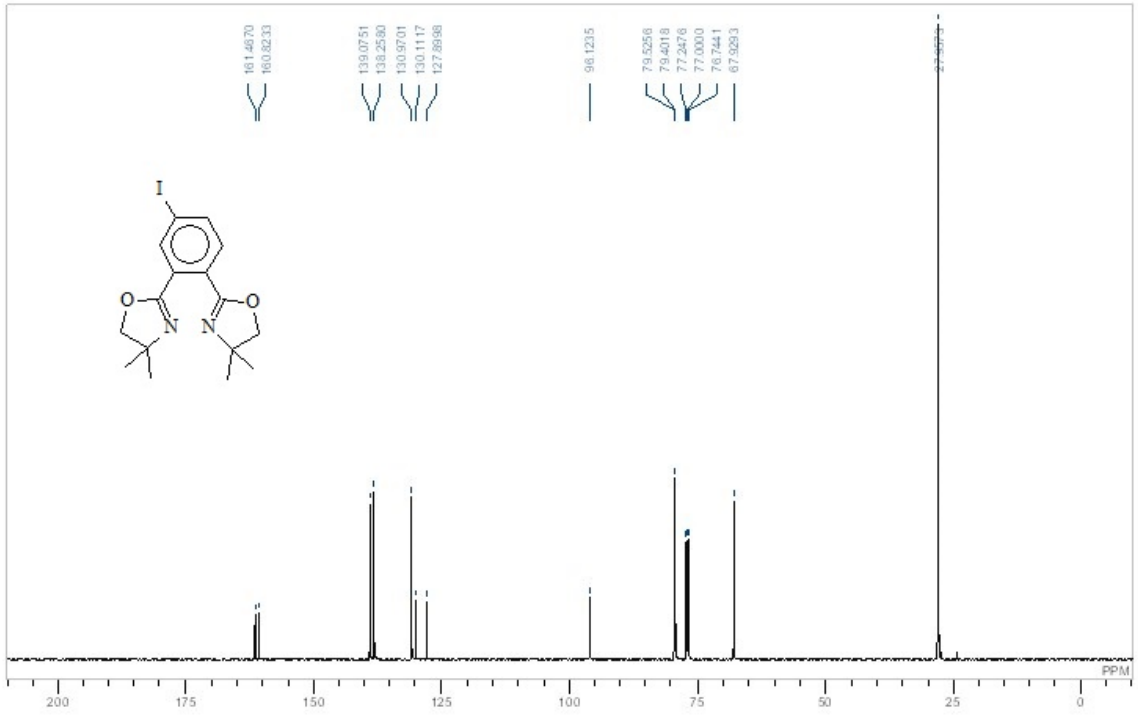

Figure A-I-14:[1]H NMR Spectrum of BOX-7

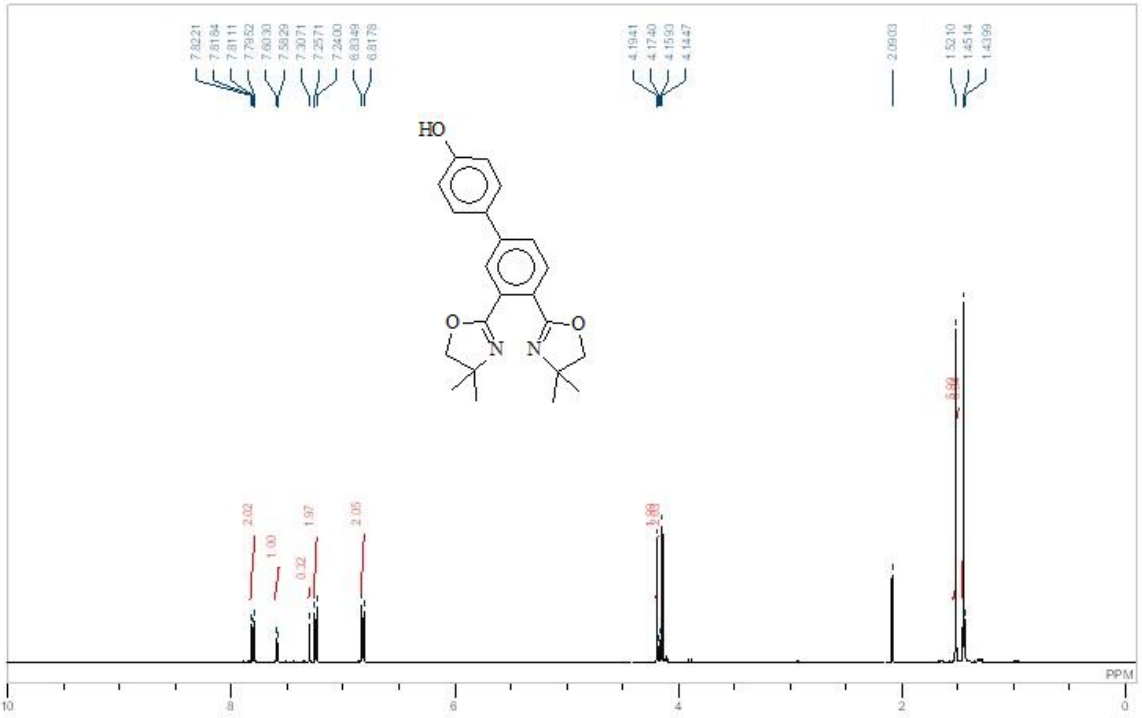

Figure A-I-15:[1]H NMR Spectrum of BOX-8

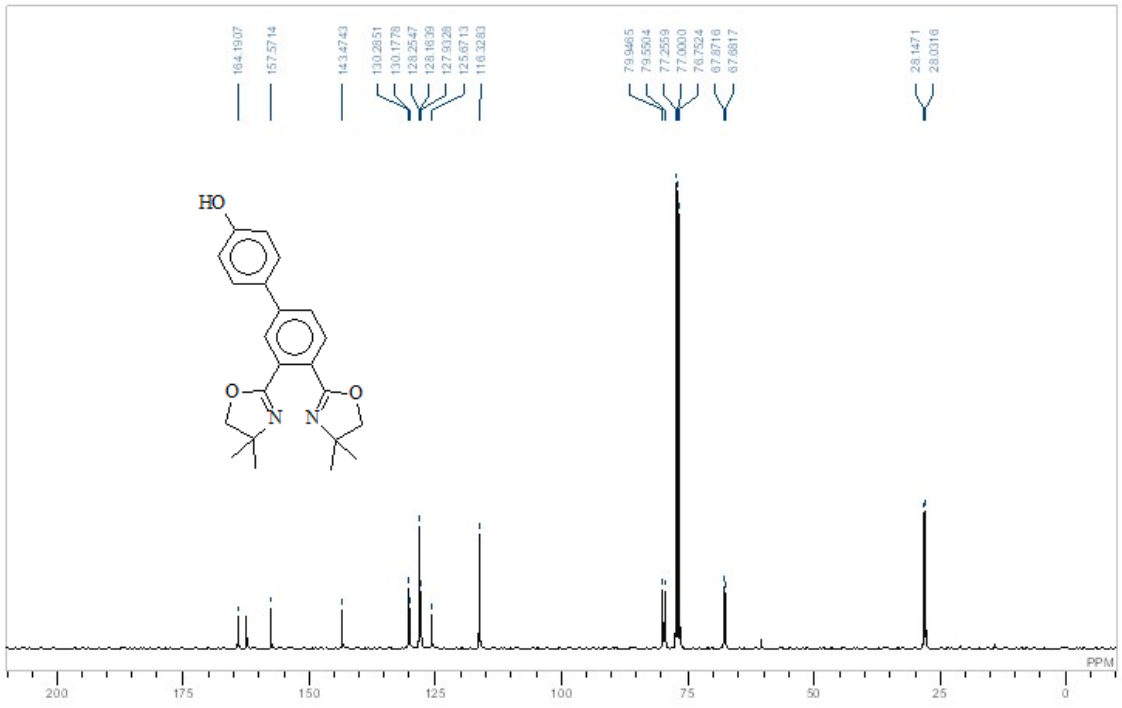

Figure A-I-16:[13]C NMR Spectrum of BOX-8

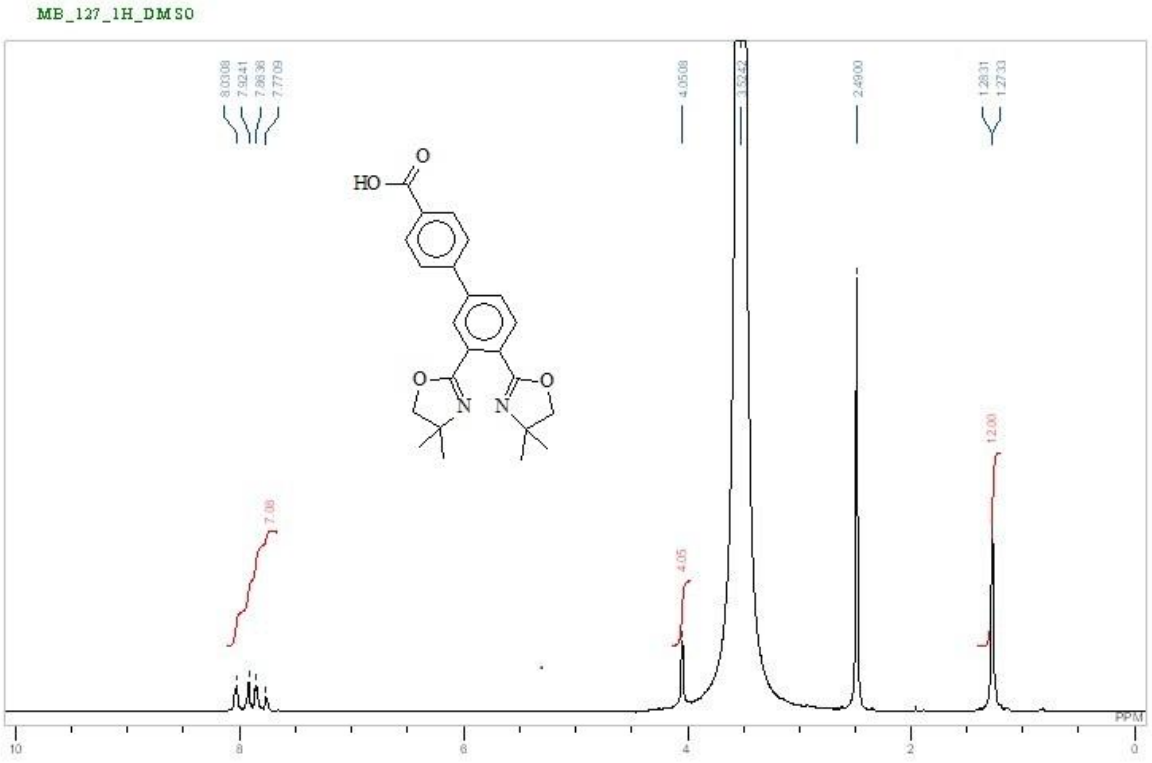

Figure A-I-17:[1]H NMR Spectrum of BOX-9

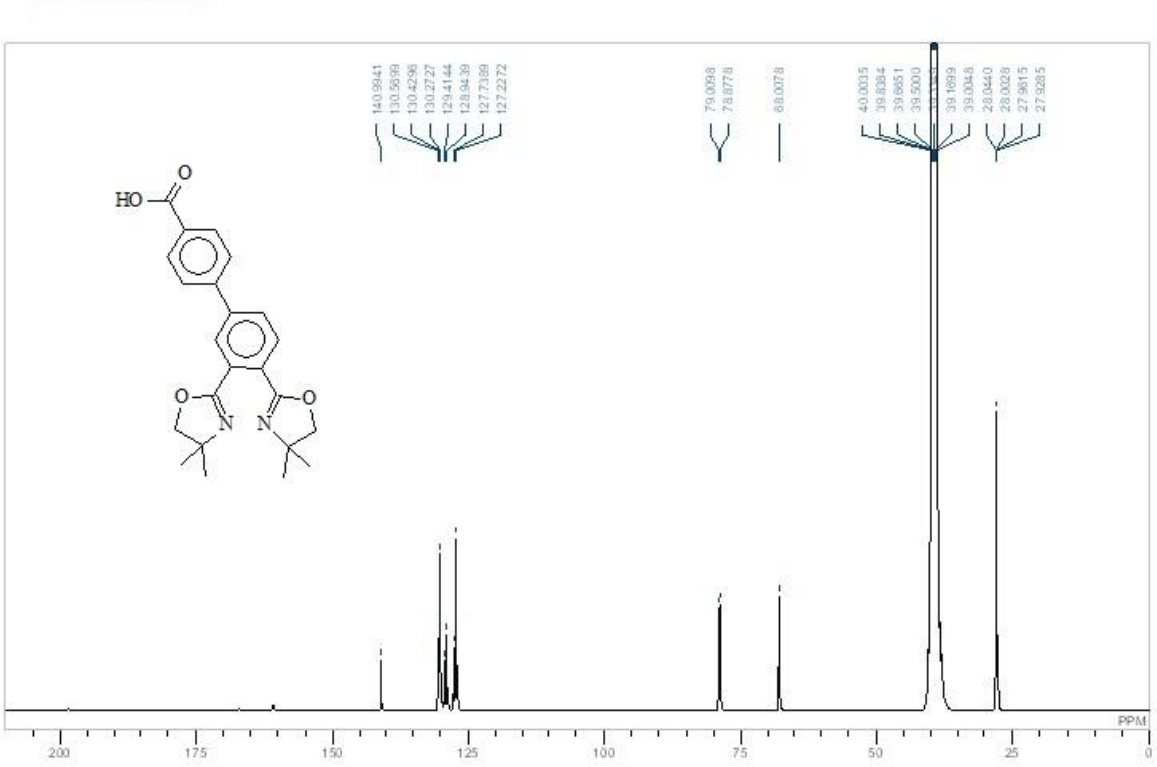

Figure A-I-18:[13]C NMR Spectrum of BOX-9

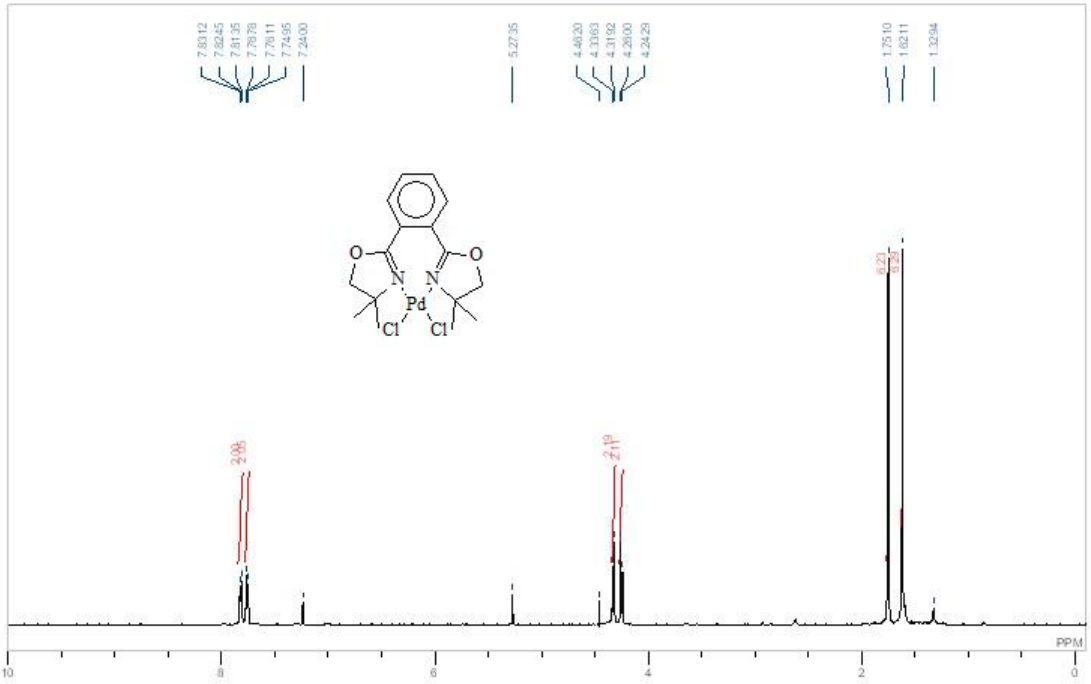

Figure A-I-19:[1]H NMR Spectrum of Pd-BOX-1

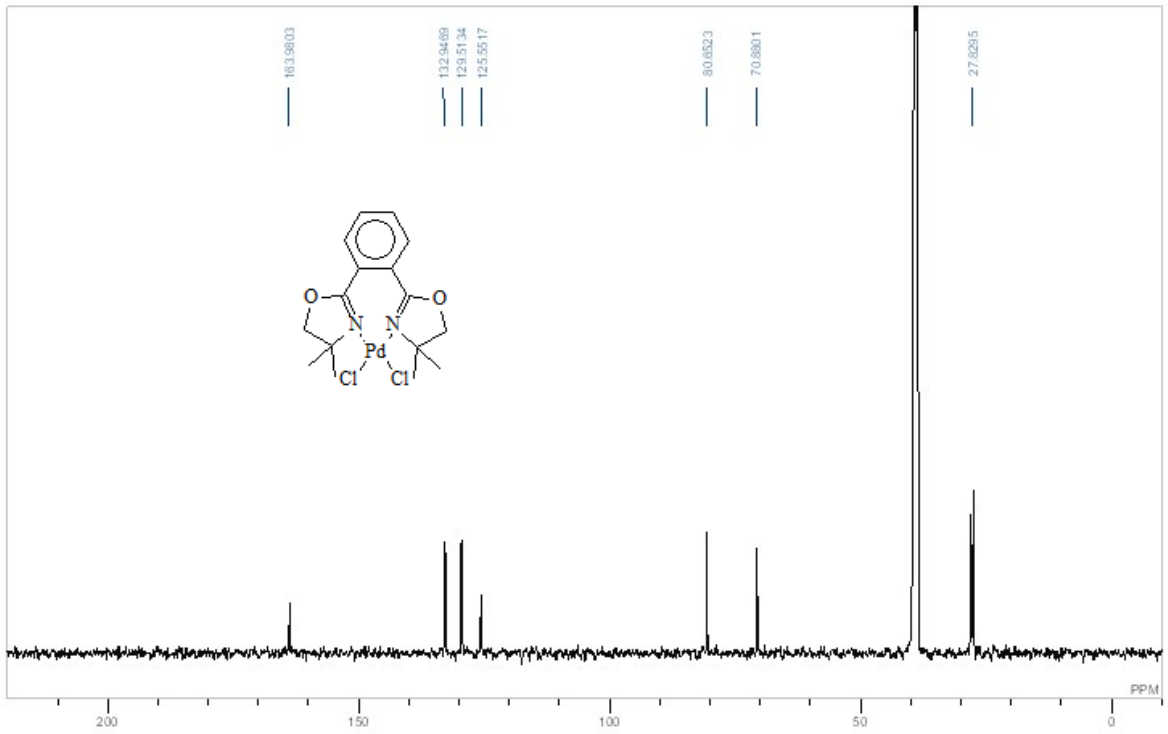

Figure A-I-20:[13]C NMR Spectrum of Pd-BOX-1

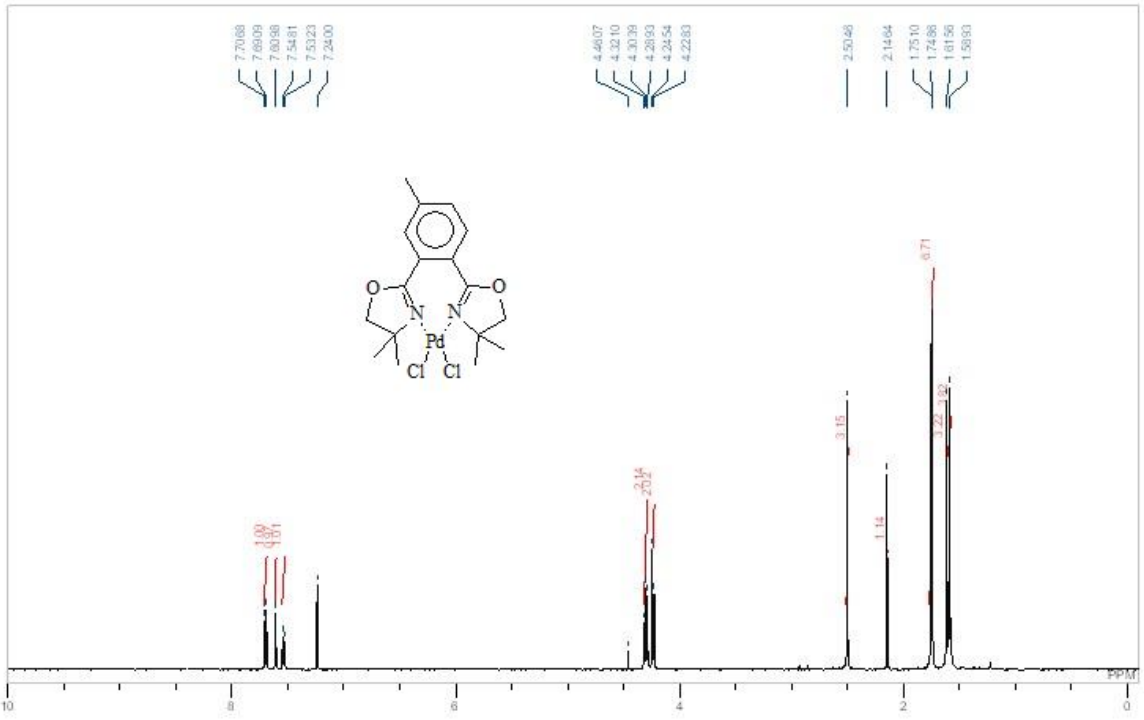

Figure A-I-21:[1]H NMR Spectrum of Pd-BOX-2

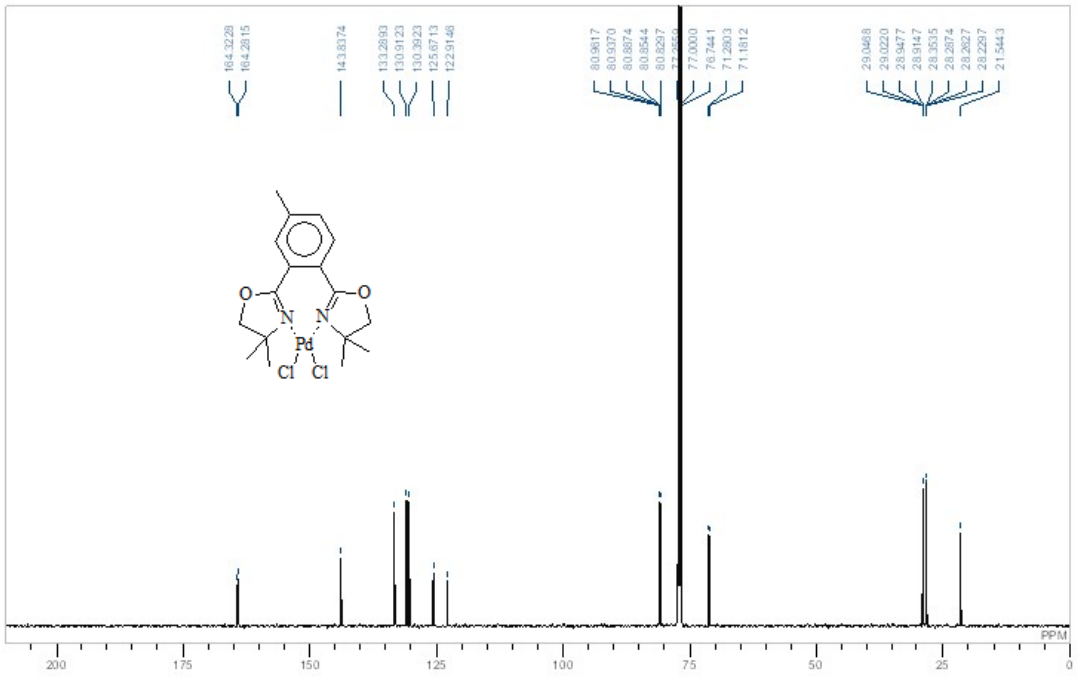

Figure A-I-22:[13]C NMR Spectrum of Pd-BOX-2

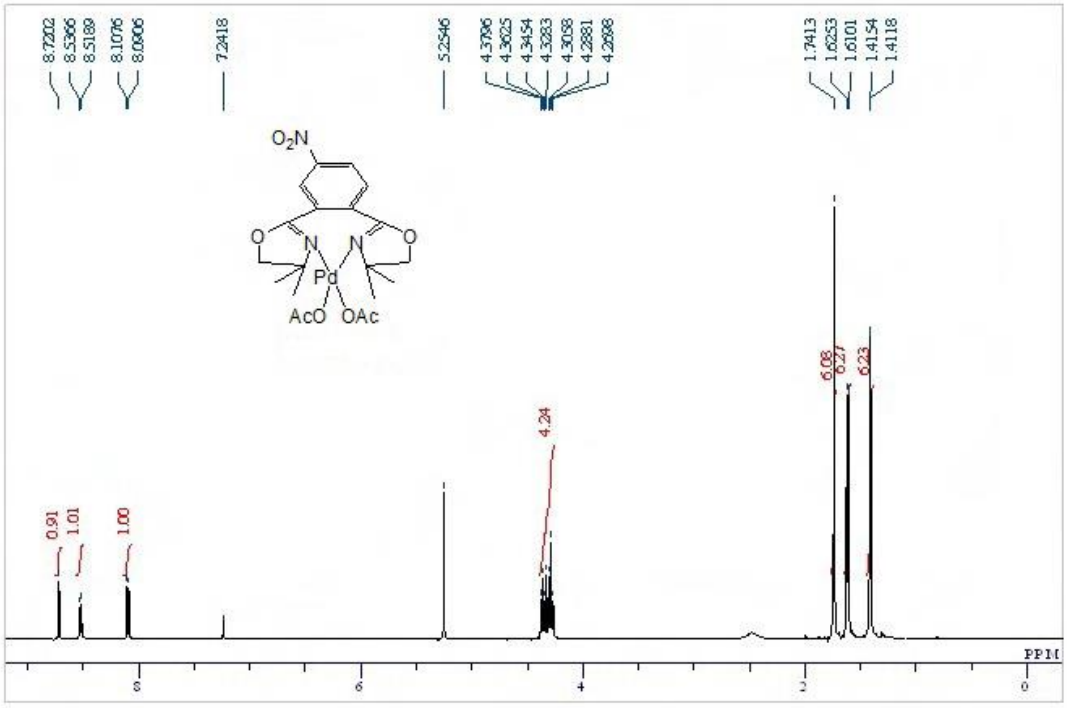

Figure A-I-23: ^{1}H NMR Spectrum of Pd-BOX-3

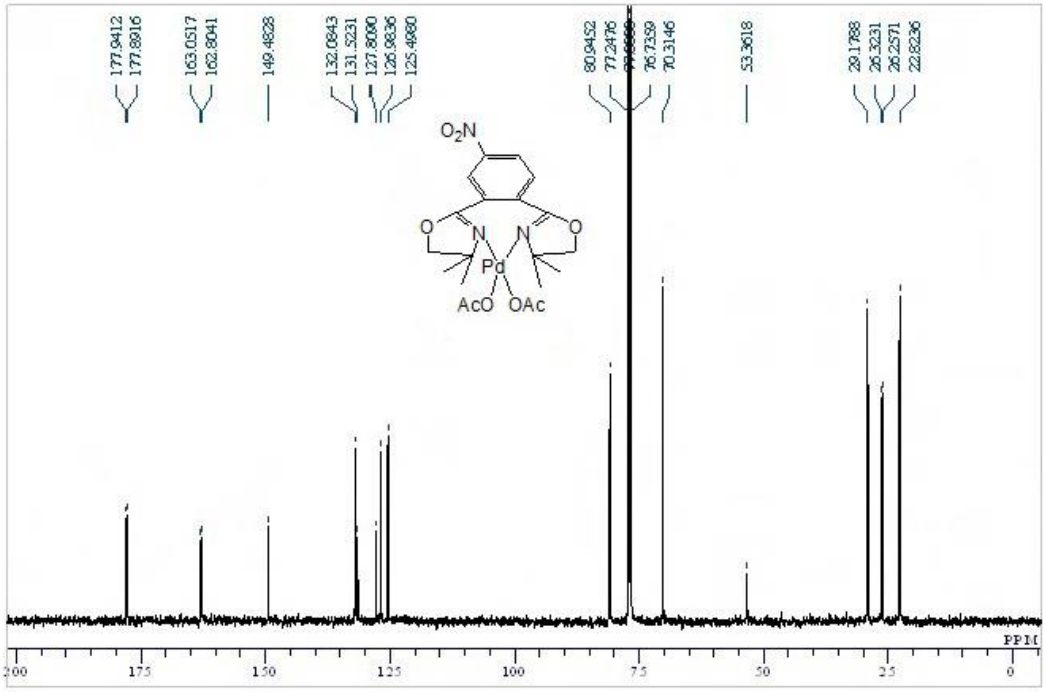

Figure A-I-24: ^{13}C NMR Spectrum of Pd-BOX-3

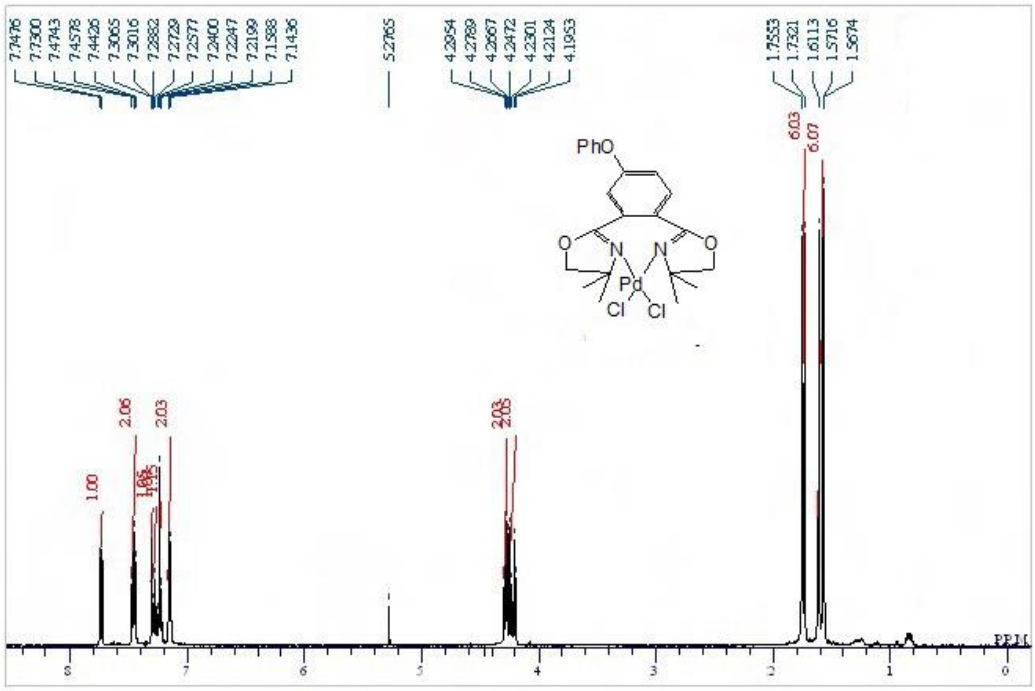

Figure A-I-25:[1]H NMR Spectrum of Pd-BOX-4

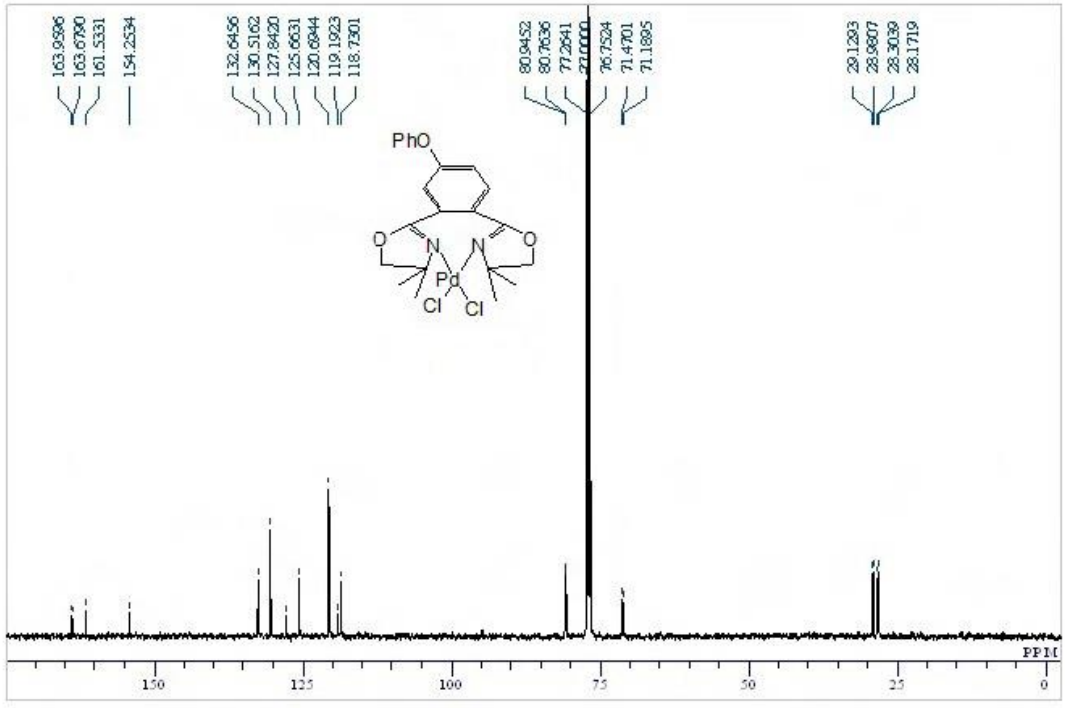

Figure A-I-26:[13]C NMR Spectrum of Pd-BOX-4

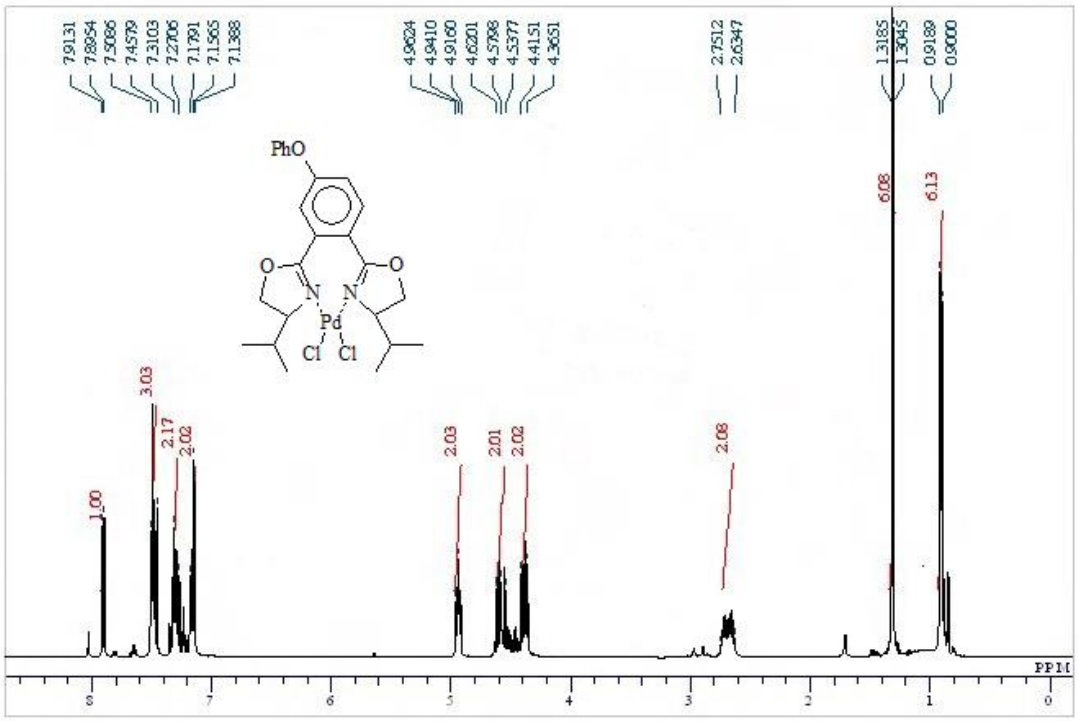

Figure A-I-27:[1]H NMR Spectrum of Pd-BOX-5

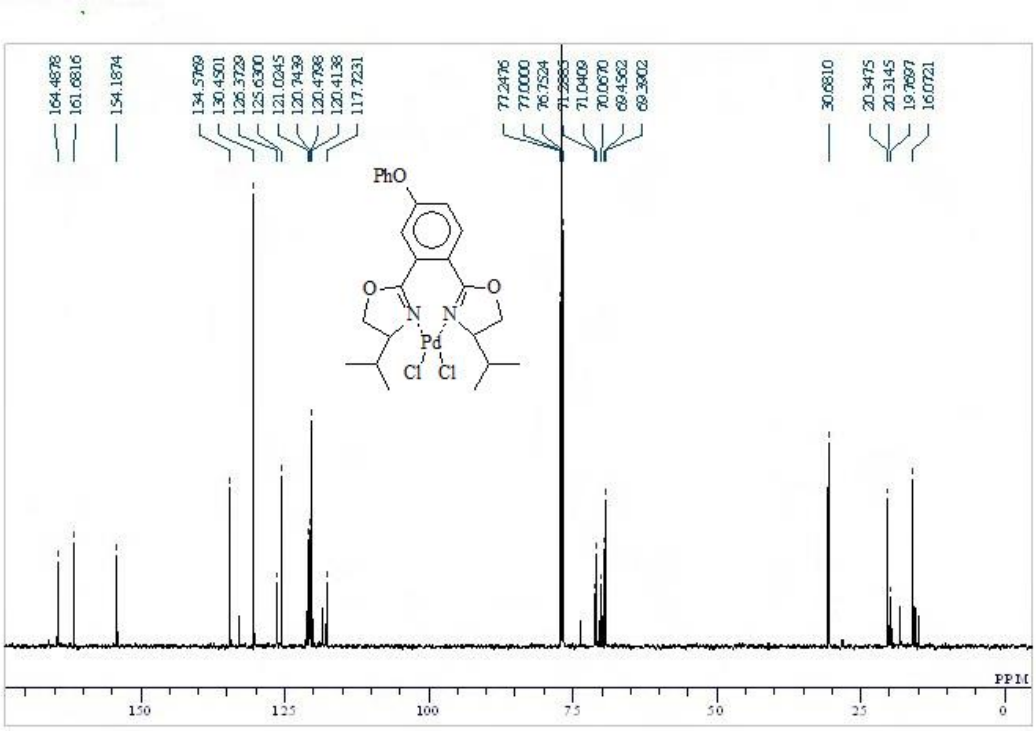

Figure A-I-28:[1]H NMR Spectrum of Pd-BOX-5

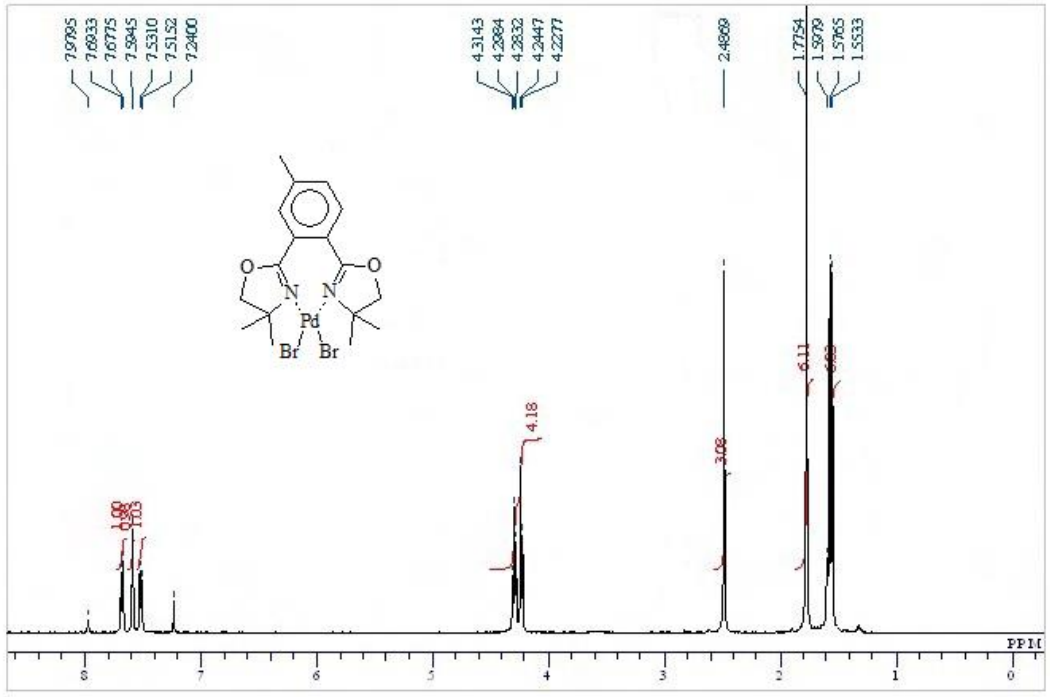

Figure A-I-29:[1]H NMR Spectrum of Pd-BOX-6

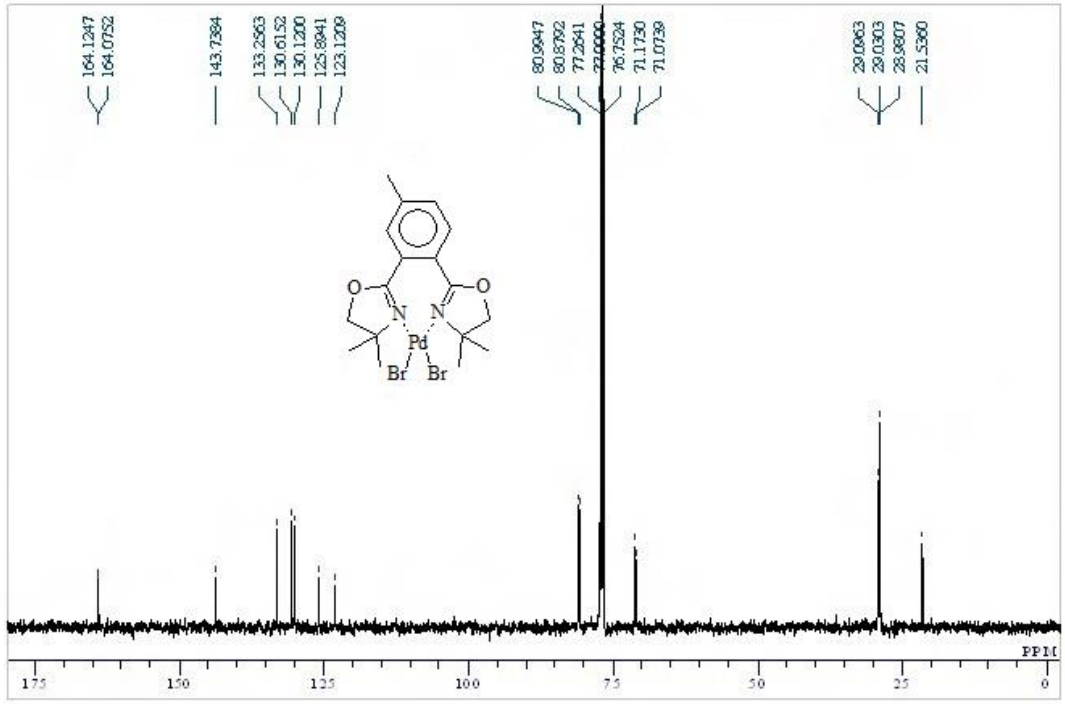

Figure A-I-30:[1]H NMR Spectrum of Pd-BOX-6

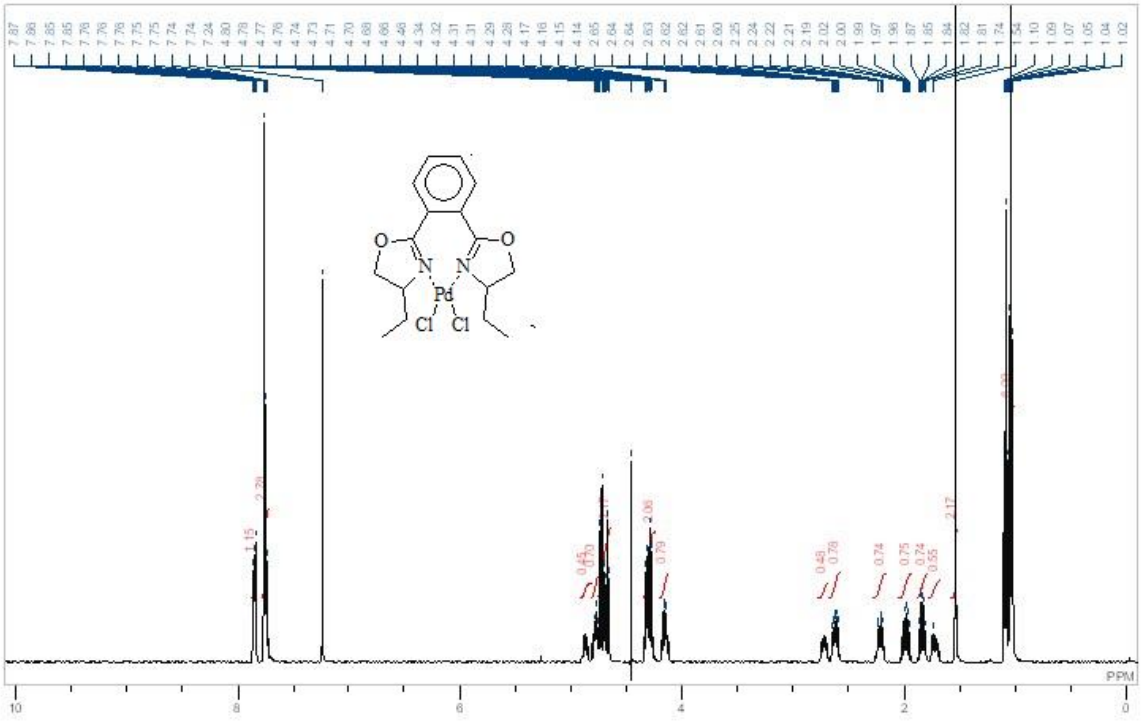

Figure A-I-31:[1]H NMR Spectrum of Pd-BOX-7

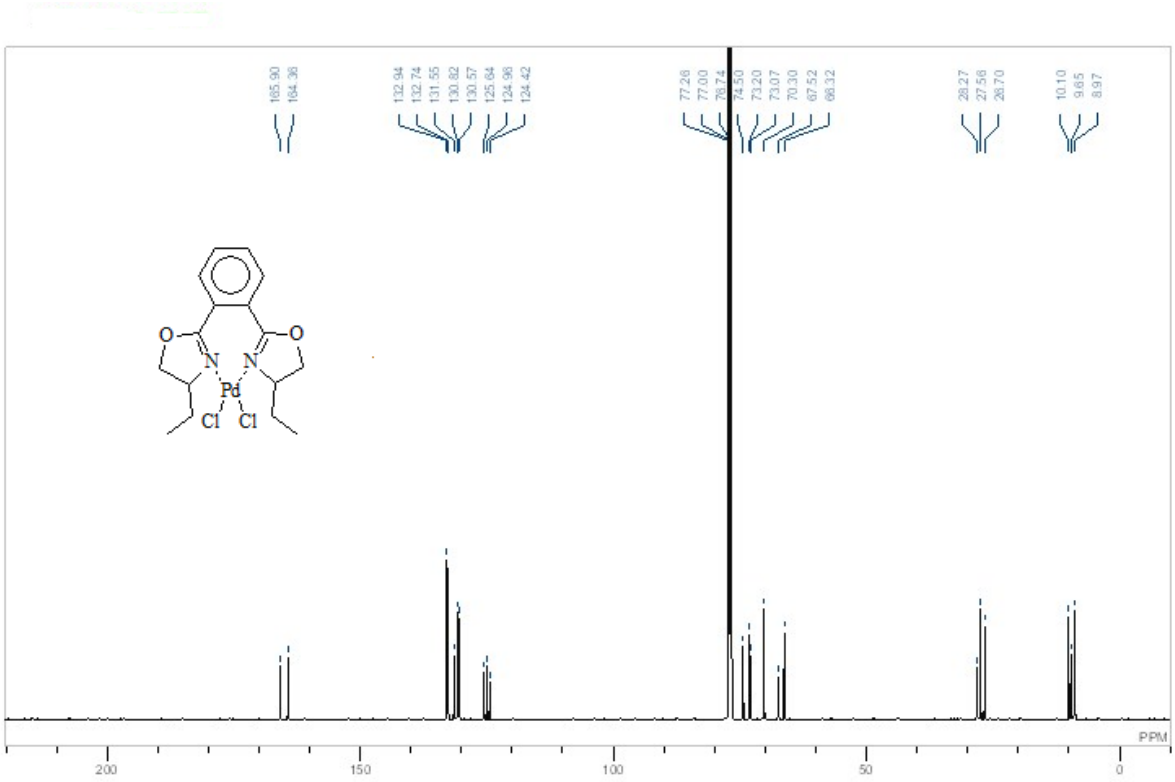

Figure A-I-32:[1]H NMR Spectrum of Pd-BOX-7

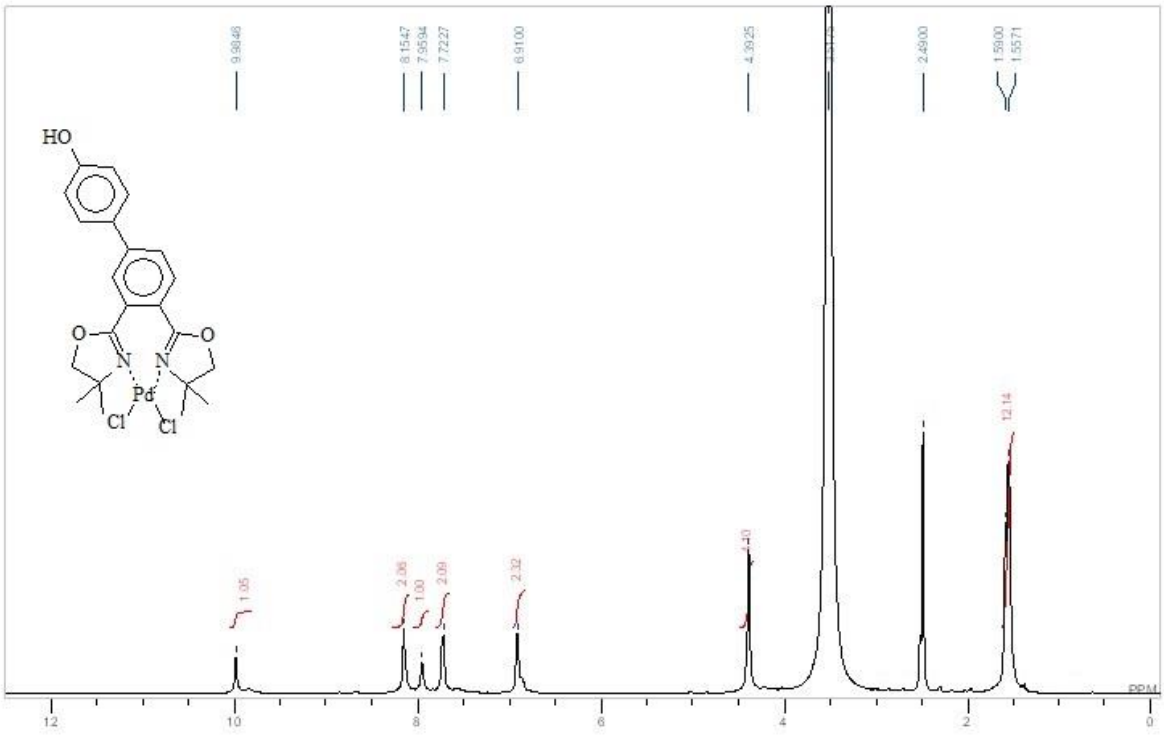

Figure A-I-33:[1]H NMR Spectrum of Pd-BOX-8

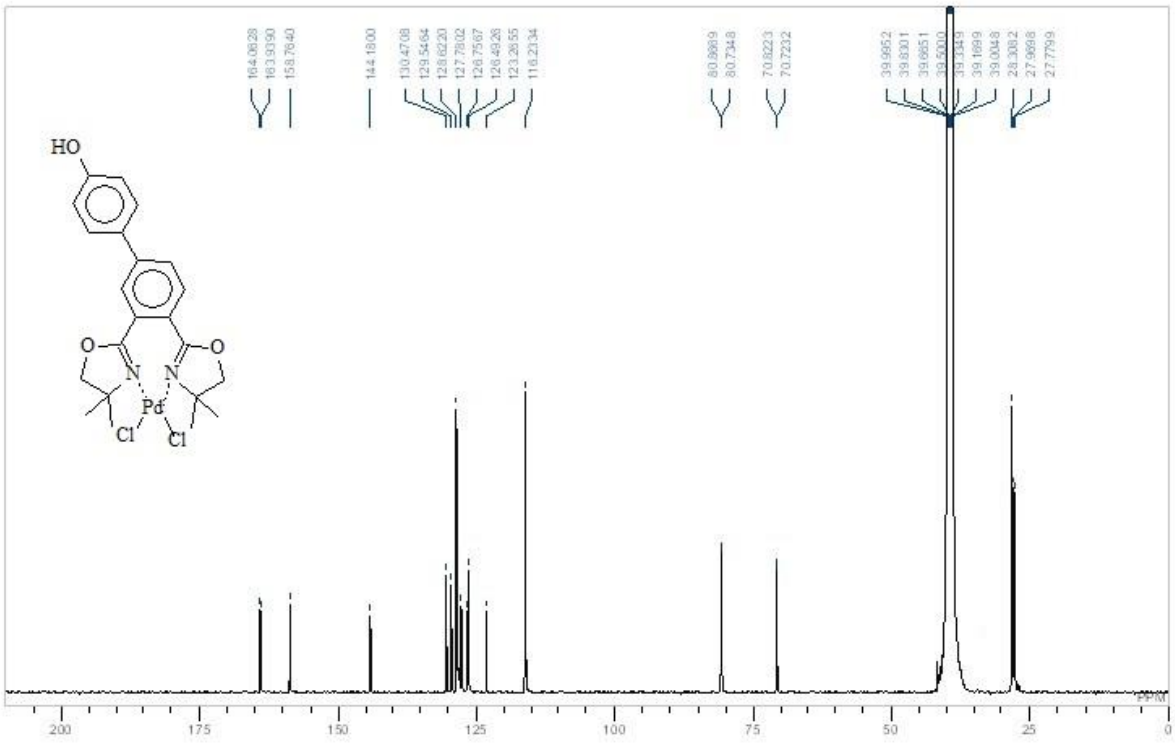

Figure A-I-34:[1]H NMR Spectrum of Pd-BOX-8

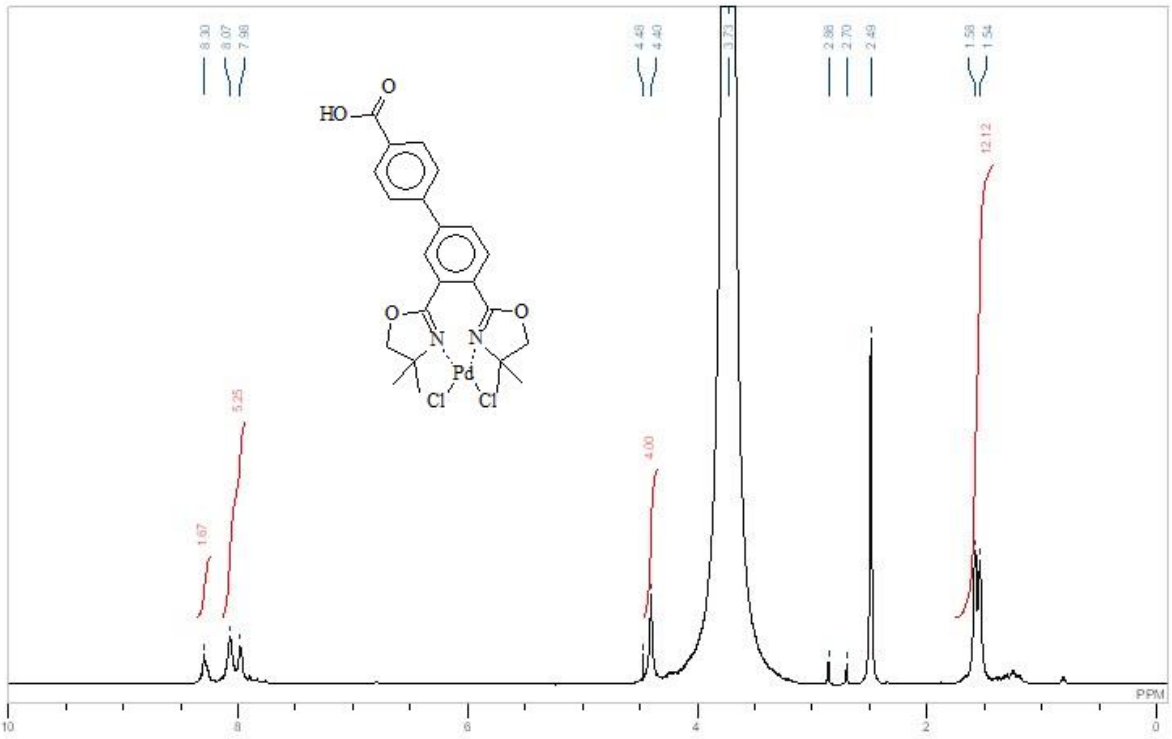

Figure A-I-35: ^{1}H NMR Spectrum of Pd-BOX-9

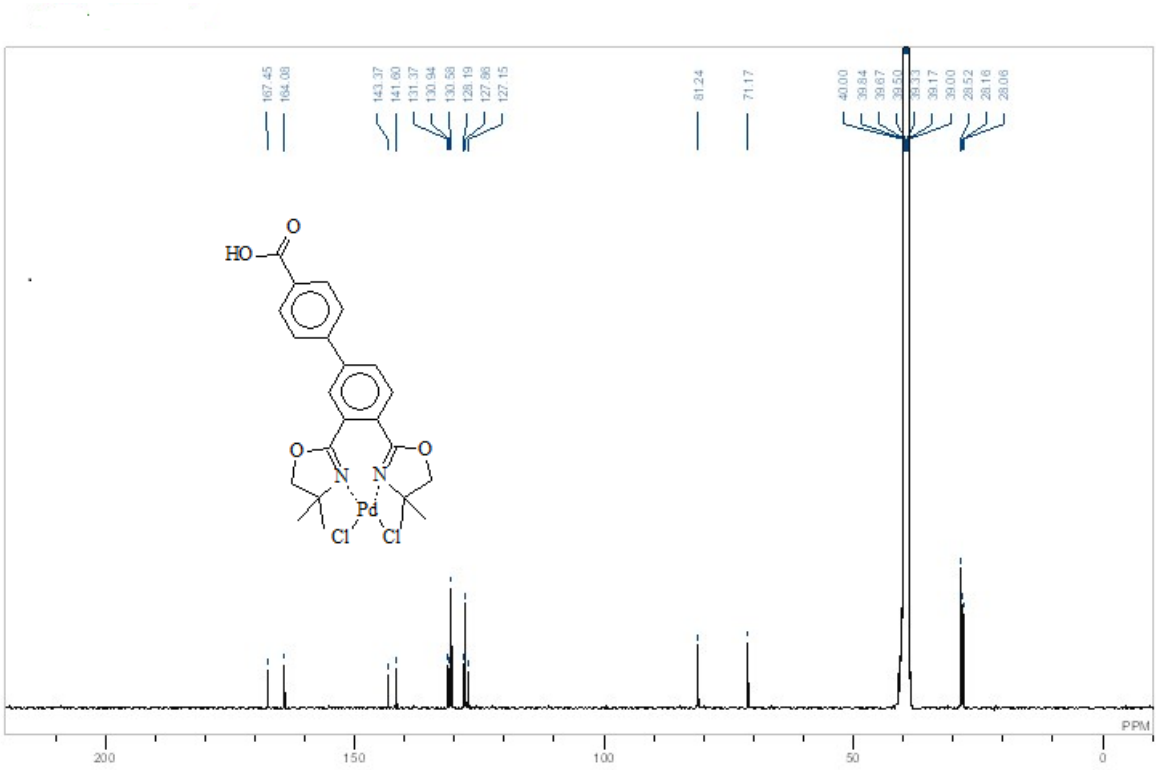

Figure A-I-36: ^{13}C NMR Spectrum of Pd-BOX-9

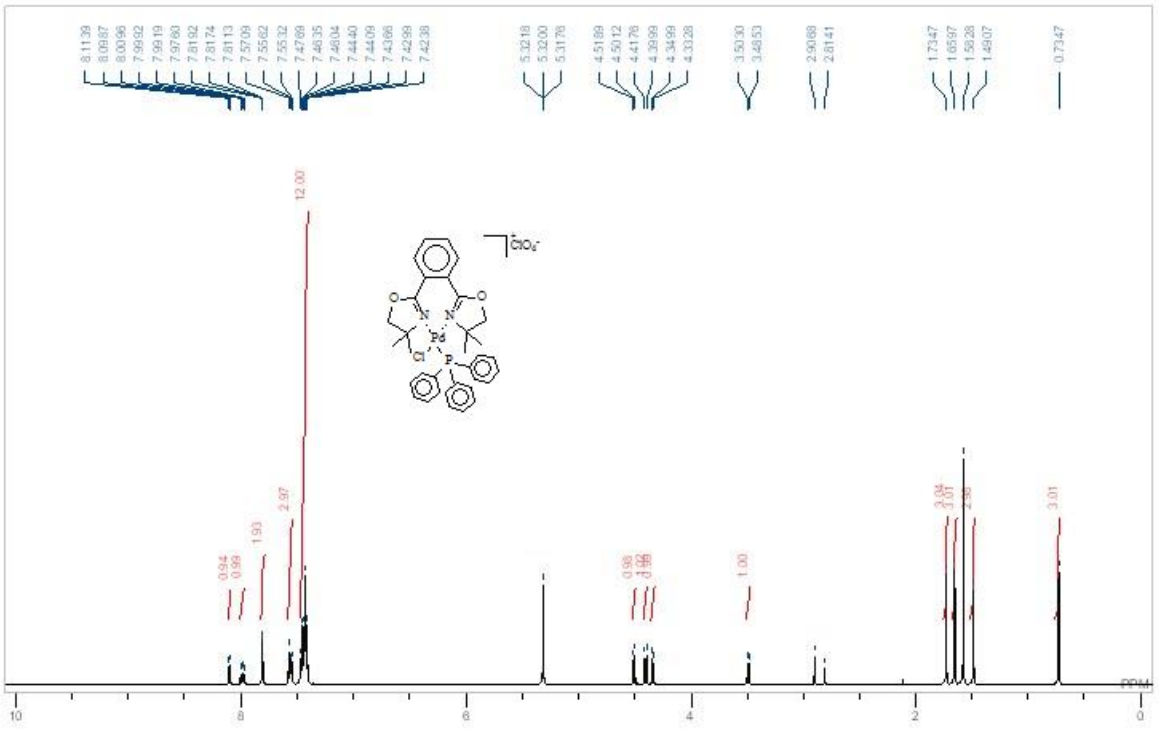

Figure A-I-37:[1]H NMR Spectrum of Pd-BOX-10

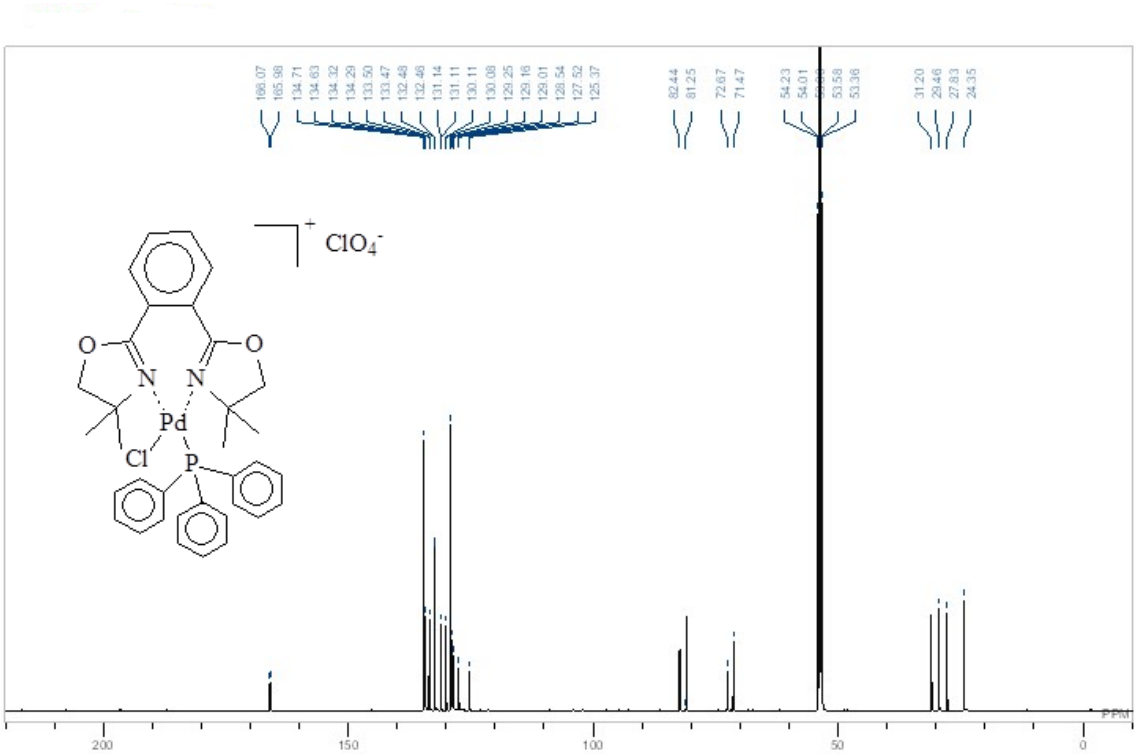

Figure A-I-38:13C NMR Spectrum of Pd-BOX-10

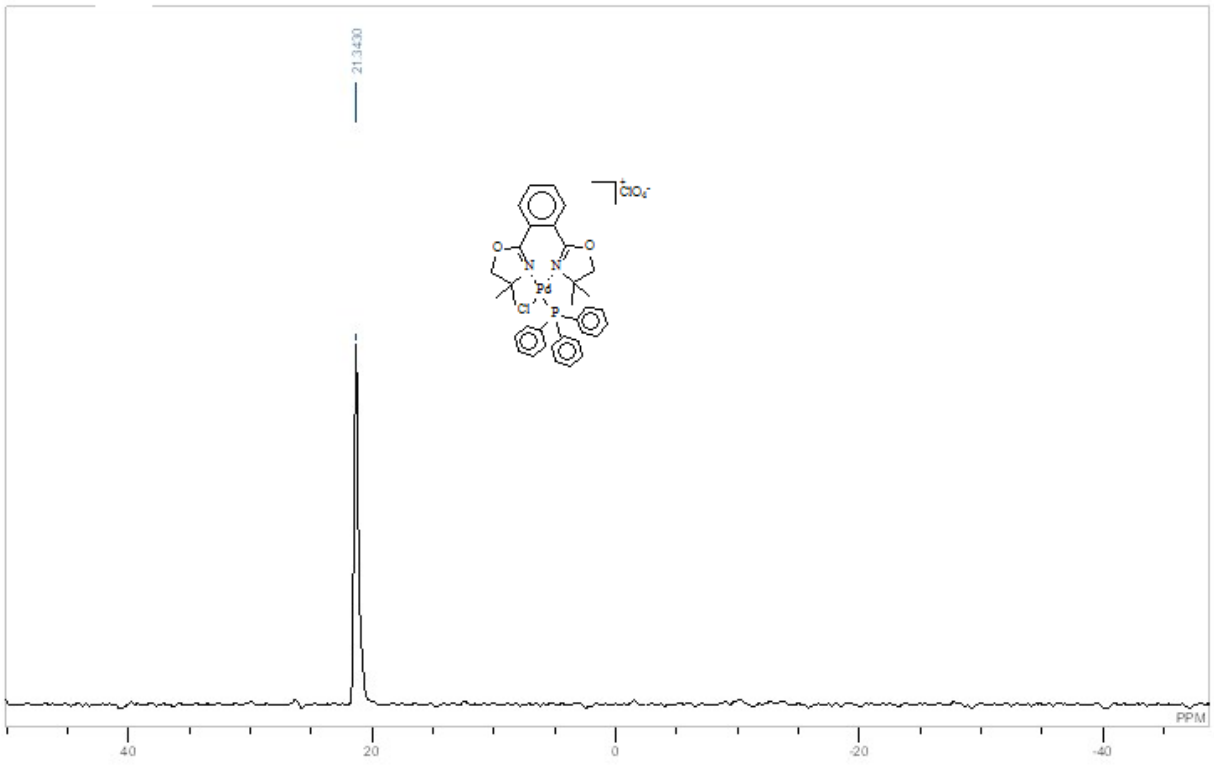

Figure A-I-39: ^{31}P NMR Spectrum of Pd-BOX-10

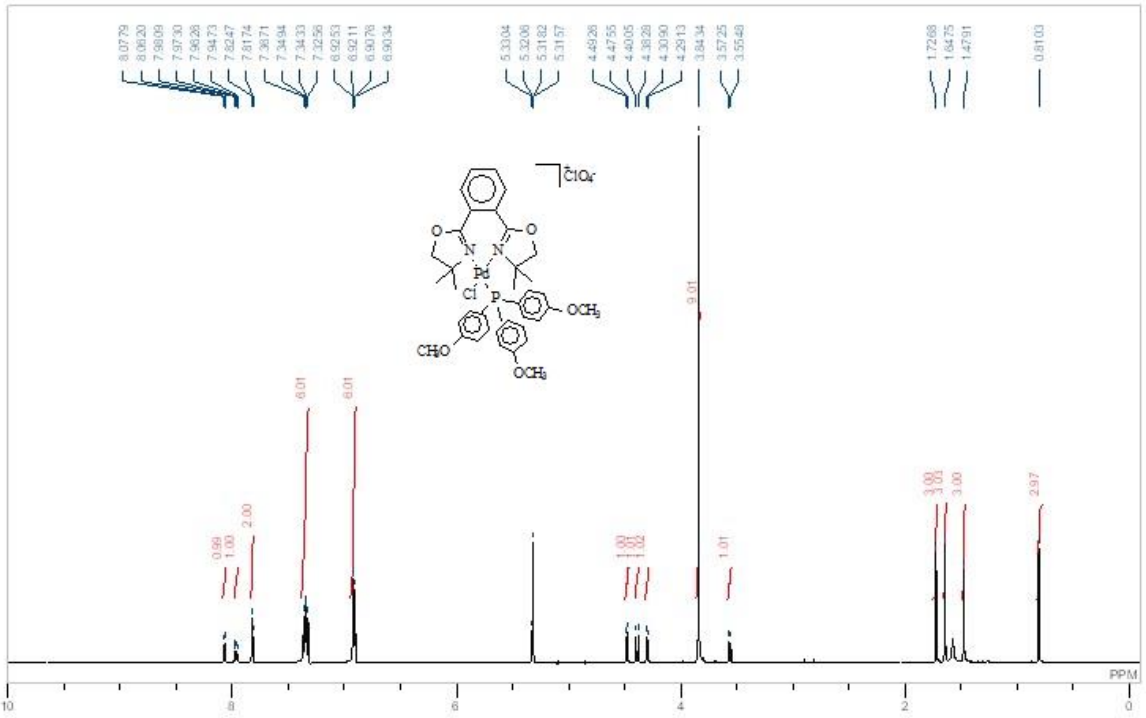

Figure A-I-40:[1]H NMR Spectrum of Pd-BOX-11

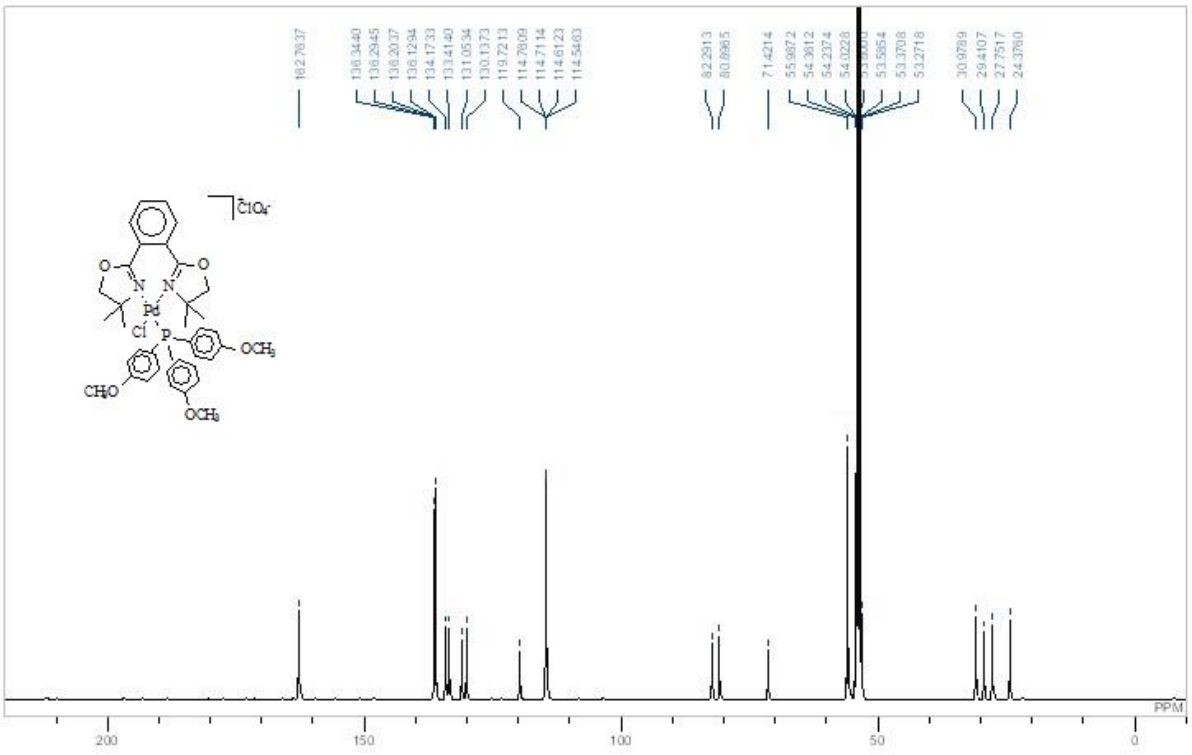

Figure A-I-41:[13]C NMR Spectrum of Pd-BOX-11

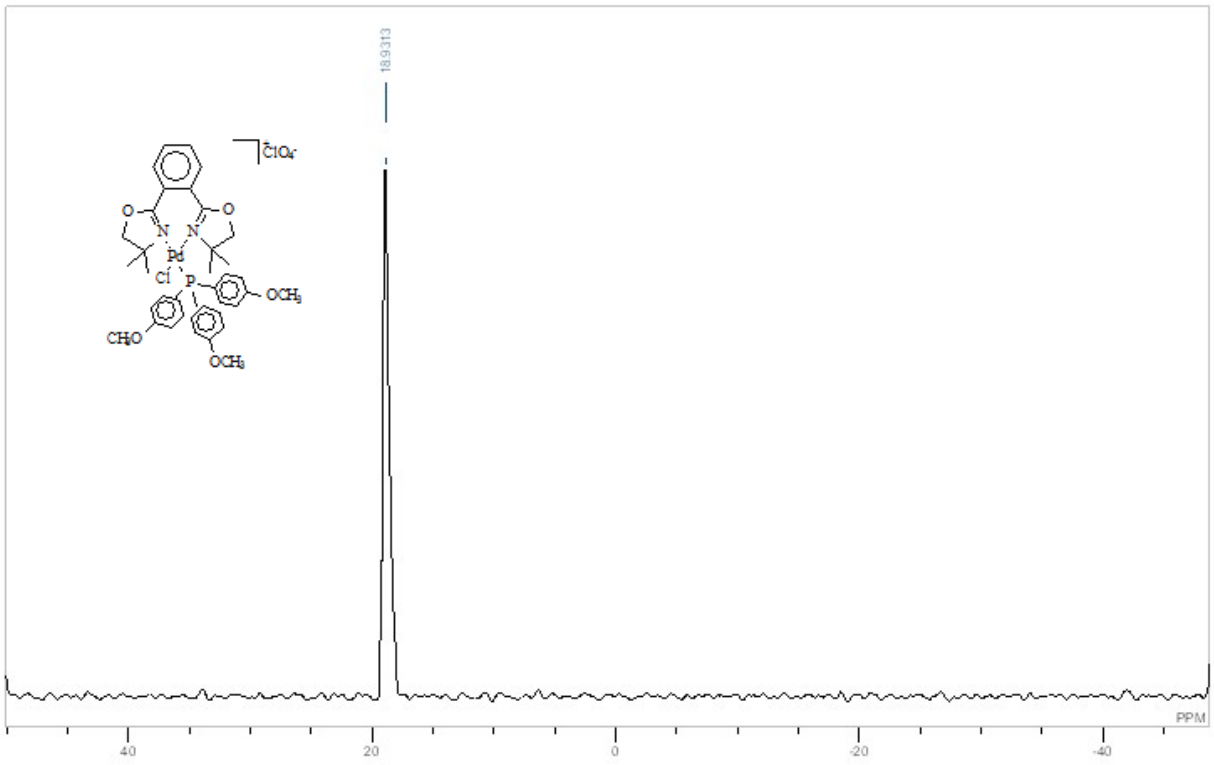

Figure A-I-42: ^{31}P NMR Spectrum of Pd-BOX-11

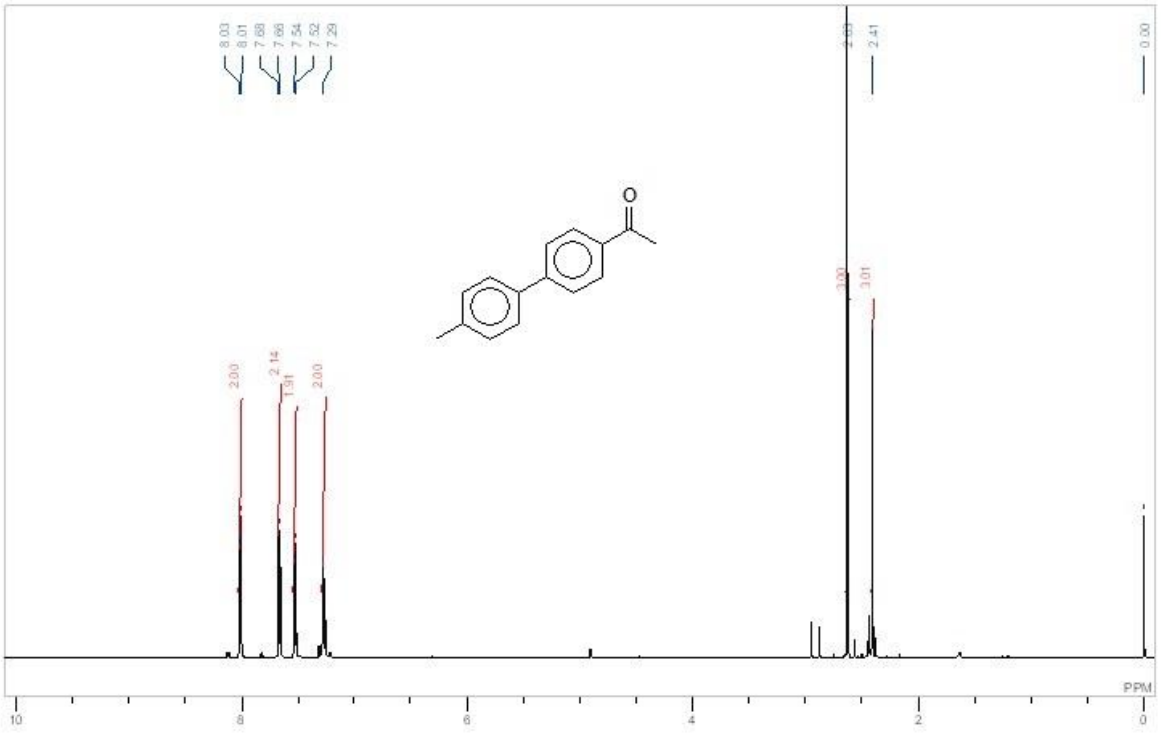

Figure A-I-43: ^{1}H NMR Spectrum of 3b

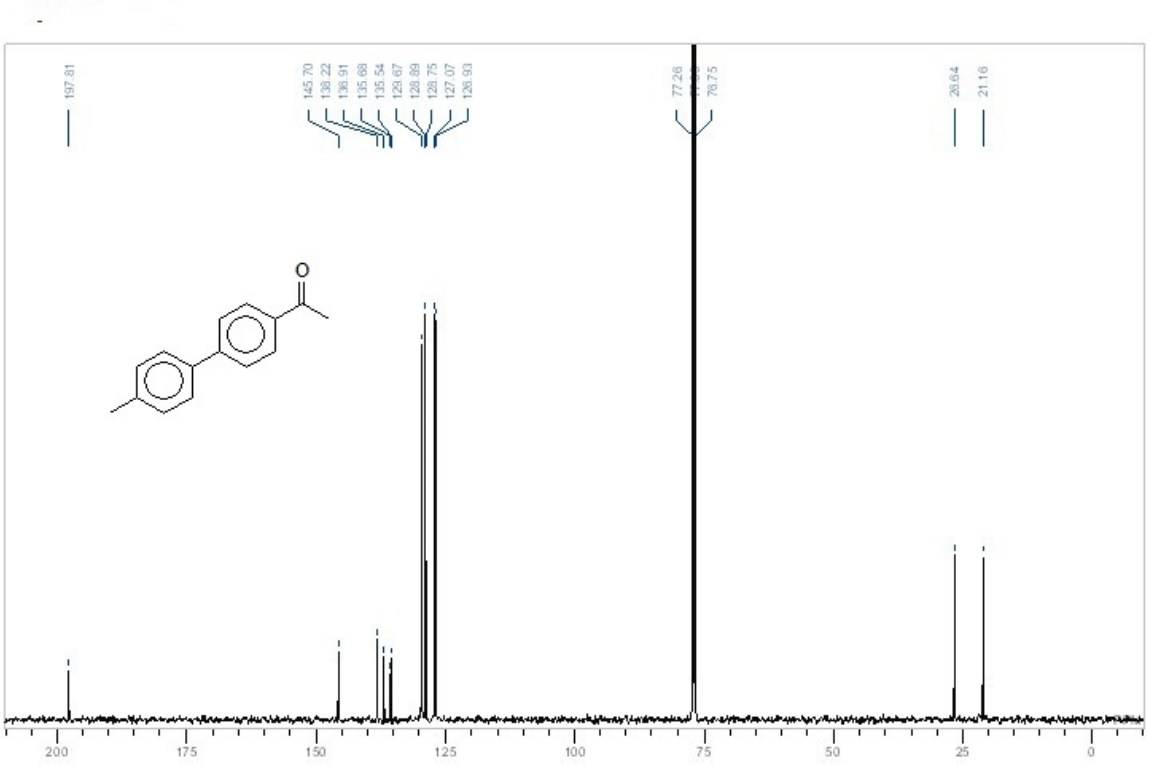

Figure A-I-44: ^{13}C NMR Spectrum of 3b

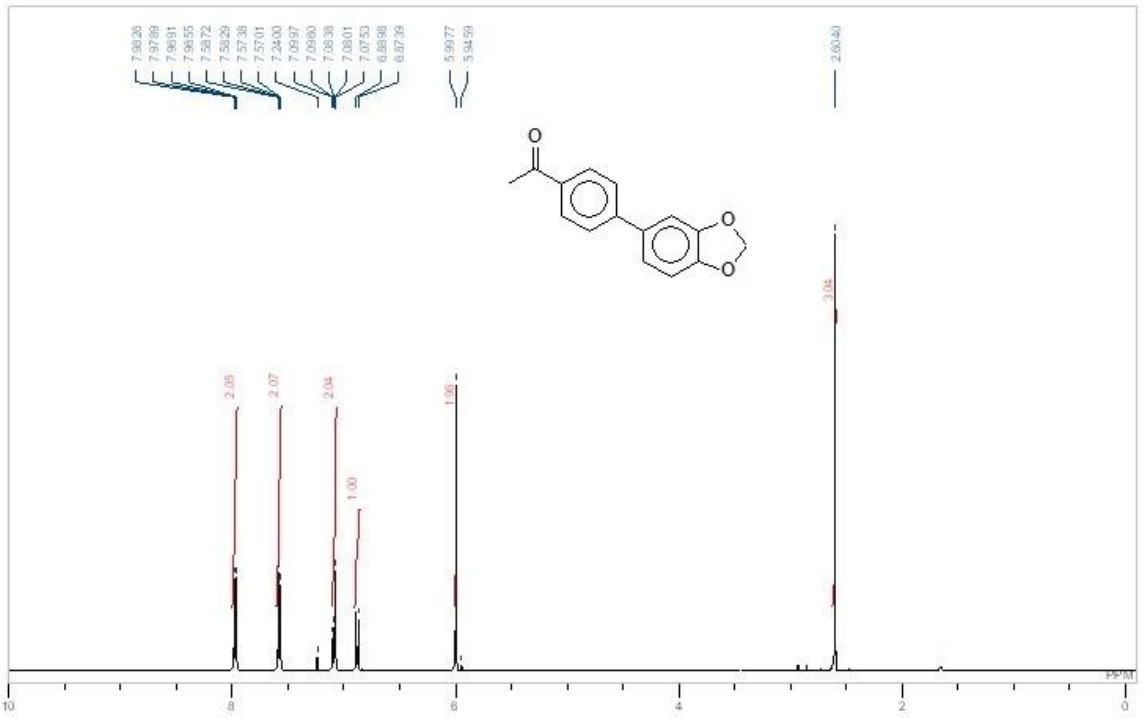

Figure A-I-45:[1]H NMR Spectrum of 3d

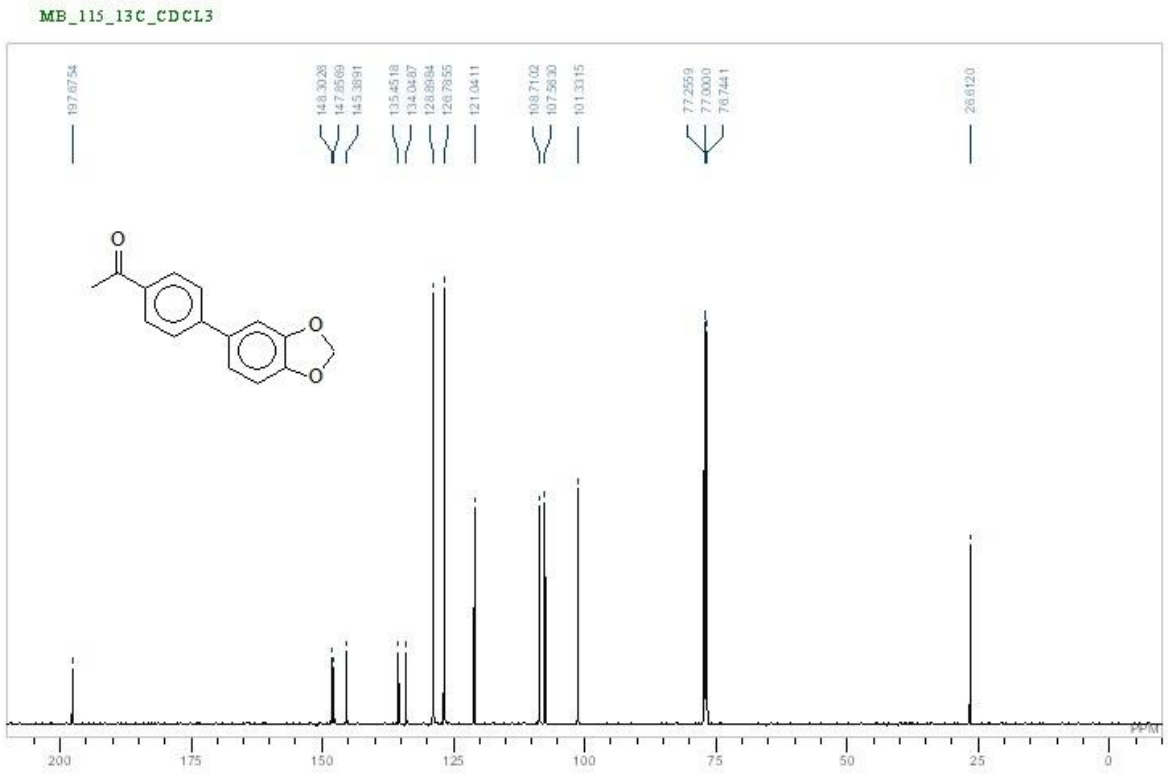

Figure A-I-46:[13]C NMR Spectrum of 3d

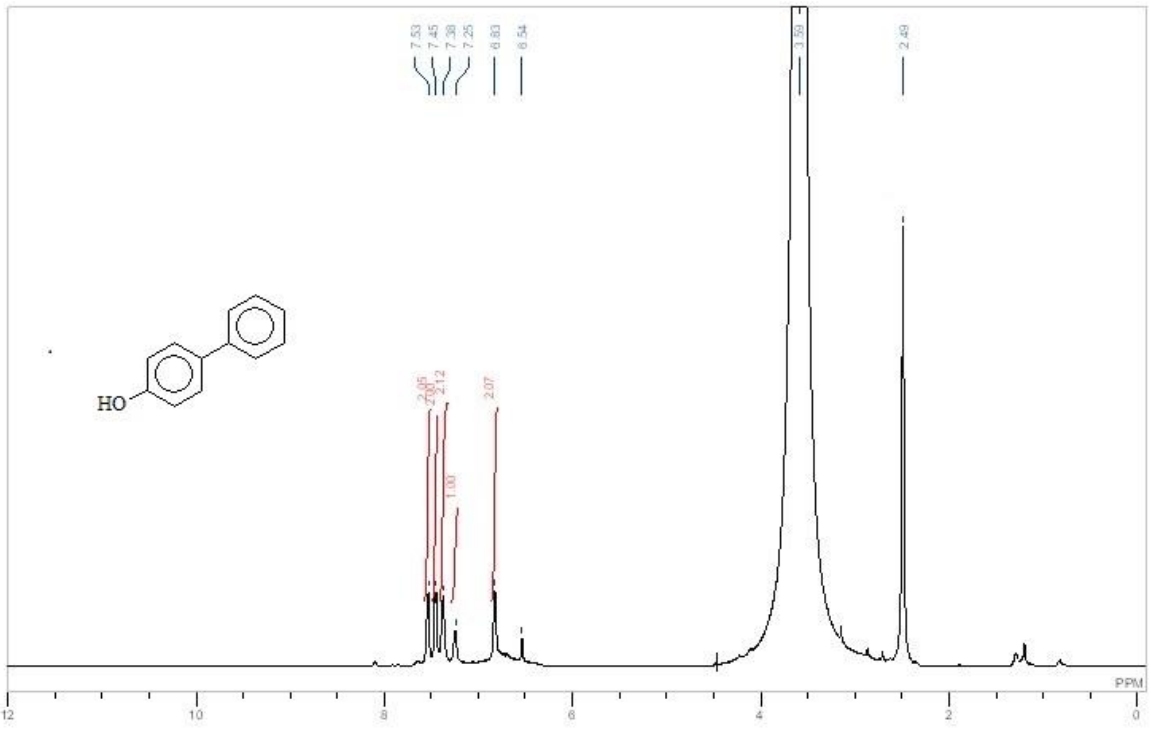

Figure A-I-47:[1]H NMR Spectrum of 3f

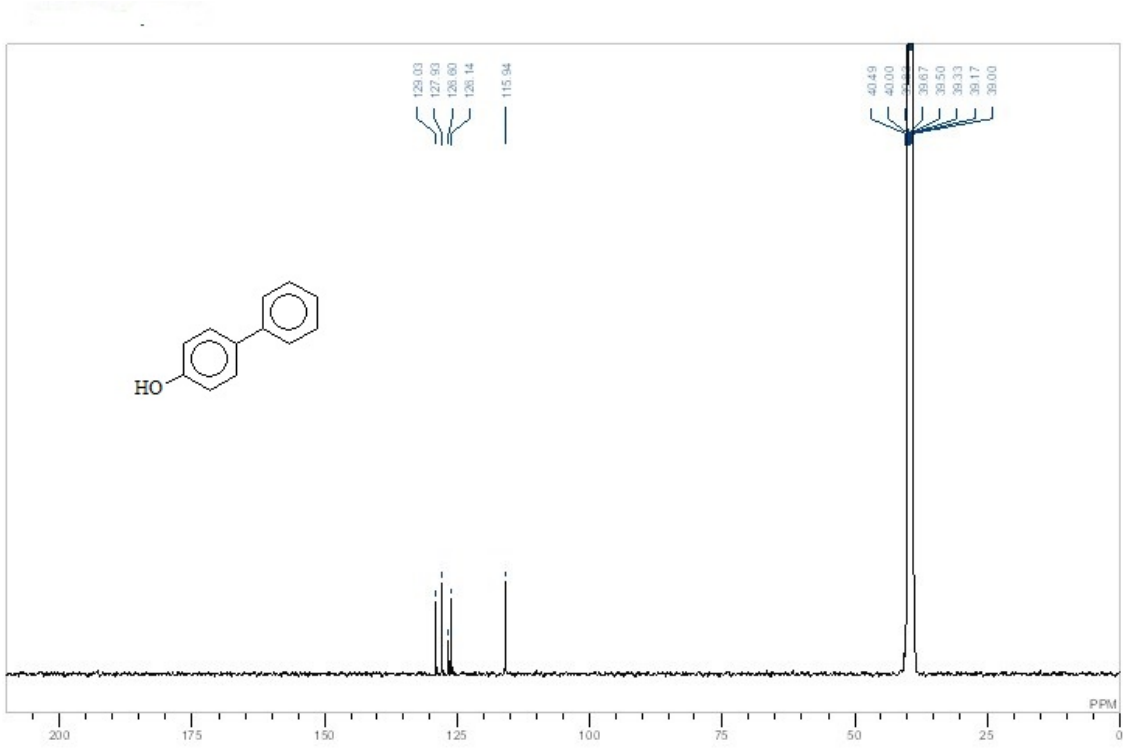

Figure A-I-48:13C NMR Spectrum of 3f

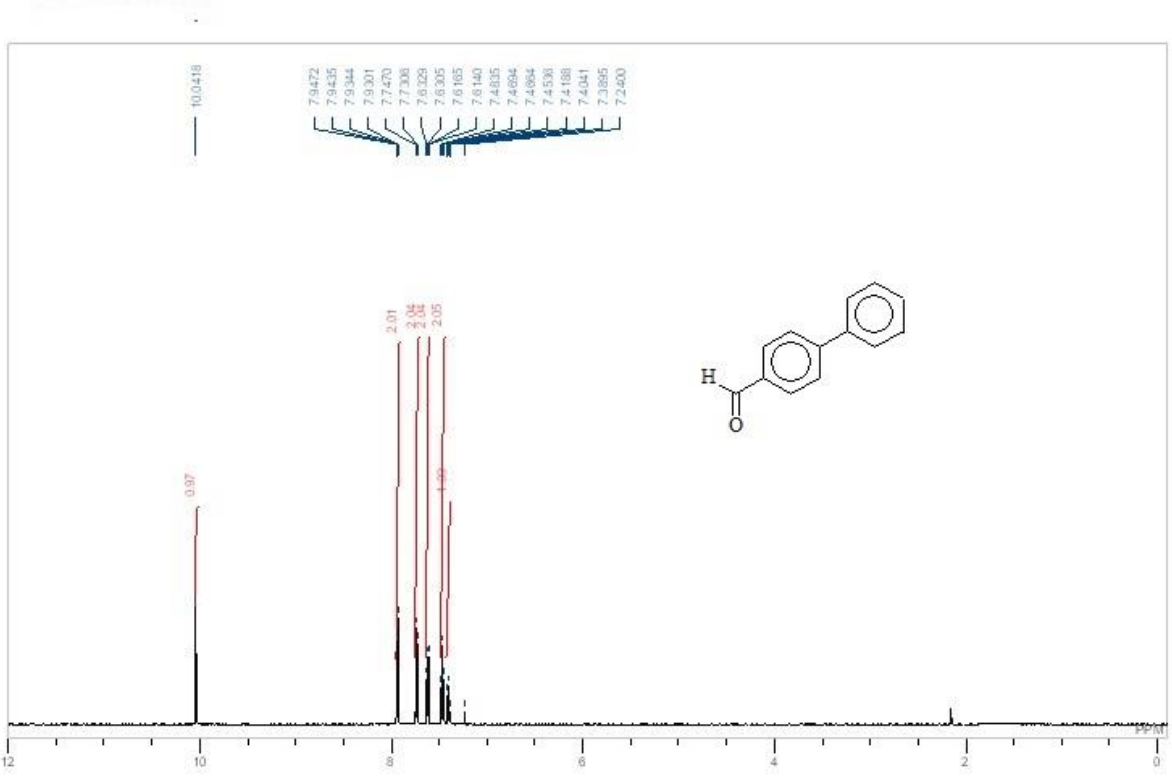

Figure A-I-49:[1]H NMR Spectrum of 3k

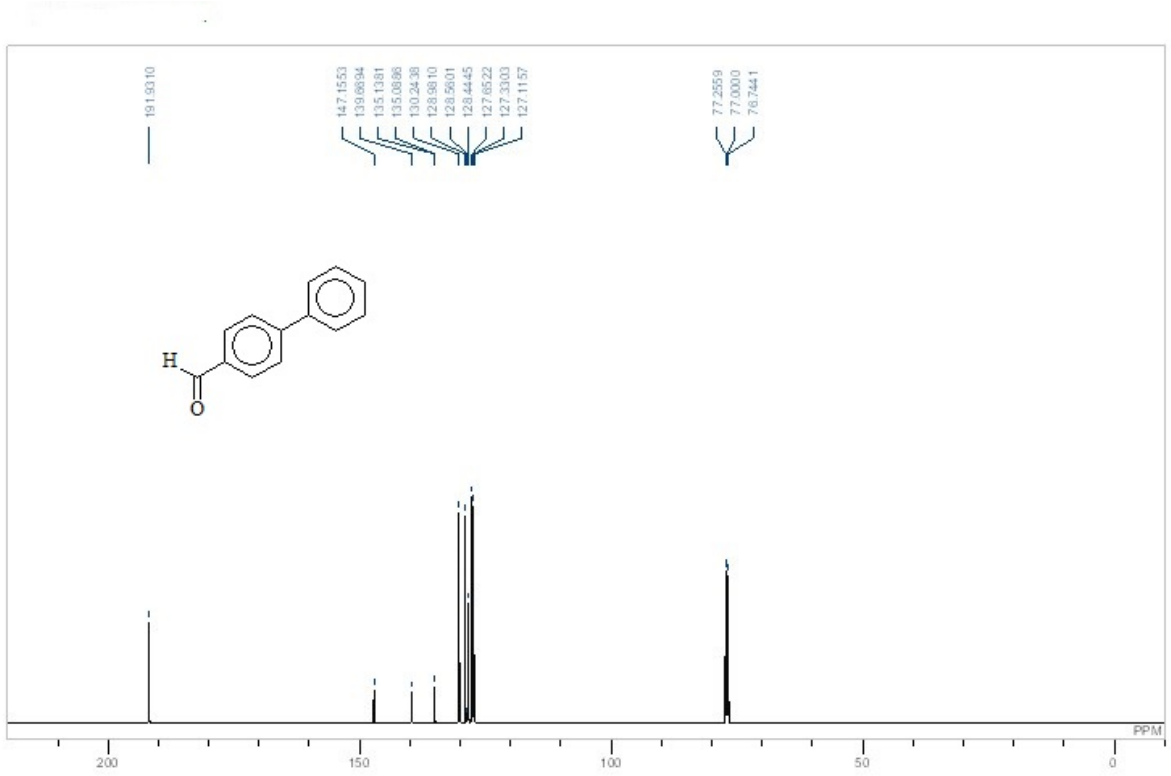

Figure A-I-50:[13]C NMR Spectrum of 3k

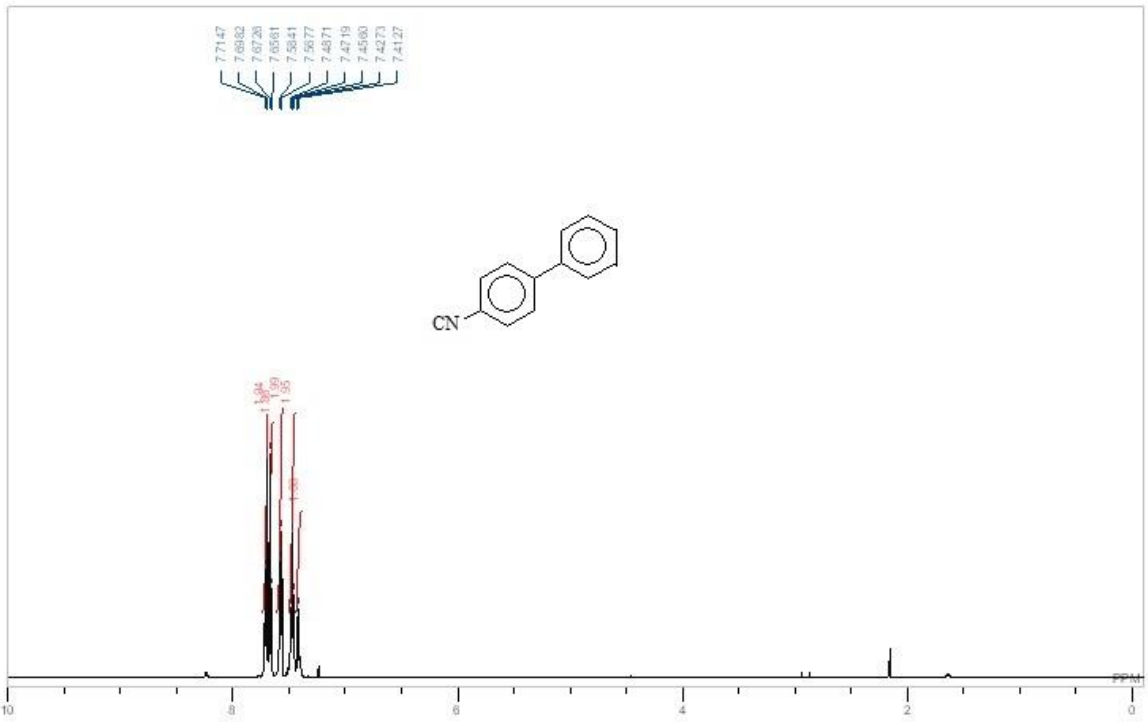

Figure A-I-51:[1]H NMR Spectrum of 3l

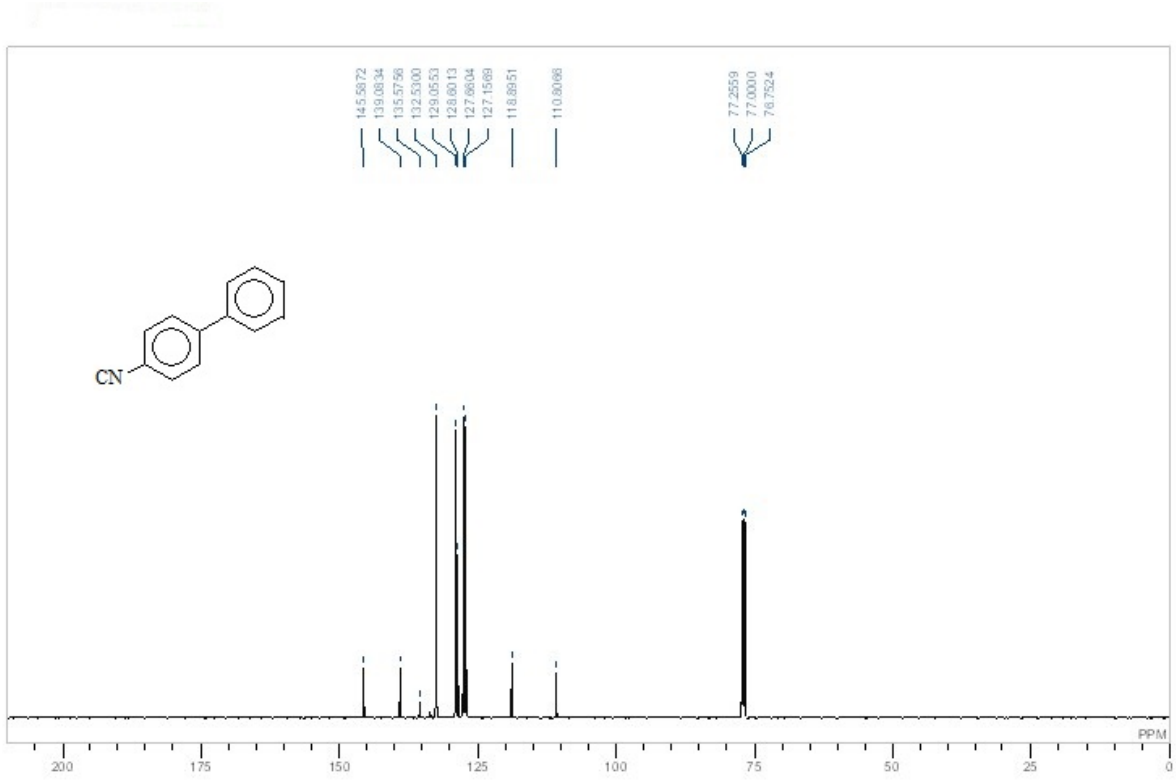

Figure A-I-52:[1]H NMR Spectrum of 3l

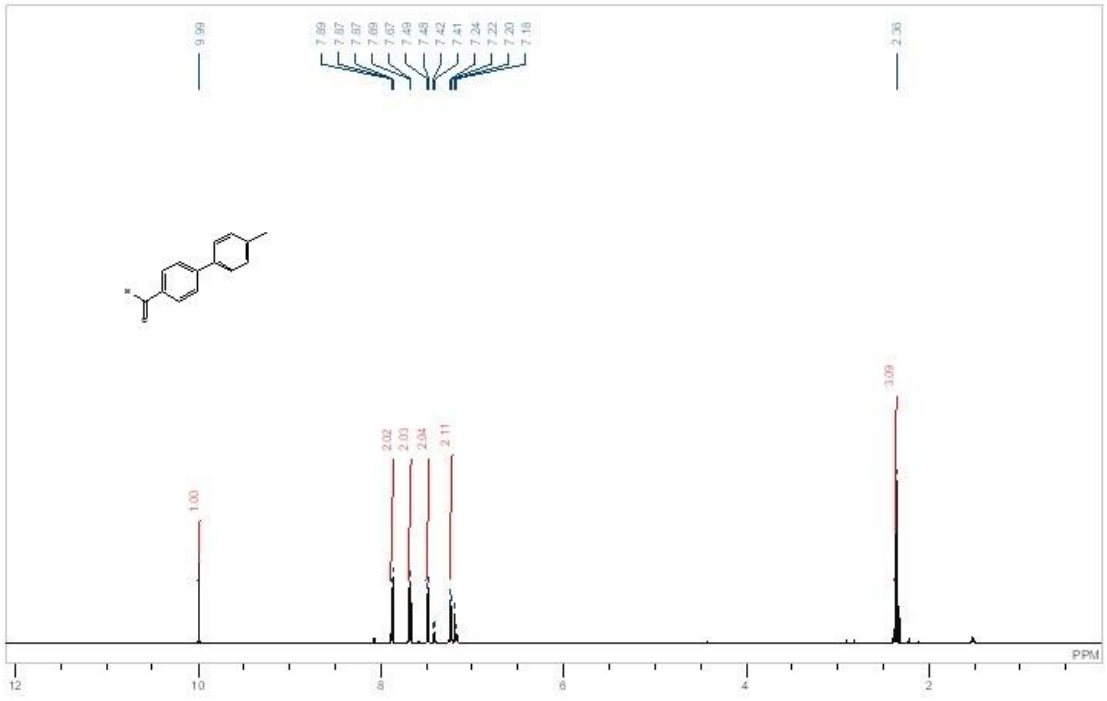

Figure A-I-53:[1]H NMR Spectrum of 3o

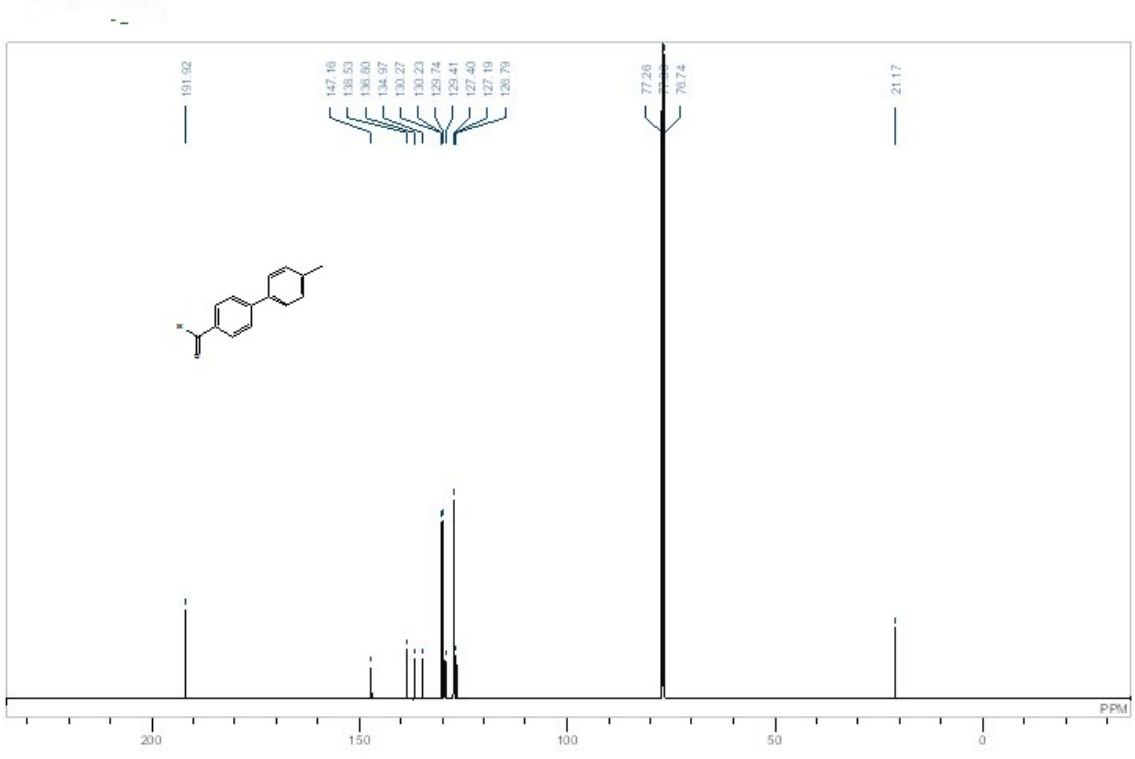

Figure A-I-54:[13]C NMR Spectrum of 3o

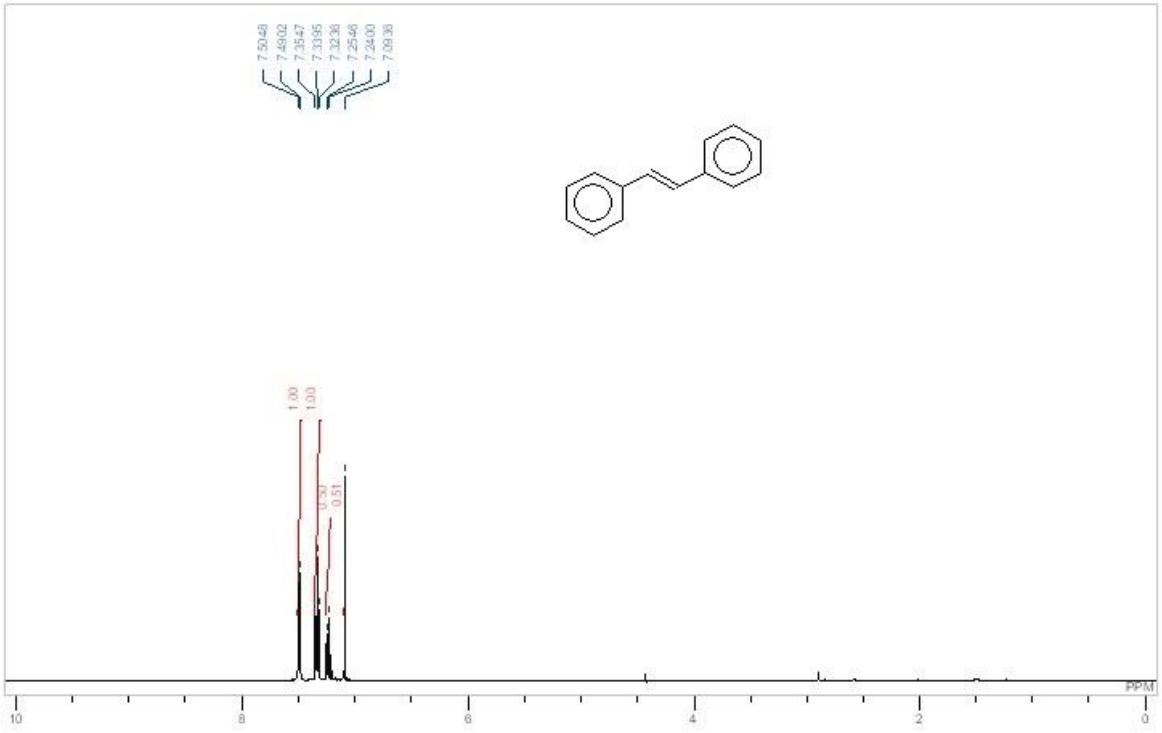

Figure A-I-55:[1]H NMR Spectrum of 5a

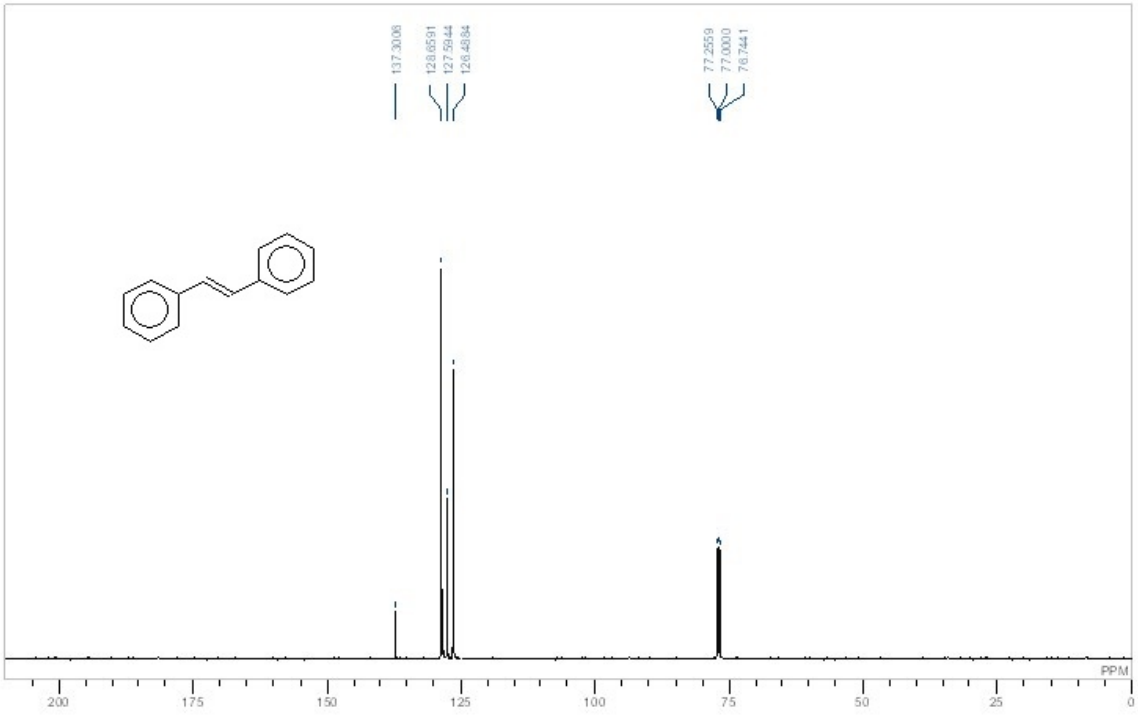

Figure A-I-56:[13]C NMR Spectrum of 5a

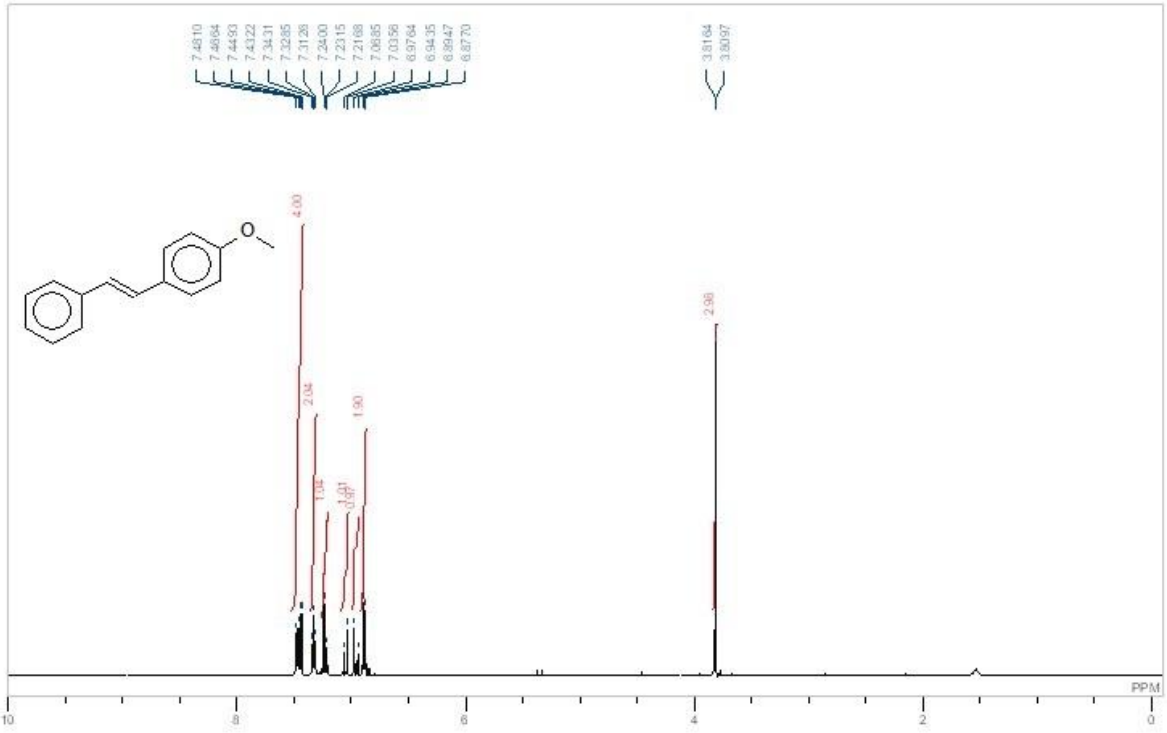

Figure A-I-57:[1]H NMR Spectrum of 5b

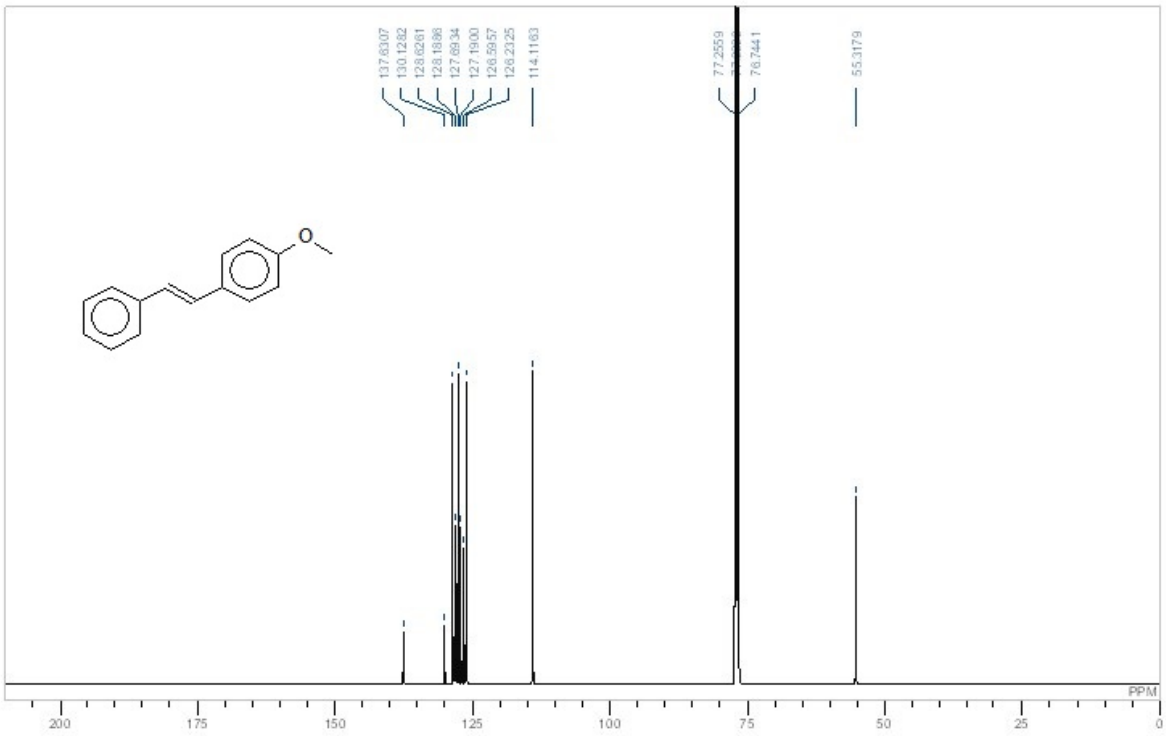

Figure A-I-58:[13]C NMR Spectrum of 5b

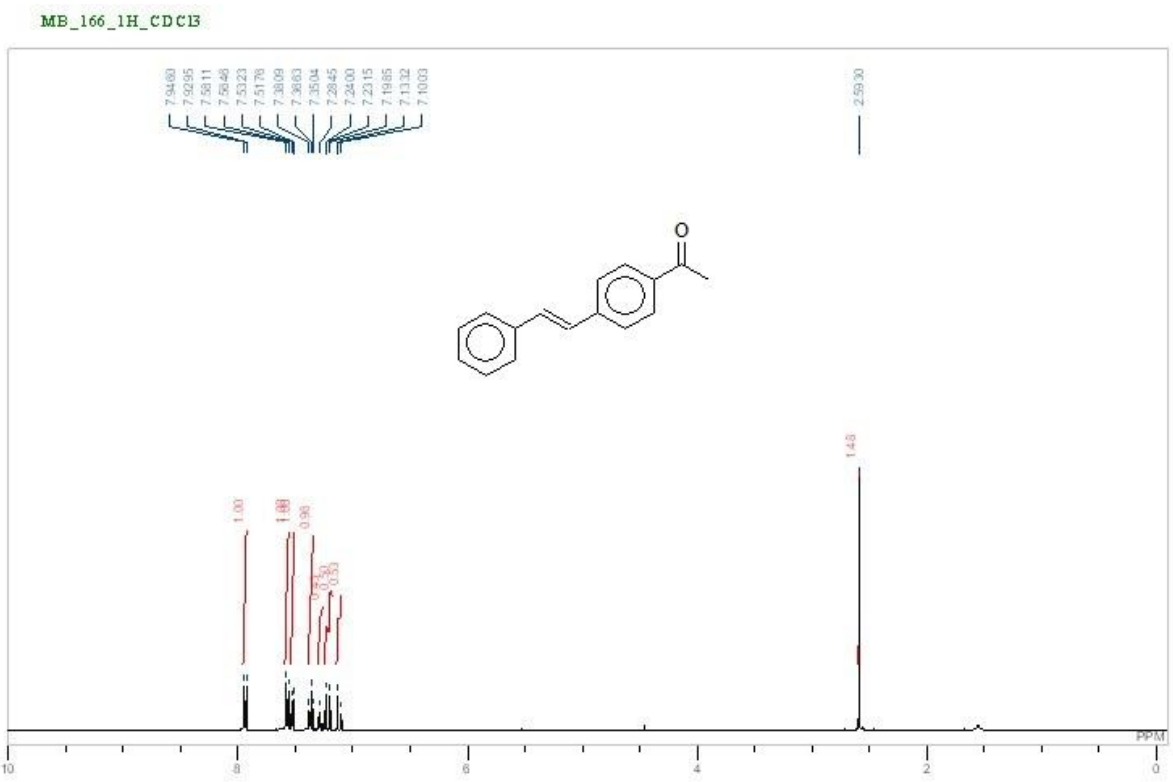

Figure A-I-59:[1]H NMR Spectrum of 5c

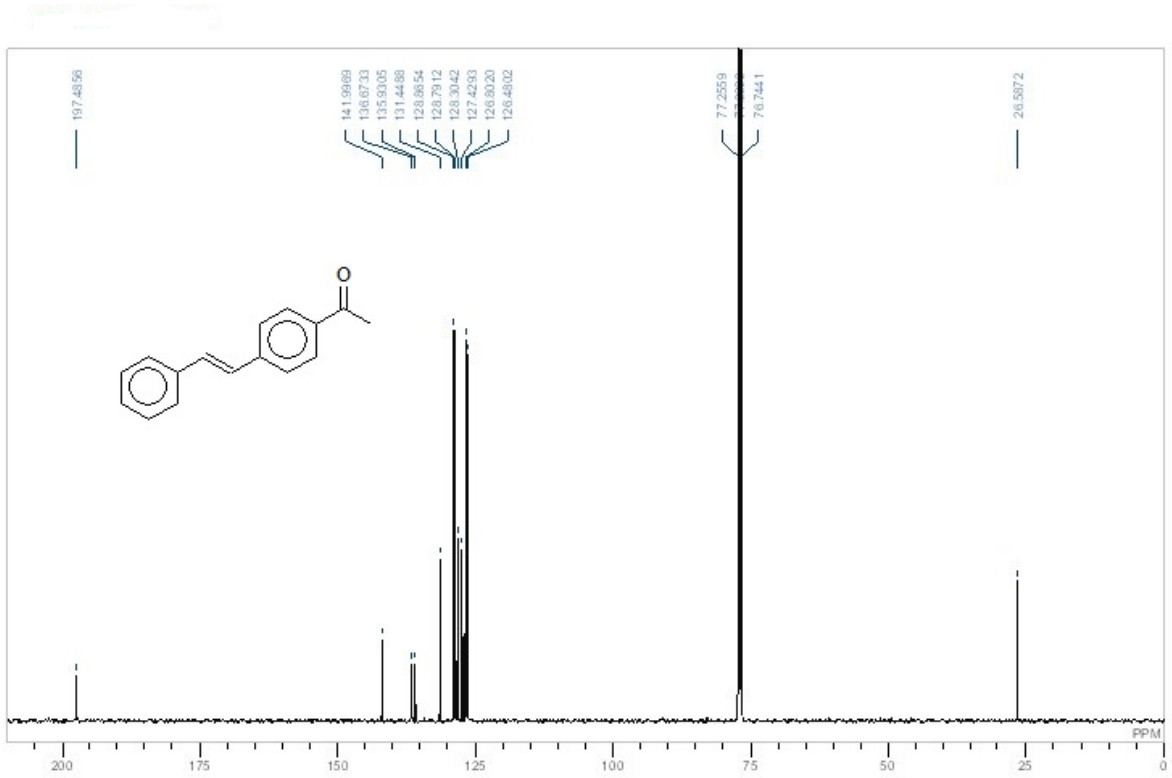

Figure A-I-60:[13]C NMR Spectrum of 5c

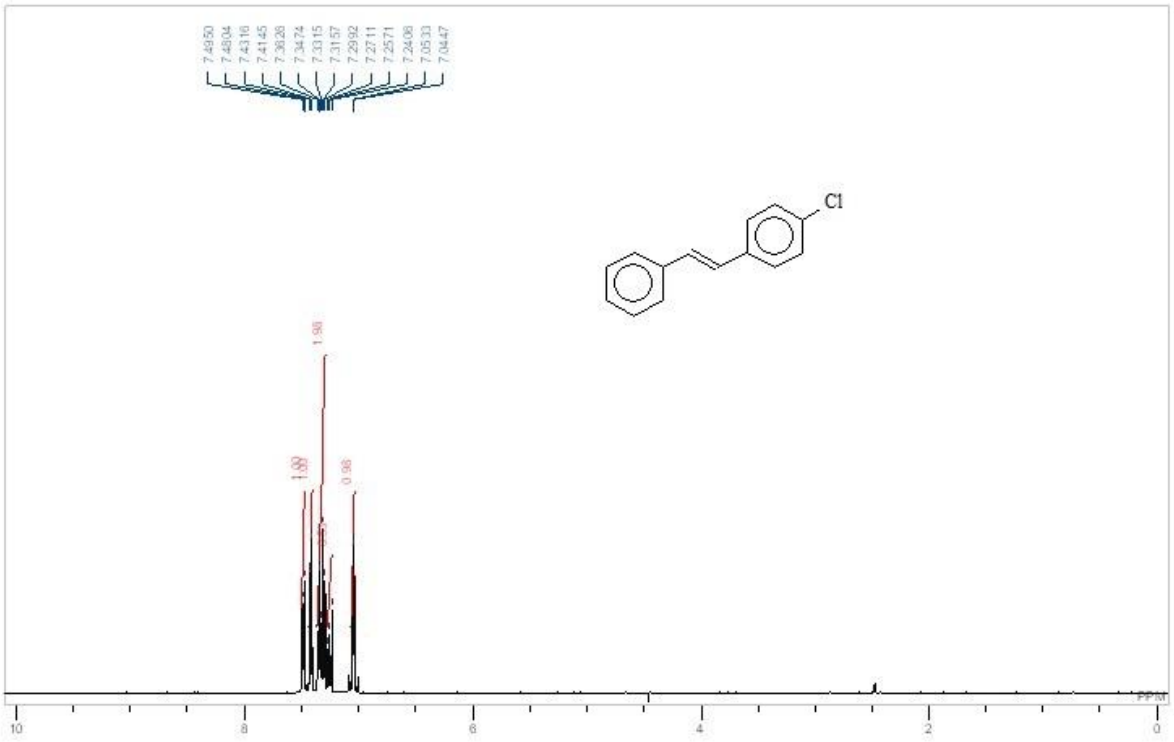

Figure A-I-61:[1]H NMR Spectrum of 5d

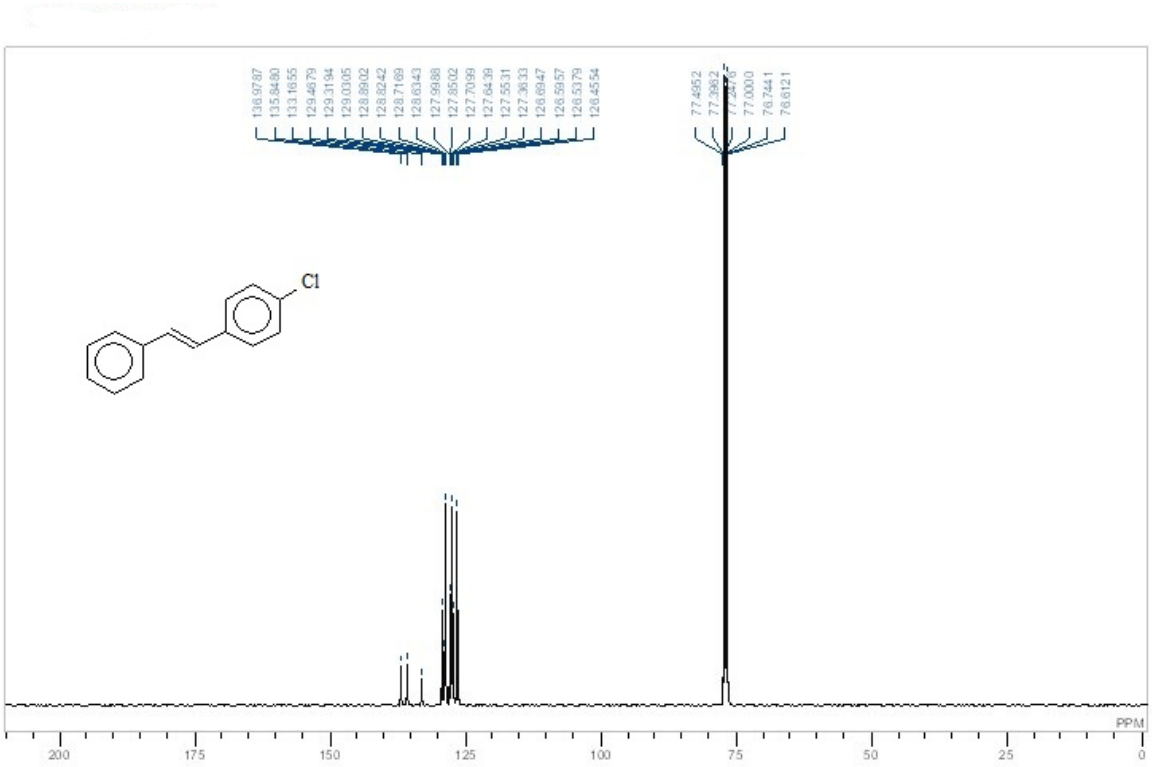

Figure A-I-62:[13]C NMR Spectrum of 5d

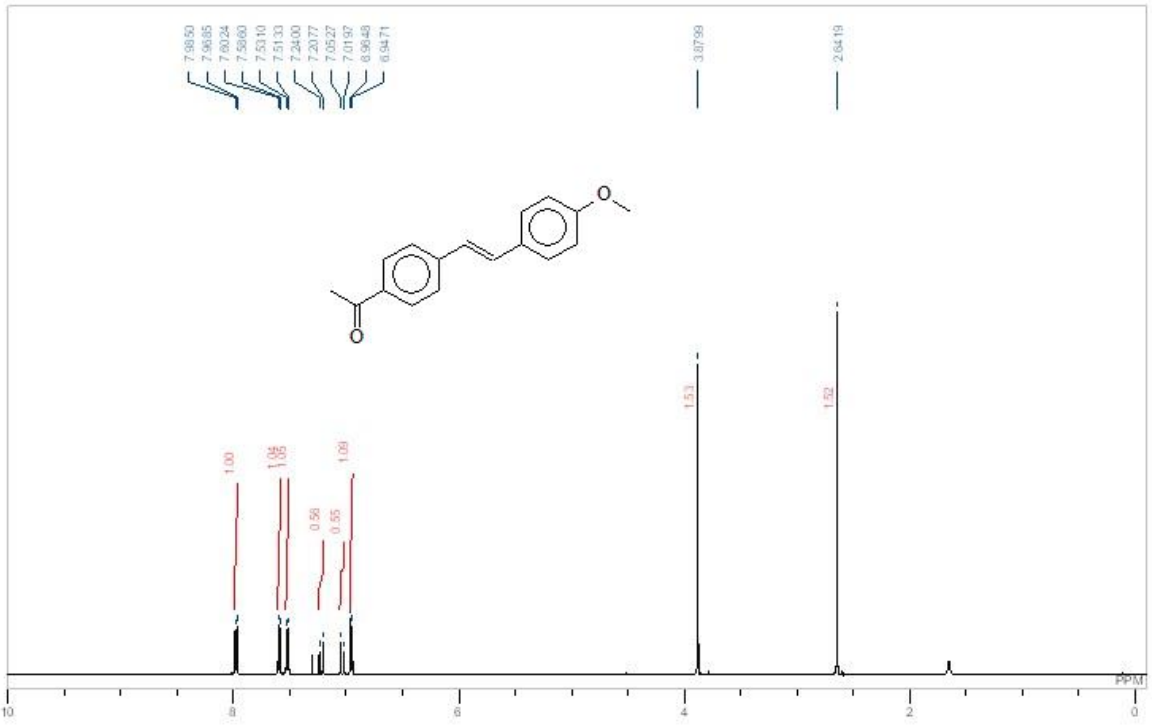

Figure A-I-63:[1]H NMR Spectrum of 5e

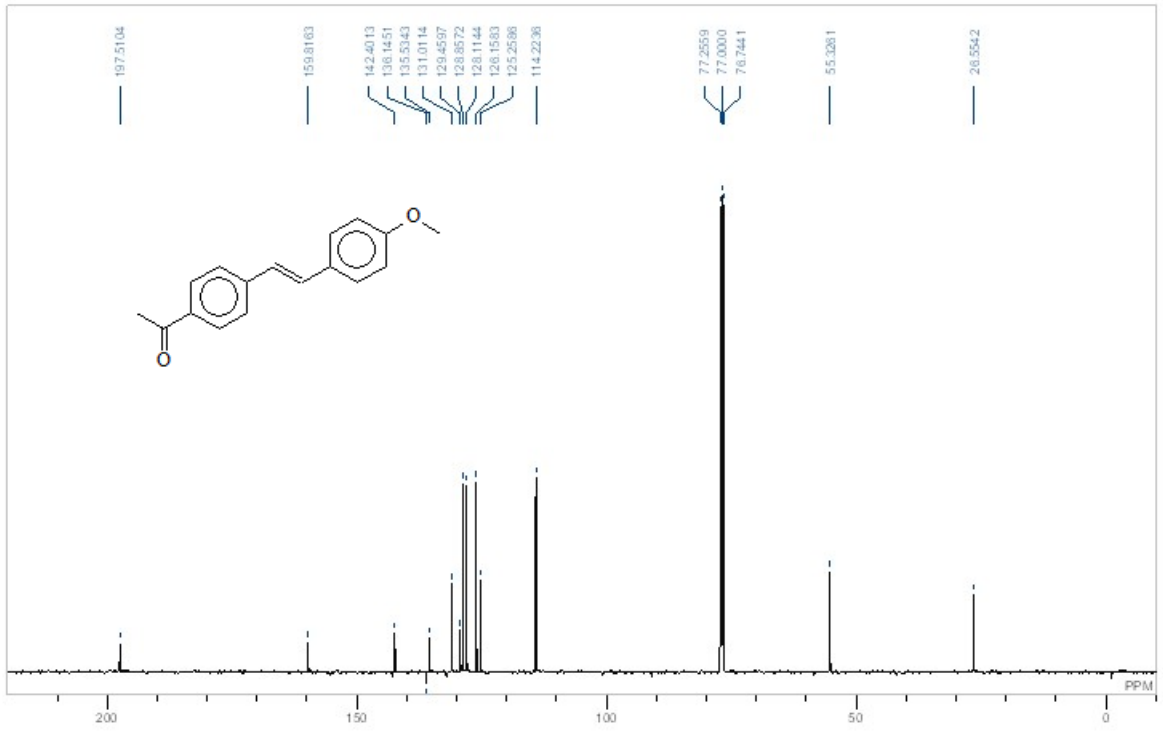

Figure A-I-64:[13]C NMR Spectrum of 5e

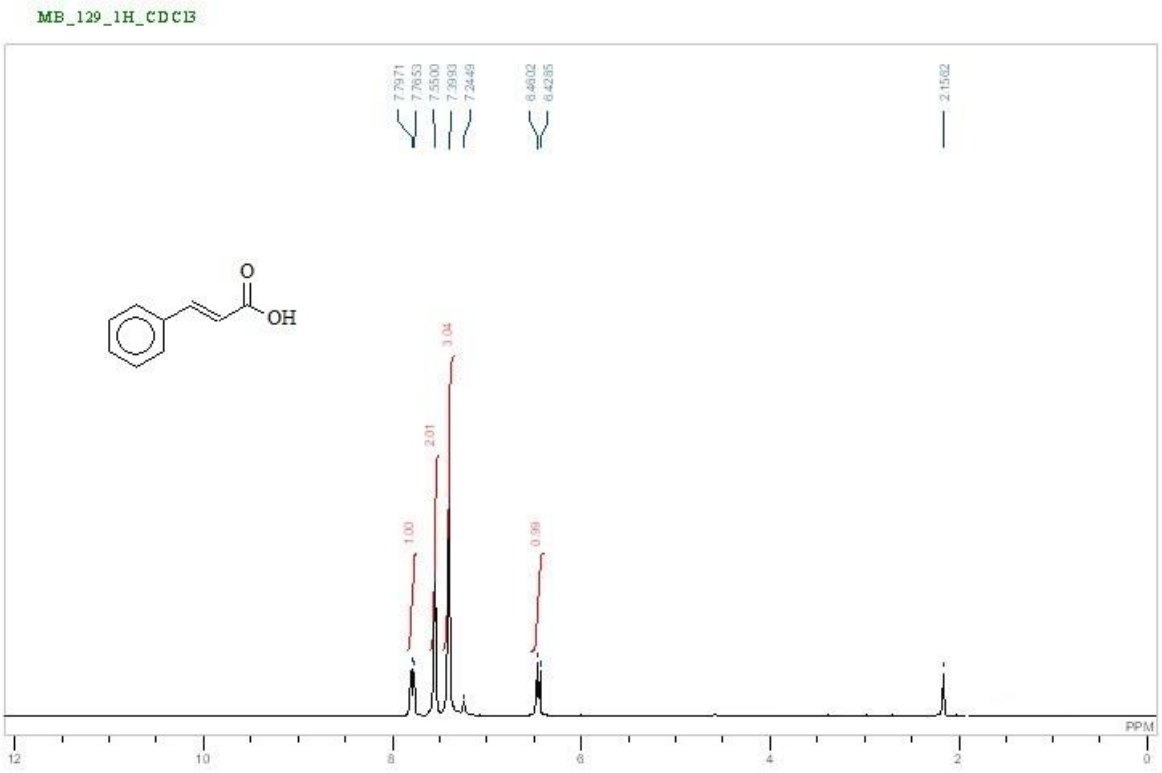

Figure A-I-65: ^{1}H NMR Spectrum of 5g

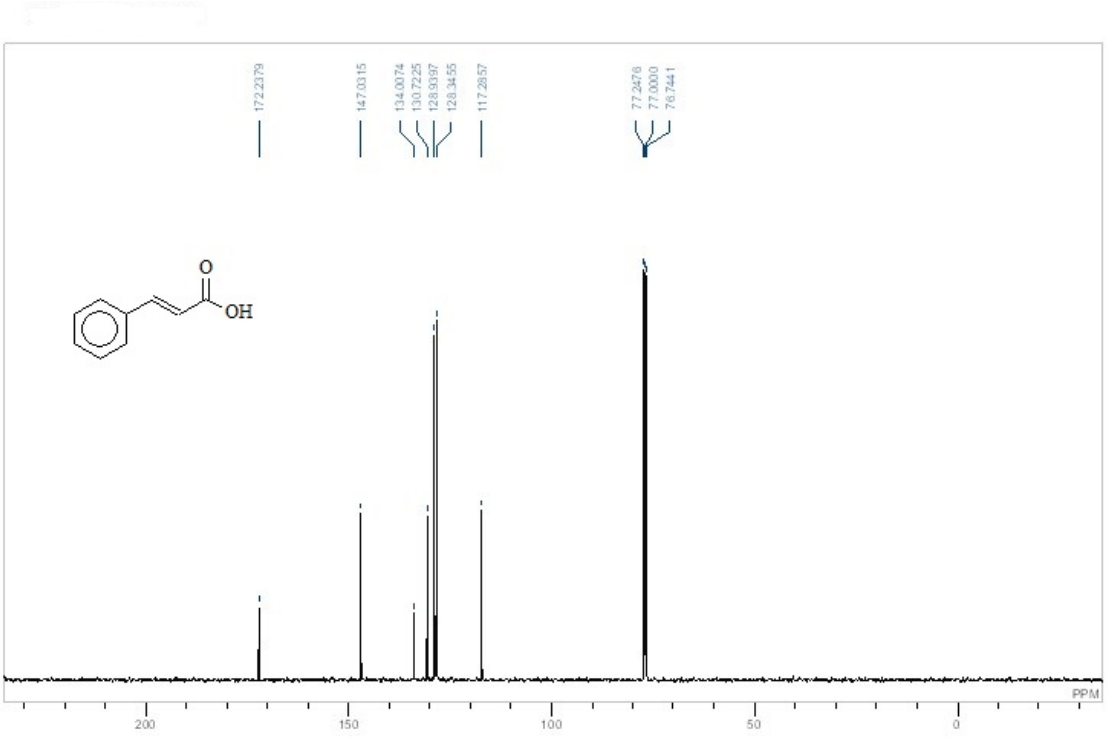

Figure A-I-66: ^{13}C NMR Spectrum of 5g

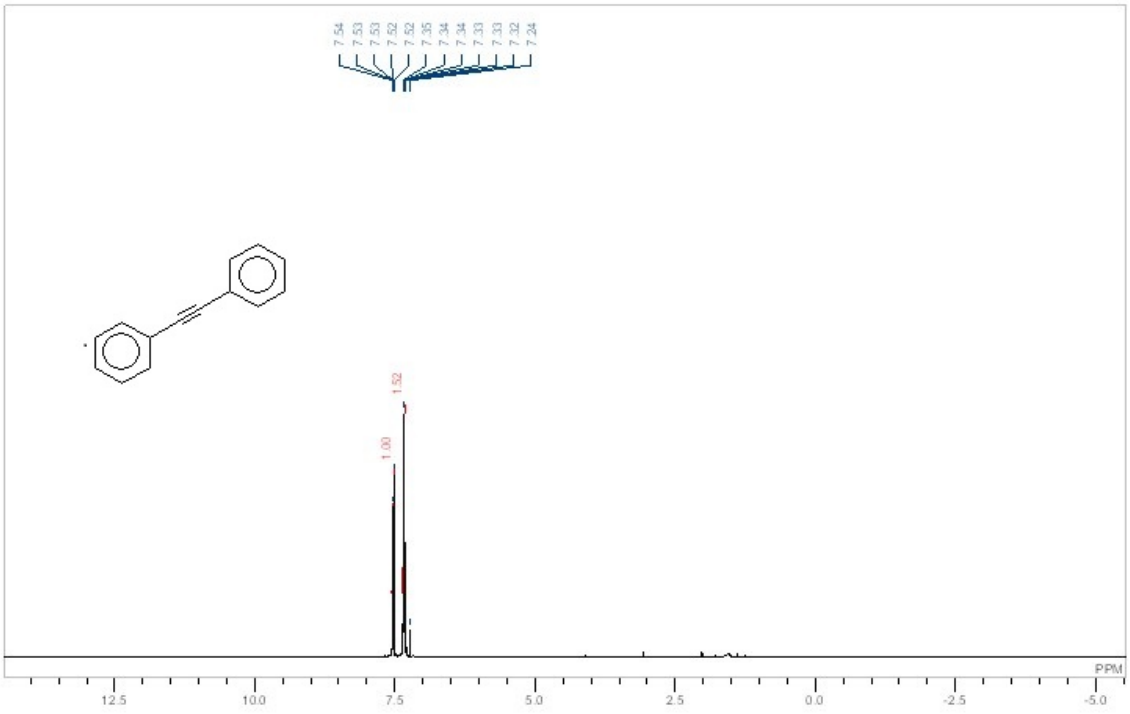

Figure A-I-67:[1]H NMR Spectrum of 7a

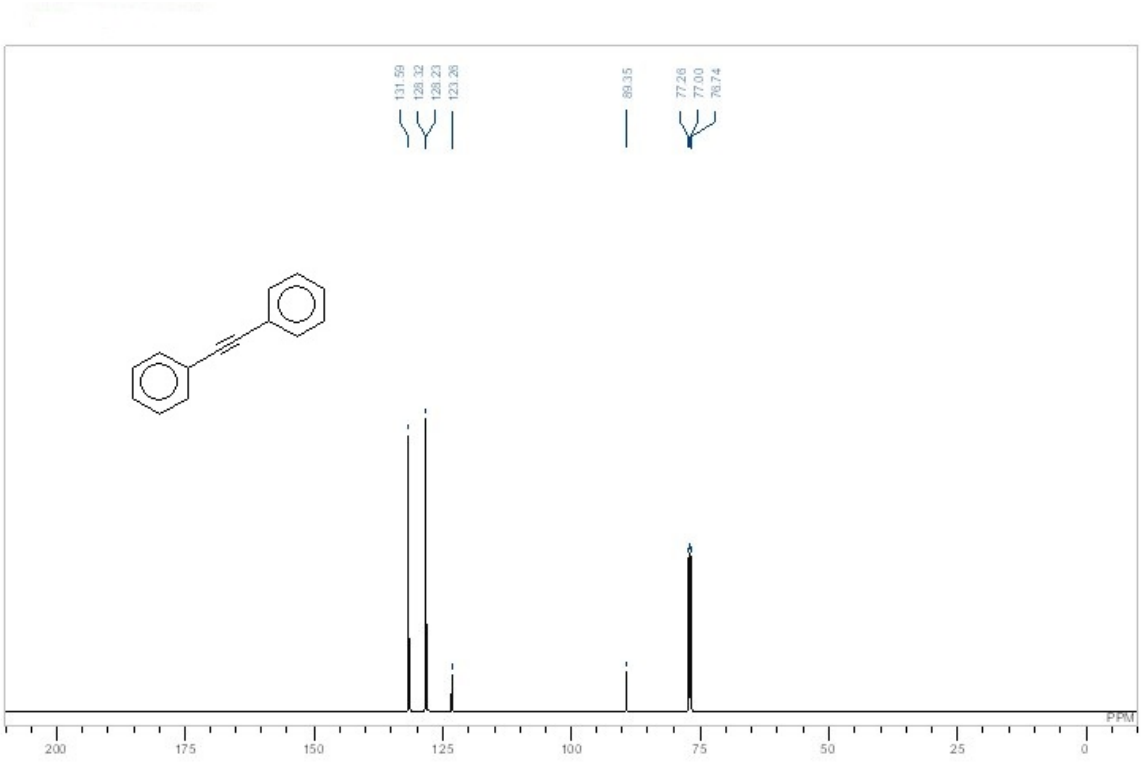

Figure A-I-68:[13]C NMR Spectrum of 7a

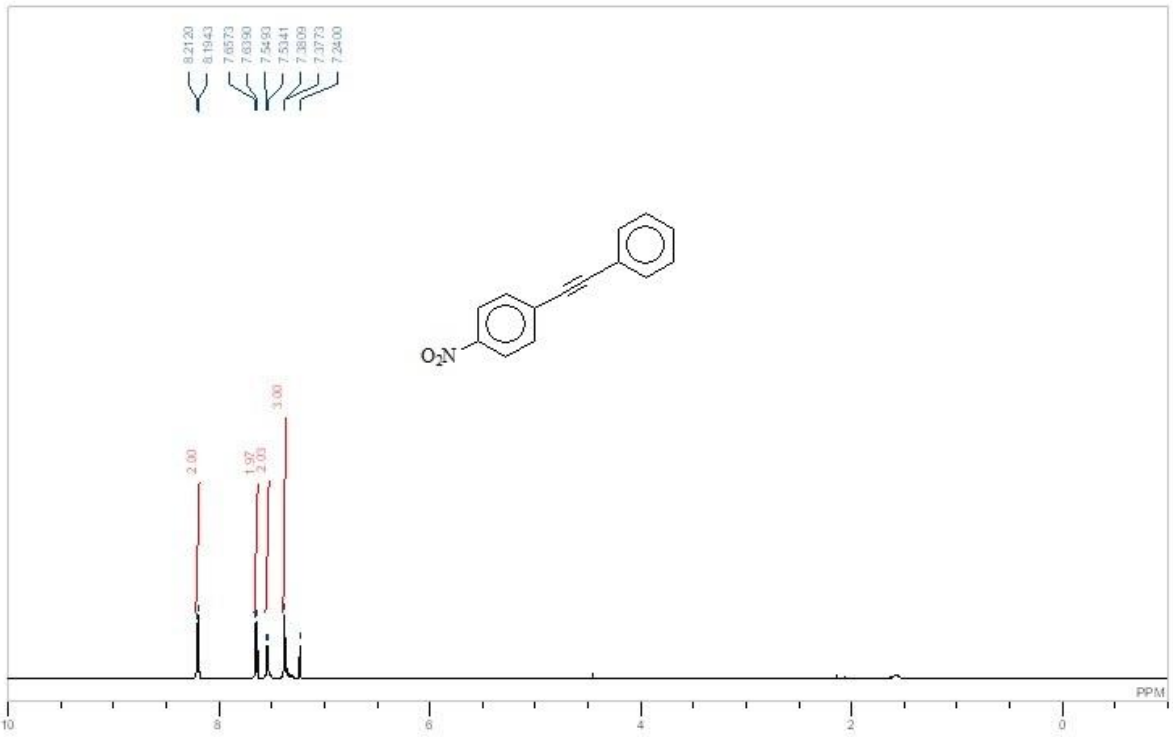

Figure A-I-69: ^{1}H NMR Spectrum of 7b

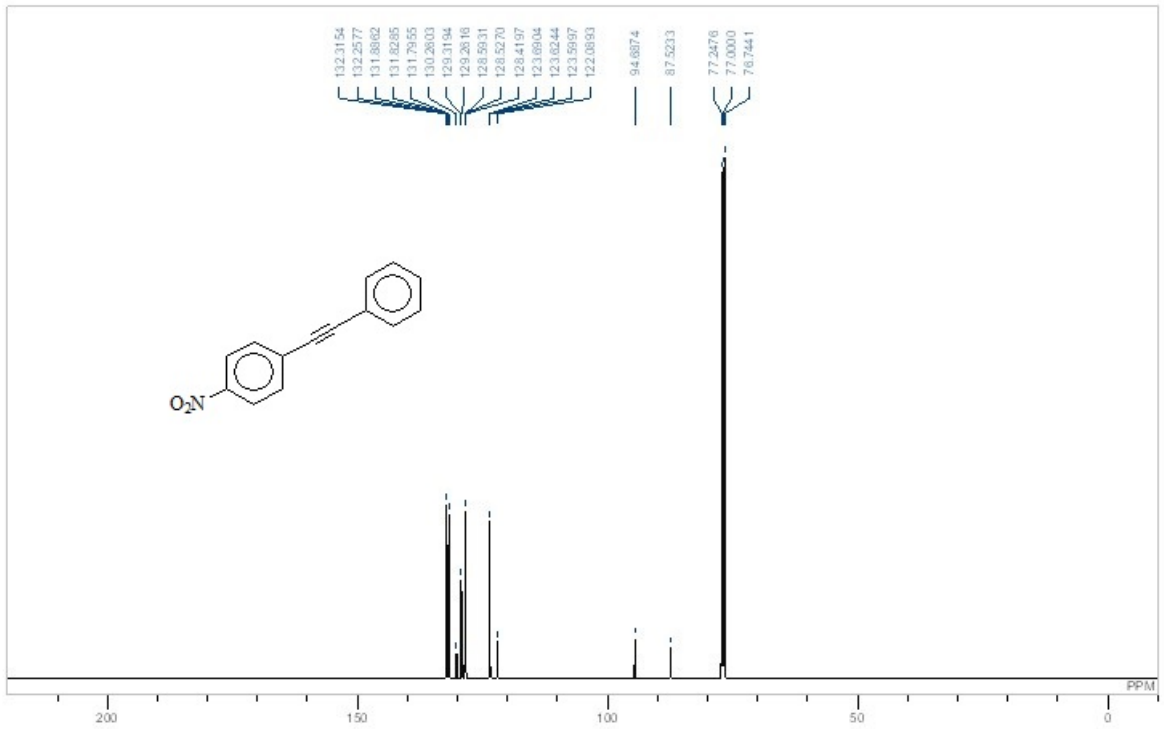

Figure A-I-70: ^{13}C NMR Spectrum of 7b

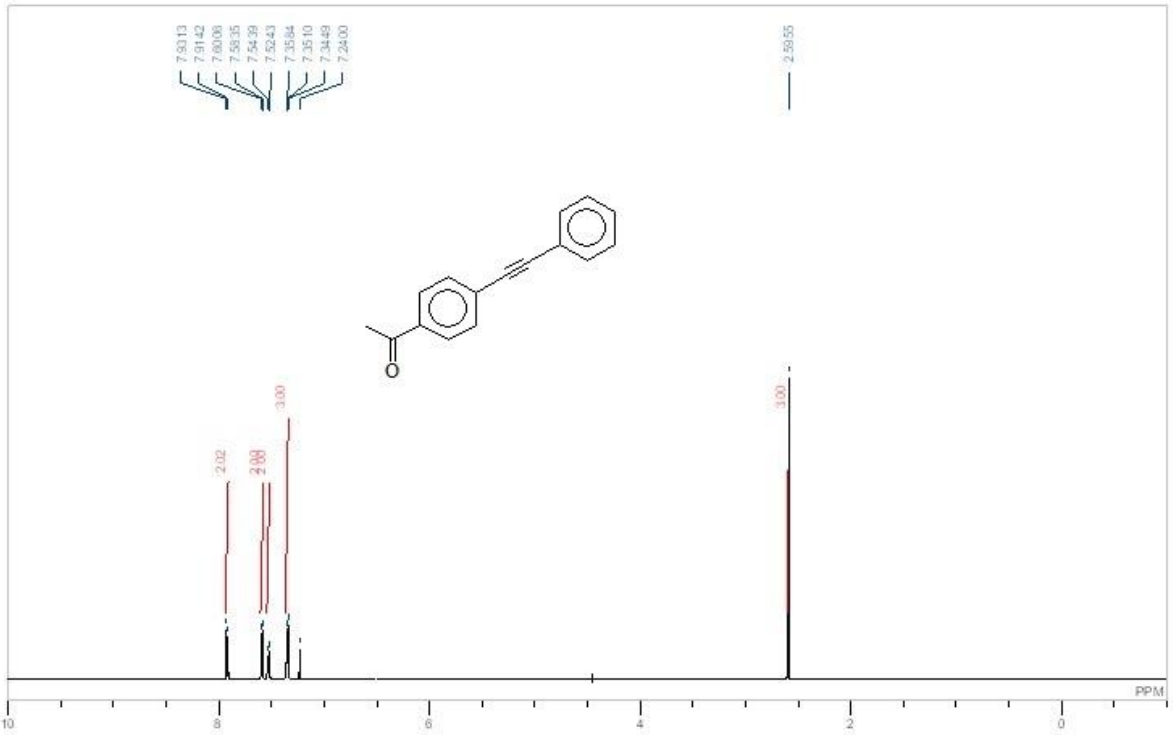

Figure A-I-71:[1]H NMR Spectrum of 7c

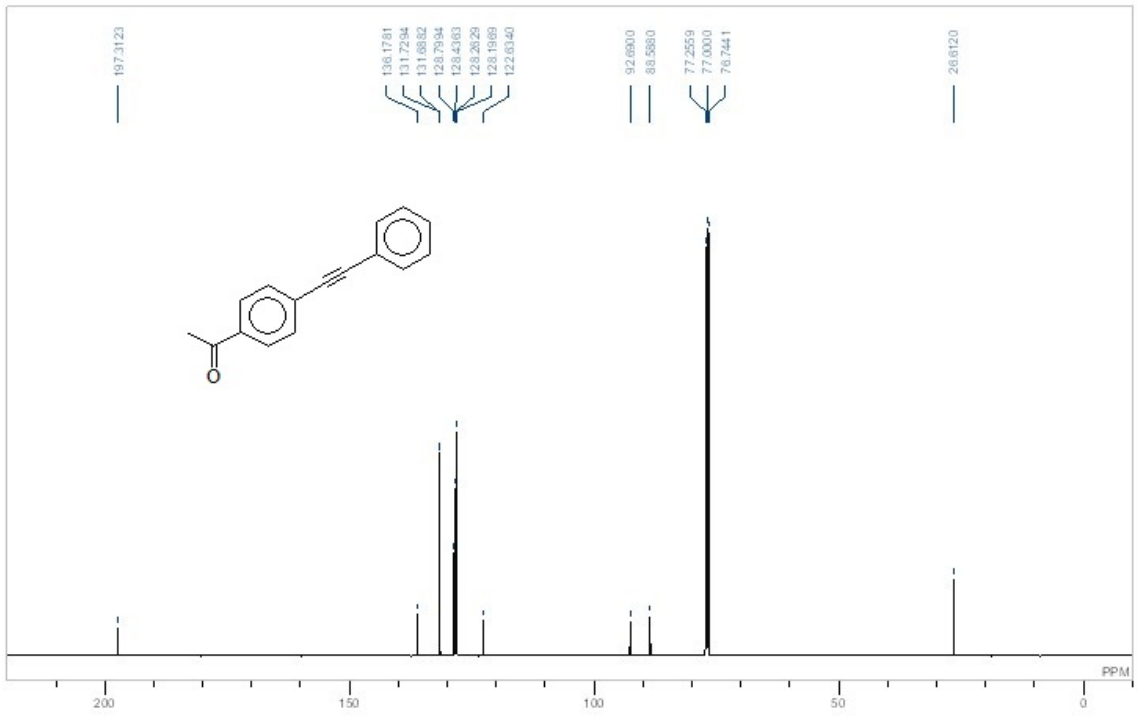

Figure A-I-72:[13]C NMR Spectrum of 7c

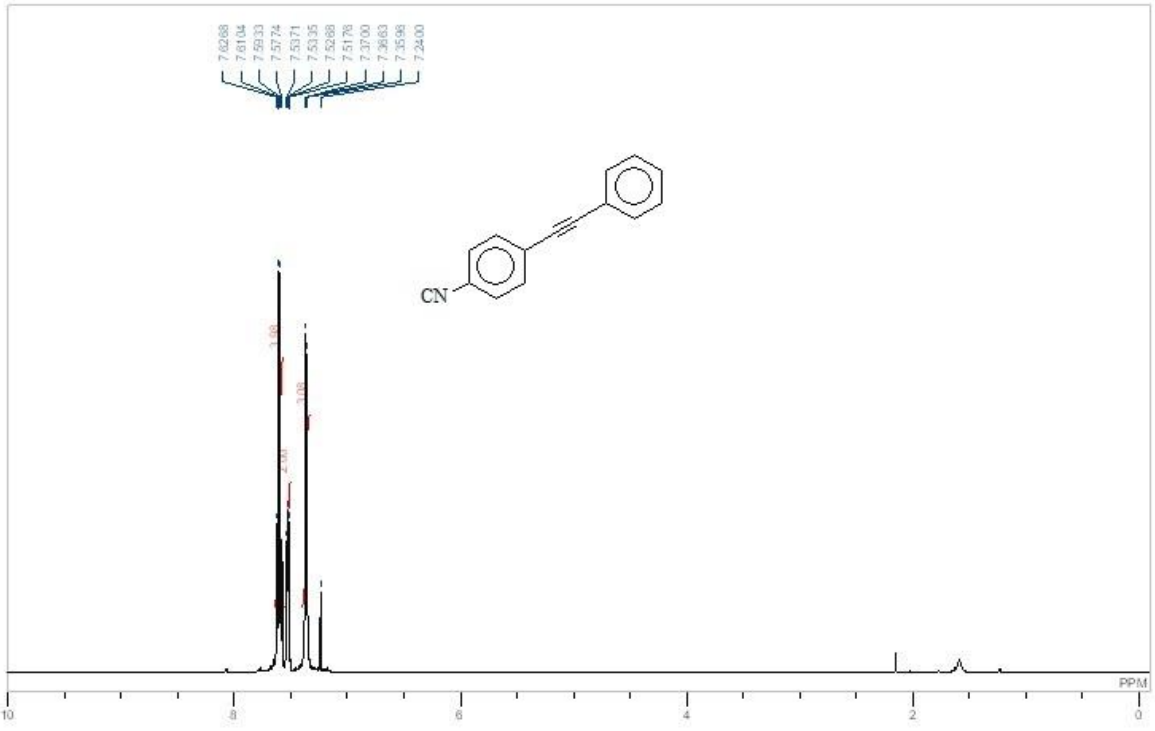

Figure A-I-73:[1]H NMR Spectrum of 7d

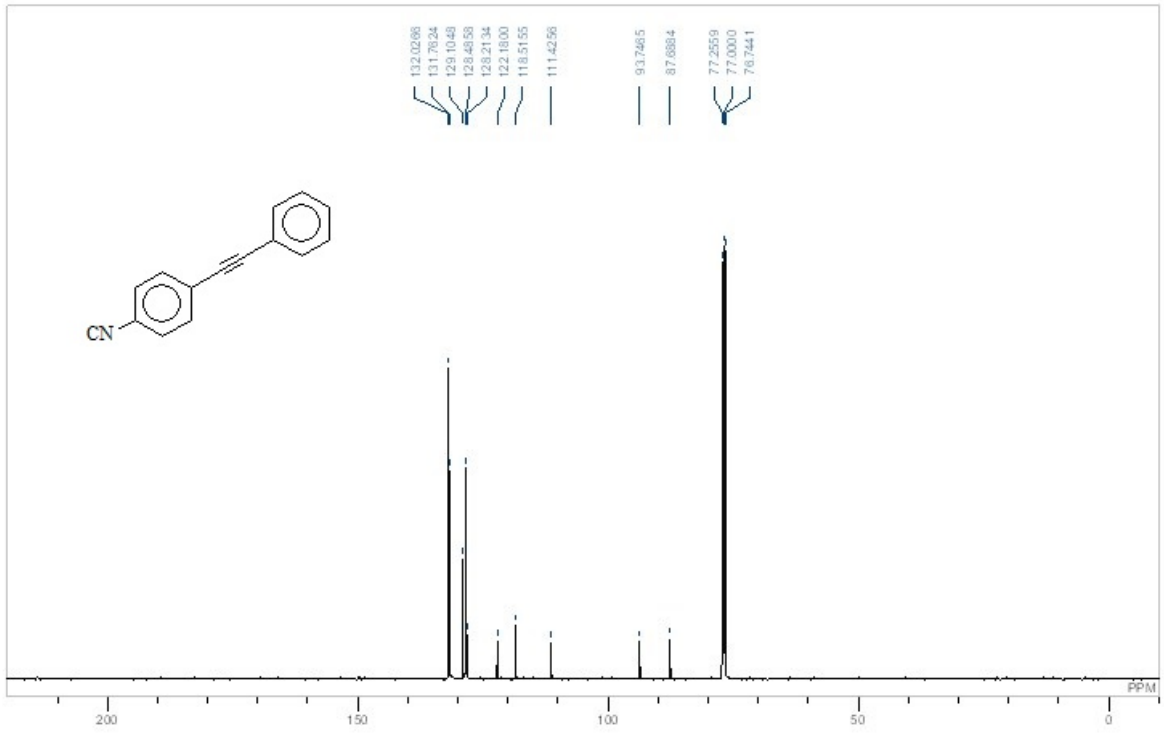

Figure A-I-74:[13]C NMR Spectrum of 7d

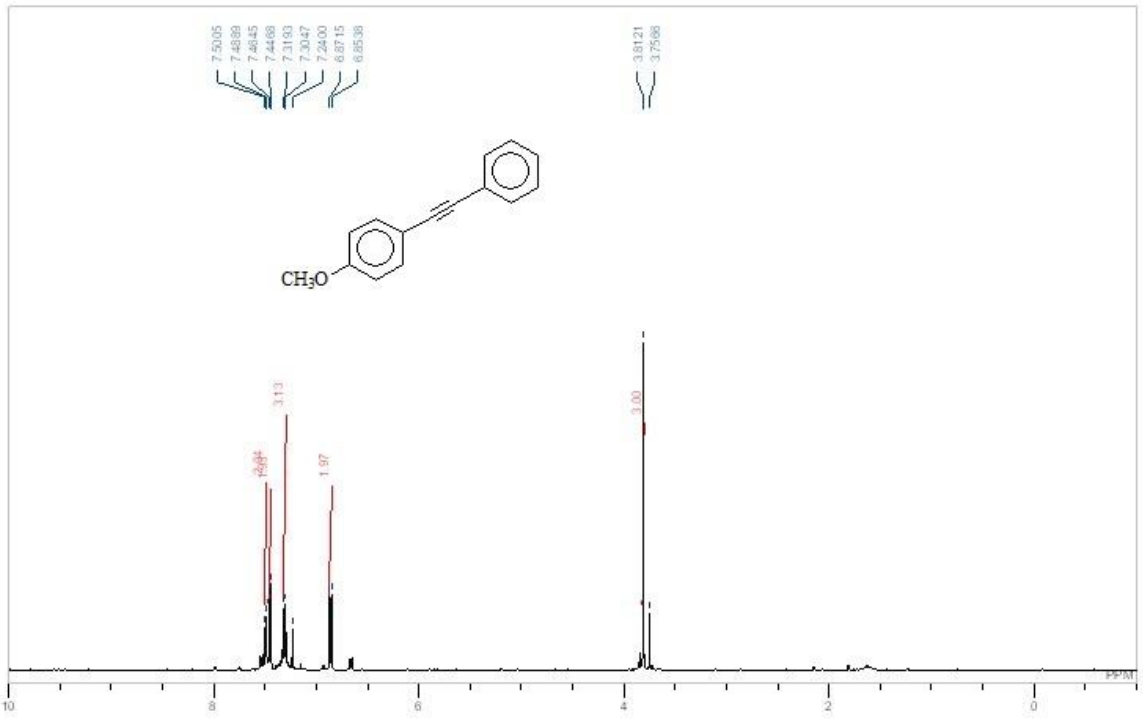

Figure A-I-75:[1]H NMR Spectrum of 7h

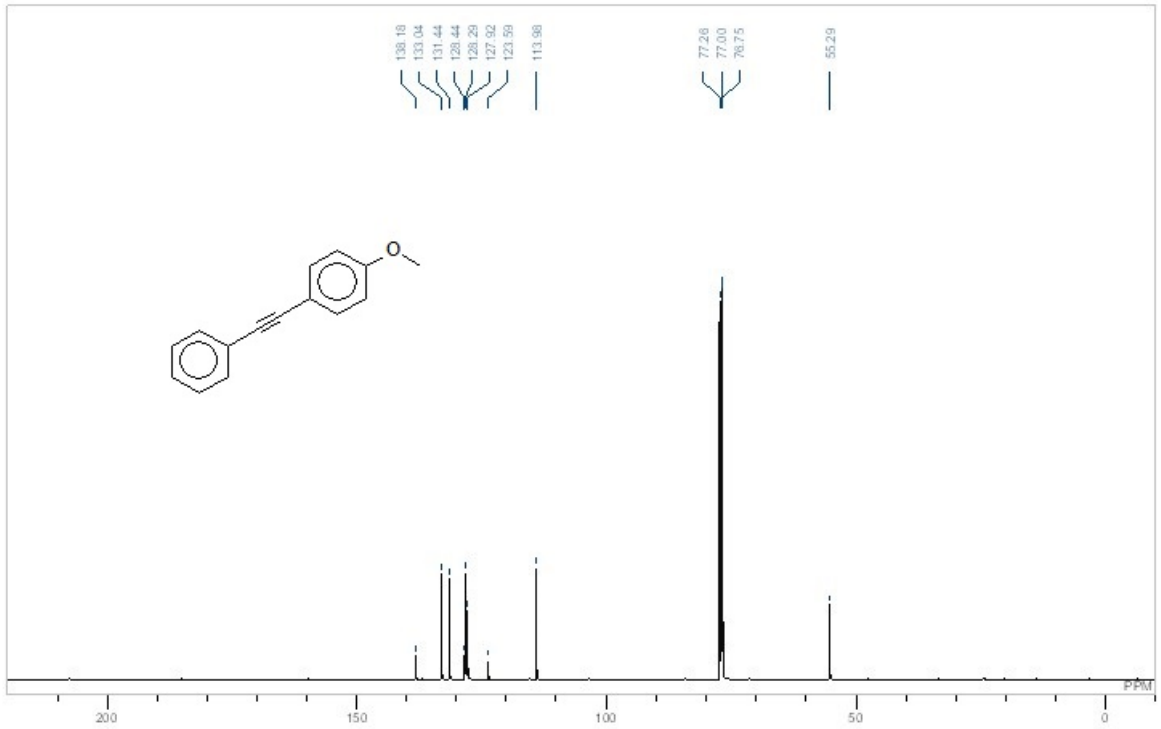

Figure A-I-76:[13]C NMR Spectrum of 7h

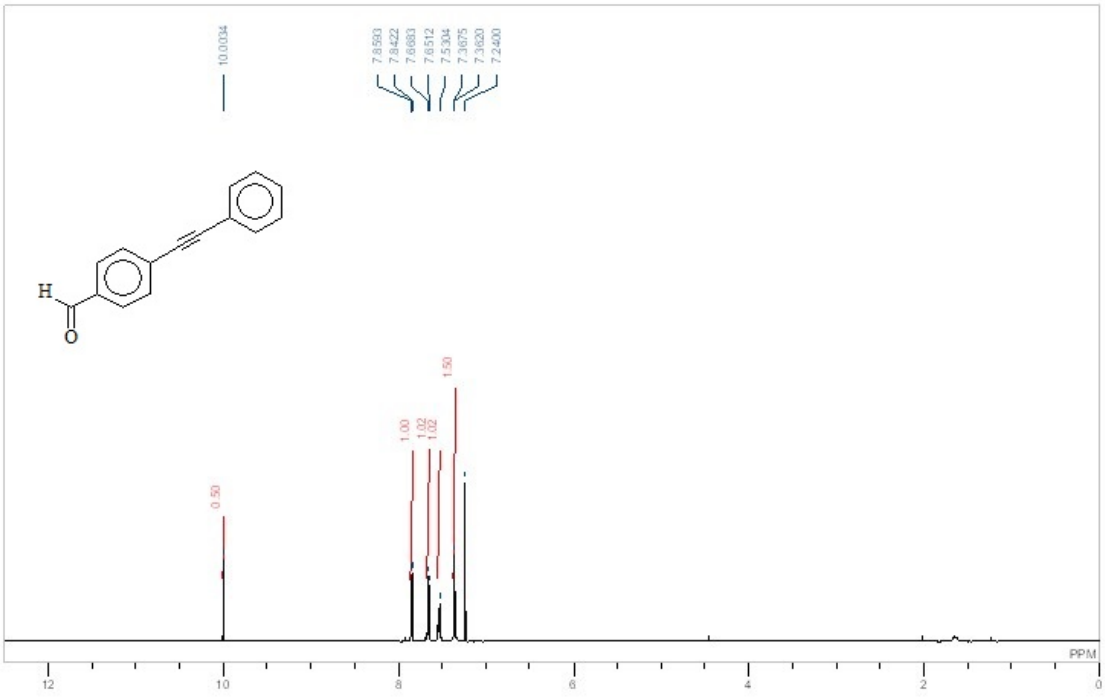

Figure A-I-77:[1]H NMR Spectrum of 7e

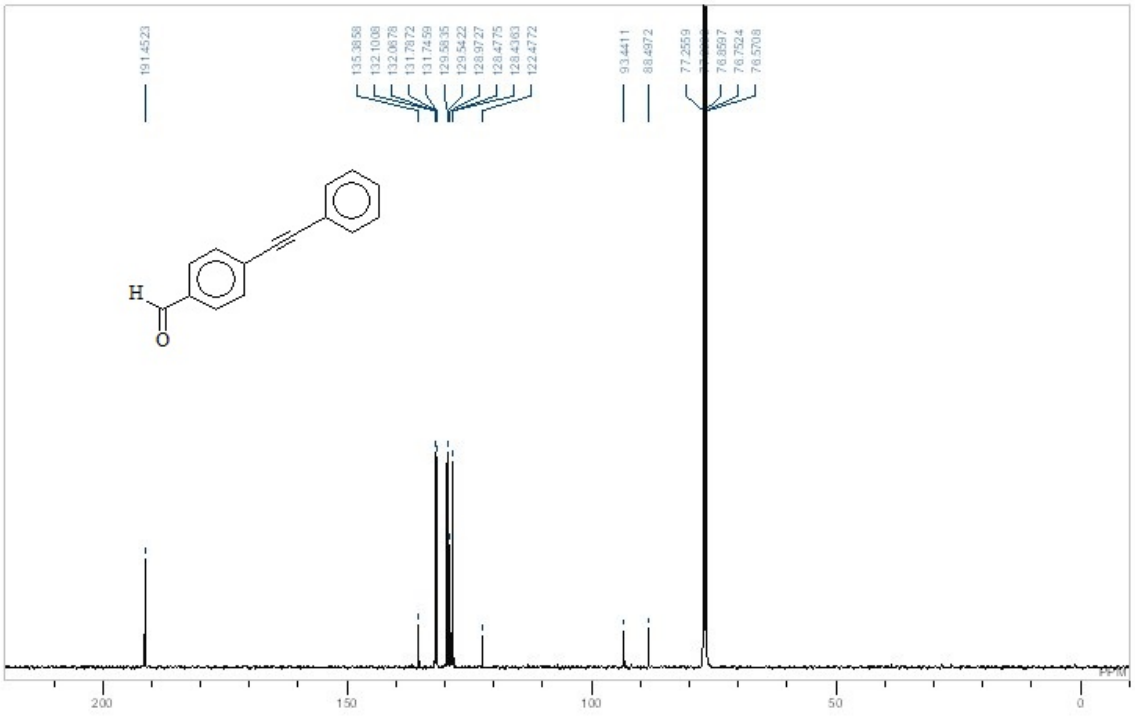

Figure A-I-78:[13]C NMR Spectrum of 7e

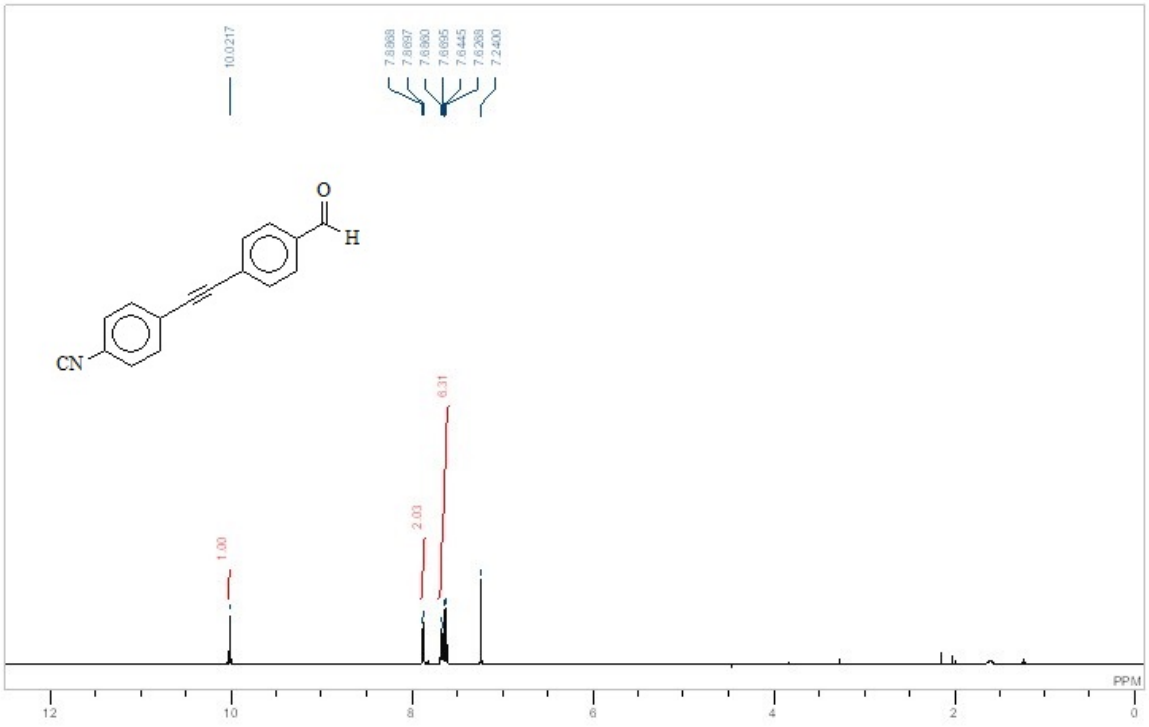

Figure A-I-79:[1]H NMR Spectrum of 7f

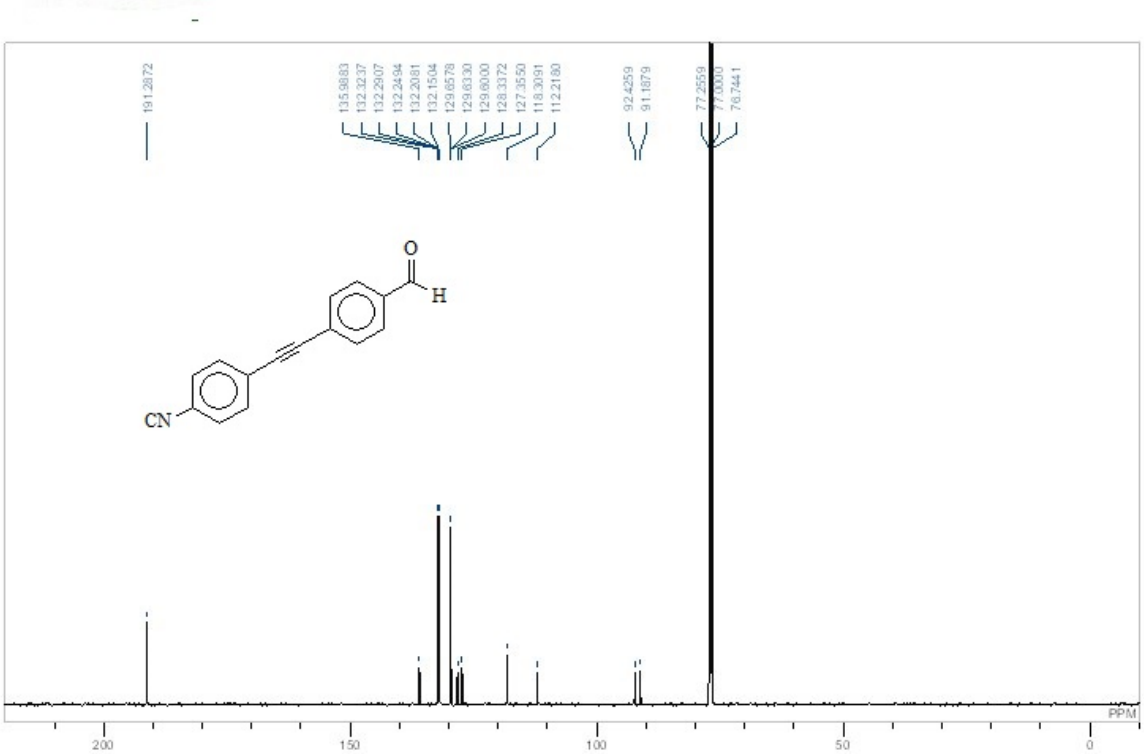

Figure A-I-80:[13]C NMR Spectrum of 7f

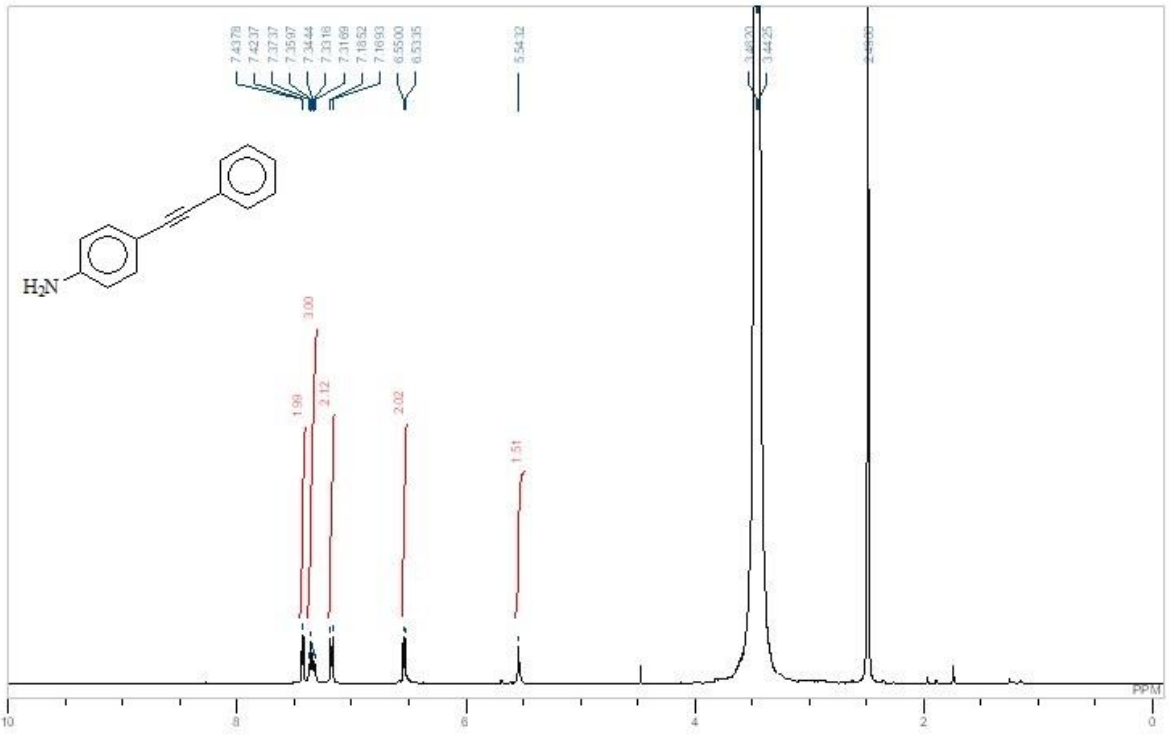

Figure A-I-81:[1]H NMR Spectrum of 7i

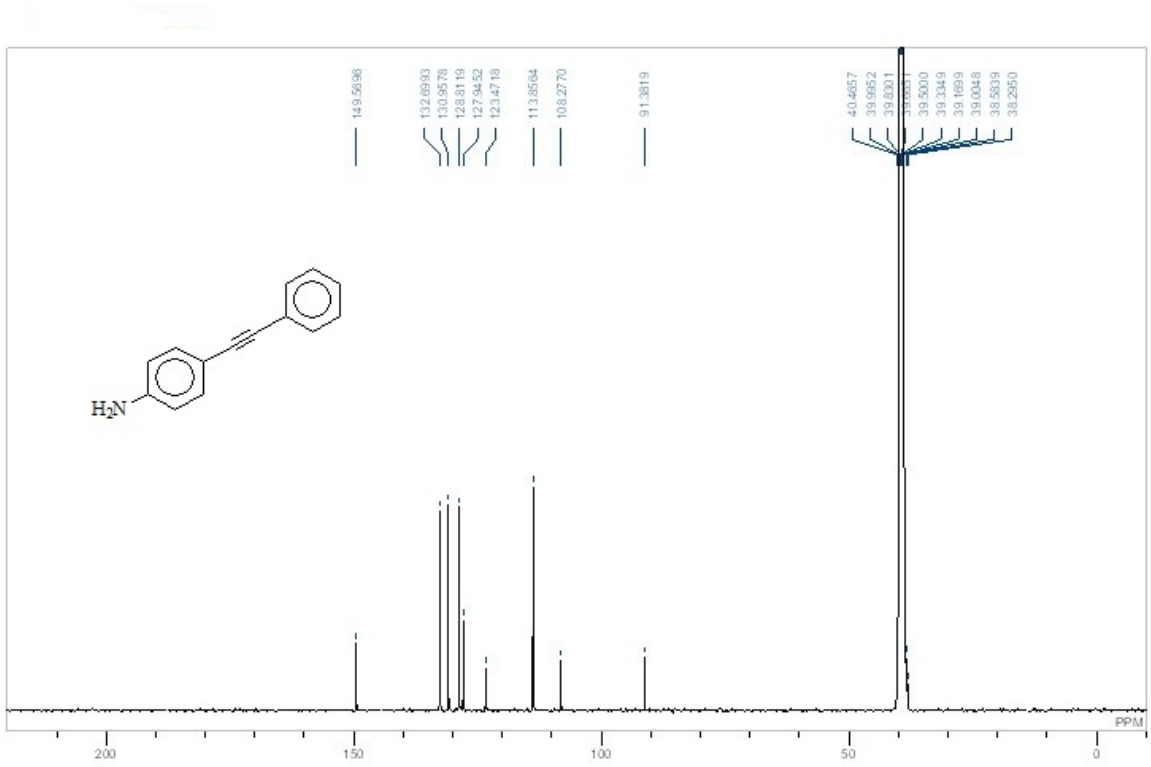

Figure A-I-82:13C NMR Spectrum of 7i

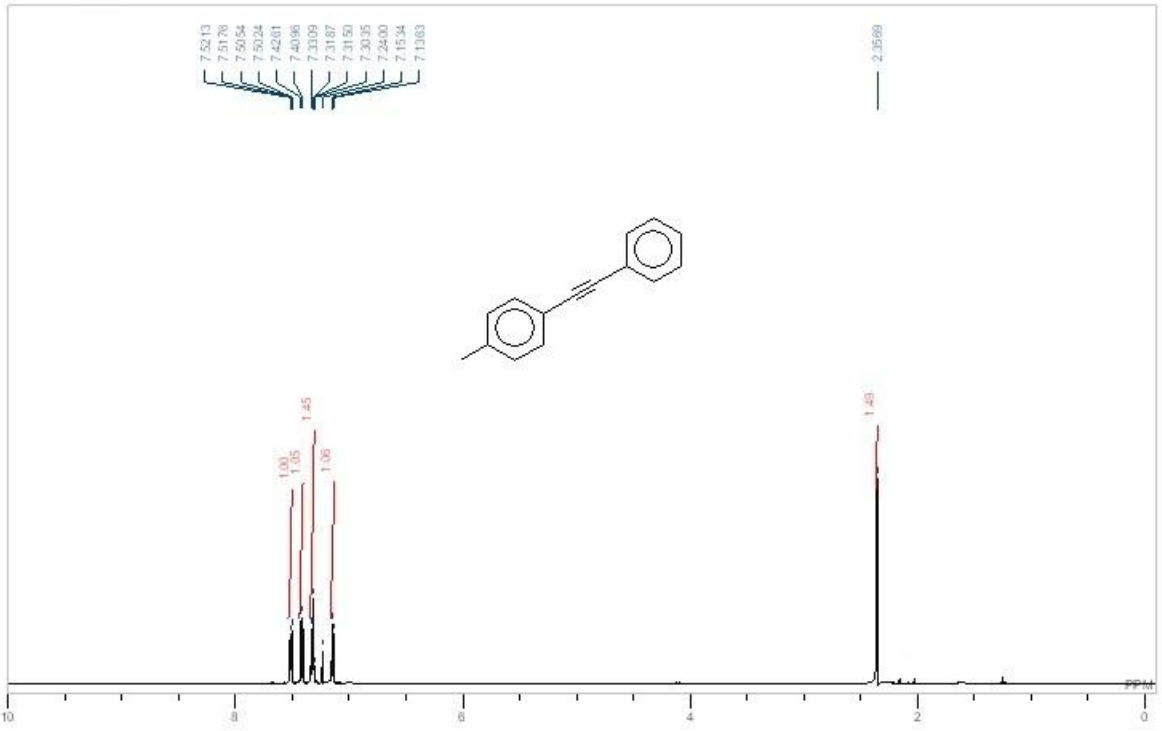

Figure A-I-83:[1]H NMR Spectrum of 7j

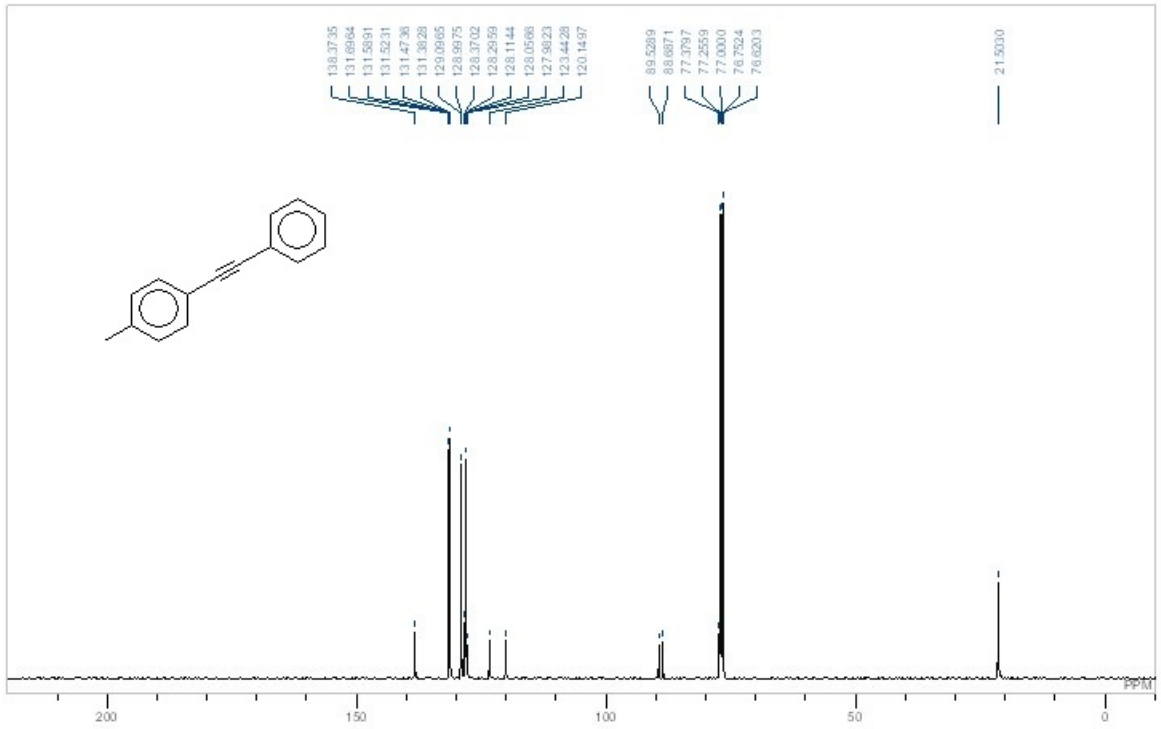

Figure A-I-84:[13]C NMR Spectrum of 7j

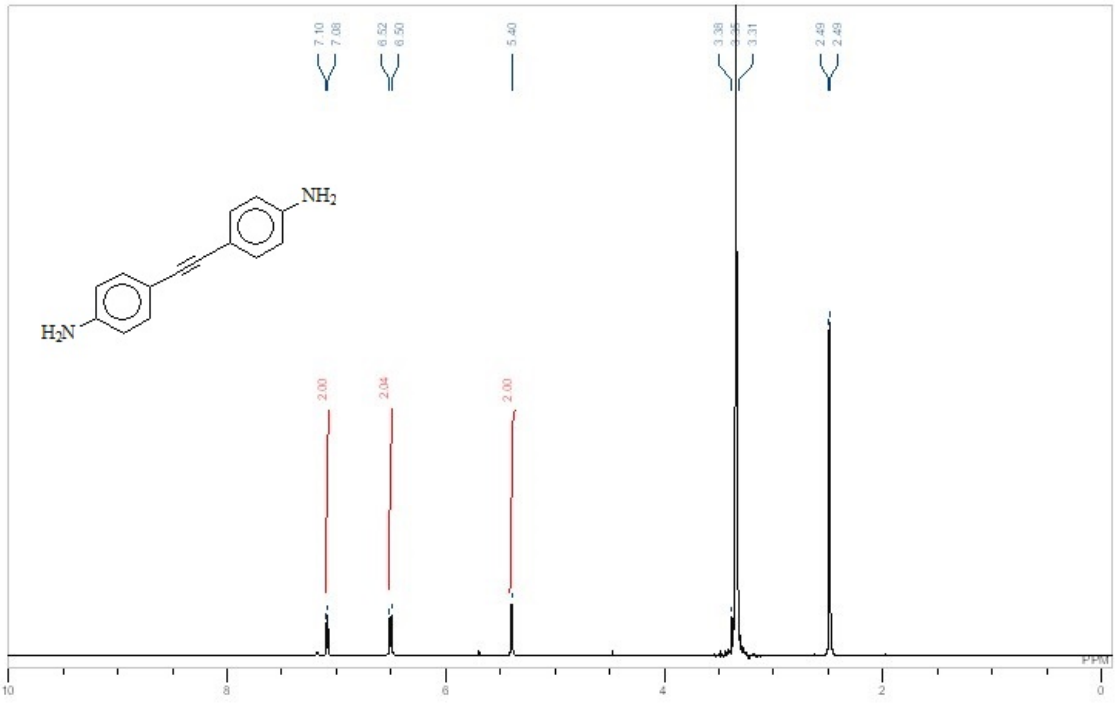

Figure A-I-85:[1]H NMR Spectrum of 7l

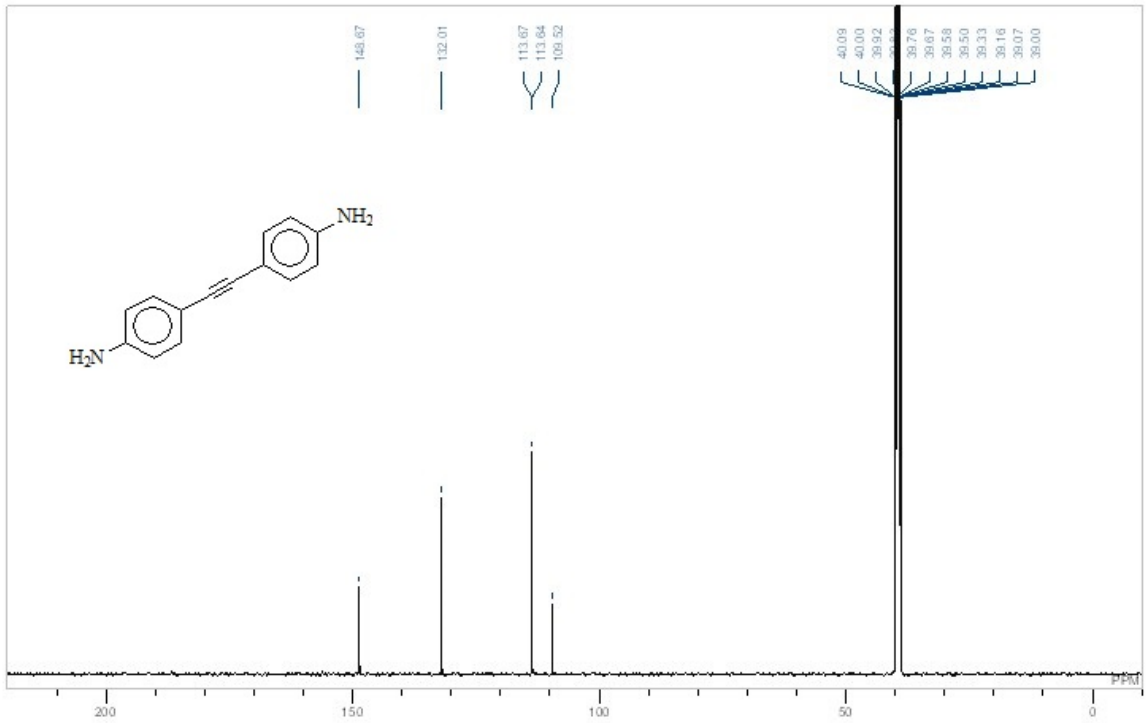

Figure A-I-86:[1]H NMR Spectrum of 7l

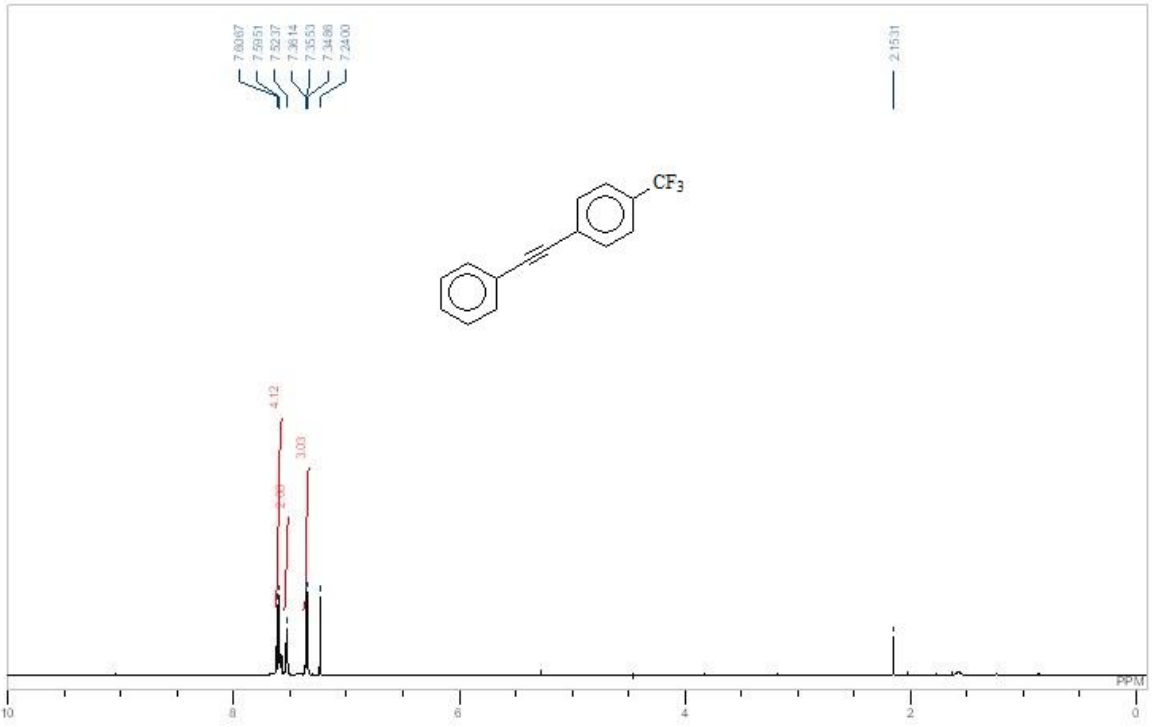

Figure A-I-87:[1]H NMR Spectrum of 7k

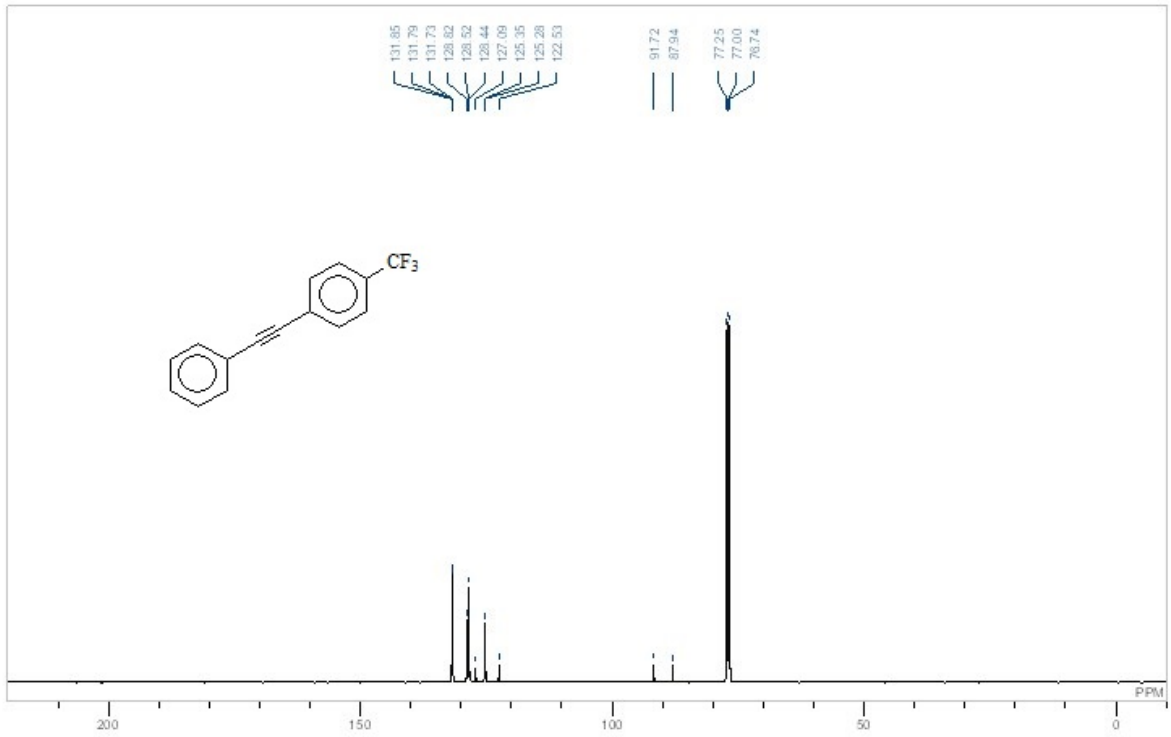

Figure A-I-88[1]H NMR Spectrum of 7k

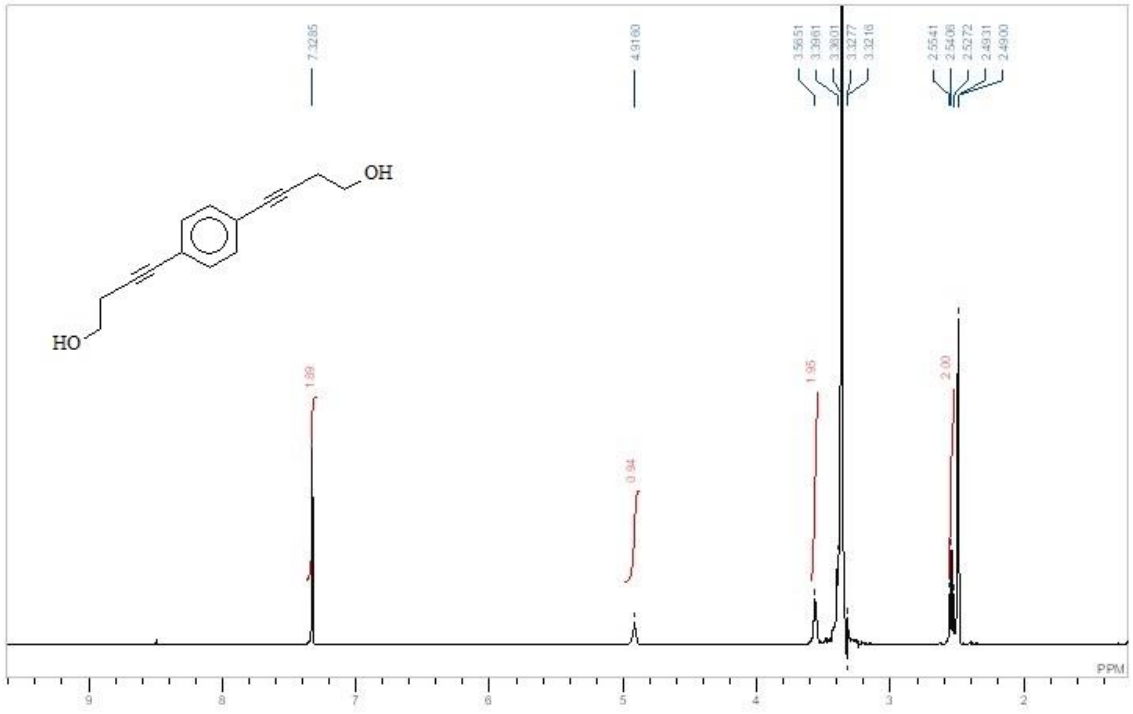

Figure A-I-89: ^{1}H NMR Spectrum of 4,4'-benzene-1,4-diylbisbut-3-yn-1-ol

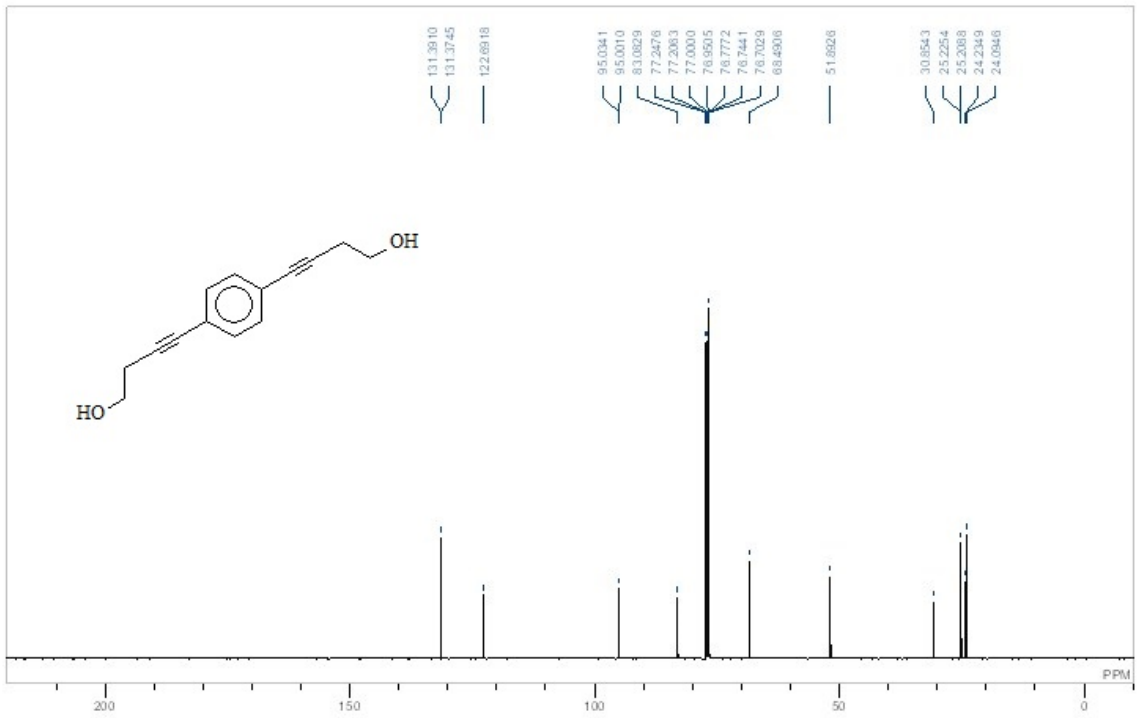

Figure A-I-90: ^{13}C NMR Spectrum of 4,4'-benzene-1,4-diylbisbut-3-yn-1-ol

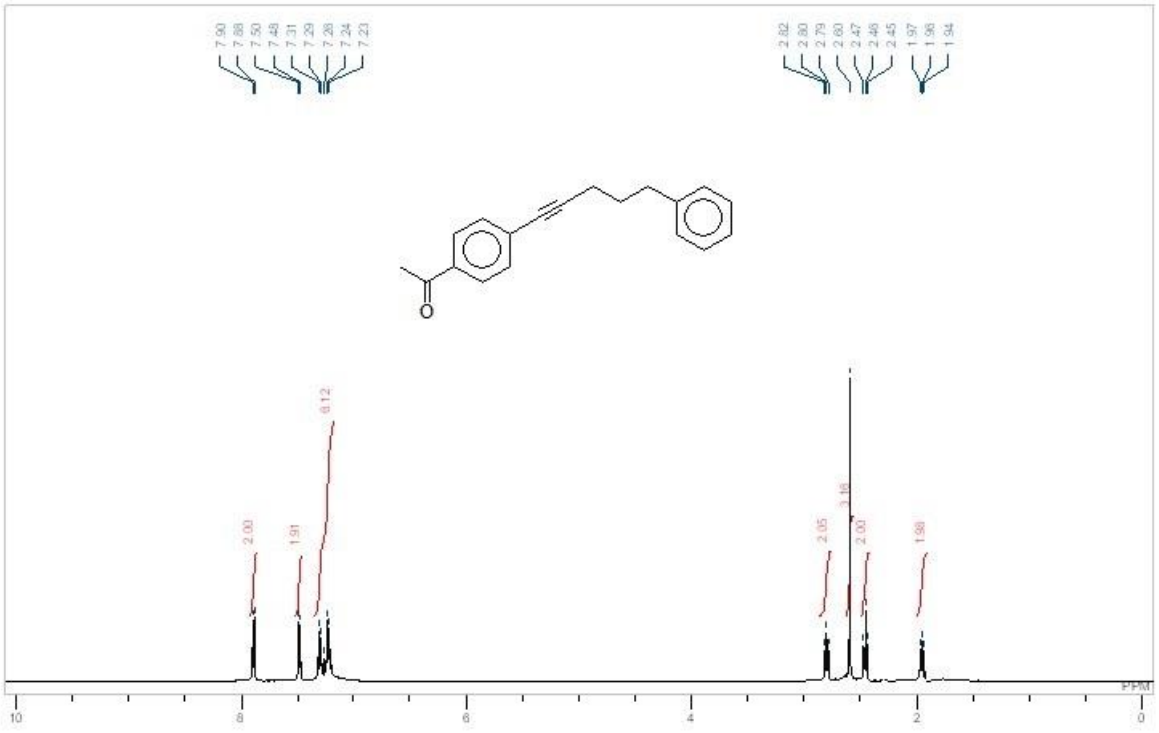

Figure A-I-91: ^{1}H NMR Spectrum of 1-[4-(5-phenylpent-1-yn-1-yl)phenyl]ethanone

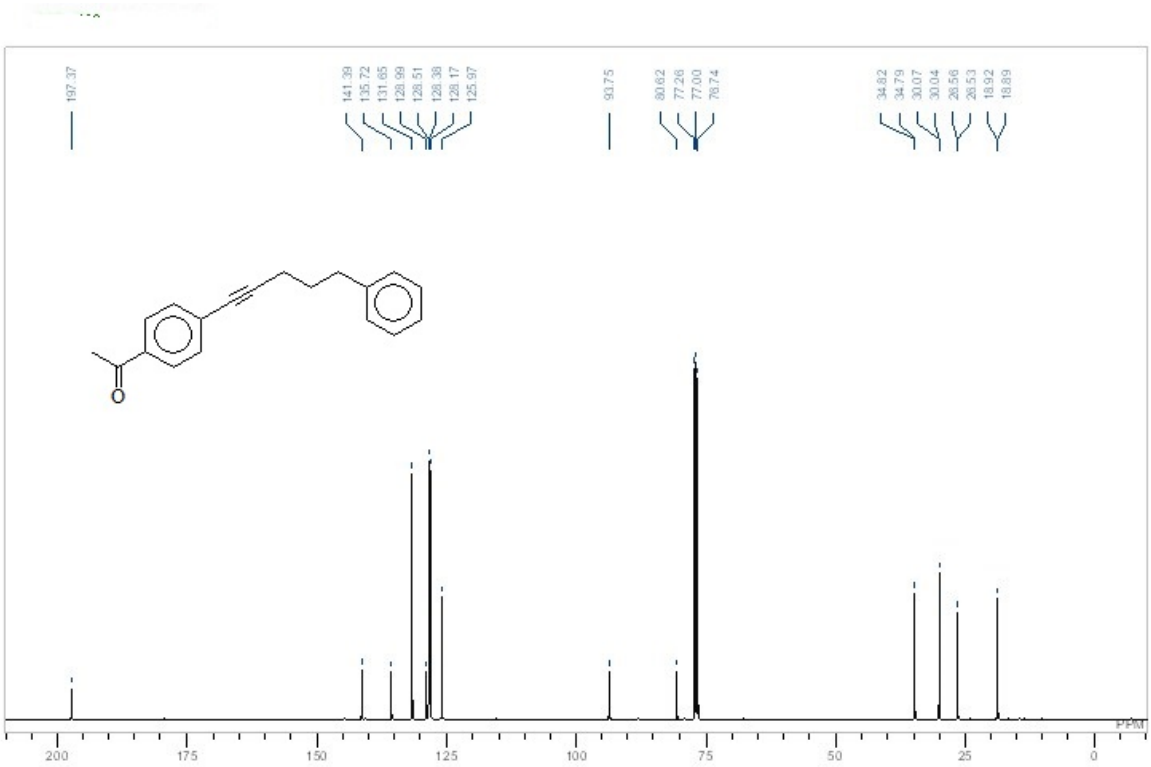

Figure A-I-92: ^{13}C NMR Spectrum of 1-[4-(5-phenylpent-1-yn-1-yl)phenyl]ethanone

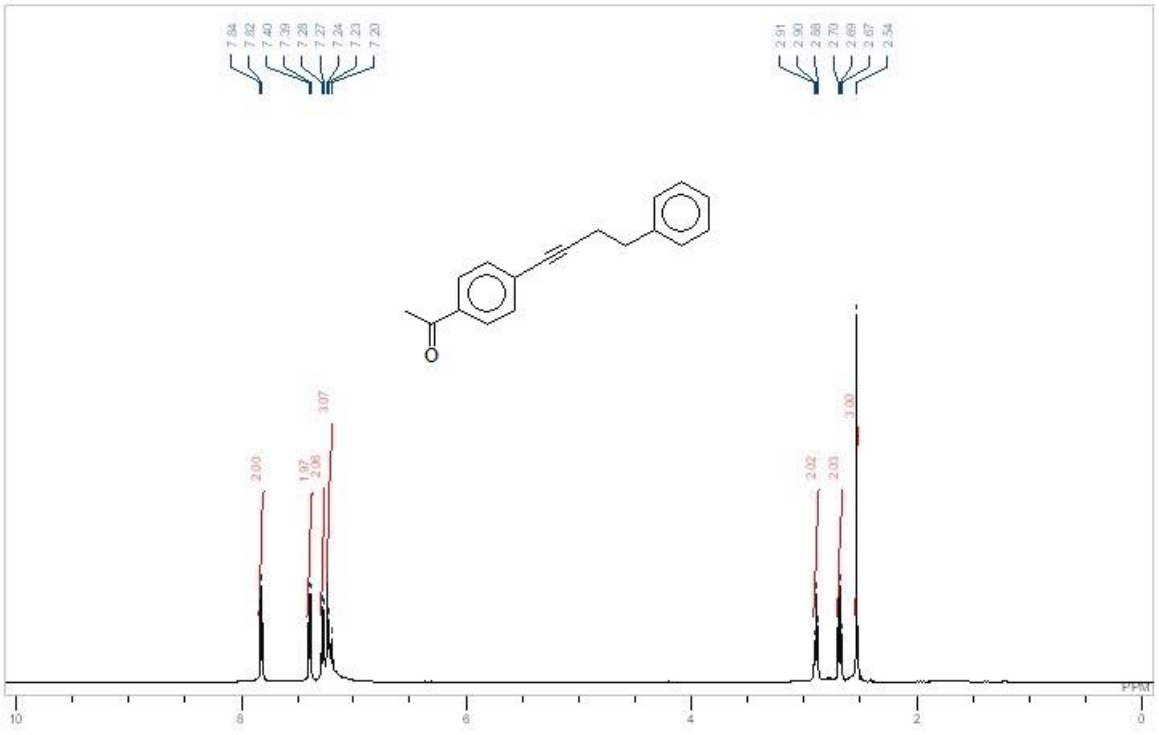

Figure A-I-93:[1]H NMR Spectrum of 1-[4-(4-phenylbut-1-yn-1-yl)phenyl]ethanone

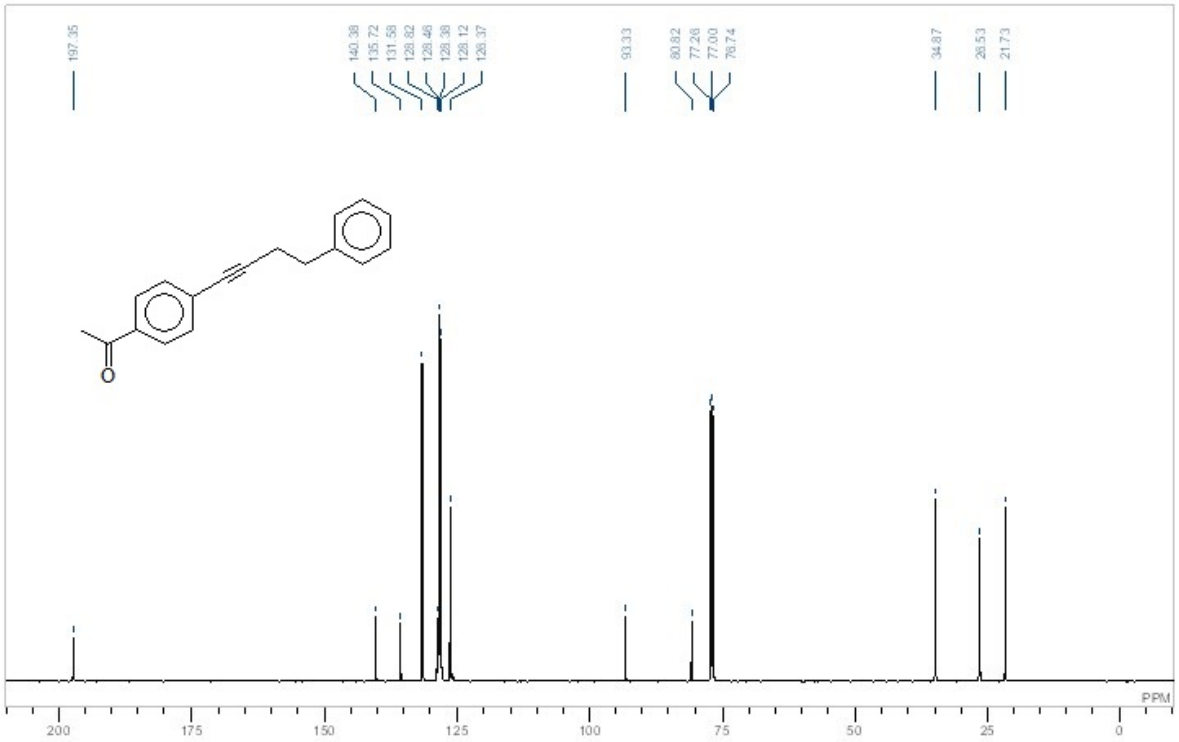

Figure A-I-94:[13]C NMR Spectrum of 1-[4-(4-phenylbut-1-yn-1-yl)phenyl]ethanone

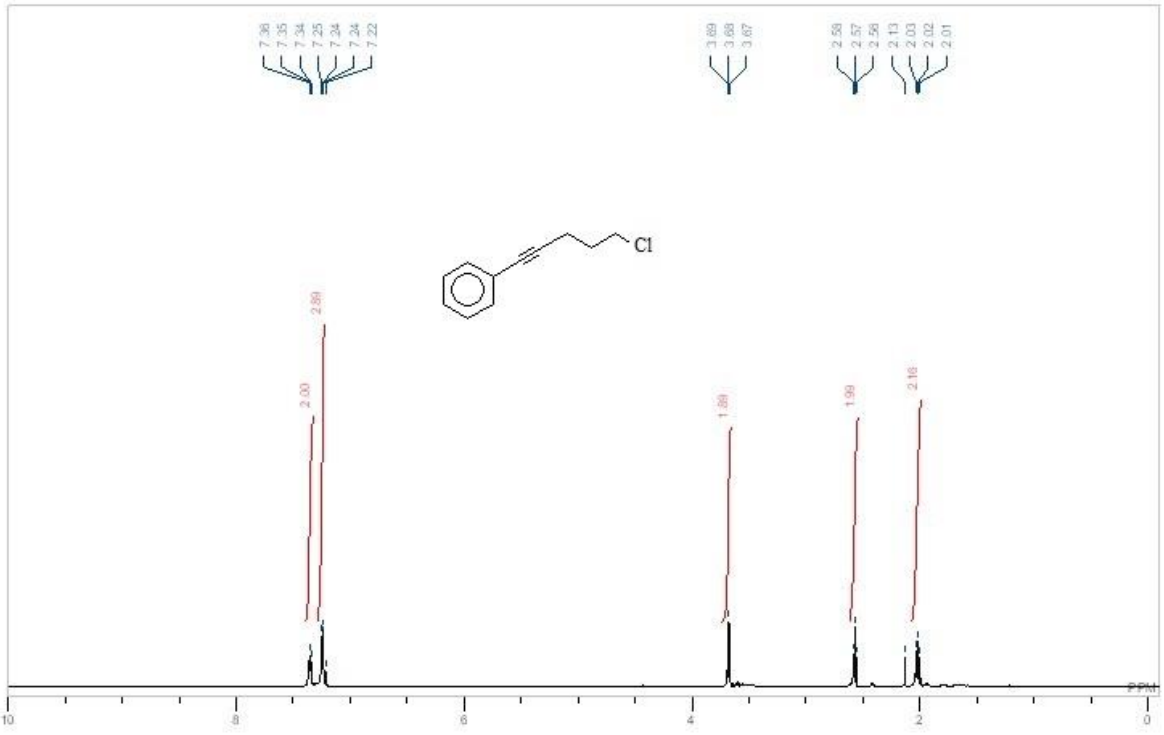

Figure A-I-95:[1]H NMR Spectrum of (5-chloropent-1-yn-1-yl)benzene

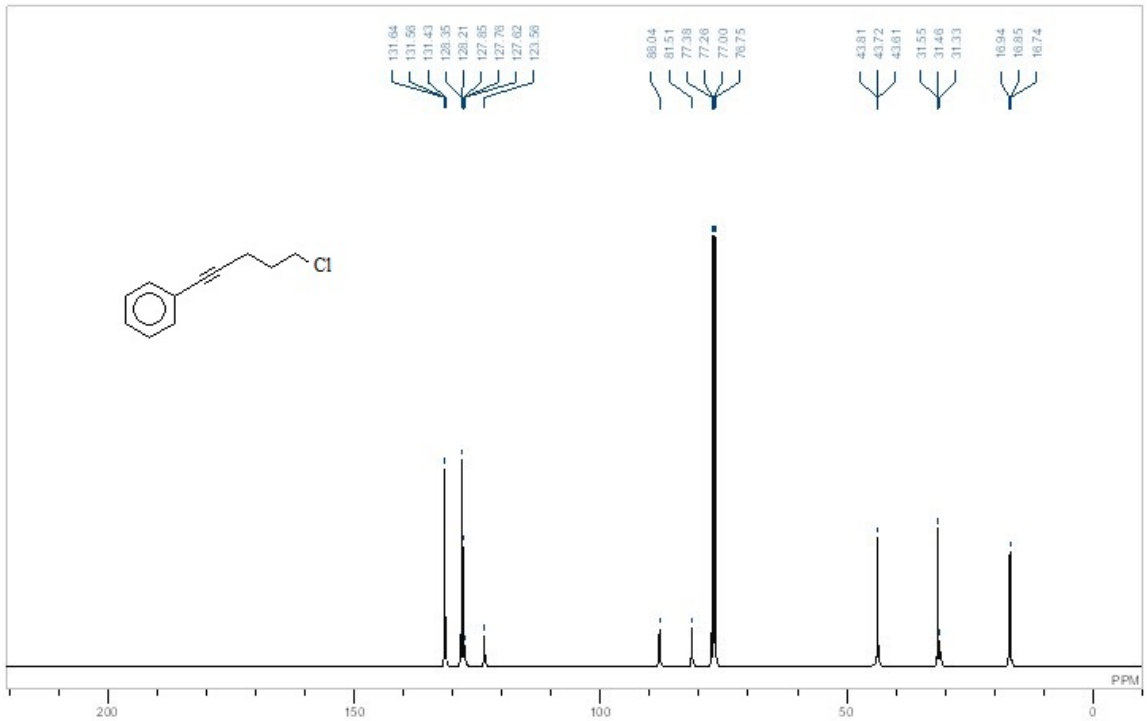

Figure A-I-96:[13]C NMR Spectrum of (5-chloropent-1-yn-1-yl)benzene

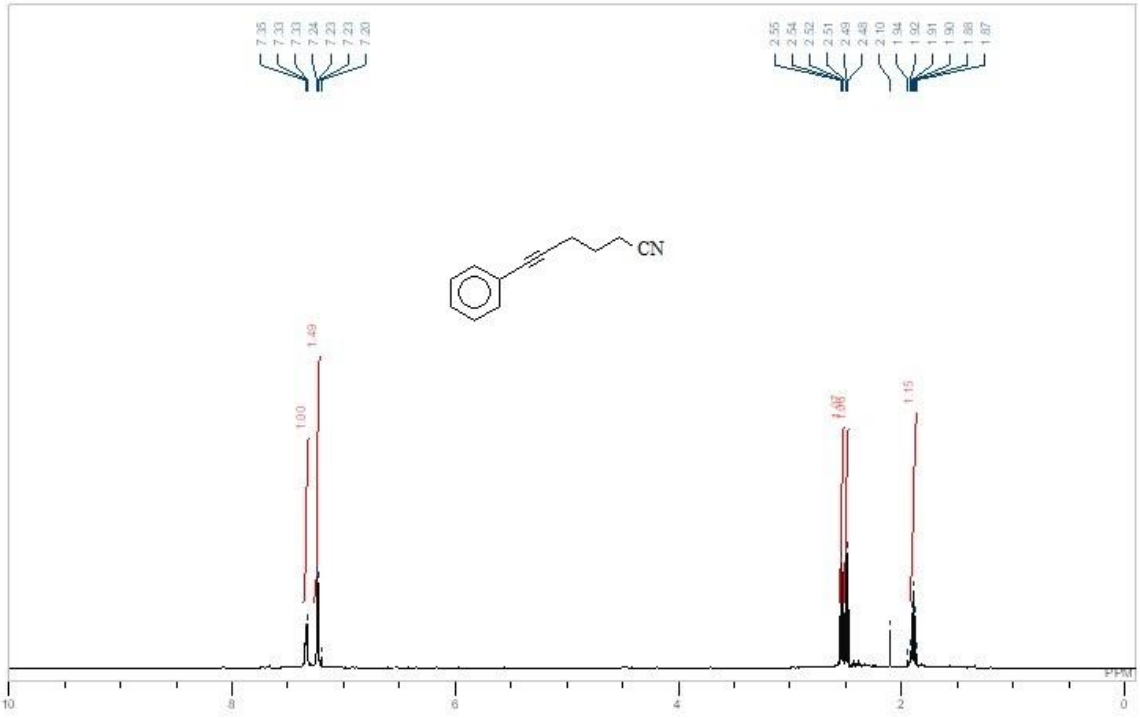

Figure A-I-97:[1]H NMR Spectrum of 6-phenylhex-5-ynenitrile

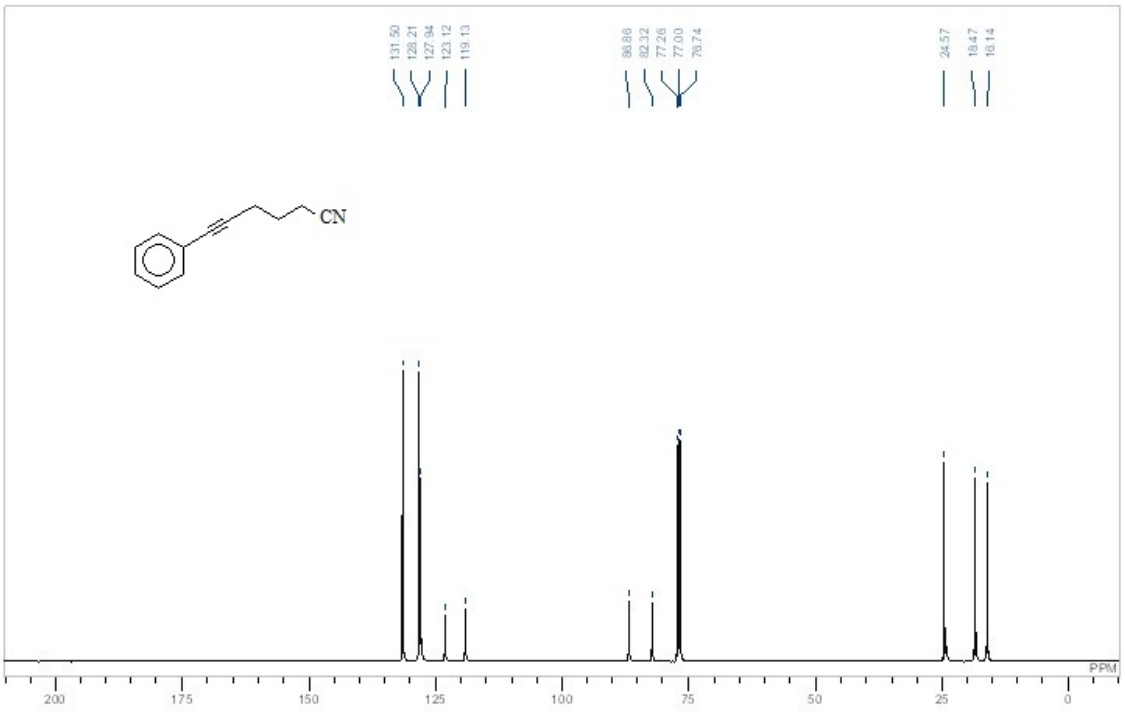

Figure A-I-98:[13]C NMR Spectrum of 6-phenylhex-5-ynenitrile

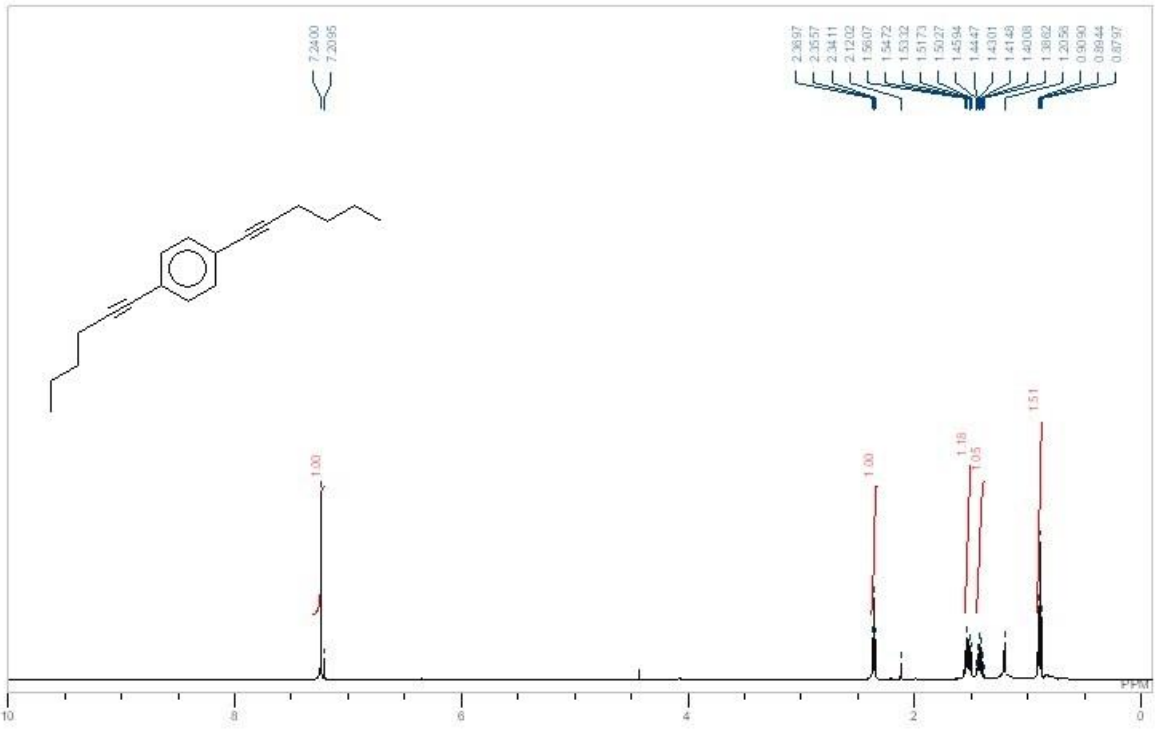

Figure A-I-99: ^{1}H NMR Spectrum of 1,4-di(hex-1-yn-1-yl)benzene

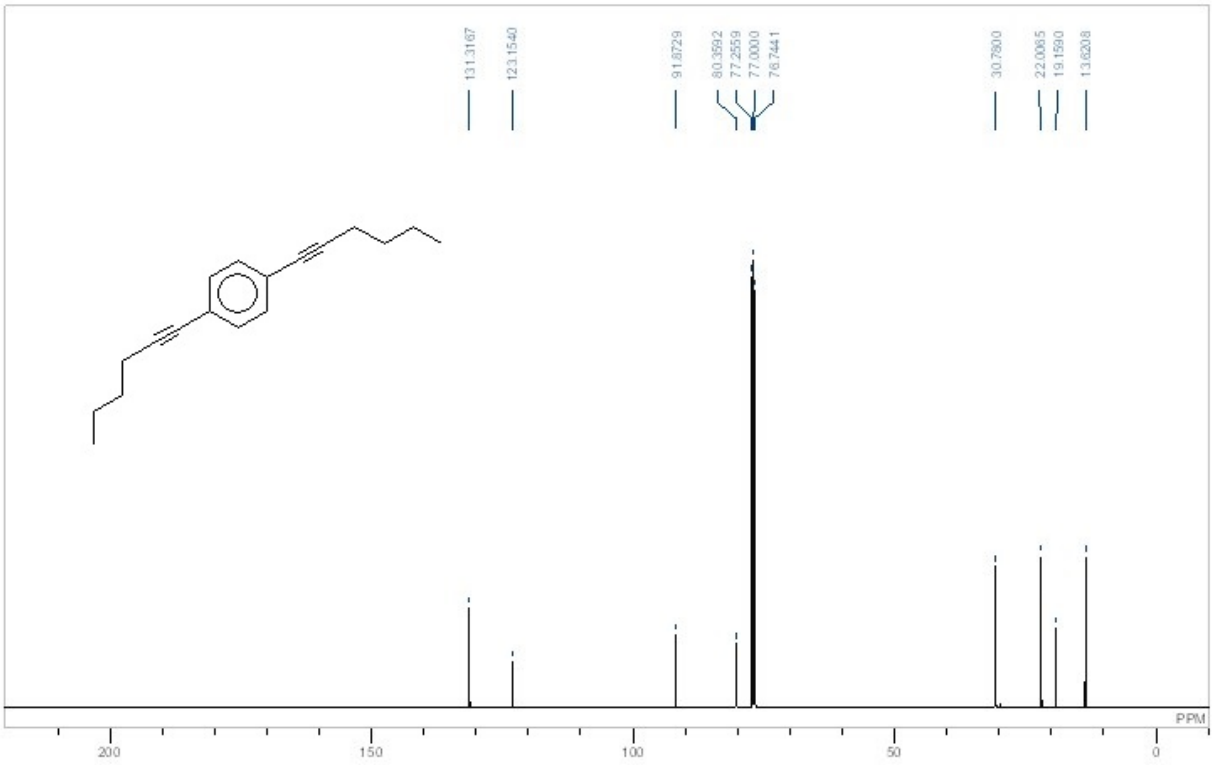

Figure A-I-100: ^{13}C NMR Spectrum of 1,4-di(hex-1-yn-1-yl)benzene

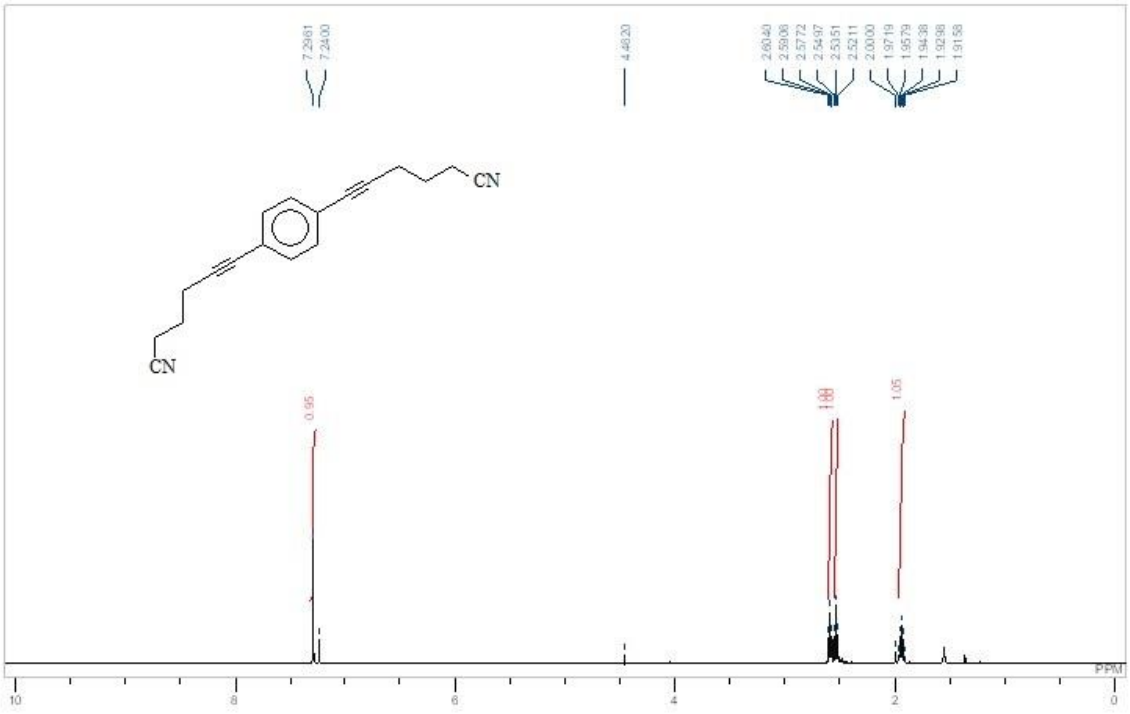

Figure A-I-101: ^{1}H NMR Spectrum of 6, 6'-benzene-1,4-diylbishex-5-ynenitrile

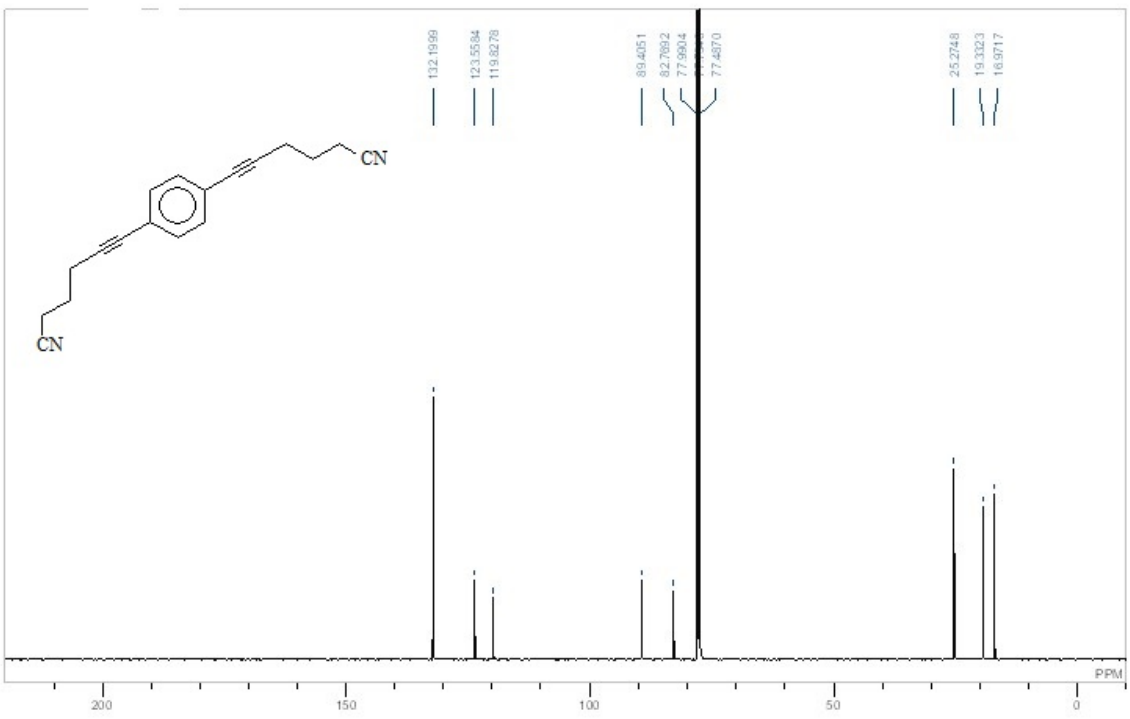

Figure A-I-102: ^{13}C NMR Spectrum of 6, 6'-benzene-1,4-diylbishex-5-ynenitrile

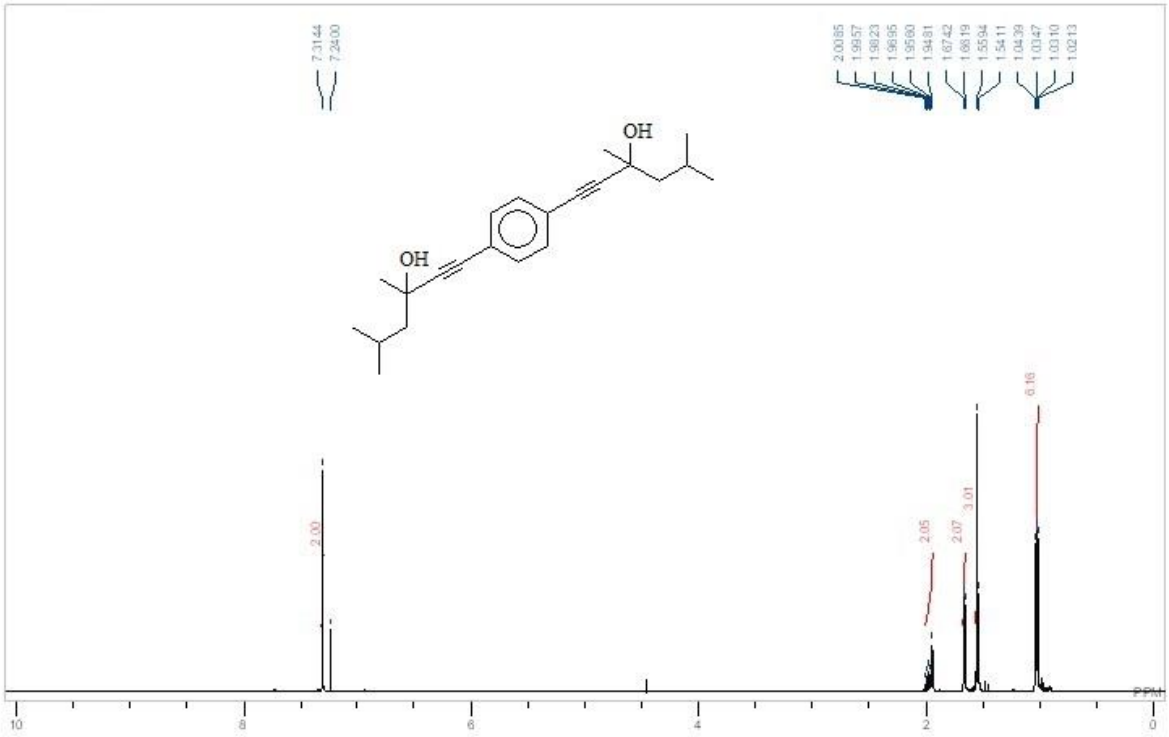

Figure A-I-103: ^{1}H NMR Spectrum of 1,4-bis(3,5-dimethyl-1-hex-1-yn-3-ol)benzene

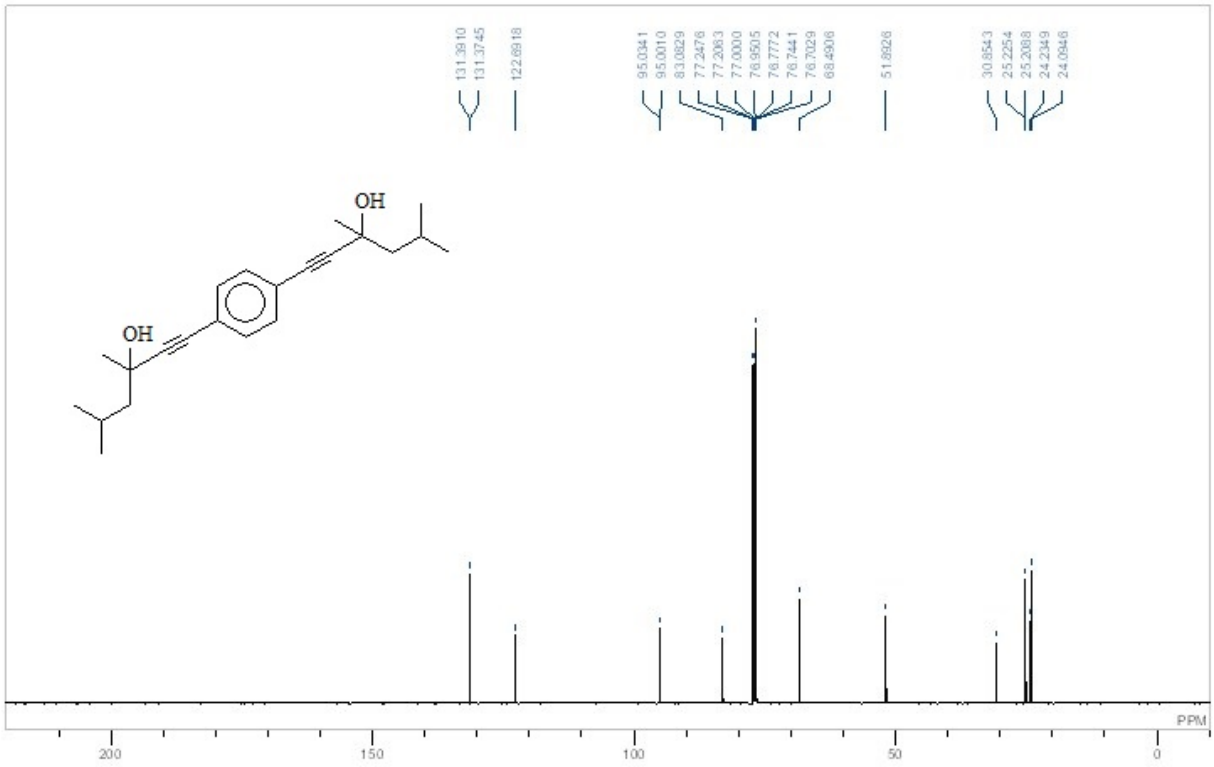

Figure A-I-104: ^{13}C NMR Spectrum of 1,4-bis(3,5-dimethyl-1-hex-1-yn-3-ol)benzene

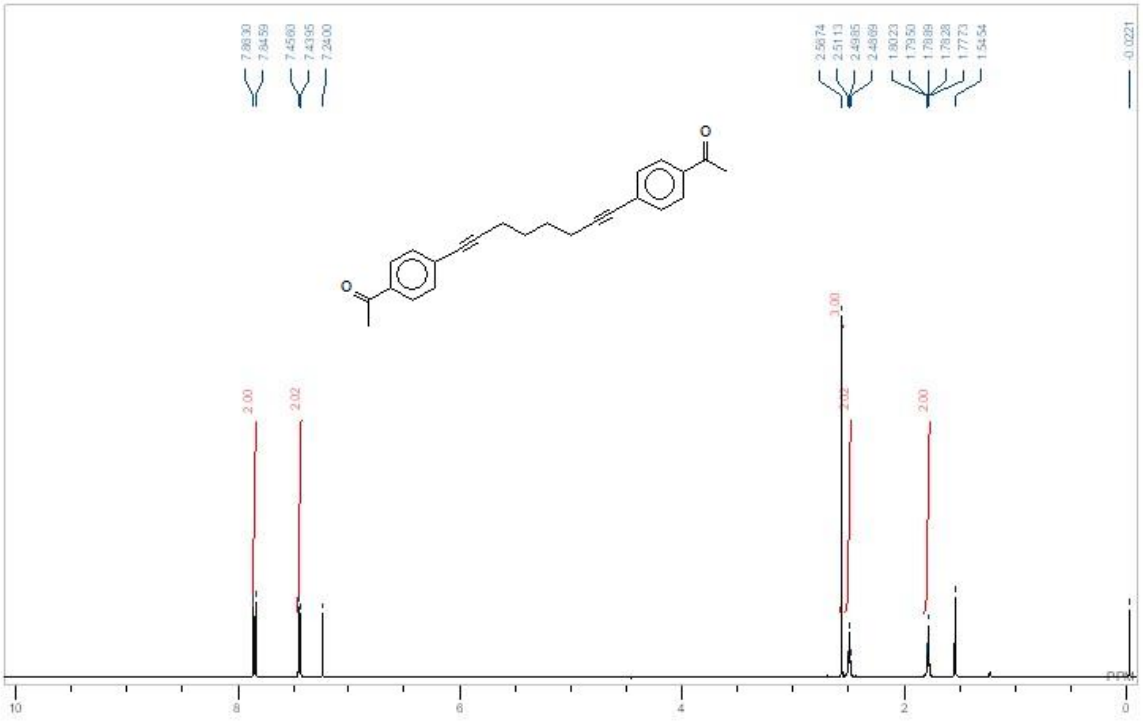

Figure A-I-105:[1]H NMR Spectrum of 1,1'-(octa-1,7-diyne-1,8-diyldibenzene-4,1-diyl)diethanone

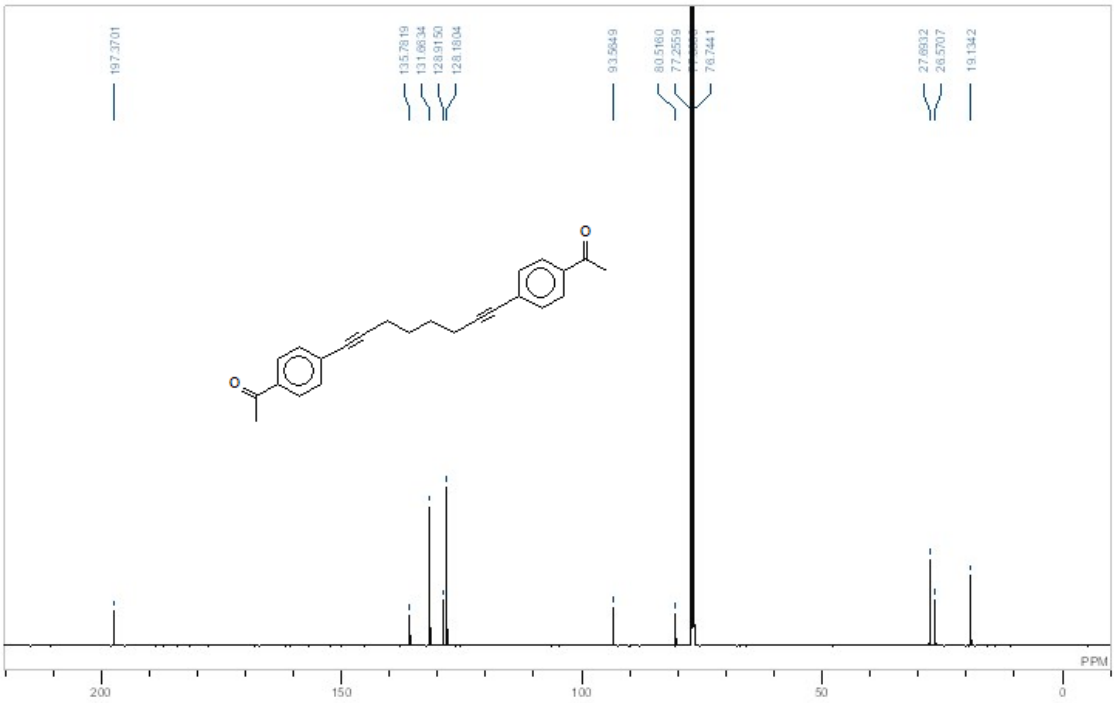

Figure A-I-106:[1]H NMR Spectrum of 1,1'-(octa-1,7-diyne-1,8-diyldibenzene-4,1-diyl)diethanone

A-II- FT-IR Spectrum of some ligands and complexes

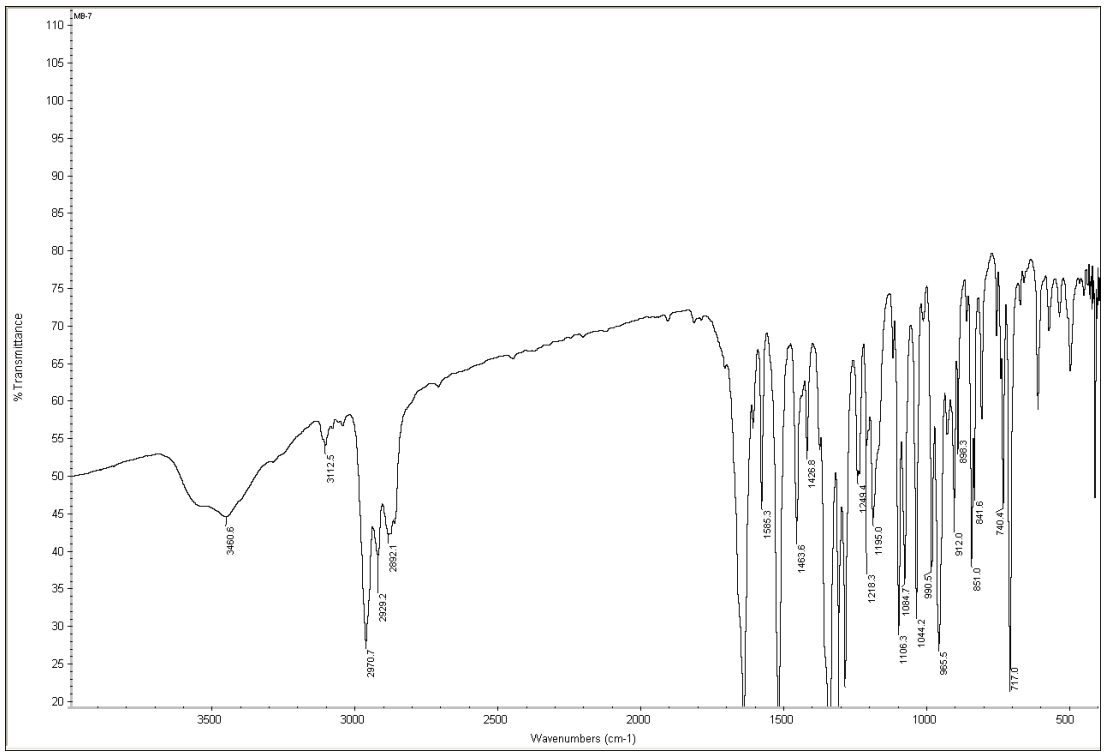

Figure A-II-1:FT-IR Spectrum of BOX-3

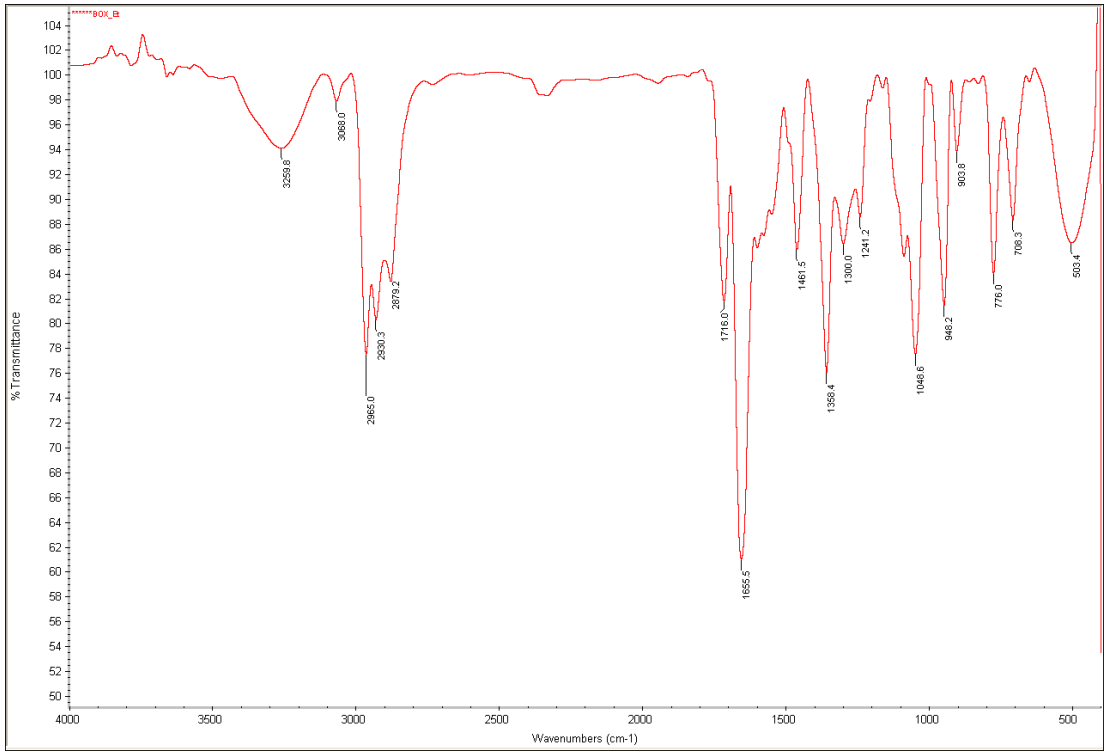

Figure A-II-2:FT-IR Spectrum of BOX-7

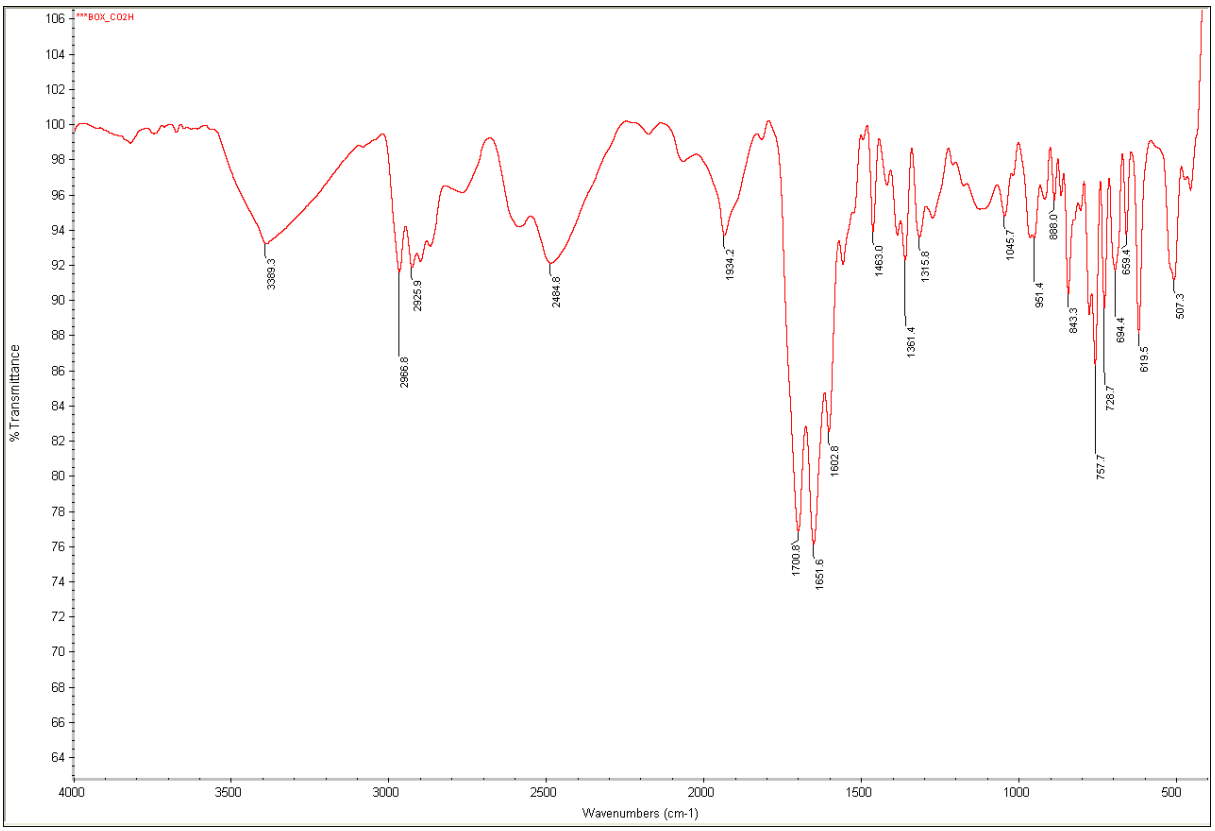

Figure A-II-3:FT-IR Spectrum of BOX-9

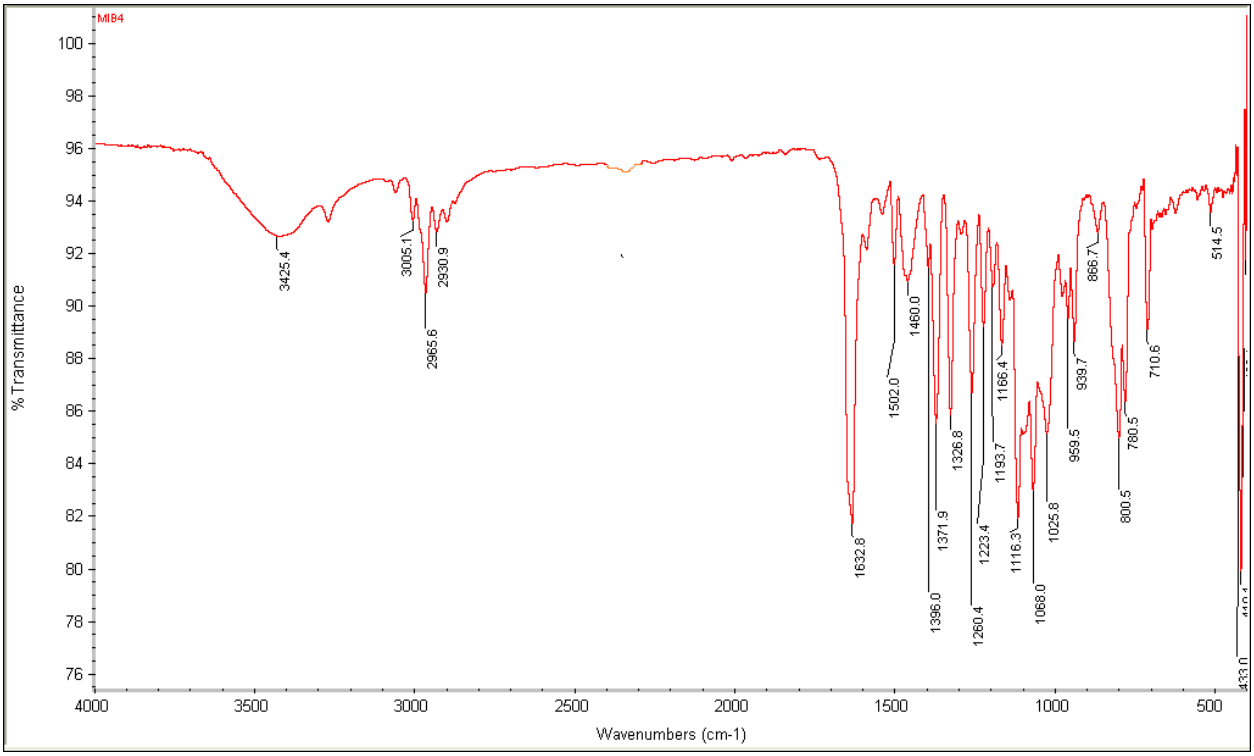

Figure A-II-4:FT-IR Spectrum of Pd-BOX-1

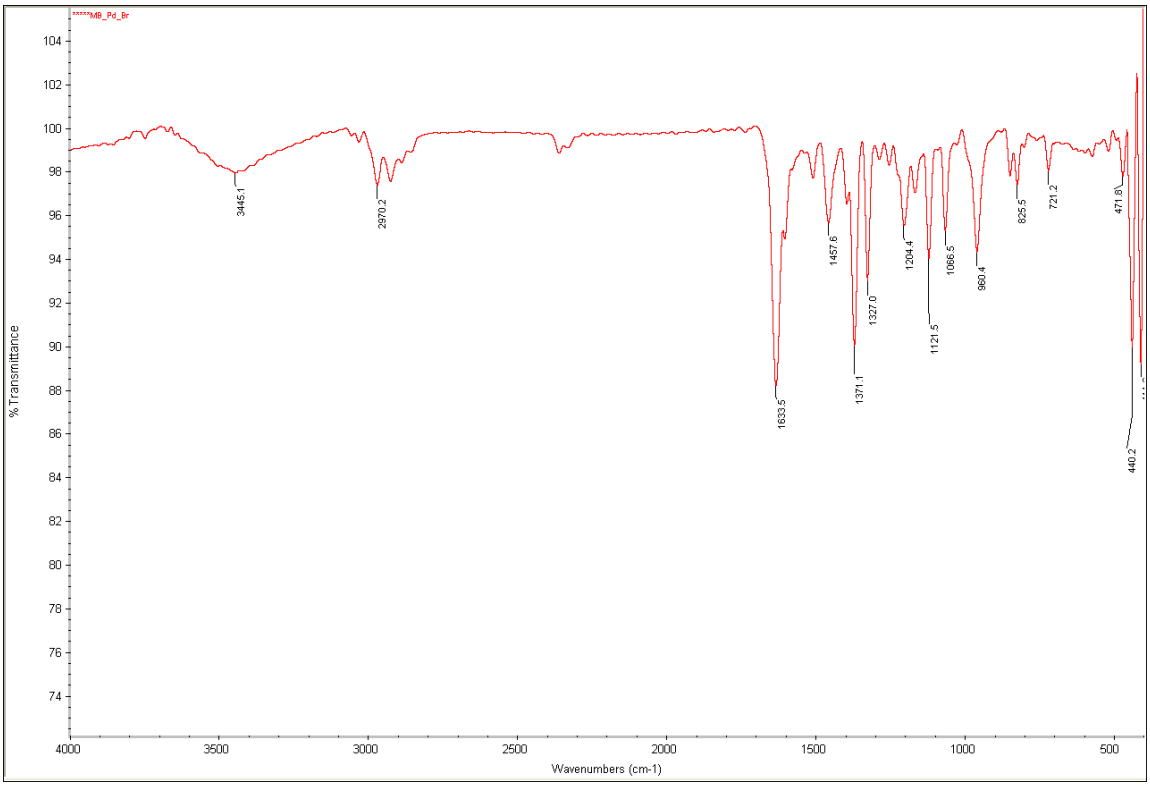

Figure A-II-5:FT-IR Spectrum of Pd-BOX-6

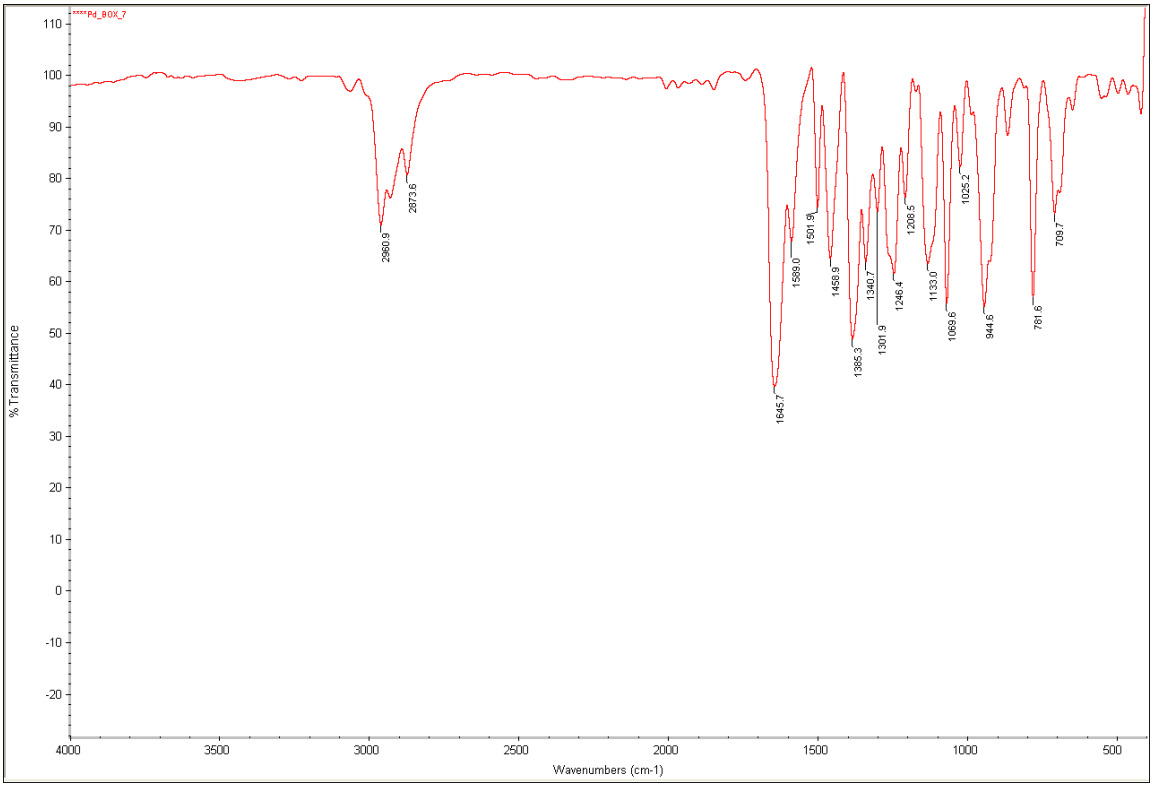

Figure A-II-6:FT-IR Spectrum of Pd-BOX-7

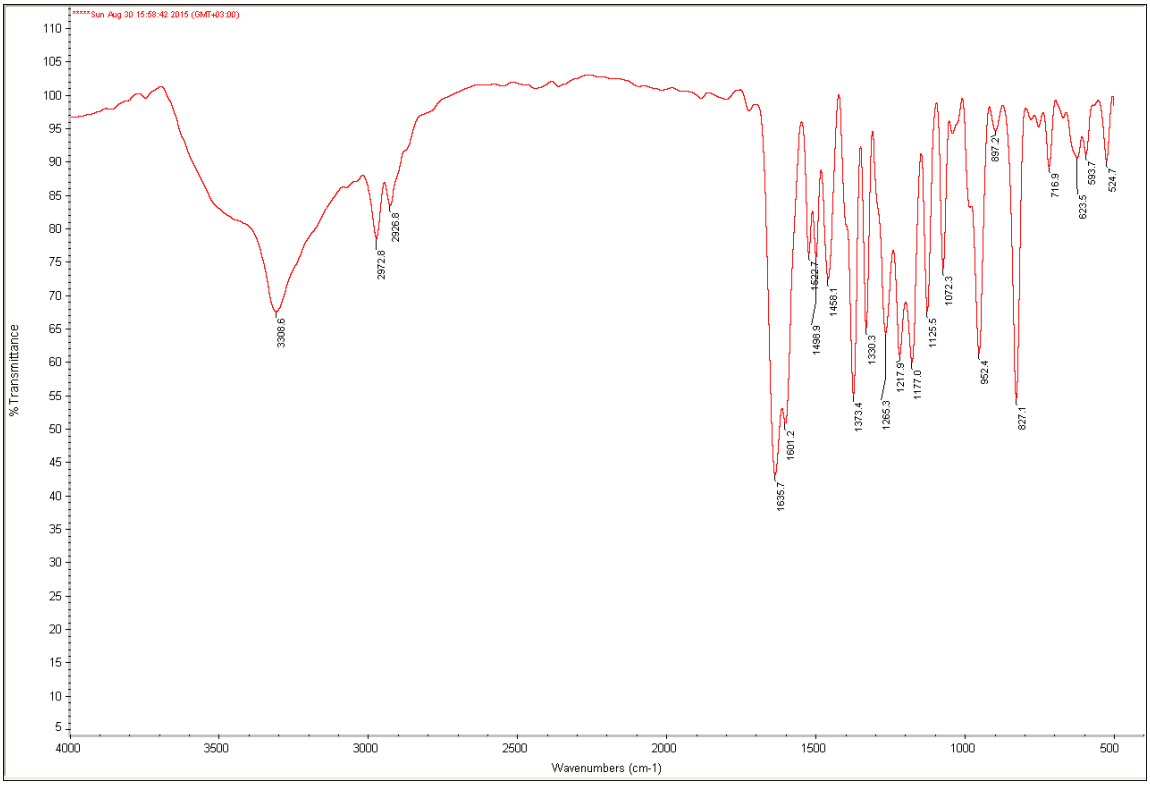

Figure A-II-7:FT-IR Spectrum of Pd-BOX-8

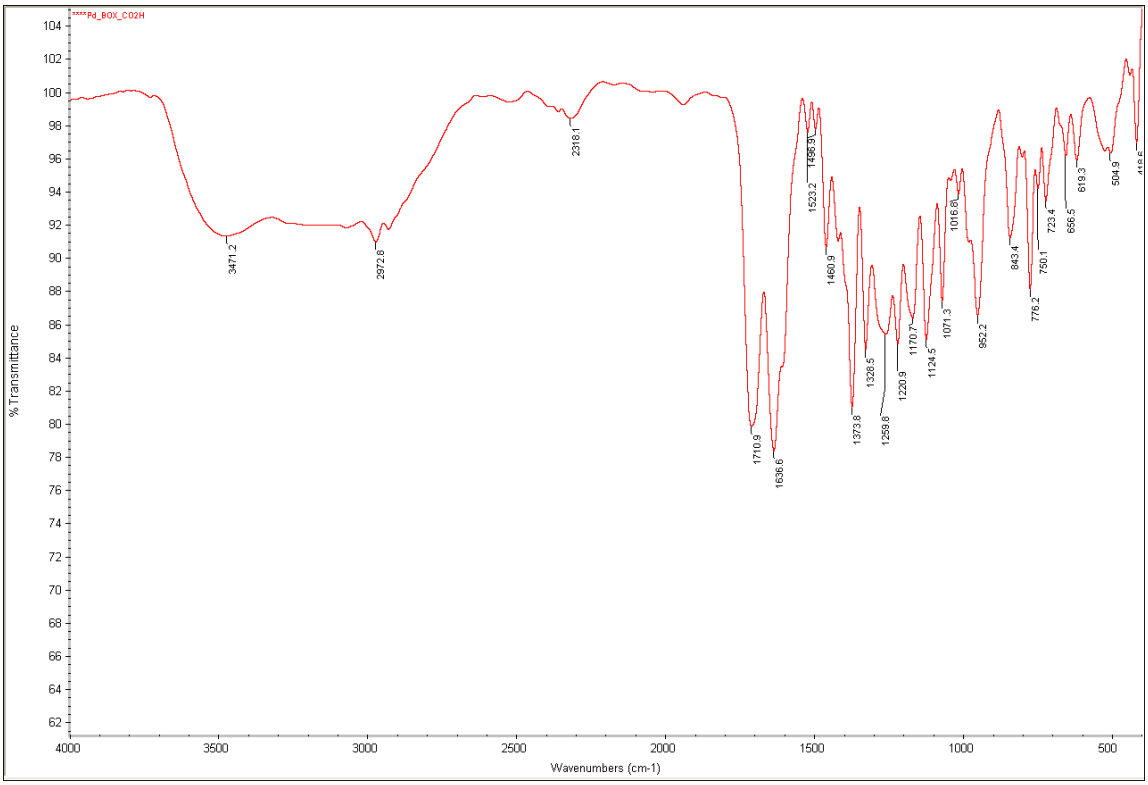

Figure A-II-8:FT-IR Spectrum of Pd-BOX-9

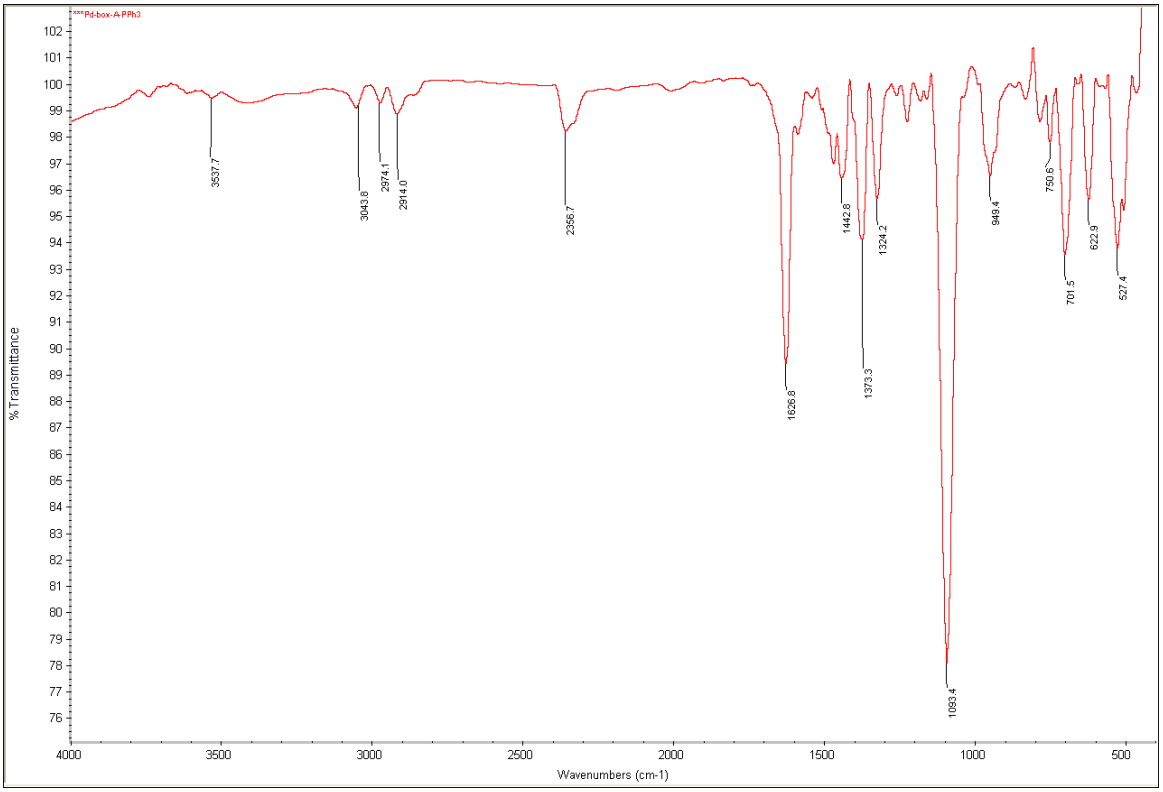

Figure A-II-9:FT-IR Spectrum of Pd-BOX-10

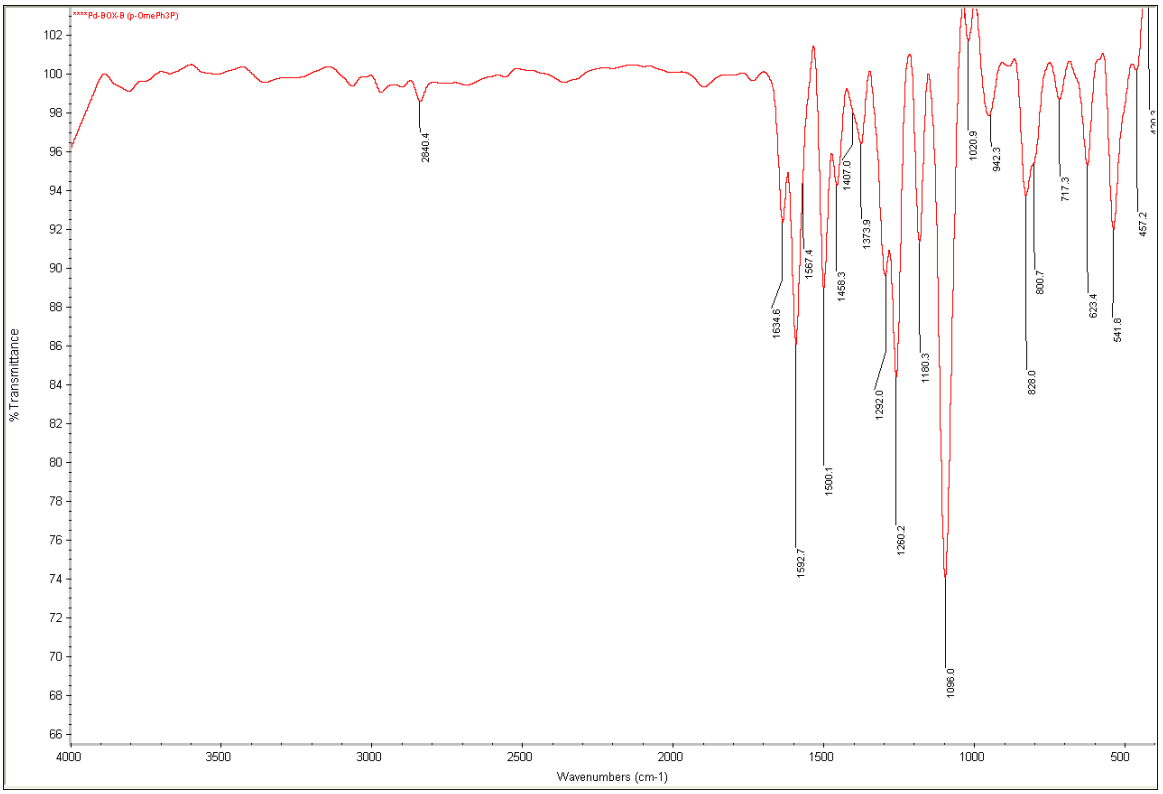

Figure A-II-10:FT-IR Spectrum of Pd-BOX-11

A-III: TGA Spectra of supported ligands and complexes

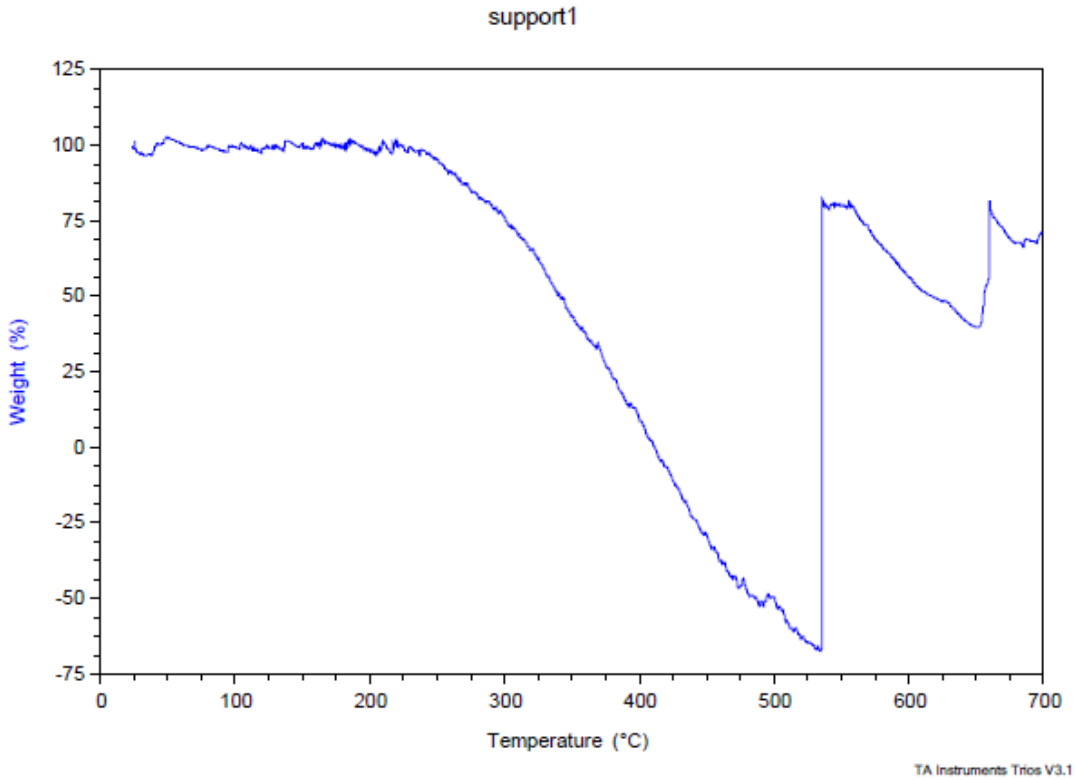

Figure A-III-1:TGA Spectrum of Merifield's resin support

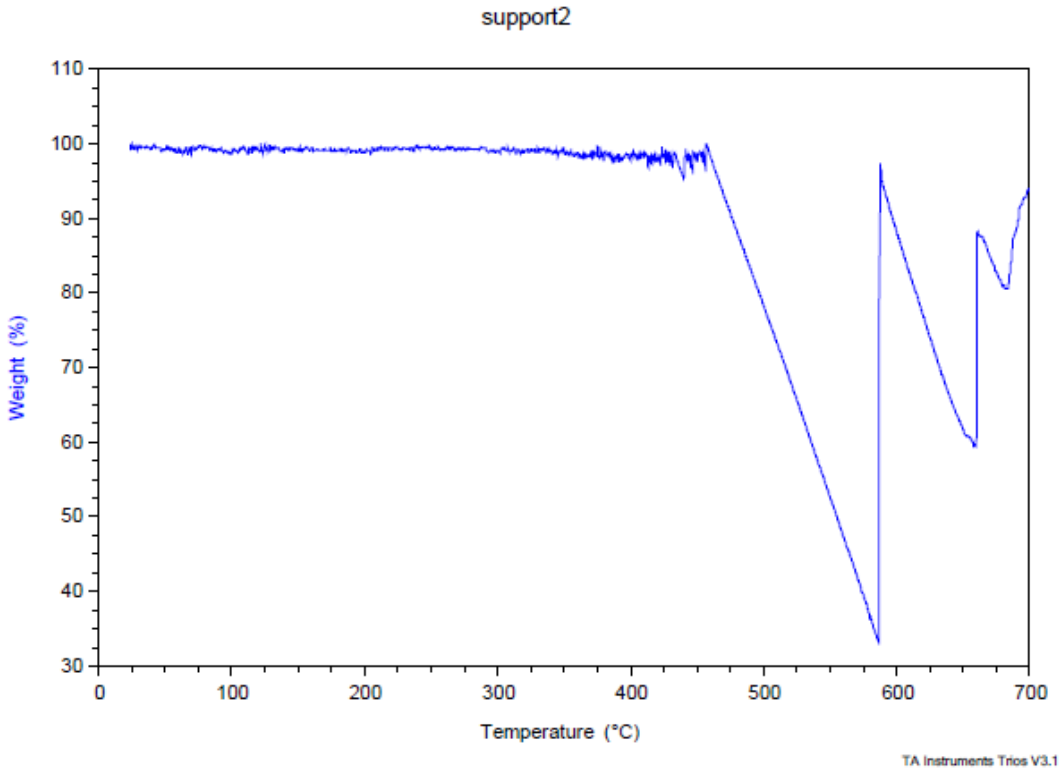

Figure A-III-2:TGA Spectrum of Benzyl silica support

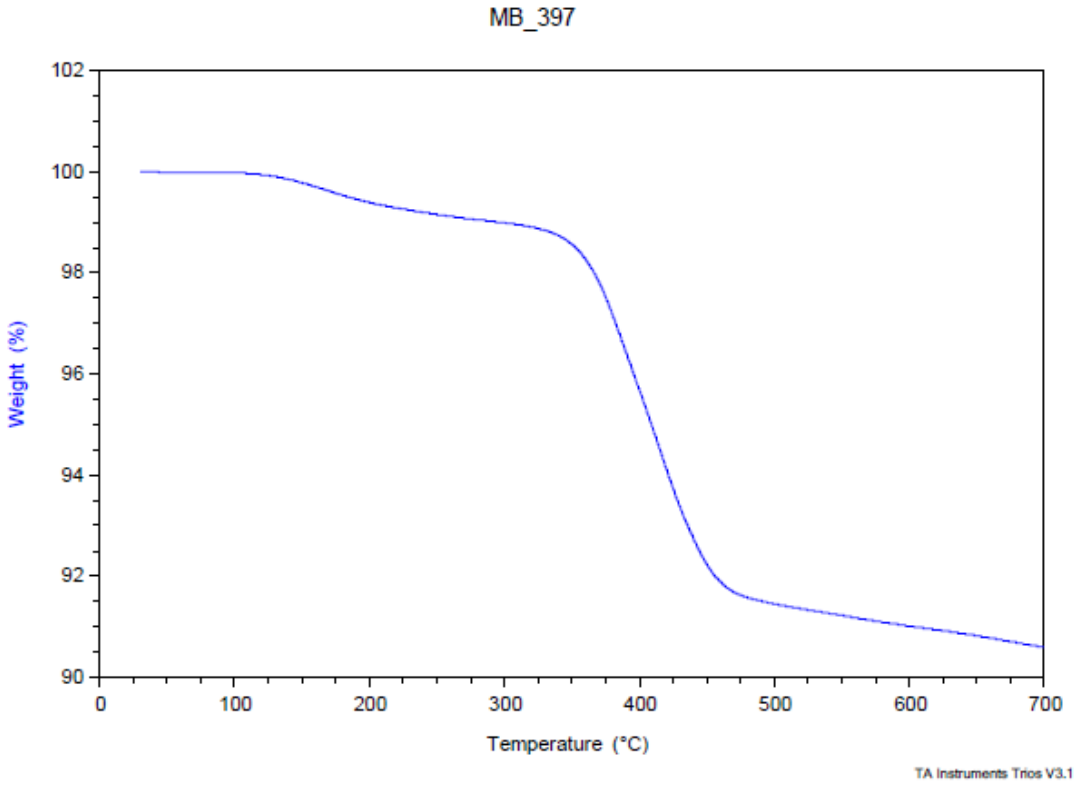

Figure A-III-3:TGA Spectrum of BOX10

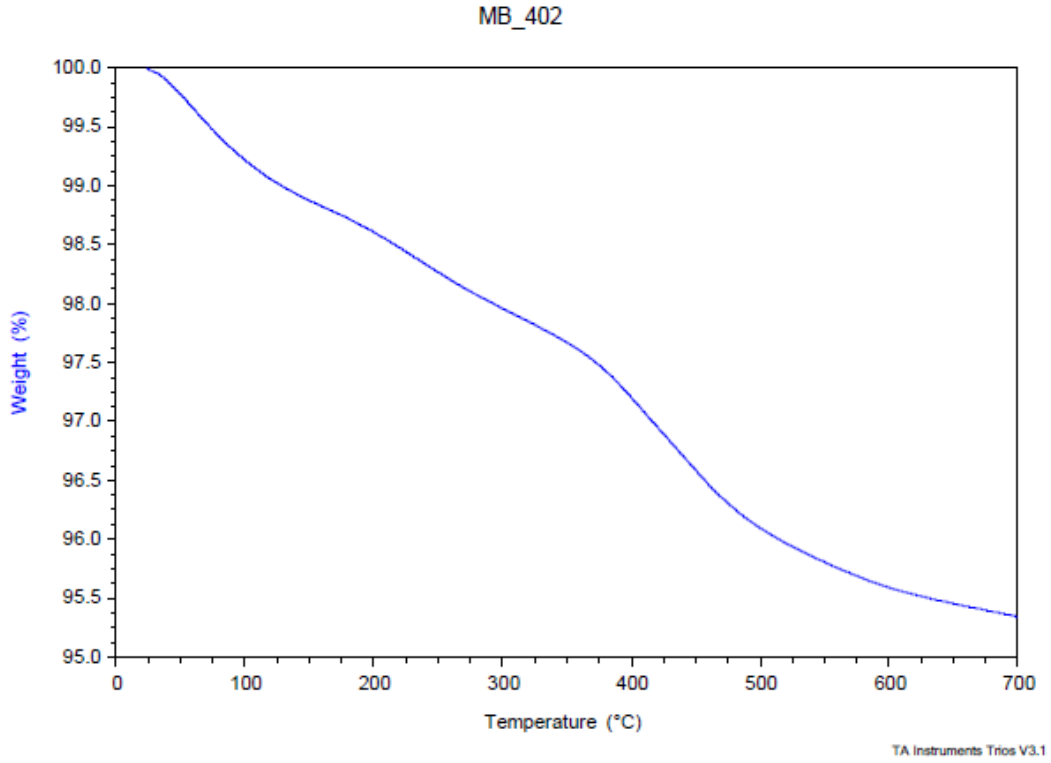

Figure A-III-4:TGA Spectrum of BOX-11

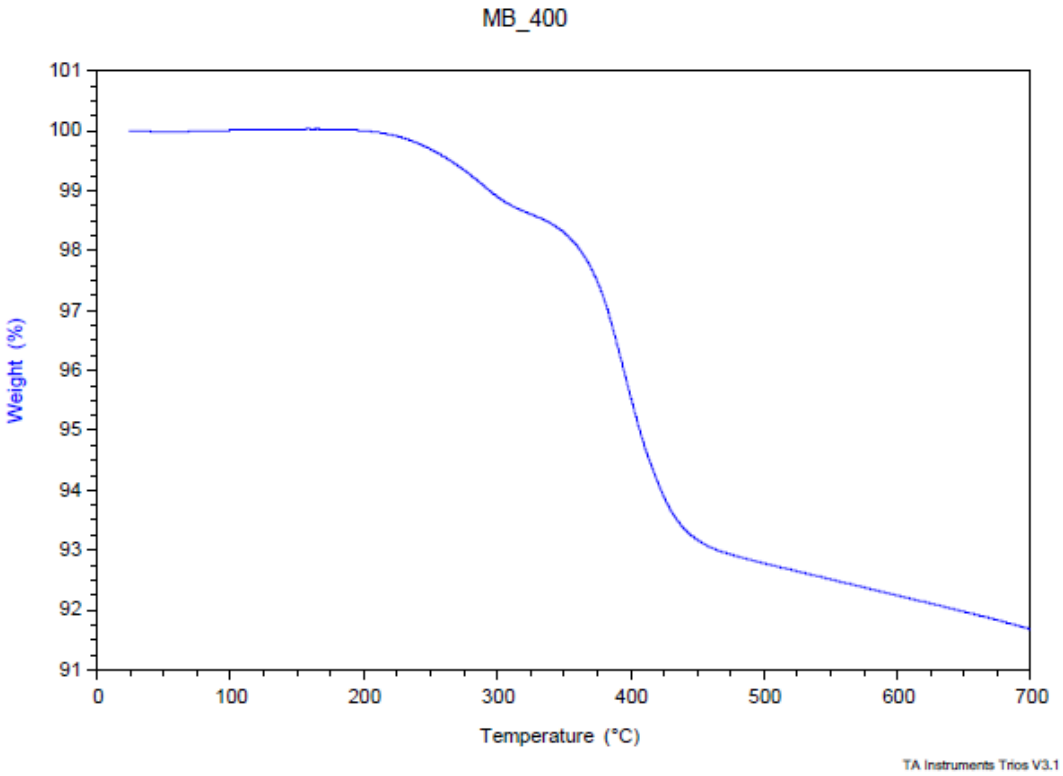

Figure A-III-5:TGA Spectrum of Pd-BOX-12

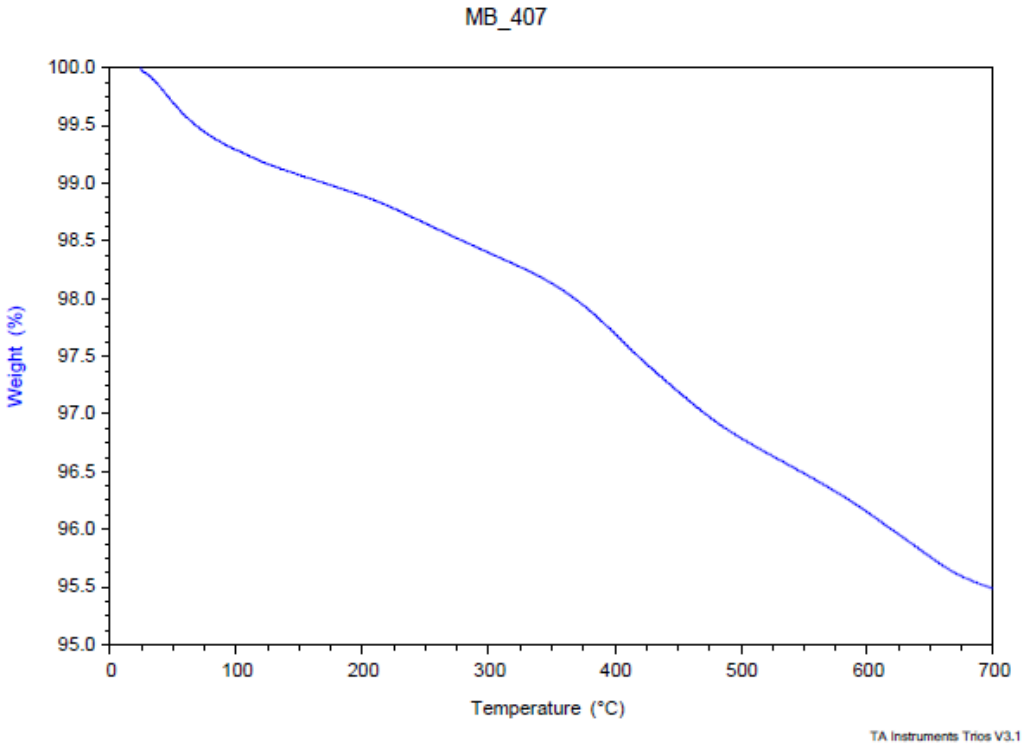

Figure A-III-6:TGA Spectrum of Pd-BOX-13

Vitae

Name	Mansur Bala Ibrahim
Nationality	Nigeria
Date of Birth	6/11/1983
Marital Status	Married with a daughter
Academic Background	B.Sc Chemistry, B.U.K (2005);
	M. Sc Chemistry (Colour Chemistry), B. U. K (2011);
	PhD Chemistry (Organic Chemistry), KFUPM (2015)
Publications	Co-author in 10 publications in international journals.
	Co-author in 5 conference papers
Address	Department of Chemistry, B. U. K, Nigeria
Email	mails4mb@yahoo.com, ibrahimm4571@buk.edu.ng
Mobile	+2348032203171, +966533693626